frontiers | Research Topics

Interactions between bioactive food ingredients and intestinal microbiota, volume II

Edited by
Zheng Ruan, Xiaodong Xia and Fengjie Sun

Published in
Frontiers in Microbiology

ISSN 1664-8714
ISBN 978-2-8325-5487-6
DOI 10.3389/978-2-8325-5487-6

About Frontiers

Frontiers is more than just an open access publisher of scholarly articles: it is a pioneering approach to the world of academia, radically improving the way scholarly research is managed. The grand vision of Frontiers is a world where all people have an equal opportunity to seek, share and generate knowledge. Frontiers provides immediate and permanent online open access to all its publications, but this alone is not enough to realize our grand goals.

Frontiers journal series

The Frontiers journal series is a multi-tier and interdisciplinary set of open-access, online journals, promising a paradigm shift from the current review, selection and dissemination processes in academic publishing. All Frontiers journals are driven by researchers for researchers; therefore, they constitute a service to the scholarly community. At the same time, the *Frontiers journal series* operates on a revolutionary invention, the tiered publishing system, initially addressing specific communities of scholars, and gradually climbing up to broader public understanding, thus serving the interests of the lay society, too.

Dedication to quality

Each Frontiers article is a landmark of the highest quality, thanks to genuinely collaborative interactions between authors and review editors, who include some of the world's best academicians. Research must be certified by peers before entering a stream of knowledge that may eventually reach the public - and shape society; therefore, Frontiers only applies the most rigorous and unbiased reviews. Frontiers revolutionizes research publishing by freely delivering the most outstanding research, evaluated with no bias from both the academic and social point of view. By applying the most advanced information technologies, Frontiers is catapulting scholarly publishing into a new generation.

What are Frontiers Research Topics?

Frontiers Research Topics are very popular trademarks of the *Frontiers journals series*: they are collections of at least ten articles, all centered on a particular subject. With their unique mix of varied contributions from Original Research to Review Articles, Frontiers Research Topics unify the most influential researchers, the latest key findings and historical advances in a hot research area.

Find out more on how to host your own Frontiers Research Topic or contribute to one as an author by contacting the Frontiers editorial office: frontiersin.org/about/contact

Interactions between bioactive food ingredients and intestinal microbiota, volume II

Topic editors

Zheng Ruan — Nanchang University, China

Xiaodong Xia — Dalian Polytechnic University, China

Fengjie Sun — Georgia Gwinnett College, United States

Citation

Ruan, Z., Xia, X., Sun, F., eds. (2024). *Interactions between bioactive food ingredients and intestinal microbiota, volume II*. Lausanne: Frontiers Media SA.

doi: 10.3389/978-2-8325-5487-6

Table of contents

frontiers | Frontiers in Microbiology

TYPE Editorial
PUBLISHED 17 September 2024
DOI 10.3389/fmicb.2024.1490884

OPEN ACCESS

EDITED AND REVIEWED BY
Aldo Corsetti,
University of Teramo, Italy

*CORRESPONDENCE
Fengjie Sun
fsun@ggc.edu

RECEIVED 03 September 2024
ACCEPTED 05 September 2024
PUBLISHED 17 September 2024

CITATION
Ruan Z, Xia X and Sun F (2024) Editorial: Interactions between bioactive food ingredients and intestinal microbiota, volume II. *Front. Microbiol.* 15:1490884. doi: 10.3389/fmicb.2024.1490884

Editorial: Interactions between bioactive food ingredients and intestinal microbiota, volume II

Zheng Ruan[1], Xiaodong Xia[2] and Fengjie Sun[3]*

[1]School of Food Science, Nanchang University, Nanchang, China, [2]School of Food Science and Technology, Dalian Polytechnic University, Dalian, China, [3]Department of Biological Sciences, School of Science and Technology, Georgia Gwinnett College, Lawrenceville, GA, United States

KEYWORDS

bioactive food ingredients, gut health, gut microbiota, microbe-microbe interactions, metabolomics

Editorial on the Research Topic
Interactions between bioactive food ingredients and intestinal microbiota, volume II

To date, human health has been greatly benefited from the rapid development of the multiple "omics" techniques (Babu and Snyder, 2023; Karczewski and Snyder, 2018; Dai and Shen, 2022; Mohr et al., 2024; Yurkovich et al., 2024; Hao et al., 2022), in combination with various application strategies, such as the use of dietary nutrients in the regulation of intestinal microbiota (Nayak et al., 2021; Si et al., 2021; Hasin et al., 2017). It is well-known that numerous biological functions, e.g., immune system, energy and intestinal homeostasis of the host, and metabolic activities, involved in human health are regulated by the human gut microbiota, which includes diverse groups of bacteria, fungi, viruses, and protozoa inhabiting the gastrointestinal tract (Fan and Pedersen, 2021; Gebrayel et al., 2022). Therefore, it is extremely important to determine how different diets shape the composition and function of gut microbiome and to explore the associations between diet (nutrition), host, and microbes for the development of precision nutrition and microbiome-based therapies for various medical disorders (Van Hul et al., 2024; Ross et al., 2024; Dmytriv et al., 2024; Jacquier et al., 2024; Li et al., 2024; Pires et al., 2024; Duffuler et al., 2024; Wu et al., 2024; Osawa et al., 2024; Singh et al., 2021; Wang et al., 2019: Han et al., 2021; Ray and Mukherjee, 2021; Deehan et al., 2020). Currently, the molecular mechanisms underlying the interactions among food nutrients, prebiotics, gut microbiota, and host health remain largely unknown.

Considering the rapid advancements in exploring of the associations among food nutrients, gut microbiota, and human health, we emphasize the significance of enhancing global scientific research on the interactions between food nutrient and gut microbiota, and their roles in developing dysbiosis and low-grade inflammation during the intestinal barrier dysfunction and metabolic disorders in hosts and in developing effective dietary treatments for various medical disorders in human.

Building on the success of our Research Topic titled "*Interactions between bioactive food ingredients and intestinal microbiota*" in the journal *Frontiers in Microbiology* (Ruan et al., 2022), we summarize the main results of a total of 15 publications contributed by 115 contributors in Volume II of this Research Topic with the same topics widely explored. Most of the contributions collected in this Research Topic were performed

based mainly on animal models, i.e., eight articles on mouse models of a total of six medical disorders, and humans of either healthy subjects or patients of two medical disorders (i.e., colorectal cancer and kidney disease), using various well-established "omics" analyses. The main outcomes of these contributions are summarized below.

First, a total of five contributions were based on healthy human subjects to explore the effects of various substances on the gut microbiome. Vizioli et al. investigated the potential effect of probiotics, yogurt supplemented with *Streptococcus thermophilus*, *Lactobacillus delbrueckii*, and *Bifidobacterium animalis* subsp. *lactis* strain BB-12, on the gut microbiome and metabolome of a total of 59 healthy children using untargeted metabolomics and shotgun metagenomics analyses. Their results showed that in 10 days, the relative abundances of these probiotics were significantly increased, indicating the impact of probiotics on the bacteria of interest in the gut microbiome. However, the protective gastrointestinal effect of the functional metabolite changes would be verified by longer intervention durations in children at risk for gastrointestinal disorders. Corrêa et al. studied the effects of Moro orange (*Citrus sinensis* L. Osbeck) juice (MOJ) on gut microbiota composition and subsequent changes in the levels of cardiometabolic biomarkers in a total of 12 overweight women, demonstrating the importance of orange juice intake duration, as observed in the evident variations in the beneficial changes (e.g., blood pressure improvement) between 2- and 4-week interval of MOJ intake. This study provided strong experimental evidence to support that changes in specific operational taxonomic units (OTUs) of the gut microbiota in response to MOJ intake were associated with significant improvements in some cardiometabolic biomarkers and short-chain fatty acid (SCFA) levels in overweight women with insulin resistance. Gu et al. explored the potential effects of citrus pectin-type polysaccharides, including (1) the pectin polysaccharide (PEC), which was the partially hydrolyzed pectin (PPH), and (2) the pectin oligosaccharide (POS), on the improvement of aging-associated dysbiosis and the levels of SCFAs of the gut microbiota using five healthy elderly volunteers (70–75 years) and five younger adults (30–35 years). The main results showed that these pectins boosted various bacterial groups differently from the reference prebiotic substrate (inulin), and the *in vitro* modulating effects of pectins on elderly gut microbiota revealed significant potential of using pectins to improve age-related dysbiosis. The authors indicated that further human intervention studies were necessary to verify the potential effects of pectins observed in this study. Rawi et al. identified the putative primary degraders (i.e., gum-fermenting bacteria) of commercial acacia (*Acacia senegal*) gum, which was composed of arabinogalactan branched polysaccharide and was marketed as a functional dietary fiber to improve overall human gut health, in the gut ecosystem of three healthy human subjects based on enrichment culture fermentation in an anaerobic chamber for 144 h. Based on the *16S RNA* sequencing, a total of five bacterial strains were found to be gum-fermenting bacteria and matched to butyrate-producing *Escherichia fergusonii*, ATCC 35469. This study confirmed the use of acacia gum as a potential prebiotic and an alternative approach for mediating gut illness. Lan et al. screened strains of *Bifidobacterium animalis* subsp. *lactis* with differential oligosaccharide metabolism to subsequently perform genome-wide resequencing and real time quantitative PCR (RT-qPCR) analyses in mothers and their infants. The authors further explored the mechanism underlying the differences in *B. animalis* subsp. *lactis* oligosaccharide metabolism, revealing that the variations in the gene transcription levels led to intraspecies differences in the ability of the strains to metabolize oligosaccharides even when they belonged to the same subspecies, providing strong experimental evidence to support the utilization of *B. animalis* subsp. *lactis* strains as probiotics and the development of synbiotic products.

Second, two publications were based on patients of two diseases, colorectal cancer and kidney disease. Kim et al. assessed the effects of a modified microbiota-accessible carbohydrate (mMAC) (high-fiber) diet on gut microbiota composition and clinical symptoms in two groups of a total of 40 colon cancer patients who underwent surgical resection, those who received adjuvant chemotherapy and those who did not. The main results included the distinct differences in gut microbial composition after the mMAC diet in both the chemotherapy and non-chemotheraphy groups, providing valuable insights into the potential benefits of the mMAC diet, specifically its impact on the gut microbiome and clinical symptoms in postoperative colorectal cancer patients. Lazarevic et al. explored the alternations in gut barrier, composed of gut microbiota and playing pivotal roles in chronic kidney disease (CKD) progression and nutritional status, in a total of 22 hemodialyzed (HD) patients and 11 non-HD (NHD) CKD patients. The main results included that compared to healthy group, HD patients exhibited significant alterations in fecal microbiota composition, a higher systemic inflammation, and a modification in plasma levels of appetite mediators. This study underscored the multifaceted interplay among gut microbiota, physiological markers, and kidney function. It was noted that further investigations in larger cohorts were necessary to verify the findings revealed in this study.

Third, a total of three articles were based on mouse models of colitis. Xia et al. investigated the influence of *Litsea cubeba* essential oil (LCEO) on lipopolysaccharides (LPS)-induced mouse intestinal inflammation model and associated changes in the gut microbiota, i.e., the therapeutic potential of LCEO for gut health, with particular emphasis on its gut protective properties, as well as the anti-inflammatory properties and modulation of the gut microbiome. This study identified LCEO as a promising natural compound for ameliorating diarrhea and intestinal inflammation, highlighting the need to further explore the complex interplay among the host, gut microbiome, and natural products in the context of inflammatory diseases. Wu et al. examined the effects of an intervention with fructooligosaccharides (FOS), *Saccharomyces boulardii*, and their combination in a mouse model of colitis and to explore the mechanisms underlying these effects. The results revealed enhanced anti-inflammatory effects of the combined administration of FOS and *S. boulardii* in treating colitis and colitis-induced intestinal dysbiosis, in comparison to the application of FOS alone. In particular, the combination significantly increases the abundance of beneficial bacteria such as *lactobacilli* and *Bifidobacteria* and effectively regulated the gut microbiota composition, providing a scientific rationale for the prevention and treatment of colitis using a combination of FOS and

S. boulardii and for the development of nutraceutical preparations containing both FOS and *S. boulardii*. Zou et al. applied network pharmacology to mine and verify the single active ingredient, puerarin, in *Radis puerariae*. The authors found that puerarin was a potential ingredient that could improve the crypt deformation and inflammatory infiltration in mice, as observed in the decreased levels of various inflammation related factors, while the results of correlation network and metabolic function prediction analysis of the microbiota revealed a tightly connected network widely involved in carbohydrate metabolism and amino acid metabolism. This study revealed high therapeutic effect of puerarin on ulcerative colitis, which was partially achieved by restoring the composition and abundance of gut microbiota and their metabolism.

Lastly, a total of five contributions were based on mouse models of five different medical disorders. Tian et al. investigated the effect of ursolic acid on obesity depending on the regulation of gut microbiota and metabolism based on the mouse model of obesity established with a high-fat diet using intestinal microbiome and metabolomics analyses. The results revealed that the roles of ursolic acid in the anti-obesity process depended in part on alterations in the gut microbiota and metabolism, highlighting the potential therapeutic effect of ursolic acid on the improvement of diet-induced obesity in humans. Zang et al. explored the mechanism of red quinoa polysaccharide (RQP), which was a complex polysaccharide containing more glucose, galactose and acarbose, in alleviating type 2 diabetes (T2D) through both *in vivo* and *in vitro* experiments using the mouse model of T2D induced by high-fat diet. The results showed strong anti-diabetic effects of RQP on T2D and transformed intestinal microbiota composition in diabetic mice, revealing that RQP could inhibit the development of diabetes by correcting the imbalance of intestinal microbiota. Hsiao et al. investigated the use of okra (containing a viscous substance rich in water-soluble material, including fibers, pectin, proteoglycans, gum, and polysaccharides) polysaccharides by microorganisms and their potential to improve microbiota by assessing the regulation of microcapsules prepared from okra polysaccharides with or without *Lactiplantibacilus plantarum* encapsulation on intestinal microbiota through 16S rRNA metagenomic analysis and SCFAs in the mouse model of Alzheimer's disease (AD). Interestingly, the authors found that both microcapsules prepared from okra polysaccharides either with or without *L. plantarum* encapsulation improved intestinal microbiota by elevating *Lactobacillus* levels in AD mice. Feng et al. explore the effects of alcohol intake at different concentrations on gouty arthritis based on the gut microbiota in the mouse model of acute gouty arthritis established by injection of monosodium urate crystals. Based on various morphological and biochemical factors, it was concluded that alcohol of high concentration altered the gut microbiota structure in gouty mice, possibly exacerbating gouty symptoms by enhancing pro-inflammatory pathways. Hua et al. investigated the mechanisms underlying the attenuation effect of hemp seed (HS) and its water-ethanol extract on mice with loperamide-induced constipation. The gut microbiome studies showed that the structure and abundance of intestinal microbiome were altered, as observed in the changed relatively abundances of *Odoribacter, Bacteroide, Lactobacillus,* and *Prevotella.* This study revealed the potential of HS to stimulate the proliferation of beneficial gut microbes and promote intestinal motility, thereby improving gut health and relieving symptoms of constipation.

In summary, this Research Topic of contributions highlights recent progress in the relevant fields of human health discussed in this Research Topic and suggests future research directions with potential avenues for scholars to explore. Given the rapid development of techniques for exploring the interactions between bioactive food ingredients and intestinal microbiota, it is expected that significant achievements related to human health will soon emerge from the topics covered in this Research Topic.

Author contributions

ZR: Writing – original draft, Writing – review & editing. XX: Writing – review & editing. FS: Writing – original draft, Writing – review & editing.

Funding

The author(s) declare that no financial support was received for the research, authorship, and/or publication of this article.

Conflict of interest

The authors declare that the research was conducted in the absence of any commercial or financial relationships that could be construed as a potential conflict of interest.

The author(s) declared that they were an editorial board member of Frontiers, at the time of submission. This had no impact on the peer review process and the final decision.

Publisher's note

References

Babu, M., and Snyder, M. (2023). Multi-omics profiling for health. *Mol. Cell. Proteom.* 22:100561. doi: 10.1016/j.mcpro.2023.100561

Dai, X., and Shen, L. (2022). Advances and trends in omics technology development. *Front. Med.* 9:911861. doi: 10.3389/fmed.2022.911861

Deehan, E. C., Yang, C., Perez-Muñoz, M. E., Nguyen, N., Cheng, C. C., Triador, L., et al. (2020). Precision microbiome modulation with discrete dietary fiber structures directs short-chain fatty acid production. *Cell Host Microbe* 27, 389–404. doi: 10.1016/j.chom.2020.01.006

Dmytriv, T. R., Storey, K. B., and Lushchak, V. I. (2024). Intestinal barrier permeability: the influence of gut microbiota, nutrition, and exercise. *Front. Physiol.* 15:1380713. doi: 10.3389/fphys.2024.1380713

Duffuler, P., Bhullar, K. S., and Wu, J. (2024). Targeting gut microbiota in osteoporosis: impact of the microbial based functional food ingredients. *Food Sci. Hum. Wellness* 13, 1–15. doi: 10.26599/FSHW.2022.9250001

Fan, Y., and Pedersen, O. (2021). Gut microbiota in human metabolic health and disease. *Nat. Rev. Microbiol.* 19, 55–71. doi: 10.1038/s41579-020-0433-9

Gebrayel, P., Nicco, C., Khodor, S. A., Bilinski, J., Caselli, E., Comelli, E. M., et al. (2022). Microbiota medicine: towards clinical revolution. *J. Transl. Med.* 20:111. doi: 10.1186/s12967-022-03296-9

Han, S., Lu, Y., Xie, J., Fei, Y., Zheng, G., Wang, Z., et al. (2021). Probiotic gastrointestinal transit and colonization after oral administration: a long journey. *Front. Cell. Infect. Microbiol.* 11:609722. doi: 10.3389/fcimb.2021.609722

Hao, X., Cheng, S., Jiang, B., and Xin, S. (2022). Applying multi-omics techniques to the discovery of biomarkers for acute aortic dissection. *Front. Cardiovasc. Med.* 9:961991. doi: 10.3389/fcvm.2022.961991

Hasin, Y., Seldin, M., and Lusis, A. (2017). Multi-omics approaches to disease. *Genome Biol.* 18:83. doi: 10.1186/s13059-017-1215-1

Jacquier, E. F., van de Wouw, M., Nekrasov, E., Contractor, N., Kassis, A., and Marcu, D. (2024). Local and systemic effects of bioactive food ingredients: is there a role for functional foods to prime the gut for resilience? *Foods* 13:739. doi: 10.3390/foods13050739

Karczewski, K., and Snyder, M. (2018). Integrative omics for health and disease. *Nat. Rev. Genet.* 19, 299–310. doi: 10.1038/nrg.2018.4

Li, S., Feng, W., Wu, J., Cui, H., Wang, Y., Liang, T., et al. (2024). A narrative review: immunometabolic interactions of host–gut microbiota and botanical active ingredients in gastrointestinal cancers. *Int. J. Mol. Sci.* 25:9096. doi: 10.3390/ijms25169096

Mohr, A. E., Ortega-Santos, C. P., Whisner, C. M., Klein-Seetharaman, J., and Jasbi, P. (2024). Navigating challenges and opportunities in multi-omics integration for personalized healthcare. *Biomedicines* 12:1496. doi: 10.3390/biomedicines12071496

Nayak, S. N., Aravind, B., Malavalli, S. S., Sukanth, B. S., Poornima, R., Bharati, P., et al. (2021). Omics technologies to enhance plant based functional foods: an overview. *Front. Genet.* 12, 742095. doi: 10.3389/fgene.2021.742095

Osawa, R., Fukuda, I., and Shirai, Y. (2024). Evaluating functionalities of food components by a model simulating human intestinal microbiota constructed at Kobe University. *Curr. Opin. Biotechnol.* 87:103103. doi: 10.1016/j.copbio.2024.103103

Pires, L., Gonzlez-Params, A. M., Heleno, S. A., and Calhelha, R. C. (2024). Exploring therapeutic advances: a comprehensive review of intestinal microbiota modulators. *Antibiotics* 13:720. doi: 10.3390/antibiotics13080720

Ray, S. K., and Mukherjee, S. (2021). Evolving interplay between dietary polyphenols and gut microbiota—an emerging importance in healthcare. *Front. Nutr.* 8:634944. doi: 10.3389/fnut.2021.634944

Ross, F. C., Patangia, D., Grimaud, G., Lavelle, A., Dempsey, E. M., Ross, R. P., et al. (2024). The interplay between diet and the gut microbiome: implications for health and disease. *Nat. Rev. Microbiol.* doi: 10.1038/s41579-024-01068-4

Ruan, Z., Sun, F., Xia, X., and Zhang, G. (2022). Editorial: interactions between bioactive food ingredients and intestinal microbiota. *Front. Microbiol.* 13:902962. doi: 10.3389/fmicb.2022.902962

Si, W., Zhang, Y., Li, X., Du, Y., and Xu, Q. (2021). Understanding the functional activity of polyphenols using omics-based approaches. *Nutrients* 13:3953. doi: 10.3390/nu13113953

Singh, R., Zogg, H., Wei, L., Bartlett, A., Ghoshal, U. C., Rajender, S., et al. (2021). Gut microbial dysbiosis in the pathogenesis of gastrointestinal dysmotility and metabolic disorders. *J. Neurogastroenterol. Motil.* 27, 19–34. doi: 10.5056/jnm20149

Van Hul, M., Neyrinck, A. M., Everard, A., Abot, A., Bindels, L. B., Delzenne, N. M., et al. (2024). Role of the intestinal microbiota in contributing to weight disorders and associated comorbidities. *Clin. Microbiol. Rev.* 0, e00045–e00023. doi: 10.1128/cmr.00045-23

Wang, G., Huang, S., Wang, Y., Cai, S., Yu, H., Liu, H., et al. (2019). Bridging intestinal immunity and gut microbiota by metabolites. *Cell. Mol. Life Sci.* 76, 3917–3937. doi: 10.1007/s00018-019-03190-6

Wu, J., Singleton, S. S., Bhuiyan, U., Krammer, L., and Mazumder, R. (2024). Multi-omics approaches to studying gastrointestinal microbiome in the context of precision medicine and machine learning. *Front. Mol. Biosci.* 10:1337373. doi: 10.3389/fmolb.2023.1337373

Yurkovich, J. T., Evans, S. J., Rappaport, N., Boore, J. L., Lovejoy, J. C., Price, N., et al. (2024). The transition from genomics to phenomics in personalized population health. *Nat. Rev. Genet.* 25, 286–302. doi: 10.1038/s41576-023-00674-x

frontiers | Frontiers in Microbiology

TYPE Original Research
PUBLISHED 12 May 2023
DOI 10.3389/fmicb.2023.1165771

OPEN ACCESS

EDITED BY
Xiaodong Xia,
Dalian Polytechnic University, China

REVIEWED BY
Chunlong Mu,
University of Calgary, Canada
Mohammad Altamimi,
An-Najah National University, Palestine

*CORRESPONDENCE
Paule V. Joseph
✉ paule.joseph@nih.gov

†These authors share senior authorship

RECEIVED 14 February 2023
ACCEPTED 17 April 2023
PUBLISHED 12 May 2023

CITATION
Vizioli C, Jaime-Lara R, Daniel SG, Franks A, Diallo AF, Bittinger K, Tan TP, Merenstein DJ, Brooks B, Joseph PV and Maki KA (2023) Administration of *Bifidobacterium animalis* subsp. *lactis* strain BB-12® in healthy children: characterization, functional composition, and metabolism of the gut microbiome. *Front. Microbiol.* 14:1165771. doi: 10.3389/fmicb.2023.1165771

Administration of *Bifidobacterium animalis* subsp. *lactis* strain BB-12® in healthy children: characterization, functional composition, and metabolism of the gut microbiome

Carlotta Vizioli[1,2], Rosario Jaime-Lara[2,3,4], Scott G. Daniel[5], Alexis Franks[3], Ana F. Diallo[6], Kyle Bittinger[5], Tina P. Tan[7], Daniel J. Merenstein[7], Brianna Brooks[3], Paule V. Joseph[2,3*†] and Katherine A. Maki[8†]

[1]Department of Health and Human Services, National Institute of Neurological Disorders and Stroke, National Institutes of Health, Bethesda, MD, United States, [2]Department of Health and Human Services, National Institute on Alcohol Abuse and Alcoholism, National Institutes of Health, Bethesda, MD, United States, [3]Department of Health and Human Services, National Institute of Nursing Research, National Institutes of Health, Bethesda, MD, United States, [4]UCLA School of Nursing, University of California, Los Angeles, Los Angeles, CA, United States, [5]Division of Gastroenterology, Hepatology, and Nutrition, Children's Hospital of Philadelphia, Philadelphia, PA, United States, [6]Family and Community Health Nursing, School of Nursing, Institute of Inclusion, Inquiry and Innovation (iCubed), Virginia Commonwealth University, Richmond, VA, United States, [7]Department of Family Medicine, Georgetown University Medical Center, Washington, DC, United States, [8]Translational Biobehavioral and Health Disparities Branch, National Institutes of Health, Clinical Center, Bethesda, MD, United States

Introduction: The consumption of probiotics may influence children's gut microbiome and metabolome, which may reflect shifts in gut microbial diversity composition and metabolism. These potential changes might have a beneficial impact on health. However, there is a lack of evidence investigating the effect of probiotics on the gut microbiome and metabolome of children. We aimed to examine the potential impact of a two (*Streptococcus thermophilus* and *Lactobacillus delbrueckii*; S2) *vs.* three (S2+ *Bifidobacterium animalis* subsp. *lactis* strain BB-12) strain-supplemented yogurt.

Methods: Included in this study were 59 participants, aged one to five years old, recruited to phase I of a double-blinded, randomized controlled trial. Fecal samples were collected at baseline, after the intervention, and at twenty days post-intervention discontinuation, and untargeted metabolomics and shotgun metagenomics were performed.

Results: Shotgun metagenomics and metabolomic analyses showed no global changes in either intervention group's gut microbiome alpha or beta diversity indices, except for a lower microbial diversity in the S2 + BB12 group at Day 30. The relative abundance of the two and three intervention bacteria increased in the S2 and S2 + BB12 groups, respectively, from Day 0 to Day 10. In the S2 + BB12 group, the abundance of several fecal metabolites increased at Day 10, including alanine, glycine, lysine, phenylalanine, serine, and valine. These fecal metabolite changes did not occur in the S2 group.

Discussion: In conclusion, there were were no significant differences in the global metagenomic or metabolomic profiles between healthy children receiving two (S2) *vs.* three (S2 + BB12) probiotic strains for 10 days. Nevertheless, we observed a significant increase (Day 0 to Day 10) in the relative abundance of the two and three probiotics administered in the S2 and S2 + BB12 groups, respectively,

indicating the intervention had a measurable impact on the bacteria of interest in the gut microbiome. Future research using longer probiotic intervention durations and in children at risk for gastrointestinal disorders may elucidate if functional metabolite changes confer a protective gastrointestinal effect.

KEYWORDS

probiotics, gut microbiome, *L. delbrueckii*, *B. animalis* BB-12, metagenomics, *S. thermophilus*, children, metabolomics

Introduction

The gut microbiome is comprised of the entire gastrointestinal (GI) microbial community, including bacteria, fungi, viruses, and their genes. Metagenomic analysis captures a comprehensive summary of the microbiome, *i.e.*, microbial diversity and their ecological niches (microbial function) (Wang et al., 2015). Gut colonization starts prenatally and continues after birth. The gut microbiome in early infancy begins to stabilize early in life (Bäckhed et al., 2015). Several mechanisms, including birth mode (Yuan et al., 2016), type of milk received (Mayer-Davis et al., 2006), and environmental factors (Yatsunenko et al., 2012), shape the development of the gut microbiome from infancy to adulthood. The environment and diet during the first two to five years turn an immature microbiota into a more stable, resilient, adult-like gut microbial community (Yatsunenko et al., 2012). The human gut microbiome influences nutritional absorption, immune health, and behavior (Jungersen et al., 2014). Pre-clinical and clinical studies suggest that the gut microbiota-immune system crosstalk may be responsible for long-term health (Kostic et al., 2015; Stiemsma and Michels, 2018). Disruptions to a healthy gut microbiome are observed during disease states and across chronic illnesses, including inflammatory and immune disorders (Neis et al., 2015; Boulangé et al., 2016; Stinson et al., 2017).

Probiotics are defined by the International Scientific Association for Probiotics and Prebiotics as "live microorganisms that, when administered in adequate amounts, confer a health benefit on the host (Hill et al., 2014)." Probiotics are increasingly used in commercial products because of their potential benefits on the gut microbiota that have been shown to exert positive effects on host physiology (Hill et al., 2014; Hojsak et al., 2018). The mechanism of action by which probiotics confer health benefits are diverse and include: colonization and normalization of perturbed intestinal microbial populations, competitive exclusion of pathogens, and modulation of the immune system via production of anti-inflammatory factors (Plaza-Diaz et al., 2019).

Probiotics have been used in treatment of GI symptoms and prevention or management of GI disorders. Several studies have shown that probiotic strains from the *Bifidobacterium* genus promote the growth of beneficial bacteria, inhibit pathogenic microorganisms by secreting antibacterial factors (Moroni et al., 2006), competitive adhesion to intestinal epithelial cells (Plaza-Diaz et al., 2019) improve GI barrier (Srutkova et al., 2015; Schroeder et al., 2018), promoting the formation of mucous layers maintaining of intestinal immune homeostasis (Artis, 2008), and lower inflammatory cytokines (Xue et al., 2017). Moreover, consumption of *Lactobacillus* and *Bifidobacterium* genera have been associated with improved mental health and memory function in pre-clinical and human studies (Savignac et al., 2015; Mörkl et al., 2020; Sharma et al., 2021; Griffin et al., 2022).

There is increasing interest in using probiotics as a tool to maintain and restore a healthy gut microbiota. While evidence supports their use in some GI diseases, the impact of probiotics on healthy gut microbiota and its metabolism is still unclear in both adults and children (Wilkins and Sequoia, 2017; Suez et al., 2018, 2019; Merenstein et al., 2021). Few studies have examined the effect of probiotics in healthy adults (McKean et al., 2017; Suez et al., 2018; Merenstein et al., 2021), and even fewer have studied the effect of probiotics in healthy children (Łukasik et al., 2018). Although *Bifidobacterium animalis* subsp. *lactis* BB-12 (BB-12) is among the most common probiotic supplements and has previously been demonstrated to be well-tolerated by healthy children (Tan et al., 2017), there are limited studies examining the effects of BB-12 on structural and functional characteristics of the gut microbiome in children ages one to five years old (Tan et al., 2017).

Metabolites produced by gut microorganisms have been identified in modulating human health, including the immune system, metabolic, and neurobehavioral traits (Arpaia et al., 2013; LeBlanc et al., 2017; McKean et al., 2017; Plaza-Diaz et al., 2019; Mörkl et al., 2020). Furthermore, emerging studies suggest that probiotics' effects on intestinal metabolites may contribute to intestinal health and immune function (Dai et al., 2011; den Besten et al., 2013; Conlon and Bird, 2015; LeBlanc et al., 2017; Lee et al., 2018). Thus, there is growing interest in the link between probiotic administration and the subsequent impact on metabolite changes in the context of human health and disease. Shotgun metagenomics sequencing and untargeted metabolomics technologies have grown exponentially in the last decade providing a key tool to closer examine the microbial characterization, function, and metabolism in a sample (e.g., fecal or tissue samples). Therefore, metabolomics offers an efficient and accurate strategy of exploring the biological role of how probiotics may impact the pediatric gut microbiome, including how these metabolites respond to different combinations of symbiotic bacteria administration (*i.e.*, *Bifidobacterium vs. Lactobacillus* spp. probiotic genera) (Riekeberg and Powers, 2017).

Abbreviations: FC, Fold change; FDR, False discovery rate; GI, Gastrointestinal; PCA, Principal component analysis; PCoA, Principal coordinate analysis; PERMANOVA, Permutational analysis of variance; RA, Relative abundance; S2, Two-strain (*Streptococcus thermophilus* and *Lactobacillus delbrueckii*) yogurt group; S2+BB12, Two-strain (*Streptococcus thermophilus* and *Lactobacillus delbrueckii*) plus *Bifidobacterium animalis* subsp. *lactis* strain BB-12 yogurt group; TMAO, Trimethylamine N-oxide.

Exploring the effect of probiotics on the gut microbiome and metabolome in healthy children may provide more extensive insight into the relationship between probiotics, gut microbiota, metabolites, and human health. This may aid in developing more effective methods of assessing gut health by simultaneously characterizing the gut microbiome and functional impacts of microbiome community changes on the metabolome. Furthermore, GI disorders are among the most common ailments reported in pediatric primary care. Therefore, utilizing our approach including microbiome and metabolome analyses to characterize structural and functional responses of gut microbiota to two probiotics combinations (*Streptococcus thermophilus* and *Lactobacillus delbrueckii* [S2] *vs. Streptococcus thermophilus, Lactobacillus delbrueckii*, and *Bifidobacterium animalis* subsp. *lactis* strain BB-12 [S2 + BB12]) in children is an important first step to design future research evaluating the efficacy of probiotics in the prevention of dysbiosis–associated GI disorders.

To date, few studies have been conducted to examine the effect of probiotics on gut microbial compositional and functional structure combined with associated fecal metabolome changes in healthy children. Thus, this study uses shotgun metagenomic sequencing and untargeted fecal metabolomics to examine the effects induced by the consumption of yogurt with and without the BB-12 probiotic strain (BB12) in healthy children aged one to five years old. This study builds upon findings by Tan et al. (2017) using shotgun metagenomics sequencing for microbiome analysis and the integration of metabolomic data.

Results

Participant characteristics

A total of 59 healthy participants between the ages of one and five years (mean age = 2.38 ± 1.22) were included in the study (Figure 1A). The yogurt was administered to the participants for ten consecutive days. Fecal samples were analyzed at baseline (Day 0), ten (Day 10), and 30 (Day 30) days from both S2 + BB12 (n = 25, 28, and 25, respectively) and S2 (n = 31, 31, and 30, respectively) groups (Figure 1B).

Participants were relatively divided equally between males and females (n = 28 males and n = 31 females). Most of the participants included were White (n = 40). Additional demographic information from the included participants is displayed in Table 1.

Metagenomic analyses

The administration of BB-12, in addition to *S. thermophilus* and *L. delbrueckii*, influenced the composition of the gut microbiome, although there were no overt global microbiome changes quantified by alpha and beta diversity indices. Species richness and Shannon indices were not significantly different between the S2 and S2 + BB12 groups at Day 10 (p = 0.65 and p = 0.24, respectively; Figures 2A,B). At Day 30, there were no significant differences in species richness between S2 and S2 + BB12 groups (p = 0.669), but Shannon diversity was significantly lower in the S2 + BB12 group compared to the S2 group (p = 0.044; Figures 2A,B). There were no between group differences in beta diversity (based on Bray–Curtis dissimilarity) at Day 10 (R^2 = 0.02, p = 0.31; Figure 2C) or Day 30 (R^2 = 0.02, p = 0.427; Supplementary Figure S1). Age was a significant predictor of alpha diversity measures in the Day 0 and Day 10 samples, irrespective of treatment group (species richness p = 0.001, Shannon index p = 0.045). These findings agree with previously reported results by Tan et al. (2017) using 16S rRNA analysis.

We built upon these findings by using shotgun metagenomics, which allowed us to observe differential abundant taxa at the species level. As expected, the metagenomic analysis showed an increase of *B. animalis* in the S2 + BB12 group. *B. animalis* abundance was significantly impacted by the administration of the BB12 supplemented yogurt (group × time p < 0.001; Figure 2D). We observed an effect of time, but not group, in *L. delbrueckii* (time

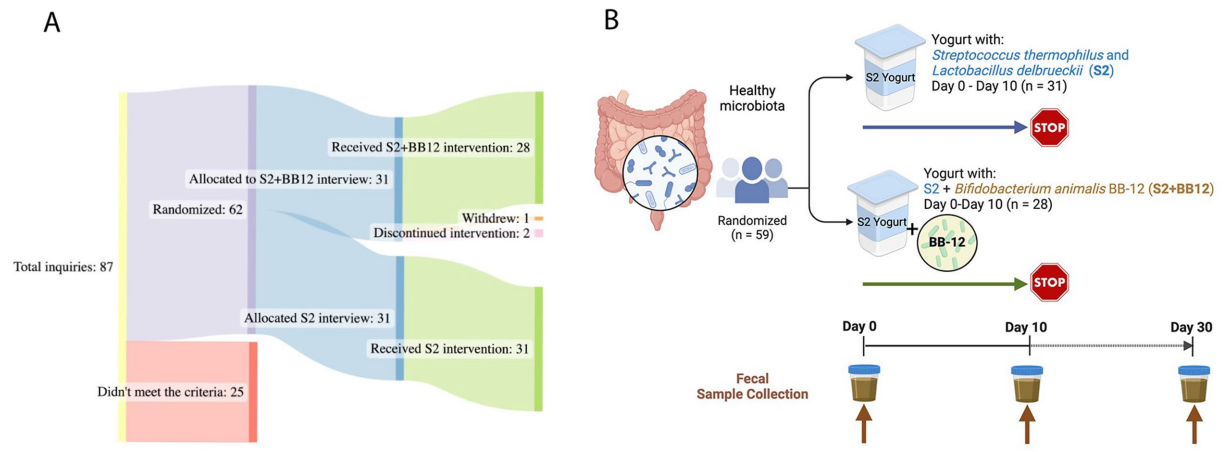

FIGURE 1
Study Design: a total of 59 children, aged one to five years old, were analyzed for this double-blinded, randomized controlled study **(A)**. The participants consumed yogurt with two (S2 group) *vs.* three (S2+BB12 group) probiotics' strains **(B)**. The participants consumed yogurt during ten consecutive days. Fecal samples were collected before the intervention (Day 0), after ten days of yogurt consumption (Day 10), and after 20days of yogurt consumption discontinuation (Day 30). Created with BioRender.com and SankeyMATIC.com.

TABLE 1 Participants demographics.

		Overall	S2	S2+BB12
		n =59	*n* =31	*n* =28
Age	Mean (SD)	2.38 (1.22)	2.42 (1.21)	2.35 (1.26)
Gender (*n*)	Male	28	13	15
	Female	31	18	13
Race (*n*)	Indian/Alaskan	1		1
	Black or African	8	4	4
	White/Caucasian	40	17	23
	Other/more than one race	7	6	1
Ethnicity (*n*)	Hispanic/Latino	8	5	3

$p < 0.001$; group $p = 0.405$). *S. thermophilus*'s relative abundance were significantly different in time and group × time interaction (time $p < 0.001$; group $p = 0.349$; group x time $p = 0.020$) (Figures 2E,F). As expected, *post hoc* testing showed in the S2 + BB12 group a statistically significant increase comparing Day 0 *vs.* Day 10 in BB-12 ($p < 0.001$), *S. thermophilus* ($p < 0.001$), and *L. delbrueckii* ($p = 0.018$) abundances. Similarly, Day 10 *vs.* Day 30 comparison showed a statistically significant decrease in BB-12 ($p < 0.001$), *S. thermophilus* ($p = 0.001$), and *L. delbrueckii* ($p = 0.004$) abundances (Figures 2D–F). In the S2 group, we found statistically significant differences in Day 0 *vs.* Day 10 comparison of *S. thermophilus* ($p < 0.001$) and *L. delbrueckii* ($p = 0.005$) abundances. Interestingly, BB-12 increased comparing Day 0 to Day 30 in the same group ($p = 0.016$).

We then focused our analyses on within-group differences in both groups from Day 0 to Day 10, as both groups received a probiotic intervention (S2 *vs.* S2 + BB12) and were healthy children. The 25 taxa with the greatest change in relative abundance between Day 0 and Day 10 were evaluated to observe the effect on individual microbial taxa following a ten-day administration of two (S2) *vs.* three (S2 + BB12) strains of probiotics. *S. thermophilus*, one of the intervention bacteria, was significantly increased in the S2 group at Day 10 compared to Day 0 (FDR $p = 0.003$; Figure 2G). Interestingly, the other intervention bacteria *L. delbrueckii* was absent among the 25 most changing taxa in the S2 group. In the S2 + BB12 group, all three intervention bacteria (*i.e.*, *B. animalis, S. thermophilus,* and *L. delbrueckii*) were significantly increased at Day 10 (FDR $p < 0.001$, FDR $p < 0.0001$, and FDR $p = 0.048$, respectively), but the S2 + BB12 intervention did not significantly influence the abundance of any other taxa when FDR correction was applied (Figure 2G; Supplementary Table S1). In both groups most of the top changing taxa were decreased in Day 10 compared to Day 0 (19/25 and 20/25 taxa in S2 and S2 + BB12 groups respectively), but many of these differences were not significant before or after FDR correction (Figures 2G,H; Supplementary Table S1). We also saw an influence of race and ethnicity on within group taxonomic response to the S2 and S2 + BB12 interventions; *E. cloacae complex* sp. 35734 and *K. michiganensis* were both decreased in Asian children compared to Black or African American children (FDR $p = 0.015$ and 0.032, respectively, S2 group) and *B. pseudocatenulatum* was decreased in non-Hispanic children (FDR $p = 0.022$, S2 + BB12 group; Supplementary Table S2).

When we analyzed the differential abundance of gene orthologs, we found that the relative abundance of the glucan 1,4-alpha-glucosidase, chondroitin-sulfate-ABC endolyase/exolyase, and response regulator HydG genes decreased from Day 0 to Day 10 in both groups, (Figures 2I,J). These differences were also not statistically significant before or after FDR correction (Supplementary Table S1). Except for two orthologs, fatty acid synthase [K11533] and KUP potassium uptake protein, the 23 remaining orthologs among the 25 top changing ones between groups were decreased in the S2 group after ten days of probiotics administration, although these decreases were not statistically significant (Figure 2I; Supplementary Table S1). An overall trend of decreased orthologs relative abundance from Day 0 to Day 10 was similar in the S2 + BB12 group, except for four orthologs that had a non-statistically significant increase following BB12 administration, including *fliC* (flagellin), *msbA*; ATP-binding cassette, subfamily B, bacterial MsbA, *sstT*; serine/threonine transporter, and chondroitin-sulfate-ABC endolyase/exolyase (Figure 2J; Supplementary Table S1). There were two orthologs that changed significantly with age in the S2 + BB12 group; hexuronate transporter decreased (FDR $p = 0.025$) and aspartyl-tRNA synthetase increased (FDR $p = 0.022$; Supplementary Table S3). No significant changes were found with the other covariates in the S2 group.

We selected 18 known probiotic strains identified through literature search (Supplementary Table S4), to observe if the administration of two (S2) *vs.* three (S2 + BB12) probiotic strains would influence the abundance other known probiotics. Most of the identified probiotic-associated taxa belonged to *Lactobacillus*, *Bacteroides*, and *Bifidobacterium* genera, and were commonly used as probiotic supplements in the food industry or clinical trials (see Supplementary Table S4 for references). We observed that the abundance of targeted probiotic-associated bacteria increased from Day 0 to Day 10 in 61% (11/18) of selected taxa in the S2 group (Figure 3A) and 72% (13/18) of taxa in the S2 + BB12 (Figure 3B) group, but most of the differences did not reach statistical significance. Nevertheless, cumulative bacterial responses changes of probiotic-associated bacteria differed according to intervention group. For example, we observed no pattern in samples distribution in the S2 group (Figure 3C), while in the S2 + BB12 group we can observe a separation of Day 0 *vs.* Day 10 samples (Figure 3D). In the S2 + BB12 group, many of the Day 10 probiotic-associated bacteria clustered with *B. animalis*, indicating similar response to the probiotic (Figure 3D).

Metabolomic analyses

The untargeted metabolomic analysis identified 734 metabolites. To evaluate the impact of S2 *vs.* S2 + BB12 probiotics on the metabolome, we performed both exploratory analyses quantifying differences in all annotated metabolites and hypothesis-driven metabolomics analyses focused on amino acid-associated and short chain fatty acid metabolites.

After excluding xenobiotics, we conducted exploratory metabolomic analyses on 601 biochemicals. We analyzed the differences between Day 0 *vs.* Day 10, Day 10 *vs.* Day 30, and Day 0 *vs.* Day 30 within the S2 and S2 + BB12 groups (Supplementary Table S5). After correcting for multiple comparisons, we did not find statistically significant differences between groups for any metabolite evaluated. Nevertheless, there were clinically relevant metabolites that were

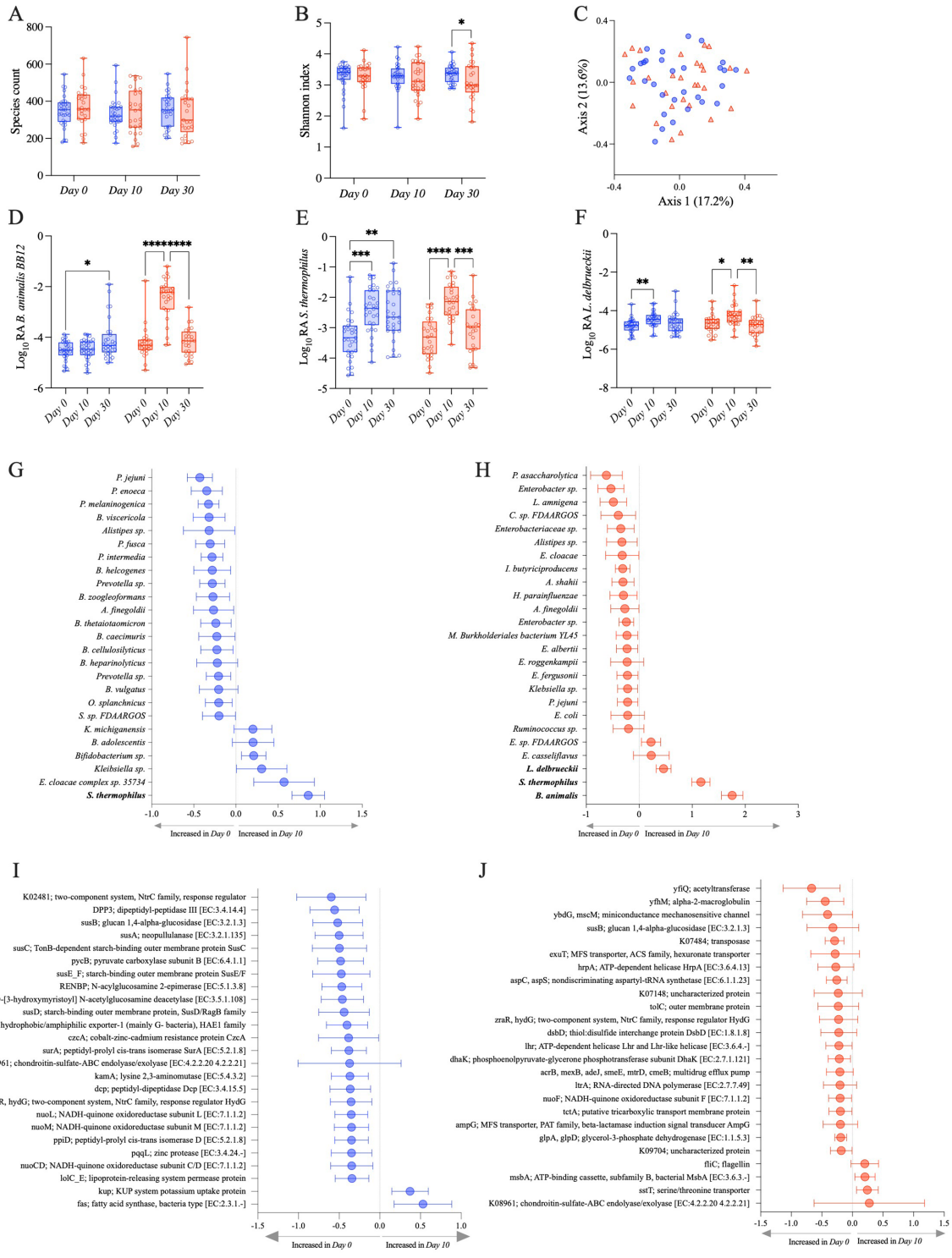

FIGURE 2
Observed species **(A)** and Shannon **(B)** alpha diversity indexes in S2 (blue) and S2+BB12 (red) groups at Day 0, Day 10, and Day 30. PCoA based on Bray–Curtis dissimilarity followed by a PERMANOVA (p =0.318) showing no separation among samples **(C)**. Relative abundances of the three strains used in the S2 and S2+BB12 interventions: *B animalis* **(D)**, *S. thermophilus* **(E)**, and *L. delbrueckii* **(F)** during time comparing S2 (blue) and S2+BB12 groups (red). Top 25 changing taxa **(G,H)** and gene orthologs **(I,J)** between Day 0 and Day 10 in S2 **(G–I)** and S2+BB12 **(H–J)** groups identified by linear model.

differentially abundant during the probiotic intervention within groups, but did not survive correction for multiple testing (raw and FDR corrected p-values, along with FC response are listed in Supplementary Table S5). Therefore, metabolites with a FC response ≥ |2| and raw p-value <0.05 comparing Day 0 *vs.* Day 10 and Day 0 *vs.* Day 30 in S2 (Figures 4A,C,E) and S2 + BB12 (Figures 4B,D,F) groups are presented. We found greater changes in the S2 + BB12 group compared to the S2 group (14 *vs.* three metabolites). After ten days of yogurt

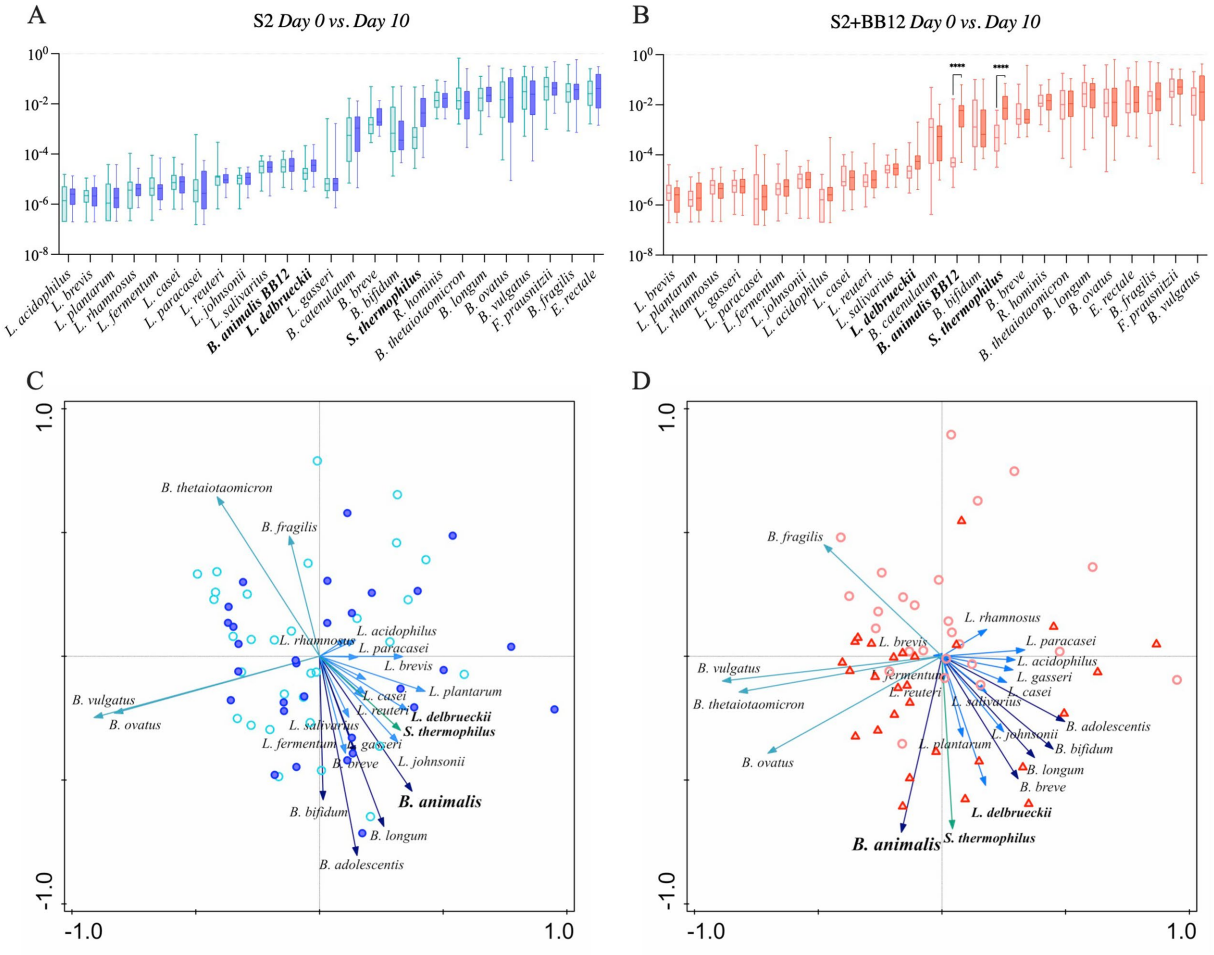

FIGURE 3
Relative abundances of selected probiotic taxa are plotted in S2 **(A)** and S2+BB12 **(B)** groups after ten days of probiotic intervention (Day 0 *vs.* Day 10). Post-selection PCA shows selected probiotics following ten days of probiotics administration in S2 **(C)** and S2+BB12 **(D)** groups. The difference in *S. thermophilus* and *B. animalis* between Day 0 and Day 10 abundances are statistically significant different (p <0.0001 for both) in S2+BB12 group. Day 10 is represented by the darkest color all plots. In PCA, different arrows colors refer to different genera: Blue, light blue, dark green, and green represent *Bifidobacterium*, *Lactobacillus*, *Bacteroides*, and *Streptococcus* genera, respectively. Each arrow points in the direction of the steepest increase of the values for the corresponding feature. The angle between arrows indicates the correlation between the different features (positive when the angle is sharp and negative when the angle is larger than 90 degrees). The length of the arrow is a measure of fit for the feature.

consumption, we found an increase of N-acetylvaline (FDR $p = 0.974$, FC = 2.151) and a decrease of arachidoylcarnitine (C20) * (FDR $p = 0.974$, FC = 0.436). Day 0 *vs.* Day 30 comparison exhibited several changes in lipids decreased at Day 30 belonging to diacyglicerol metabolism: linoleoyl-linoleoyl-glycerol (18:2/18:2) (Wang et al., 2015)* (FDR $p = 0.216$, FC = 0.29), palmitoyl-linoleoyl-glycerol (16:0/18:2) (Bäckhed et al., 2015)* (FDR $p = 0.188$, FC = 0.311), palmitoyl-linoleoyl-glycerol (16:0/18:2) (Wang et al., 2015)* (FDR $p = 0.216$, FC = 0.263), oleoyl-linoleoyl-glycerol (18:1/18:2) (Bäckhed et al., 2015) (FDR $p = 0.188$, FC = 0.295), palmitoyl-oleoyl-glycerol (16:0/18:1) (Bäckhed et al., 2015)* (FDR $p = 0.188$, FC = 0.252), and oleoyl-linoleoyl-glycerol (18,1/18:2) (Wang et al., 2015) (FDR $p = 0.166$, FC = 0.221). The glycerolipids 2-palmitoyl-galactosylglycerol (16:0)* (FDR $p = 0.166$, FC = 2.358) and 1-palmitoyl-galactosylglycerol (16,0)* (FDR $p = 0.166$ FC = 2.319), were increased together with 3-hydroxybutyrate (BHBA) (FDR $p = 0.906$, FC = 2.821).

In the S2 group, the amino acid (R)-salsolinol was decreased after ten days of intervention (Day 0 *vs.* Day 10) (FDR $p = 1.000$, FC = 0.38) and 20 days after yogurt consumption discontinuation (Day 0 *vs.* Day 30) (FDR $p = 0.995$, FC = 0.423). Lactate and indolelactate were also decreased looking at Day 0 *vs.* Day 30 comparison (FC = 0.222, FDR $p = 0.999$ and FC = 0.165, FDR $p = 0.999$, respectively). PCA of untargeted metabolites showed no separation between the time points in any group (Supplementary Figures S2 A–F).

Next, we focused on evaluating differences in specific metabolites associated with amino acid metabolism or biosynthesis, as we hypothesized that they would be impacted by probiotic intervention and associated with the gut microbiome in both groups. There were several amino-acid associated metabolites that differed as a result of time in both groups (Supplementary Table S6) including 3-methyl-2-oxobutyrate ($p = 0.004$), 3-methyl-2-oxovalerate ($p = 0.025$), alanine ($p = 0.001$), glutamate ($p = 0.034$), isoleucine ($p = 0.020$), and valine ($p = 0.004$), among others. Conversely, glycine ($p = 0.025$), indolelactate ($p = 0.034$), N-acetylserine ($p = 0.049$), and pyroglutamine ($p = 0.007$) had significant group × time effects as a result of the S2 and S2 + BB12 probiotic interactions

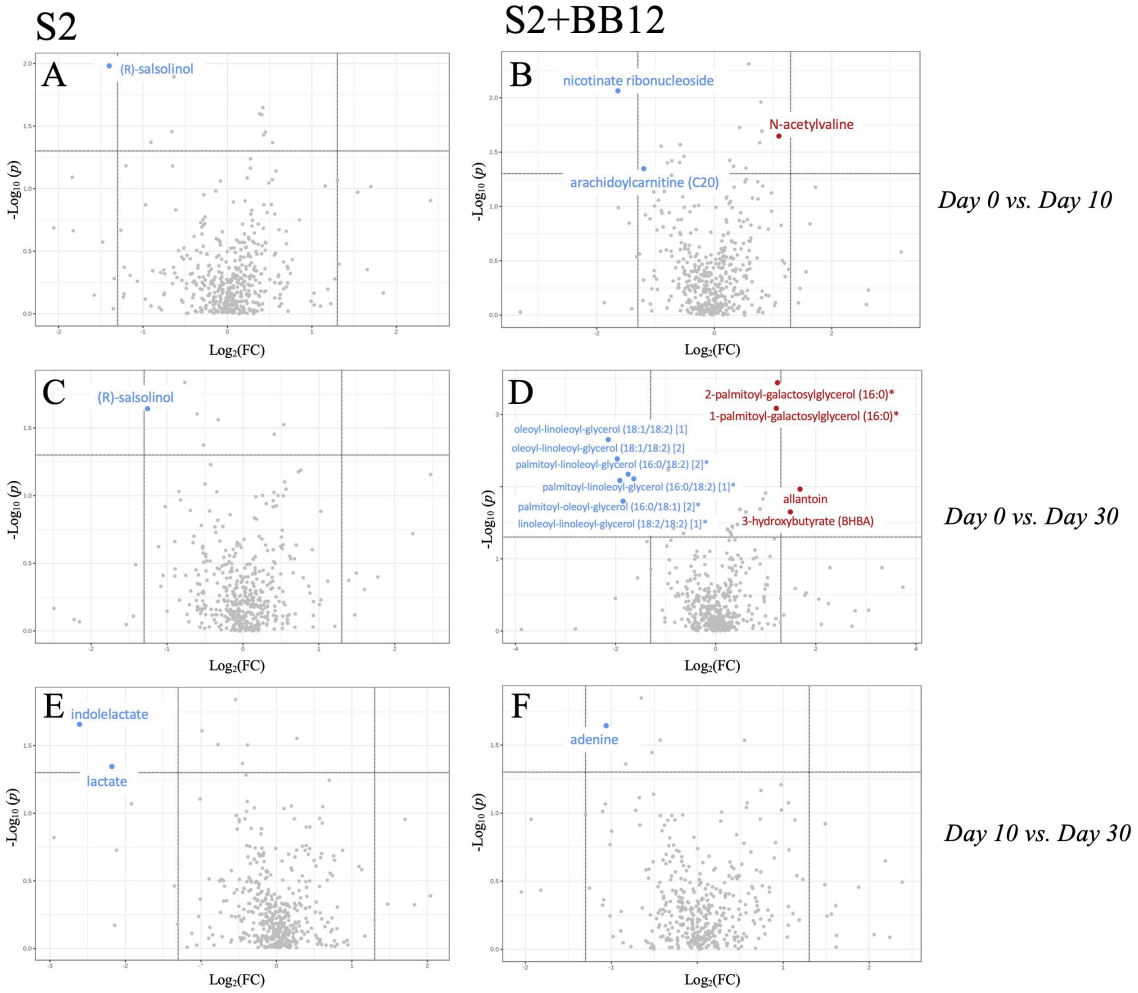

FIGURE 4
Volcano plot (p <0.05, FC>2) comparing Day 0 *vs.* Day 10 **(A,B)**, Day 0 *vs.* Day 30 **(C,D)**, and Day 10 *vs.* Day 30 **(E,F)** within S2 and S2+BB12, respectively. Metabolites in red/blue represent metabolites increased/decreased at Day 10 **(A,B)** and Day 30 **(C–F)**.

(Supplementary Table S6). In the S2 + BB12 group, average fecal metabolite abundances of 4-methyl-2-oxopentanoate, alanine, cysteine s-sulfate, glycine, histidine, lysine, N-acetylalanine, N-acetylglutamine, N-acetylleucine, phenylalanine, serine and valine were significantly higher at Day 10 (versus baseline Day 0; Figures 5A–N). Alanine, glycine, and N-acetylglutamine metabolite levels continued to be lower 20 days after the S2 + BB12 probiotic was discontinued (Day 30) *vs.* baseline (Figures 5B,D,H), while fecal cysteine s-sulfate levels increased back to baseline levels after probiotic discontinuation.

Integration of metagenomics and metabolomics datasets

Microbe-metabolite interactions were tested through correlation matrices and visualized with network graphs. After filtering, 26 microbial taxa and 79 metabolites were tested for associations (Figure 6; Supplementary Tables S7, S8).

Metabolites that were significantly positively correlated with *Enterobacteriaceae* and *Escherichia coli* included trimethylamine N-oxide (TMAO), ursodeoxycholate, 7-ketodeoxycholate, and glycine (Figure 7). Other taxa that had multiple significant positive associations with metabolites included *Akkermansia muciniphila, Eubacterium hallii, Roseburia hominis*, and *Clostridiales*. Of the supplemented probiotic bacteria, *B. animalis* was positively associated with uracil, *S. thermophilus* with deoxycarnitine and phenylalanine, and *L. delbrueckii* with thymine. Known products of bacteria such as nicotinate (vitamin B3), pantothenate (vitamin B5) correlated positively with *Clostridiales*, *R. hominis*, *F. prausnitzii*, and *E. eligens* (Figure 7A).

Several amino acids correlated negatively with *F. prausnitzii* and *R. hominis*, including glutamine, lactate, threonine, tryptophan and TMAO (Figure 7B). Lactate was also negatively associated with *A. rectalis*, *R. bicirculans*, *E. hallii,* and *Clostridiales*; glucose with *R. bicirculans*, *E. hallii*, and *A. muciniphila*; and glycerate with *A. muciniphila* and *B. longum*. Among the probiotics of interest, *B. animalis* correlated negatively with arginine and *L. delbrueckii* with 1-palmitoyl-GPE (16:0). Uracil was positively associated with *Clostridiales*, *A. finegoldii*, and *E. rectale*. Uracil was also negatively correlated with *B. dorei*, *F. plautii*, Enterobacteriaceae and *E. coli*.

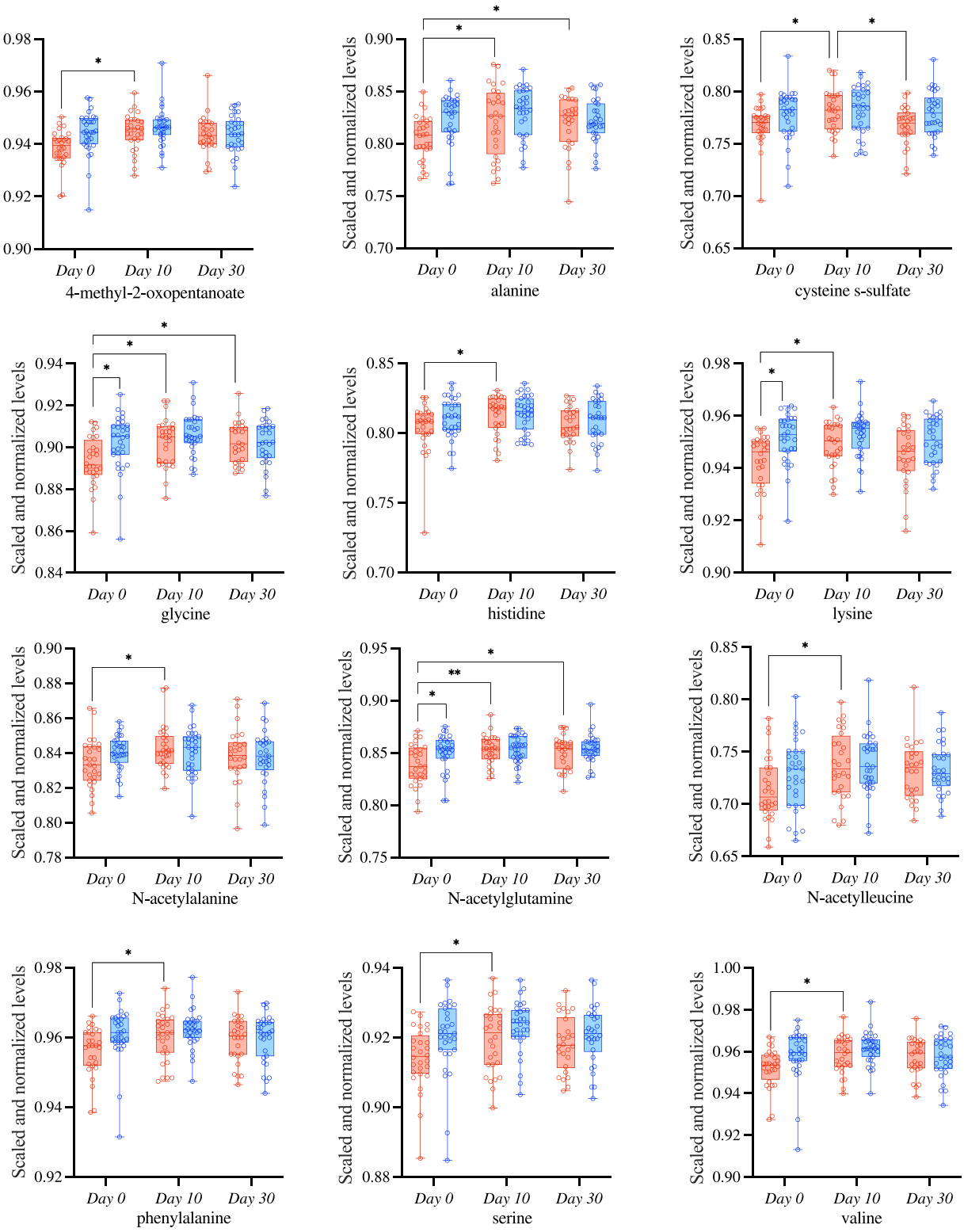

FIGURE 5
Targeted metabolomic analysis on amino acids was used to study the differences comparing Day 0 *vs.* Day 10, Day 0 *vs.* Day 30, and Day 10 *vs.* Day 30 within S2 (blue) and S2+BB12 (red) groups. Linear mixed-effects model followed by *post hoc* pairwise testing with Tukey's correction (when appropriate) were performed. All mixed model results of selected amino acid-associated metabolites and *post hoc* testing results (when group, time, or group * time model results were significant) are listed in Supplementary Table S6.

10.3389/fmicb.2023.1165771

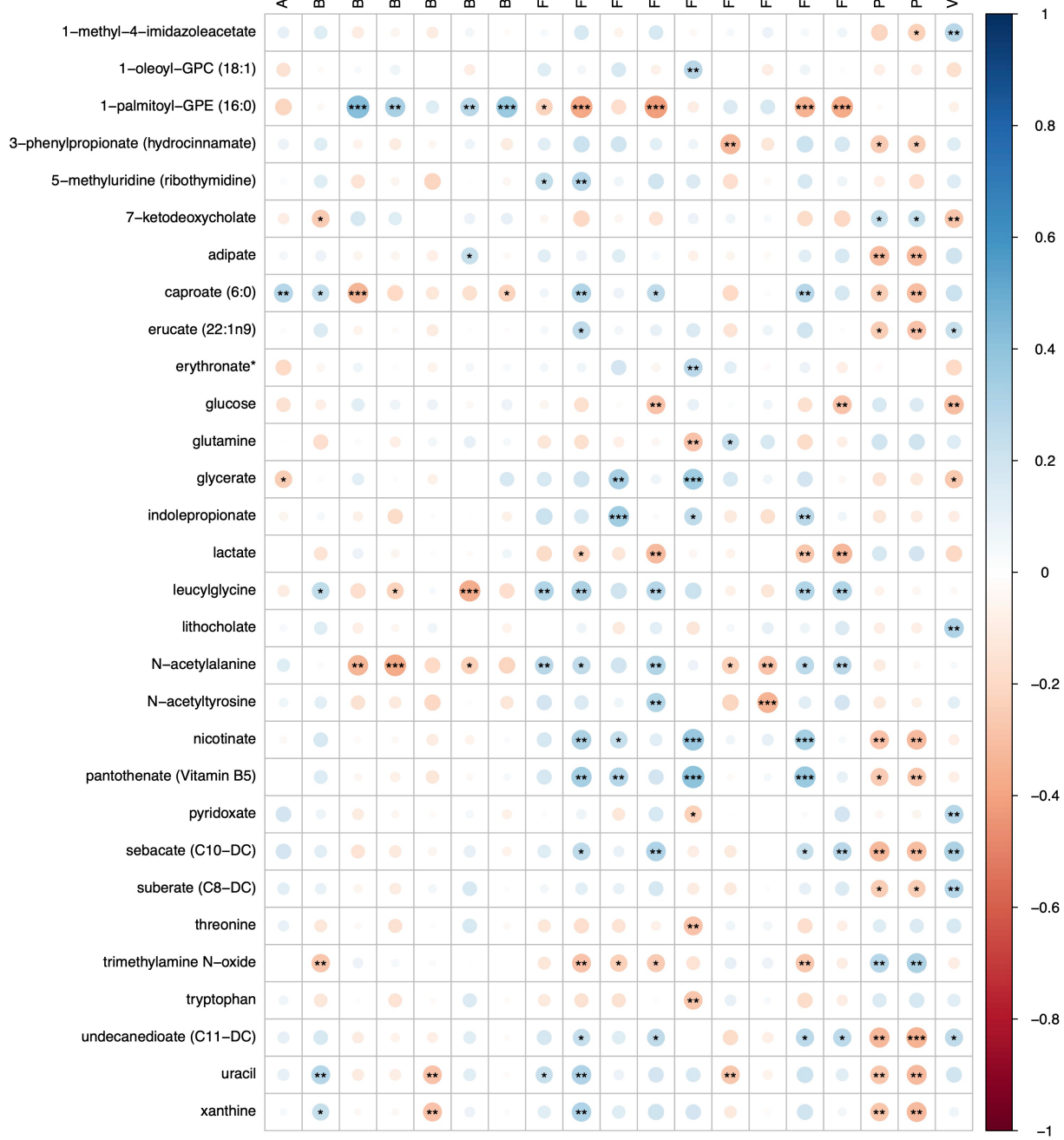

FIGURE 6
Heatmap representing FDR corrected correlations between microbial taxa and metabolites in S2 and S2+BB12 groups. Red and blue represent negative and positive correlations, respectively. Stars indicate FDR values: *=FDR<0.05, **=FDR<0.01, and ***=FDR<0.001.

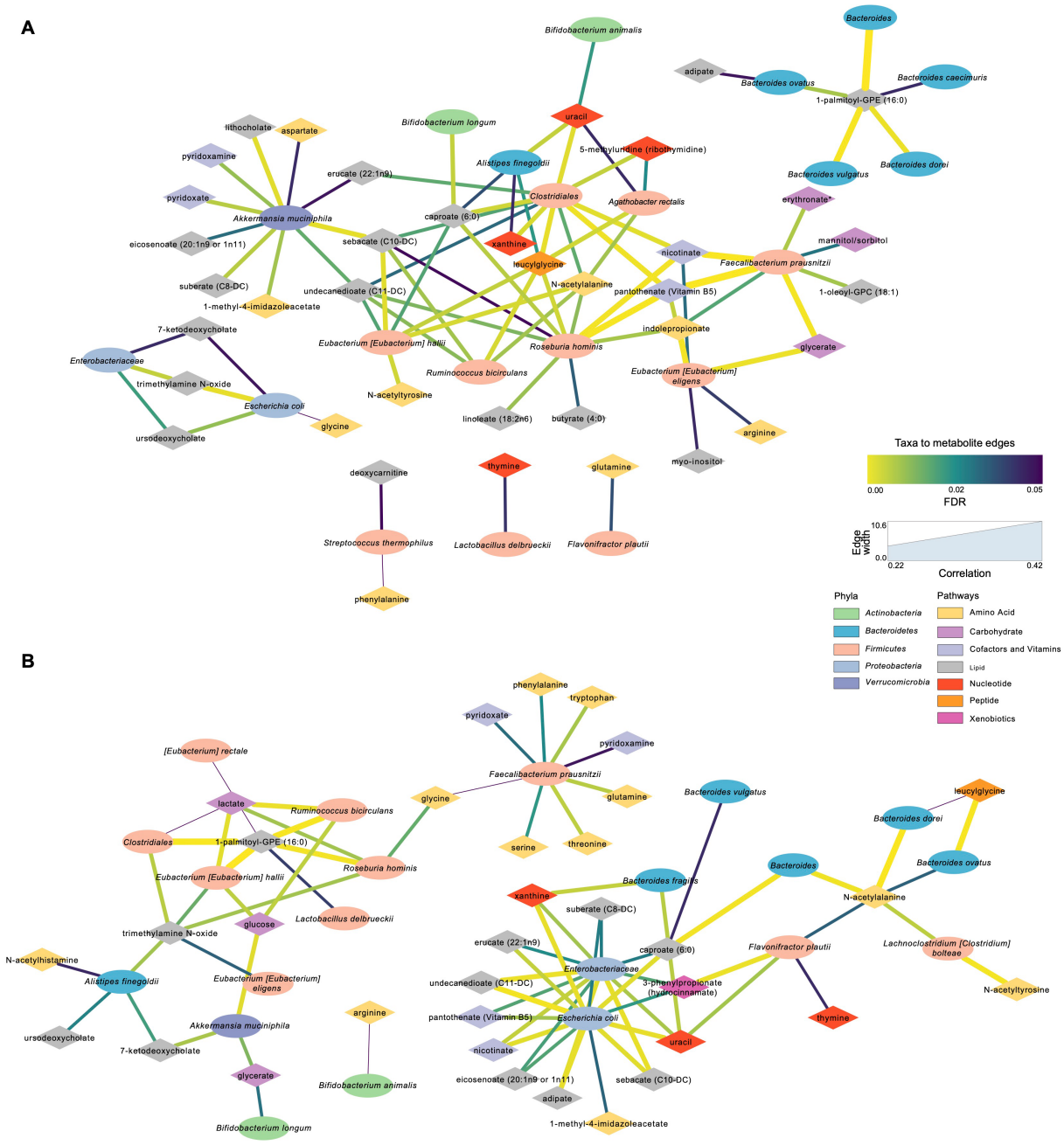

FIGURE 7
Significant microbial taxa and metabolite associations: Network analyses in samples across Day 0, Day 10, and Day 30 within S2 and S2+BB12 groups. **(A)** Network generated from microbial taxa (ellipses) that passed filtering and microbial-associated metabolites (diamonds) identified from previous work (Tanes et al., 2021) showing only positive correlations. **(B)** Same network but showing only negative correlations. Width of edges is proportional to Spearman correlation coefficient and edge color is mapped to the FDR value or the correlation test. All correlations between selected taxa and metabolites and statistical significance testing results are listed in Supplementary Table S5.

Discussion

This randomized, controlled study aimed to observe the differences following the administration of yogurt supplemented with two (S2) *vs.* three (S2 + BB12) probiotic strains in healthy children. We studied probiotics consumption effects on the fecal microbiome and metabolome comparing baseline, post-ten days (Day 10), and post-30 days (Day 30) following yogurt administration. There were no significant differences in the global metagenomic or metabolomic profiles between healthy children receiving two (S2) *vs.* three (S2 + BB12) probiotic strains for 10 days. Nevertheless, we observed a significant increase (Day 0 to Day 10) in the relative abundance of the two and three probiotics administered in the S2 and S2 + BB12 groups, respectively, indicating the intervention had a measurable impact on the bacteria of interest in the gut microbiome. Interestingly, in the S2 group, *S. thermophilus* species appear to maintain a sustained increase

over time, maintaining the significant increase in relative abundance from Day 0 *vs.* Day 30 As both cohorts of children received a probiotic cocktail and the intervention lasted over a short period of time, the lack of strong association between groups in global microbiome changes is not surprising and suggests a resilient and stable gut microbiota in this cohort of healthy children ages one to five. Nevertheless, existing literature reports about infant's and children's gut microbiota stability are conflicting (Bäckhed et al., 2015; Kumbhare et al., 2019). Infant and children's gut microbiota are thought to be immature and therefore more susceptible to perturbations. In line with other studies (Laursen et al., 2017; Wang et al., 2021) our data show short-term effects of probiotic administrations in both groups on the gut microbiome and metabolome. The children's gut microbiota stability observed in this study is consistent with the parent study's findings (Tan et al., 2017).

Most studies examining the health benefits of probiotics have focused on people with pathologies. However, few studies have examined the effects of probiotics on healthy individuals and even fewer have examined the use of probiotics in children. A review of probiotic supplementation in healthy adults found that probiotic supplementation led to a transient increase in the concentration of supplement-specific bacteria but failed to support the ability of probiotics to cause persistent changes in gut microbiota (Khalesi et al., 2019). This is consistent with our results finding a significant increase in the concentration of the supplement-specific bacteria BB-12, following 10 days of BB-12 supplementation. Importantly, as reported in adults, these results were temporary. On Day 30 (20 days following the termination of the BB-12 supplementation), there were no significant differences in the concentration of BB-12 in the S2 + BB12 group.

As yogurts and other dairy products commonly supplemented with probiotics often possess other beneficial characteristics, such as a high calcium content, these properties of probiotics could allow consumers to benefit from the nutritional components without risking disruption to their microbiota and health. This potential beneficial shift to probiotic-associated bacteria that we demonstrated in the S2 + BB12 group (Figure 3) supports the theory that a probiotic intervention may provide a net positive contribution to the gut microbiome ecosystem without conferring strong effects on specific individual bacteria. These findings are also consistent with the concept of emergent properties which postulates that individual properties cannot entirely be explained by their individual components (Ponge, 2005). Therefore, in the context of the current study, although no significant differences following the interventions were observed, there was a global shift towards the increase of bacteria belonging to *Bifidobacterium* and *Lactobacillus* genera, commonly used probiotics. The combined effects of these bacteria could have more functional implications and protective effects than individual bacterial changes supporting the use of probiotics to maintain a healthy gut ecosystem in hopes to prevent gastrointestinal disorders in children, although more research is needed to directly test and validate this notion. Importantly, as this study was conducted on healthy children, these findings should not be extrapolated to children with gastrointestinal disorders or subjects seeking intervention for other diseases or disorders.

Species belonging to *Bifidobacterium* genus were highly abundant in both groups at the three time points. Bifidobacteria are highly represented in children, as they use milk oligosaccharides as a carbon source and to restrict human milk oligosaccharides availability to other microorganisms (Turroni et al., 2011). In addition to the parent study findings, our metagenomic approach allowed a low-level taxonomic affiliation, revealing differences among species belonging to the same genus as in the case of *Bifidobacterium*. It explains why *Bifidobacterium* genus was not among the differentially abundant species in the previous study, *i.e.*, because different *Bifidobacterium* species were abundant in the experimental group (S2 + BB12) and in the control group S2 (e.g., *B. catenulatum*, *B. pseudocatenulatum*). Additionally, this metagenomic approach adds to the existing literature of the genomic potential of the microbial community underlying microbiome-host interactions.

Because the fecal metabolome is influenced by different factors, these changes could reflect shifts of dietary intake, digestion, microbial degradation, and host absorption. When we analyzed the fecal metabolome and microbial diversity using both participant groups, we found associations between metabolites (e.g., uracil, deoxycarnitine, and thymine) and microorganisms. Uracil was positively associated with Clostridiales family, *A. finegoldii, B. animalis,* and *E. rectale*. *B. dorei*, *F. plautii*, *Enterobacteriaceae* family, and *E. coli* were negatively correlated with uracil. During infections, the immune response triggered by uracil promotes pathogen bacteria elimination, intestinal cell repair, and host homeostasis (Lee et al., 2013). Thymine was positively associated with *L. delbrueckii*, the probiotic used in both interventions, and negatively correlated to *F. plautii.* Thymine was found to accelerate microbial metabolisms and ROS production improving antibiotic efficacy both *in vitro* and *in vivo* (Liu et al., 2021). Deoxycarnitine, positively associated with *S. thermophilus*, was linked to increased intestinal permeability (Ghonimy et al., 2018). This suggests that the fecal metabolome may influence gut immune function, permeability, and homeostasis.

A strength of our study is that it was a randomized, blinded controlled trial conducted on children ages one to five years old, an age group that is rarely studied in probiotic research. Additionally, we incorporated and integrated both metagenomic and metabolomic analyses to characterize the effect of BB-12 supplemented yogurt on the children's gut-microbiome and metabolism. This unique integration allowed us to test more system-wide and functional effects on the gut microbiome as a result of two probiotic interventions, providing more comprehensive data on gut health. However, this study examined short-term changes of probiotics over a 10-day period, and more studies should be conducted to investigate the long-term effects on probiotic consumption in this age group. An additional limitation is that we did not incorporate information of dietary intake in the current analysis, as it was not collected in the original study procedures as described by Tan et al. (2017). Diet is an important driver of microbiome composition and an important covariate when evaluating the impact of an intervention, such as probiotics, on gut microbiome communities (Maki et al., 2019). Dietary intake recall and assessment has been historically challenging in children and ongoing work is being performing to improve the validity of dietary reporting in study cohorts with age ranges such as the ones in this study (Livingstone et al., 2004; Livingstone, 2022). Future work evaluating the impact of interventions on gut microbiome composition in children should aim to collect dietary intake should be performed, likely with the assistance of a caregiver or parent (Walker et al., 2018), in order to adequately control for the impact of food consumption on study measures. Novel metagenomics-based methods are being

developed to validate self-report tools, such as using metabarcoding to quantify plant components of human diets (Reese et al., 2019). While these methods are outside of the scope of the current research, they will be useful tools to validate and quantify different dietary components in future microbiome studies.

More studies are needed to elucidate the mechanistic pathways by which probiotics such as BB-12 can affect mucosal barrier functions and innate immunity. Future studies should expand upon the findings presented in this double-blinded, randomized controlled trial and examine the interplay of diet and probiotics on metabolites and microbiota in children. Additionally, further research is needed to investigate environmental factors that influence the impacts of probiotics on children's health status and behavior. The long-term supplementation BB-12 on this population and its longitudinal effects during development should also be examined. This would allow for more in-depth knowledge of the impact that probiotics have on gut microbial communities in developing children as they age. Additionally, future research in children at risk for gastrointestinal disorders may elucidate if these functional metabolite changes as a result of S2 + BB12 probiotic intervention confer a protective gastrointestinal effect.

In conclusion, the results from this deep metagenomic and metabolomic characterization of the gut microbiome and metabolome of children following BB-12 consumption did not show statistically significant differences between the groups, although net positive emergent property effects were witnessed in the S2 + BB12 group over time. The functional redundancy in healthy microbial systems and metabolic stability reflects no changes in the microbial diversity, although we did observe a separation effect in the S2 + BB12 group as a result of the three-strain intervention when we focused on probiotic-associated and beneficial bacteria reported the literature. Our study validated previous results from Tan et al. (2017) and allowed a more in-depth taxonomic characterization of the microorganisms, their genes, and their metabolites. We detected higher abundances of two of the probiotic intervention bacterial taxa (*B. animalis* and *S. thermophilus*) in study subjects receiving the based S2 probiotic intervention + BB12, but no individual taxonomic changes occurred in the S2 only group. Finally, although we did not see global fecal metabolome response to either probiotic, several fecal metabolites were increased in the S2 + BB12 group, indicating a net functional impact of the addition of BB12 to the probiotic intervention. Future research replicating these results across different patient populations will confirm the therapeutic use of BB12 as a probiotic intervention to exert beneficial impacts on the pediatric gastrointestinal system.

Materials and methods

Study design, participants, and setting

Participants ages one to five years old were recruited through the Capital Area Primary Care Research Network for phase I of a double-blinded, randomized controlled study (protocol NCT001652287). Participants included in this study were children whose parents/caregivers were able to read, write, and speak either English or Spanish and had access to a telephone and refrigerator. Eligible participants provided written informed consent were enrolled and randomized as described by Tan et al. to either the BB-12® or control yogurt drink by family cluster. The study protocol was approved by the Georgetown University Institutional Review Board (IRB No. 2012-1,112, Washington, DC). The independent Data Safety Monitoring Board reviewed the protocol before study initiation and checked adverse event data at approximately 33, 50 and 66% data completion. Additional monitoring was conducted by the FDA/CBER, under IND#13691 and the National Institutes of Health (NIH), National Center for Complementary and Integrative Health (NCCIH), including its Office of Clinical and Regulatory Affairs. Participants' eligibility criteria are described in Tan et al. (2017) which included the absence of lactose intolerance and chronic conditions, such as diabetes and asthma. The participants were asked not to consume any products containing probiotics for 14 days before initiating the yogurt intervention and throughout the entire intervention period. The base yogurt drink was prepared with live yogurt starter cultures of *Streptococcus thermophilus* and *Lactobacillus delbrueckii* probiotics [referred to as the two strain [S2] yogurt group (Nagaoka, 2019)], as described in Tan et al. (2017). At baseline, the children were randomized into two groups called S2 or S2 + BB12. Participants in the S2 group ($n = 31$) were administered 112 g of the base yogurt beverage (containing *Streptococcus thermophilus* and *Lactobacillus delbrueckii* only) with no additions to the drink. In contrast, participants in the S2 + BB12 group ($n = 28$) were administered the base yogurt beverage that was supplemented with an additional 1×10^{10} colony-forming units of BB12 per serving per day. BB12 was chosen as the interventional probiotic of interest as it has been widely studied in infants and children (Merenstein et al., 2010, 2011; Goldenberg et al., 2015; Merenstein et al., 2021), and is associated with positive gastrointestinal protective mechanisms including maintenance of tight junction function and immune regulation in the gut (Uusitupa et al., 2020; Cheng et al., 2021). The yogurt was administered to the participants in both groups for ten consecutive days.

Sample collection and processing

Fecal samples were collected at baseline (Day 0), following 10 days of yogurt consumption (Day 10), and 20 days following discontinuation of yogurt administration (Day 30), and immediately stored after collection at −80°C. Samples from days 0, 10 and 30 were then thawed, and approximately 100 mg of the samples were sent to Microbiome Center of the Children's Hospital of Philadelphia ($n = 169$) for microbiome analysis and another 100 mg were sent to Metabolon Inc. (Morrisville, NC, United States; $n = 174$) for metabolomic analyses.

Metagenomic profiling

The DNA used for the metagenomic analysis was extracted using the DNeasy PowerSoil Kit (Qiagen, Hilden, Germany) and quantified with the Quant-iT PicoGreen Assay Kit (Molecular Probes). Shotgun libraries were generated from 0.5 ng DNA using the Nextera XT Library Prep Kit (Illumina, San Diego, CA, United States) and libraries were sequenced on an Illumina HiSeq 2500 in High Output mode to produce paired-end 125 bp sequence reads. Extraction blanks and nucleic acid-free water were processed along with experimental

samples to empirically assess environmental and reagent contamination. A laboratory-generated mock community consisting of DNA from *Vibrio campbellii* and Lambda phage was included as a positive sequencing control.

Metabolomic analysis

The metabolomic analysis was performed using untargeted ultra-performance liquid chromatography-tandem mass spectrometry (UPLC/MS/MS, Waters ACQUITY, Milford, MA, United States), as described previously (Vizioli et al., 2021). Briefly, the fecal samples were prepared using the automated MicroLab STAR system (Hamilton Company, Franklin, MA, United States) and extracted at a constant per-mass basis. Proteins were removed using methanol precipitation (Glen Mills GenoGrinder 2000), followed by centrifugation. The samples were processed using four methods: reverse phase (RP)-UPLC/MS/MS with electrospray ionization (ESI), in both positive (optimized for hydrophilic and hydrophobic compounds, respectively) and negative modes, and hydrophilic interaction chromatography (HILIC)-UPLC/MS/MS-ESI in negative ion mode. The raw UPLC/MS/MS data were integrated into ion peaks organized by mass, retention time/index, and peak area. Metabolites were annotated by comparison of individual spectra to a standard reference library, and area-under-the-curve analysis was performed for peak quantification.

Statistical analysis

For gut microbiome and metabolome analyses, we studied within and between group differences after 10 days of probiotic consumption (Day 10) and 20 days post probiotic discontinuation (Day 30). Shotgun metagenomic data were analyzed using Sunbeam (Clarke et al., 2019). The abundance of bacteria was estimated using Kraken. (Wood and Salzberg, 2014). Taxa that were above 0.1% abundance in any sample were used for differential abundance testing, along with including the microbial taxa at the species level that were included in the probiotic interventions (*i.e., L. delbrueckii, S. thermophilus*, and *B. animalis*). Differential abundance analysis was performed using linear models of Log_{10} transformed relative abundances. Reads were mapped to the KEGG database (Ogata et al., 1999) using DIAMOND (Buchfink et al., 2015) to estimate the abundance of bacterial gene orthologs. Differences between groups for gene and pathways abundances were found by applying linear models to logit transformed relative abundances. Alpha diversity within samples in the S2 and S2 + BB12 groups were assessed by computing the expected number of species at a sequencing depth of 1,000 reads and the Shannon index. To evaluate community-level differences between S2 and S2 + BB12 group fecal samples, beta diversity was calculated using Bray–Curtis dissimilarity matrices, visualized using Principal Coordinates Analysis (PCoA) plots, and relationships within and between S2 and S2 + BB12 groups were compared using the PERMANOVA test.

The top 25 most abundant bacterial taxa and gene orthologs from shotgun metagenomics sequencing were selected using linear models to evaluate the taxa with greatest estimated change in Log_{10} transformed relative abundance for the given comparison. Probiotic-associated bacteria, previously demonstrated to be short chain fatty acid (SCFA)-producers and beneficial for GI health (Markowiak-Kopeć and Śliżewska, 2020), were determined from the literature (Supplementary Table S4). The impact of the S2 *vs.* S2 + BB12 probiotic strains on overall probiotic-associated bacterial relative abundance was additionally measured and visualized by CANOCO version 5 (Braak and Milauer, 1998) in a post-selection PCA to evaluate the effect of targeted probiotic strain administration on bacterial responses of taxa known to be linked to gut microbiome health.

Exploratory and hypothesis-driven metabolite analyses were performed with untargeted metabolite data processed by Metabolon Inc. using MetaboAnalyst 5.0[1] (Chong et al., 2018) and R. (R Development Core Team, 2013) Metabolites with 20% or more missing values were excluded from the exploratory analyses. Missing values, if any, were imputed as 1/5 of the minimum positive value of each feature. Metabolite values were median-scaled and Log_{10} transformed. Wilcoxon rank-sum test, fold change (FC) analyses (FC threshold = 2), and Principal Component Analysis (PCA) were performed to analyze differences between Day 0 *vs.* Day 10, Day 0 *vs.* Day 30, and Day 0 *vs.* Day 30 within the S2 and S2 + BB12 groups and between groups within each time point.

Hypothesis-driven metabolite analyses were additionally performed in metabolites associated with the amino acid super pathways (*i.e.*, glycine, serine and threonine metabolism, alanine and aspartate metabolism, etc.), and SCFAs, as these metabolites are strongly associated with gut microbial community characteristics (Neis et al., 2015). Linear mixed-effects model followed by *post hoc* pairwise testing (when appropriate) and Tukey's correction were performed in JMP statistical analysis platform (Ye et al., 2000).

To create a network of metabolite-taxa correlation pairs, filtering was applied to metabolites as above as well as restricting to bacterial substrates and products based on previous work (Tanes et al., 2021). Briefly, metabolite substrates were defined as those that were increased after treatment with antibiotics and products were those that decreased (Tanes et al., 2021). Microbial taxa at the species level were filtered to include taxa present at >0.01% mean relative abundance, along with including the microbial taxa at the species level that were included in the probiotic interventions (*i.e.*, *L. delbrueckii, S. thermophilus*, and *B. animalis*). Spearman correlation testing was then performed on each microbe-metabolite pair with FDR correction applied to *p*-values. Network diagrams of bacteria and metabolites were generated using Cytoscape v3.9.1 (Shannon et al., 2003). Metabolites that significantly correlated with *L. delbrueckii*, *S. thermophilus,* and BB-12 were additionally tested for intervention-associated change over time. Statistical significance was defined as *p*-values or FDR corrected *p*-values <0.05 for all statistical analyses. All statistical tests were adjusted for the following covariates: age, race, gender, ethnicity, and total number of housemates except for correlations between genes and metabolites.

Author's note

The content is solely the responsibility of the authors and does not necessarily represent the official views of the National Institutes of Health.

1 https://www.metaboanalyst.ca/

Data availability statement

The datasets presented in this study can be found in the NCBI repository, accession number PRJNA929986: https://www.ncbi.nlm.nih.gov/bioproject/PRJNA929986.

Ethics statement

The studies involving human participants were reviewed and approved by Georgetown University Institutional Review Board. Written informed consent to participate in this study was provided by the participants' legal guardian/next of kin.

Author contributions

DM and PJ: concept and design, obtained funding, and study supervision. TT, DM, AF, and BB: acquisition of data and sample processing. CV, AF, SD, KB, RJ-L, KM, and PJ: statistical analysis or interpretation of data. CV, AD, AF, BB, RJ-L, KM, and PJ: drafting of the manuscript. AF, DM, TT, BB, PV, SD, and KB: critical revision of the manuscript for important intellectual content. PJ: administrative, technical, or material support. All authors contributed to the article and approved the submitted version.

Funding

PJ is supported by National Institute of Alcohol Abuse and Alcoholism under award number, Z01AA000135, the National Institute of Nursing Research and the Rockefeller University Heilbrunn Nurse Scholar Award. PJ is supported by the Office of Workforce Diversity, and the Office of Workforce Diversity, National Institutes of Health Distinguished Scholar Program. Intramural Research Training Award (to AF, RJ-L, and BB). RJ-L is supported by the Center of Compulsive Behaviors Fellowship, National Institutes of Health. Funding from Dannon to TT and DM, the Department of Family Medicine, Georgetown University Medical Center, Washington, DC. KM is supported by intramural research funds at the National Institutes of Health, Clinical Center.

Acknowledgments

The authors would like to thank Joan Austin for her review and edits and Jennifer J. Barb for bioinformatics consultative support. A special thanks to the participants of this study and the Georgetown Microbiome Group.

Conflict of interest

DM previously served as a paid expert at Howard University and Bayer. DM has done legal work for Visniome VSL#3, Golo for Life, and President of the International Scientific Association for Probiotics and Prebiotics (ISAPP) board.

The remaining authors declare that the research was conducted in the absence of any commercial or financial relationships that could be construed as a potential conflict of interest.

Publisher's note

Supplementary material

The Supplementary material for this article can be found online at: https://www.frontiersin.org/articles/10.3389/fmicb.2023.1165771/full#supplementary-material

SUPPLEMENTARY FIGURE S1
Metagenomics PCoA day 30.

SUPPLEMENTARY FIGURE S2
Metabolite PCA.

SUPPLEMENTARY TABLE S1
Top 25 taxa genes within group.

SUPPLEMENTARY TABLE S2
Covariate results taxa.

SUPPLEMENTARY TABLE S3
Covariate results gene.

SUPPLEMENTARY TABLE S4
Probiotics selection.

SUPPLEMENTARY TABLE S5
Metabolites and pathways volcano plot.

SUPPLEMENTARY TABLE S6
Selected metabolite model results.

SUPPLEMENTARY TABLE S7
26 taxa to 479 metab correlations.

SUPPLEMENTARY TABLE S8
26 taxa to 79 metab network.

References

Arpaia, N., Campbell, C., Fan, X., Dikiy, S., van der Veeken, J., deRoos, P., et al. (2013). Metabolites produced by commensal bacteria promote peripheral regulatory T-cell generation. *Nature* 504, 451–455. doi: 10.1038/nature12726

Artis, D. (2008). Epithelial-cell recognition of commensal bacteria and maintenance of immune homeostasis in the gut. *Nat. Rev. Immunol.* 8, 411–420. doi: 10.1038/nri2316

Bäckhed, F., Roswall, J., Peng, Y., Feng, Q., Jia, H., Kovatcheva-Datchary, P., et al. (2015). Dynamics and stabilization of the human gut microbiome during the first year of life. *Cell Host Microbe* 17, 690–703. doi: 10.1016/j.chom.2015.04.004

Boulangé, C. L., Neves, A. L., Chilloux, J., Nicholson, J. K., and Dumas, M. E. (2016). Impact of the gut microbiota on inflammation, obesity, and metabolic disease. *Genome Med.* 8:42. doi: 10.1186/s13073-016-0303-2

Braak, C.T. and Milauer, P. *CANOCO Reference Manual and User's Guide to Canoco for Windows: Software for Canonical Community Ordination* (Version 4). (1998).

Buchfink, B., Xie, C., and Huson, D. H. (2015). Fast and sensitive protein alignment using DIAMOND. *Nat. Methods* 12, 59–60. doi: 10.1038/nmeth.3176

Cheng, J., Laitila, A., and Ouwehand, A. C. (2021). *Bifidobacterium animalis* subsp. *lactis* HN019 effects on gut health: a review. *Front. Nutr.* 8:790561. doi: 10.3389/fnut.2021.790561

Chong, J., Soufan, O., Li, C., Caraus, I., Li, S., Bourque, G., et al. (2018). MetaboAnalyst 4.0: towards more transparent and integrative metabolomics analysis. *Nucleic Acids Res.* 46, W486–w494. doi: 10.1093/nar/gky310

Clarke, E. L., Taylor, L. J., Zhao, C., Connell, A., Lee, J. J., Fett, B., et al. (2019). Sunbeam: an extensible pipeline for analyzing metagenomic sequencing experiments. *Microbiome* 7:46. doi: 10.1186/s40168-019-0658-x

Conlon, M. A., and Bird, A. R. (2015). The impact of diet and lifestyle on gut microbiota and human health. *Nutrients* 7, 17–44. doi: 10.3390/nu7010017

Dai, Z. L., Wu, G., and Zhu, W. Y. (2011). Amino acid metabolism in intestinal bacteria: links between gut ecology and host health. *Front. Biosci.* 16, 1768–1786. doi: 10.2741/3820

den Besten, G., van Eunen, K., Groen, A. K., Venema, K., Reijngoud, D. J., and Bakker, B. M. (2013). The role of short-chain fatty acids in the interplay between diet, gut microbiota, and host energy metabolism. *J. Lipid Res.* 54, 2325–2340. doi: 10.1194/jlr.R036012

Ghonimy, A., Zhang, D., Farouk, M., and Wang, Q. (2018). The impact of carnitine on dietary fiber and gut bacteria metabolism and their mutual interaction in monogastrics. *Int. J. Mol. Sci.* 19:1008. doi: 10.3390/ijms19041008

Goldenberg, J. Z., Goldenberg, J. Z., Humphrey, C., El Dib, R., and Johnston, B. C. (2015). Probiotics for the prevention of pediatric antibiotic-associated diarrhea. *Cochrane Database Syst. Rev.* 12:Cd004827. doi: 10.1002/14651858.CD004827.pub5

Griffin, S. M., Lehtinen, M. J., Meunier, J., Ceolin, L., Roman, F. J., and Patterson, E. (2022). Restorative effects of probiotics on memory impairment in sleep-deprived mice. *Nutr. Neurosci.* 26, 254–264. doi: 10.1080/1028415X.2022.2042915

Hill, C., Guarner, F., Reid, G., Gibson, G. R., Merenstein, D. J., Pot, B., et al. (2014). Expert consensus document. The International Scientific Association for Probiotics and Prebiotics consensus statement on the scope and appropriate use of the term probiotic. *Nat. Rev. Gastroenterol. Hepatol.* 11, 506–514. doi: 10.1038/nrgastro.2014.66

Hojsak, I., Fabiano, V., Pop, T. L., Goulet, O., Zuccotti, G. V., Çokuğraş, F. C., et al. (2018). Guidance on the use of probiotics in clinical practice in children with selected clinical conditions and in specific vulnerable groups. *Acta Paediatr.* 107, 927–937. doi: 10.1111/apa.14270

Jungersen, M., Wind, A., Johansen, E., Christensen, J., Stuer-Lauridsen, B., and Eskesen, D. (2014). The science behind the probiotic strain *Bifidobacterium animalis* subsp. *lactis* BB-12®. *Microorganisms* 2, 92–110. doi: 10.3390/microorganisms2020092

Khalesi, S., Bellissimo, N., Vandelanotte, C., Williams, S., Stanley, D., and Irwin, C. (2019). A review of probiotic supplementation in healthy adults: helpful or hype? *Eur. J. Clin. Nutr.* 73, 24–37. doi: 10.1038/s41430-018-0135-9

Kostic, A. D., Gevers, D., Siljander, H., Vatanen, T., Hyötyläinen, T., Hämäläinen, A. M., et al. (2015). The dynamics of the human infant gut microbiome in development and in progression toward type 1 diabetes. *Cell Host Microbe* 17, 260–273. doi: 10.1016/j.chom.2015.01.001

Kumbhare, S. V., Patangia, D. V., Patil, R. H., Shouche, Y. S., and Patil, N. P. (2019). Factors influencing the gut microbiome in children: from infancy to childhood. *J. Biosci.* 44:49. doi: 10.1007/s12038-019-9860-z

Laursen, M. F., Laursen, R. P., Larnkjær, A., Michaelsen, K. F., Bahl, M. I., and Licht, T. R. (2017). Administration of two probiotic strains during early childhood does not affect the endogenous gut microbiota composition despite probiotic proliferation. *BMC Microbiol.* 17:175. doi: 10.1186/s12866-017-1090-7

LeBlanc, J. G., Chain, F., Martín, R., Bermúdez-Humarán, L. G., Courau, S., and Langella, P. (2017). Beneficial effects on host energy metabolism of short-chain fatty acids and vitamins produced by commensal and probiotic bacteria. *Microb. Cell Fact.* 16:79. doi: 10.1186/s12934-017-0691-z

Lee, S. H., Joo, N. S., Kim, K. M., and Kim, K. N. (2018). The therapeutic effect of a multistrain probiotic on diarrhea-predominant irritable bowel syndrome: a pilot study. *Gastroenterol. Res. Pract.* 2018:8791916. doi: 10.1155/2018/8791916

Lee, K. A., Kim, S. H., Kim, E. K., Ha, E. M., You, H., Kim, B., et al. (2013). Bacterial-derived uracil as a modulator of mucosal immunity and gut-microbe homeostasis in *Drosophila*. *Cells* 153, 797–811. doi: 10.1016/j.cell.2013.04.009

Liu, Y., Yang, K., Jia, Y., Shi, J., Tong, Z., Wang, Z., et al. (2021). Thymine sensitizes gram-negative pathogens to antibiotic killing. *Front. Microbiol.* 12:622798. doi: 10.3389/fmicb.2021.622798

Livingstone, M. B. E. (2022). Issues in dietary intake assessment of children and adolescents. *Br. J. Nutr.* 127, 1426–1427. doi: 10.1017/S0007114522000770

Livingstone, M. B., Robson, P. J., and Wallace, J. M. (2004). Issues in dietary intake assessment of children and adolescents. *Br. J. Nutr.* 92, S213–S222. doi: 10.1079/BJN20041169

Łukasik, J., Salminen, S., and Szajewska, H. (2018). Rapid review shows that probiotics and fermented infant formulas do not cause d-lactic acidosis in healthy children. *Acta Paediatr.* 107, 1322–1326. doi: 10.1111/apa.14338

Maki, K. A., Diallo, A. F., Lockwood, M. B., Franks, A. T., Green, S. J., and Joseph, P. V. (2019). Considerations when designing a microbiome study: implications for nursing science. *Biol. Res. Nurs.* 21, 125–141. doi: 10.1177/1099800418811639

Markowiak-Kopeć, P., and Śliżewska, K. (2020). The effect of probiotics on the production of short-Chain fatty acids by human intestinal microbiome. *Nutrients* 12:1107. doi: 10.3390/nu12041107

Mayer-Davis, E. J., Rifas-Shiman, S. L., Zhou, L., Hu, F. B., Colditz, G. A., and Gillman, M. W. (2006). Breast-feeding and risk for childhood obesity: does maternal diabetes or obesity status matter? *Diabetes Care* 29, 2231–2237. doi: 10.2337/dc06-0974

McKean, J., Naug, H., Nikbakht, E., Amiet, B., and Colson, N. (2017). Probiotics and subclinical psychological symptoms in healthy participants: a systematic review and meta-analysis. *J. Altern. Complement. Med.* 23, 249–258. doi: 10.1089/acm.2016.0023

Merenstein, D., Fraser, C. M., Roberts, R. F., Liu, T., Grant-Beurmann, S., Tan, T. P., et al. (2021). *Bifidobacterium animalis* subsp. *lactis* BB-12 protects against antibiotic-induced functional and compositional changes in human fecal microbiome. *Nutrients* 13:2814. doi: 10.3390/nu13082814

Merenstein, D., Gonzalez, J., Young, A. G., Roberts, R. F., Sanders, M. E., and Petterson, S. (2011). Study to investigate the potential of probiotics in children attending school. *Eur. J. Clin. Nutr.* 65, 447–453. doi: 10.1038/ejcn.2010.290

Merenstein, D. J., Smith, K. H., Scriven, M., Roberts, R. F., Sanders, M. E., and Petterson, S. (2010). The study to investigate the potential benefits of probiotics in yogurt, a patient-oriented, double-blind, cluster-randomised, placebo-controlled, clinical trial. *Eur. J. Clin. Nutr.* 64, 685–691. doi: 10.1038/ejcn.2010.30

Mörkl, S., Butler, M. I., Holl, A., Cryan, J. F., and Dinan, T. G. (2020). Probiotics and the microbiota-gut-brain Axis: focus on psychiatry. *Curr. Nutr. Rep.* 9, 171–182. doi: 10.1007/s13668-020-00313-5

Moroni, O., Kheadr, E., Boutin, Y., Lacroix, C., and Fliss, I. (2006). Inactivation of adhesion and invasion of food-borne *Listeria monocytogenes* by bacteriocin-producing *Bifidobacterium* strains of human origin. *Appl. Environ. Microbiol.* 72, 6894–6901. doi: 10.1128/AEM.00928-06

Nagaoka, S. (2019). Yogurt production. *Methods Mol. Biol.* 1887, 45–54. doi: 10.1007/978-1-4939-8907-2_5

Neis, E. P., Dejong, C. H., and Rensen, S. S. (2015). The role of microbial amino acid metabolism in host metabolism. *Nutrients* 7, 2930–2946. doi: 10.3390/nu7042930

Ogata, H., Goto, S., Sato, K., Fujibuchi, W., Bono, H., and Kanehisa, M. (1999). KEGG: Kyoto Encyclopedia of Genes And Genomes. *Nucleic Acids Res.* 27, 29–34. doi: 10.1093/nar/27.1.29

Plaza-Diaz, J., Ruiz-Ojeda, F. J., Gil-Campos, M., and Gil, A. (2019). Mechanisms of action of probiotics. *Adv. Nutr.* 10, S49–S66. doi: 10.1093/advances/nmy063

Ponge, J. F. (2005). Emergent properties from organisms to ecosystems: towards a realistic approach. *Biol. Rev. Camb. Philos. Soc.* 80, 403–411. doi: 10.1017/S146479310500672X

R Development Core Team (2013). *R: A Language and Environment for Statistical Computing* R Foundation for Statistical Computing: Vienna, Austria.

Reese, A. T., Kartzinel, T. R., Petrone, B. L., Turnbaugh, P. J., Pringle, R. M., and David, L. A. (2019). Using DNA metabarcoding to evaluate the plant component of human diets: a proof of concept. *mSystems* 4:e00458. doi: 10.1128/mSystems.00458-19

Riekeberg, E., and Powers, R. (2017). New frontiers in metabolomics: from measurement to insight. *F1000Res* 6:1148. doi: 10.12688/f1000research.11495.1

Savignac, H. M., Tramullas, M., Kiely, B., Dinan, T. G., and Cryan, J. F. (2015). Bifidobacteria modulate cognitive processes in an anxious mouse strain. *Behav. Brain Res.* 287, 59–72. doi: 10.1016/j.bbr.2015.02.044

Schroeder, B. O., Birchenough, G. M. H., Ståhlman, M., Arike, L., Johansson, M. E. V., Hansson, G. C., et al. (2018). Bifidobacteria or Fiber protects against diet-induced microbiota-mediated colonic mucus deterioration. *Cell Host Microbe* 23, 27–40.e7. doi: 10.1016/j.chom.2017.11.004

Shannon, P., Markiel, A., Ozier, O., Baliga, N. S., Wang, J. T., Ramage, D., et al. (2003). Cytoscape: a software environment for integrated models of biomolecular interaction networks. *Genome Res.* 13, 2498–2504. doi: 10.1101/gr.1239303

Sharma, R., Gupta, D., Mehrotra, R., and Mago, P. (2021). Psychobiotics: the next-generation probiotics for the brain. *Curr. Microbiol.* 78, 449–463. doi: 10.1007/s00284-020-02289-5

Srutkova, D., Schwarzer, M., Hudcovic, T., Zakostelska, Z., Drab, V., Spanova, A., et al. (2015). *Bifidobacterium longum* CCM 7952 promotes epithelial barrier function and prevents acute DSS-induced colitis in strictly strain-specific manner. *PLoS One* 10:e0134050. doi: 10.1371/journal.pone.0134050

Stiemsma, L. T., and Michels, K. B. (2018). The role of the microbiome in the developmental origins of health and disease. *Pediatrics* 141:e20172437. doi: 10.1542/peds.2017-2437

Stinson, L. F., Payne, M. S., and Keelan, J. A. (2017). Planting the seed: origins, composition, and postnatal health significance of the fetal gastrointestinal microbiota. *Crit. Rev. Microbiol.* 43, 352–369. doi: 10.1080/1040841X.2016.1211088

Suez, J., Zmora, N., Segal, E., and Elinav, E. (2019). The pros, cons, and many unknowns of probiotics. *Nat. Med.* 25, 716–729. doi: 10.1038/s41591-019-0439-x

Suez, J., Zmora, N., Zilberman-Schapira, G., Mor, U., Dori-Bachash, M., Bashiardes, S., et al. (2018). Post-antibiotic gut mucosal microbiome reconstitution is impaired by probiotics and improved by autologous FMT. *Cells* 174, 1406–1423.e16. doi: 10.1016/j.cell.2018.08.047

Tan, T. P., Ba, Z., Sanders, M. E., D'Amico, F. J., Roberts, R. F., Smith, K. H., et al. (2017). Safety of *Bifidobacterium animalis* subsp. *lactis* (*B. lactis*) strain BB-12-supplemented yogurt in healthy children. *J. Pediatr. Gastroenterol. Nutr.* 64, 302–309. doi: 10.1097/MPG.0000000000001272

Tanes, C., Bittinger, K., Gao, Y., Friedman, E. S., Nessel, L., Paladhi, U. R., et al. (2021). Role of dietary fiber in the recovery of the human gut microbiome and its metabolome. *Cell Host Microbe* 29, 394–407.e5. doi: 10.1016/j.chom.2020.12.012

Turroni, F., van Sinderen, D., and Ventura, M. (2011). Genomics and ecological overview of the genus *Bifidobacterium*. *Int. J. Food Microbiol.* 149, 37–44. doi: 10.1016/j.ijfoodmicro.2010.12.010

Uusitupa, H. M., Rasinkangas, P., Lehtinen, M. J., Mäkelä, S. M., Airaksinen, K., Anglenius, H., et al. (2020). *Bifidobacterium animalis* subsp. *lactis* 420 for metabolic health: review of the research. *Nutrients* 12:892. doi: 10.3390/nu12040892

Vizioli, C., Jaime-Lara, R. B., Franks, A. T., Ortiz, R., and Joseph, P. V. (2021). Untargeted metabolomic approach shows no differences in subcutaneous adipose tissue of diabetic and non-diabetic subjects undergoing bariatric surgery: an exploratory study. *Biol. Res. Nurs.* 23, 109–118. doi: 10.1177/1099800420942900

Walker, J. L., Ardouin, S., and Burrows, T. (2018). The validity of dietary assessment methods to accurately measure energy intake in children and adolescents who are overweight or obese: a systematic review. *Eur. J. Clin. Nutr.* 72, 185–197. doi: 10.1038/s41430-017-0029-2

Wang, W. L., Xu, S. Y., Ren, Z. G., Tao, L., Jiang, J. W., and Zheng, S. S. (2015). Application of metagenomics in the human gut microbiome. *World J. Gastroenterol.* 21, 803–814. doi: 10.3748/wjg.v21.i3.803

Wang, S., Xun, Y., Ahern, G. J., Feng, L., Zhang, D., Xue, Y., et al. (2021). A randomized, double blind, parallel, placebo-controlled study to investigate the efficacy of *Lactobacillus paracasei* N1115 in gut development of young children. *Food Sci. Nutr.* 9, 6020–6030. doi: 10.1002/fsn3.2533

Wilkins, T., and Sequoia, J. (2017). Probiotics for gastrointestinal conditions: a summary of the evidence. *Am. Fam. Physician* 96, 170–178.

Wood, D. E., and Salzberg, S. L. (2014). Kraken: ultrafast metagenomic sequence classification using exact alignments. *Genome Biol.* 15:R46. doi: 10.1186/gb-2014-15-3-r46

Xue, L., He, J., Gao, N., Lu, X., Li, M., Wu, X., et al. (2017). Probiotics may delay the progression of nonalcoholic fatty liver disease by restoring the gut microbiota structure and improving intestinal endotoxemia. *Sci. Rep.* 7:45176. doi: 10.1038/srep45176

Yatsunenko, T., Rey, F. E., Manary, M. J., Trehan, I., Dominguez-Bello, M. G., Contreras, M., et al. (2012). Human gut microbiome viewed across age and geography. *Nature* 486, 222–227. doi: 10.1038/nature11053

Ye, C., Liu, J., Ren, F., and Okafo, N. (2000). Design of experiment and data analysis by JMP® (SAS institute) in analytical method validation. *J. Pharm. Biomed. Anal.* 23, 581–589. doi: 10.1016/S0731-7085(00)00335-6

Yuan, C., Gaskins, A. J., Blaine, A. I., Zhang, C., Gillman, M. W., Missmer, S. A., et al. (2016). Association between cesarean birth and risk of obesity in offspring in childhood, adolescence, and early adulthood. *JAMA Pediatr.* 170:e162385. doi: 10.1001/jamapediatrics.2016.2385

frontiers | Frontiers in Microbiology

TYPE Original Research
PUBLISHED 04 July 2023
DOI 10.3389/fmicb.2023.1199383

OPEN ACCESS

EDITED BY
Xiaodong Xia,
Dalian Polytechnic University, China

REVIEWED BY
Hengjun Du,
University of Massachusetts Amherst, United States
Jisun Lee,
Chung-Ang University, Republic of Korea

*CORRESPONDENCE
Eric de Castro Tobaruela
✉ erictobaruela@usp.br

†These authors have contributed equally to this work and share first authorship

RECEIVED 03 April 2023
ACCEPTED 19 June 2023
PUBLISHED 04 July 2023

CITATION
Corrêa TAF, Tobaruela EC, Capetini VC, Quintanilha BJ, Cortez RV, Taddei CR, Hassimotto NMA, Hoffmann C, Rogero MM and Lajolo FM (2023) Blood orange juice intake changes specific bacteria of gut microbiota associated with cardiometabolic biomarkers. *Front. Microbiol.* 14:1199383. doi: 10.3389/fmicb.2023.1199383

Blood orange juice intake changes specific bacteria of gut microbiota associated with cardiometabolic biomarkers

Telma Angelina Faraldo Corrêa[1,2†], Eric de Castro Tobaruela[1,2*†], Vinicius Cooper Capetini[2,3], Bruna Jardim Quintanilha[2,3], Ramon Vitor Cortez[4], Carla R. Taddei[4], Neuza Mariko Aymoto Hassimotto[1,2], Christian Hoffmann[1,2], Marcelo Macedo Rogero[2,3] and Franco Maria Lajolo[1,2]

[1]Department of Food and Experimental Nutrition, School of Pharmaceutical Sciences, University of São Paulo, São Paulo, Brazil, [2]Food Research Center (FoRC), São Paulo, Brazil, [3]Department of Nutrition, School of Public Health, University of São Paulo, São Paulo, Brazil, [4]Department of Clinical Analyses and Toxicology, School of Pharmaceutical Sciences, University of São Paulo, São Paulo, Brazil

Blood orange juice is an important source of flavanones and anthocyanins, mainly hesperidin, narirutin, and cyanidin-3-*O*-glucoside. The benefits of these bioactive compounds have been reported, but the mechanistic details behind their biological effects are not well established. This study investigated the effects of Moro orange (*Citrus sinensis* L. Osbeck) juice (MOJ) on gut microbiota composition and cardiometabolic biomarkers in overweight women. In this study, 12 overweight women (BMI from 25.0 to 29.9 kg/m^2), aged 18–37 years, consumed 500 mL of MOJ every day for 4 weeks. We assessed the gut microbiota composition, levels of short-chain fatty acids (SCFAs), cardiometabolic biomarkers, and insulin resistance (HOMA-IR) at baseline and after 2 weeks and 4 weeks of MOJ intake. The results suggested that MOJ intake affected the abundance of specific operational taxonomic units (OTUs) of the gut microbiota but did not significantly alter the diversity and general composition of the gut microbiota. However, MOJ intake increased the production of SCFAs, especially propionic and isobutyric acids, and significantly improved cardiometabolic biomarkers such as blood pressure and plasma VCAM-1 levels in the overweight women. Additionally, we observed significant associations between gut microbiota OTUs belonging to the Bacteroidetes phyla and *Prevotella 9* genera and the cardiometabolic biomarkers. Furthermore, MOJ reduced fasting glucose and insulin levels and HOMA-IR values, thereby enhancing insulin sensitivity in the insulin-resistant overweight women. Finally, we highlighted the importance of orange juice intake duration because some beneficial changes such as blood pressure improvements were evident at the 2-week time interval of the intervention, but other changes became significant only at the 4-week interval of MOJ intake. In conclusion, our study demonstrated that changes in specific OTUs of the gut microbiota in response to MOJ intake were associated with significant improvements in some cardiometabolic biomarkers and SCFA levels in overweight women with insulin resistance.

KEYWORDS

microbiome, short-chain fatty acids, flavanones, anthocyanins, cardiometabolic diseases

1. Introduction

Cardiovascular diseases (CVDs) and diabetes are the main causes of mortality worldwide, accounting for nearly 31% of all deaths globally. The development of CVDs is associated with risk factors such as dietary patterns, diabetes mellitus, dyslipidemia, hypertension, and obesity, whereas insulin resistance is directly associated with diabetes (World Health Organization, 2020).

Orange juice is an important source of bioactive compounds such as flavonoids, vitamin C, and carotenoids. Hesperidin and naringin are the most abundant flavanones in orange juice (Yi et al., 2017). Furthermore, blood orange (*Citrus sinensis* L. Osbeck var. Moro) juice also contains higher levels of anthocyanins, especially cyanidin-3-*O*-glucoside. These nutrients and bioactive compounds may act as antioxidants, anti-inflammatories and improve glucose and lipid metabolism and blood pressure (D'Elia et al., 2021). Animal studies have shown that orange juice reduces the risk of CVDs by improving lipid and glucose metabolism, fat storage, inflammation and hypertension (Al-Okbi et al., 2018; Berger et al., 2020; Mas-Capdevila et al., 2020; Yang et al., 2022). However, human studies are not conclusive regarding the beneficial role of orange juice in reducing the risk of CVD (Corrêa et al., 2019; Lima et al., 2019; Stevens et al., 2019; Fidélix et al., 2020; Mas-Capdevila et al., 2020).

Gut microbiota is involved in several cardiometabolic diseases (Fan and Pedersen, 2021). Disruption of gut microbiota may extract more energy from the diet, reduce satiety, promote changes in lipid and glucose metabolism, increase the production of branched-chain fatty acids (BCFAs) and trimethylamine oxide (TMAO), and increase gut permeability. The disturbance of the intestinal barrier function activates the immune system, triggering metabolic endotoxemia, low-grade inflammation, and insulin resistance (Fan and Pedersen, 2021). Gut microbiota has emerged as a modifiable therapeutic target to reduce cardiometabolic risk (Chambers et al., 2018).

Recent evidence has shown that orange flavanones could modulate the gut microbiota composition and reduce the risk of metabolic diseases (Lima et al., 2019; Fidélix et al., 2020; Nishioka et al., 2021; Santana et al., 2022). However, only one clinical trial has investigated the effects of blood orange juice on the gut microbiota composition and its effects on the host (Santana et al., 2022). In view of the above, this study evaluated the effects of daily consumption of blood orange juice (*Citrus sinensis* L. Osbeck var. Moro) on the microbiota composition and subsequent changes in the levels of cardiometabolic biomarkers in overweight women.

2. Materials and methods

2.1. Blood orange juice

The pasteurized blood orange juice (*Citrus sinensis* L. Osbeck var. Moro) was provided by Fundecitrus (Araraquara, São Paulo, Brazil) in 500 mL bottles. Moro orange juice (MOJ) was prepared as described by Brasili et al. (2017) from fruits grown in the Minas Gerais state (Brazil). Since blood oranges require low temperature for anthocyanin production, Moro orange fruits (MOJ) were stored at 9°C until the pulp reached a darker purple color, as described by Carmona et al. (2017). The detailed chemical characterization of the MOJ (quality parameters, soluble sugars, organic acids, total phenolic compounds, dietary fiber, and flavonoids) was performed according to the methods described in the Supplementary material, and the results are shown in Supplementary Tables S1, S2. The orange juice bottles were stored at −80°C until the beginning of trial.

2.2. Study population

This study enrolled 12 women (18–37 years) who were overweight (body mass index–BMI ranged from 25.0 to 29.9 kg/m^2). The study subjects did not have any history of metabolic diseases and were nonsmokers, non-pregnant, non-vegetarians, and non-athletes. They also did not have any history of receiving drug therapies or dietary supplements (e.g., vitamins and minerals). The study volunteers were provided with the orange juice bottles and instructed to store their bottles in a refrigerator. The study was conducted in accordance with the Declaration of Helsinki and written informed consent was provided by volunteers. This study was approved by the Ethics Board, School of Public Health, University of São Paulo (CAAE 69382217.9.0000.5421), and was registered at the Brazilian Registry of Clinical Trials (UTN: U1111-1241-4,665).

2.3. Study protocol

The volunteers were instructed to restrict their intake of citrus (orange, lemon, grapefruit) and their derivatives for 3 consecutive days before the 4-week longitudinal intervention study. On the first day of the intervention (baseline; A), blood samples were collected from all the volunteers after 12 h overnight fasting. A stool sample was obtained by each volunteer the day before blood collection, stored under refrigeration and delivered to the laboratory at the time of blood collection. Blood pressure (Omron HEM-7113, Kyoto, Japan) and the anthropometric parameters were also measured. The 24 h dietary recall (R24h) was the method conducted to collect diet data, to evaluate the consumption of food nutrients and to check for possible variations in food intake. Subsequently, the volunteers consumed 500 mL of pasteurized MOJ every day for 4 weeks. We further collected blood and stool samples, and assessed the blood pressure and anthropometric assessments at the 2-week (B) and 4-week (C) time points during the MOJ intake. Volunteers were instructed to maintain their usual dietary habits and lifestyle throughout the intervention period and avoid intake of any citrus-derived foods or beverages in addition to the MOJ intake as part of the study protocol. This study protocol is detailed in Figure 1.

2.4. Anthropometric and dietary intake measurements

Height, weight, and abdominal circumference of all the volunteers were measured at baseline (A) and at 2-week (B) and 4-week (C) times points during the MOJ intake. BMI classification was performed according to the World Health Organization (2000). The dietary intake of macronutrients and micronutrients was determined using the diet data obtained from the R24h conducted at each time point during MOJ intake and the Avanutri® 4.0 software (Rio de Janeiro, Brazil).

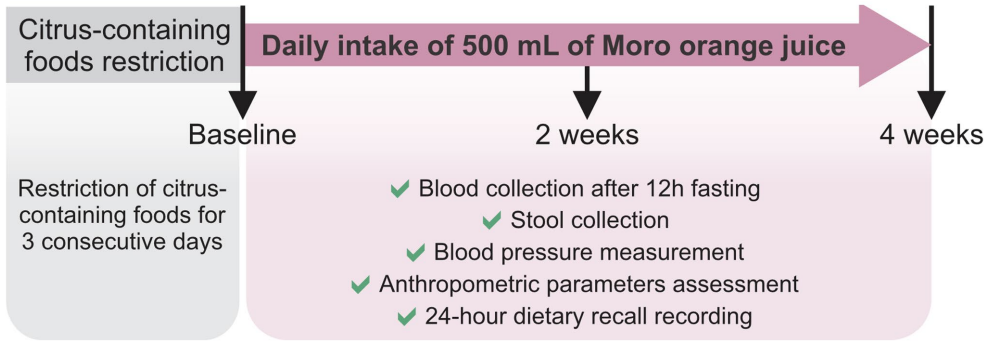

FIGURE 1
Study protocol. Twelve overweight women were selected to daily intake of 500 mL of Moro orange juice for 4 weeks. Blood and stool samples were obtained in baseline, and after 2 weeks and 4 weeks of the intervention. Blood pressure and anthropometric parameters were also measured in the same time points. Twenty-four-hour dietary recalls were recorded to food intake evaluation.

2.5. Characterization of cardiometabolic biomarkers

Plasma samples were obtained from the blood samples that were collected from the volunteers at baseline (A) and at the 2-week (B) and 4-week (C) time points of MOJ intake. Plasma samples were aliquoted and stored at −80°C until analyzes. Plasma samples were used to measure the levels of fasting glucose, insulin, total cholesterol, high-density lipoprotein (HDL), triglycerides, and inflammatory biomarkers such as C-reactive protein (CRP), interleukin 6 (IL-6), tumoral necrosis factor alpha (TNF-α), soluble vascular cellular adhesion molecule 1 (VCAM-1), soluble intercellular adhesion molecule 1 (ICAM-1), and lipopolysaccharide (LPS). Low-density lipoprotein (LDL) concentrations were calculated using the Friedewald equation (Friedewald et al., 1972). The value of 2.71 for the Homeostasis Model Assessment for Insulin Resistance (HOMA-IR) was considered as a cutoff for classifying subjects with insulin resistance and was based on a previous study on the Brazilian population (Geloneze and Tambascia, 2006).

2.6. Gut microbiota profiling

Fecal samples were collected by the volunteers on the day before each interview using the ColOff® (Stoll Collection Device; Zymo Research, CA, United States). The refrigerated samples were delivered to the laboratory, aliquoted in sterilized microtubes, and stored at−80°C until further analyzes.

The gut microbiota composition was evaluated by performing 16S rRNA gene sequencing analysis. Firstly, total DNA was extracted from the fecal samples using the QIAamp DNA Stool Mini kit (Qiagen, CA, United States) according to the manufacturer's instructions. DNA quantity was estimated by measuring the absorbance of the samples at 260 nm in a NanoDrop ND-1000 spectrophotometer (Thermo Scientific, MA, United States) and using the Qubit® dsDNA HS (High Sensitivity) Assay (Life Tecnologies, CA, United States).

The 16S rRNA gene library was prepared using the 16S Metagenomic Sequencing Library Preparation Kit (Illumina, CA, United States). The V4 region of the 16S rRNA gene (25 cycles) was amplified by polymerase chain reaction (PCR) using the following primer set: 341F (5'-TCGTCGGCAGCGTCAGATGTGTATAAGAGACAG-3′) and 785R (5'-GTCTCGTGGGCTCGGAGATGTGTATAAGAGACAG-3′) (Klindworth et al., 2013). The Illumina adapter was used to build the 16S sequence library according to the protocol provided by Illumina. AccuPrime Taq DNA Polymerase System (Life Technologies) was used for the PCR. The PCR protocol for amplifying 16S rDNA was as follows: denaturation for 2 min at 94°C; 25 cycles of denaturation for 30 s at 94°C, primer annealing for 30 s at 55°C, and extension for 1 min at 68°C; final maintenance of the PCR amplified samples at 4°C. PCR was performed in a Veriti PCR Thermal cycler (Applied Biosystems, CA, United States). The PCR products were cleaned up with 10 mM Tris pH 8.5, AMPure XP beads, and 80% ethanol followed by an index PCR using the 2x KAPA HiFi HotStart ReadyMix and Nextera XT index primers (N7XX and S5XX; Nextera XT Index kit, Illumina). The clean-up was repeated again using the same reagents. The amplicons were pooled and paired-end 250 sequencing with a density of 820 k·mm^{-2} was performed on the Illumina MiSeq (Illumina, CA, USA) using the Illumina MiSeq clamshell style cartridge kit V2 for 500 cycles.

Bioinformatics analysis was performed using the Brazilian Microbiome Project (BMP) pipeline (Pylro et al., 2014) that included a combination of the VSEARCH (Rognes et al., 2016) and QIIME (Caporaso et al., 2010) software. VSEARCH software was used to remove barcodes and primer sequences from the fastq file, filter sequences by length (fastq_trunclen 400) and quality (fastq_maxee 0.5), sort by abundance, and remove singletons. Subsequently, the Operational Taxonomic Units (OTUs) were clustered and the chimeras were removed. We generated a fastq file with filtered sequences and an OTU table in.txt. Taxonomy assignments for the OTUs were performed using the uclust method in the QIIME software (version 1.9.0) and the SILVA 16S Database (version n132) was used for the reference sequences (Quast et al., 2012). The OTU table file was then converted to BIOM, and taxonomy metadata was added. The sequences were aligned and filtered, and the phylogenetic tree was constructed. QIIME software was then used to calculate alpha and beta diversity. The nucleotide sequence data was reported in the NCBI database and is available under BioProject PRJNA508648.

2.7. Analysis of short-chain fatty acids

The analysis of SCFAs was performed as previously described (Menezes et al., 2010) with some modifications. Frozen fecal samples (500 mg) were extracted with 1.5 mL of acetonitrile that included 0.05% 2-methyl-valeric acid (internal standard) (Sigma-Aldrich, WI, United States) and 12% $HClO_4$, centrifuged at 11,000 × g for 20 min at 4°C, and filtered with the 0.2 μm PVDF filters (Millipore, MA, United States). The supernatants were injected (3 μL; split 1:10) into a Plus HP 6890 CG system (Hewlett-Packard, DE, United States) coupled to a flame ionization detector (FID) and a capillary-fused silica column (CP7747, Varian, CA, United States). The injector and FID temperatures were maintained at 270°C and 300°C, respectively. The analysis was performed using a temperature ramp from 115°C to 250°C (13 min) under constant pressure. Identification and quantification of the SCFAs was performed by comparing with a mixture of external standards (Volatile free acid mix, Supelco, PA, United States).

2.8. Statistical analysis

Statistical analyzes were performed using the GraphPad Prism software version 8.1.2 (GraphPad Prism software, California, United States) and the R statistical software (R Development Core Team, 2014). Normality of the data distribution was verified using the Kolmogorov–Smirnov test. The normally distributed data was analyzed using the analysis of variance (ANOVA) for repeated measurements and subsequently verified using the Tukey test. The non-normally distributed data was analyzed using the Friedman test.

The mean observed richness, Chao1, Shannon, Simpson, and Equitability values were compared between the groups using the Wilcoxon-Mann Whitney test (Fay and Proschan, 2010). A heatmap was constructed for the 20 most abundant OTUs using the Ward's hierarchical clustering method (ward. d2) (Murtagh and Legendre, 2014). Principal Coordinates Analysis (PCoA) was used to compare the similarities between samples, and the differences were estimated using the Permutational analysis of variance (PERMANOVA) (Anderson, 2001). The analyzes were performed with the R statistical software (R Development Core Team, 2014) using the qiimer, ggplot2 (Wickham, 2016), phyloseq (McMurdie and Holmes, 2013), and vegan (Oksanen et al., 2019) packages.

Spearman correlation analysis was performed to evaluate the association between changes in the cardiometabolic biomarkers and changes in the specific groups of bacteria in response to MOJ intake. $p < 0.05$ was considered as statistically significant.

3. Results

3.1. Characterization of Moro orange juice composition

Twelve overweight women (BMI 27.86 ± 0.41 kg/m^2) consumed 500 mL/day of blood orange juice (*Citrus sinensis* L. Osbeck var. Moro) for 4 weeks. The chemical composition of MOJ is presented in Supplementary Tables S1–S3. The concentrations of sucrose (14.00 ± 0.72 mg/500 mL) and citric acid (5.81 ± 0.23 g/500 mL) were highest among the soluble sugars (31.95 mg/500 mL) and organic acids (7.47 g/500 mL), respectively. The total dietary fiber content was 1.70 g/500 mL, including 0.40 ± 0.03 g/500 mL of soluble dietary fiber and 1.30 ± 0.06 g/500 mL of insoluble dietary fiber. The total concentration of flavonoids in the MOJ was 290.95 mg/500 mL including high concentrations of hesperidin (182.25 mg/500 mL) and narirutin (20.95 mg/500 mL). Cyanidin-3-*O*-glucoside (61.15 ± 8.80 mg/500 mL) as the main anthocyanin in the MOJ. Overall, our analysis showed that each study volunteer consumed 215.35 mg of flavanones and 75.60 mg of anthocyanins per day.

3.2. Moro orange juice intake alters specific OTUs of the gut microbiota composition

The relative abundance of OTUs was analyzed to evaluate the effects of the daily intake of MOJ on the gut microbiota profile. We obtained 5,735,751 sequences and 12,413 clustered OTUs with 97% similarity from the fecal samples of 12 overweight women after quality control and bioinformatics analysis. The number of sequences varied significantly between the samples and ranged from 42,445 to 269,320 sequences per sample. Therefore, all the samples were rarefied to 38,000 reads and were subjected to alpha and beta-diversity analysis.

The sequence analysis identified the following phyla: Bacteroidetes (52.5%), Firmicutes (40.6%), Proteobacteria (3.5%), Actinobacteria (0.7%), and Verrucomicrobia (0.4%). *Bacteroides* (37.9%) was the most abundant genera followed by *Prevotella 9* (5.3%), *Faecalibacterium* (4.9%), *Alistipes* (3.0%), *Ruminococcaceae UCG-002* (2.8%), and *Phascolarctobacterium* (2.6%) (Figure 2). We observed significant variability in the microbial communities between the volunteers (Supplementary Figure S1). Therefore, we selected three most abundant OTUs and compared their microbiota profiles throughout the intervention. Two of the three OTUs belonged to *Bacteroides* (OTU1 and OTU2) whereas OTU3 belonged to the *Prevotella 9* (Figure 3). These three OTUs represented 21.4% (OTU1: 8%; OTU2: 10.1%; OTU3: 3.3%) of the total microbial communities. In summary, gut microbiota profiles of 9 volunteers were similar, and showed high relative abundance of OTU1, low abundance of OTU3, and variable abundance of OTU2. The gut microbiota profiles of the remaining three volunteers (S02, S21, and S22) showed variations from this pattern. The gut microbiota profile of volunteer S22 showed similar pattern at baseline but higher OTU3 abundance after 4 weeks of MOJ intake, whereas the gut microbiota profiles of the remaining 2 volunteers (S02 and S21) showed higher abundance of OTU3 and lower abundance of OTU1 throughout the intervention.

Alpha-diversity analysis showed that the number of gut microbial species ranged from 312 to 2,752 (Supplementary Table S6). Chao1 index ranged from 418 to 4,005 species for the study samples; Shannon index of species diversity ranged from 3.54 to 8.17; and the Simpson diversity index ranged from 0.77 to 0.99. We did not observe significant differences in alpha-diversity between the gut microbiota profiles at baseline (A) and at 2-weeks (B) and 4-weeks (C) after MOJ intake (Supplementary Table S6). Beta-diversity also showed high stability of the gut microbiota composition in each volunteer throughout the intervention. This suggested that the 4-week timeline of MOJ intake (500 mL) may not have been sufficient to assess changes in the gut microbiota diversity, based on the metrics used in this study which are shown in Supplementary Figures S2, S3.

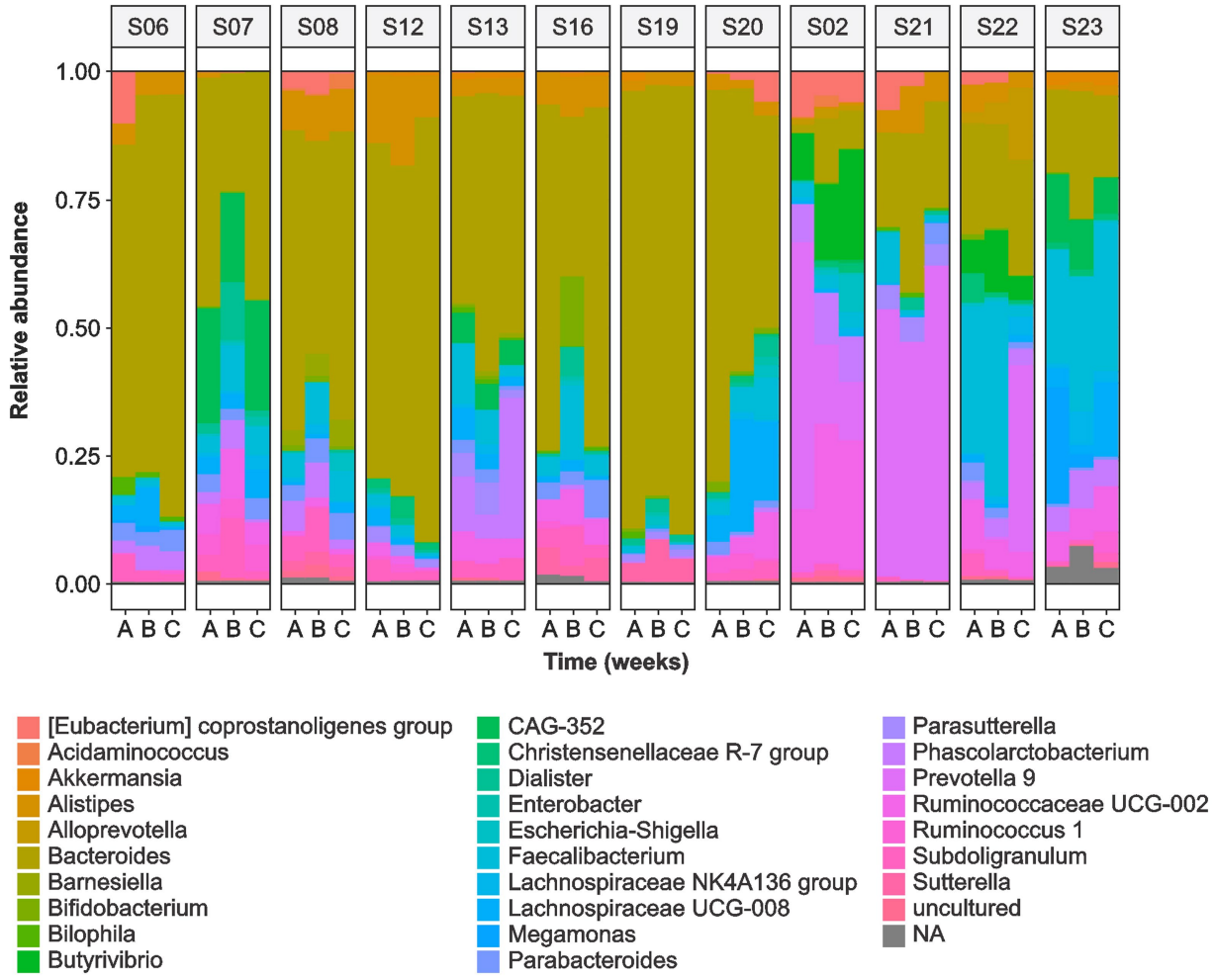

FIGURE 2
Relative abundance of the top 60 gut microbiota genera in the fecal samples of 12 overweight women at baseline **(A)**, at 2-weeks **(B)** and 4 weeks **(C)** of daily blood orange juice intake.

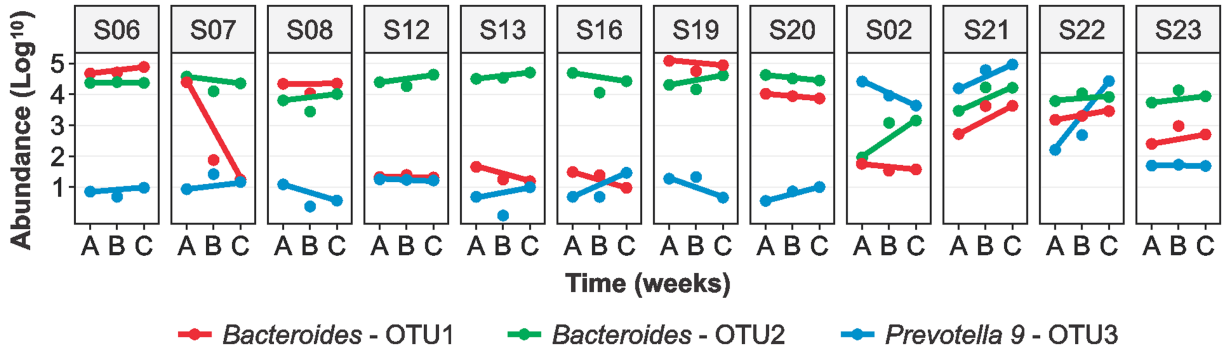

FIGURE 3
Logarithmic (log10) abundance of the top 3 OTUs in fecal samples of the 12 overweight women at baseline **(A)**, at 2-weeks **(B)** and 4-weeks **(C)** of daily blood orange juice intake. OTU: Operational Taxonomic Unit.

Procrustes analysis was performed using weighted UniFrac distance matrix and PCoA ordination and the gut microbiota communities was clustered into two groups during all the time points of the experiment. Procrustes analysis between ordinations from samples A (baseline) and B (2 weeks), and samples B and C (4 weeks) showed significant differences ($p = 0.001$ and 0.001, respectively). The samples with high abundance of *Bacteroides* and *Prevotella* were clustered in Group 1 (red) and Group 2 (blue), respectively. The

samples clustered in Group 1 tended to remain within the same group at both A and B time points (Supplementary Figure 3A). However, samples in Group 2 showed variations at different time points. Volunteers 2 and 21 remained in Group 2, whereas volunteers S22 and S23 changed from Group 2 to Group 1 (red arrows). Similar results were observed between time points B to C. However, volunteer S22 changed from Group 1 to Group 2 between time points B to C (Supplementary Figure 3B).

3.3. Moro orange juice intake significantly alters metabolism of the gut microbiota

The intake of MOJ did not significantly alter the gut microbiota composition in the study volunteers but affected metabolism of the gut microbiota as evidenced by the changes in the concentrations of SCFAs in the fecal samples. The levels of SCFAs including acetic acid, propionic acid, butyric acid, isobutyric acid, isovaleric acid, valeric acid, and hexanoic acid in the fecal samples at baseline and at 2-weeks and 4-weeks after MOJ intake is shown in Table 1. Acetic acid, propionic acid, and butyric acid were the most abundant SCFAs (74.5%) in the fecal samples. MOJ intake increased the levels of all SCFAs except for hexanoic acid. The concentration of acetic acid in the fecal samples increased at 2 weeks compared to the baseline but was restored to baseline levels at 4-weeks after intake of MOJ. The levels of propanoic acid and isobutyric acid were significantly higher in the 4-week time interval of the MOJ intake compared to the baseline ($p < 0.05$). The levels of other SCFAs also increased after MOJ intake but did not show statistically significant differences when compared with the baseline concentrations. Furthermore, the total SCFAs levels were elevated in the fecal samples after MOJ intake but did not show statistically significant differences when compared with the baseline concentrations.

3.4. Moro orange juice intake alters anthropometric parameters and levels of few cardiometabolic biomarkers

Recent studies reported that changes in the gut microbiota composition are associated with metabolic changes in the human body including body composition parameters and cardiometabolic biomarkers in response to specific changes in the gut microbiota (Lima et al., 2019; Fidélix et al., 2020; Kahleova et al., 2020; Asnicar et al., 2021).

In this study, we analyzed anthropometric parameters, cardiometabolic biomarkers, and consumption of food nutrients (R24h) at baseline and at 2-weeks and 4-weeks of MOJ intake. The daily intake of energy, macronutrients, and micronutrients were comparable between the baseline and the intervention time-points ($p > 0.05$), but we observed changes in the intake of dietary fiber, vitamin C, and potassium (Supplementary Table S7). The dietary fiber levels were significantly reduced at 4 weeks of MOJ intake compared to the baseline (20.26 ± 2.70 to 13.51 ± 1.52 g/100 g; $p = 0.039$), whereas we observed significant increase in the levels of vitamin C (66.55 ± 27.95 to 278.13 ± 18.55 mg/100 g; $p < 0.001$) and potassium (2.26 ± 0.23 to 2.82 ± 0.11 g/100 g; $p = 0.039$) at 2 weeks of MOJ intake compared to the baseline.

The effects of MOJ intake for 4 weeks on the anthropometric variables and the cardiometabolic biomarkers are shown in Table 2.

We observed significant reduction ($p = 0.02$) in the diastolic blood pressure (DBP) after 2 weeks of MOJ intake (73.08 ± 2.35 to 69.25 ± 2.77 mmHg) and this effect was maintained at the 4-week time point. We also observed reduced systolic blood pressure (SBP) at 2-weeks and 4-weeks of MOJ intake compared to the baseline (118.67 ± 2.55 to 113.83 ± 4.42 mmHg), but the differences were not statistically significant. MOJ intake also reduced the levels of biomarkers of the glucose and lipid metabolism, but the differences were not significant because of large variations in the values between the study volunteers. The intake of MOJ reduced the levels of plasma glucose and insulin from 79.58 ± 3.36 to 74.75 ± 3.36 mg/dL and from 17.05 ± 1.96 to 14.21 ± 1.22 μUI/mL, respectively ($p > 0.05$). HOMA-IR values also reduced from 3.43 ± 0.52 at baseline to 2.56 ± 0.17 at the 4-week MOJ intake time points ($p > 0.05$).

Based on the HOMA-IR values, 8 out of 12 volunteers showed insulin resistance and 4 showed normal insulin sensitivity. We assessed the effects of MOJ intake on the insulin resistance by comparing the fasting glucose, fasting insulin and HOMA-IR values in the volunteers with or without insulin resistance (Figure 4). Furthermore, we analyzed the effects of the MOJ intake on the SBP and DBP values in the normal and the insulin-resistant women. The intake of MOJ reduced the HOMA-IR (from 4.12 ± 0.65 to 2.62 ± 0.24, $p = 0.012$) and DBP (from 72.13 ± 3.32 to 68.38 ± 2.01 mmHg, $p = 0.026$) in women with insulin resistance. Women without insulin resistance did not show any

TABLE 1 Effect of blood orange juice intake on the levels of short-chain fatty acids in the fecal samples.

Fecal SCFAs (μmol/g)	Baseline	2 weeks	4 weeks	Value of *p*
Acetic acid	11.01 ± 1.22	12.25 ± 0.94	11.51 ± 0.85	0.338
Propionic acid	**5.23 ± 0.47^{b}**	**6.55 ± 0.81^{ab}**	**6.60 ± 0.52^{a}**	**0.028**
Butyric acid	7.01 ± 1.18	9.67 ± 1.71	9.33 ± 1.38	0.264
Isobutyric acid	**1.75 ± 0.15^{b}**	**2.26 ± 0.27^{ab}**	**2.46 ± 0.27^{a}**	**0.019**
Valeric acid	2.08 ± 0.15	2.35 ± 0.18	2.43 ± 0.19	0.076
Isovaleric acid	2.42 ± 0.26	3.15 ± 0.44	3.03 ± 0.43	0.264
Hexanoic acid	1.80 ± 0.20	1.66 ± 0.16	1.71 ± 0.17	0.517
Total SCFAs	31.29 ± 2.88	37.90 ± 3.40	37.07 ± 3.04	0.205

Results are expressed as the mean ± standard error. The value of *p*s were calculated using the Friedman test. Values in bold and different superscript letters indicate statistical significance ($p < 0.05$) among values obtained in the baseline and after 2 and 4 weeks of blood orange juice intake.

TABLE 2 Anthropometric, biochemical, and cardiometabolic biomarkers of overweight women at baseline and at 2-week and 4-week time points during the intake of blood orange juice.

Variables	Baseline	2 weeks	4 weeks	Value of *p*
Body weight (kg)	73.65 ± 6.36	73.88 ± 6.37	73.99 ± 6.69	0.722
BMI (kg/m^2)	27.86 ± 0.41	27.95 ± 0.45	27.99 ± 0.52	0.938
Abdominal circumference (cm)	90.00 ± 1.55	88.75 ± 1.50	88.92 ± 1.51	0.741
Blood pressure (mmHg)				
Systolic	118.67 ± 2.55	113.92 ± 3.93	113.83 ± 4.42	0.338
Diastolic	**73.08 ± 2.35^a**	**69.25 ± 2.77^b**	**69.25 ± 1.89^b**	**0.020**
Glucose (mg/dL)	79.58 ± 3.36	75.08 ± 2.40	74.75 ± 3.36	0.537
Insulin (μUI/mL)	17.05 ± 1.96	15.25 ± 1.37	14.21 ± 1.22	0.558
HOMA-IR	3.43 ± 0.52	2.83 ± 0.27	2.56 ± 0.17	0.338
Cholesterol (mg/dL)				
HDL	50.08 ± 4.39	47.75 ± 3.42	49.83 ± 4.44	0.112
LDL	70.83 ± 6.97	76.17 ± 8.03	78.50 ± 6.36	0.338
Total	138.42 ± 9.32	144.08 ± 9.77	150.50 ± 9.02	0.717
Triglycerides (mg/dL)	88.00 ± 10.91	100.67 ± 13.67	104.75 ± 15.31	0.205
C-reactive protein (mg/dL)	2.23 ± 0.38	2.84 ± 0.57	2.20 ± 0.49	0.405
TNF-α (pg/mL)	3.10 ± 0.12	3.12 ± 0.13	3.10 ± 0.12	0.723
IL-6 (pg/mL)	3.95 ± 0.67	3.96 ± 0.72	4.15 ± 0.76	0.236
IL-10 (pg/mL)	3.83 ± 0.19	3.88 ± 0.23	3.92 ± 0.18	0.976
VCAM-1 (ng/mL)	**554.99 ± 15.63^a**	**553.62 ± 14.31^{ab}**	**545.31 ± 14.65^b**	**0.039**
ICAM-1 (ng/mL)	367.57 ± 25.73	353.73 ± 28.89	349.34 ± 27.69	0.920
Fibrinogen (mg/dL)	301.17 ± 23.91	273.33 ± 21.25	297.75 ± 26.81	0.205
LPS (EU/mL)	0.07 ± 0.00	0.08 ± 0.01	0.07 ± 0.00	0.875

BMI, body mass index; HOMA-IR, Homeostasis model assessment for insulin resistance; HDL, high-density lipoprotein; LDL, low-density lipoprotein; TNF-α, tumor necrosis factor-alpha; IL, interleukin; VCAM-1, vascular cellular adhesion molecule 1; ICAM-1, intercellular adhesion molecule 1; LPS, lipopolysaccharide. The *p*-values were calculated using the Friedman test. Values in bold and different superscript letters indicate statistical significance ($p < 0.05$) among values ($n = 12$) obtained in the baseline and after 2 and 4 weeks of blood orange juice intake.

significant changes in the cardiometabolic biomarkers. Furthermore, in the women with insulin resistance, intake of MOJ for 4 weeks reduced the plasma VCAM-1 levels (554.99 ± 15.63 to 545.31 ± 14.65 ng·mL^{-1}, $p = 0.039$) but the plasma levels of ICAM-1, C-reactive protein, TNF-α, IL-6, and IL-10 were not significantly altered.

3.5. Cardiometabolic biomarkers show significant correlation with specific gut microbiota OTUs

We performed Spearman's correlation analysis to determine the association between the levels of cardiometabolic biomarkers and the gut microbiota OTUs, and the results are shown in Figures 5, 6. In general, OTUs classified within the Firmicutes and Bacteroidetes phyla showed negative correlations with the levels of IL-10, TNF-α, LPS, and propionic acid at the 2-week time-point during MOJ intake. Furthermore, at this time-point, only one OTU in the Firmicutes showed positive correlation with the IL-6 levels. In contrast, correlational analysis showed only positive associations between OTUs in the Firmicutes and Bacteroidetes and levels of the cardiometabolic biomarkers. Furthermore, Proteobacteria and Lentisphaerae showed positive correlations with the IL-10 levels at the 4-week time-point during MOJ intake (Figure 5).

At the genera level (Figure 6), *Bacteroides* showed positive correlations and *Prevotella 9* showed negative correlations with the levels of SCFAs (propionic and hexanoic acids), insulin, HOMA-IR, IL-6, and IL-10 at the 2-and 4-week time-points during MOJ intake. We also observed correlations between other bacterial genera and specific biomarkers measured in this study. The genus *Lachnoclostridium* showed positive correlation ($p < 0.05$) with the levels of propionic acid and negative correlation with HOMA-IR at the 4-week time-point of MOJ intake. Furthermore, the genus *Ruminococcaceae UCG-014* showed significant negative correlation with insulin levels and HOMA-IR at the 4-week time-point of MOJ intake, whereas *Ruminococcaceae UCG-002*, *Ruminococcaceae UCG-003*, and *Ruminococcaceae UCG-005* showed negative correlation with the plasma IL-6 levels.

4. Discussion

Blood orange juice is an important source of anthocyanins and flavanones such as hesperidin and naringin. The benefits of these bioactive compounds are well known but the mechanisms of action underlying their biological effects are not well established. The bioavailability and beneficial effects of orange juice flavonoids are significantly influenced by their chemical structure, food matrix

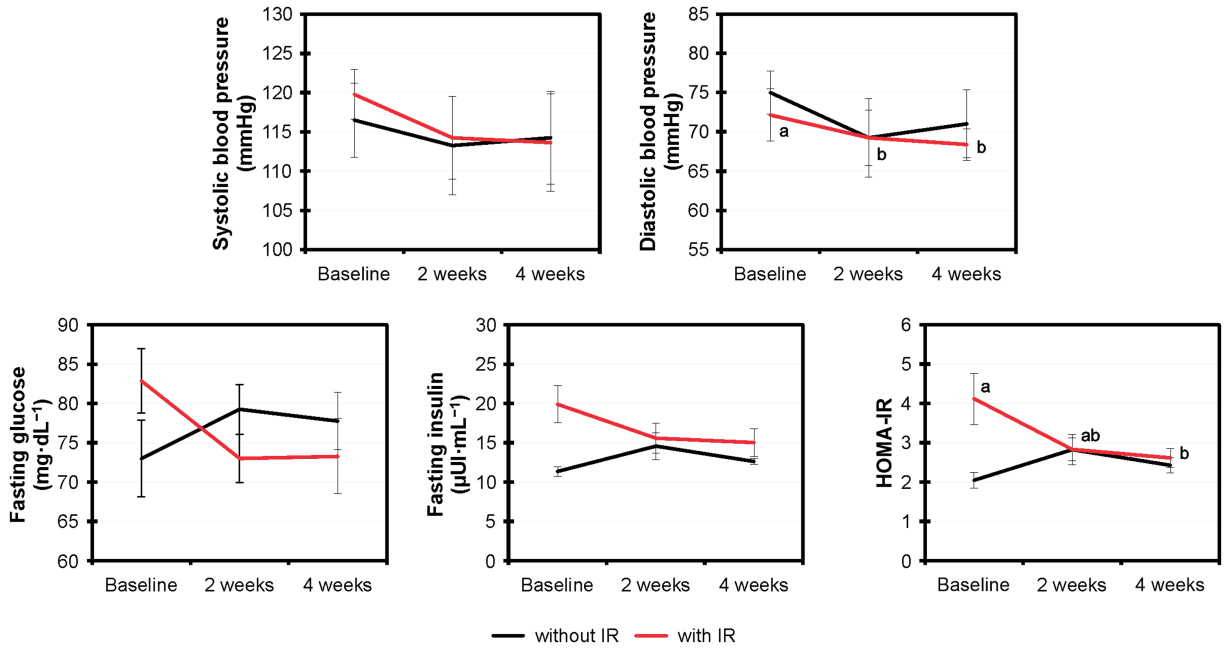

FIGURE 4
Comparative variation of the systolic and diastolic blood pressure, fasting glucose and fasting insulin levels, and HOMA-IR values in the overweight women with (n=8) and without (n=4) insulin resistance that drank Moro orange juice (500 mL per day) for 4 weeks. Different superscript letters indicate statistical significance calculated using the Friedman test (p<0.05) by comparing the experimental values (n=12) at baseline and those at 2-weeks and 4-weeks of Moro orange juice intake. HOMA-IR, Homeostasis model assessment for insulin resistance.

effects, and composition of the host gut microbiota. Hesperidin and naringin are resistant to enzymatic breakdown in the stomach and the small intestine (Mas-Capdevila et al., 2020). In the colon, these flavanones are broken down by the α-rhamnosidases and β-glucosidases secreted by the gut microbiota and are converted into aglycones, hesperetin and naringenin. Aglycones are then absorbed through the intestinal epithelium or further metabolized into phenolic acids by bacterial enzymes (Mas-Capdevila et al., 2020). The two-way interaction between the flavonoids and the gut microbiota improves metabolism and reduces the risk of cardiometabolic diseases. Gut microbiota enhance the bioavailability and bioactivity of the dietary flavonoids through enzymatic metabolism. On the other hand, flavonoids act as prebiotics altering the gut microbiota composition and activity. Flavonoids suppress the growth of pathobionts and promote the growth of commensals (Corrêa et al., 2019). Recent studies have shown that flavonoids from orange juice alter the composition and activity of the gut microbiota (Stevens et al., 2019; Fidélix et al., 2020; Mas-Capdevila et al., 2020; Santana et al., 2022). The present study aimed to evaluate the effects of MOJ on the gut microbiota composition and the cardiometabolic biomarkers in overweight women.

Several recent studies have investigated the benefits of blood orange juice intake, especially of the Moro variety (Dorna et al., 2021; Nishioka et al., 2021; Ribeiro et al., 2021; Briskey et al., 2022; Santana et al., 2022; Capetini et al., 2023). However, the effects of MOJ on the gut microbiota profiles have not been investigated in detail. Nishioka et al. (2021) performed a clinical trial with MOJ by analyzing the gut microbiota composition, but stratified the volunteers based on the fecal profile of the flavanones. Santana et al. (2022) performed a randomized crossover study with obese patients that consumed 'Pera' orange juice (POJ) or MOJ and reported improved gut microbiota profile (initially with obesity-associated alterations) after 15 days. The improvements were significantly higher for patients who consumed MOJ than those who consumed POJ, especially in patients with higher obesity classes. The authors reported significant effects of MOJ on the gut microbiota and on several oxidative stress and inflammatory response biomarkers but did not clearly define the association between bacterial OTUs and the biomarker levels. This is the first study to report the correlation between the gut microbiota composition and the cardiometabolic biomarkers.

Gut microbiota belonged predominantly to the Bacteroidetes and Firmicutes phyla, with the *Bacteroides* genera being the most prevalent. The Firmicutes/Bacteroidetes (F/B) ratio did not change significantly throughout the study. A higher F/B ratio are positive correlated with the development of obesity and insulin resistance in overweight subjects (Liu et al., 2021). A similar profile was reported in our previous studies (Nishioka et al., 2021; Santana et al., 2022). However, these studies did not identify *Prevotella 9* as the predominant OTU. We did not classify the bacterial OTUs at the species level. However, previous studies showed that *Bacteroides dorei* and *B. vulgatus*, which belong to the phylum Bacteroidetes, are depleted in subjects with obesity. These species play an important role in maintaining a healthy gut ecosystem, protecting role against atherosclerosis, and reducing LPS activity (Yoshida et al., 2021). Yoshida et al. (2021) also showed that these species promote the catabolism of branched-chain amino acids (BCAAs), protecting against obesity. Moreover, some species of *Bacteroides* including *B. ovatus*, *B. fragilis*, *B. distasonis*, and *B. uniformis* are involved in polyphenol metabolism (*O*-deglycosylation) (Braune and Blaut, 2016; Cortés-Martín et al., 2020). *O*-deglycosylation by human gut bacteria

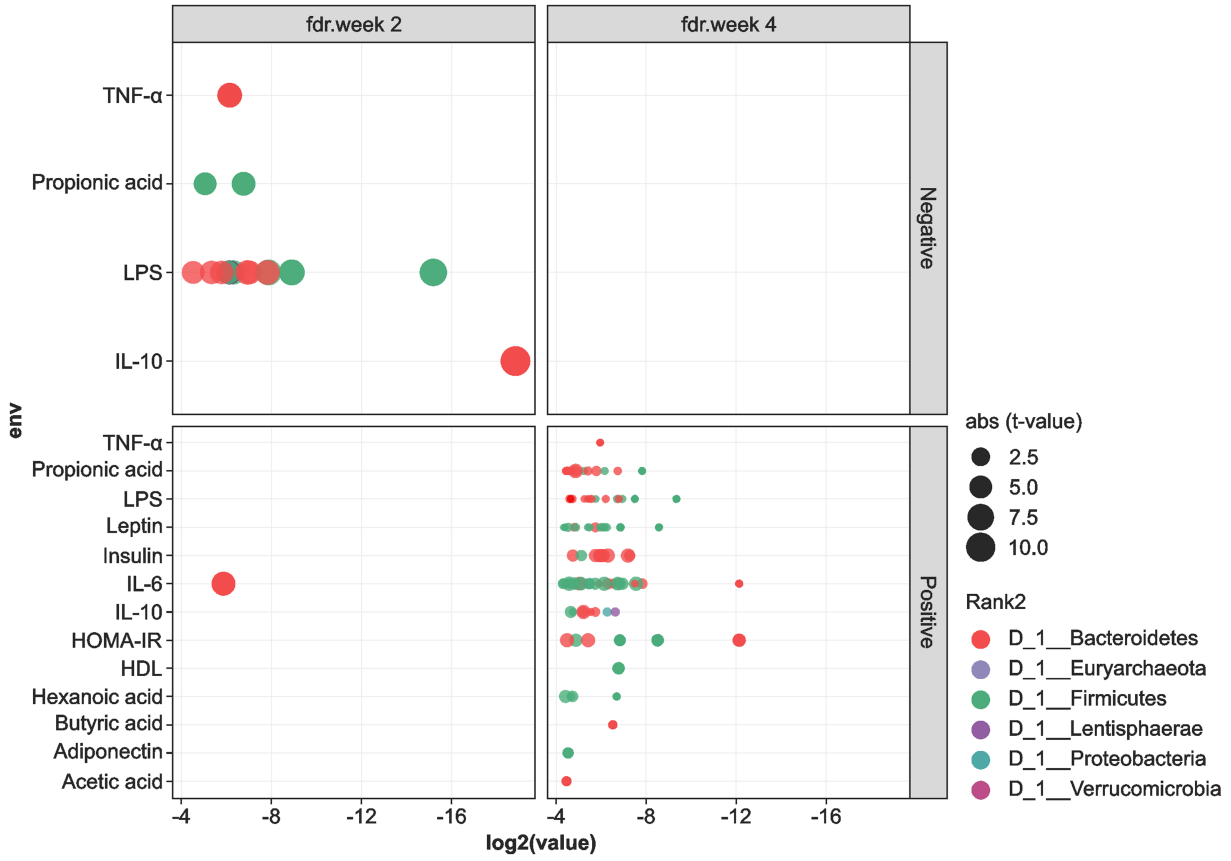

FIGURE 5
Correlation between cardiometabolic parameters and the 6 most abundant phyla in the fecal samples of the 12 overweight women volunteers that drank Moro orange juice (500mL per day) for 4 weeks. BMI, body mass index; HOMA-IR, Homeostasis model assessment for insulin resistance; HDL, high-density lipoprotein; LDL, low-density lipoprotein; CRP, C-reactive protein; TNF-α, tumor necrosis factor alpha; IL, interleukin; VCAM-1, vascular cellular adhesion molecule 1; ICAM-1, intercellular adhesion molecule 1; LPS, lipopolysaccharide.

is attributed to the activity of a specific *Parabacteroides* species, namely *P. distasonis*. Two *Parabacteroides* OTUs in the fecal samples showed significant correlation with the levels of propionic acid (Al-Ishaq et al., 2021). In contrast, none of the known *Prevotella* species have been reported to play a role in flavonoid metabolism. However, the abundance of *Prevotella* is strongly associated with plant-based diets, rich in fiber, and *Prevotella copri* is considered an important biomarker for diet (Precup and Vodnar, 2019).

Subjects with obesity generally have lower gut microbiota diversity and richness than the lean subjects (Liu et al., 2021). Low microbiota richness is associated with dyslipidemia, fat storage, insulin resistance, and inflammation (Lin et al., 2023). As well as in obesity, in prediabetes, gut microbiota composition is altered and exhibits reduced bacterial richness and reduced bacterial butyrate producers and increased species with a pro-inflammatory potential (Fan and Pedersen, 2021). Significant changes in gut microbiota composition were not observed in overweight women after 4 weeks of MOJ intake. However, significant correlations were identified between specific OTUs and cardiometabolic biomarkers, thereby highlighting the role of the gut microbiota on flavanone metabolism, and the health benefits of MOJ. MOJ intake did not significantly alter the gut microbiota diversity but increased the production of SCFAs, especially propionic acid and isobutyric acid, and induced significant improvements in several cardiometabolic biomarkers such as DBP and VCAM-1. Furthermore, *Bacteroides* and *Prevotella 9* and other specific OTUs showed positive and negative correlations with several biomarkers including SCFAs, insulin, HOMA-IR, IL-6, and IL-10. SCFAs modulate CVD risk factors by regulating appetite and improving systolic and diastolic pressure, glucose and lipid homeostasis, adiposity and inflammation. SCFAs maintain epithelium integrity and restore gut barrier function preventing the translocation of LPS. Furthermore, SCFAs induce the production of mucin which creates a physical barrier between luminal bacteria and epithelial cells (Chambers et al., 2018). SCFAs bind to G-protein-coupled receptor (GPR) 41 and GPR 43 enhancing the release of anorexigenic peptides glucagon-like peptide-1 (GLP-1) and peptide YY (PYY) from enteroendocrine cells. GLP-1 and PYY contribute to satiety, reduction of plasma glucose and lipids, insulin resistance and inflammation, and increased lipid oxidation (Van Hul and Cani, 2023). A differential association of OTUs classified under the same bacterial genus with the same biomarkers was observed. This highlighted complexity of the gut microbiota response to the orange juice intake. Moreover, although some associations were evident within 2 weeks of MOJ intake, they became significant only at the end of the intervention (4 weeks). This suggested that the changes in the OTUs in response to the

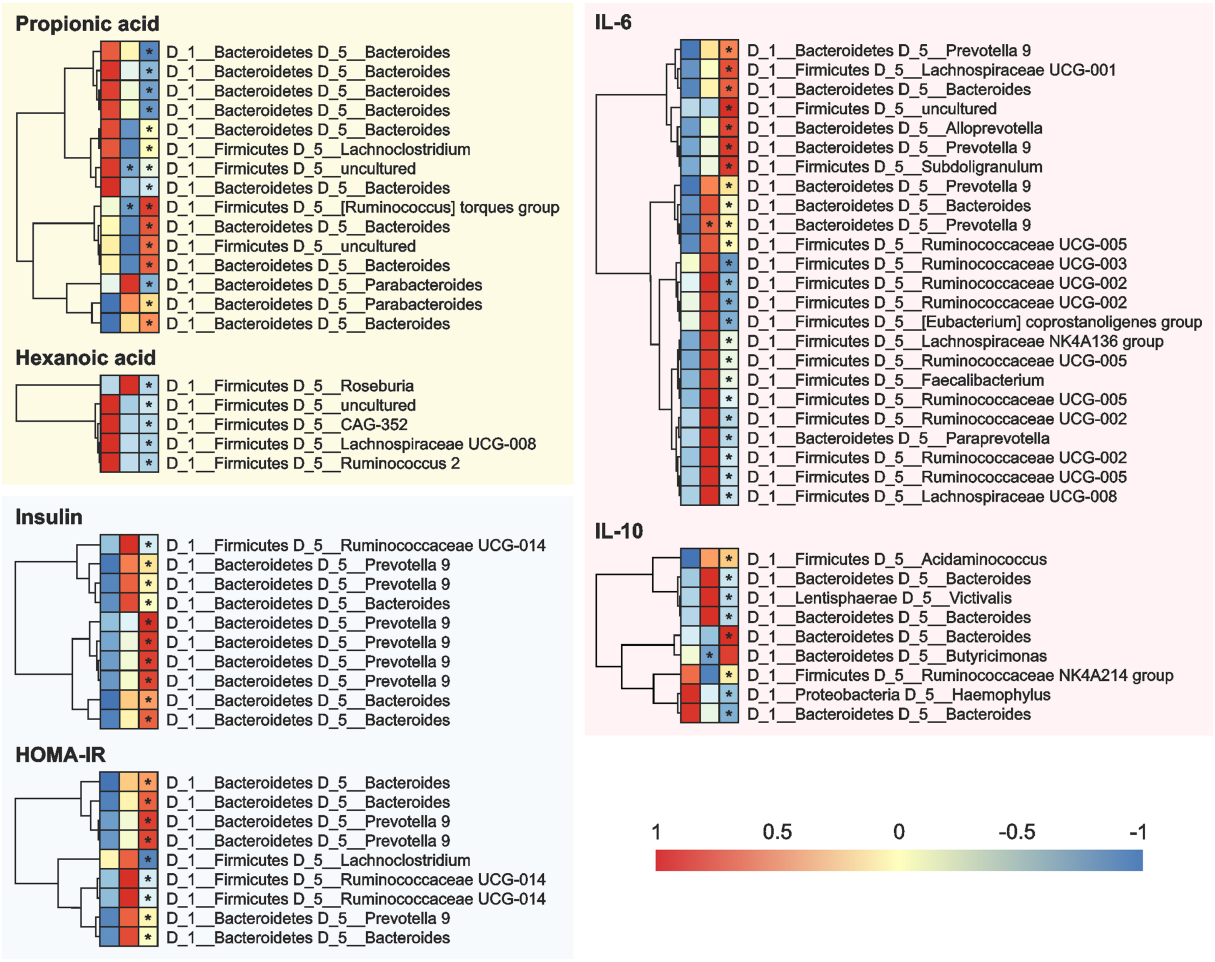

FIGURE 6
Correlation between the cardiometabolic parameters and the OTUs in the fecal samples of the 12 overweight women volunteers that drank Moro orange juice (500mL per day) for 4 weeks. A=Baseline, B=2 weeks, and C=4 weeks. OUT, Operational Taxonomic Unit; HOMA-IR, Homeostasis model assessment for insulin resistance; IL, interleukin.

constituents of the MOJ were not instantaneous but occurred gradually over a longer period of time.

MOJ intake significantly reduced DBP in the overweight women. This was consistent with the previous findings in eutrophic and overweight adults (Fraga et al., 2021) and obese adults (Santana et al., 2022; Santos et al., 2022) after Pera orange juice and MOJ intake. The relative risk of all the major CVD is significantly reduced by a reduction of 5 mmHg in DBP (Zanchetti, 2016). It is plausible that hesperidin exerts antihypertensive effects through the vascular nitric oxide (NO) synthase pathway. A previous study reported that hesperidin and its metabolites enhance NO bioavailability and protect the endothelial function by reducing the levels of the reactive oxygen species (Mas-Capdevila et al., 2020). DBP improvement may also be associated with the metabolic products of citrus flavanones such as flavanones-phase II conjugates and the phenolic acids, which are generated by the gut bacteria (Fraga et al., 2021). The flavanone composition of MOJ is comparable to that of POJ. Therefore, the health benefits of MOJ intake in the overweight women volunteers in this study may be attributed to the hesperidin and naringin metabolites.

The reduced levels of plasma VCAM-1 after MOJ intake suggested that the bioactive compounds from the MOJ reduced cardiometabolic risk by targeting the endothelium. Anthocyanins in MOJ (75.60 mg/500 mL) are metabolized by the gut microbiota and their metabolites are potentially responsible for the beneficial effects on the endothelium (Hidalgo et al., 2012; Kuntz et al., 2015; Krga and Milenkovic, 2019). A recent systematic review and meta-analysis reported that hesperidin significantly reduced the levels of VCAM-1 but did not alter the circulating E-selectin, IL-6, and ICAM-1 levels (Lorzadeh et al., 2019) similar to our findings.

The reduction in the cardiometabolic biomarkers was significantly higher in the insulin resistant women, similarly to the findings of Santana et al. (2022). This suggested significantly higher health benefits of regular MOJ intake for individuals with insulin resistance. The comparison of the effects of MOJ intake in women with or without insulin resistance showed the beneficial effects of MOJ on the cardiometabolic disorder including reduced levels of glucose, insulin, and HOMA-IR, as well as greater reduction of SBP and DBP in the insulin-resistant women. As observed in the correlation analyzes, some changes (as in blood pressure parameters) were significant at the

2-week time-point of the MOJ intake, whereas other parameters were significant only after 4 weeks. This highlighted the importance of the intake duration. Silveira et al. (2015) reported similar results in eutrophic and overweight volunteers who consumed 750 mL daily of blood orange juice for 8 weeks. The blood orange juice intake enhanced insulin sensitivity and reduced total cholesterol and LDL levels as well as SBP and DBP.

Gut microbiota is involved in the regulation of energy homeostasis, control of body weight, and inflammation. The changed microbiota composition in overweight subjects extracts more energy from the diet and increases lipogenesis. This microbiota provides lipogenic substrates to the liver and increases the lipoprotein lipase activity, as a consequence of the Fasting-Induced Adipose Factor (FIAF) suppression in the gut. Consequently, fatty acids and triacylglycerol are released from circulating lipoprotein in muscle, and adipose tissue, increasing the adiposity and body weight gain. This microbiota can also reduce the AMP-activated protein kinase (AMPK) activation and fatty acid oxidation (Kobyliak et al., 2016). Although the literature reports increasing in weight gain and adiposity, we did not observe significant change in anthropometric parameters throughout the study. Briskey et al. (2022) and Cardile et al. (2015) showed significant reduction of body mass, BMI, hip and waist circumferences, fat mass, and fat distribution in overweight adults however these studies used Moro orange extract daily for 3 or 6 months. As in these studies, we also observed significant changes in the cardiometabolic markers in response to MOJ intake, especially in women with insulin resistance. This can also be easily explained by the ability of the bioactive compounds in the MOJ to regulate metabolism (Lima and Barbosa, 2021).

Recent studies have identified novel polymorphisms (Fraga et al., 2022) and microRNAs (Dorna et al., 2021; Quintanilha et al., 2022; Capetini et al., 2023), which regulate cellular processes and mechanisms that are associated with the benefits of orange juice intake. This is one of the few studies that has evaluated the effects of MOJ on the gut microbiota composition and is the first study to report the correlation between the gut microbiota composition and the cardiometabolic biomarkers. Our results showed that specific OTUs play a significant role in the cardiometabolic disease process.

The main limitation of this study was small sample size (12 volunteers). Although we observed clear correlation between several biomarkers and bacterial OTUs, there were large variations in the gut microbiota composition between individuals. This may have affected the significance of several responses and limited the identification of some effects of MOJ intake. Therefore, future studies with larger sample sizes are required to confirm our findings, improve the gut microbiota results, and further explore the benefits associated with MOJ intake.

5. Conclusion

In conclusion, MOJ intake had effects on specific OTUs, although significant changes in the gut microbiota composition of overweight women were not observed. MOJ intake increased the production of SCFAs, especially propanoic and isobutyric acids, and improved cardiometabolic biomarkers such as DBP and plasma VCAM-1. The gut microbiota was associated with the levels of SCFAs and cardiometabolic biomarkers. Positive and negative correlations were observed between specific gut microbiota OTUs belonging to the *Bacteroides* and *Prevotella 9* genera, and the cardiometabolic biomarkers at 2-weeks and 4-weeks of MOJ intake. This shows that the gut microbiota played a significant role in flavanone metabolism and influenced the biological processes responsible for the health benefits of MOJ intake.

Finally, the improvements in the cardiometabolic biomarkers were significantly higher in insulin-resistant women including a significant improvement in insulin resistance. The MOJ intake time was important since some changes were significant after 2 weeks of MOJ intake, but others became significant only after 4 weeks. However, future studies are required to confirm our findings and investigate further the effects of MOJ on the gut microbiota and the role of gut microbiota in the health benefits of orange juice.

Data availability statement

The datasets presented in this study can be found in online repositories. The names of the repository/repositories and accession number(s) can be found at: https://www.ncbi.nlm.nih.gov/, PRJNA508648.

Ethics statement

The studies involving human participants were reviewed and approved by School of Public Health, University of São Paulo (CAAE 69382217.9.0000.5421), and was registered at the Brazilian Registry of Clinical Trials (UTN: U1111-1241-4665). The patients/participants provided their written informed consent to participate in this study.

Author contributions

FL, NH, MR, CT, and CH: conceptualization. TC, BQ, and VC: investigation and formal analysis. TC and ECT: data curation. TC, BQ, VC, and RC: methodology. FL, NH, and MR: resources. FL: supervision. TC and ET: writing–original draft. TC, ET, NH, FL, MR, and RC: writing–review and editing. All the authors have read and agreed to the published version of the manuscript.

Funding

This research was funded by the National Council for Scientific and Technological Development (CNPq) (Grant No. 434713/2018–0) and the São Paulo Research Foundation (FAPESP) (Grant No. 2013/07914–8). The authors are grateful for the scholarships provided by the FAPESP (Grant No. 2020/06467–1) and the CNPq (Grant No. 153624/2018–3).

Acknowledgments

The authors thank all the study volunteers and Fundecitrus for providing the orange juice used in this study. They also thank the

GENIAL (Genome Investigation and Analysis Laboratory) facility for sequencing the gut microbiome; Luciano Lopes Queiroz for performing biostatistical analyzes of gut microbiome data; Luana Moreira for collaborating to obtain the libraries; Geni Sampaio for collaborating to analyze the SCFAs; and Elizabeth Torres for providing the gas chromatography set-up.

Conflict of interest

The authors declare that the research was conducted in the absence of any commercial or financial relationships that could be construed as a potential conflict of interest.

Publisher's note

Supplementary material

The Supplementary material for this article can be found online at: https://www.frontiersin.org/articles/10.3389/fmicb.2023.1199383/full#supplementary-material

References

Al-Ishaq, R. K., Liskova, A., Kubatka, P., and Büsselberg, D. (2021). Enzymatic metabolism of flavonoids by gut microbiota and its impact on gastrointestinal Cancer. *Cancers* 13:3934. doi: 10.3390/cancers13163934

Al-Okbi, S. Y., Mohamed, D. A., Abd-Elhady, E. E., Hussein, A. M. S., and Al-Siedy, E. S. K. (2018). Comparative study of Orange and its Main bioactive constituents as remedy for non-alcoholic fatty liver in rats. *Pak. J. Biol. Sci.* 21, 359–368. doi: 10.3923/pjbs.2018.359.368

Anderson, M. J. (2001). A new method for non-parametric multivariate analysis of variance. *Austral Ecol.* 26, 32–46. doi: 10.1111/j.1442-9993.2001.01070.pp.x

Asnicar, F., Berry, S. E., Valdes, A. M., Nguyen, L. H., Piccinno, G., Drew, D. A., et al. (2021). Microbiome connections with host metabolism and habitual diet from 1,098 deeply phenotyped individuals. *Nat. Med.* 27, 321–332. doi: 10.1038/s41591-020-01183-8

Berger, E., Colosetti, P., Jalabert, A., Meugnier, E., Wiklander, O. P. B., Jouhet, J., et al. (2020). Use of Nanovesicles from Orange juice to reverse diet-induced gut modifications in diet-induced obese mice. *Mol. Ther. Methods Clin. Dev.* 18, 880–892. doi: 10.1016/j.omtm.2020.08.009

Brasili, E., Chaves, D. F., Xavier, A. A., Mercadante, A. Z., Hassimotto, N. M., and Lajolo, F. M. (2017). Effect of pasteurization on flavonoids and carotenoids in *Citrus sinensis* (L.) Osbeck cv. 'Cara Cara' and 'Bahia' juices. *J. Agric. Food Chem.* 65, 1371–1377. doi: 10.1021/acs.jafc.6b05401

Braune, A., and Blaut, M. (2016). Bacterial species involved in the conversion of dietary flavonoids in the human gut. *Gut Microbes* 7, 216–234. doi: 10.1080/19490976.2016.1158395

Briskey, D., Malfa, G. A., and Rao, A. (2022). Effectiveness of "Moro" blood Orange *Citrus sinensis* Osbeck (Rutaceae) standardized extract on weight loss in overweight but otherwise healthy men and women—a randomized double-blind placebo-controlled study. *Nutrients* 14:427. doi: 10.3390/nu14030427

Capetini, V. C., Quintanilha, B. J., Oliveira, D. C., Nishioka, A. H., Matos, L. A., Ferreira, L. R. P., et al. (2023). Blood orange juice intake modulates plasma and PBMC microRNA expression in overweight and insulin-resistant women: impact on MAPK and NFκB signaling pathways. *J. Nutr. Biochem.* 112:109240. doi: 10.1016/j.jnutbio.2022.109240

Caporaso, J. G., Kuczynski, J., Stombaugh, J., Bittinger, K., Bushman, F. D., Costello, E. K., et al. (2010). QIIME allows analysis of high-throughput community sequencing data. *Nat. Methods* 7, 335–336. doi: 10.1038/nmeth.f.303

Cardile, V., Graziano, A. C. E., and Venditti, A. (2015). Clinical evaluation of Moro (*Citrus sinensis* (L.) Osbeck) orange juice supplementation for the weight management. *Nat. Prod. Res.* 29, 2256–2260. doi: 10.1080/14786419.2014.1000897

Carmona, L., Alquézar, B., Marques, V. V., and Peña, L. (2017). Anthocyanin biosynthesis and accumulation in blood oranges during postharvest storage at different low temperatures. *Food Chem.* 237, 7–14. doi: 10.1016/j.foodchem.2017.05.076

Chambers, E. S., Preston, T., Frost, G., and Morrison, D. J. (2018). Role of gut microbiota-generated short-chain fatty acids in metabolic and cardiovascular health. *Curr. Nutr. Rep.* 7, 198–206. doi: 10.1007/s13668-018-0248-8

Corrêa, T. A. F., Rogero, M. M., Hassimotto, N. M. A., and Lajolo, F. M. (2019). The two-way polyphenols-microbiota interactions and their effects on obesity and related metabolic diseases. *Front. Nutr.* 6:188. doi: 10.3389/fnut.2019.00188

Cortés-Martín, A., Selma, M. V., Tomás-Barberán, F. A., González-Sarrías, A., and Espín, J. C. (2020). Where to look into the puzzle of polyphenols and health? The Postbiotics and gut microbiota associated with human Metabotypes. *Mol. Nutr. Food Res.* 64:1900952. doi: 10.1002/mnfr.201900952

D'Elia, L., Dinu, M., Sofi, F., Volpe, M., and Strazzullo, P.SINU Working Group, Endorsed by SIPREC (2021). 100% fruit juice intake and cardiovascular risk: a systematic review and meta-analysis of prospective and randomised controlled studies. *Eur. J. Nutr.* 60, 2449–2467. doi: 10.1007/s00394-020-02426-7

Dorna, M. S., Barbosa, E. M. S., Callegari, M. A., Tanni, S. E., Chiuso-Minicucci, F., Felix, T. F., et al. (2021). Orange juice attenuates circulating miR-150-5p, miR-25-3p, and miR-451a in healthy smokers: a randomized crossover study. *Front. Nutr.* 8:775515. doi: 10.3389/fnut.2021.775515

Fan, Y., and Pedersen, O. (2021). Gut microbiota in human metabolic health and disease. *Nat. Rev. Microbiol.* 19, 55–71. doi: 10.1038/s41579-020-0433-9

Fay, M. P., and Proschan, M. A. (2010). Wilcoxon-Mann-Whitney or t-test? On assumptions for hypothesis tests and multiple interpretations of decision rules. *Stat. Surv.* 4, 1–39. doi: 10.1214/09-SS051

Fidélix, M., Milenkovic, D., Sivieri, K., and Cesar, T. (2020). Microbiota modulation and effects on metabolic biomarkers by orange juice: a controlled clinical trial. *Food Funct.* 11, 1599–1610. doi: 10.1039/C9FO02623A

Fraga, L. N., Coutinho, C. P., Rozenbaum, A. C., Tobaruela, E. C., Lajolo, F. M., and Hassimotto, N. M. A. (2021). Blood pressure and body fat % reduction is mainly related to flavanone phase II conjugates and minor extension by phenolic acid after long-term intake of orange juice. *Food Funct.* 12, 11278–11289. doi: 10.1039/d1fo02664j

Fraga, L. N., Milenkovic, D., Lajolo, F. M., and Hassimotto, N. M. A. (2022). Association between single nucleotide polymorphisms of SULT1A1, SULT1C4, ABCC2 and phase II flavanone metabolites excretion after Orange juice intake. *Nutrients* 14:3770. doi: 10.3390/nu14183770

Friedewald, W. T., Levy, R. I., and Fredrickson, D. S. (1972). Estimation of the concentration of low-density lipoprotein cholesterol in plasma, without use of the preparative ultracentrifuge. *Clin. Chem.* 18, 499–502. doi: 10.1093/clinchem/18.6.499

Geloneze, B., and Tambascia, M. A. (2006). Avaliação laboratorial e diagnóstico da resistência insulínica. *Arq. Bras. Endocrinol. Metab.* 50, 208–215. doi: 10.1590/S0004-27302006000200007

Hidalgo, M., Oruna-Concha, M. J., Kolida, S., Walton, G. E., Kallithraka, S., Spencer, J. P. E., et al. (2012). Metabolism of anthocyanins by human gut microflora and their influence on gut bacterial growth. *J. Agric. Food Chem.* 60, 3882–3890. doi: 10.1021/jf3002153

Kahleova, H., Rembert, E., Alwarith, J., Yonas, W. N., Tura, A., Holubkov, R., et al. (2020). Effects of a low-fat vegan diet on gut microbiota in overweight individuals and relationships with body weight, body composition, and insulin sensitivity. A randomized clinical trial. *Nutrients* 12:2917. doi: 10.3390/nu12102917

Klindworth, A., Pruesse, E., Schweer, T., Peplies, J., Quast, C., Horn, M., et al. (2013). Evaluation of general 16S ribosomal RNA gene PCR primers for classical and next-generation sequencing-based diversity studies. *Nucleic Acids Res.* 41:e1. doi: 10.1093/nar/gks808

Kobyliak, N., Virchenko, O., and Falalyeyeva, T. (2016). Pathophysiological role of host microbiota in the development of obesity. *Nutr. J.* 15:43. doi: 10.1186/s12937-016-0166-9

Krga, I., and Milenkovic, D. (2019). Anthocyanins: from sources and bioavailability to cardiovascular-health benefits and molecular mechanisms of action. *J. Agric. Food Chem.* 67, 1771–1783. doi: 10.1021/acs.jafc.8b06737

Kuntz, S., Asseburg, H., Dold, S., Römpp, A., Fröhling, B., Kunz, C., et al. (2015). Inhibition of low-grade inflammation by anthocyanins from grape extract in an in vitro epithelial-endothelial co-culture model. *Food Funct.* 6, 1136–1149. doi: 10.1039/C4FO00755G

Lima, L. P., and Barbosa, A. P. (2021). A review of the lipolytic effects and the reduction of abdominal fat from bioactive compounds and Moro orange extracts. *Heliyon* 7:e07695. doi: 10.1016/j.heliyon.2021.e07695

Lima, A. C. D., Cecatti, C., Fidélix, M. P., Adorno, M. A. T., Sakamoto, I. K., Cesar, T. B., et al. (2019). Effect of daily consumption of Orange juice on the levels of blood glucose, lipids, and gut microbiota metabolites: controlled clinical trials. *J. Med. Food* 22, 202–210. doi: 10.1089/jmf.2018.0080

Lin, Y., Xu, Z., Yeoh, Y. K., Tun, H. M., Huang, W., Jiang, W., et al. (2023). Combing fecal microbial community data to identify consistent obesity-specific microbial signatures and shared metabolic pathways. *iScience.* 26:106476. doi: 10.1016/j.isci.2023.106476

Liu, B. N., Liu, X. T., Liang, Z. H., and Wang, J. H. (2021). Gut microbiota in obesity. *World J. Gastroenterol.* 27, 3837–3850. doi: 10.3748/wjg.v27.i25.3837

Lorzadeh, E., Ramezani-Jolfaie, N., Mohammadi, M., Khoshbakht, Y., and Salehi-Abargouei, A. (2019). The effect of hesperidin supplementation on inflammatory markers in human adults: a systematic review and meta-analysis of randomized controlled clinical trials. *Chem. Biol. Interact.* 307, 8–15. doi: 10.1016/j.cbi.2019.04.016

Mas-Capdevila, A., Teichenne, J., Domenech-Coca, C., Caimari, A., Bas, J. M. D., Escoté, X., et al. (2020). Effect of hesperidin on cardiovascular disease risk factors: the role of intestinal microbiota on hesperidin bioavailability. *Nutrients* 12:1488. doi: 10.3390/nu12051488

McMurdie, P. J., and Holmes, S. (2013). Phyloseq: an R package for reproducible interactive analysis and graphics of microbiome census data. *PLoS One* 8:e61217. doi: 10.1371/journal.pone.0061217

Menezes, E. W., Dan, M. C. T., Cardenette, G. H. L., Goñi, I., Bello-Pérez, L. A., and Lajolo, F. M. (2010). In vitro colonic fermentation and glycemic response of different kinds of unripe Banana flour. *Plant Foods Hum. Nutr.* 65, 379–385. doi: 10.1007/s11130-010-0190-4

Murtagh, F., and Legendre, P. (2014). Ward's hierarchical agglomerative clustering method: which algorithms implement Ward's criterion? *J. Classif.* 31, 274–295. doi: 10.1007/s00357-014-9161-z

Nishioka, A., Tobaruela, E. C., Fraga, L. N., Tomás-Barberán, F. A., Lajolo, F. M., and Hassimotto, N. M. A. (2021). Stratification of volunteers according to flavanone metabolite excretion and phase II metabolism profile after single doses of 'Pera' Orange and 'Moro' blood Orange juices. *Nutrients* 13:473. doi: 10.3390/nu13020473

Oksanen, J., Blanchet, F. G., Friendly, M., Kindt, R., Legendre, P., McGlinn, D., et al. (2019). *Vegan: Community ecology package*. R package version 1.8-5.

Precup, G., and Vodnar, D.-C. (2019). Gut Prevotella as a possible biomarker of diet and its eubiotic versus dysbiotic roles: a comprehensive literature review. *Br. J. Nutr.* 122, 131–140. doi: 10.1017/S0007114519000680

Pylro, V. S., Roesch, L. F. W., Ortega, J. M., Amaral, A. M., Tótola, M. R., Hirsch, P. R., et al. (2014). Brazilian microbiome project: revealing the unexplored microbial diversity—challenges and prospects. *Microb. Ecol.* 67, 237–241. doi: 10.1007/s00248-013-0302-4

Quast, C., Pruesse, E., Yilmaz, P., Gerken, J., Schweer, T., Yarza, P., et al. (2012). The SILVA ribosomal RNA gene database project: improved data processing and web-based tools. *Nucleic Acids Res.* 41, D590–D596. doi: 10.1093/nar/gks1219

Quintanilha, B. J., Chaves, D. F. S., Brasili, E., Corrêa, T. A. F., Capetini, V. C., Ferreira, F. M., et al. (2022). Ingestion of orange juice prevents hyperglycemia and increases plasma miR-375 expression. *Clin. Nutr. ESPEN* 47, 240–245. doi: 10.1016/j.clnesp.2021.12.003

R Development Core Team. (2014). *R: A Language and Environment for Statistical Computing*. Vienna, Austria: R Foundation for Statistical Computing.

Ribeiro, A. P. D., Pereira, A. G., Todo, M. C., Fujimori, A. S. S., Santos, P. P., Dantas, D., et al. (2021). Pera orange (*Citrus sinensis*) and Moro orange (*Citrus sinensis* (L.) Osbeck) juices attenuate left ventricular dysfunction and oxidative stress and improve myocardial energy metabolism in acute doxorubicin-induced cardiotoxicity in rats. *Nutrition* 91-92:111350. doi: 10.1016/j.nut.2021.111350

Rognes, T., Flouri, T., Nichols, B., Quince, C., and Mahé, F. (2016). VSEARCH: a versatile open source tool for metagenomics. *PeerJ.* 4:e2584. doi: 10.7717/peerj.2584

Santana, A. A., Tobaruela, E. C., Santos, K. G., Sparvoli, L. G., Amaral, C. K., Magnoni, C. D., et al. (2022). 'Pera' Orange and 'Moro' blood Orange juice improves oxidative stress and inflammatory response biomarkers and modulates the gut microbiota of individuals with insulin resistance and different obesity classes. *Obesities* 2, 389–412. doi: 10.3390/obesities2040033

Santos, K. G., Yoshinaga, M. Y., Glezer, I., Chaves-Filho, A. B., Santana, A. A., Kovacs, C., et al. (2022). Orange juice intake by obese and insulin-resistant subjects lowers specific plasma triglycerides: a randomized clinical trial. *Clin. Nutr. ESPEN* 51, 336–344. doi: 10.1016/j.clnesp.2022.08.005

Silveira, J. Q., Dourado, G. K. Z. S., and Cesar, T. B. (2015). Red-fleshed sweet orange juice improves the risk factors for metabolic syndrome. *Int. J. Food Sci. Nutr.* 66, 830–836. doi: 10.3109/09637486.2015.1093610

Stevens, Y., Rymenant, E. V., Grootaert, C., Camp, J. V., Possemiers, S., Masclee, A., et al. (2019). The intestinal fate of citrus flavanones and their effects on gastrointestinal health. *Nutrients* 11:1464. doi: 10.3390/nu11071464

Van Hul, M., and Cani, P. D. (2023). The gut microbiota in obesity and weight management: microbes as friends or foe?. Na.T rev. *Endocrinol.* 19, 258–271. doi: 10.1038/s41574-022-00794-0

Wickham, H.. (2016). *ggplot2: Elegant graphics for data analysis*. Second. Springer.

World Health Organization. (2000). *Obesity: preventing and managing the global epidemic. Report of a WHO consultation*. Geneva: World Health Organization, 1–253.

World Health Organization. (2020). *The top 10 causes of death*. Geneva: World Health Organization.

Yang, Y., Trevethan, M., Wang, S., and Zhao, L. (2022). Beneficial effects of citrus flavanones naringin and naringenin and their food sources on lipid metabolism: an update on bioavailability, pharmacokinetics, and mechanisms. *J. Nutr. Biochem.* 104:108967. doi: 10.1016/J.JNUTBIO.2022.108967

Yi, L., Ma, S., and Ren, D. (2017). Phytochemistry and bioactivity of Citrus flavonoids: a focus on antioxidant, anti-inflammatory, anticancer and cardiovascular protection activities. *Phytochem. Rev.* 16, 479–511. doi: 10.1007/s11101-017-9497-1

Yoshida, N., Yamashita, T., Osone, T., Hosooka, T., Shinohara, M., Kitahama, S., et al. (2021). *Bacteroides* spp. promotes branched-chain amino acid catabolism in brown fat and inhibits obesity. *iScience* 24:103342. doi: 10.1016/j.isci.2021.103342

Zanchetti, A. (2016). Lower or higher blood-pressure targets for high-risk patients? *Nat. Rev. Cardiol.* 13, 637–638. doi: 10.1038/nrcardio.2016.165

frontiers | Frontiers in Microbiology

TYPE Original Research
PUBLISHED 05 July 2023
DOI 10.3389/fmicb.2023.1207837

OPEN ACCESS

EDITED BY
Fengjie Sun,
Georgia Gwinnett College, United States

REVIEWED BY
Seungha Kang,
The University of Queensland, Australia
Paula Jauregi,
Centro tecnológico experto en innovación marina y alimentaria (AZTI), Spain

*CORRESPONDENCE
Fangjie Gu
✉ fangjie.gu@food.ku.dk

RECEIVED 18 April 2023
ACCEPTED 13 June 2023
PUBLISHED 05 July 2023

CITATION
Gu F, Larsen N, Pascale N, Petersen SA, Khakimov B, Respondek F and Jespersen L (2023) Age-related effects on the modulation of gut microbiota by pectins and their derivatives: an *in vitro* study. *Front. Microbiol.* 14:1207837. doi: 10.3389/fmicb.2023.1207837

Age-related effects on the modulation of gut microbiota by pectins and their derivatives: an *in vitro* study

Fangjie Gu[1,2]*, Nadja Larsen[1], Nélida Pascale[2], Sune Allan Petersen[2], Bekzod Khakimov[1], Frederique Respondek[3] and Lene Jespersen[1]

[1]Department of Food Science, Faculty of Science, University of Copenhagen, Frederiksberg, Denmark, [2]CP Kelco ApS, Lille Skensved, Denmark, [3]CP Kelco, Levallois-Perret, France

Introduction: The present study investigates whether supplementation with pectin-type polysaccharides has potential to improve aging-associated dysbiosis of the gut microbiota. The influence of different types of pectins on the gut microbiota composition and short-chain fatty acids (SCFAs) profiles of elderly was compared to younger adults.

Methods: Pectins studied included a pectin polysaccharide (PEC), a partially hydrolyzed pectin (PPH), and a pectin oligosaccharide (POS). Additionally, inulin was used as a reference prebiotic substrate. Individual fecal samples were collected from healthy elderly volunteers (70–75 years) and younger adults (30–35 years). *In vitro* fermentations were performed using the CoMiniGut model with controlled temperature and pH. Samples were withdrawn at baseline and after 24h fermentation for measurement of SCFAs production and microbiota composition by 16S rRNA gene sequencing.

Results and Discussion: The results showed that fermentations with PEC and PPH resulted in a specific stimulation of *Faecalibacterium prausnitzii* regardless of the age groups. *Collinsella aerofaciens* became a dominating species in the young adult group with fermentations of all three pectins, which was not observed in the elderly group. No significant differences in SCFAs production were found among the pectins, indicating a high level of functional redundancy. Pectins boosted various bacterial groups differently from the reference prebiotic substrate (inulin). We also found inulin had reduced butyrogenic and bifidogenic effects in the elderly group compared to the younger adult group. In conclusion, the *in vitro* modulating effects of pectins on elderly gut microbiota showed potential of using pectins to improve age-related dysbiosis.

KEYWORDS

prebiotic, pectin, inulin, elderly, aging, gut microbiota, short chain fatty acids

1. Introduction

The large microbial community residing in the human intestine, often named as human gut microbiota, plays a vital role in maintaining the health status of human beings (Holscher, 2017). The gut microbiota is dynamic over lifetime, with an assembly phase starting just after birth for about 2 years, followed by relative stability during adulthood until distinct changes appearing with aging (Castanys-Muñoz et al., 2016; Greenhalgh et al., 2016). Despite interindividual variations,

several aging-associated bacterial groups have been identified (An et al., 2018). Major shifts included a lower abundance of *Bifidobacterium* and a higher abundance of *Enterobacteriaceae* family being found in elderly fecal microbiota compared to young adults (An et al., 2018). A functional metagenomic analysis reported aging-related loss of genes responsible for saccharolytic potential and short-chain fatty acids (SCFAs) production, accompanied by an increased proteolytic activity (Rampelli et al., 2013). Although the exact mechanism behind the alterations in the elderly gut microbiota has not been fully unraveled, changes in diet and physical activity, antibiotic administration and altered gut physiology are supposed to be contributors (Buford, 2017). Taking into consideration that the elderly population is rapidly increasing (projected to reach 1.4 billion globally by 2030) as well as a generally longer lifespan of individuals (WHO, 2021), a healthy gut microbiota in elderly is of increasing significance. Dietary supplementation with prebiotics could be a promising approach to beneficially modulate the gut microbiota and thereby to improve health conditions of the elderly. According to the expert consensus of the International Scientific Association for Probiotics and Prebiotics (ISAPP; Gibson et al., 2017), a prebiotic is defined as "a substrate that is selectively utilized by host microorganisms conferring a health benefit." Most well-known prebiotics so far include β-fructans (fructo-oligosaccharides (FOS) and inulin), and other oligosaccharides from various origins, e.g., galacto-oligosaccharides (GOS), arabino-oligosaccharides and more recently human milk oligosaccharides (HMOs; Roberfroid et al., 2010; Gibson et al., 2017). The benefits of inulin on improvement of bowel function is the first authorized health claim for prebiotics in Europe following a positive European Food Safety Authority (EFSA) opinion (EFSA Panel on Dietetic Products and Allergies, 2015). Inulins are polysaccharides composed of linear β(2→1)-linked fructose with a terminal α-glucose (EFSA Panel on Dietetic Products and Allergies, 2015). Fermentation of inulin in the gut promotes the growth of beneficial microbes, especially *Bifidobacterium* spp., inhibits enteropathogenic microorganisms and generates abundant SCFAs, especially butyrate (González-Herrera et al., 2015; Teferra, 2021). *Bifidobacterium* is the most commonly recognized genus with myriad benefits, e.g., healthy gut microbiota modulation, immunomodulation, anti-cholesterolemic effects, and protection against pathogens (Roberts et al., 2020). Butyrate is one key SCFAs in regulating the immune system and maintaining a healthy epithelial barrier (Baxter et al., 2019).

Recently, pectins have been suggested as a type of emerging prebiotic due to increasing scientific evidence on their capacities to selectively modulate human gut microbiota (Pascale et al., 2022; Rastall et al., 2022). Pectins are complex heteropolysaccharides that are naturally present in plant cell walls. Traditionally, pectins are extracted from fruit and vegetable sources, e.g., citrus, apple, and sugar beet, to be applied in the food industry as gelling or thickening agents (Elshahed et al., 2021). Pectins are considered as dietary fibers, as they pass indigestible through the upper gastrointestinal tract (Ferreira-Lazarte et al., 2019), and are fermented by the human gut microbiota resulting in the production of SCFAs (Holloway et al., 1983; Holscher, 2017). Molecular structures of pectins are varied, depending on their origins and extraction methods (Naqash et al., 2017; Pascale et al., 2022). Although not fully elucidated, a direct link between the structures of non-digestible carbohydrates and their functional effect on the gut microbiota has been reported (Rastall et al., 2022). In a recent study, the impact of pectin structures on the composition of the human gut microbiota was investigated using an *in vitro* experimental setup (Larsen et al., 2019). Promotion of *Faecalibacterium prausnitzii*, *Bifidobacterium* spp., and several other health-related bacterial groups were found to be associated with the structural features of pectins, including sugar composition and degree of esterification (Larsen et al., 2019). Fermentation of the high-methylated citrus pectin stimulated higher abundances of *F. prausnitzii* and resulted in higher production of propionate (Larsen et al., 2019). Furthermore, differences in molecular weight (MW) of pectins led to different fermentation effects, although MW was not covered by Larsen et al. (2019). For instance, *Bifidobacterium* spp., equipped with more exo-acting enzymes, are known to preferentially utilize oligosaccharides of lower MW (Sarbini and Rastall, 2011; Rastall et al., 2022). Likewise, an increased bifidogenic effect of lower MW pectins in comparison with pectin polysaccharides was observed in several *in vitro* studies and at least one human study (Olano-Martin et al., 2002; Gómez et al., 2016; Ferreira-Lazarte et al., 2018).

Limited number of studies have explored the ability of pectins to modulate the elderly gut microbiota. Wilkowska et al. (2021) studied the prebiotic effect of a pectin oligosaccharide (POS) derived from apple in relation to the different ages of the fecal donors, and concluded that the donors´ age was a determinant on the growth of lactic acid bacteria, SCFAs production, and lactic acid profiles from POS fermentation. Another *in vitro* fermentation study compared the effects of POS from lemon peel and fructo-oligosaccharide (FOS) on pooled fecal inoculum of elderly, and found similar microbial profiles and butyrate production (Míguez et al., 2020). However, the aforementioned study lacks a reference assessment with a fecal inoculum from younger adults under a similar fermentation setting. A recent human intervention study with elderly and younger adults found that a daily supplementation of 15 g of sugar beet pectin for 4 weeks resulted in no significant changes in the fecal microbiota profiles or metabolic activity for neither of the groups (An et al., 2019).

Previous studies have explored either the impact of pectins with different structural characteristics or age of fecal donors on the gut microbiota composition and SCFA production (Larsen et al., 2019; Wilkowska et al., 2021). However, there is still a need to investigate how molecular sizes of pectins influence the human gut microbiota and, especially, how they differentially impact age-related differences in microbiota composition, particularly linked to the microbiota of the elderly. The aim of the current study was therefore to investigate how molecular sizes of HM citrus-derived pectins, i.e., a pectin polysaccharide (PEC), a partially hydrolyzed pectin (PPH), and a pectin oligosaccharide (POS), modulate the gut microbiota of elderly vs. younger adults, using an *in vitro* colon model. The main effects driven by the fermentation of the pectins in terms of relative abundances and diversity of the gut microbial community, as well as the cumulative production of SCFAs were evaluated and compared with chicory inulin (INU) as a reference prebiotic substrate.

2. Materials and methods

2.1. Substrates

Lemon pectin (PEC) with a degree of methyl-esterification of 68.2%, partially hydrolyzed pectin, also called modified pectin (PPH), and pectic oligosaccharides (POS) were provided by CP Kelco ApS (Denmark). Both PPH and POS were derived from the same batch of PEC, but they were produced to have clear differences in MW. PEC had

the largest average MW of 419 kDa (76.7% mass recovery), followed by PPH with an average MW of 24 kDa (78.6% mass recovery). POS had the smallest molecules, with an average MW of 2.3 kDa of the major fraction (55.1% mass recovery). Additionally, POS also contained a smaller fraction with an average MW of 0.4 kDa (24.1% mass recovery) and a minor fraction of large molecules with average MW of 372 kDa (13.5% mass recovery). More details of the absolute MW and corresponding weight fraction of the three pectins were shown in Supplementary Figure 1. Commercial inulin (INU) from chicory (purity >95%) was purchased from Carbosynth Limited (United Kingdom) and included in the experimental setup as a reference.

2.2. Determination of molecular weight by size exclusion chromatography

The molecular weight (MW) distribution of PEC, PPH and POS were analyzed by injecting 100 µL of 2.5 mg/mL substrate to Agilent 1,260 Infinity II liquid chromatography system (Agilent, United States) equipped with PSS precolumn 10 µm 8 × 50 mm, PSS Suprema Lux analytical Ultrahigh, and PSS Suprema Lux 30 Å (PSS, Germany). The separation was performed using 0.3 M lithium acetate buffer as eluent at flow rate 1.0 mL/min, and column temperature was 37°C. Wyatt Dawn 8+ light scattering instrument and Wyatt Optilab T-rex refractive index detector (Wyatt, United States) were used for detection. MW and concentrations were converted from the detector signals by the software ASTRA 7 (Wyatt).

2.3. Fecal sample collection and inoculum preparation

Fecal samples were provided by ten human donors with consent. All the donors were self-reported healthy Caucasian males who did not receive pharmaceutical supplementation of pro-, pre-or antibiotics at least 90 days prior to stool collection. The donors were divided into two groups based on their ages, elderly group ($n = 5$, age range 70–75 years old) and young group ($n = 5$, age range 30–35 years old). The studies involving human participants were reviewed and approved by the Ethical Committee of the Capital Region of Denmark (H-15001754; Wiese et al., 2018). Written informed consent to participate in this study was provided by the participants.

The collected fecal samples were processed individually within the same day as described earlier (Wiese et al., 2018). Briefly, fresh feces were mixed with equal weight of phosphate buffered saline (PBS, pH 5.6) containing 20% glycerol, followed by homogenization using a Stomacher 400 (Seward, United Kingdom) at normal speed for 2 min (Wiese et al., 2018). The homogenized fecal slurries were then aliquoted, snap frozen in liquid nitrogen and stored at –60°C until further use. The abovementioned preparation procedures were performed in a vinyl anaerobic chamber (Coy Lab, United States) filled with 5% H_2, 5% CO_2 and 90% N_2 (ALPHAGAZ, Air Liquide, France).

2.4. *In vitro* fermentation using CoMiniGut system

Batch fermentations of INU, PEC, PPH and POS with individual fecal inoculum were performed in triplicates using the CoMiniGut system with five parallel reactor units (Wiese et al., 2018). The current study followed the operation protocol of the CoMiniGut model as described (Wiese et al., 2018), with adjustment of several parameters. The homogenized fecal slurries were thawed and further diluted with four volumes of PBS. Each anaerobic reactor unit contained 0.5 mL of PBS-diluted fecal inoculum and 4.5 mL of basal colon medium (2 g/L peptone, 0.5 g/L bile salts, 1 g/L yeast extract, 0.1 g/L NaCl, 0.04 g/L K_2HPO_4, 0.04 g/L KH_2PO_4, 0.01 g/L $MgSO_4 \bullet 7H_2O$, 0.01 g/L $CaCl_2 \bullet 2H_2O$, 0.2 g/L $NaHCO_3$, 0.005 g/L hemin, 0.001% (v/v) vitamin K1, 0.2% (v/v) Tween 80, 0.5 g/L L-Cysteine HCl; Wiese et al., 2018). The fermentation mixtures had a final concentration of 1% (*w/v*) inulin or pectins. The concentrations of the original fecal matter and glycerol were 1 and 0.2%, respectively. Anaerobic conditions in the reactor units were maintained and monitored by placing the Oxoid™ AnaeroGen™ Compact Sachets and Oxoid™ Resazurin Anaerobic Indicator (both from Thermo Fisher Scientific, United States) in the reaction compartments. Fermentations were performed at 37°C, and the pH gradually increased from 5.6 to 6.8 in 24 h, with computer-controlled addition of 1 M sodium hydroxide solution. Fermentations were terminated at 24 h endpoint and samples were stored in aliquots at -60°C until further analysis.

2.5. Analysis of short-and branched-chain fatty acids (SCFAs/BCFAs)

Concentrations of SCFAs and BCFAs of the fermentation samples taken at 24 h endpoint were determined by GC–MS as described previously (Wiese et al., 2018, 2021). The fermentation samples were mixed at 1:2 ratio with 0.3 M oxalic acid containing 2 mM 2-ethylbutyrate as internal standard, followed by centrifugation and filtration. One µL of the supernatant was injected into Agilent 7890A GC (Agilent) equipped with a Phenomenex Zebron ZB-WAXplus column (30 m × 250 µm × 0.25 µm, Phenomenex, United States). Agilent 5,973 series MSD mass spectrometer was employed to identity and quantify SCFAs and BCFAs. Selected Ion Monitoring (SIM) mode was used to scan ions with mass–to–charge (*m/z*) ratios of 41, 43, 45, 57, 60, 73, 74, and 84. These *m/z* ions are specific for SCFA and BCFA quantified in this study including acetic acid (*m/z* 43, 45, 60), propionic acid (*m/z* 45, 57, 73, 74), butyric acid (*m/z* 41, 43, 45, 60, 73), isobutyric acid (*m/z* 41, 43, 45, 73), 2-methylbutyric acid (*m/z* 74), valeric acid (*m/z* 41, 45, 60,73), and isovaleric acid (*m/z* 60). Prior to quantification, a calibration curve was constructed for each compound using authentic standards of SCFAs and BCFAs. GC–MS data was analyzed using MATLAB scripts (version R2015A; MathWorks, United States) written by authors. The concentration values were corrected by subtracting the concentrations found in the corresponding blank control (inoculum at baseline) samples.

2.6. DNA extraction and 16S rRNA gene amplicon sequencing

DNA was extracted from the fermentation samples taken at 24 h endpoint, and from the blank control samples (inoculum), using the Bead – Beat Micro AX Gravity Kit (A&A Biotechnology, Poland) according to the manufacturer's instruction. The concentrations of extracted DNA were determined using Qubit™ 1X dsDNA High Sensitivity (HS) Assay Kit (Thermo Fisher Scientific) on a Varioskan

Flash multimode reader (Thermo Fisher Scientific), followed by a dilution to 1 ng/μL for library preparation.

Library preparation procedures for nanopore based sequencing of V1V3–V8V9 hypervariable regions of 16S rRNA gene amplicon using MinION (Oxford Nanopore Technologies, United Kingdom) were conducted as previously described with several adaptions (Hui et al., 2021). Shortly, in the first round of PCR, 5 μL of the diluted DNA was mixed with 6 μL of nuclease-free water, 12 μL of PCRBIO Ultra Mix (PCR Biosystems Ltd., United Kingdom), and 2 μL of Primers Mix, which contained 5 μM of a unique combination of forward and reverse primers, which sequences were given in Supplementary Table 1 (Kårhus et al., 2022). The mixtures were subjected to the first PCR amplification in a Thermocycler Agilent SureCycler 8800 (Agilent) with the temperature profile as follows: denaturation at 95°C for 5 min; 2 cycles of 95°C for 20 s, 48°C for 30 s, 65°C for 10 s, and 72°C for 45 s; followed by final elongation at 72°C for 4 min. s.

The first PCR products were purified with AMPure XP beads (Beckman Coulter, United States) before the second PCR amplification. The second PCR reaction mixtures contained 11 μL of the first PCR clean products, 12 μL of PCRBIO Ultra Mix, and 2 μL of ONT UMI barcodes at 10 μM that were custom designed for tag encoding multiple samples in one run. The second PCR temperature profile included denaturation at 95°C for 2 min; 33 cycles of 95°C for 20 s, 55°C for 20 s, and 72°C for 40 s; followed by final elongation at 72°C for 4 min. The size of second PCR products (around 1,500 bp) were checked by agarose gel electrophoresis, followed by purification using AMPure XP beads and equimolar pooling. The library preparation was finalized by using the 1D Genomic DNA by Ligation kit (SQK–LSK109, Oxford Nanopore Technologies) according to the manufacturer's protocol, and was loaded on a R9.4.1 flow cell.

The sequencing data generated by MinION was processed as outlined elsewhere (Hui et al., 2021). MinKnow software v19.06.8,[1] Guppy v3.2.2 basecalling toolkit (see footnote 1), Porechop v0.2.2,[2] NanoFilt (qq ≥ 10; read length > 1Kb) were used for data collection, base calling, adapter trimming, demultiplexing and quality correction (Hui et al., 2021). Greengenes (13.8) was used for taxonomy assignment with implementation of parallel_assign_taxonomy_uclust.py in QIIME v1.9.1. Individual Amplicon Sequence Variant (ASV) was treated as individual "seeds." The reads that were annotated to at least phylum level was included in further analysis. Due to taxonomic reorganization, three features annotated as [*Eubacterium*] *biforme*, *Lactobacillus ruminis*, and *Lactobacillus zeae* were updated manually to *Holdemanella biformis* (De Maesschalck et al., 2014), *Ligilactobacillus ruminis* (Zheng et al., 2020) and *Lacticaseibacillus zeae* (Zheng et al., 2020), respectively.

2.7. Data analysis and statistics

Analysis and visualization of SCFAs/BCFAs concentrations and microbiome data was conducted in RStudio v.1.4.1717 integrated in R v.4.1.3. The average SCFAs/BCFAs concentrations of triplicates were taken to check normality and homogeneity of variances using Shapiro–Wilk test and Levene's test. Comparisons of specific acids among the four substrates were conducted using one-way ANOVA with Tukey's HSD *post hoc* test. Student's *t*-test was performed to compare the values between the elderly and the young group. R packages rstatix v.0.7.0, tidy verse v1.3.1, and multcompView v.0.1–8 were used to perform the abovementioned tests.

Microbiome data was imported to R followed by microbial diversity analysis using the package phyloseq v1.38.0 (McMurdie and Holmes, 2013). All the samples were rarefied to an even library depth of 10,000 reads/sample and triplicates were averaged to the nearest integers. One sample using PPH as substrate and fecal inoculum from one elderly donor was discarded due to inadequate library size (< 10,000 counts). Alpha diversity (observed features index and Shannon diversity index) was compared among substrates using one-way ANOVA with Tukey's HSD *post hoc* test, or between the two age groups using Student's *t*-test, after checking normality and homogeneity of variances. Beta diversity was evaluated by Jaccard (unweighted) and Bray–Curtis distance matrices. Differences between the substrates as well as between the two age groups were determined by PERMANOVA test using the package vegan v2.5–7 (Dixon, 2003) with *p*-values corrected by Benjamini – Hochberg method. Differentially enriched taxa (summarized at species level) among the substrates were identified by DESeq2 method (Love et al., 2014) with a preset *p*-value lower than 0.05. The taxa occurring at a minimum relative abundance of 1% in at least 10% samples were visualized in a heatmap. Differentially enriched taxa between elderly and young groups were also identified using DESeq2 method (Love et al., 2014). Relative abundance of the responding taxa which fulfilled the abovementioned criteria were compared using Kruskal–Wallis rank sum test. Three features of interest, *s_Faecalibacterium prausnitzii*, *s_Escherichia coli*, and *g_Dorea.s* were also included in the between-age comparison. Pearson's correlation analysis between centered log-ratio (clr) transformed microbial relative abundance and short-/ branched-chain fatty acid concentrations were performed with Rhea package (Lagkouvardos et al., 2017). Zeros in taxonomic variables were excluded from the correlation analysis. Core taxa were selected with a prevalence cut-off value set as 30%, with at least four pair of observations supporting each calculated correlation. Microbial co-occurrence network based on SPIEC-EASI method was constructed using the unrarefied counts from all the fermentation and fecal inoculum samples ($n = 129$), with R package NetCoMi v.1.0.2 (Peschel et al., 2021). Samples with total reads less than 10,000 were filtered out. Taxa were included in the analysis if prevalence ≥ 30% and mean relative abundance ≥ 0.1%. Other R packages used for visualization included corrplot v0.92 (Wei and Simko, 2021), ggplot2 v.3.3.5 (Wickham, 2016), circlize v.0.4.14 (Gu et al., 2014) and complexheatmap v.2.8.0 (Gu et al., 2016).

3. Results

3.1. Alpha and beta diversity of microbiota

In total, 157 microbial features were summarized at species level. The alpha diversity indices of the fermentations with PEC and PPH were comparable to those of the blank control (inoculum), including observed features (Figure 1A) and Shannon index (Figure 1B). A significant lower Shannon index was observed with POS compared to

1 https://nanoporetech.com

2 https://github.com/rrwick/Porechop

that with PEC. Fermentation with INU significantly decreased both the observed features and the Shannon diversity index (alpha diversity) compared to the blank control, while POS only had a significantly lower Shannon index than the blank control. The decreased Shannon diversity indices of POS and INU indicated that the two substrates stimulated certain bacterial groups that dominated the corresponding microbial communities. No difference was found between the elderly and young adult groups in terms of alpha diversity (Supplementary Figure 2).

Principal coordinate analysis (PCoA) of beta diversity was performed based on weighted Bray–Curtis and unweighted Jaccard distance matrices (Figures 2A,B). Both plots showed a shift in community structures of the fermentation samples after 24 h compared to the blank control. Separated clusters corresponding to each substrate were formed in the weighted PCoA, indicating shifts in dominant bacterial groups among the microbial communities. However, the fermentation samples at 24 h clustered closely in the unweighted PCoA, which represented the presence and absence of bacterial groups in the microbial communities. Based on PERMANOVA results, the substrate factor explained 37% of the variances on Bray–Curtis matrix (Figure 2C), compared to 22% of the same factor on Jaccard (Figure 2D). Age had a smaller effect on both matrices than substrate, explaining 10 and 7% on Bray–Curtis and Jaccard, respectively (Figures 2C,D). Differences or similarities in microbial community structures between each substrate and the blank control were further explored by pairwise PERMANOVA (Figures 2E,F). For both weighted and unweighted matrices, all the fermentation samples at 24 h were significantly different from the blank control. PEC and PPH showed comparable community structures, while POS and INU had distinct microbiota profiles compared to PEC and PPH based on the weighted matrix.

3.2. Abundances of bacterial groups and co-occurrence network

The average relative abundances of bacterial phyla and genera (abundances ≥ 1%) at 24 h of fermentation as well as the blank control (inoculum) samples are shown in Figures 3A,B. There were 4 phyla and 20 genera with average relative abundances not lower than 1% in all the fermentation samples. Despite the inter-individual differences, Firmicutes was the most abundant phylum in the blank controls in both age groups, dominated by unidentified species from families *Ruminococcaceae* and *Lachnospiraceae*, *Blautia* spp. and *F. prausnitzii*. After 24 h fermentation with INU, the relative abundance of Firmicutes dropped by almost half, while the phylum Actinobacteria increased, represented mainly by *Bifidobacterium adolescentis* in both age groups, and by *Bifidobacterium* spp. in the young adult group only. The decreased relative abundance of Firmicutes was also observed for the pectins, compensated by an increased relative abundance of *Bacteroides* spp., and *B. adolescentis* in both age groups, together with *Collinsella aerofaciens* that was particularly increased in the young adult group. Furthermore, higher levels of phylum Proteobacteria were detected in fermentations with pectins in the elderly group, as well as with POS in the young adult group, which mainly contained an unidentified species from family *Enterobacteriaceae* and a minor fraction of *Escherichia coli*.

Figure 4A visualizes the relative abundances of different taxa between substrates including both age groups. Results of the adapted DESeq2 analysis with *p*-values lower than 0.05 are listed in Supplementary Table 2. In general, PEC and PPH fermentations led to comparable relative abundances of the bacterial groups, except for *Bacteroides* spp., which were more abundant in PEC samples. Fermentations with PEC and PPH favored the growth of *F. prausnitzii*, *Dorea* spp., *Blautia* spp. and *Clostridium* spp., while POS promoted the growth of distinct species, including *Lachnospira* spp., *Parabacteroides distasonis*, *Bacteroides* spp., and *B. ovatus*. Furthermore, fermentation with POS resulted in significantly reduced levels of *Prevotella copri* and *Catenibacterium* spp., along with increased levels of the unidentified species from the *Enterobacteriaceae* family and *E. coli*. Compared to pectins, fermentation with INU was characterized by significantly higher relative abundances of *B. uniformis*, *B. adolescentis*, *Coprococcus* spp., *Blautia* spp. and unidentified species from the families *Lachnospiraceae* and *Erysipelotrichaceae*.

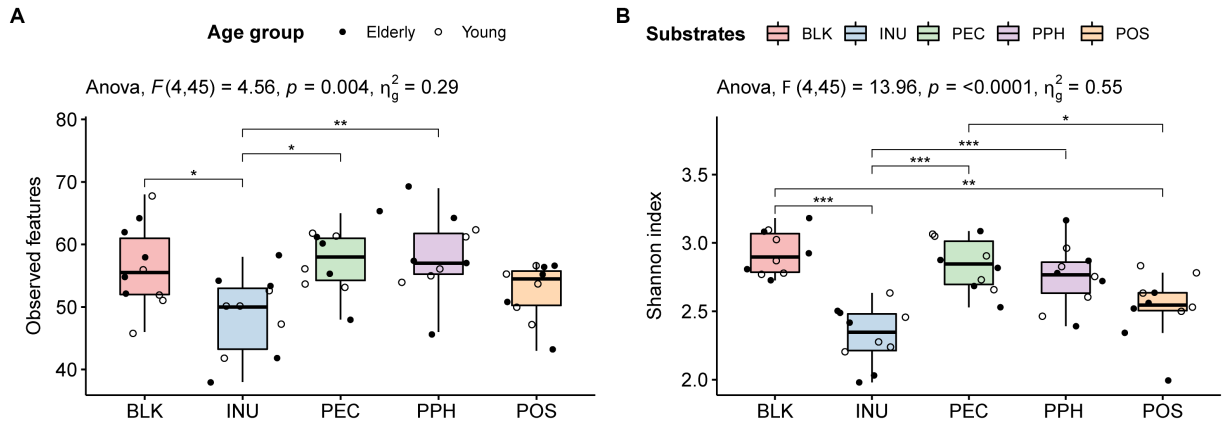

FIGURE 1
The effect of substrates (BLK, blank control; INU, inulin; PEC, pectin; PPH, partly hydrolyzed pectin; POS, pectin oligosaccharides) and age of fecal inoculum donors (elderly group, *n* = 5; young group, *n* = 5) on the microbial alpha diversity at 24 h end point of CoMiniGut fermentation: observed features summarized at species level **(A)** and Shannon diversity index **(B)**. The labels of *, **, and *** indicate *value of ps* < 0.05, < 0.01, and < 0.001, respectively.

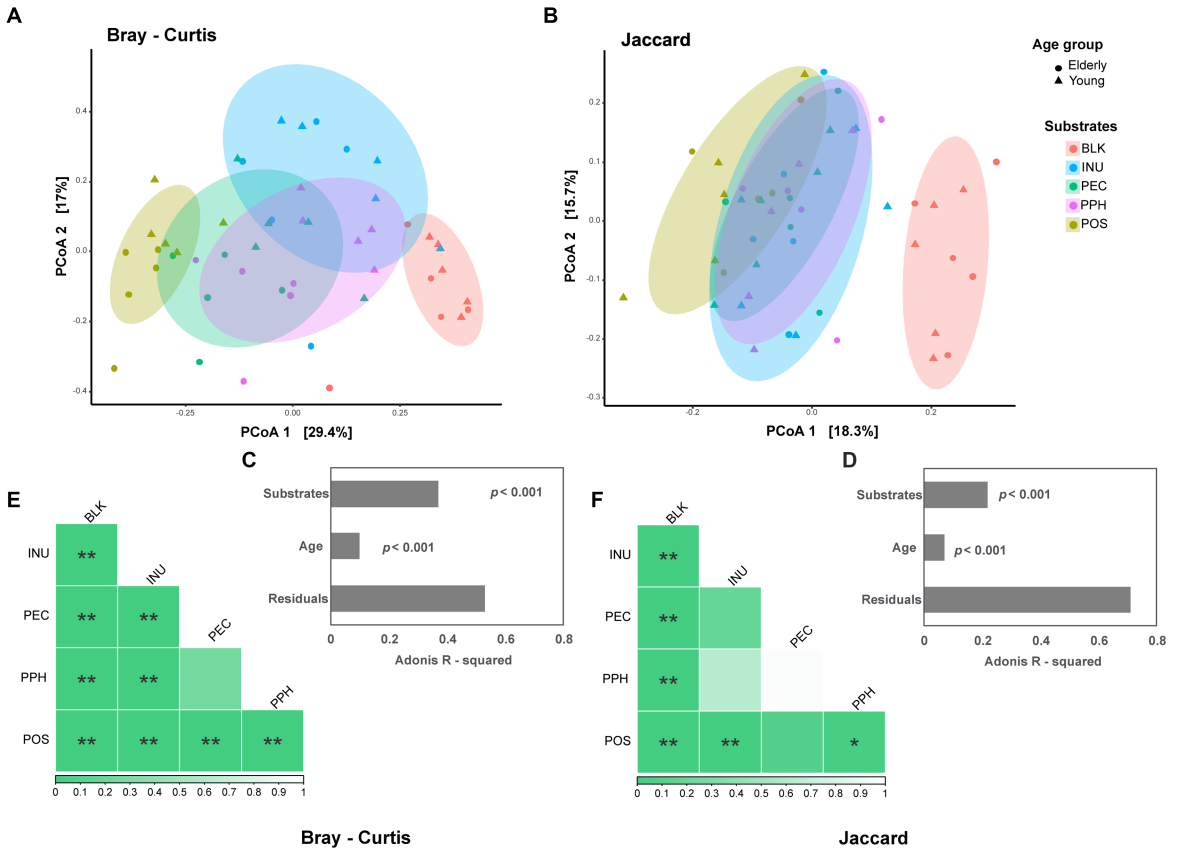

FIGURE 2
The effect of substrates (BLK, blank control; INU, inulin; PEC, pectin; PPH, partly hydrolyzed pectin; POS, pectin oligosaccharides) and age of fecal inoculum donors (elderly group, n = 5; young group, n = 5) on the microbial beta diversity at 24 h end point of CoMiniGut fermentation. Principal Coordinates analysis (PCoA) plots based on Bray–Curtis (weighted, **A**) and Jaccard (unweighted, **B**) distance matrices, with their corresponding adonis R-squared values listed in **(C)** and **(D)**. The ellipses illustrate the 80% confidential area assuming a multivariable t-distribution. Pairwise PERMANOVA tests visualized as heatmaps for Bray–Curtis **(E)** and Jaccard **(F)**, with the *value of ps* indicated by the color codes underneath. The labels of *, **, and indicate p-values < 0.05 and < 0.01, respectively.

Figure 4B shows the comparison between all the samples from the elderly group to those from the young adult group. Four species with average relative abundances over 1% were significantly different between the groups as based on the DESeq2 analysis, namely *C. aerofaciens*, *Bifidobacterium* spp., *Lachnospira* spp. and the unidentified species from family *Enterobacteriaceae*. The young adult group showed much higher relative abundance of *C. aerofaciens* in response to all the pectins compared to the elderly group. High abundances of *Bifidobacterium* spp. were only detected in the young adult group, especially in fermentations with INU. In contrast, fermentations in the elderly group with almost all the substrates led to increased levels of the unidentified species from family *Enterobacteriaceae* and *E. coli* (Figure 4B). Additionally, the levels of *F. prausnitzii* were significantly lower in the elderly samples compared to the young adult ones in the blank controls (inoculum at baseline; Figure 4B). However, the relative abundances of *F. prausnitzii* became comparable between the elderly and the young groups after 24 h fermentation with PEC and PPH, while it became almost absent with INU and POS.

A microbial co-occurrence network was constructed based on all the samples to explore positive and negative direct connections among bacterial groups (Figure 5). Strong positive associations were commonly found between nodes from the same phylum, for instance, one cluster was formed by several species from the phylum Firmicutes with two unidentified species from families *Ruminococcaceae* and *Lachnospiraceae* as the hubs. Cross-phyla clusters were also observed, e.g., *Bacteroides* spp., *Lachnospira* spp., the unidentified species from family *Enterobacteriaceae* and *E. coli* were co-occurring microbes, which were negatively associated with *Bifidobacterium* spp., *Roseburia* spp., *C. aerofaciens*, *Oscillospira* spp. and *[Ruminococcus]* spp. Despite the phylogenetic similarities, *Bifidobacterium* spp. were seldomly connected, possibly implying low niche overlap and functional diversity within the genus.

3.3. Acid production and correlations with microbial taxa

The cumulative production of SCFAs and branched-chain fatty acids (BCFAs) after 24 h fermentation with the four substrates are listed in Table 1. For all the samples, acetic acid, propionic acid, and butyric acid, were present as the dominant acids, while BCFAs (isobutyric acid, isovaleric acid, 2-methylbutyric acid) and valeric acid were detected in minor amounts. Acetic acid was the principal SCFA

10.3389/fmicb.2023.1207837

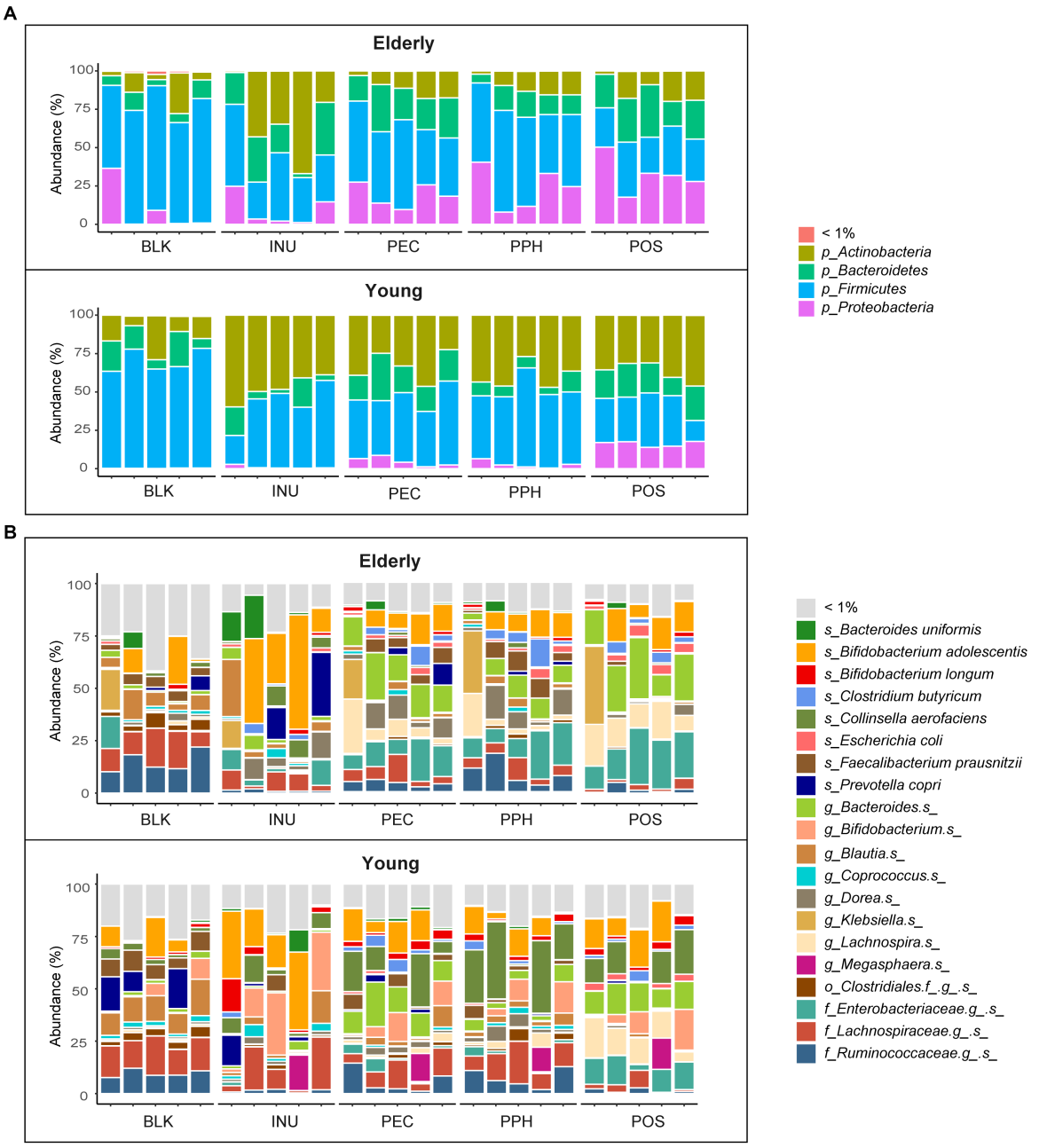

FIGURE 3
Microbiota composition of blank control (BLK) and at 24 h end point of CoMiniGut fermentation of: INU, inulin; PEC, pectin; PPH, partly hydrolyzed pectin; POS, pectin oligosaccharides. Fecal inoculums used for CoMiniGut fermentation were either from the elderly group (n = 5), or the young group (n = 5). Relative abundances of detected taxa are summarized at phylum **(A)** and species **(B)** level. Taxa with average relative abundance less than 1% are grouped as "< 1%."

produced from pectins, followed by butyric acid, and propionic acid produced in least amount. Fermentation with INU led to the highest level of total SCFAs, butyric acid and propionic acid within the young adult group. Interestingly, the SCFAs levels became statistically insignificant between INU and the pectins after 24 h fermentation by the elderly microbiota. When comparing the two age groups, elderly microbiota showed lower capability of utilizing inulin for butyric acid production, but no difference utilizing pectins, compared to young adults. The fact that microbiota of the young adult group generated significantly higher concentrations of butyric acid than that of the elderly with INU indicated that the bifidogenic effect of inulin is age dependent. Furthermore, no significant differences were identified on BCFAs and valeric acid production among substrates or between age groups (p-values listed in Supplementary Table 3).

Pearson's correlation between cumulative acid production and microbial taxa at species level are summarized in Figure 6.

10.3389/fmicb.2023.1207837

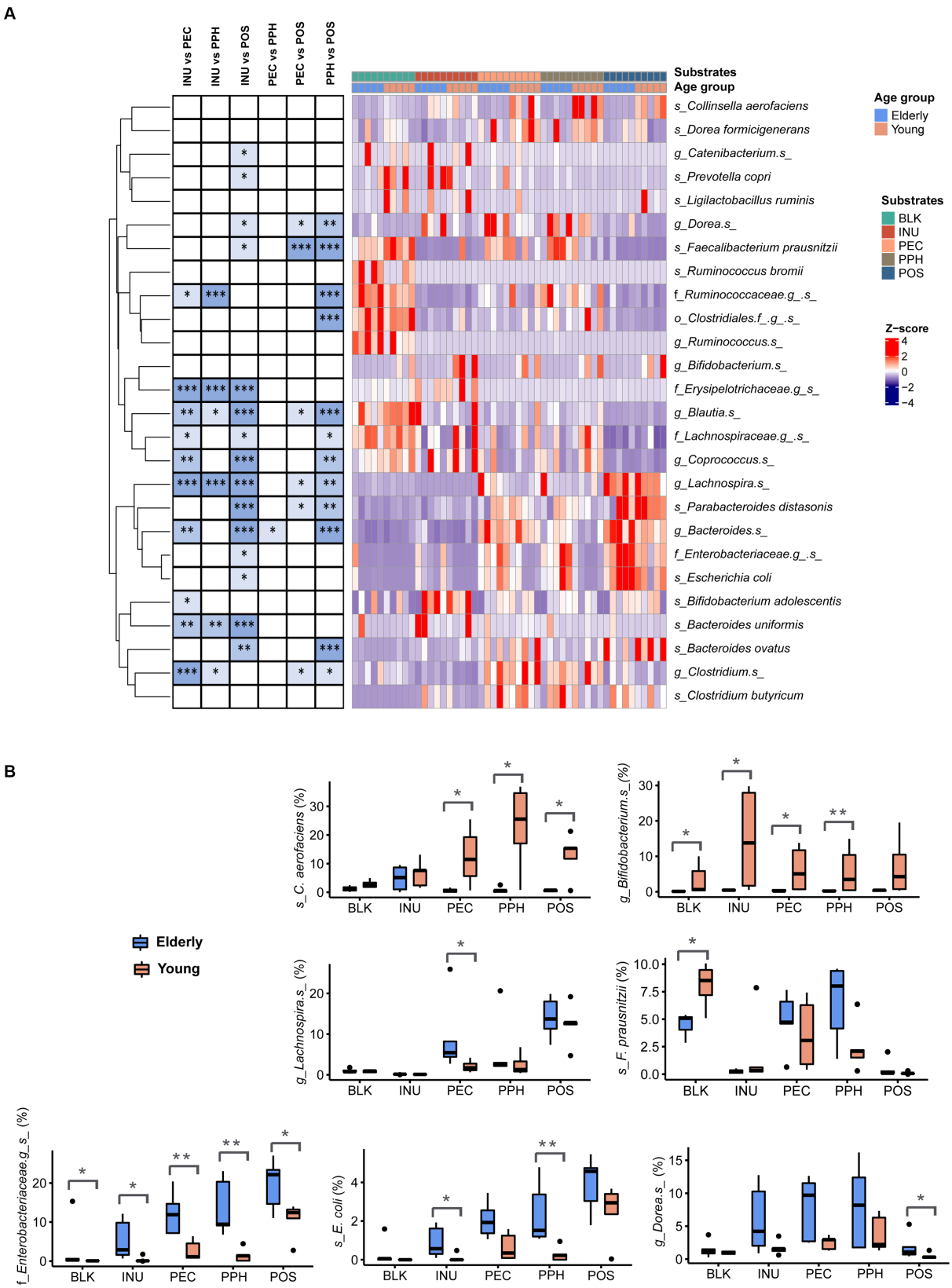

FIGURE 4
(A) Differentially abundant taxa (summarized at species level) from pairwise comparisons between the substrates at 24 h end point of CoMiniGut fermentation, as determined by DESeq 2 analysis. Relative abundances of the taxa were row-wise scaled and visualized in heatmap, where significant *p*-values were indicated with asterisks on the left. **(B)** Relative abundances of selected taxa shown by box plots and compared between elderly group (n = 5) and young group (n = 5). BLK, blank control; INU, inulin; PEC, pectin; PPH, partly hydrolyzed pectin; POS, pectin oligosaccharides. The labels of *, **, or *** indicate *p*-values < 0.05, < 0.01, or < 0.001, respectively.

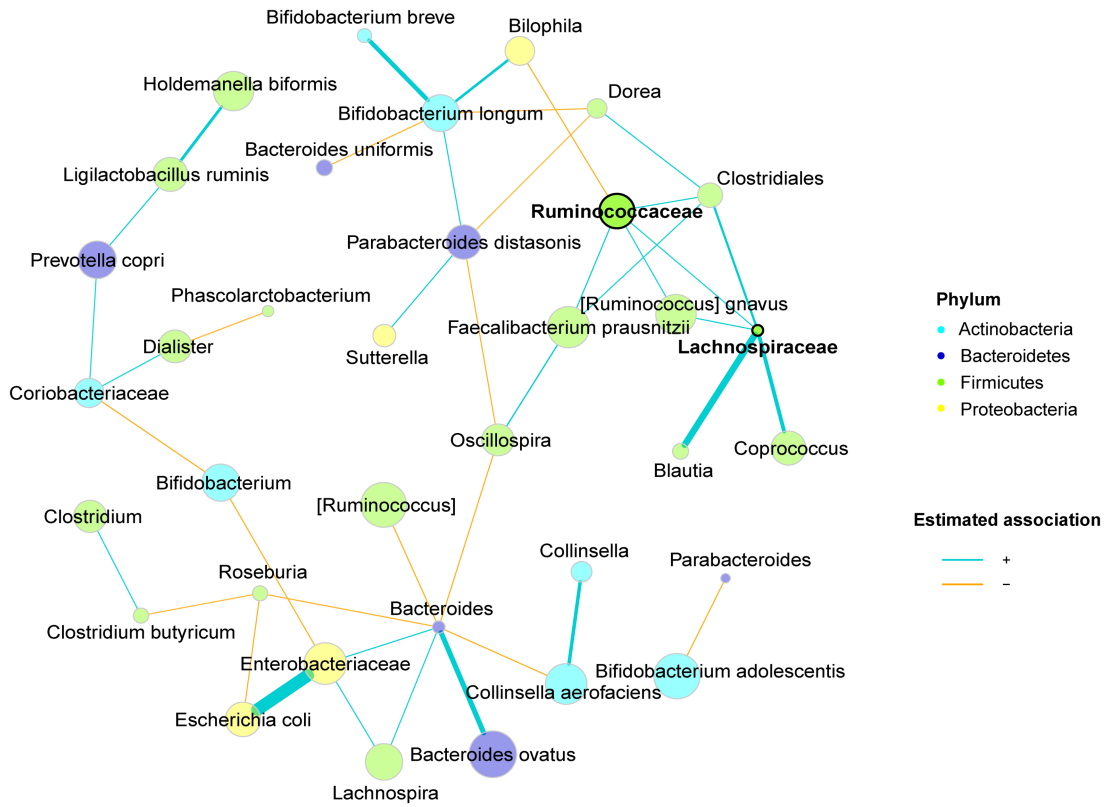

FIGURE 5
Microbiota co-occurrence network of CoMiniGut fermentation of inulin and pectins using fecal inoculums from either elderly donors (n = 5), or young donors (n = 5). Taxa are summarized at species level, with phylum level information indicated by node colors. Nodes are defined as hubs based on eigenvector centrality and are highlighted by bold text and borders. Edge thickness and node sizes correspond to similarity values, and centered log-ratio transformed relative abundances of corresponding taxa, respectively.

Interestingly, butyric acid, propionic and valeric acid showed similar correlations with specific species, whereas acetic acid often showed opposite correlations with the same species. Positive correlation with acetic acid levels were observed for *F. prausnitzii* and *Clostridium* spp., which were highly abundant species in PEC and PPH fermentations. The species favored by POS, such as *Lachnospira* spp., *P. distasonis*, *Bacteroides* spp., and *B. ovatus*, correlated negatively with butyric and/or propionic acid production. Abundances of *B. adolescentis*, *Coprococcus* spp., *Blautia* spp. and *P. copri*, which were enriched species in INU fermentations, positively correlated with the levels of butyric and/or propionic acid. Finally, *C. aerofaciens* and *Bifidobacterium* spp., which were found significantly abundant in the young adult group, correlated positively with butyric acid. *E. coli* and the unidentified species from family *Enterobacteriaceae*, specifically found in the elderly group, correlated negatively with butyric acid.

4. Discussion

4.1. Effects of pectins on the gut microbiota in relation to structural differences

PEC and its derivatives, PPH and POS, were included in the same experimental setup to study the impact of MW of pectin on their fermentation by gut microbiota. Fermentation of PPH resulted in similar fermentation profiles as the parent pectin polysaccharide PEC, in terms of both microbial diversity and relative abundances of bacterial groups. Both substrates selectively promoted the abundances of *F. prausnitzii*, *Dorea* spp., *Blautia* spp. and *Clostridium* spp. after 24 h *in vitro* fermentation, probably due to their capacity to degrade the polysaccharide backbones of pectin (Lopez-Siles et al., 2012). *F. prausnitzii* is one important primary pectin-degrader, whose activity releases sugar units from the pectin backbone for further consumption by secondary metabolizers (Elshahed et al., 2021). In addition to being one of the most abundant species present in the gut microbiota of healthy humans, *F. prausnitzii* is considered a beneficial bacterium to treat gut inflammation (Lopez-Siles et al., 2012; Miquel et al., 2013; Heinken et al., 2014). The ability of PEC and PPH to promote the growth of *F. prausnitzii* is promising for the elderly population, who are vulnerable to age-related inflammation (An et al., 2018; Míguez et al., 2020). In accordance with the present findings, our previous *in vitro* study exploring the effects of pectins (Larsen et al., 2019), found that the abundances of *F. prausnitzii*, together with family *Ruminococcaceae*, were most stimulated by high methylated lemon pectin. Furthermore, we found a positive correlation between acetic acid production and *F. prausnitzii*, which agreed with a previous study showing that *in vitro* growth of *F. prausnitzii* was stimulated by presence of acetate in the medium (Heinken et al., 2014).

TABLE 1 Cumulative production of short-and branched-chain fatty acids (SCFAs/BCFAs) in mmol or μmol per gram of substrates (INU, inulin; PEC, pectin; PPH, partly hydrolyzed pectin; POS, pectin oligosaccharides) at 24 h end point of CoMiniGut fermentation[#].

Organic acids	Substrates				
	INU	PEC	PPH	POS	*p*-Value*
ELDERLY					
Major SCFAs (mmol/g)					
Acetic acid	1.86 (0.26)	2.34 (0.28)	2.32 (0.37)	2.14 (0.26)	0.07
Propionic acid	1.11 (0.88)	0.76 (0.09)	0.72 (0.11)	0.66 (0.28)	0.45
Butyric acid	1.60 (0.75)[†]	1.04 (0.61)	1.15 (0.63)	0.98 (0.53)	0.44
Total	4.56 (1.12)[†]	4.15 (0.3)[†]	4.2 (0.77)	3.78 (0.65)	0.48
BCFAs (μmol/g)					
Isobutyric acid	9.17 (1.40)	10.87 (5.49)	15.78 (7.24)	11.21 (13.89)	0.29
Isovaleric acid	3.68 (2.76)	7.95 (4.3)	9.34 (6.16)	8.95 (13.23)	0.26
2-Methylbutyric acid	2.98 (1.75)	4.99 (2.82)	6.67 (5.17)	6.26 (8.46)	0.51
Total	15.83 (5.09)	23.8 (12.22)	31.8 (17.71)	26.43 (35.55)	0.36
Other (μmol/g)					
Valeric acid	33.61 (34.65)	13.33 (12.61)	19.38 (17.38)	2.93 (1.89)	0.16
YOUNG					
Major SCFAs (mmol/g)					
Acetic acid	1.91 (0.73)	2.31 (0.42)	2.27 (0.47)	1.89 (0.38)	0.44
Propionic acid	1.3 (0.43)[a]	0.78 (0.27)[ab]	0.82 (0.37)[ab]	0.6 (0.2)[b]	**0.02**
Butyric acid	2.84 (0.76)[a]	1.47 (0.35)[b]	1.69 (0.49)[b]	1.45 (0.48)[b]	**0.002**
Total	6.05 (0.5)[a]	4.56 (0.24)[b]	4.78 (0.25)[b]	3.94 (0.22)[c]	**<0.001**
BCFAs (μmol/g)					
Isobutyric acid	16.43 (8.8)	21.89 (13.48)	22.41 (5.41)	11.61 (8.51)	0.27
Isovaleric acid	6.37 (4.07)	15.62 (12.51)	13.48 (4.18)	8 (7.56)	0.24
2-Methylbutyric acid	5.93 (4.45)	10.04 (7.84)	9.54 (3.76)	6.05 (5)	0.51
Total	28.73 (16.38)	47.56 (33.53)	45.42 (11.89)	25.66 (20.16)	0.31
Other (μmol/g)					
Valeric acid	14.65 (19.59)	42.84 (76.64)	74.62 (125.54)	50.2 (105.93)	0.65

[#]Values with different superscript letters were significantly different from each other in the same row, with their averages ranked from higher to lower following the order a to c.
*Difference in specific acid concentrations among the four substrates within the same age group.
[†]Significantly different concentrations of the same acids between elderly and young on the same substrates ($p < 0.05$).The results are shown as means (standard deviations).

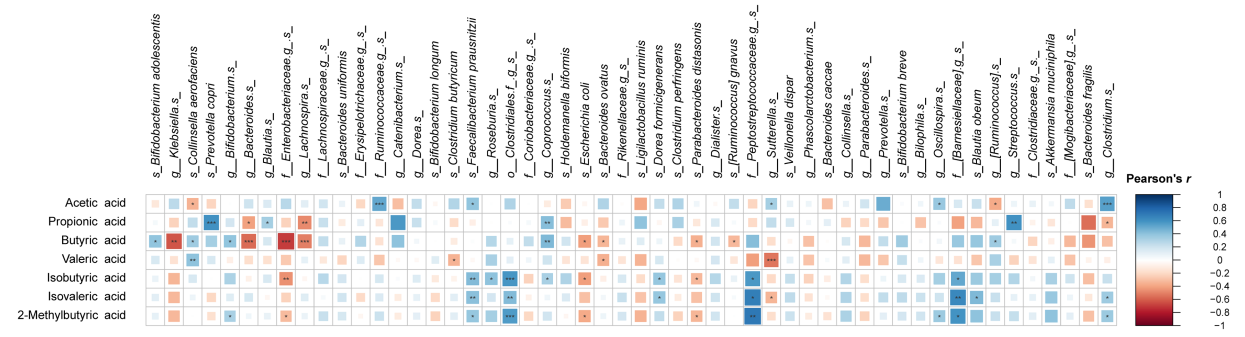

FIGURE 6
Pearson's correlation between relative abundances of microbial taxa (summarized at species level) and short-and branched-chain fatty acid concentrations at 24 h end point of CoMiniGut fermentation. The areas of colored squares correspond to the absolute values of correlation coefficients (*r*). The labels of *, **, or *** indicate *p*-values <0.05, <0.01, or <0.001, respectively.

Fermentation with POS, having the lowest MW, resulted in the lowest Shannon diversity index and a significantly different beta diversity based on Bray-Curtis compared to PEC and PPH. The Shannon diversity index estimates richness and evenness of a microbial community, and a lower value is related to lower stability or less homeostasis of the human microbiome (An et al., 2018). Although several previous *in vitro* studies have reported an increased bifidogenic effect of lower MW pectins and POS (Olano-Martin et al., 2002; Gómez et al., 2016; Ferreira-Lazarte et al., 2018), we did not observe such effects in fermentations with POS in the current set-up. The lower bifidogenic effects of POS from our study than the previous studies could be due to structural differences of POS since they were derived from different parent pectins (Pascale et al., 2022). The species that were promoted by POS in the current study included *Lachnospira* spp., *P. distasonis*, *Bacteroides* spp., and *B. ovatus*. In contrast to PEC and PPH, the beneficial species *F. prausnitzii*, was almost depleted after 24 h fermentation with POS. Microbial utilization of large pectin polysaccharides requires extracellular breakdown of the backbone by pectinolytic activities before intracellular consumption (Elshahed et al., 2021). We speculate that the capability of *F. prausnitzii* to degrade the polymer backbone of PEC and PPH might account for its specificity to pectin polysaccharides instead of oligosaccharides.

Another reason for the differences observed in microbiota profiles could be a slower fermentation of PEC and PPH compared to POS, due to the time needed to degrade the polymer structures of PEC and PPH. The relatively faster fermentation of POS by the primary pectin-degraders could be already followed by enrichment of the secondary metabolizers by cross-feeding interactions within 24 h (Bang et al., 2018), leading to different microbiota composition compared to PEC and PPH. This hypothesis of slow fermentation is supported by one *in vitro* study that showed a trend from rise to decline of relative abundances of *F. prausnitzii* during fermentation with methylated pectin oligosaccharides (Onumpai et al., 2011). A slow fermentation of pectins may be more promising in the sense that the beneficial saccharolytic activities could be prolonged to the distal colon (Tingirikari, 2018). Nevertheless, the SCFAs and BCFAs profiles of all three pectins were comparable in this study, implying functional redundancy of the gut microbiome on pectin fermentation pathways (Reichardt et al., 2018).

4.2. Effects of pectins on the gut microbiota in relation to donor age

Donors' age was another factor affecting the fermentation profiles. The fecal microbiota of the elderly group in the blank control (inoculum) had lower levels of *F. prausnitzii* and *Bifidobacterium* spp., while the family *Enterobacteriaceae* was enriched, compared to the young adult group. After 24 h fermentation with pectins, the phylum Bacteroidetes, which is often equipped with pectinolytic enzymes, was increased relatively more in the elderly group. In contrast, the young adult group exhibited a higher enrichment of the phylum Actinobacteria, which generally includes secondary metabolizers instead of primary pectin-degraders (Chung et al., 2017; Tingirikari, 2018). The different microbial profiles at 24 h of fermentation between the two age groups may indicate a slower fermentation of pectins by elderly gut microbiota, as the elderly microbiota were still dominated by the primary pectin-degraders.

Interestingly, the relative abundances of *F. prausnitzii*, although lower in the elderly inoculum, were equally abundant in both age groups, after 24 h fermentation with PEC and PPH. Several other bacterial taxa were found to be associated with donor age. Among them, *C. aerofaciens*, which levels were comparably low in the inoculum of both age groups, was promoted by all pectins in the young adult group, while almost absent in the elderly group. In contrast, species from family *Enterobacteriaceae* and *E. coli* were much more abundant in the elderly group at the end of fermentation. In accordance, we found a negative correlation between *C. aerofaciens* and the cluster comprising *Enterobacteriaceae* and *E. coli* in the microbial network. These findings are in line with those of Miguez et al., who reported an increased growth of *F. prausnitzii* and near absence of genus *Collinsella* in POS *in vitro* fermentations with a pooled elderly fecal inoculum (Míguez et al., 2020). The species *C. aerofaciens* showed a positive correlation with butyric acid production, and in accordance with our results, Qin et al. (2019) reported it as a butyrate-producing strain. Several studies found higher prevalence of *C. aerofaciens* in healthy controls, compared to patients with cystic fibrosis or inflammatory bowel disease (IBD; Miragoli et al., 2017; Malham et al., 2019; Quagliariello et al., 2020), suggesting its association with a healthy microbiome. The family *Enterobacteriaceae*, including *E. coli*, have been reported to possess genes encoding pectinases, however, *in vitro* studies demonstrated non-promoting and anti-adhesive properties of pectins against pathogenic *E. coli* strains in human cell models (Di et al., 2017; Prandi et al., 2018).

Unlike other *Bifidobacterium* spp., *B. adolescentis* was equally stimulated by pectins in both age groups, and it was isolated from other species in the microbial network. The high relative abundance of *B. adolescentis* among elderly has also been observed in previous studies (Míguez et al., 2020). A recent review has listed evidence showing that *B. adolescentis* has a potential key role in modulating gut-brain axis interactions by producing gamma aminobutyric acid (GABA), which inhibits anxiety and depression (Barrett et al., 2012; Sharma et al., 2021). Furthermore, *B. adolescentis* was found to be anti-inflammatory and had an anti-viral effect against Noroviruses (Li et al., 2016; Sharma et al., 2021).

Despite the different microbiota composition observed between the two age groups, their microbial richness and evenness were similar. The 24 h cumulative production of SCFAs and BCFAs from the pectins were also comparable, except for a slightly lower total SCFAs level observed in fermentations with PEC. This finding further confirmed the high level of functional redundancy of pectin fermentation for SCFA production by microbes in the human gut levels out the age effect.

4.3. Comparative effects of pectins and inulin on the gut microbiota composition and SCFA production

In the present study, we found the well-known bifidogenic and butyrogenic effects of inulin drastically reduced in fermentations with the gut microbiota of the elderly population, in an *in vitro* experimental setup. The reduced bifidogenic effect of inulin with elderly gut microbiota has also been reported in literature. An et al. (2021) noticed less consistent increase of *Bifidobacterium* spp. abundances with fermentation of traditional bifidogenic ingredients,

including inulin, by pre-frail elderly compared to adult controls, which the authors suggested was due to a reduced efficiency in carbohydrate degradation of the pre-frail elderly gut microbiota. Furthermore, they found that the lower level of *Bifidobacterium* spp. allowed utilization of inulin by other bacterial groups, e.g., *Blautia* spp. (An et al., 2021). Some human intervention studies found an increase in bifidobacterial prevalence with inulin supplementation (Marteau et al., 2011; Kiewiet et al., 2021). However, these intervention studies only included elderly participants, without a control group of younger adults while it is therefore difficult to compare the two age groups. In the current study, enriched *Enterobacteriaceae* family and *E.coli* were detected in elderly group with inulin, which had negative correlations with butyrate production, as well as negative relationships with *Bifidobacterium* spp. Production of SCFAs from carbohydrates is believed to be highly reproducible despite inter-individual variations in gut microbiota compositions (Reichardt et al., 2018). The drastic reduction of the butyrogenic effect of inulin observed in the current study indicates a loss of functional genes in the elderly gut microbiota which encodes SCFA synthesis, and possibly a lower level of functional redundancy of the gut microbiota in utilizing inulin, compared to that of pectins. *F. prausnitzii* was reported to be another degrader of inulin in the human gut in literature (Park et al., 2022). However, the selective stimulating effects of inulin on *F. prausnitzii* was not observed in the current study. The inulin-utilizing capabilities varied among different strains of *F. prausnitzii* (Lopez-Siles et al., 2017). The strains of *F. prausnitzii* found in the current study could not be those efficient degraders of inulin. As limited by the sequencing technique used, we were not able to study the gut microbes at strain level.

Overall, both inulin and pectins led to distinct fermentation profiles for both the elderly and the young adult groups. In general, effects of pectins on the gut microbiota were more specific and less dependent on the initial microbiota of the fecal inoculum compared to inulin, confirming the results obtained by a previous study (Cantu-Jungles et al., 2021). Pectin fermentations were characterized with enriched *Bacteroides* spp., *P. distasonis*, *Lachnospira* spp. and *Clostridium* spp., with a specific promotion of *F. prausnitzii* by pectin polymer structures, as well as a specific increase in *C. aerofaciens* found in gut microbiota from young donors. Out of the aforementioned species, *Bacteroides* spp., *P. distasonis*, *Lachnospira* spp. and *F. prausnitzii* are primary pectin-degraders equipped with pectinases, while the remaining ones would utilize released sugars for metabolite conversion such as SCFA production (Elshahed et al., 2021). *Bifidobacterium* spp. are known to encode enzymes like β-fructosidase for inulin degradation (Gibson et al., 2017). However, this genus is not able to degrade pectins and may function as secondary metabolizers via cross-feeding interactions (Yang et al., 2013). Although *Bifidobacterium* is not a butyrate-producer (Sarbini and Rastall, 2011), its abundance positively correlated with butyrate levels in the current study, indicating the existence of cross-feeding interactions between *Bifidobacterium* and butyrate-producing microbes. As a result, we found that inulin fermentations generated more butyric acid by the young adult group compared to pectins, which generated mainly acetic acid, and this finding is in accordance with previous *in vitro* studies (Johnson et al., 2015; Chung et al., 2016; Bang et al., 2018; Chung et al., 2019; Yu et al., 2020). Clinical trials confirming the consistently induced acetate levels by pectin supplementation are so far rare. Acetic acid might play a role in protecting against pathogens and inflammation (Míguez et al., 2020), which is often associated with aging.

5. Conclusion

By using an *in vitro* colonic fermentation set-up, we showed how the molecular sizes of HM citrus pectins impacted their colonic fermentation by the human gut microbiota. Pectins of large and medium-size molecules led to more similar fermentation profiles compared to pectin oligosaccharides, in terms of the gut microbiota compositions and SCFA productions. The commonly known beneficial gut microbe, *F. prausnitzii*, was specifically stimulated by fermentation of pectin polysaccharides (both large and medium sizes) instead of pectin oligosaccharides. As to the SCFA production, acetic acid was the main SCFA product from all the pectins. Fermentations with inulin led to microbial profiles different from those of the pectin substrates, in particular higher increase in *Bifidobacterium* spp. and production of butyric acid were seen. Donor age also influenced the fermentation results of both inulin and pectins. However, in contrast to the obviously reduced bifidogenic and butyrogenic effects of inulin on the elderly gut microbiota, fermentations of pectins were less dependent on the donor age. Therefore, HM citrus pectins of high and medium molecular sizes showed the most potential to improve age-related dysbiosis of the elderly gut microbiota. Although an *in vitro* experimental setup is an efficient screening tool to evaluate and compare the potential effects of different substrates on the human gut microbiota, the observed effects should be further confirmed by human intervention studies.

Data availability statement

The data presented in the study are deposited in the NCBI database under BioProject PRJNA985075, https://www.ncbi.nlm.nih.gov/bioproject/PRJNA985075.

Ethics statement

The studies involving human participants were reviewed and approved by the Ethical Committee of the Capital Region of Denmark (H-15001754; Wiese et al., 2018). Written informed consent to participate in this study was provided by the participants.

Author contributions

LJ and NL: conceptualization and supervision. FG: experiments, data analysis, and writing—draft preparation. BK: SCFA analysis. NL, NP, FR, SP, BK, and LJ: writing—review and editing. All authors contributed to the article and approved the submitted version.

Funding

This project was financially supported by the Innovation Fund Denmark (Case Number 0154-00018A).

Acknowledgments

We acknowledge all the donors who generously provided the fecal samples. We would like to thank Britta Pugholm (CP Kelco,

Denmark) for helping with the analytical characterization of pectin structures; Janne Riis Hansen and Helle Bech Olsen (both from CP Kelco, Denmark) for helping with POS preparation; Denitsa Vladimirova Stefanova for her help with 16S rRNA gene sequencing; and Beinta Unni Marr, Birgit Michelsen and Dennis Sandris Nielsen for their valuable suggestions to the study.

Conflict of interest

FG, NP, FR, and SP are employees of CP Kelco Inc., a producer of commercial pectin.

The remaining authors declare that the research was conducted in the absence of any commercial or financial relationships that could be construed as a potential conflict of interest.

Publisher's note

Supplementary material

The Supplementary material for this article can be found online at: https://www.frontiersin.org/articles/10.3389/fmicb.2023.1207837/full#supplementary-material

References

An, R., Wilms, E., Logtenberg, M. J., Van Trijp, M. P. H., Schols, H. A., Masclee, A. A. M., et al. (2021). *In vitro* metabolic capacity of carbohydrate degradation by intestinal microbiota of adults and pre-frail elderly. *ISME Commun.*:1. doi: 10.1038/s43705-021-00065-5

An, R., Wilms, E., Masclee, A. A., Smidt, H., Zoetendal, E. G., and Jonkers, D. (2018). Age-dependent changes in Gi physiology and microbiota: time to reconsider? *Gut* 67, 2213–2222. doi: 10.1136/gutjnl-2017-315542

An, R., Wilms, E., Smolinska, A., Hermes, G. D. A., Masclee, A. A. M., De Vos, P., et al. (2019). Sugar beet pectin supplementation did not Alter profiles of fecal microbiota and exhaled breath in healthy young adults and healthy elderly. *Nutrients* 11, 61–72. doi: 10.3390/nu11092193

Bang, S.-J., Kim, G., Lim, M. Y., Song, E.-J., Jung, D.-H., Kum, J.-S., et al. (2018). The influence of in vitro pectin fermentation on the human fecal microbiome. *AMB Express* 8, 1–9. doi: 10.1186/s13568-018-0629-9

Barrett, E., Ross, R., O'toole, P. W., Fitzgerald, G. F., and Stanton, C. (2012). Γ-aminobutyric acid production by Culturable Bacteria from the human intestine. *J. Appl. Microbiol.* 113, 411–417. doi: 10.1111/j.1365-2672.2012.05344.x

Baxter, N. T., Schmidt, A. W., Venkataraman, A., Kim, K. S., Waldron, C., and Schmidt, T. M. (2019). Dynamics of human gut microbiota and short-chain fatty acids in response to dietary interventions with three fermentable fibers. *MBio* 10, E02566–E02518. doi: 10.1128/mBio.02566-18

Buford, T. W. (2017). (dis)trust your gut: the gut microbiome in age-related inflammation, health, and disease. *Microbiome* 5:80. doi: 10.1186/s40168-017-0296-0

Cantu-Jungles, T. M., Bulut, N., Chambry, E., Ruthes, A., Iacomini, M., Keshavarzian, A., et al. (2021). Dietary Fiber hierarchical specificity: the missing link for predictable and strong shifts in gut bacterial communities. *MBio* 12, E01028–E01021. doi: 10.1128/mBio.01028-21

Castanys-Muñoz, E., Martin, M. J., and Vazquez, E. (2016). Building a beneficial microbiome from birth. *Adv. Nutr.* 7, 323–330. doi: 10.3945/an.115.010694

Chung, W. S. F., Meijerink, M., Zeuner, B., Holck, J., Louis, P., Meyer, A. S., et al. (2017). Prebiotic potential of pectin and Pectic oligosaccharides to promote anti-inflammatory commensal Bacteria in the human Colon. *FEMS Microbiol. Ecol.* 93, 127–135. doi: 10.1093/femsec/fix127

Chung, W. S. F., Walker, A. W., Louis, P., Parkhill, J., Vermeiren, J., Bosscher, D., et al. (2016). Modulation of the human gut microbiota by dietary fibres occurs at the species level. *BMC Biol.* 14, 1–13. doi: 10.1186/s12915-015-0224-3

Chung, W. S. F., Walker, A. W., Vermeiren, J., Sheridan, P. O., Bosscher, D., Garcia-Campayo, V., et al. (2019). Impact of carbohydrate substrate complexity on the diversity of the human colonic microbiota. *FEMS Microbiol. Ecol.* 95:Fiy201. doi: 10.1093/femsec/fiy201

De Maesschalck, C., Van Immerseel, F., Eeckhaut, V., De Baere, S., Cnockaert, M., Croubels, S., et al. (2014). Faecalicoccus Acidiformans gen. Nov., Sp. Nov., isolated from the chicken Caecum, and reclassification of *Streptococcus Pleomorphus* (Barnes et Al. 1977), *Eubacterium Biforme* (Eggerth 1935) and *Eubacterium Cylindroides* (Cato et Al. 1974) as Faecalicoccus Pleomorphus comb. Nov., Holdemanella Biformis gen. Nov., comb. Nov. and Faecalitalea Cylindroides gen. Nov., comb. Nov., respectively, within the family Erysipelotrichaceae. *Int. J. Syst. Evol. Microbiol.* 64, 3877–3884. doi: 10.1099/ijs.0.064626-0

Di, R., Vakkalanka, M. S., Onumpai, C., Chau, H. K., White, A., Rastall, R. A., et al. (2017). Pectic oligosaccharide structure-function relationships: prebiotics, inhibitors of *Escherichia Coli* O157: H7 adhesion and reduction of Shiga toxin cytotoxicity in Ht29 cells. *Food Chem.* 227, 245–254. doi: 10.1016/j.foodchem.2017.01.100

Dixon, P. (2003). Vegan, a package of R functions for community ecology. *J. Veg. Sci.* 14, 927–930. doi: 10.1111/j.1654-1103.2003.tb02228.x

EFSA Panel on Dietetic Products and Allergies (2015). Scientific opinion on the substantiation of a health claim related to "native chicory inulin" and maintenance of Normal defecation by increasing stool frequency pursuant to article 13.5 of regulation (Ec) no 1924/2006. *EFSA J.* 13:3951. doi: 10.2903/j.efsa.2015.3951

Elshahed, M. S., Miron, A., Aprotosoaie, A. C., and Farag, M. A. (2021). Pectin in diet: interactions with the human microbiome, role in gut homeostasis and nutrient–drug interactions. *Carbohydr. Polym.* 255:117388. doi: 10.1016/j.carbpol.2020.117388

Ferreira-Lazarte, A., Kachrimanidou, V., Villamiel, M., Rastall, R. A., and Moreno, F. J. (2018). In vitro fermentation properties of pectins and enzymatic-modified pectins obtained from different renewable bioresources. *Carbohydr. Polym.* 199, 482–491. doi: 10.1016/j.carbpol.2018.07.041

Ferreira-Lazarte, A., Moreno, F. J., Cueva, C., Gil-Sánchez, I., and Villamiel, M. (2019). Behaviour of Citrus pectin during its gastrointestinal digestion and fermentation in a dynamic simulator (Simgi®). *Carbohydr. Polym.* 207, 382–390. doi: 10.1016/j.carbpol.2018.11.088

Gibson, G. R., Hutkins, R., Sanders, M. E., Prescott, S. L., Reimer, R. A., Salminen, S. J., et al. (2017). Expert consensus document: the international scientific association for probiotics and prebiotics (Isapp) consensus statement on the definition and scope of prebiotics. *Nat. Rev. Gastroenterol. Hepatol.* 14, 491–502. doi: 10.1038/nrgastro.2017.75

Gómez, B., Gullón, B., Yáñez, R., Schols, H., and Alonso, J. L. (2016). Prebiotic potential of Pectins and Pectic oligosaccharides derived from lemon Peel wastes and sugar beet pulp: a comparative evaluation. *J. Funct. Foods* 20, 108–121. doi: 10.1016/j.jff.2015.10.029

González-Herrera, S. M., Herrera, R. R., López, M. G., Rutiaga, O. M., Aguilar, C. N., Esquivel, J. C. C., et al. (2015). Inulin in food products: prebiotic and functional ingredient. *Br. Food J.* 117, 371–387. doi: 10.1108/BFJ-09-2013-0238

Greenhalgh, K., Meyer, K. M., Aagaard, K. M., and Wilmes, P. (2016). The human gut microbiome in health: establishment and resilience of microbiota over a lifetime. *Environ. Microbiol.* 18, 2103–2116. doi: 10.1111/1462-2920.13318

Gu, Z., Eils, R., and Schlesner, M. (2016). Complex Heatmaps reveal patterns and correlations in multidimensional genomic data. *Bioinformatics* 32, 2847–2849. doi: 10.1093/bioinformatics/btw313

Gu, Z., Gu, L., Eils, R., Schlesner, M., and Brors, B. (2014). Circlize implements and enhances circular visualization in R. *Bioinformatics* 30, 2811–2812. doi: 10.1093/bioinformatics/btu393

Heinken, A., Khan, M. T., Paglia, G., Rodionov, D. A., Harmsen, H. J., and Thiele, I. (2014). Functional Metabolic Map Of *Faecalibacterium Prausnitzii*, A Beneficial Human Gut Microbe. *J. Bacteriol.* 196, 3289–3302. doi: 10.1128/JB.01780-14

Holloway, W. D., Tasman-Jones, C., and Maher, K. (1983). Pectin digestion in humans. *Am. J. Clin. Nutr.* 37, 253–255. doi: 10.1093/ajcn/37.2.253

Holscher, H. D. (2017). Dietary Fiber and prebiotics and the gastrointestinal microbiota. *Gut Microbes* 8, 172–184. doi: 10.1080/19490976.2017.1290756

Hui, Y., Tamez-Hidalgo, P., Cieplak, T., Satessa, G. D., Kot, W., Kjaerulff, S., et al. (2021). Supplementation of a lacto-fermented rapeseed-seaweed blend promotes gut microbial-and gut immune-modulation in weaner piglets. *J Anim Sci Biotechnol* 12:85. doi: 10.1186/s40104-021-00601-2

Johnson, L. P., Walton, G. E., Psichas, A., Frost, G. S., Gibson, G. R., and Barraclough, T. G. (2015). Prebiotics modulate the effects of antibiotics on gut microbial diversity and functioning in vitro. *Nutrients* 7, 4480–4497. doi: 10.3390/nu7064480

Kårhus, M. L., Sonne, D. P., Thomasen, M., Ellegaard, A.-M., Holst, J. J., Rehfeld, J. F., et al. (2022). Enterohepatic, Gluco-metabolic, and gut microbial characterization of individuals with bile acid malabsorption. *Gastro. Hep. Adv.* 1, 299–312. doi: 10.1016/j.gastha.2021.12.007

Kiewiet, M. B. G., Elderman, M. E., El Aidy, S., Burgerhof, J. G. M., Visser, H., Vaughan, E. E., et al. (2021). Flexibility of gut microbiota in ageing individuals during dietary Fiber long-chain inulin intake. *Mol. Nutr. Food Res.* 65:E2000390. doi: 10.1002/mnfr.202000390

Lagkouvardos, I., Fischer, S., Kumar, N., and Clavel, T. (2017). Rhea: a transparent and modular R pipeline for microbial profiling based on 16s Rrna gene amplicons. *PeerJ* 5:E2836. doi: 10.7717/peerj.2836

Larsen, N., Bussolo De Souza, C., Krych, L., Barbosa Cahú, T., Wiese, M., Kot, W., et al. (2019). Potential of Pectins to beneficially modulate the gut microbiota depends on their structural properties. *Front. Microbiol.* 10:223. doi: 10.3389/fmicb.2019.00223

Li, D., Breiman, A., Le Pendu, J., and Uyttendaele, M. (2016). Anti-viral effect of *Bifidobacterium Adolescentis* against noroviruses. *Front. Microbiol.* 7:864. doi: 10.3389/fmicb.2016.00864

Lopez-Siles, M., Duncan, S. H., Garcia-Gil, L. J., and Martinez-Medina, M. (2017). *Faecalibacterium Prausnitzii*: from microbiology to diagnostics and prognostics. *ISME J.* 11, 841–852. doi: 10.1038/ismej.2016.176

Lopez-Siles, M., Khan, T. M., Duncan, S. H., Harmsen, H. J., Garcia-Gil, L. J., and Flint, H. J. (2012). Cultured representatives of two major Phylogroups of human colonic *Faecalibacterium Prausnitzii* can utilize pectin, uronic acids, and host-derived substrates for growth. *Appl. Environ. Microbiol.* 78, 420–428. doi: 10.1128/AEM.06858-11

Love, M. I., Huber, W., and Anders, S. (2014). Moderated estimation of fold change and dispersion for RNA-Seq data with Deseq2. *Genome Biol.* 15, 1–21. doi: 10.1186/s13059-014-0550-8

Malham, M., Lilje, B., Houen, G., Winther, K., Andersen, P. S., and Jakobsen, C. (2019). The microbiome reflects diagnosis and predicts disease severity in Paediatric onset inflammatory bowel disease. *Scand. J. Gastroenterol.* 54, 969–975. doi: 10.1080/00365521.2019.1644368

Marteau, P., Jacobs, H., Cazaubiel, M., Signoret, C., Prevel, J. M., and Housez, B. (2011). Effects of chicory inulin in constipated elderly people: a double-blind controlled trial. *Int. J. Food Sci. Nutr.* 62, 164–170. doi: 10.3109/09637486.2010.527323

Mcmurdie, P. J., and Holmes, S. (2013). Phyloseq: An R package for reproducible interactive analysis and graphics of microbiome census data. *PLoS One* 8:E61217. doi: 10.1371/journal.pone.0061217

Míguez, B., Vila, C., Venema, K., Parajó, J. C., and Alonso, J. L. (2020). Prebiotic effects of Pectooligosaccharides obtained from lemon Peel on the microbiota from elderly donors using An in vitro continuous Colon model (Tim-2). *Food Funct.* 11, 9984–9999. doi: 10.1039/D0FO01848A

Miquel, S., Martin, R., Rossi, O., Bermúdez-Humarán, L., Chatel, J., Sokol, H., et al. (2013). Faecalibacterium Prausnitzii and human intestinal health. *Curr. Opin. Microbiol.* 16, 255–261. doi: 10.1016/j.mib.2013.06.003

Miragoli, F., Federici, S., Ferrari, S., Minuti, A., Rebecchi, A., Bruzzese, E., et al. (2017). Impact of cystic fibrosis disease on archaea and bacteria composition of gut microbiota. *FEMS Microbiol. Ecol.* 93, 230–242, Fiw230. doi: 10.1093/femsec/fiw230

Naqash, F., Masoodi, F. A., Rather, S. A., Wani, S. M., and Gani, A. (2017). Emerging concepts in the nutraceutical and functional properties of pectin-a review. *Carbohydr. Polym.* 168, 227–239. doi: 10.1016/j.carbpol.2017.03.058

Olano-Martin, E., Gibson, G. R., and Rastall, R. (2002). Comparison of the in vitro bifidogenic properties of pectins and pectic-oligosaccharides. *J. Appl. Microbiol.* 93, 505–511. doi: 10.1046/j.1365-2672.2002.01719.x

Onumpai, C., Kolida, S., Bonnin, E., and Rastall, R. A. (2011). Microbial utilization and selectivity of pectin fractions with various structures. *Appl. Environ. Microbiol.* 77, 5747–5754. doi: 10.1128/AEM.00179-11

Park, J.-H., Song, W.-S., Lee, J., Jo, S.-H., Lee, J.-S., Jeon, H.-J., et al. (2022). An integrative multiomics approach to characterize prebiotic inulin effects on *Faecalibacterium Prausnitzii*. *Front. Bioeng. Biotechnol.* 10. doi: 10.3389/fbioe.2022.825399

Pascale, N., Gu, F., Larsen, N., Jespersen, L., and Respondek, F. (2022). The potential of Pectins to modulate the human gut microbiota evaluated by in vitro fermentation: a systematic review. *Nutrients* 14:3629. doi: 10.3390/nu14173629

Peschel, S., Müller, C. L., Von Mutius, E., Boulesteix, A.-L., and Depner, M. (2021). Netcomi: network construction and comparison for microbiome data in R. *Brief. Bioinform.* 22:Bbaa290. doi: 10.1093/bib/bbaa290

Prandi, B., Baldassarre, S., Babbar, N., Bancalari, E., Vandezande, P., Hermans, D., et al. (2018). Pectin oligosaccharides from sugar beet pulp: molecular characterization and potential prebiotic activity. *Food Funct.* 9, 1557–1569. doi: 10.1039/C7FO01182B

Qin, P., Zou, Y., Dai, Y., Luo, G., Zhang, X., and Xiao, L. (2019). Characterization a novel butyric acid-producing bacterium *Collinsella aerofaciens* Subsp. Shenzhenensis Subsp. Nov. *Microorganisms* 7, 78–87. doi: 10.3390/microorganisms7030078

Quagliariello, A., Del Chierico, F., Reddel, S., Russo, A., Onetti Muda, A., D'argenio, P., et al. (2020). Fecal microbiota transplant in two ulcerative colitis pediatric cases: gut microbiota and clinical course correlations. *Microorganisms* 8, 1486–1497. doi: 10.3390/microorganisms8101486

Rampelli, S., Candela, M., Turroni, S., Biagi, E., Collino, S., Franceschi, C., et al. (2013). Functional metagenomic profiling of intestinal microbiome in extreme ageing. *Aging (Albany NY)* 5, 902–912. doi: 10.18632/aging.100623

Rastall, R., Diez-Municio, M., Forssten, S., Hamaker, B., Meynier, A., Moreno, F. J., et al. (2022). Structure and function of non-digestible carbohydrates in the gut microbiome. *Benefic. Microbes* 13, 95–168. doi: 10.3920/BM2021.0090

Reichardt, N., Vollmer, M., Holtrop, G., Farquharson, F. M., Wefers, D., Bunzel, M., et al. (2018). Specific substrate-driven changes in human faecal microbiota composition contrast with functional redundancy in short-chain fatty acid production. *ISME J.* 12, 610–622. doi: 10.1038/ismej.2017.196

Roberfroid, M., Gibson, G. R., Hoyles, L., Mccartney, A. L., Rastall, R., Rowland, I., et al. (2010). Prebiotic effects: metabolic and health benefits. *Br. J. Nutr.* 104, S1–S63. doi: 10.1017/S0007114510003363

Roberts, J. L., Liu, G., Darby, T. M., Fernandes, L. M., Diaz-Hernandez, M. E., Jones, R. M., et al. (2020). *Bifidobacterium Adolescentis* supplementation attenuates fracture-induced systemic sequelae. *Biomed. Pharmacother.* 132:110831. doi: 10.1016/j.biopha.2020.110831

Sarbini, S. R., and Rastall, R. A. (2011). Prebiotics: metabolism, structure, and function. *Funct. Food Rev.* 3, 93–106. doi: 10.2310/6180.2011.00004

Sharma, M., Wasan, A., and Sharma, R. K. (2021). Recent developments in probiotics: An emphasis on Bifidobacterium. *Food Biosci.* 41, 100993–101002. doi: 10.1016/j.fbio.2021.100993

Teferra, T. F. (2021). Possible actions of inulin as prebiotic polysaccharide: a review. *Food Front.* 2, 407–416. doi: 10.1002/fft2.92

Tingirikari, J. M. R. (2018). Microbiota-accessible Pectic poly-and oligosaccharides in gut health. *Food Funct.* 9, 5059–5073. doi: 10.1039/C8FO01296B

Wei, T., and Simko, V. (2021). R package 'Corrplot': Visualization of a correlation matrix. (Version 0.92), https://github.com/taiyun/corrplot

WHO (2021). *Ageing and Health [Online]*. Geneva, Switzerland: World Health Organization.

Wickham, H. (2016). *Ggplot2: Elegant graphics for data analysis*, Cham, Springer International Publishing.

Wiese, M., Hui, Y., Holck, J., Sejberg, J. J. P., Daures, C., Maas, E., et al. (2021). High throughput in vitro characterization of Pectins for pig(let) nutrition. *Anim. Microbiome* 3:69. doi: 10.1186/s42523-021-00129-w

Wiese, M., Khakimov, B., Nielsen, S., Sorensen, H., Van Den Berg, F., and Nielsen, D. S. (2018). Cominigut-a small volume in vitro Colon model for the screening of gut microbial fermentation processes. *PEERJ* 6:E4268. doi: 10.7717/peerj.4268

Wilkowska, A., Motyl, I., Antczak-Chrobot, A., Wojtczak, M., Nowak, A., Czyżowska, A., et al. (2021). Influence of human age on the prebiotic effect of pectin-derived oligosaccharides obtained from apple pomace. *Fermentation* 7, 224–236. doi: 10.3390/fermentation7040224

Yang, J., Martínez, I., Walter, J., Keshavarzian, A., and Rose, D. J. (2013). In vitro characterization of the impact of selected dietary fibers on fecal microbiota composition and short chain fatty acid production. *Anaerobe* 23, 74–81. doi: 10.1016/j.anaerobe.2013.06.012

Yu, X., Gurry, T., Nguyen, L. T. T., Richardson, H. S., and Alm, E. J. (2020). Prebiotics and community composition influence gas production of the human gut microbiota. *MBio* 11, E00217–E00220. doi: 10.1128/mBio.00217-20

Zheng, J., Wittouck, S., Salvetti, E., Franz, C., Harris, H. M. B., Mattarelli, P., et al. (2020). A taxonomic note on the genus *Lactobacillus*: description of 23 novel genera, emended description of the genus *Lactobacillus beijerinck* 1901, and union of Lactobacillaceae and Leuconostocaceae. *Int. J. Syst. Evol. Microbiol.* 70, 2782–2858. doi: 10.1099/ijsem.0.004107

frontiers | Frontiers in Microbiology

TYPE Original Research
PUBLISHED 06 July 2023
DOI 10.3389/fmicb.2023.1183598

OPEN ACCESS

EDITED BY
Xiaodong Xia,
Dalian Polytechnic University, China

REVIEWED BY
Sidharth Prasad Mishra,
University of South Florida, United States
Fengjie Sun,
Georgia Gwinnett College, United States

*CORRESPONDENCE
Yan Bao
✉ by_1977@163.com
Long Gao
✉ 15804717362@163.com

†These authors have contributed equally to this work and share first authorship

RECEIVED 14 March 2023
ACCEPTED 12 June 2023
PUBLISHED 06 July 2023

CITATION
Tian C, Li J, Bao Y, Gao L, Song L, Li K and Sun M (2023) Ursolic acid ameliorates obesity of mice fed with high-fat diet via alteration of gut microbiota and amino acid metabolism.
Front. Microbiol. 14:1183598.
doi: 10.3389/fmicb.2023.1183598

Ursolic acid ameliorates obesity of mice fed with high-fat diet via alteration of gut microbiota and amino acid metabolism

Chunfeng Tian[1†], Jie Li[2†], Yan Bao[1,3*], Long Gao[1*], Lixin Song[4], Kai Li[1] and Ming Sun[1]

[1]School of Public Health, Baotou Medical College, Inner Mongolia University of Science and Technology, Baotou, China, [2]School of Public Health, Jiamusi University, Jiamusi, China, [3]Institute of Nutrition and Food Health, Baotou Medical College, Baotou, China, [4]Baotou Disease Prevention Control Center, Baotou, China

Obesity has been regarded as one of the major health problems worldwide. Studies demonstrated that ursolic acid (UA) can significantly ameliorate the progress of obesity. However, whether the effect of UA on obesity depends on the regulation of gut microbiota and metabolism is uncertain. To investigate the regulatory role of UA in obese mice from the perspective of intestinal microbiome and metabolomics analyses, an obese mice model was established with a high-fat diet, and the effect of UA on obesity was evaluated. The alterations of gut microbiota and metabolism related to obesity were evaluated by bioinformatic analysis. The results of the gut microbiota analysis showed that UA intervention could shift the Firmicutes to Bacteroidetes ratio at the phylum level and increase in the genera of *Lactobacillus*, *Bacteroides,* and *Akkermansia*. Additionally, metabolomics analysis showed that the beneficial influence of UA on obesity partly depended on amino acid metabolism. The current study demonstrated the roles of UA in the anti-obesity process, which depends in part on alterations in the gut microbiota and metabolism. Therefore, our findings highlight the potential therapeutic effect of UA on the improvement of diet-induced obesity in humans.

KEYWORDS

ursolic acid, obesity, gut microbiota, metabolism, high-fat diet, metabolomics

1. Introduction

Obesity the third most prevalent isepidemiological factor affecting human health after smoking and AIDS. It is also intimately connected to several chronic illnesses, including cancer, type 2 diabetes, renal disease, liver disease, and heart disease, all of which are detrimental to human health (Medanić and Pucarin-Cvetković, 2012;

Abbreviations: HFD, high-fat diet; TC, total cholesterol; TG, total triglyceride; HDL-C, high-density lipoprotein cholesterol; LDL-C, low-density lipoprotein cholesterol; LEfSe, linear discriminant analysis effect size; OPLS-DA, orthogonal partial least-squares discriminant analysis; UA, ursolic acid; BCAA, branched-chain amino acids; KEGG, Kyoto Encyclopedia of Genes and Genomes; PCoA, principal coordinates analysis.

Pan et al., 2018; Ojulari et al., 2019). Therefore, the search for effective solutions to improve obesity is extremely important. There are several preventive or therapeutic strategies for combating obesity, including lifestyle changes, such as diet and exercise, drug treatment, and surgery. However, these approaches can be less satisfactory in the long term, especially drug therapies, which may have serious adverse effects that lead to their successive withdrawal in recent years (Khera et al., 2016; Clément et al., 2018). Therefore, a more effective method should be explored to improve obesity.

The gut microbiota refers to a complex ecosystem in the human digestive tract that includes bacteria, fungi, viruses, archaea, and protists. It could participate in the regulation of multiple physiological functions that maintain the metabolic homeostasis of the host (Qu et al., 2018; Li et al., 2020; Sun et al., 2022). Gut dysbiosis has various adverse effects on the host and may result in metabolic diseases, especially in the obesity condition, which has been revealed by growing evidence over the last two decades. In mice, *Candida parapsilosis* expansion in the gut has been shown to contribute to the promotion of obesity, mainly in terms of higher body weight, accumulation of fungal lipase, and alteration of serum biochemical indicators (Sun S. et al., 2021). Yu et al. (2022) found that the onset of diabetes type 2 mellitus in obese mice was impeded by gut microbiota disturbance, and glucose decomposition may be the primary mechanism by which the jejunal bacteria control the host metabolism. Meanwhile, Wang et al. (2019) demonstrated the numerous metabolic benefits of orally administering live *Parabacteroides distasonis* in high-fat diet (HFD)-induced obese mice, mainly via controlling weight gain, lowering hyperglycemia and hyperlipidemia, and improving hepatic steatosis through the production of succinate and secondary bile acids. According to the findings, effective regulation of host metabolism by intestinal flora is crucial to the development of obesity.

Plant-derived biologically active products have various biological functions in the regulation of a wide spectrum of diseases (Diarra et al., 2016; de Freitas Junior and de Almeida, 2017; Sehrawat et al., 2017). Ursolic acid (UA) is commonly found in fruits and vegetables. According to reports, UA controls a variety of biological functions, including the modulation of several signaling pathways that may stop the onset of chronic diseases (Seo et al., 2018). Recently, the relation of UA to obesity has been documented extensively. Tang et al. (2022) examined the anti-obesity impact of UA in obese rats induced by high fat and streptozotocin via altering insulin and c-Jun N-terminal kinase signaling pathways. Sun A. et al. (2021) demonstrated the crucial role of UA in improving the obesity and metabolic status of obese mice via increasing irisin production, promoting white adipose tissue beigeing, and lowering weight. Moreover, UA has been shown to have potential therapeutic utility in obesity and diabetes via preventing insulin resistance and hyperinsulinemia and by reversing hyperinsulinemia induced by obesity in rats fed with a HFD (González-Garibay et al., 2020). However, the function of UA on the metabolism and gut microbiota during obesity is largely unexplored, so more studies are needed to ascertain whether UA can affect host metabolic pathways.

The objective of this study was to identify the interrelationship among UA, gut microbiota, and metabolites in obese mice induced by diet. 16S rRNA sequencing was conducted to analyze the gut microbiota in mice receiving a HFD, and a metabolomics analysis was used to investigate the mechanism of UA in obesity from the perspective of microbiome changes. This study provides a useful exploration of the potential mechanisms of UA in the regulation of obesity though microbiomics and metabolomics analysis and further demonstrated the beneficial effect of UA on obesity improvement.

2. Materials and methods

2.1. Animals and diets

In the current research, C57BL/6J male mice ordered form SiPeiFu Biotechnology Co., Ltd (Beijing, China). Then 5-week-old mice were firstly housed under a 12 h light/dark cycle with unrestricted access to food and water, the temperature and humidity of the feeding environment were controlled at 24 ± 1°C and 55 ± 5%, respectively. After 1 week adaptive feeding, the mice were separated equally into three groups for treatment (8 mice per group): (1) control group (fed with the normal diet), (2) HFD group (fed with the HFD), (3) HFD + UA group (fed with the HFD and given a moderate dose of UA, 100 mg/kg/d). The UA was purchased from Xi'an Ruilin Biotechnology Co., Ltd. (Xi'an, China). The normal-fat diet (10 kcal% fat, 20 kcal% protein, and 70 kcal% carbohydrate, catalog no. D12450B) and the HFD (60 kcal% fat, 20 kcal% protein, and 20 kcal% carbohydrate, catalog no. D12492) were Research Diets purchased from Xiaoshuyoutai Biotechnology Co., Ltd. (Beijing, China). During the experiment, the body weight of the mice was record once per week. The treatment were continued for 8 weeks.

2.2. Sample collection and preparation

Fresh fecal samples were obtained after an 8-week treatment and stored at −80°C for the gut microbiota and metabolite analyses. After the last treatment administration, mice were allowed with free access to water but no food for 12 h, then were anesthetized via intraperitoneal injection of 1.25% tribromoethanol and the blood samples from the eye orbit were collected. The liver, epididymal white adipose tissue (eWAT), perirenal white adipose tissue (pWAT), and mesenteric fat were stripped and weighed immediately at 4°C after mice were sacrificed, and then maintained at −80°C for the experiment. The collected blood was then centrifuged at 3,000 rpm for 15 min to obtain the serum. After being frozen at −80°C, the serum biochemical indexes were tested using assay kits (Jiancheng, China), including total cholesterol (TC), total triglyceride (TG), high-density lipoprotein cholesterol (HDL-C), and low-density lipoprotein cholesterol (LDL-C). The following formula was used to calculate the index:

$$\text{Fat/body weight ratio} = \text{Visceral fat weight (g)}/\text{Body weight (g)} \times 100\%$$

$$\text{Visceral fat (g)} = \text{eWAT weight (g)} + \text{pWAT weight (g)} + \text{Mesenteric fat weight (g)}$$

2.3. Histological analysis of liver

After being treated in 4% formaldehyde solution for paraffin sections, partial liver samples were cut into 5-μm-thick slices for hematoxylin-eosin staining. An optical microscope was used to take pictures of the dyed liver sections (Olympus, Tokyo, Japan).

2.4. Bioinformatic analysis of gut microbiota

We extracted genomic DNA from fecal samples using the DNA Extraction Kit (Nobleryder, China) following the manufacturer's instructions. The 16S rRNA gene's hypervariable region V3–4 was amplified through PCR using a specific primer. Wekemon Biotechnology Co., Ltd. (Guangzhou, China) carried out the sequencing using the NovaSeq 6000 platform. Quantitative Insights Into Microbial Ecology (QIIME, version 2.0) software was used to obtain quality filter raw sequences. Paired-end reads were assembled using FLASH. Following the detection of chimeras, the remaining high-quality sequences were clustered into operational taxonomic units (OTUs) at 97% sequence identity by UCLUST. A representative sequence was selected from each OTU using default parameters. OTU taxonomic classification was then conducted by BLAST searching the representative sequences set against the Green Genes Database. Based on the emergence of OTUs between groups a Venn diagram was generated using the R package to visualize the shared and unique OTUs between groups. The core-diversity plugin within the open-source QIIME 2 platform was used to calculate the alpha and beta diversity. The specific gut microbiota was analyzed through linear discriminant analysis (LDA) and effect size (LEfSe) analyses. A non-parametric factorial Kruskal–Wallis sum-rank test was used for LEfSe to determine the differences in abundance between groups and used LDA to assess the effect size of each feature, and the threshold on the logarithmic score of LDA analysis was set to 2.0. Spearman's analysis was used to determine the relationship between microbial communities and serum biochemical parameters based on the relative abundance of microbial species at various taxon levels. All settings were set to default, unless otherwise stated.

2.5. Metabolomic profiling analysis

To obtain the supernatant for LC-MS analysis, fecal samples (100 mg) were mixed with extract solution (methanol:water = 4:5, v:v) and centrifuged. A Vanquish UHPLC System from Wekemon Biotechnology Co., Ltd. (Guangzhou, China) was used to perform the LC separation. Orthogonal partial least-squares discriminant analysis (OPLS-DA) was used to compare metabolites in different groups. The variable influence on projection value together with the p-value obtained using the two-tailed t-test (VIP value > 1.0 and p-value < 0.05) were used to select the potential biomarkers. The Human Metabolome Database[1] was selected to compare the typical MS/MS fragments. The MetaboAnalyst website[2] based on the Kyoto Encyclopedia of Genes and Genomes (KEGG) database[3] was used for pathway enrichment analyses.

2.6. Statistical analysis

All data were analyzed using one-way ANOVA in SPSS 24.0 (IBM), and Prism 8.0.2 software (GraphPad Software, La Jolla, CA, USA) was used to create all graphics. Spearman correlation was used to examine the correlation between significant microbial communities and metabolism; p-value < 0.05 indicated significance.

3. Results

3.1. Effects of UA administration on physiological, serological, and liver histopathological changes

In this study, we investigated the effects of UA on obese mice by constructing an obesity model as shown in **Figure 1A**. According to **Figure 1B**, the body weight of mice in the HFD group increased rapidly relative to that of those in the control group over the course of 8 weeks. Nevertheless, UA supplementation decreased this increment ($p < 0.05$). In addition, the HFD could significantly increase the ratio of fat to body weight and visceral fat in contrast to the control, and the UA treatment also reduced the elevated levels but still remained above the normal level ($p < 0.05$) (**Figures 1C, D**).

Additionally, the levels of TC, TG, HDL-C, and LDL-C were measured to ascertain the potential contribution of UA to the reduction of lipid buildup in mice (**Figures 1E–H**). The HFD-fed mice had higher TC, TG, and LDL-C levels in serum after 8 weeks of feeding relative to the control group ($p < 0.05$), and these increases were lowered by UA administration, but still remained above normal levels. Interestingly, HDL-C presented high levels of expression in the HFD group relative to those in the control group and remained significantly higher after UA intervention.

Hematoxylin-eosin staining of liver samples was used to assess the triacylglycerol accumulation. The result showed that following the 8-week treatment period, the HFD-fed mice had substantial lipid droplet buildup relative to those in the control group. This accumulation was greatly alleviated after UA intervention (**Figures 1I–K**), suggesting that UA can successfully limit the buildup of liver lipids and slow the onset of fatty liver in HFD-group mice.

3.2. Effects of UA on gut microbiota diversity of mice

For the 16S rRNA sequencing results included Sparsity curve analysis and OTUs Venn diagram were shown in

1 https://hmdb.ca/

2 https://www.metaboanalyst.ca/

3 https://www.kegg.jp/kegg/pathway.html

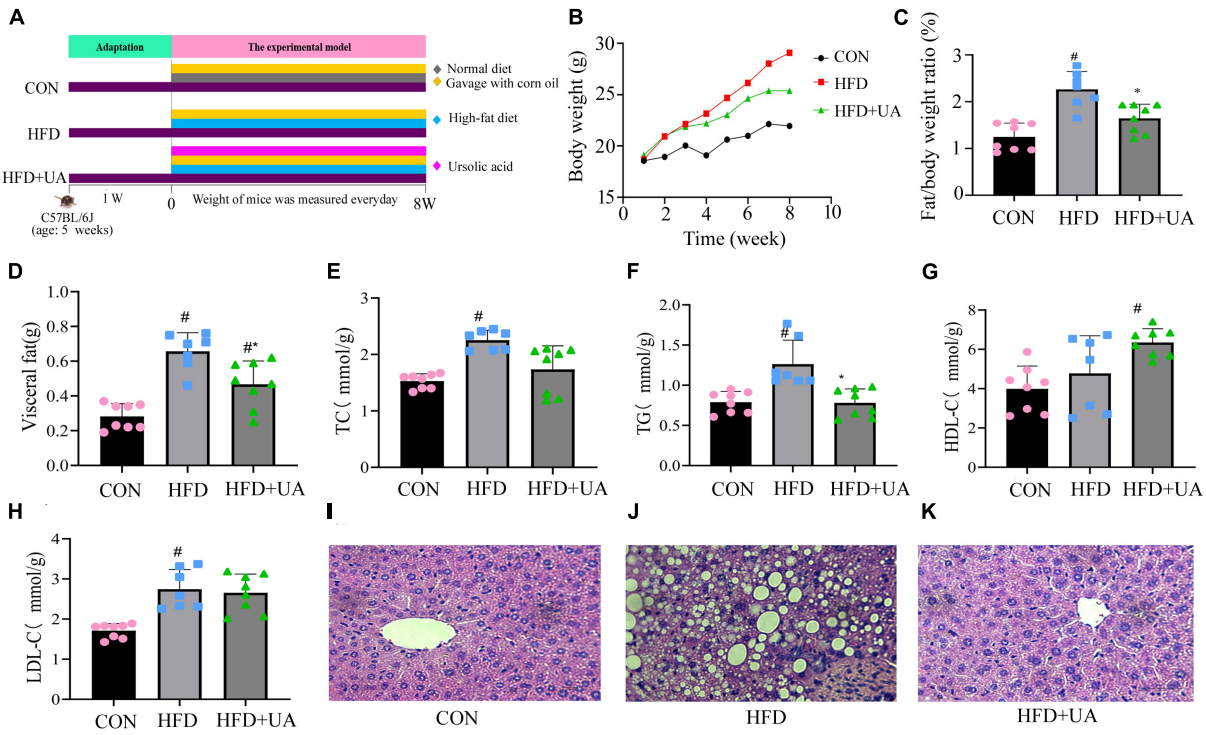

FIGURE 1
Effect of ursolic acid administration on physiological, serological, and liver histopathological changes. **(A)** Experimental design **(B)** Body weight growth; **(C)** ratio of fat to body weight; **(D)** visceral fat; **(E–H)** Changes in serum biochemical indexes in each group of mice; **(I–K)** hemotoxin-eosin staining of liver tissue sections of mice in different groups ($^{\#}P < 0.05$ compared to control group, $^{*}p < 0.05$ relative to the high-fat diet group).

Supplementary Figures 1, 2. Alpha diversity analysis was used to evaluate the diversity of the microbiota community in each sample, which was presented by diversity indices including Shannon, Ace, and Chao1. The Shannon index reflects the richness and evenness of a community, whereas the Ace and Chao1 indices were positively correlated with community richness (Figures 2A–C). In contrast to those in the control group, the Ace and Chao1 indexes in the HFD group were considerably lower ($p < 0.05$) and greatly increased after UA supplementation. According to the Shannon index, less diversity was present in the HFD group, and there was no improvement as a result of UA supplementation.

Beta diversity analysis in mice was explained using the Principal Coordinates Analysis (PCoA). According to Figure 2D, there was a clear division in the microbiota community among the control and HFD groups, whereas in the HFD and UA treatment groups, the structure of the microbiota community was closer, suggesting that UA and HFD may influence the structure of the gut microbiota.

3.3. Effects of UA on the taxonomic composition of the gut microbiota

The relative bacterial abundance of the different groups was evaluated to identify specific taxa in the UA treatment group. According to Figure 3A, Firmicutes and Bacteroidetes were the dominant phyla in all groups. HFD treatment significantly changed the gut microbiota composition and structure compared with control group. For example, Firmicutes and Proteobacteria increased significantly, which was accompanied with decreased Bacteroidetes and Verrucomicrobia. Notably, the Firmicutes to Bacteroidetes (F/B) ratio was 0.93 in the control group, and increased rapidly to 2.82 after the HFD treatment, but the changes were reversed after UA supplementation, resulting in a lower F/B ratio of 2.22, which was accompanied by an increase in Verrucomicrobia.

At the genus level, the relative abundance of *Akkermansia*, *Allobaculum,* and *Lactobacillus* decreased and that of *Oscillospira*, *Ruminococcus*, *Parabacteroides,* and *Erysipelotrichaceae-Clostridium* increased in the HFD group (Figure 3B). However, UA supplementation increased the abundance of *Lactobacillus*, *Bacteroides,* and *Akkermansia,* which is inconsistent with the results from the HFD group.

3.4. Treatment effects on specific phylotypes in the gut microbiota of mice

By using LEfSe to look for variations in the abundance of bacterial taxa between three groups, the features of microbiota in the mice were examined. As presented in Figures 4A, B, 10 significant discriminative features were uncovered in the HFD group and eight were revealed in the UA treatment groups. The indicator microorganisms in the HFD group were identified as belonging to Clostridia, Clostridiales, Lachnospiraceae, Micrococcaceae, Aerococcaceae, *Holdemania*, *Facklamia*, *Ruminococcus*, *Pseudoramibacter-Eubacterium,* and

10.3389/fmicb.2023.1183598

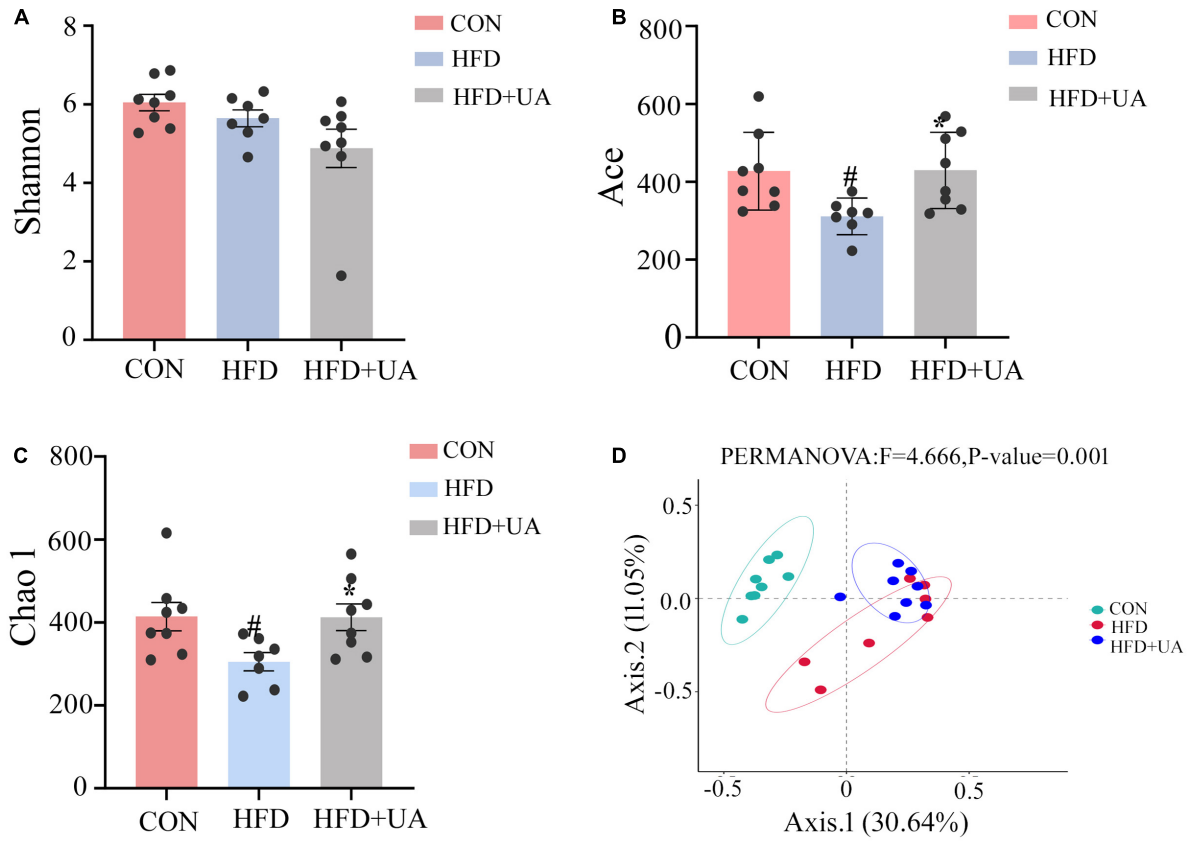

FIGURE 2
Analysis of alpha and beta diversity of intestinal flora in three groups of mice: **(A)** Shannon index; **(B)** Ace index; **(C)** Chao1 index; **(D)** Principal coordinates analysis (PCoA) ($^{\#}p < 0.05$ compared to control group, $^{*}p < 0.05$ relative to the high-fat diet group).

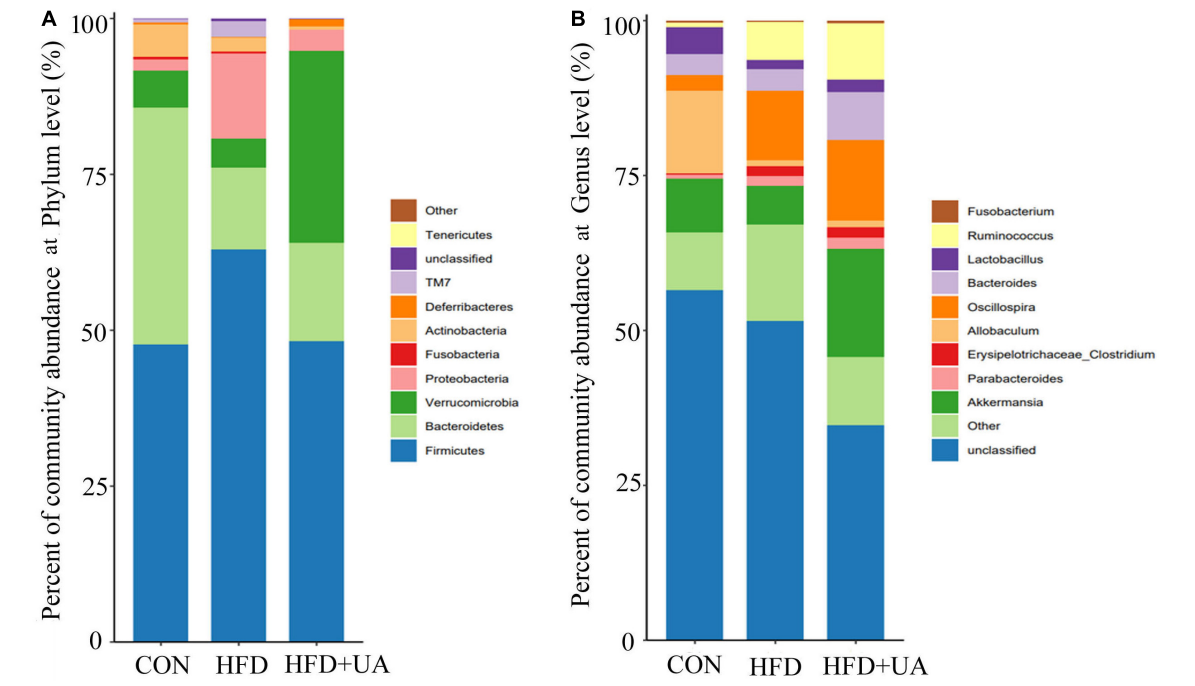

FIGURE 3
Abundance of intestinal bacteria at the **(A)** phylum and **(B)** the genus levels.

Clostridium; likewise, Rhodobacterales, Methylobacteriaceae, Rhodobacteraceae, *Methylobacterium*, *Coprobacillus*, *Clostridium*, *Serratia,* and *Clostridium* were the dominant microbes in the UA treatment group (linear discriminant analysis score > 2, Figure 4A).

3.5. Correlations between major microbial communities and biochemical parameters

As shown in Figure 4C, Spearman's correlation analysis revealed that obesity-related indicators were strongly correlated with the microbial communities. *Parabacteroides*, *Anaerotruncus,* and *Erysipelotrichaceae_Clostridium* were significantly positively associated with LDL-C, and *Bacteroides*, *Mucispirillum*, *Oscillospira,* and *Ruminococcus* were positively correlated with LDL-C. Meanwhile, *Odoribacter*, *Lactobacillus*, *Bifidobacterium,* and *Allobaculum* showed a significant negative correlation with LDL-C. HDL-C was positively correlated with *Akkermansia*, *Lactococcus*, *Erysipelotrichaceae_Clostridium,* and *Ruminococcus*; *Parabacteroides* also showed a positive correlation with TG, but *Bifidobacterium* and *Allobaculum* were negatively correlated with TG.

3.6. Effect of UA on metabolic profiles

To examine the impact of UA on obesity from the viewpoint of host metabolism, the metabolic profiles of mice in the HFD and UA treatment groups were analyzed using non-targeted metabolomics. As shown in Figure 5A, OPLS-DA was conducted to analyze the effect of UA on classification, and the results showed a clear distribution for each group, as the R^2Y and Q^2 values of the OPLS-DA score analysis were 0.976 and 0.766, respectively, demonstrating a stable and precise prediction from the existing models. Moreover, the intercepts of R^2 and Q^2 were + 0.777 and −0.501, showing that the statistical models are valid and not overfit (Figure 5B).

3.7. Changes in metabolites induced by UA

Metabolite changes in the feces of mice are presented in Figure 6, showing that the HFD led to 490 metabolite changes (>1-fold, $p < 0.05$) relative to the control group, with 258 increasing and 232 decreasing (Figure 6A). Moreover, the intervention with UA led to 38 metabolite changes (>1-fold, $p < 0.05$) relative to the HFD group, with 18 increasing and 20 decreasing (Figure 6B). These findings indicted that the HFD and UA intervention caused the changes in metabolites in the feces of mice.

A hierarchical clustering heatmap was used to display the relative level of metabolites between three groups. We found that there were eight up-regulated metabolites, mainly including L-norleucine, L-methionine, isoleucine, valine, L-phenylalanine, 2-hydroxycinnamic acid, and L-tyrosine, in mice fed with the HFD relative to those in the control group, and the level decreased after UA intervention. Moreover, there were six down-regulated differential metabolites, 7-ketolithocholic acid, oleamide, hexadecanamide, ursodeoxycholic acid, oleoyl ethylamide, and nicotinic acid in mice fed with the HFD, and the level increased after UA intervention except for that of ursodeoxycholic acid (Figure 6C). Interestingly, correlation analysis of the differential metabolite expression and obese-related indicators using a hierarchical clustering heatmap revealed that the amino acids negatively correlated with UA levels were all positively correlated with TC except for L-norleucine, which was positively correlated with TG. Meanwhile, oleamide and oleoyl ethylamide was negatively correlated with TC, and nicotinic acid showed a significant negative correlation with LDL-C. Notably, these three amino acids also have been showed a positive correlation with UA (Figure 6D). These findings indicated that UA may influence the expression levels of obese-related indicators by regulating amino acid metabolism.

3.8. Correlations between gut microbiota and metabolites

To further explore the changes in metabolites after UA intervention, the KEGG database was used for pathway enrichment analysis to identify the relevant pathways and functions of differential metabolites between the HFD and UA treatment groups. According to Figure 7A, the KEGG analysis showed 39 annotated pathways, and the most representative pathways were steroid hormone biosynthesis, phenylalanine, tyrosine and tryptophan biosynthesis, ubiquinone and other terpenoid-quinone biosynthesis, and vitamin B6 metabolism.

Spearman's correlation analysis was used to reveal the functional correlation of the key microbial phylotypes to the altered fecal metabolites. As shown in Figure 7B, UA and glycolithocholic acid both had a positive correlation with *Akkermansia*, but glycolithocholic acid had a negative correlation with *Pseudoramibacter-Eubacterium*; 1-(3-phenylpropanoy)-4-piperidinecarboxylic acid was positively correlated with *Pseudoramibacter-Eubacterium* and *Corynebacterium* but was negatively associated with *Akkermansia*; betulin had a negative correlation with *Clostridium*, *Facklamia*, *Pseudoramibacter-Eubacterium,* and *Corynebacterium*.

4. Discussion

Obesity is regarded as a worldwide public health problem, significantly affecting the health of people in all age groups, and the major factor causing obesity is a high-fat diet (Hariri and Thibault, 2010). UA has multiple biological functions and plays a positive regulatory role in metabolic diseases, especially diabetes and obesity (González-Garibay et al., 2020), but few studies have focused on its impacts on the gut microbiota and metabolites in the disease process. In the present study, we established an obesity model by feeding mice a HFD with or without UA supplement for 8 weeks to explore the effects of UA on the gut microbiota and metabolites in the obesity process.

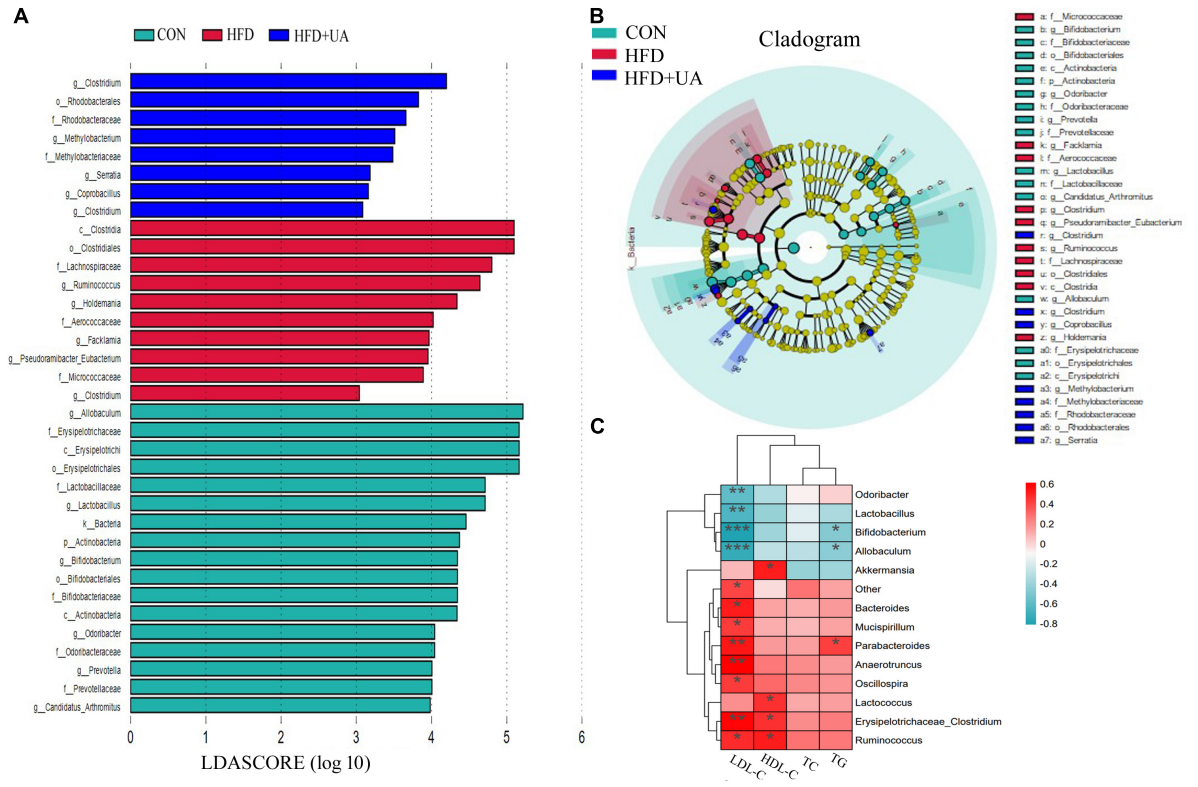

FIGURE 4
(A) Bacterial populations with a linear discriminant analysis score > 2 are displayed. **(B)** Taxonomy cladogram from linear discriminant analysis effect size analysis. **(C)** Heatmap depicting the correlation between major microbial communities and obese-related indicators. *$p < 0.05$; **$p < 0.01$; ***$p < 0.001$.

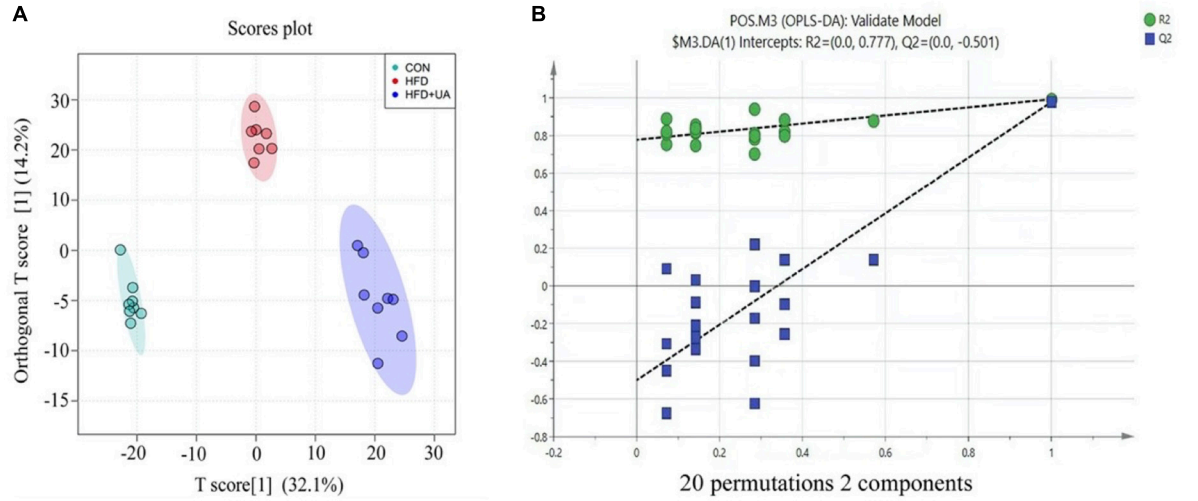

FIGURE 5
(A) Score plots of fecal samples derived from the LC-MS metabolite profiles. Samples from control (green circles), HFD (red circles) and HFD + UA (purple circles) groups. **(B)** Permutation tests were conducted with 20 random permutations in the OPLS-DA model.

4.1. UA treatment altered obesity-related serum biochemical indicators

We found that several serum biochemical indicators closely related to obesity increased in the HFD group as documented by previous research (Kim et al., 2018; Guo et al., 2020), and the level was rapidly reduced by UA intervention. A previous study demonstrated that UA could decreased the lipid accumulation in the adipose tissues and liver. Meanwhile, the TG and LDL concentrations also decreased while the HDL concentration was

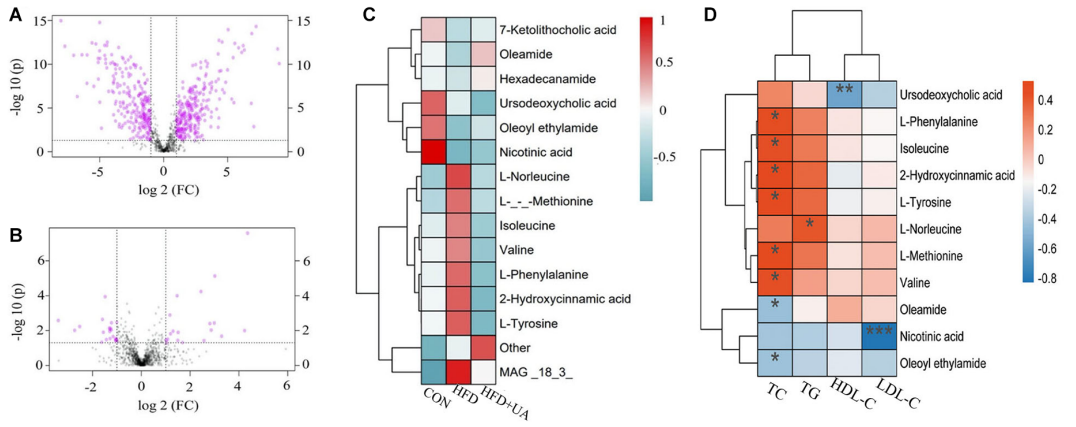

FIGURE 6
Metabolites in mice feces between groups. **(A)** Univariate statistical analysis of metabolites in fecal samples in the control and HFD groups (multiple > 1 and $p < 0.05$). **(B)** Univariate statistical analysis of metabolites in fecal samples in the HFD and UA treatment groups (multiple > 1 and $p < 0.05$). **(C)** Cluster analysis of the difference in metabolite expression among different groups using hierarchical clustering heatmap. **(D)** Heatmap depicting the correlation between differential metabolites and obese-related indicators. *$p < 0.05$; **$p < 0.01$; ***$p < 0.001$.

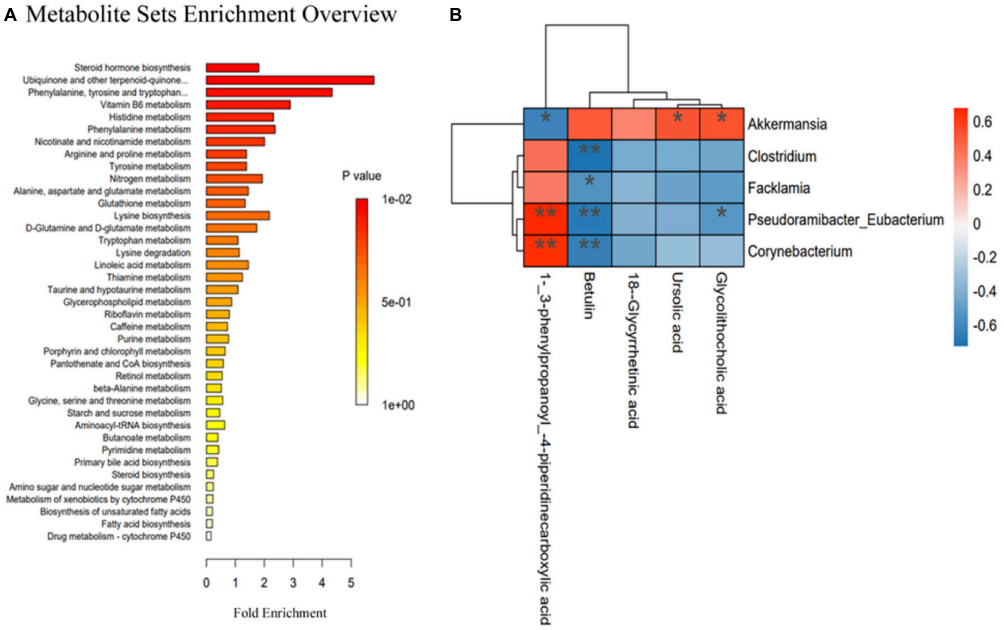

FIGURE 7
(A) Relevant pathways and functions of differential metabolites in Kyoto Encyclopedia of Genes and Genomes analysis; **(B)** Spearman's correlation heatmap reveals the relationship between the gut microbiota and metabolites. *$p < 0.05$; **$p < 0.01$.

increased significantly in mice administrated by UA, which is consistent with our results (Jia et al., 2015). Additionally, The similar results were also reported in other studies that UA treatment significantly decreased the concentration of TG (Li et al., 2014; Chu et al., 2015). Evidence from an animal study indicated that the elevated levels of TC, TG, and LDL-C in serum could improve atherosclerosis and associated cardiovascular disease (Sathyapalan et al., 2018). Moreover, recent research showed that TC, TG, LDL-C and HDL-C could be used as a specific lipid biomarkers to assess the risk of cardiovascular disease among different population groups (Georgoulis et al., 2022). Based on these results, we proposed that UA could regulate lipid metabolism and reduce the risk of atherosclerosis as well as related cardiovascular disease induced by obesity.

4.2. General effects of UA on gut microbiota

To explore the effect of UA on the composition of the intestinal flora of obese mice, we analyzed the gut microbiota structure of mice in the HFD and UA treatment groups. It was found that UA intervention shifted the Firmicutes to Bacteroidetes (F/B) ratio in fecal samples of the HFD-induced mice at the phylum level.

Recent research demonstrated that Firmicutes has more efficient sugar metabolism relative to Bacteroidetes, which promotes energy absorption and weight gain that contribute to obesity (Bai et al., 2019; Lu et al., 2021; Li F. et al., 2022). Thus, a lower F/B ratio may reduce obesity through energy metabolism, and a similar effect of the F/B ratio on obesity in mice has been further demonstrated in a study that focused on the function of *Rosa roxburghii* Tratt fruit vinegar in the prevention of obesity (Li J. et al., 2022).

The crucial roles of the gut microbiota in obtaining energy from the diet and influencing the pathophysiology of obesity by modulating lipid or glucose metabolism have been demonstrated (Wang and Jia, 2016). In particular, *Akkermansia muciniphila* was shown to participate in the regulation of obesity and could serve as an indicator to evaluate the body's metabolic status, especially in terms of glucose or lipid metabolism homeostasis (Dao et al., 2016; Wu et al., 2020). Moreover, *A. muciniphila* has a beneficial impact on liver disorders, systemic inflammation, and gut disruption caused by obesity (Xu et al., 2020). Our research found that UA had a positive correlation with *Akkermansia*, and supplementation with UA could significantly increase the abundance of *Akkermansia* relative to that of mice in the HFD group. These findings suggested that the function of UA in the improvement of obesity, at least in part, depends on increasing the abundance of *Akkermansia*, which is beneficial for the steady state of the host's basal metabolism. In addition, recent research has demonstrated that *Lactobacillus*, as a beneficial bacteria in gut, could alleviate the process of HFD-induced obesity by regulating the intestinal flora (Cai et al., 2020; Hussain et al., 2020; Liu et al., 2022). Our results showed that the abundance of *Lactobacillus* increased after UA intervention, so we further speculated that the anti-obesity action of UA in mice was realized though increasing the commensal gut beneficial microbes and improving the gut barrier integrity.

4.3. General effects of UA on amino acid metabolism

Obesity can lead to various degrees of metabolic imbalance, particularly in terms of lipid and carbohydrate metabolism, but amino acid metabolism is also affected. Altered amino acid profiles in the obesity condition are often accompanied by concomitant changes in the resistance and secretion of insulin (Simonson et al., 2020). In particular, the branched-chain amino acids (BCAAs), including leucine, isoleucine, and valine, play vital roles in the pathogenesis of metabolic disorders observed in obesity, and increased BCAA circulating levels are related to insulin resistance (Ridaura et al., 2013; Lynch and Adams, 2014; Pedersen et al., 2016). Mice fed a diet with a lower level of BCAA could quickly lose weight and fat mass before achieving a normal weight, and glucoregulatory control is improved (Cummings et al., 2018). Likewise, ginsenoside Rb1 has been demonstrated to ameliorate glycemic disorder in obese mice partly by decreasing the level of BCAAs, especially isoleucine and leucine (Yang et al., 2021). This provides additional support for our results. Our results showed that UA supplementation could decrease the level of amino acids like BCAAs, tyrosine and others relative to the HFD group, indicating a positive effect of UA on obesity. Furthermore, previous reports showed that BCAAs are partly produced and metabolized by the intestinal microbiome, and obese patients exhibit an imbalanced intestinal microbiome with increased BCAA synthesis and decreased BCAA catabolism (Gill et al., 2006; Liu et al., 2017). Thus, we speculated that the beneficial influence of UA on obesity partly depends on amino acid metabolism and the intestinal microbiome and their interaction.

Notably, besides the BCAAs, obesity risk was also associated with aromatic amino acids, especially tryptophan, which influences host metabolism and has become another potential obesity treatment (Aron-Wisnewsky et al., 2021). As described recently, moderate tryptophan restriction can cause loss of appetite and thermogenesis, whereas severe tryptophan restriction causes hypophagia and weight loss (Zapata et al., 2018). Together with tryptophan itself, metabolites generated from it, including indole, serotonin, and kynurenine, can also contribute to obesity (Konopelski et al., 2019; Pan et al., 2019; Simonson et al., 2020; Aron-Wisnewsky et al., 2021). Additionally, increasing evidence has shown that phenylalanine and tyrosine were also related to the increased incidence of obesity (Libert et al., 2018; Bai et al., 2020; Cheng et al., 2021). Our metabolic analysis showed that the different metabolites could participate in phenylalanine, tyrosine, and tryptophan biosynthesis, further implying that the positive effects of UA on obesity partly depend on its effect on amino acid metabolism.

5. Conclusion

In summary, the effects of UA on the microbiome structure and fecal metabolome of obese mice induced by a HFD were investigated. These results indicated that UA intervention not only changed the microbiota composition but also altered host metabolism, in particular that of amino acid metabolism. Our findings could further our understanding of the anti-obesity effects of UA and its potential as a treatment for obesity.

Data availability statement

The datasets presented in this study can be found in online repositories. The names of the repository/repositories and accession numbers can be found in the NCBI database under accession number: PRJNA960690 (https://www.ncbi.nlm.nih.gov/sra/PRJNA960690), Metabolomics raw data has been uploaded in Metabolights database under accession number: MTBLS7741 (https://www.ebi.ac.uk/metabolights/editor/study/MTBLS7741).

Ethics statement

The animal study was reviewed and approved by the Ethics Committee of Baotou Medical College.

Author contributions

CT: investigation, writing–original draft, visualization, and formal analysis. JL: methodology, validation, investigation, and writing–review and editing. LG: conceptualization, resources,

supervision, and project administration. YB: investigation, writing–review and editing, and funding acquisition. LS: investigation and supervision. KL: data curation and visualization. MS: supervision. All authors contributed to the article and approved the submitted version.

Funding

This study was supported by the Medical and Health Science and Technology Plan Project of Inner Mongolia Autonomous Region Health Commission (202201368); the Natural Science Foundation of Inner Mongolia (2021LHMS08017); the Young Scientific and Technological Talents Inner Mongolia Universities (NJYT22119); the Baotou Medical College Doctoral Research Start-up-fund Project (BSJJ201801); Heilongjiang Provincial Colleges and Universities Basic Scientific Research Projects, China (2022-KYYWF-0649); and Jiamusi University Young Innovative Talent Training Support Program Project, China (JMSUQP2022014).

Acknowledgments

We thank each author for their sincere effort in this research and the North Medicine and Functional Food Characteristic Subject Project in Heilongjiang Providence for the help provided.

Conflict of interest

The authors declare that the research was conducted in the absence of any commercial or financial relationships that could be construed as a potential conflict of interest.

Publisher's note

All claims expressed in this article are solely those of the authors and do not necessarily represent those of their affiliated organizations, or those of the publisher, the editors and the reviewers. Any product that may be evaluated in this article, or claim that may be made by its manufacturer, is not guaranteed or endorsed by the publisher.

Supplementary material

The Supplementary Material for this article can be found online at: https://www.frontiersin.org/articles/10.3389/fmicb.2023.1183598/full#supplementary-material

References

Aron-Wisnewsky, J., Warmbrunn, M. V., Nieuwdorp, M., and Clément, K. (2021). Metabolism and metabolic disorders and the microbiome: The intestinal microbiota associated with obesity, lipid metabolism, and metabolic health-pathophysiology and therapeutic strategies. *Gastroenterology* 160, 573–599. doi: 10.1053/j.gastro.2020.10.057

Bai, L., Gao, M., Cheng, X., Kang, G., Cao, X., and Huang, H. (2020). Engineered butyrate-producing bacteria prevents high fat diet-induced obesity in mice. *Microb. Cell Fact.* 19:94. doi: 10.1186/s12934-020-01350-z

Bai, Y. F., Wang, S. W., Wang, X. X., Weng, Y. Y., Fan, X. Y., Sheng, H., et al. (2019). The flavonoid-rich Quzhou *Fructus Aurantii* extract modulates gut microbiota and prevents obesity in high-fat diet-fed mice. *Nutr. Diabetes* 9:30. doi: 10.1038/s41387-019-0097-6

Cai, H., Wen, Z., Li, X., Meng, K., and Yang, P. (2020). *Lactobacillus plantarum* FRT10 alleviated high-fat diet-induced obesity in mice through regulating the PPARα signal pathway and gut microbiota. *Appl. Microbiol. Biotechnol.* 104, 5959–5972. doi: 10.1007/s00253-020-10620-0

Cheng, D., Zhao, X., Yang, S., Cui, H., and Wang, G. (2021). Metabolomic signature between metabolically healthy overweight/obese and metabolically unhealthy overweight/obese: A systematic review. *Diabetes Metab. Syndr. Obes.* 14, 991–1010. doi: 10.2147/DMSO.S294894

Chu, X., He, X., Shi, Z., Li, C., Guo, F., Li, S., et al. (2015). Ursolic acid increases energy expenditure through enhancing free fatty acid uptake and β-oxidation via an UCP3/AMPK-dependent pathway in skeletal muscle. *Mol. Nutr. Food Res.* 59, 1491–1503. doi: 10.1002/mnfr.201400670

Clément, K., Biebermann, H., Farooqi, I. S., Van der Ploeg, L., Wolters, B., Poitou, C., et al. (2018). MC4R agonism promotes durable weight loss in patients with leptin receptor deficiency. *Nat. Med.* 24, 551–555. doi: 10.1038/s41591-018-0015-9

Cummings, N. E., Williams, E. M., Kasza, I., Konon, E. N., Schaid, M. D., Schmidt, B. A., et al. (2018). Restoration of metabolic health by decreased consumption of branched-chain amino acids. *J. Physiol. (Lond.)* 596, 623–645. doi: 10.1113/JP275075

Dao, M. C., Everard, A., Aron-Wisnewsky, J., Sokolovska, N., Prifti, E., Verger, E. O., et al. (2016). *Akkermansia muciniphila* and improved metabolic health during a dietary intervention in obesity: Relationship with gut microbiome richness and ecology. *Gut* 65, 426–436. doi: 10.1136/gutjnl-2014-308778

de Freitas Junior, L. M., and de Almeida, E. B. Jr. (2017). Medicinal plants for the treatment of obesity: Ethnopharmacological approach and chemical and biological studies. *Am. J. Transl. Res.* 9, 2050–2064.

Diarra, M., El Ouahabi, H., Bouxid, H., Boujraf, S., Khabbal, Y., and Ajdi, F. (2016). Medicinal plants in type 2 diabetes: Therapeutic and economical aspects. *Int. J. Prev. Med.* 7:56. doi: 10.4103/2008-7802.178370

Georgoulis, M., Chrysohoou, C., Georgousopoulou, E., Damigou, E., Skoumas, I., Pitsavos, C., et al. (2022). Long-term prognostic value of LDL-C, HDL-C, lp(a) and TG levels on cardiovascular disease incidence, by body weight status, dietary habits and lipid-lowering treatment: The ATTICA epidemiological cohort study (2002-2012). *Lipids Health Dis.* 21:141. doi: 10.1186/s12944-022-01747-2

Gill, S. R., Pop, M., Deboy, R. T., Eckburg, P. B., Turnbaugh, P. J., Samuel, B. S., et al. (2006). Metagenomic analysis of the human distal gut microbiome. *Science* 312, 1355–1359. doi: 10.1126/science.1124234

González-Garibay, A. S., López-Vázquez, A., García-Bañuelos, J., Sánchez-Enríquez, S., Sandoval-Rodríguez, A. S., Bueno-Topete, M. R., et al. (2020). Effect of ursolic acid on insulin resistance and Hyperinsulinemia in rats with diet-induced obesity: Role of adipokines expression. *J. Med. Food* 23, 297–304. doi: 10.1089/jmf.2019.0154

Guo, W. L., Guo, J. B., Liu, B. Y., Lu, J. Q., Chen, M., Liu, B., et al. (2020). Ganoderic acid A from *Ganoderma lucidum* ameliorates lipid metabolism and alters gut microbiota composition in hyperlipidemic mice fed a high-fat diet. *Food Funct.* 11, 6818–6833. doi: 10.1039/d0fo00436g

Hariri, N., and Thibault, L. (2010). High-fat diet-induced obesity in animal models. *Nutr. Res. Rev.* 23, 270–299. doi: 10.1017/S0954422410000168

Hussain, A., Kwon, M. H., Kim, H. K., Lee, H. S., Cho, J. S., and Lee, Y. I. (2020). Anti-obesity effect of *Lactobacillus plantarum* LB818 is associated with regulation of gut microbiota in high-fat diet-fed obese mice. *J. Med. Food* 23, 750–759. doi: 10.1089/jmf.2019.4627

Jia, Y., Kim, S., Kim, J., Kim, B., Wu, C., Lee, J. H., et al. (2015). Ursolic acid improves lipid and glucose metabolism in high-fat-fed C57BL/6J mice by activating peroxisome proliferator-activated receptor alpha and hepatic autophagy. *Mol. Nutr. Food Res.* 59, 344–354. doi: 10.1002/mnfr.201400399

Khera, R., Murad, M. H., Chandar, A. K., Dulai, P. S., Wang, Z., Prokop, L. J., et al. (2016). Association of pharmacological treatments for obesity with weight loss

and adverse events: A systematic review and metaanalysis. *JAMA* 315, 2424–2434. doi: 10.1001/jama.2016.7602

Kim, H. M., Kim, Y., Lee, E. S., Huh, J. H., and Chung, C. H. (2018). Caffeic acid ameliorates hepatic steatosis and reduces ER stress in high fat diet-induced obese mice by regulating autophagy. *Nutrition* 55–56, 63–70. doi: 10.1016/j.nut.2018.03.010

Konopelski, P., Konop, M., Gawrys-Kopczynska, M., Podsadni, P., Szczepanska, A., and Ufnal, M. (2019). Indole-3-propionic acid, a tryptophan-derived bacterial metabolite, reduces weight gain in rats. *Nutrients* 11:591. doi: 10.3390/nu11030591

Li, S., Liao, X., Meng, F., Wang, Y., Sun, Z., Guo, F., et al. (2014). Therapeutic role of ursolic acid on ameliorating hepatic steatosis and improving metabolic disorders in high-fat diet-induced non-alcoholic fatty liver disease rats. *PLoS One* 29:e86724. doi: 10.1371/journal.pone.0086724

Li, F., Yang, S., Zhang, L., Qiao, L., Wang, L., He, S., et al. (2022). Comparative metagenomics analysis reveals how the diet shapes the gut microbiota in several small mammals. *Ecol. Evol.* 12:e8470. doi: 10.1002/ece3.8470

Li, H., Fang, Q., Nie, Q., Hu, J., Yang, C., Huang, T., et al. (2020). Hypoglycemic and hypolipidemic mechanism of tea polysaccharides on type 2 diabetic rats via gut microbiota and metabolism alteration. *J. Agric. Food Chem.* 68, 10015–10028. doi: 10.1021/acs.jafc.0c01968

Li, J., Zhang, J., Zhang, Y., Shi, Y., Feng, D., Zuo, Y., et al. (2022). Effect and correlation of *Rosa roxburghii* tratt fruit vinegar on obesity, dyslipidemia and intestinal microbiota disorder in high-fat diet mice. *Foods* 11:4108. doi: 10.3390/foods11244108

Libert, D. M., Nowacki, A. S., and Natowicz, M. R. (2018). Metabolomic analysis of obesity, metabolic syndrome, and type 2 diabetes: Amino acid and acylcarnitine levels change along a spectrum of metabolic wellness. *PeerJ* 6:e5410. doi: 10.7717/peerj.5410

Liu, R., Hong, J., Xu, X., Feng, Q., Zhang, D., Gu, Y., et al. (2017). Gut microbiome and serum metabolome alterations in obesity and after weight-loss intervention. *Nat. Med.* 23, 859–868. doi: 10.1038/nm.4358

Liu, Z., Zhou, X., Wang, W., Gu, L., Hu, C., Sun, H., et al. (2022). *Lactobacillus paracasei* 24 attenuates lipid accumulation in high-fat diet-induced obese mice by regulating the gut microbiota. *J. Agric. Food Chem.* 70, 4631–4643. doi: 10.1021/acs.jafc.1c07884

Lu, X., Jing, Y., Li, Y., Zhang, N., Zhang, W., and Cao, Y. (2021). The differential modulatory effects of *Eurotium cristatum* on the gut microbiota of obese dogs and mice are associated with improvements in metabolic disturbances. *Food Funct.* 12, 12812–12825. doi: 10.1039/d1fo02886c

Lynch, C. J., and Adams, S. H. (2014). Branched-chain amino acids in metabolic signalling and insulin resistance. *Nat. Rev. Endocrinol.* 10, 723–736. doi: 10.1038/nrendo.2014.171

Medanić, D., and Pucarin-Cvetković, J. (2012). Pretilost–javnozdravstveni problem i izazov [Obesity–a public health problem and challenge]. *Acta Med. Croatica* 66, 347–355. Croatian

Ojulari, O. V., Lee, S. G., and Nam, J. O. (2019). Beneficial effects of natural bioactive compounds from *Hibiscus sabdariffa* L. on obesity. *Molecules* 24:210. doi: 10.3390/molecules24010210

Pan, H., Fu, C., Huang, L., Jiang, Y., Deng, X., Guo, J., et al. (2018). Anti-obesity effect of chitosan oligosaccharide capsules (COSCs) in obese rats by ameliorating leptin resistance and adipogenesis. *Mar. Drugs* 16:198. doi: 10.3390/md16060198

Pan, Q., Liu, Q., Wan, R., Kalavagunta, P. K., Liu, L., Lv, W., et al. (2019). Selective inhibition of intestinal 5-HT improves neurobehavioral abnormalities caused by high-fat diet mice. *Metab. Brain Dis.* 34, 747–761. doi: 10.1007/s11011-019-0392-x

Pedersen, H. K., Gudmundsdottir, V., Nielsen, H. B., Hyotylainen, T., Nielsen, T., Jensen, B. A., et al. (2016). Human gut microbes impact host serum metabolome and insulin sensitivity. *Nature* 535, 376–381. doi: 10.1038/nature18646

Qu, W., Nie, C., Zhao, J., Ou, X., Zhang, Y., Yang, S., et al. (2018). Microbiome-metabolomics analysis of the impacts of long-term dietary advanced-glycation-end-product consumption on C57BL/6 mouse fecal microbiota and metabolites. *J. Agric. Food Chem.* 66, 8864–8875. doi: 10.1021/acs.jafc.8b01466

Ridaura, V. K., Faith, J. J., Rey, F. E., Cheng, J., Duncan, A. E., Kau, A. L., et al. (2013). Gut microbiota from twins discordant for obesity modulate metabolism in mice. *Science* 341:1241214. doi: 10.1126/science.1241214

Sathyapalan, T., Aye, M., Rigby, A. S., Thatcher, N. J., Dargham, S. R., Kilpatrick, E. S., et al. (2018). Soy isoflavones improve cardiovascular disease risk markers in women during the early menopause. *Nutr. Metab. Cardiovasc. Dis.* 28, 691–697. doi: 10.1016/j.numecd.2018.03.007

Sehrawat, A., Roy, R., Pore, S. K., Hahm, E. R., Samanta, S. K., Singh, K. B., et al. (2017). Mitochondrial dysfunction in cancer chemoprevention by phytochemicals from dietary and medicinal plants. *Semin. Cancer Biol.* 47, 147–153. doi: 10.1016/j.semcancer.2016.11.009

Seo, D. Y., Lee, S. R., Heo, J. W., No, M. H., Rhee, B. D., Ko, K. S., et al. (2018). Ursolic acid in health and disease. *Korean J. Physiol. Pharmacol.* 22, 235–248. doi: 10.4196/kjpp.2018.22.3.235

Simonson, M., Boirie, Y., and Guillet, C. (2020). Protein, amino acids and obesity treatment. *Rev. Endocr. Metab. Disord.* 21, 341–353. doi: 10.1007/s11154-020-09574-5

Sun, A., Hu, X., Chen, H., Ma, Y., Yan, X., Peng, D., et al. (2021). Ursolic acid induces white adipose tissue beiging in high-fat-diet obese male mice. *Food Funct.* 12, 6490–6501. doi: 10.1039/d1fo00924a

Sun, S., Sun, L., Wang, K., Qiao, S., Zhao, X., Hu, X., et al. (2021). The gut commensal fungus, *Candida parapsilosis*, promotes high fat-diet induced obesity in mice. *Commun. Biol.* 4:1220. doi: 10.1038/s42003-021-02753-3

Sun, X., Wen, J., Guan, B., Li, J., Luo, J., Li, J., et al. (2022). Folic acid and zinc improve hyperuricemia by altering the gut microbiota of rats with high-purine diet-induced hyperuricemia. *Front. Microbiol.* 29:907952. doi: 10.3389/fmicb.2022.907952

Tang, S., Fang, C., Liu, Y., Tang, L., and Xu, Y. (2022). Anti-obesity and anti-diabetic Effect of ursolic acid against streptozotocin/high fat induced obese in diabetic rats. *J. Oleo Sci.* 71, 289–300. doi: 10.5650/jos.ess21258

Wang, J., and Jia, H. (2016). Metagenome-wide association studies: Fine-mining the microbiome. *Nat. Rev. Microbiol.* 14, 508–522. doi: 10.1038/nrmicro.2016.83

Wang, K., Liao, M., Zhou, N., Bao, L., Ma, K., Zheng, Z., et al. (2019). *Parabacteroides distasonis* alleviates obesity and metabolic dysfunctions via production of succinate and secondary bile acids. *Cell Rep.* 26, 222–235.e5. doi: 10.1016/j.celrep.2018.12.028

Wu, F., Guo, X., Zhang, M., Ou, Z., Wu, D., Deng, L., et al. (2020). An *Akkermansia muciniphila* subtype alleviates high-fat diet-induced metabolic disorders and inhibits the neurodegenerative process in mice. *Anaerobe* 61:102138. doi: 10.1016/j.anaerobe.2019.102138

Xu, Y., Wang, N., Tan, H. Y., Li, S., Zhang, C., and Feng, Y. (2020). Function of *Akkermansia muciniphila* in obesity: Interactions with lipid metabolism, immune response and gut systems. *Front. Microbiol.* 11:219. doi: 10.3389/fmicb.2020.00219

Yang, X., Dong, B., An, L., Zhang, Q., Chen, Y., Wang, H., et al. (2021). Ginsenoside Rb1 ameliorates glycemic disorder in mice with high fat diet-induced obesity via regulating gut microbiota and amino acid metabolism. *Front. Pharmacol.* 12:756491. doi: 10.3389/fphar.2021.756491

Yu, Z., Yu, X. F., Kerem, G., and Ren, P. G. (2022). Perturbation on gut microbiota impedes the onset of obesity in high fat diet-induced mice. *Front. Endocrinol. (Lausanne)* 13:795371. doi: 10.3389/fendo.2022.795371

Zapata, R. C., Singh, A., Ajdari, N. M., and Chelikani, P. K. (2018). Dietary tryptophan restriction dose-dependently modulates energy balance, gut hormones, and microbiota in obesity-prone rats. *Obesity (Silver Spring)* 26, 730–739. doi: 10.1002/oby.22136

frontiers | Frontiers in Microbiology

TYPE Original Research
PUBLISHED 14 August 2023
DOI 10.3389/fmicb.2023.1233934

OPEN ACCESS

EDITED BY
Xiaodong Xia,
Dalian Polytechnic University, China

REVIEWED BY
Bangxing Han,
West Anhui University, China
Zheng Ruan,
Nanchang University, China

*CORRESPONDENCE
Ran Li
✉ wwwlr@sgu.edu.cn
Zhanghua Sun
✉ sysuszh@126.com
Changqiong Xu
✉ 406453188@qq.com

†These authors have contributed equally to this work

RECEIVED 03 June 2023
ACCEPTED 28 July 2023
PUBLISHED 14 August 2023

CITATION
Xia L, Li R, Tao T, Zhong R, Du H, Liao Z, Sun Z and Xu C (2023) Therapeutic potential of *Litsea cubeba* essential oil in modulating inflammation and the gut microbiome. *Front. Microbiol.* 14:1233934. doi: 10.3389/fmicb.2023.1233934

Therapeutic potential of *Litsea cubeba* essential oil in modulating inflammation and the gut microbiome

Liqiong Xia[1], Ran Li[2,3*†], Ting Tao[3], Ruimin Zhong[2], Haifang Du[4], Ziling Liao[3], Zhanghua Sun[2*†] and Changqiong Xu[3,5*†]

[1]Department of Pharmacy, Loudi Central Hospital, Loudi, Hunan, China, [2]Guangdong Provincial Key Laboratory of Utilization and Conservation of Food and Medicinal Resources in Northern Region, Shaoguan University, Shaoguan, Guangdong, China, [3]Hunan Yueyang Maternal and Child Health-Care Hospital, Yueyang, Hunan, China, [4]The Second Clinical Medical College, Guangzhou University of Chinese Medicine, Guangzhou, China, [5]Medical College of Shaoguan University, Shaoguan, Guangdong, China

Inflammation, a sophisticated and delicately balanced physiological mechanism, is paramount to the host's immunological defense against pathogens. However, unfettered and excessive inflammation can be instrumental in engendering a plethora of chronic ailments and detrimental health repercussions, notably within the gastrointestinal tract. Lipopolysaccharides (LPS) from bacteria are potent endotoxins capable of instigating intestinal inflammation through the disruption of the intestinal epithelial barrier and the stimulation of a pro-inflammatory immune response. In this study, we sought to investigate the influence of *Litsea cubeba* essential oil (LCEO) on LPS-induced intestinal inflammation and associated changes in the gut microbiota. We investigated the therapeutic potential of LCEO for gut health, with particular emphasis on its gut protective properties, anti-inflammatory properties and modulation of the gut microbiome. LCEO exhibited protective effects on colonic tissue by protecting crypts and maintaining epithelial integrity, and anti-inflammatory properties by reducing TNF-α, IL-6, and IL-1β levels in the liver and intestine. Citral, a major component of LCEO, showed robust binding to IL-1β, IL-6, and TNF-α, exerting anti-inflammatory effects through hydrogen bonding interactions. Using community barplot and LEfSe analyses, we detected significant variation in microbial composition, identified discrete biomarkers, and highlighted the influence of essential oils on gut microbial communities. Our research suggests that LCEO may be a promising natural compound for ameliorating diarrhea and intestinal inflammation, with potential implications for modulating the gut microbiome. These observations provide invaluable insight into the potential therapeutic role of LCEO as a natural anti-inflammatory agent for treating intestinal inflammatory disorders, particularly in the setting of a dysregulated immune response and altered gut microbiota. Furthermore, our findings highlight the need to understand the complex interplay between the host, the gut microbiome and natural products in the context of inflammatory diseases.

KEYWORDS

inflammation, essential oils, gut microbiome, LPS, *Litsea cubeba*, citral

1. Introduction

Inflammation manifests as a physiological response to injury or infection, serving as a pervasive pathological mechanism underlying a myriad of diseases. The immune system, primarily mediated by macrophages, releases inflammatory mediators, including nitric oxide (NO), tumor necrosis factor-α (TNF-α), interleukin-6 (IL-6), and interleukin-1β (IL-1β), in its endeavor to combat pathogens. However, an exaggerated inflammatory response can give rise to acute and chronic conditions and, in severe cases, can precipitate shock or even mortality (Barton, 2008). Bacterial lipopolysaccharides (LPS), which constitute the outer membrane of Gram-negative bacteria, exert profound pro-inflammatory effects and have been implicated in gut inflammation (Candelli et al., 2021). LPS have demonstrated its capacity to instigate intestinal damage across diverse animal models through the upregulation of pro-inflammatory mediators and the imposition of oxidative stress (Wu et al., 2018; Zhu et al., 2018; Zhuang et al., 2019). Some investigations have proposed that excessive immune reactions to pathogens, characterized by an amplified release of pro-inflammatory cytokines, can impede the functionality of the intestinal barrier, resulting in increased epithelial apoptosis and reduced expression of junctional proteins. Notably, the gut microbiome serves as a substantial reservoir of LPS in both humans and animals. Previous studies have elucidated that alterations in the microbial composition of the host's gut can induce persistent intestinal inflammation and metabolic dysfunction (Sommer and Backhed, 2013). Currently, there are three primary categories of conventional medications used in the management of inflammatory bowel disease, namely aminosalicylic acid derivatives, glucocorticoids, and immunosuppressants. Nonetheless, the necessity for novel therapeutic alternatives arises from the potential long-term adverse effects associated with these treatments. Indeed, herbal medicine is extensively applied worldwide for the treatment of inflammatory bowel disease, and substantial progress has been achieved in both clinical and fundamental research in recent decades (Zheng et al., 2021).

Essential oils (EOs) are a diverse group of volatile compounds synthesized by aromatic plants as secondary metabolites. They occur in various plant organs and are primarily intended to shield plants from aggression by bacteria, fungi, and viruses, as well as insects. There are vast amounts of EOs from different plants worldwide, most of which have been at least partially characterized for their antimicrobial activity against Gram-positive and Gram-negative bacteria, fungi, and viruses. The composition of EOs was chosen by nature over millions of years of evolution, during which, competitive selection processes acted on their antibacterial, antifungal, and antiviral activities in an evolutionary conflict between plant survival and microbial aggressions. EOs have adopted multi-target mechanisms of action that make it challenging for microorganisms to develop resistance to these compounds, making them a promising therapeutic intervention (Sharma et al., 2019). EOs and their molecules are capable of modulating various signaling pathways that are dysregulated during acute or chronic inflammatory responses. The complex relationships between the human intestinal microbiota, consisting of bacteria, fungi, and viruses, and its intricate pathophysiological interactions with the immune system and the enteric nervous system make EOs particularly intriguing for their antimicrobial activity, which is often selective for different microbial components. From this viewpoint, EOs have the potential to be potent modulators of the intestinal microbiota (De Fazio et al., 2016).

Among the plants that produce EOs, *Litsea cubeba*, also known as Lour. Pers. (Lauraceae), is a species widely distributed across the eastern and southern regions of China and other parts of Southeast Asia, is renowned for its essential oil, which is extracted from the plant's fruits and has a distinctive crisp lemon aroma. This oil has a wealth of potential health benefits, including anti-inflammatory, antimicrobial and antioxidant properties (Feng et al., 2009). In recent years, a growing number of studies have reported that extracts and compounds derived from *L. cubeba* possess a diverse range of pharmacological properties, including anticancer, antibacterial, antioxidant, and anti-inflammatory activities (Lin et al., 2013). One of the most notable bioactive components of *L. cubeba* essential oil (LCEO) is citral, which is widely used in a variety of industries, including medicine, food, and chemicals. Despite the growing interest in *L. cubeba* and its potential therapeutic properties, the effects of LCEO on intestinal inflammation remain largely unknown. Therefore, further research is required to investigate the efficacy of LCEO and its potential to modulate the intestinal microbiota.

In this study, we endeavored to explore the impact of *L. cubeba* essential oil (LCEO) on LPS-induced intestinal inflammation and the consequent alterations in the gut microbiome. Our investigation divulged that LCEO administration effectively alleviated LPS-induced gut inflammation, thereby substantiating its potential therapeutic utility in the management of intestinal inflammatory diseases. Furthermore, our findings suggest that LCEO's anti-inflammatory action is intricately linked to its modulatory effects on the composition and diversity of the gut microbiota. These insightful results bolster the notion that LCEO could serve as a promising candidate for the treatment of intestinal inflammation, and potentially other gastrointestinal ailments that afflict the human population.

2. Methods

2.1. Chemicals

The essential oil of *Litsea cubeba* was procured from Jiangxi Baicao Pharmaceutical Co., Ltd. The lipopolysaccharides (LPS) were obtained from Beijing Solarbio Science & Technology Co. Ltd. The genes for IL-6, IL-1β, and TNF-α were acquired from Sangon Biotech Co., Ltd. The Trizol and RT Mix Kit with gDNA Clean for qPCR were supplied by Accurate Biology. The SYBR Green reagent was obtained from Roche. The C57BL/6J and SPF chow were obtained from Changsha Tianqin Biotechnology Co. Ltd. All other chemicals utilized were of the highest analytical grade.

2.2. Experimental design and induction of colitis

In accordance with the established guidelines of the Animal Ethics Committee at Loudi Central Hospital (LCH2022015), a cohort of 50 male C57BL/6J mice was acquired from Hunan SJA Laboratory

Animal Co. The mice, which weighed 18–20 grams and were 8 weeks old, were randomly assigned to five groups [control, model, low-dose LCEO (LCEO-L, 100 mg/kg), medium-dose LCEO (LCEO-M, 200 mg/kg), and high-dose LCEO (LCEO-H, 400 mg/kg)], and housed in a controlled environment characterized by consistent temperatures, humidity, and light–dark cycles. On the 21nd day, the fresh fecal samples were collected to assess the safety and efficacy of LCEO by microbiota analysis. On the 22nd day, the control group was administered PBS, while the other groups were given an intraperitoneal injection of LPS at a dose of 10 mg/kg. Following a 6-h fast, the mice were weighed and then sacrificed to obtain the tissues of liver, duodenum, jejunum, ileum and intestinal contents for further biochemical and microbiota analysis. All collected samples were stored at −80°C (Figure 1A).

2.3. Molecular docking simulation

A molecular docking simulation was performed by downloading the crystal structure of the genes from RCSB Protein Data Bank30 and the small molecules from TCMSP MENU. Autoduck software was used for molecular docking, and PyMol2.3.0 software was used for visualizing the binding model. In summary, this study used various tools and databases for prediction of the targets, protein–protein interaction analyses, KEGG pathway analyses, GO functional analyses, construction of the network, and the molecular docking simulation. The results provided valuable insights into the molecular mechanisms underlying the effects of compounds on the targets of citral related to inflammation.

2.4. Anti-inflammatory gene expression levels determined via RT-qPCR

RNA was extracted from the liver and duodenum using Trizol reagent. Primers were specially designed for the RT-qPCR analysis of IL-1β, TNF-α, and IL-6. The RT-qPCR assay was performed using an analytical qTOWER3G instrument (Germany), with a reaction volume of 10 μL, including 1 μL of the cDNA template and 5 μL of SYBR® Green real-time PCR master mix (solarbio, China). The PCR protocol consisted of an initial denaturation phase at 95°C for 10 min, followed by 40 cycles of denaturation at 95°C for 15 s, annealing at 60°C for 60 s, and a dissociation phase comprising denaturation at 95°C for 10 s, annealing at 65°C for 1 min, extension at 97°C for 1 s, and cooling at 37°C for 1 min. The threshold cycle values for each gene were obtained, and the genes' expression levels were calculated using the $2^{-\Delta\Delta CT}$ method. The primer sequences are provided in Table 1.

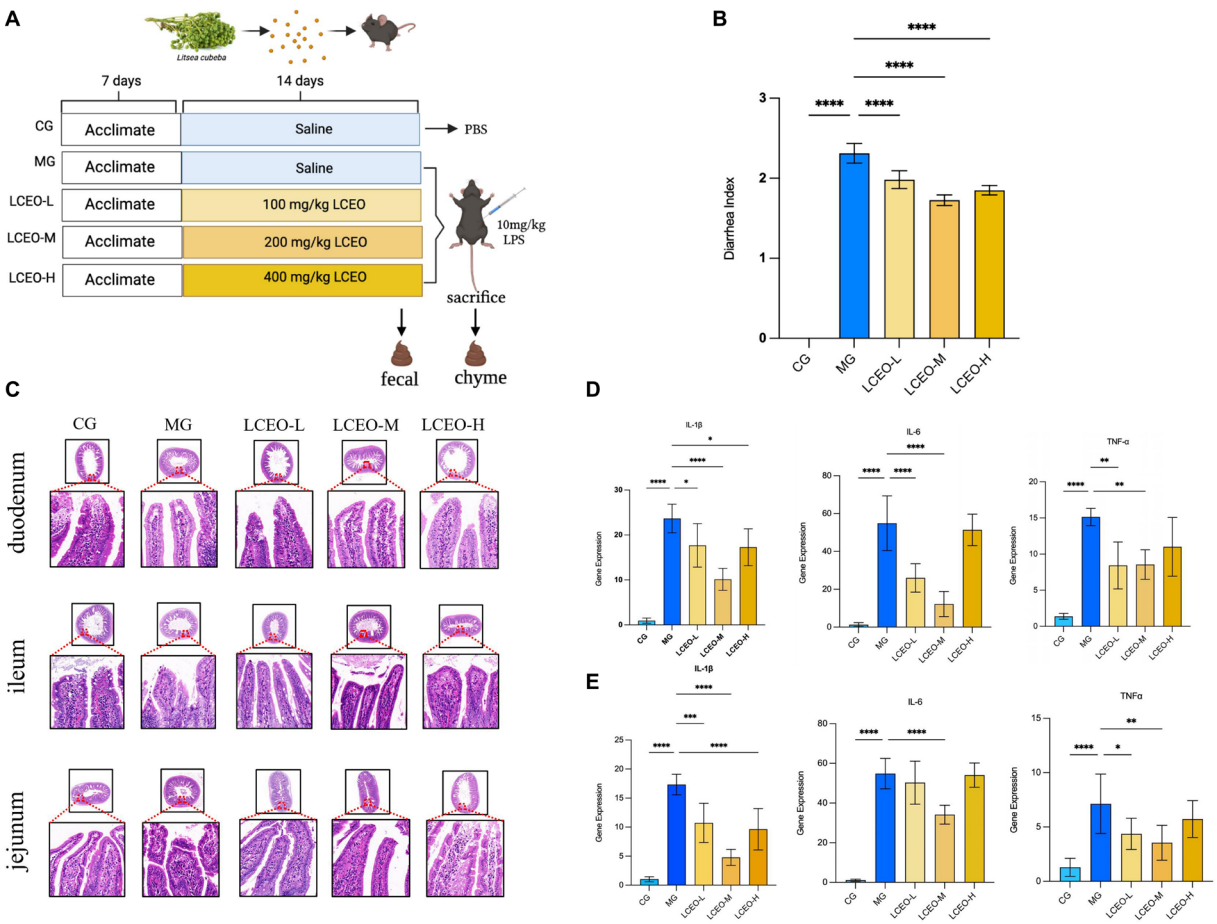

FIGURE 1
(A) Experimental design in mice. **(B)** The effect of LCEO of DAI index in all groups. **(C)** Pathological sections of the intestinal of various groups of mice (20×). **(D)** Effect of LCEO on the level of liver inflammatory cytokines. **(E)** Effect of LCEO on the level of duodenum inflammatory cytokines. *$p < 0.05$, **$p < 0.01$, ***$p < 0.005$, ****$p < 0.001$.

TABLE 1 Sequences of primers used for real-time polymerase chain reaction.

Gene	Accession number	Primer sequence (5′–3′)
GAPDH	NM_008084.2	CCTCGTCCCGTAGACAAAATG TGAGGTCAATGAAGGGGTCGT
TNF-α	NM_013693.3	ATGTCTCAGCCTCTTCTCATTC GCTTGTCACTCGAATTTTGAGA
IL-6	NM_001314054.1	AGACTTCCATCCAGTTGCCT CAGGTCTGTTGGGAGTGGTA
IL-1β	NM_008361.4	ACTCATTGTGGCTGTGGAGA TTGTTCATCTCGGAGCCTGT

2.5. Histological studies

The duodenum, jejunum, and ileum from the mice were subjected to a washing procedure using phosphate-buffered saline (PBS), followed by fixation in 4% formaldehyde for a duration of 1 h at 4°C. The tissues underwent dehydration through sequential immersion in solutions of alcohol and xylene prior to being embedded in paraffin. Subsequently, 5 μm sections were obtained from the paraffin-embedded specimens, stained with hematoxylin–eosin (H&E), and examined under a digital light microscope to evaluate the length of the intestinal villi.

2.6. Collection of fecal and intestinal contents and 16S rRNA sequencing

The microbial DNA from fecal and intestinal samples was extracted using the E.Z.N.A. Stool DNA Kit, with the purity of the extracted DNA verified through agarose gel electrophoresis. A paired-end library was then generated in accordance with Illumina's genomic DNA library preparation protocols, utilizing the NEXTFLEX Rapid DNASeq Kit. The hypervariable V3–V4 regions of the 16S rRNA gene were amplified using the 338F and 806R primer sets. Subsequently, the amplification pyrosequencing was conducted on the Illumina HiSeq 2000 at Shanghai Majorbio Bio-pharm Technology Co., Ltd. in accordance with the manufacturer's instructions. Raw sequencing data were subjected to quality control by Fastp, and the raw data were merged using FLASH. The operational taxonomic units were clustered on the basis of a 97% sequence identity threshold, utilizing UPARS. Taxonomic labels were assigned by the RDP classifier. Taxonomic classification was performed from the phylum to genus and species levels, with the UniFrac method being used for clustering the high-quality sequences in the R software package. Alpha diversity was calculated from the OTUs' sparsity and Simpson's index of evenness, while the beta diversity was compared through the UniFrac metric via principal coordinate analysis (PCoA).

2.7. Statistical analysis

A statistical analysis was performed using SPSS 20.0 software, and the results were presented as the mean ± SD ($x \pm s$). The level of statistical significance was established at $p < 0.05$. To evaluate the statistical and biological differences, Graphpad 9 software was utilized, which used one-way ANOVA for parametric data and Kruskal–Wallis tests for non-normal data. The gut microbiota (GM) was analyzed through the application of the linear discriminant analysis effect size (LEfSe), while changes in the microbial communities before and after the treatments were visualized by partial least squares discriminant analysis (PLS-DA). The alpha diversity values were set at a threshold of 0.05, with a logarithmic score of linear discriminant analysis of ≥2.0 and a confidence level of 95% ($p < 0.05$).

3. Results

3.1. Intestinal section and diarrhea index

Figure 1B displays the results of the study, which indicated a statistically significant increase ($P < 0.001$) in the diarrhea activity index (DAI) for the model group. However, the administration of LCEO at low, medium, and high doses produced a significant reduction ($P < 0.001$) in the DAI compared with the model group. These findings suggested that LCEO might have potential as a therapeutic intervention for the management of diarrhea. Nonetheless, further investigations are warranted to delineate the underlying mechanisms of action by which LCEO mitigates DAI and to evaluate its safety and efficacy in clinical settings. To demonstrate the protective effects of LCEO on the intestine, an assessment of intestinal structural damage was also performed. In the LPS-treated model group, granulation tissue formed in the duodenum, accompanied by a large amount of villous desquamation in the ileum, a shortened villus length, and a reduced number of goblet cells, resulting in the formation of granulation tissue. The epithelial cells of the jejunum also desquamated, with villous rupture and leakage of the blood cells. Conversely, a significant improvement in LPS-induced pathological changes in the colonic tissue and partial restoration of the structure of glandular and goblet cells was observed at doses of 200 and 400 mg/kg LCEO, suggesting a role in protecting crypts and the epithelial integrity of the colon. The results demonstrated that LPS could cause damage to intestinal tissue's morphology, while LCEO had a protective effect on intestinal tissue, with the highest efficacy observed at high doses of LCEO (Figure 1C). To further assess the impact of LCEO on inflammation, we investigated the cytokine levels in the liver and intestines. The low and medium doses of LCEO significantly lowered the levels of TNF-α, IL-6, and IL-1β in liver in LPS-treated mice (Figure 1D). The medium dose of LCEO also significantly decreased TNF-α, IL-1β, and IL-6 mRNA levels in the duodenum compared with those in the LPS group. Additionally, the low dose of LCEO also significantly decreased the mRNA levels of TNF-α and IL-1β in the duodenum compared with the LPS group. All the results showed the anti-inflammatory effect of LCEO, and the medium dose had the best effect (Figure 1E).

3.2. Molecular docking of LCEO

Table 2 lists the binding energies of nine different docking methods between citral and 4 inflammatory compounds. Binding

TABLE 2 Molecular docking binding energy.

Ingredient	Chemical formula	Protein	Binding energy (kcal/mol)
Citral	C10H16O	IL-1β	−4.489
Citral	C10H17O	IL-1β	−4.283
Citral	C10H18O	IL-1β	−4.237
Citral	C10H19O	IL-1β	−4.175
Citral	C10H20O	IL-1β	−4.171
Citral	C10H21O	IL-1β	−4.141
Citral	C10H22O	IL-1β	−4.14
Citral	C10H23O	IL-1β	−4.125
Citral	C10H24O	IL-1β	−4.115
Citral	C10H25O	IL-6	−4.637
Citral	C10H26O	IL-6	−4.601
Citral	C10H27O	IL-6	−4.415
Citral	C10H28O	IL-6	−4.266
Citral	C10H29O	IL-6	−4.184
Citral	C10H30O	IL-6	−4.18
Citral	C10H31O	IL-6	−4.144
Citral	C10H32O	IL-6	−4.143
Citral	C10H33O	IL-6	−4.131
Citral	C10H34O	TNF-α	−3.759
Citral	C10H35O	TNF-α	−3.466
Citral	C10H36O	TNF-α	−3.416
Citral	C10H37O	TNF-α	−3.402
Citral	C10H38O	TNF-α	−3.343
Citral	C10H39O	TNF-α	−3.207
Citral	C10H40O	TNF-α	−3.042
Citral	C10H41O	TNF-α	−2.991
Citral	C10H42O	TNF-α	−2.98
Citral	C10H43O	Nrf2	−4.992
Citral	C10H44O	Nrf2	−4.45
Citral	C10H45O	Nrf2	−4.41
Citral	C10H46O	Nrf2	−4.37
Citral	C10H47O	Nrf2	−4.348
Citral	C10H48O	Nrf2	−4.334
Citral	C10H49O	Nrf2	−4.311
Citral	C10H50O	Nrf2	−4.3
Citral	C10H51O	Nrf2	−4.283

energy indicates the affinity of the ligand to the receptor, and less than 0 kcal/mol indicates that these ligands and receptors can bind spontaneously. The lower the binding capacity, the more stable the binding of the ligand to the receptor. The docking result is shown in Figure 2. In molecular docking, the higher the absolute value of the binding energy, the more stable the binding. The molecular docking of citral and the inflammatory factors showed that citral can bind well with IL-1β, IL-6, TNF-α, and Nrf2, and citral has an anti-inflammatory function. Citral binds to the LYS-209 and GLN-164 of IL-1β through hydrogen bonds, binds to the ARG-196 of IL-6 through hydrogen bonds, binds to the SER-197 of IL-6 through a hydrophobic interaction, binds to the GLN-137 of TNF-α through hydrogen bonds, binds to the GLN-225 of TNF-α through a hydrophobic interaction, and binds to the LYS-50 of Nrf2 through hydrogen bonds (Figure 2).

3.3. Analysis of the intestinal microbial community after the essential oil intervention

The community barplot analysis elucidated pronounced disparities in microbiological constitution between fecal samples procured prior to LPS injection, and intestinal content samples succeeding LPS injection. Nonetheless, the deviation in microbiological composition between fecal samples and the intestinal content of the control group was marginal (Figures 3A–C). Within the quintet of fecal material groups, an array of microbial taxa, encompassing *Bacteroides*, *Blautia*, *Staphylococcus*, *Akkermansia*, *unclassified_k_norank_d_Bacteria*, *Parasutterella*, *unclassified_f_Ruminococcaceae*, *Erysipelatoclostridium*, *Ruminococcus_gnavus*_group, *norank_f__Oscillospiraceae*, *anaerotruncus*, *unclassified_f__Oscillospiraceae*, *unclassified_o_Bacteroidales*, and *norank_f__Desulfovibrionaceae*, demonstrated considerable disparities. It is noteworthy that *Staphylococcus*, *Akkermansia*, and *Klebsiella* were conspicuously absent in the LCEO cohorts. In contrast, the essential oil intervention group exhibited a substantial upsurge in *Lactobacillaceae*, *Lachnospiraceae*, *Eggerthellaceae*, and *Marinifilaceae* (Figures 3D,E).

In pursuit of delineating the effects of essential oils on intestinal flora, a ternary diagram was leveraged, elucidating variations in community structure abundance at the family echelon among distinct treatment groups (control, model, and essential oil). Each dot embodied an OTU, with its size, hue, and position denoting the relative abundance, taxonomy, and cluster classification of the OTUs, correspondingly. Scrutiny of gut contents manifested pronounced disparities in flora abundance between the trinity of essential oil doses and the model and control groups (Figures 3F,G). The MG group manifested the utmost abundance of *Bacteroidales*, whereas the CG group disclosed heightened prevalence of *Lactobacillales*, accompanied by *Lachnospiraceae* bacteria in the LCEO-L group, *Lactobacillaceae* in the CG group, and *Muribaculaceae* bacteria in the MG group. Notably, no explicit bacterial predilection was discernible among the trio of essential oil groups. An ensuing ternary analysis was undertaken using fecal samples, which presented a more intricate composition. However, marked differences in fecal flora were discernible between the essential oil cohorts and the model and control groups. In comparing disparate doses of essential oils, the FLCEO-L group was typified by heightened abundance of *Rikenellaceae*, the FLCEO-M group by abundant *Lachnospiraceae* and *Marinifilaceae*, while the FLCEO-H group by prevalence of *Helicobacteraceae* and *Bacteroidaceae*. In contrasting the essential oil and control groups with the model group, the control group exhibited diminished abundance of associated flora in their feces, whereas the model group revealed a heightened abundance of *Lachnospiraceae* and *Lachnospiraceae*. These findings underscore significant discrepancies in the intestinal

10.3389/fmicb.2023.1233934

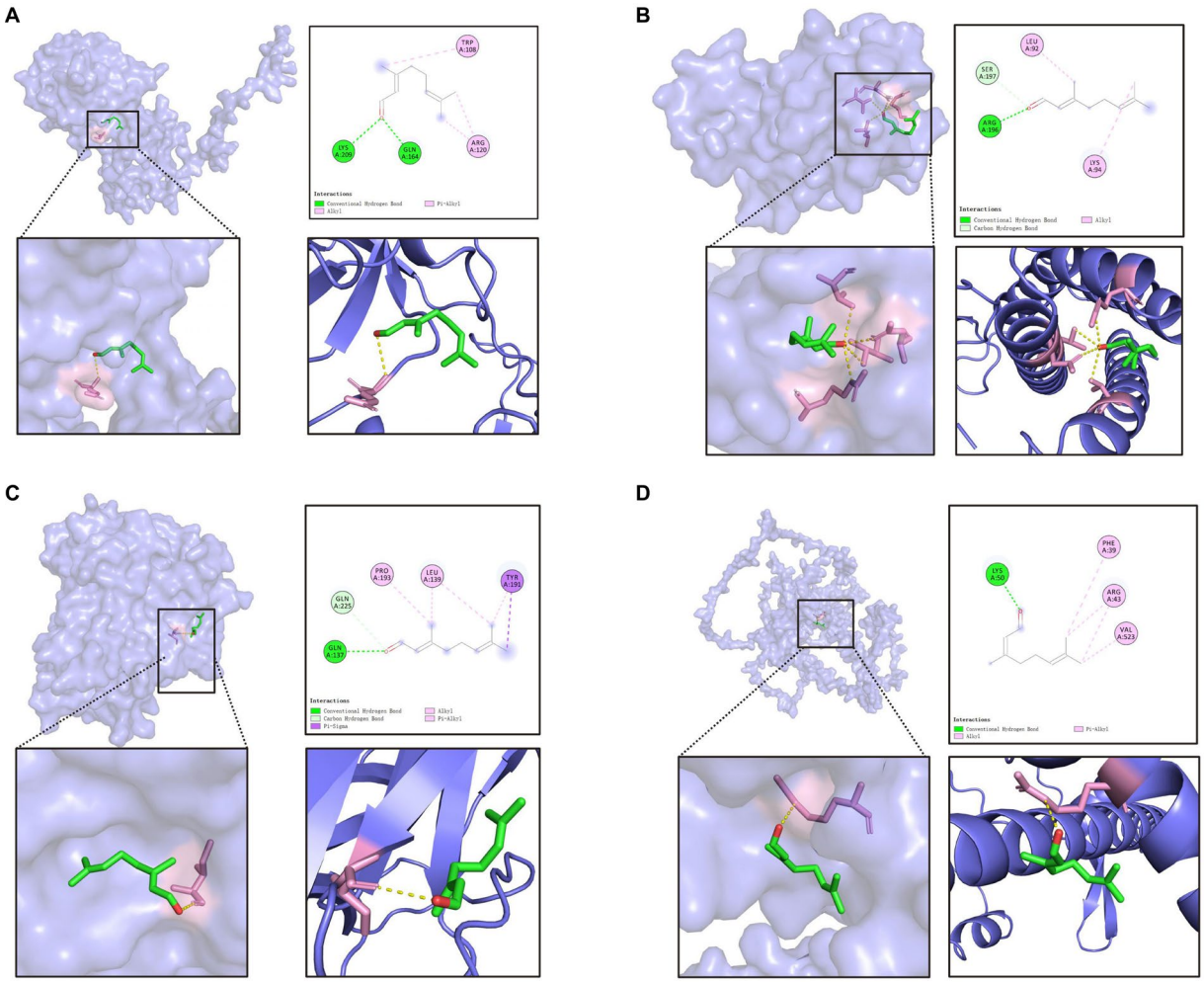

FIGURE 2
Molecular docking of LCEO **(A)** Molecular docking of citral with IL-1β. **(B)** Molecular docking of citral with IL-6. **(C)** Molecular docking of citral with TNF-α. **(D)** Molecular docking of citral with Nrf-2.

microbial community structure between intestinal contents and fecal matter.

3.4. Analysis of the association between the gut microbiota and factors of intestinal inflammation

Our preliminary analysis of the flora in the feces and intestinal contents using bubble plots revealed that three genera, namely *Lachnospiraceae*, *Muribaculaceae*, and *Helicobacter*, were more affected in both sample types. In the intestinal contents, the abundance of *Lachnospiraceae* was significantly higher in the essential oil groups than in the other groups, indicating that essential oils had an important effect on the abundance of *Lachnospiraceae*. In contrast, the abundance of *Muribaculaceae* was inhibited by the intervention of essential oils, particularly in the intestinal contents (Figure 4A). By creating co-occurrence network diagrams to visualize the co-occurrence of the species in the different samples, we confirmed the differences in the effects of different doses of essential oils on the gut microbiota (Figure 4B). The present study aimed to explore the intricate relationships between inflammatory factors and selected species at both the genus and species level. To achieve this, we used a correlation heatmap analysis, which revealed that the correlation between the two was dynamic, with some interactions exhibiting a positive correlation (depicted in blue) and others showing a negative correlation (depicted in red) (Figure 4C). This analysis was performed to gain more insight into the protective effects of essential oil on the gut microbiota and the parameters of LPS-induced inflammation in mice. The result showed that the potential correlations between the gut microbiota at the species level and the expression levels of specific genes, including IL-1β, IL-6, and TNF-α in the duodenum. The results showed that the groups of bacteria that showed a negative correlation with inflammatory factors were *Peptostreptococcaceae, Lactobacillaceae, Erysipelotrichaceae,* and *Bifidobacteriaceae*. Conversely, the groups that showed a positive correlation with inflammatory factors were *Anaerovoracaceae, Ruminococcaceae, Eggerthellaceae, Acholeplasmataceae, Marinifilaceae, Clostridia, Lachnospiraceae, Oscillospiraceae Butyricicoccaceae, Corynebacteriaceae, Prevotellaceae, Peptococcaceae, Monoglobaceae, Desulfovibrionaceae, Enterococcaceae, Deferribacteraceae,* and *UCG-010*. Overall, this analysis provided a comprehensive understanding

10.3389/fmicb.2023.1233934

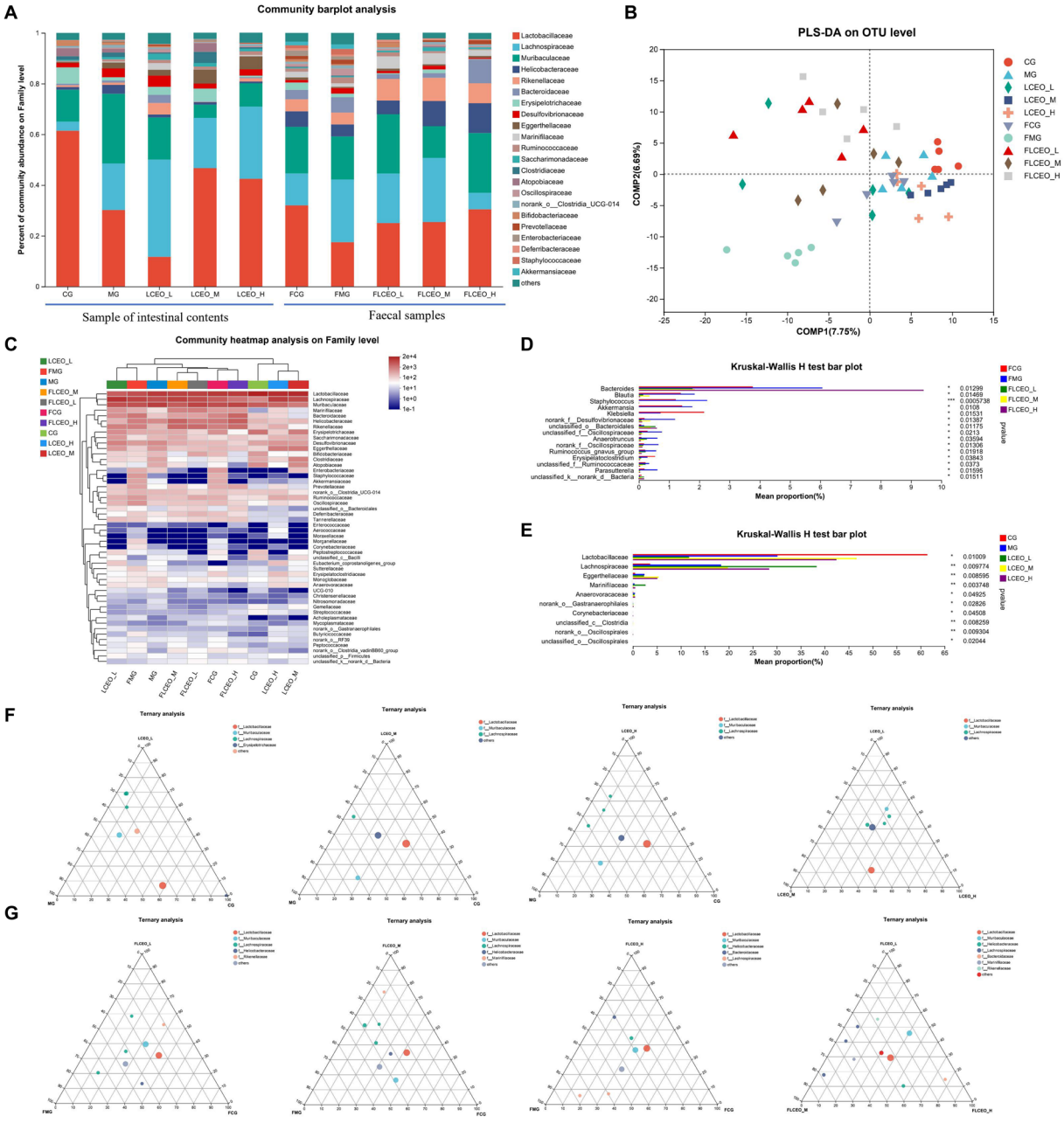

FIGURE 3
Composition of the gut microbiota and fecal samples. **(A)** bacterial taxonomic compositions at the levels of genus in the intestinal digesta and the feces. **(B)** PLS-DA score plots. **(C)** Community heatmap analysis on Family level. **(D)** KrusKal-Wallis H test bar plot of fecal samples. **(E)** KrusKal-Wallis H test bar plot of intestinal content. **(F)** Ternary analysis of intestinal content. **(G)** Ternary analysis of fecal samples.

of the intricate relationships between inflammatory factors and selected species on the genus and species level, thus emphasizing the importance of considering both factors in the context of inflammation. In addition, we used a redundancy analysis (RDA) or canonical correspondence analysis (CCA) to analyze the complex interplay between the microbiota and environmental factors. The RDA/CCA analysis had red arrows to represent the quantitative environmental factors, with the length of each arrow reflecting the degree of the environmental factor's influence on the species. The angles between the arrows of the environmental factors were used to signify positive and negative correlations, with an acute angle indicating a positive correlation, an obtuse angle signifying a negative correlation, and a right angle implying no correlation between the environmental factors and the species. The results showed that IL-1β, IL-6, and TNF-α were positively related to each other, and that the MG group was greatly affected by inflammatory factors (Figure 4D).

3.5. Specific bacterial taxa in the feces and intestinal contents

The histogram depicting the distribution of the LDA values and the evolutionary branch diagram were meticulously crafted through the LDA effect size (LEfSe) analysis. These insightful visualizations

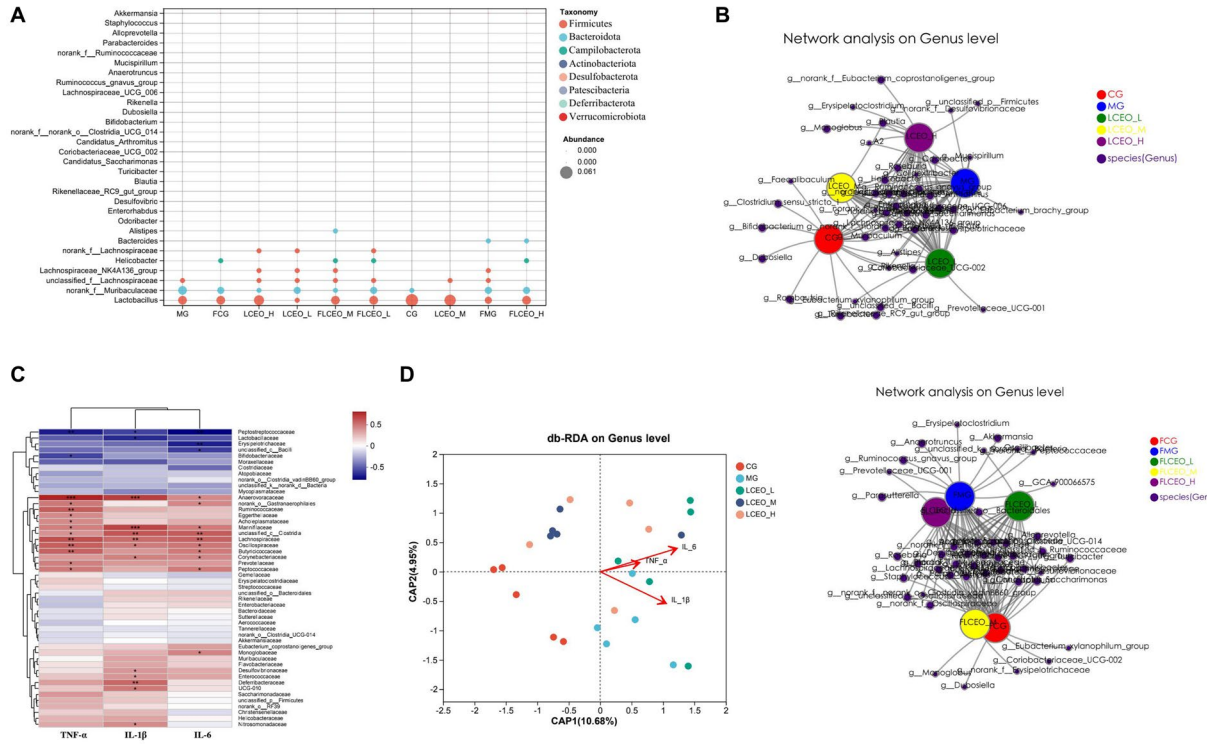

FIGURE 4
(A) The composition of the intestinal and fecal samples in bubble chart. **(B)** The network analysis on genus level intestinal and fecal samples. **(C)** Correlation heatmap between inflammatory factors and selected species on Genus and Species level. **(D)** RDA/CCA analysis of the relationship between microbiota and inflammatory factor.

enabled the exploration of biomarkers, showcasing statistical disparities among the experimental cohorts. The taxonomic cladogram of LEfSe offers a captivating portrayal of the pivotal bacterial modifications, using diverse hues to represent the distinct groups, while the sizes of the circles reflect their relative abundance. The outcomes revealed notable divergence in the composition of the gut microbiota among the different groups. Notably, the LEfSe analysis successfully discerned numerous genera that serve as noteworthy biomarkers, delineating taxonomic discrepancies among the five cohorts. In the intestinal contents samples, 16 genera were identified as discriminating biomarkers, one in the CG group (*Lactobacillus*), eight in the LCEO-L group (*Ruminococcus_gnavus_group, unclassified_f_Lachnospiraceae, Lachnoclostridium, norank_f_Lachnospiraceae unclassified_c_Clostridia, Colidextribacter, norank_f_Oscillospiraceae,* and *Odoribacter*), two in the LCEO-M group (*unclassified_f_Eggerthellaceae,* and *Enterorhabdus*), five in yjr LCEO-H group (*Ruminococcus_gnavus_group, Lachnospiraceae_UCG-006, A2, Eubacterium_brachy_group*, and *norank_f_norank_o_Gastranaerophilales*) (Figure 5A). Additionally, 16 genera were identified as discriminating biomarkers only in the fecal samples (*Ruminococcus_gnavus_group, Lachnospiraceae_FCS020_group, Tuzzerella, Blautia, GCA-900066575, unclassified_f_Ruminococcaceae, Candidatus_soleaferrea, Anaerotruncus, UBA1819, UCG-009, Oscillibacter, norank_f_Oscillospiraceae, unclassified_f_Oscillospiraceae, Eubacterium_nodatum_group, Family_XIII_AD3011_group,* and *norank_f_Peptococcaceae*) (Figure 5B). Subsequently, we performed an evolutionary tree analysis of the gut microbes and found that *Lactobacillus* was the most abundant of all groups, followed by *Muribaculaceae* (Figure 5C).

4. Discussion

The therapeutic potential of essential oils, especially their role in inflammation modulation, is well-documented. In a rigorous analysis, mice subjected to geranium oil treatment showed an increased incidence of yeast-form cells in vaginal smears, indicating the potential of geranium oil and its component, geraniol, to prevent vaginal candidiasis. *In vitro* evaluations revealed geranium oil and geraniol's efficacy in inhibiting fungal filament growth at a modest concentration (25 μg/mL), despite a lack of impact on yeast growth (Maruyama et al., 2008). Concurrently, kanuka and manuka essential oils demonstrated potent antimicrobial and anti-inflammatory properties, suggesting potential utility as pharmaceutical antibiotics, cosmeceutical agents, and dietary supplements (Chen et al., 2016). Furthermore, investigations into the biological activities of 10 essential oils (nine individual and one blend) within a human dermal fibroblast system simulating chronic inflammation revealed notable anti-inflammatory, tissue remodeling, and immunomodulation effects. These findings reinforce the therapeutic potential of essential oils as potential adjunct treatments for a range of conditions (Han et al., 2017).

Historically, the essential oil derived from *L. cubeba* has primarily been investigated for its anti-inflammatory and antibacterial attributes. Notably, Lin elucidated the oil's potential prophylactic

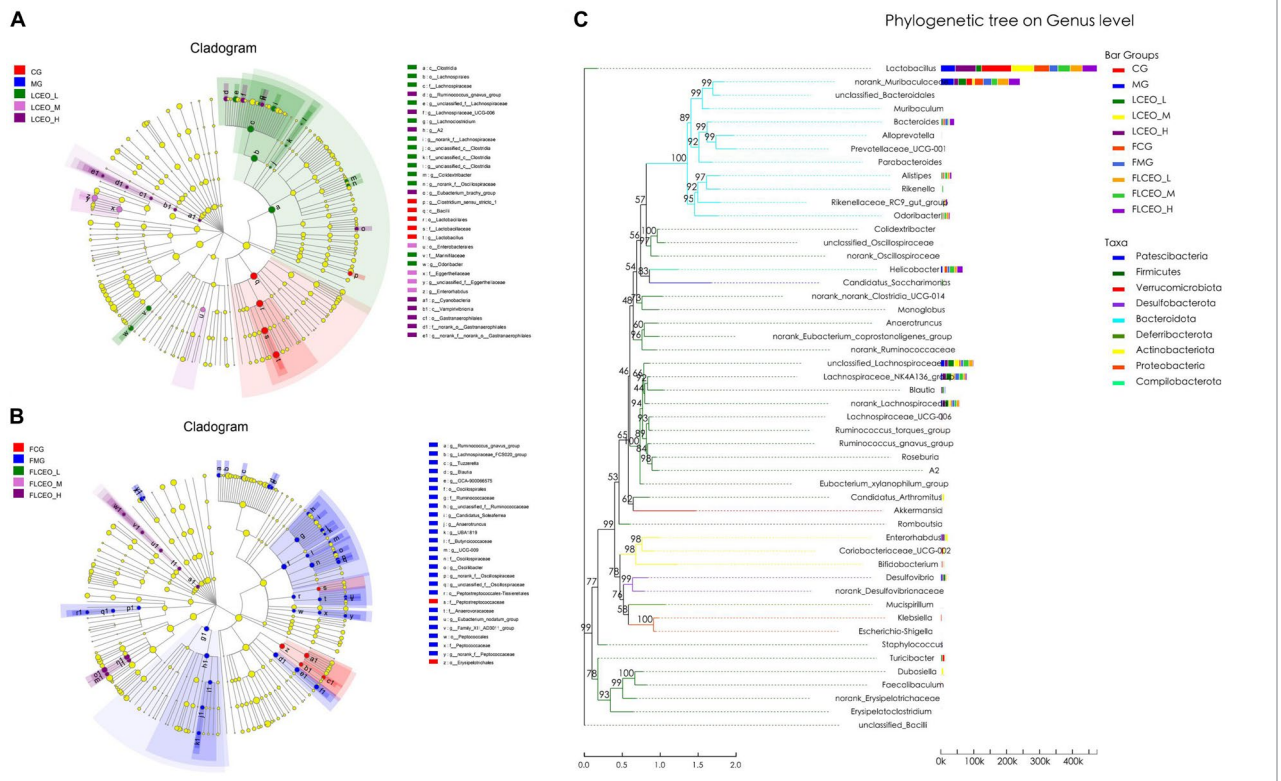

FIGURE 5
The specific microbiota taxa in samples **(A)** Species with significant differential effects at different taxonomic levels in LEfsa analysis in intestinal. **(B)** Species with significant differential effects at different taxonomic levels in LEfsa analysis in fecal. **(C)** polygenetic tree on genus level.

capabilities in mitigating rheumatoid arthritis, employing a rat model with Freund's complete adjuvant-induced arthritis (Lin et al., 2013). The consequential discoveries underscored a substantial mitigation of arthritis via downregulation of pro-inflammatory cytokines and inflammatory enzymes, concurrently with an increase in anti-inflammatory cytokine IL-10 levels, thereby implying prospective applications of *L. cubeba* roots in human arthritis therapeutics. Our research subsequently emphasizes LCEO's impact on gastrointestinal health. Our analysis revealed the oil's potential as a treatment for diarrhea and its protective effect on gut integrity, with evidence of reduced intestinal tissue damage and maintained crypt and colon epithelial integrity. Moreover, the oil displayed anti-inflammatory characteristics, as evidenced by reduced TNF-α, IL-6, and IL-1β levels in hepatic and intestinal tissues. A prior study on the antibacterial action and kinetics of LCEO identified aldehydes—comprising about 70% of the total constituents—as the key contributors to its antibacterial efficacy, with minor components synergistically enhancing this effect. Therefore, given its antimicrobial properties, *L. cubeba* oil exhibits broad utility in industries ranging from flavoring and spicing to antimicrobial interventions (Li et al., 2014).

Previous research has shed light on the significant interactions between citral, a major component of *Litsea cubeba* essential oil, and the Nrf2 pathway. For instance, a study by Ka et al. showed that citral could ameliorate the severity of lupus nephritis by enhancing Nrf2 activation and inhibiting the activation signal of the NLRP3 inflammasome (Ka et al., 2015). Another research conducted by Yang et al. highlighted the renoprotective effect of citral in a model of focal segmental glomerulosclerosis, partly attributed to the activation of the Nrf2 pathway (Yang et al., 2013). Furthermore, a recent study demonstrated the protective effects of citral against LPS-induced endometritis, finding that these effects were exerted through inhibiting ferroptosis and activating the Nrf2 signaling pathway (Zhao et al., 2023). Given these compelling evidences of citral's interaction with the Nrf2 pathway, and the pivotal role this pathway plays in regulating oxidative stress and inflammation, we selected it as a primary focus of our research. This added context underpins our investigation into the impacts of LCEO, and particularly citral, on gut health. Citral, as the main natural compound of LCEO, which is also found in citrus fruits and essential oils such as lemongrass and lemon verbena, possesses various beneficial properties. One notable function of citral is its potential anti-inflammatory activity. We also found that citral exhibited anti-inflammatory effects by modulating inflammatory factors involved in the immune response. In our study, citral showed strong binding to IL-1β, IL-6, and TNF-α, and exerted anti-inflammatory effects via hydrogen-bonding interactions. It was found to bind effectively to inflammatory factors such as interleukin-1β (IL-1β), interleukin-6 (IL-6), and tumor necrosis factor-alpha (TNF-α), which were key mediators in the inflammatory process. Through these hydrogen-bonding interactions, citral interacts with specific amino acid residues in these inflammatory factors, thereby inhibiting their activity. By binding to IL-1β, IL-6, and TNF-α, citral may interfere with the signaling pathways that promote inflammation, thereby reducing the production and release of pro-inflammatory cytokines. Overall, citral shows promise as a natural compound with anti-inflammatory properties. Moreover, some researchers have investigated its *in vitro* effects on the production of cytokines (IL-1β,

IL-6, and IL-10) both before and after LPS incubation, demonstrating the anti-inflammatory effects and potential role of citral in inhibiting the production of cytokines through suppression of the transcription factor NF-KB (Bachiega and Sforcin, 2011). In addition, citral was found to activate PPAR-γ, and its anti-inflammatory effects were reversed by the PPAR-γ antagonist GW9662. Using a well-established rat model of systemic LPS administration, Ka et al. (2015) reported the *in vivo* antipyretic effects of citral, suggesting that its protective mechanism in the mouse ASLN model involved inhibiting the activation of the NLRP3 inflammasome signal and enhancing the Nrf2 antioxidant signal. Muñoz-Pérez (Munoz-Perez et al., 2021) further investigated the modulatory role of citral in inflammation resulting from infection with *S. aureus* and discovered a significant inhibition of PGF-2α-induced contractions, a concentration-dependent increase in myometrial cAMP levels, and a concentration-dependent decrease in the LPS-induced production of TNFα and IL-1β, while the production of IL-10 was significantly increased. In conclusion, according to the findings of others and the present study, we have reason to believe that citral plays a key role in alleviating LPS-induced intestinal inflammation in mice, and that these studies have contributed to a comprehensive understanding of the potential therapeutic applications of citral and the underlying mechanisms of various biological processes.

In addition to its inflammatory effect, essential oils have an important impact on the abundance of intestinal flora and bacteria. Previous studies found that a mixture of organic acids and essential oils had a beneficial effect on the gut microflora and improved the immune response and disease resistance of *L. vannamei* (He et al., 2017). In another study, the researchers evaluated the effects of three essential oils, namely cinnamon bark oil (CNO), clove bud oil (CLO), and ajwain seed oil (AJO), with different major chemical structures as alternatives to antibiotic growth promoters (AGPs) on the gut health, immune response, and antioxidant status of broiler chickens (Chowdhury et al., 2018). In our research, we used community barplot analysis to discern significant disparities in the microbiological composition within fecal samples and intestinal contents before and after the essential oil intervention. Prominent variations in the taxa were identified, revealing marked differences in the abundance of flora among the essential oil groups, the model group, and the control group. The MG group displayed the highest abundance *of Bacteroidales*, the CG group exhibited the most substantial abundance of *Lactobacillales*, and the LCEO-L group was characterized by the dominance of *Lachnospiraceae*. Analyses of the fecal flora revealed heterogeneity among the essential oil groups, the model group, and the control group. When we compared the different doses of essential oil, FLCEO-L had increased *Rikenellaceae,* FLCEO-M had an abundance of *Lachnospiraceae* and *Marinifilaceae*, and FLCEO-H had an abundance of *Helicobacteraceae* and *Bacteroidaceae*. The control group had a reduced abundance of flora in the feces, whereas the model group had an increased abundance of *Lachnospiraceae*. Our findings unveil significant alterations in the composition of gut microbiota consequent to the administration of essential oils, underscoring the substantial variations observed between intestinal contents and feces. Essential oils were shown to augment the population of *Lachnospiraceae* in the intestinal contents while inhibiting *Muribaculaceae*. This demonstrates the substantial influence these oils may exert on intestinal microbial communities. Further, these modulations were observed to be dose-dependent, corroborated by co-occurrence networks. The discovery of bacterial groups inversely correlated with inflammation, such as *Peptostreptococcaceae, Lactobacillaceae, Erysipelotrichaceae*, and *Bifidobacteriaceae,* as well as those showing positive correlation, like *Anaerovoracaceae, Ruminococcaceae*, and *Eggerthellaceae,* suggests an intriguing potential for essential oils to modulate inflammation via microbiota manipulation. Future exploration could delve into investigating this anti-inflammatory potential and the precise mechanisms of action. LEfSe analysis revealed discriminatory biomarkers, including the genera *Lactobacillus, Ruminococcus_gnavus*_group, and *Lachnoclostridium* among others. Notably, *Lactobacillus*, the most abundant genus, and *Muribaculaceae* revealed distinct divergence in their distributions within the evolutionary tree, presenting potential targets for future investigation. The stark divergence in the gut microbiota composition demands further exploration to elucidate the possible impacts on host health and disease resistance. The findings of this study suggest that essential oils can cause significant changes in the composition of gut microbiota. Importantly, essential oils were found to increase the population of Lachnospiraceae while decreasing Muribaculaceae. This suggests that essential oils may have a significant influence on the balance of microbial communities within the intestine, and these changes appear to be dose-dependent. Another key aspect of this research was the discovery of bacterial groups that correlated negatively with inflammation, including *Peptostreptococcaceae, Lactobacillaceae*, *Erysipelotrichaceae*, and *Bifidobacteriaceae*, as well as bacterial groups that correlated positively with inflammation, such as *Anaerovoracaceae*, *Ruminococcaceae*, and *Eggerthellaceae*. This finding could have significant implications for the development of essential oil-based treatments or preventive strategies for inflammatory diseases, suggesting a potential mechanism through which essential oils might exert their effects by modulating the gut microbiota.

Overall, this study propounds a comprehensive understanding of the potential applications and mechanisms of essential oils in various animal production settings. However, the far-reaching implications of these findings go beyond the realm of animal health. Given the burgeoning interest in the human gut microbiome's role in health and disease, our insights could pioneer new avenues for employing essential oils in manipulating gut microbiota for promoting human health, with possible applications in disease treatment, health maintenance, and even personalized nutrition. In this study, we explored the effects of LCEO on LPS-induced intestinal inflammation and the gut microbiome. Our findings demonstrated that the LCEO treatment alleviated gut inflammation and suggested its potential in the treatment of intestinal inflammation. However, there are certain limitations to consider in our study. Firstly, our study focused on the effects of LCEO on LPS-induced intestinal inflammation in experimental models. Further investigations are needed to evaluate its efficacy in clinical settings, as well as its safety profile. Secondly, while we observed changes in the composition of the gut microbiome following the LCEO intervention, our study only provided a snapshot of the microbial community at a specific time point. Longitudinal studies would provide a more comprehensive understanding of the dynamic changes in the gut microbiome over time. Thirdly, the mechanisms underlying the anti-inflammatory effects of LCEO and its interaction with the gut microbiome remain to be fully elucidated. Additional research is warranted to explore the specific pathways and molecular mechanisms involved in the observed

effects. Moreover, our study focused on the evaluation of citral as the main natural compound in LCEO. While citral has demonstrated anti-inflammatory properties, further studies are needed to investigate its specific mechanisms of action and its potential as a therapeutic agent. Lastly, our study primarily relied on animal models and *in vitro* experiments. The translation of these findings to human subjects may vary, and clinical studies are needed to validate the efficacy and safety of LCEO in human populations. In conclusion, while our study provides valuable insights into the anti-inflammatory effects of LCEO and its impact on the gut microbiome, further research is necessary to address the limitations and fully understand the therapeutic potential of LCEO in the management of intestinal inflammation.

Data availability statement

The datasets presented in this study can be found in online repositories. The names of the repository/repositories and accession number(s) can be found in the article/supplementary material.

Ethics statement

The animal study was reviewed and approved by the Animal Ethics Committee at Loudi Central Hospital (LCH2022015).

Author contributions

LX: writing—original draft, methodology, data curation, visualization, software, formal analysis, resources, investigation, and validation. TT: methodology, validation, and writing—review and editing. HD: methodology and resources. RZ and ZL: methodology, validation, and writing—review and editing. RL, ZS, and CX: conceptualization, methodology, writing—review and editing, supervision, project administration, and funding acquisition. All authors contributed to the article and approved the submitted version.

Funding

This work was supported by the Research and Development Plan in Key Fields of Hunan Province (2022SK2126), Research Foundation of Hunan Administration of Traditional Chinese Medicine (A2023054, 2019101), Shaoguan University Doctoral Research Fund (142-9900064602), Research Foundation of Natural Science Foundation of Hunan Province (2022JJ30041, 2021JJ40550, 2022JJ80098, and 2022JJ50101), Scientific Research Project of Hunan Provincial Health Commission (202103101455 and 202102081835), Clinical Innovation Leading Scientific Research Projects of Hunan Science and Technology Department (2020SK52603 and 2021SK52901), Guangdong Basic and Applied Basic Research Foundation (2022A1515111127), Science and Technology Program of Guangzhou (2023A04J0468), and China Postdoctoral Science Foundation (2022M710908).

Conflict of interest

The authors declare that the research was conducted in the absence of any commercial or financial relationships that could be construed as a potential conflict of interest.

Publisher's note

All claims expressed in this article are solely those of the authors and do not necessarily represent those of their affiliated organizations, or those of the publisher, the editors and the reviewers. Any product that may be evaluated in this article, or claim that may be made by its manufacturer, is not guaranteed or endorsed by the publisher.

References

Bachiega, T. F., and Sforcin, J. M. (2011). Lemongrass and citral effect on cytokines production by murine macrophages. *J. Ethnopharmacol.* 137, 909–913. doi: 10.1016/j.jep.2011.07.021

Barton, G. M. (2008). A calculated response: control of inflammation by the innate immune system. *J. Clin. Invest.* 118, 413–420. doi: 10.1172/JCI34431

Candelli, M., Franza, L., Pignataro, G., Ojetti, V., Covino, M., Piccioni, A., et al. (2021). Interaction between lipopolysaccharide and gut microbiota in inflammatory bowel diseases. *Int. J. Mol. Sci.* 22:6242. doi: 10.3390/ijms22126242

Chen, C. C., Yan, S. H., Yen, M. Y., Wu, P. F., Liao, W. T., Huang, T. S., et al. (2016). Investigations of kanuka and manuka essential oils for *in vitro* treatment of disease and cellular inflammation caused by infectious microorganisms. *J. Microbiol. Immunol. Infect.* 49, 104–111. doi: 10.1016/j.jmii.2013.12.009

Chowdhury, S., Mandal, G. P., Patra, A. K., Kumar, P., Samanta, I., Pradhan, S., et al. (2018). Different essential oils in diets of broiler chickens: 2. Gut microbes and morphology, immune response, and some blood profile and antioxidant enzymes. *Anim. Feed Sci. Technol.* 236, 39–47. doi: 10.1016/j.anifeedsci.2017.12.003

De Fazio, L., Spisni, E., Cavazza, E., Strillacci, A., Candela, M., Centanni, M., et al. (2016). Dietary geraniol by oral or enema administration strongly reduces dysbiosis and systemic inflammation in dextran sulfate sodium-treated mice. *Front. Pharmacol.* 7:38. doi: 10.3389/fphar.2016.00038

Feng, T., Zhang, R. T., Tan, Q. G., Zhang, X. Y., Liu, Y. P., Cai, X. H., et al. (2009). Two new isoquinoline alkaloids from *Litsea cubeba*. *J Chem Sci* 64, 871–874. doi: 10.1515/znb-2009-0717

Han, X., Beaumont, C., and Stevens, N. (2017). Chemical composition analysis and *in vitro* biological activities of ten essential oils in human skin cells. *Biochim Open* 5, 1–7. doi: 10.1016/j.biopen.2017.04.001

He, W., Rahimnejad, S., Wang, L., Song, K., Lu, K., and Zhang, C. (2017). Effects of organic acids and essential oils blend on growth, gut microbiota, immune response and disease resistance of Pacific white shrimp (*Litopenaeus vannamei*) against *Vibrio parahaemolyticus*. *Fish Shellfish Immunol.* 70, 164–173. doi: 10.1016/j.fsi.2017.09.007

Ka, S. M., Lin, J. C., Lin, T. J., Liu, F. C., Chao, L. K., Ho, C. L., et al. (2015). Citral alleviates an accelerated and severe lupus nephritis model by inhibiting the activation signal of NLRP3 inflammasome and enhancing Nrf2 activation. *Arthritis Res. Ther.* 17:331. doi: 10.1186/s13075-015-0844-6

Li, W. R., Shi, Q. S., Liang, Q., Xie, X. B., Huang, X. M., and Chen, Y. B. (2014). Antibacterial activity and kinetics of *Litsea cubeba* oil on *Escherichia coli*. *PLoS One* 9:e110983. doi: 10.1371/journal.pone.0110983

Lin, B., Zhang, H., Zhao, X. X., Rahman, K., Wang, Y., Ma, X. Q., et al. (2013). Inhibitory effects of the root extract of *Litsea cubeba* (lour.) pers. on adjuvant arthritis in rats. *J. Ethnopharmacol.* 147, 327–334. doi: 10.1016/j.jep.2013.03.011

Maruyama, N., Takizawa, T., Ishibashi, H., Hisajima, T., Inouye, S., Yamaguchi, H., et al. (2008). Protective activity of geranium oil and its component, geraniol, in combination with vaginal washing against vaginal candidiasis in mice. *Biol. Pharm. Bull.* 31, 1501–1506. doi: 10.1248/bpb.31.1501

Munoz-Perez, V. M., Ortiz, M. I., Salas-Casa, A., Perez-Guerrero, J., Castillo-Pacheco, N., Barragan-Ramirez, G., et al. (2021). *In vitro* effects of citral on the human myometrium: potential adjunct therapy to prevent preterm births. *Birth Defects Res* 113, 613–622. doi: 10.1002/bdr2.1873

Sharma, M., Koul, A., Sharma, D., Kaul, S., Swamy, M. K., and Dhar, M. K. (2019). Metabolic engineering strategies for enhancing the production of bio-active compounds from medicinal plants. *Nat. Bio-act. Comp.* 3, 287–316. doi: 10.1007/978-981-13-7438-8_12

Sommer, F., and Backhed, F. (2013). The gut microbiota - masters of host development and physiology. *Nat. Rev. Microbiol.* 11, 227–238. doi: 10.1038/nrmicro2974

Wu, W., Wang, S., Liu, Q., Shan, T., and Wang, Y. (2018). Metformin protects against LPS-induced intestinal barrier dysfunction by activating AMPK pathway. *Mol. Pharm.* 15, 3272–3284. doi: 10.1021/acs.molpharmaceut.8b00332

Yang, S. M., Hua, K. F., Lin, Y. C., Chen, A., Chang, J. M., Kuoping Chao, L., et al. (2013). Citral is renoprotective for focal segmental glomerulosclerosis by inhibiting oxidative stress and apoptosis and activating Nrf2 pathway in mice[J]. *PLoS One* 8:e74871. doi: 10.1371/journal.pone.0074871

Zhao, W., Wang, J., Li, Y., and Ye, C. (2023). Citral protects against LPS-induced endometritis by inhibiting ferroptosis through activating Nrf2 signaling pathway. *Inflammopharmacology* 31, 1551–1558. doi: 10.1007/s10787-023-01211-2

Zheng, H., Jin, S., Shen, Y. L., Peng, W. Y., Ye, K., Tang, T. C., et al. (2021). Chinese herbal medicine for irritable bowel syndrome: a meta-analysis and trial sequential analysis of randomized controlled trials. *Front. Pharmacol.* 12:694741. doi: 10.3389/fphar.2021.694741

Zhu, H., Wang, H., Wang, S., Tu, Z., Zhang, L., Wang, X., et al. (2018). Flaxseed oil attenuates intestinal damage and inflammation by regulating necroptosis and TLR4/NOD signaling pathways following lipopolysaccharide challenge in a piglet model. *Mol. Nutr. Food Res.* 62:e1700814. doi: 10.1002/mnfr.201700814

Zhuang, S., Zhong, J., Bian, Y., Fan, Y., Chen, Q., Liu, P., et al. (2019). Rhein ameliorates lipopolysaccharide-induced intestinal barrier injury via modulation of Nrf2 and MAPKs. *Life Sci.* 216, 168–175. doi: 10.1016/j.lfs.2018.11.048

frontiers | Frontiers in Microbiology

TYPE Original Research
PUBLISHED 13 September 2023
DOI 10.3389/fmicb.2023.1257701

OPEN ACCESS

EDITED BY
Fengjie Sun,
Georgia Gwinnett College, United States

REVIEWED BY
Hongkai Bi,
Nanjing Medical University, China
Zhangran Chen,
Xiamen University, China

*CORRESPONDENCE
Yundong Sun
✉ syd@sdu.edu.cn
Dawei Wang
✉ wangdawei@sdu.edu.cn

†These authors have contributed equally to this work and share first authorship

RECEIVED 12 July 2023
ACCEPTED 30 August 2023
PUBLISHED 13 September 2023

CITATION
Feng Y, Sun H, Zhu R, Tao J, Su R, Sun Y and Wang D (2023) Effects of alcohol on the symptoms of gouty arthritis and taxonomic structure of gut microbiota in C57BL/6 mice. *Front. Microbiol.* 14:1257701. doi: 10.3389/fmicb.2023.1257701

Effects of alcohol on the symptoms of gouty arthritis and taxonomic structure of gut microbiota in C57BL/6 mice

Yu Feng[1†], Haihui Sun[2†], Ruilou Zhu[1], Jianxing Tao[1], Rui Su[3], Yundong Sun[4*] and Dawei Wang[1*]

[1]Department of Orthopedic, Shandong Provincial Hospital Affiliated to Shandong First Medical University, Jinan, China, [2]Department of Cardiology, Shandong Provincial Hospital Affiliated to Shandong First Medical University, Jinan, China, [3]Department of Clinical Laboratory, Shandong Provincial Hospital Affiliated to Shandong First Medical University, Jinan, China, [4]Key Laboratory for Experimental Teratology of Ministry of Education, Department of Microbiology, School of Basic Medicine, Cheeloo College of Medicine, Shandong University, Jinan, China

Gout is an acute arthritis caused by the elevated levels of serum uric acid (UA), and its prevalence has been rapidly increasing. Alcohol abuse could lead to a series of health problems. Multiple pieces of evidence suggest that alcohol intake affects the development and progression of gout, while the gut microbiota plays an important role in the development of gout and the long-term alcohol consumption could affect the stability of the gut microbiota. This study aimed to explore the effects of alcohol intake at different concentrations on gouty arthritis based on the gut microbiota. We investigated the effects of different concentrations of alcohol on gouty arthritis in mouse models of acute gouty arthritis established by injection of monosodium urate (MSU) crystals into C57BL/6 mice. The results indicated that the high-alcohol consumption not only exacerbated joint swelling and pain, increased the levels of UA, tumor necrosis factor-α (TNF-α), interleukin-1β (IL-1β), and interleukin-6 (IL-6), but also showed dramatic effects on the composition and structure of the gut microbiota in gouty mice. Two key microorganisms, *Parasutterella* and *Alistipes*, could aggravate gout symptoms through lipopolysaccharide biosynthesis, riboflavin metabolism, phenylalanine metabolism, and arginine and proline metabolisms. In conclusion, our study suggested that high-concentrations of alcohol altered the gut microbiota structure in gouty mice induced by MSU crystals, which could exacerbate gouty symptoms by enhancing pro-inflammatory pathways.

KEYWORDS

alcohol, gouty arthritis, gut microbiota, purine metabolism, pro-inflammatory cytokine

1. Introduction

Gout is an acute arthritis caused by elevated serum uric acid (UA) levels, activation of inflammatory mediators, and cytokine release, ultimately leading to deposition of monosodium urate (MSU) crystals in the joints (So and Martinon, 2017). In addition, gout can lead to kidney diseases such as uric acid nephrolithiasis and chronic nephropathy (Singh and Gaffo, 2020). In recent years, the prevalence of gout has been rapidly increasing worldwide due to the changes in dietary habits and lifestyle (Kuo et al., 2015). The overall estimated prevalence of gout is 2.6%, with a significantly higher proportion in males (3:1 to 4:1) (Ankli and Daikeler, 2023). Alcohol

is generally considered a potential risk factor for acute gouty arthritis and recurrent gout attacks (Neogi et al., 2014).

Alcohol abuse could lead to a range of health problems (Barbería-Latasa et al., 2022). For example, it has been reported that an increase in alcohol consumption is closely associated with an increased risk of gout, with a 1.17-fold increase in risk for every 10 grams of alcohol consumed per day (Tu et al., 2017). A cross-sectional study has shown that gout patients with consumption of 15–30 g and 30–60 g of alcohol per day gained increased risks of recurrence by 1.36-fold and 1.51-fold, respectively, compared to non-drinking gout patients (Neogi et al., 2014). Consumption of various alcoholic beverages, e.g., liquor, beer, and wine, could increase the UA levels and thereby increase the risk of gout attacks (Neogi et al., 2014). Furthermore, some of the non-alcoholic components in alcoholic beverages may contain different purine contents, thus excessive alcohol consumption could induce the progression of gouty arthritis by providing excessive exogenous purines (Liu et al., 2021). However, the molecular mechanisms underlying the exacerbation of gouty arthritis by alcohol are still not clearly known.

Studies have found that the homeostasis of the gut microbiota influences the development of human physical and mental health (Postler and Ghosh, 2017), while the gut microbiota could influence the progression of gouty arthritis (Guo et al., 2016). Recent research has shown that β-carotene and green tea powder diet could alleviate gout symptoms by modulating the structure of the gut microbiota in gouty mice (Feng et al., 2022). Furthermore, studies have shown that alcohol could increase the diversity of gut microbiota in mice and cause damages in both hepatic and colon tissues (Wang et al., 2018). Moreover, strong evidence has suggested that gut microbiota composition in alcohol abusers greatly differs from that in healthy individuals (Dubinkina et al., 2017).

Dietary habits are important factors affecting the composition and function of gut microbiota (Qin et al., 2022). Alcohol abuse could alter gut permeability, leading to bacterial translocation to mesenteric lymph nodes and hepatic tissue, further exacerbating the disease progression (Leclercq et al., 2014; Wang et al., 2016). Therefore, we hypothesized that alcohol could alter the structure of the gut microbiota in gouty mice, which could exacerbate the progression of gout. In this study, our goals were to establish a mouse model of acute gouty arthritis by injection of MSU crystals and to further investigate the effects of alcohol at different concentrations on gout symptoms, pro-inflammatory cytokines, and gut microbiota in mice. The results showed that high concentrations of alcohol changed the structures of the gut microbiota and aggravated gout symptoms in gouty mice, whereas the significant effects of low concentrations of alcohol on mice with gout were not observed.

2. Materials and methods

2.1. Consumable alcohol and MSU crystals

Consumable alcohol (ethanol and water, 98–99% of total) was purchased from Beijing Hongxing Co. (Beijing, China). MSU was purchased from Sigma Aldrich Trading Co. (Shanghai, China; Cat. U2875).

A total of 800 mg of MSU was accurately weighed and added into the boiling Milli-Q water (155 mL) with the pH of the solution adjusted to 7.2 using both NaOH (5 mL) and hydrochloric acid, and gradually cooled with stirring at room temperature. Then, MSU crystals were colledted by centrifugation at 3000 g and 4°C for 2 min (Model 5430R, Eppendorf, Germany) and stored after sterilization at 180°C for 2 h (Ruiz-Miyazawa et al., 2017).

2.2. Animals

Thirty Specific Pathogen Free (SPF) C57BL/6 male mice (4 weeks old with average weight = 15 ± 2 g) were purchased from Beijing Vital River Experimental Animal Technology Co., Ltd. (Beijing, China). All mice were continuously provided with food and water in a standard environment (12/12 h light/dark cycle, 40% humidity, and temperature of 22 ± 1°C). During the entire experiment (6 weeks), there were no deaths or other abnormal conditions observed in any of the mice. The Animal Ethics Review Board of the Provincial Hospital of Shandong First Medical University approved this study (Permit No. 2022–025).

2.3. Experimental design

After 1 week of rearing in a standardized environment, 30 mice were randomly and evenly grouped and kept in 6 cages (i.e., 5 mice per cage), including the healthy control group (CTL), the acute gouty arthritis model group (AGA), the two low-concentration alcohol experimental groups (treated with 0.3 and 0.8% alcohol, respectively), and the two high-concentration alcohol experinmental groups (treated with 10 and 20% alcohol, respectively). Previous clinical studies have confirmed a correlation between daily alcohol consumption in adults and an increased risk of gout (Tu et al., 2017). Therefore, the alcohol concentration consumed by mice in the low concentration alcohol group was calculated based on the ratio of daily alcohol consumption in adults to body weight. The concentration of alcohol consumed by mice in the high-concentration alcohol groups was determined based on previous studies (Wang et al., 2018). All six groups of mice were given a normal diet every day (protein content 18–22% Kcal, fat content 4–8% Kcal, total 3.56 Kcal/g; Wuhan Shisheng Biotechnology Co., Wuhan, China). In the CTL and AGA groups, mice were orally administered drinking water daily, while the mice in the alcohol groups were given alcohol orally. Additionally, every 10 d, mice in the CTL group were injected with 40 μL of PBS into the right hind paw pad, while 1 mg of MSU crystals mixed with 40 μL of PBS was injected into the right hind paw pad of the other five groups of mice (Figure 1A; Lin et al., 2020). During the entire experiment (6 weeks), both food and alcohol bottles were weighed every morning at 10 am to calculate the food and alcohol intakes by the mice.

2.4. Evaluation of foot joint hypersensitivity and oedema

Monosodium urate crystals were injected into the right hindfoot pads of mice at 10 a.m. each day. Starting from the second injection of MSU crystals, the thickness of the right hindfoot pads of all mice was measured using digital calipers (Meinaite, Germany) before and at 4, 24, 48, and 72 h after injection. The mechanical withdrawal threshold

10.3389/fmicb.2023.1257701

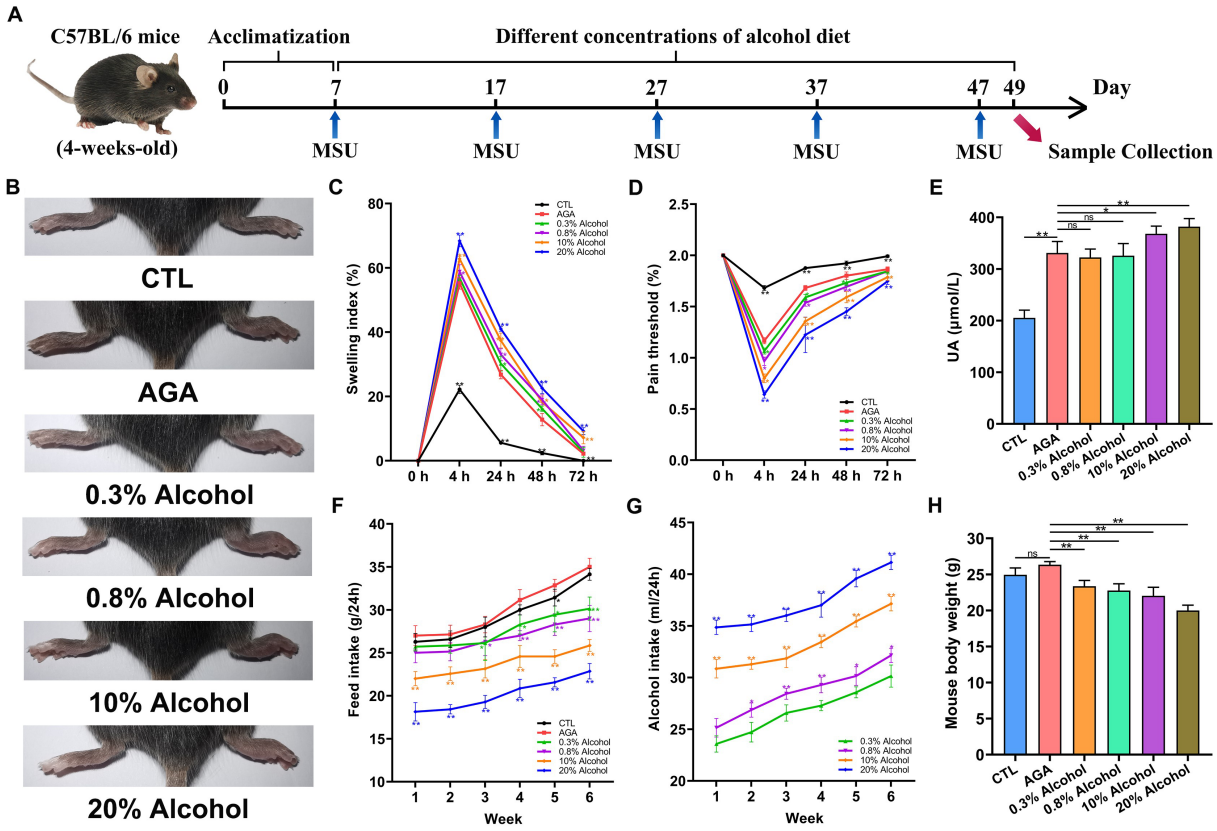

FIGURE 1
Effect of alcohol on body weight and foot joint gout symptoms in mice. **(A)** Schematic diagram of the experimental treatments. MSU, monosodium urate. **(B)** Schematic representation of the appearance of foot joints in six groups of mice. CTL, control. AGA, acute gouty arthritis. **(C)** Comparison of changes in footpad swelling in six groups of mice. **(D)** Comparison of changes in footpad pain thresholds in six groups of mice. **(E)** Comparison of changes in serum uric acid (UA) levels in six groups of mice. **(F)** Food intake of the six groups of mice. **(G)** Comparison of changes in alcohol intake in mice of the alcohol group. **(H)** Comparison of body weight changes in six groups of mice after 6 weeks of feeding. Data are presented as mean ± standard deviation. Statistical differences are determined by $p < 0.05$ (*) and $p < 0.01$ (**), respectively; "ns" represents no statistical significance.

(MWT) was quantified using von Frey monofilaments (Danmic Global LLC Co., Ltd., USA) to assess the foot pain. Foot swelling was expressed as the ratio of Δmm/mm (baseline) of the joint (Lin et al., 2020).

2.5. Sample collection

At the end of the 6 week (42 day) experiment, all mice were weighed and samples were collected. The mouse blood was collected through the orbital vein, then centrifuged to collect serum and stored at −80°C. Subsequently, all mice were exectued using CO_2 (100%) for 5 min, and fresh fecal samples were immediately collected from mouse colon tissues that were stored at −80°C. In addition, the hepatic and right foot joint tissues in mice were collected in an ice water bath environment and stored at −80°C after rapid freezing in liquid nitrogen.

2.6. Measurements of cytokines and enzymes

The mouse foot joint specimens and hepatic specimens were kept at room temperature for slow thawing, followed by homogenization of the tissues (0.05 g of tissue per 1.0 mL of buffer solution) and centrifugation of the tissues at 6,500 g and 4°C for 10 min to collect the supernatant. Previous studies have shown that xanthine oxidase (XOD) and adenosine deaminase (ADA) in the hepatic could further influence the uric acid production by participating in the purine metabolism (Lou et al., 2020). Therefore, the enzymatic activities of myeloperoxidase (MPO), XOD, and ADA were assayed using a mouse ELISA kit (Kelvin, Suzhou, China). Previous studies have shown that the pro-inflammatory cytokines IL-6, IL-1β, and TNF-α were associated with inflammatory activity in gout patients (Galozzi et al., 2021). The levels of serum UA and proinflammatory cytokines (i.e., IL-1β, IL-6, and TNF-α) in mice as well as in foot joint supernatants were measured by mouse ELISA kits (Novus, Germany).

2.7. Histopathological assessment of foot joint

Foot joint tissues of mice were thawed at room temperature and washed with PBS solution. Subsequently, the foot joints were immersed in 10% paraformaldehyde for 12 h and then decalcified with EDTA for 14 d. The decalcified foot joint tissues were embedded in paraffin for sectioning of 5 μm thickness. The sections were then

stained with hematoxylin and eosin (HE) and observed for morphological changes and degree of inflammation in the foot joint tissues.

2.8. Gut microbiota analysis

Nucleic acids were extracted from mouse fecal samples using the TGuide S96 Magnetic Soil/Fecal DNA Kit (Tiangen Biotechnology Co., Ltd., Beijing, China) according to the manufacturer's instructions. The 16S rRNA gene was amplified and sequenced on the Illumina Miseq platform using the universal bacterial primer 338F (5'-ACTCCT ACGGGAGGCAGCA-3′) and 806R (5'-GGACTACHVGGGT WTCTAAT-3′) by BioMarker Technologies Co. (Beijing, China) (Zhang et al., 2021). Sequencing libraries were quality checked for high-quality tag sequences. The 16S rRNA sequences were analyzed using QIIME version 1.9.3. Sequences were clustered at 97% similarity level (USEARCH, version 10.0), and OTUs were filtered using 0.005% of the number of all sequences as a threshold. Species annotation and classification were performed based on the Silva database[1] and RDP Classifier.[2] Alpha diversity indices were calculated using Mothur (version v. 1.30). Beta diversity analysis was performed by principal coordinate analysis (PCoA) to compare differences in community composition and structure among samples. Finally, biomarker taxa that were statistically different between groups were screened at the genus level. Spearman's correlation coefficients between microbial communities and gout symptoms were calculated using the "cort.test" function in the R statistical software, and the correlations were visualized in heat maps. In addition, the metabolic functions of the gut microbiota were predicted using Picrust (Feng et al., 2022). These predictions were precalculated based on the gene functional annotation using the Kyoto Encyclopedia of Genes and Genomes (KEGG) database.[3] The datasets used in this study are deposited in the NCBI database[4] with the accession number PRJNA990312.

2.9. Statistics

Biochemical data were plotted using GraphPad Prism (V8.0.2). Significant differences in microbial structure and gene expressions between two groups were determined using *t*-test based on $p < 0.05$.

3. Results

3.1. Gout symptoms aggravated in mice with intake of high concentration of alcohol

The effects of different concentrations of alcohol on weights and foot joint gout symptoms in mice were evaluated by measuring the daily food and alcohol intakes, foot pad swelling and pain threshold, levels of serum UA (Figure 1). Compared to the CTL group, the level of foot joint swelling in other groups of mice was significantly higher, the foot pad mechanical pain thresholds were significantly decreased, and the serum UA level were significantly increased (Figures 1B–E). The above indexes indicated that the MSU crystals were injected into the right hind paw of mice to successfully establish an acute gouty arthritis mouse model. In addition, compared to the AGA group, the mice of the alcohol groups were observed with significantly increased degree of foot joint swelling, as the concentrations of alcohol were increased, while the foot pad mechanical pain thresholds were significantly decreased (Figures 1C,D). Compared to the AGA group, the serum UA levels were significantly increased in mice fed with high concentrations of alcohol (Figure 1E).

The results of daily weighing of food and alcohol bottles showed that as the concentration of alcohol was increased, the food intake of the mice was gradually decreased and the alcohol intake was gradually increased (Figures 1F,G). After 6 weeks of feeding, all mice in the alcohol group showed a significant decrease in body weight compared to the AGA group (Figure 1H).

3.2. Gout inflammation index aggravated in mice with intake of high concentration of alcohol

To further investigate the effects of alcohol on gouty arthritis, the inflammation of gouty sites in mice was evaluated in each group of mice (Figure 2). Histological analysis showed that compared to the CTL group, the AGA group of mice exhibited significantly increased infiltration of inflammatory cells in the foot joints (Figure 2A). Compared to the AGA group, treatment of high concentrations of alcohol dramatically increased the infiltration of inflammatory cells in the foot joints of gouty mice, while the significant changes were not observed in the number of foot joint inflammatory cells of mice treated with low concentrations of alcohol (Figure 2A). Similarly, compared to the AGA group, the high alcohol concentration group showed significantly higher levels of MPO, IL-1β, IL-6, and TNF-α in the right foot joints of mice, and there were no significant changes in the levels of these inflammatory factors in the right foot joints of mice in the low-concentration alcohol group (Figure 2B).

In order to further investigate the changes in inflammatory factors associated with gout, the expression levels of IL-1β, IL-6, and TNF-α were re-examined in serum (Figure 2C). Serum IL-1β levels were significantly higher in gouty mice in the high-alcohol group compared with the AGA group, while no significant changes were detected in mice treated with low concentrations of alcohol. Conversely, as the concentrations of alcohol were increased, the serum of mice in all alcohol groups showed progressively higher levels of TNF-α and IL-6.

3.3. Intestinal microbial structure in mice altered by the intake of high concentrations of alcohol

The 16S rRNA sequencing was used to analyze fecal samples from gouty mice to study the effect of alcohol on the gut microbiota of mice. The results showed that the microbial alpha diversity of mice was gradually increased as the concentration of alcohol was increased, compared to the AGA group (Figure 3A). The microbial alpha

1 http://www.arb-silva.de/
2 http://sourceforge.net/projects/rdpclassifier/
3 https://www.genome.jp/kegg/
4 https://www.ncbi.nlm.nih.gov/sra/

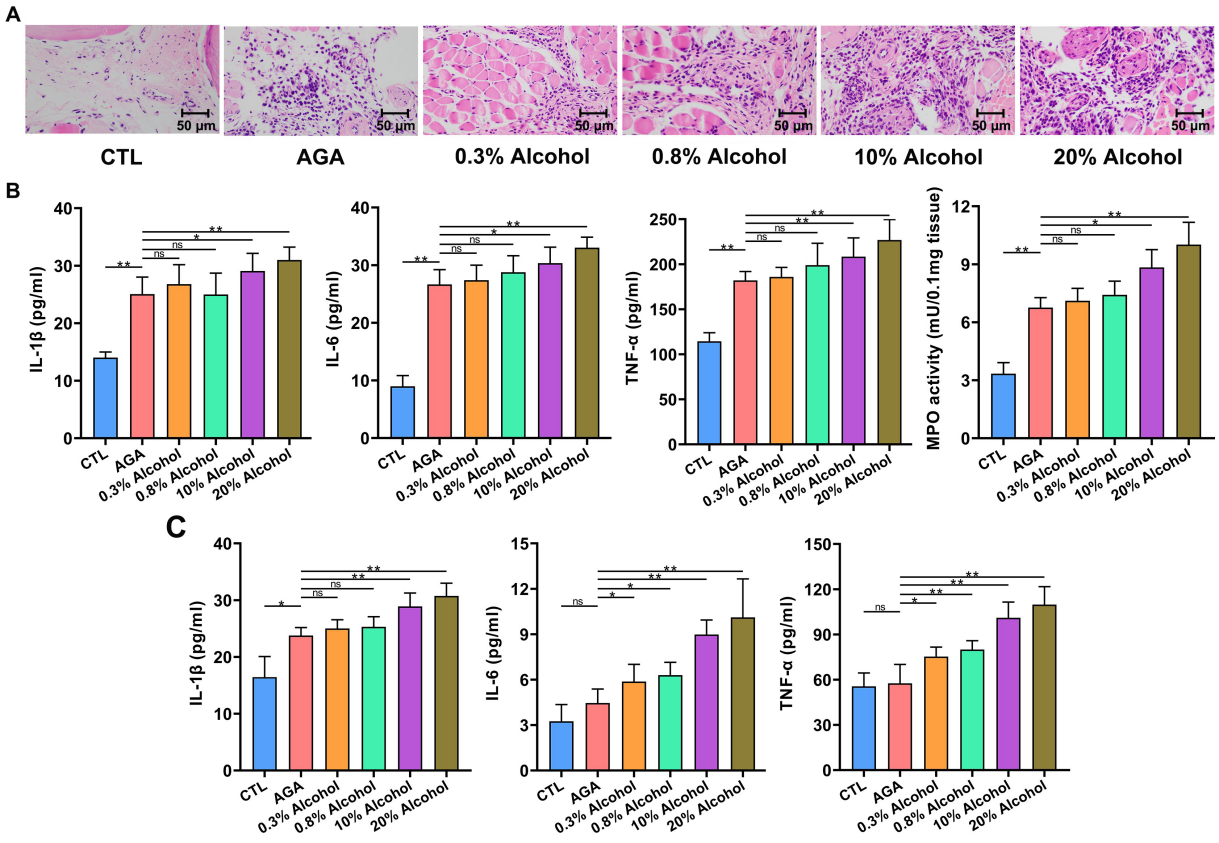

FIGURE 2
Gout-associated inflammatory markers aggravated by alcohol in mice. **(A)** HE analysis of the right hindfoot pads of six groups of mice. **(B)** Comparison of changes in the levels of cytokines interleukin-1β (IL-1β), IL-6, and tumor necrosis factor-α (TNF-α), and the enzymatic activity of myeloperoxidase (MPO), in foot joint tissues of six groups of mice. **(C)** Comparison of changes in serum cytokine (i.e., IL-1β, IL-6, and TNF-α) levels in six groups of mice (based on ELISA). Data are presented as mean ± standard deviation. Statistical differences are determined by $p < 0.05$ (*) and $p < 0.01$ (**), respectively; "ns" represents no statistical significance.

diversity was significantly increased in mice with gout treated with high concentrations of alcohol (Figure 3A; Supplementary Figure S1). PCoA results showed that the gut microbiota of mice in the high alcohol concentration group was significantly different from that of mice in the CTL and AGA groups, while the gut microbiota of mice in the low alcohol concentration group was not significantly different from that of mice in the CTL and AGA groups (Figure 3B). Analysis of the changes in the dominant bacterial groups at the phylum level showed a gradual decrease in the ratio of Firmicutes to Bacteroidota (F/B) as the concentration of alcohol was increased (Figures 3C,D). Similarly, at the genus level, there were significant differences in the structure of the gut microbiota in different groups of mice (Figure 3E). Compared to the AGA group, alcohol consumption in mice resulted in decreased relative abundances of *unclassified_Lachnospiraceae* and *Ligilactobacillusp.*, while the relative abundances of *unclassified_Muribaculaceae* and *Parasutterella* were increased (Figure 3E).

The effects of low concentrations of alcohol intake on the gut microbiota of gouty mice were found to be insignificant by α-diversity and β-diversity analyses (Figures 3A,B), only the effect of high concentration of alcohol on intestinal microbiota of mice was further explored (Figure 4). At the genus level, the relative abundances of bacteria greater than 1% were compared between the mice of AGA group and the high alcohol concentration group (Figures 4A,B). Compared to the AGA group, the relative abundances of *Parasutterella*, *Alistipes*, and *Dubosiella* were significantly decreased in the 10% alcohol group (Figure 4A), while the relative abundances of *Parasutterella*, *Alistipes*, *Parabacteroides*, and *unclassified_Oscillospiraceae* were significantly increased in the 20% alcohol group (Figure 4B). Therefore, two genera, i.e., *Parasutterella* and *Alistipes*, common to both the 10 and 20% alcohol groups of mice, were identified as the key bacteria. In addition, changes in the relative abundances of critical bacteria in each of the samples from the 4 groups of mice were visualized with the heatmaps (Figure 4C).

3.4. Intestinal microbial interactions in mice altered by the intake of high concentration of alcohol

Spearman's correlation ≥ 0.1 and $p \leq 0.05$ were used as screening criteria to select the 50 most relatively abundant microbials for further study of their correlation in the gut microbiome.The results showed that the intestinal microbes were closely associated with each other (Figure 5). The interactions among intestinal microbes were increased in mice of AGA group compared to the CTL group (Figures 5A,B). In contrast, administration of high concentrations of alcohol to mice

10.3389/fmicb.2023.1257701

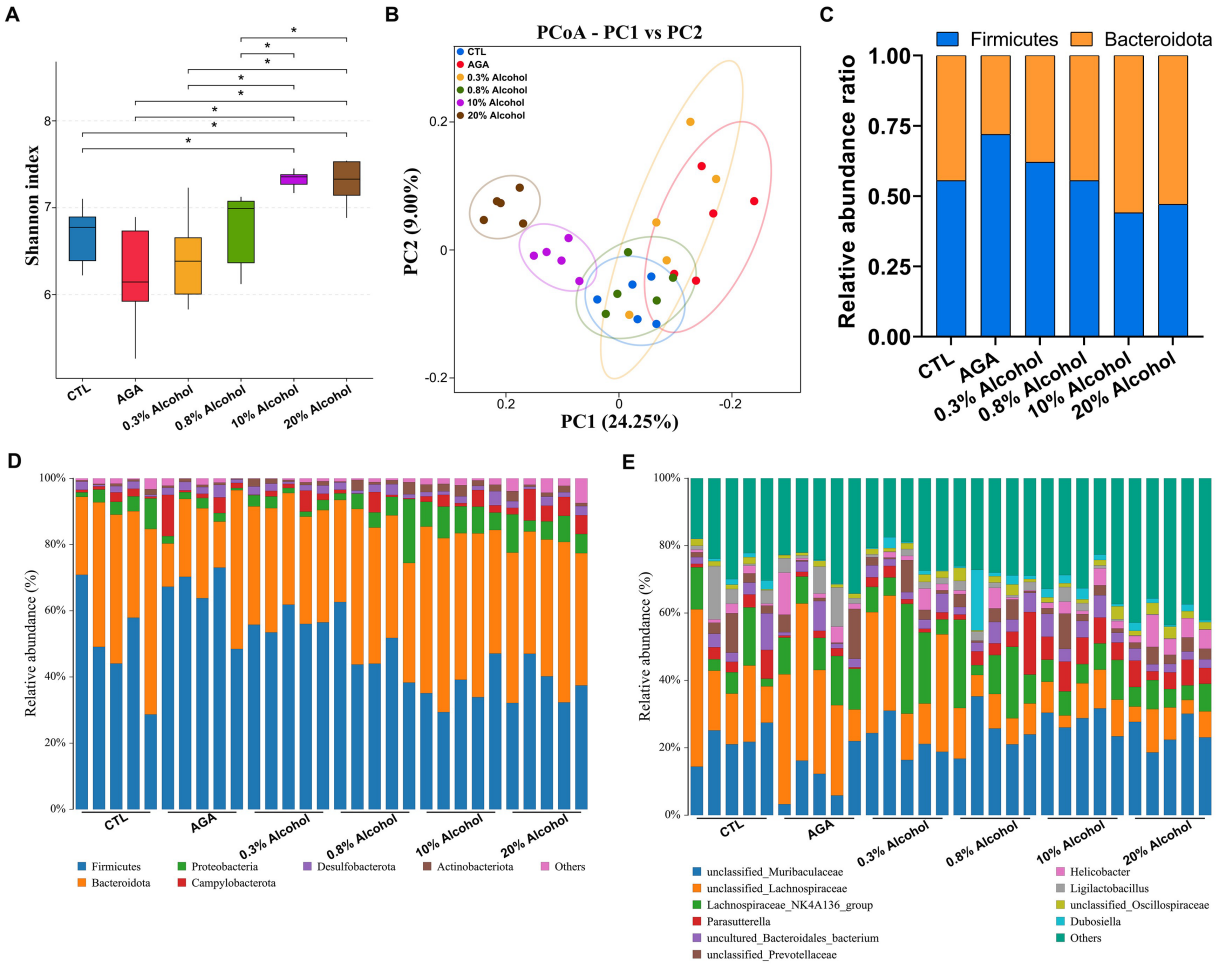

FIGURE 3
Comparison of changes in gut microbiota in six groups of mice. **(A)** Alpha diversity analysis of the intestinal microbiota in six groups of mice. **(B)** Principal coordinate analysis (PCoA) of intestinal microbiota in six groups of mice. **(C)** Variations in the relative proportions of Firmicutes and Bacteroidota in the intestines of six groups of mice. **(D)** Comparison of changes in the composition of the intestinal microflora at the phylum level in six groups of mice. **(E)** Comparison of changes in the composition of the gut microbiota at the genus level in six groups of mice. Data are presented as mean ± standard deviation. The statistical difference is determined by $p < 0.05$ (*).

significantly reduced the gut microbial interactions (Figures 5C,D). For example, in the CTL group, *Desulfovibrio* (#24) was negatively correlated with *unclassified_Lachnospiraceae* (#36) and *unclassified_Oscillospiraceae* (#1) (Figure 5A). *Desulfovibrio* (#29) was negatively correlated with *Bacteroides* (#4), *Oscillibacter* (#5), *Muribaculum* (#6), and *Prevotellaceae_UCG_001* (#10) in the AGA group (Figure 5B). In the 10% alcohol group, *Desulfovibrio* (#24) was negatively correlated with *Enterorhabdus* (#27) (Figure 5C). In the 20% alcohol group, *Desulfovibrio* (#48) was negatively correlated with *Candidatus_Arthromitus* (#29) and *Ileibacterium* (#33) (Figure 5D). The most pronounced decrease in interactions between gut microbes was observed in mice treated with 20% alcohol (Figure 5D).

3.5. Metabolic functions of the intestinal microbiota in mice altered by the intake of high concentration of alcohol

Gut microbiota functions in mice were predicted by PICRUSt based on the KEGG database (Figure 6). The results indicated that the levels of the four metabolic pathways, compared to the AGA group, namely, lipopolysaccharide biosynthesis, riboflavin metabolism, phenylalanine metabolism, and arginine and proline metabolism, were significantly elevated in the gut microbiota of mice in the high concentration alcohol group (Figures 6A,B). The levels of purine metabolic pathways, which are closely related to uric acid levels, were not significantly increased (Figure 6C). The results of activities of two enzymes (i.e., XOD and ADA) related to purine metabolism in the hepatic tissue revealed no significant changes in the hepatic enzyme activities of mouse XOD and ADA in the high-alcohol group compared to the AGA group (Supplementary Figure S2).

3.6. Correlations among key gut microorganisms, inflammatory indicators, and metabolic pathways in mice

Spearman rank correlation coefficient heatmap analysis was applied to analyze the association between key bacterial taxa, pro-inflammatory factors, serum UA, foot and joint MPO, hepatic

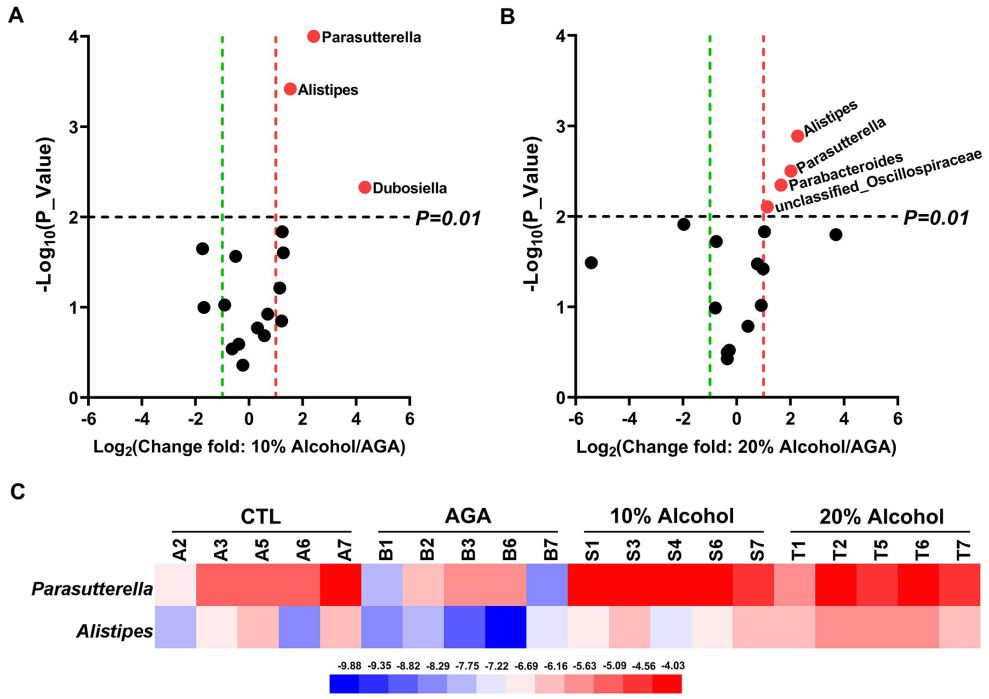

FIGURE 4
Comparative analysis of changes in the genus level of key bacteria in mice in high alcohol concentration groups. **(A)** Volcano plot analysis of changes in the intestinal microbiota of mice in the 10% Alcohol group compared to the AGA group. **(B)** Volcano plot analysis of changes in the intestinal microbiota of mice in the 20% Alcohol group compared to the AGA group. The significant difference is determined by *t*-test. Bacteria with relative abundance >1% are identified as key bacteria. **(C)** Heatmap showing the relative abundance of the key bacteria co-occurring in both **(A,B)**.

XOD, and ADA levels, and four key metabolic pathways (Figure 7). The results showed that the two key bacterial genera, *Parasutterella* and *Alistipes*, were not correlated with XOD and ADA activity levels, but were significantly and positively correlated with the levels of IL-1β, IL-6, TNF-α, UA, and MPO (Figure 7A). Both *Parasutterella* and *Alistipes* were also positively correlated with four metabolic pathways, i.e., lipopolysaccharide biosynthesis, riboflavin metabolism, phenylalanine metabolism, and arginine and proline metabolism (Figure 7A), while both lipopolysaccharide biosynthesis and riboflavin metabolism were positively correlated with the levels of IL-1β, IL-6, TNF-α, and MPO, negatively correlated with the level of ADA, and not correlated with XOD and UA levels (Figure 7B). Phenylalanine metabolism as well as arginine and proline metabolism were not significantly correlated with XOD and ADA levels, but were positively correlated with UA, IL-1β, IL-6, TNF-α, and MPO levels (Figure 7B).

4. Discussion

Acute gout attacks could severely affect people's physical and mental health (Terkeltaub, 2017). Strong evidence has suggested a close relationship between alcohol consumption and the development of gout, with intestinal microbiota playing an important role in gout (Neogi et al., 2014; Guo et al., 2016). The results of this study showed that treatment of high concentrations of alcohol exacerbated the acute gout symptoms induced by MSU crystals in mice and altered the gut microbial composition of gout mice. It is commonly known that changes in gut microbiota could lead to metabolic disorders. Our results showed that the production of abnormal metabolites enhanced the gout symptoms by promoting the release of inflammatory mediators (Figure 8).

Alcohol is an addictive substance consumed worldwide, and the alcohol consumption levels and patterns are closely associated with various types of chronic diseases (Hendriks, 2020). Many studies have suggested that moderate drinking could lower the risk of death, mainly due to reduced risks of cardiovascular diseases and diabetes (Larsson et al., 2016; Li et al., 2016). However, chronic alcohol abuse could cause alcohol use disorders and increased risks of various types of cancers and neurological diseases (Larsson et al., 2013; Hendriks, 2020). Currently, there are still a large number of significant controversies surrounding the safe intake levels of alcohol (Barbería-Latasa et al., 2022).

4.1. High concentration alcohol intake alters the structure of gut microbiota in mice

Gut microbiota, generally considered an endocrine organ, plays an important role in regulating the host immune system and maintaining the intestinal barrier integrity (Kogut et al., 2020). A healthy gut microbiota promotes host growth and development, whereas alterations in the structure of the gut microbiota could have many detrimental effects on the host (Compare et al., 2016). Furthermore, research has shown that the long-term alcohol consumption could affect the stability of the gut microbiota

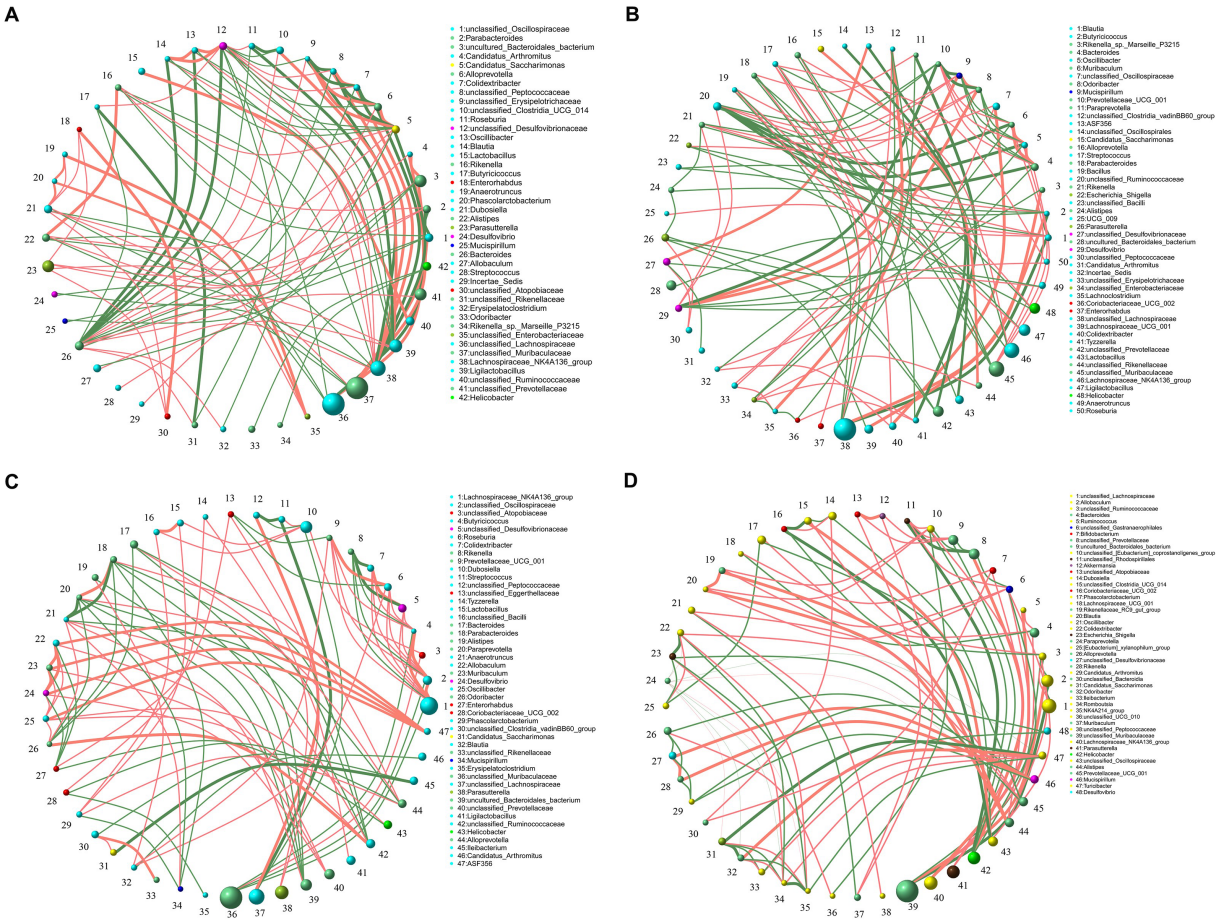

FIGURE 5
Correlation of microbiota among the top 50 taxa at the genus level in the intestines of four groups of mice, including the CTL group **(A)**, the Model group **(B)**, the 10% Alcohol group **(C)**, and the 20% Alcohol group **(D)**. The size of the circle represents the relative abundance, the line represents the correlation between the two taxa at both ends of the line, the thickness of the line represents the level of the correlation, the orange line represents positive correlation, and the green line represents negative correlation.

(Dubinkina et al., 2017), while alcohol-impaired mice have been revealed with a significantly increased diversity of gut microbiota, with varied degrees of damage to both the hepatic and colon tissues (Wang et al., 2018). Moreover, alcohol could induce osteoporosis in mice by regulating variations in the gut microbiota to further activate osteoclasts (Cheng et al., 2021).

Studies have shown that MSU crystals could alter the structure of the gut microbiota (Vieira et al., 2015). Furthermore, previous studies revealed significant changes in gut immunity and environment during the acute and recurrent phases of arthritis (Nemoto et al., 2020). Our results showed that as the concentrations of alcohol consumed by gout mice were gradually increased, the alpha diversity of gut microbiota in gout mice was also gradually increased, while the relative abundance of Firmicutes was decreased. Firmicutes is generally considered an anti-inflammatory bacterium (Natividad et al., 2015). The imbalance of the F/B ratio may lead to metabolic syndrome, such as obesity and diabetes (Turnbaugh et al., 2006). In addition, studies have found that *Lactobacillus paracasei* X11 can restore the ratio of F/B in the gut microbiota of gout mice and improve the structure and function of the gut microbiota (Cao J. et al., 2022). Therefore, we speculated that the decrease in the ratio of F/B caused by alcohol could contribute to the exacerbation of gout symptoms. At the genus level, the treatment of high concentrations of alcohol significantly increased the relative abundances of *Parasutterella* and *Alistipes* in mice. *Parasutterella*, a core member of the gut microbiota in both human and mouse, is closely associated with the development of inflammatory bowel disease (Blasco-Baque et al., 2017). Metabolomic studies have shown that *Parasutterella* affects the metabolism of aromatic amino acids, bilirubin, purines, and bile acids (Ju et al., 2019). Furhtermore, a significant increase was revealed in the relative abundance of *Parasutterella* in a chronic hepatic injury model induced by alcohol in mice (Sang et al., 2021). Moreover, feeding high-fat food to gout mice was also detected to increase the relative abundance of *Parasutterella*, exacerbating the symptoms of gout (Lin et al., 2020). Bacteroidota are often associated with chronic intestinal inflammation (Parker et al., 2020), while *Alistipes* is a genus of the phylum Bacteroidota. Previous studies have revealed the associations between *Alistipes* and various medical disorders, e.g., hepatic fibrosis, colorectal cancer, and other potential diseases (Moschen et al., 2016; Rau et al., 2018). Furthermore, *Alistipes* uses its unique way of fermentation of amino acids, i.e., putrefaction, which plays a crucial role in inflammation and diseases (Kaur et al., 2017). An increase in the relative abundance of *Alistipes*

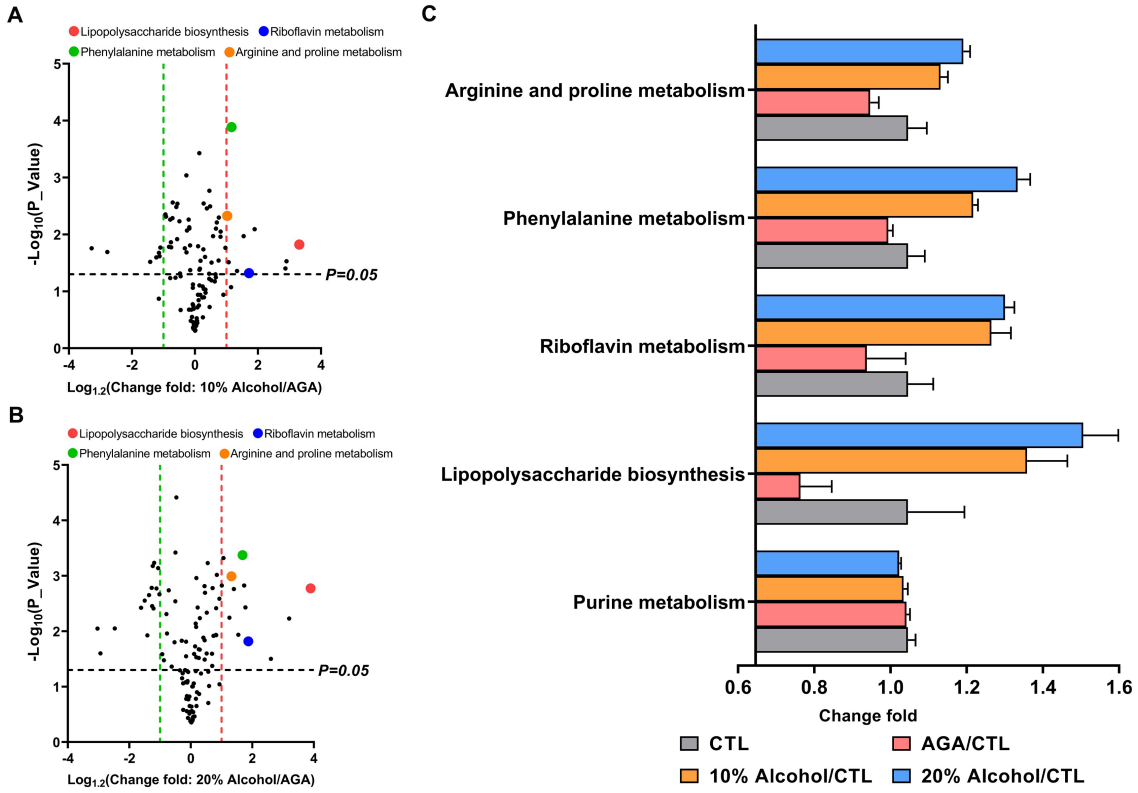

FIGURE 6
Comparison of the relative abundances of functional profiles of the intestinal microbiota of mice in high alcohol concentration groups based on Picrust. **(A)** Volcano plot analysis of altered KEGG pathways in mice of the 10% Alcohol group vs. Model group, with mean relative abundance >0.1%. **(B)** Volcano plot analysis of altered KEGG pathways in mice of the 20% Alcohol group vs. Model group, with mean relative abundance >0.1%. The significant difference is determined by *t*-test. **(C)** Relative abundance of five key metabolic pathways identified in both **(A)** and **(B)** showing the significant difference in the four groups of mice. Data are presented as mean ± standard deviation.

has also been observed in alcohol-intoxicated mice (Wang et al., 2018). Additionally, it has been found that the increased relative abundance of *Alistipes* could aggravate gout symptoms by regulating the purine metabolism (Shirvani-Rad et al., 2023).

4.2. Effects of intake of high concentration of alcohol on metabolism in mice

Our results showed that consumption of high concentrations of alcohol significantly increased the levels of lipopolysaccharide biosynthesis, riboflavin metabolism, phenylalanine metabolism, and arginine and proline metabolism. Lipopolysaccharide has been revealed with many harmful effects and has worsen the disease progression by enhancing the release of inflammatory mediators (Schaffert et al., 2009). Recent studies showed that the bacteria releasing lipopolysaccharide could participate in the pathogenesis of gout by stimulating the immune system (Shirvani-Rad et al., 2023). Furthermore, studies have shown that phenylalanine promotes the alcohol-induced oxidative stress (Hu et al., 2017), while metabolomic studies have revealed a significantly positive correlation between the level of plasma phenylalanine and gout in humans (Mahbub et al., 2017). A recent study found that fructose could aggravate the colonic inflammation by inducing dysregulation of arginine and proline metabolism (Song et al., 2023). Purine metabolism disorder could result in a significant amount of UA production, which in turn affects the progression of gout (Kuo et al., 2015). The riboflavin metabolism in gut microbiota is considered a function involved in purine metabolism (Jiménez et al., 2005), which could lead to higher levels of UA. Furthermore, metabolic studies have shown that alcohol consumption could lead to increased level of serum lactat, thereby blocking the renal excretion of urate salts and potentially leading to increased level of UA (Choi et al., 2004).

Previous studies have demonstrated that *Parasutterella* and *Alistipes* have been implicated in the pathogenesis of constipation and heart disease, respectively, through their impact on lipopolysaccharide biosynthesis and exacerbation of inflammatory responses (Wan et al., 2019; Yang et al., 2021). Studies have shown that taking the new type of synbiotics can lower the relative level of *Parasutterella*, thereby reducing the relative abundance of lipopolysaccharide biosynthesis, as well as significantly reduces the levels of serum LPS, TNF-α, and IL-6, to inhibit the inflammatory response and improve constipation in rats (Yang et al., 2021). In addition, associations between *Parasutterella* and *Alistipes* with phenylalanine metabolism have been detected in ulcerative colitis and brain-related diseases such as Alzheimer's disease and Parkinson's disease (Cao C. et al., 2022; Eicher and Mohajeri, 2022). Bacteria with pro-inflammatory characteristics (*Alistipes*) may be involved in microglial cell activation and neuroinflammatory responses by increasing the production of pro-inflammatory cytokines through the modulation of phenylalanine metabolism, thereby contributing to the

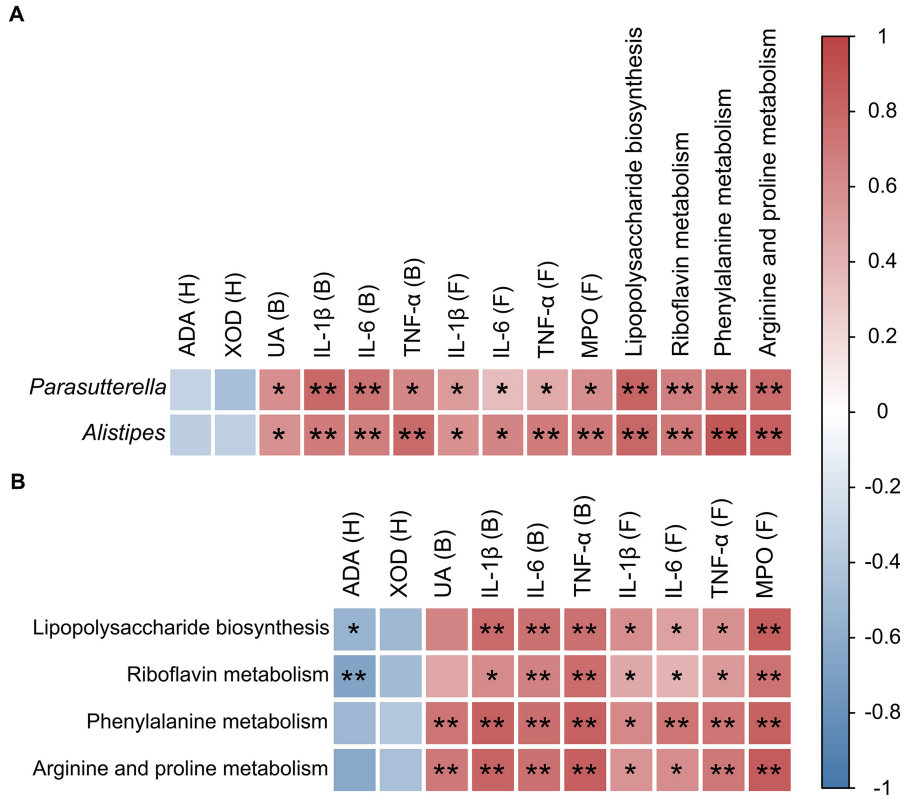

FIGURE 7
Correlation analyses between microorganisms, pro-inflammatory cytokines, enzymes, and metabolic pathways in mice. **(A)** Correlation between key intestinal microorganisms (i.e., *Parasutterella* and *Alistipes*) and pro-inflammatory cytokines, enzymes, and metabolic pathways. **(B)** Correlation between metabolic pathways and both pro-inflammatory cytokines and enzymes. The relative R values range from –1 to 1 (i.e., blue to red). B, blood; H, hepatic tissue; F, foot joint tissue. Statistical differences are determined by $p < 0.05$ (*) and $p < 0.01$ (**), respectively.

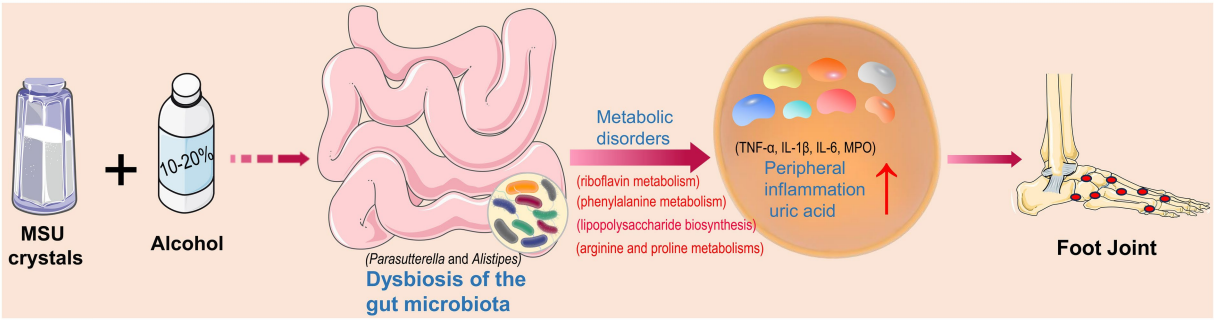

FIGURE 8
Intestinal bacterial disorders and abnormal metabolic pathways as well as increased levels of pro-inflammatory factors and uric acid caused by alcohol and monosodium urate (MSU) crystals to exacerbate gout symptoms.

pathogenesis of brain-related diseases (Eicher and Mohajeri, 2022). Furthermore, in an alcoholic hepatic injury mouse model, an association between *Parasutterella* and riboflavin metabolism was discovered (Lv et al., 2022). Our study revealed no significant effect of high-concentration alcohol consumption on purine metabolism. However, significantly positive correlations were detected among the key bacterial taxa (i.e., *Parasutterella* and *Alistipes*), UA, IL-1β, IL-6, TNF-α, and MPO, as well as the levels of four metabolic pathways (i.e., lipopolysaccharide biosynthesis, riboflavin metabolism, phenylalanine metabolism, and arginine and proline metabolism) in gout mice (Figure 7A). Therefore, it was speculated that high-concentration alcohol consumption alters the taxonomic structure of the gut microbiota and promotes an inflammatory response that could exacerbate gout symptoms. Further studies are needed to provide more evidence to support these speculations.

Considering that both ADA and XOD affect the purine metabolism, we further investigated the enzymatic activation with ADA and XOD in mouse hepatic to explore the exacerbation of gout symptoms by alcohol

via purine metabolism. Although our results showed that high alcohol consumption slightly increased the activation of ADA and XOD in mouse hepatic, the differences were not statistically significant due to the small sample size. We hypothesized that this might be related to the lower concentration of alcohol consumed and the shorter treatment time. In the high concentration alcohol group, we found that both 10 and 20% alcohol intake significantly exacerbated acute gouty arthritis symptoms and related clinical indicators, and it was difficult to differentiate the differences between the high concentration alcohol groups. Therefore, we focused on the joint effect of 10 and 20% alcohol intake. Further experimental studies are needed to analyze the differences between 10 and 20% alcohol intake. Notably, while treatment of high-concentration alcohol increased the diversity of the gut microbiota, it significantly reduced the negative correlation between the gut microbiota. We hypothesize that the decrease in negative correlation between bacteria may be responsible for the increased diversity of the gut microbiota. However, our results still need to be validated by further studies. In addition, although our research results indicate that low-concentration alcohol treatment does not have a significant impact on the gut microbiota of gout mice, it also does not have an effect in improving gout symptoms. Therefore, it is highly recommended that the alcohol consumption be avoided during the acute phase of gout.

5. Conclusion

In conclusion, our results suggested that high concentrations of alcohol altered the gut microbiota structure in gout mice induced by MSU crystals, possibly exacerbating gout symptoms by enhancing the pro-inflammatory pathways. These results recommended that alcohol consumption should be avoided during the acute phase of gout. Our study provides novel insights into the exacerbation of gouty arthritis by alcohol consumption.

Data availability statement

The datasets presented in this study can be found in online repositories. The names of the repository/repositories and accession number(s) can be found in the article/Supplementary material.

Ethics statement

The animal study was approved by the Animal Ethics Review Board of the Provincial Hospital of Shandong First Medical University approved this study (Permit No. 2022-025). The study was conducted in accordance with the local legislation and institutional requirements.

Author contributions

YF: data curation, methodology, writing – original draft. HS: methodology, software, validation, writing – original draft. RZ: data curation, investigation, writing – original draft. JT: formal analysis, project administration, writing – original draft. RS: data curation, methodology, writing – original draft. YS: conceptualization, formal analysis, funding acquisition, investigation, supervision, validation, writing – review and editing. DW: conceptualization, data curation, funding acquisition, investigation, writing – review and editing.

Funding

The author(s) declare financial support was received for the research, authorship, and/or publication of this article. This study was financially supported by the National Natural Science Foundation of China (81972057 and 82172313) and the Major Innovation Project of Shandong Province (2021GXGC011305).

Conflict of interest

The authors declare that the research was conducted in the absence of any commercial or financial relationships that could be construed as a potential conflict of interest.

Publisher's note

Supplementary material

The Supplementary material for this article can be found online at: https://www.frontiersin.org/articles/10.3389/fmicb.2023.1257701/full#supplementary-material

References

Ankli, B., and Daikeler, T. (2023). Update Gicht [update gout]. *Ther. Umsch.* 80, 17–26. doi: 10.1024/0040-5930/a001402

Barbería-Latasa, M., Gea, A., and Martínez-González, M. A. (2022). Alcohol, drinking pattern, and chronic disease. *Nutrients* 14:1954. doi: 10.3390/nu14091954

Blasco-Baque, V., Coupé, B., Fabre, A., Handgraaf, S., Gourdy, P., Arnal, J. F., et al. (2017). Associations between hepatic miRNA expression, liver triacylglycerols and gut microbiota during metabolic adaptation to high-fat diet in mice. *Diabetologia* 60, 690–700. doi: 10.1007/s00125-017-4209-3

Cao, J., Liu, Q., Hao, H., Bu, Y., Tian, X., Wang, T., et al. (2022). *Lactobacillus paracasei* X11 ameliorates hyperuricemia and modulates gut microbiota in mice. *Front. Immunol.* 13:940228. doi: 10.3389/fimmu.2022.940228

Cao, C., Wang, L., Ai, C., Gong, G., Wang, Z., Huang, L., et al. (2022). Impact of *Lycium barbarum* arabinogalactan on the fecal metabolome in a DSS-induced chronic colitis mouse model. *Food Funct.* 13, 8703–8716. doi: 10.1039/d2fo01283a

Cheng, M., Tan, B., Wu, X., Liao, F., Wang, F., and Huang, Z. (2021). Gut microbiota is involved in alcohol-induced osteoporosis in young and old rats through immune regulation. *Front. Cell. Infect. Microbiol.* 11:636231. doi: 10.3389/fcimb.2021.636231

Choi, H. K., Atkinson, K., Karlson, E. W., Willett, W., and Curhan, G. (2004). Alcohol intake and risk of incident gout in men: a prospective study. *Lancet* 363, 1277–1281. doi: 10.1016/S0140-6736(04)16000-5

Compare, D., Rocco, A., Sanduzzi Zamparelli, M., and Nardone, G. (2016). The gut Bacteria-driven obesity development. *Dig. Dis.* 34, 221–229. doi: 10.1159/000443356

Dubinkina, V. B., Tyakht, A. V., Odintsova, V. Y., Yarygin, K. S., Kovarsky, B. A., Pavlenko, A. V., et al. (2017). Links of gut microbiota composition with alcohol dependence syndrome and alcoholic liver disease. *Microbiome* 5:141. doi: 10.1186/s40168-017-0359-2

Eicher, T. P., and Mohajeri, M. H. (2022). Overlapping mechanisms of action of brain-active Bacteria and bacterial metabolites in the pathogenesis of common brain diseases. *Nutrients* 14:2661. doi: 10.3390/nu14132661

Feng, Y., Yu, Y., Chen, Z., Wang, L., Ma, J., Bai, X., et al. (2022). Effects of β-Carotin and green tea powder diets on alleviating the symptoms of gouty arthritis and improving gut microbiota in C57BL/6 mice. *Front. Microbiol.* 13:837182. doi: 10.3389/fmicb.2022.837182

Galozzi, P., Bindoli, S., Doria, A., Oliviero, F., and Sfriso, P. (2021). Autoinflammatory features in gouty arthritis. *J. Clin. Med.* 10:1880. doi: 10.3390/jcm10091880

Guo, Z., Zhang, J., Wang, Z., Ang, K. Y., Huang, S., Hou, Q., et al. (2016). Intestinal microbiota distinguish gout patients from healthy humans. *Sci. Rep.* 6:20602. doi: 10.1038/srep20602

Hendriks, H. F. J. (2020). Alcohol and human health: what is the evidence? *Annu. Rev. Food Sci. Technol.* 11, 1–21. doi: 10.1146/annurev-food-032519-051827

Hu, Q., Wei, J., Liu, Y., Fei, X., Hao, Y., Pei, D., et al. (2017). Discovery and identification of potential biomarkers for alcohol-induced oxidative stress based on cellular metabolomics. *Biomed. Chromatogr.* 31:e3907. doi: 10.1002/bmc.3907

Jiménez, A., Santos, M. A., Pompejus, M., and Revuelta, J. L. (2005). Metabolic engineering of the purine pathway for riboflavin production in ashbya gossypii. *Appl. Environ. Microbiol.* 71, 5743–5751. doi: 10.1128/AEM.71.10.5743-5751.2005

Ju, T., Kong, J. Y., Stothard, P., and Willing, B. P. (2019). Defining the role of Parasutterella, a previously uncharacterized member of the core gut microbiota. *ISME J.* 13, 1520–1534. doi: 10.1038/s41396-019-0364-5

Kaur, H., Das, C., and Mande, S. S. (2017). In silico analysis of putrefaction pathways in Bacteria and its implication in colorectal Cancer. *Front. Microbiol.* 8:2166. doi: 10.3389/fmicb.2017.02166

Kogut, M. H., Lee, A., and Santin, E. (2020). Microbiome and pathogen interaction with the immune system. *Poult. Sci.* 99, 1906–1913. doi: 10.1016/j.psj.2019.12.011

Kuo, C. F., Grainge, M. J., Zhang, W., and Doherty, M. (2015). Global epidemiology of gout: prevalence, incidence and risk factors. *Nat. Rev. Rheumatol.* 11, 649–662. doi: 10.1038/nrrheum.2015.91

Larsson, S. C., Wallin, A., Wolk, A., and Markus, H. S. (2016). Differing association of alcohol consumption with different stroke types: a systematic review and meta-analysis. *BMC Med.* 14:178. doi: 10.1186/s12916-016-0721-4

Larsson, S. C., Wallin, A., Wolk, A., Markus, H. S., Islami, F., Fedirko, V., et al. (2013). Light alcohol drinking and cancer: a meta-analysis. *Ann. Oncol.* 14, 301–308. doi: 10.1186/s12916-016-0721-4

Leclercq, S., Matamoros, S., Cani, P. D., Neyrinck, A. M., Jamar, F., Stärkel, P., et al. (2014). Intestinal permeability, gut-bacterial dysbiosis, and behavioral markers of alcohol-dependence severity. *Proc. Natl. Acad. Sci. U. S. A.* 111, E4485–E4493. doi: 10.1073/pnas.1415174111

Li, X. H., Yu, F. F., Zhou, Y. H., and He, J. (2016). Association between alcohol consumption and the risk of incident type 2 diabetes: a systematic review and dose-response meta-analysis. *Am. J. Clin. Nutr.* 103, 818–829. doi: 10.3945/ajcn.115.114389

Lin, X., Shao, T., Wen, X., Wang, M., Wen, C., and He, Z. (2020). Combined effects of MSU crystals injection and high fat-diet feeding on the establishment of a gout model in C57BL/6 mice. *Adv. Rheumatol.* 60:52. doi: 10.1186/s42358-020-00155-3

Liu, Y. R., Tantoh, D. M., Lin, C. C., Hsiao, C. H., and Liaw, Y. P. (2021). Risk of gout among Taiwanese adults with ALDH-2 rs671 polymorphism according to BMI and alcohol intake. *Arthritis Res. Ther.* 23:115. doi: 10.1186/s13075-021-02497-9

Lou, X. J., Wang, Y. Z., Lei, S. S., He, X., Lu, T. T., Zhan, L. H., et al. (2020). Beneficial effects of macroporous resin extract of Dendrobium candidum leaves in rats with hyperuricemia induced by a high-purine diet. *Evid. Based Complement. Alternat. Med.* 2020:3086106. doi: 10.1155/2020/3086106

Lv, X. C., Wu, Q., Cao, Y. J., Lin, Y. C., Guo, W. L., Rao, P. F., et al. (2022). Ganoderic acid a from Ganoderma lucidum protects against alcoholic liver injury through ameliorating the lipid metabolism and modulating the intestinal microbial composition. *Food Funct.* 13, 5820–5837. doi: 10.1039/d1fo03219d

Mahbub, M. H., Yamaguchi, N., Takahashi, H., Hase, R., Amano, H., Kobayashi-Miura, M., et al. (2017). Alteration in plasma free amino acid levels and its association with gout. *Environ. Health Prev. Med.* 22:7. doi: 10.1186/s12199-017-0609-8

Moschen, A. R., Gerner, R. R., Wang, J., Klepsch, V., Adolph, T. E., Reider, S. J., et al. (2016). Lipocalin 2 protects from inflammation and tumorigenesis associated with gut microbiota alterations. *Cell Host Microbe* 19, 455–469. doi: 10.1016/j.chom.2016.03.007

Natividad, J. M., Pinto-Sanchez, M. I., Galipeau, H. J., Jury, J., Jordana, M., Reinisch, W., et al. (2015). Ecobiotherapy rich in Firmicutes decreases susceptibility to colitis in a humanized Gnotobiotic mouse model. *Inflamm. Bowel Dis.* 21, 1883–1893. doi: 10.1097/MIB.0000000000000422

Nemoto, N., Takeda, Y., Nara, H., Araki, A., Gazi, M. Y., Takakubo, Y., et al. (2020). Analysis of intestinal immunity and flora in a collagen-induced mouse arthritis model: differences during arthritis progression. *Int. Immunol.* 32, 49–56. doi: 10.1093/intimm/dxz058

Neogi, T., Chen, C., Niu, J., Chaisson, C., Hunter, D. J., and Zhang, Y. (2014). Alcohol quantity and type on risk of recurrent gout attacks: an internet-based case-crossover study. *Am. J. Med.* 127, 311–318. doi: 10.1016/j.amjmed.2013.12.019

Parker, B. J., Wearsch, P. A., Veloo, A. C. M., and Rodriguez-Palacios, A. (2020). The genus Alistipes: gut Bacteria with emerging implications to inflammation, Cancer, and mental health. *Front. Immunol.* 11:906. doi: 10.3389/fimmu.2020.00906

Postler, T. S., and Ghosh, S. (2017). Understanding the holobiont: how microbial metabolites affect human health and shape the immune system. *Cell Metab.* 26, 110–130. doi: 10.1016/j.cmet.2017.05.008

Qin, Y., Havulinna, A. S., Liu, Y., Jousilahti, P., Ritchie, S. C., Tokolyi, A., et al. (2022). Combined effects of host genetics and diet on human gut microbiota and incident disease in a single population cohort. *Nat. Genet.* 54, 134–142. doi: 10.1038/s41588-021-00991-z

Rau, M., Rehman, A., Dittrich, M., Groen, A. K., Hermanns, H. M., Seyfried, F., et al. (2018). Fecal SCFAs and SCFA-producing bacteria in gut microbiome of human NAFLD as a putative link to systemic T-cell activation and advanced disease. *United European Gastroenterol. J.* 6, 1496–1507. doi: 10.1177/2050640618804444

Ruiz-Miyazawa, K. W., Staurengo-Ferrari, L., Mizokami, S. S., Domiciano, T. P., Vicentini, F. T. M. C., Camilios-Neto, D., et al. (2017). Quercetin inhibits gout arthritis in mice: induction of an opioid-dependent regulation of inflammasome. *Inflammopharmacology* 25, 555–570. doi: 10.1007/s10787-017-0356-x

Sang, L., Kang, K., Sun, Y., Li, Y., and Chang, B. (2021). FOXO4 ameliorates alcohol-induced chronic liver injury via inhibiting NF-κB and modulating gut microbiota in C57BL/6J mice. *Int. Immunopharmacol.* 96:107572. doi: 10.1016/j.intimp.2021.107572

Schaffert, C. S., Duryee, M. J., Hunter, C. D., Hamilton, B. C., DeVeney, A. L., Huerter, M. M., et al. (2009). Alcohol metabolites and lipopolysaccharide: roles in the development and/or progression of alcoholic liver disease. *World J. Gastroenterol.* 15, 1209–1218. doi: 10.3748/wjg.15.1209

Shirvani-Rad, S., Khatibzade-Nasari, N., Ejtahed, H. S., and Larijani, B. (2023). Exploring the role of gut microbiota dysbiosis in gout pathogenesis: a systematic review. *Front. Med.* 10:1163778. doi: 10.3389/fmed.2023.1163778

Singh, J. A., and Gaffo, A. (2020). Gout epidemiology and comorbidities. *Semin. Arthritis Rheum.* 50, S11–S16. doi: 10.1016/j.semarthrit.2020.04.008

So, A. K., and Martinon, F. (2017). Inflammation in gout: mechanisms and therapeutic targets. *Nat. Rev. Rheumatol.* 13, 639–647. doi: 10.1038/nrrheum.2017.155

Song, G., Gan, Q., Qi, W., Wang, Y., Xu, M., and Li, Y. (2023). Fructose stimulated colonic arginine and proline metabolism dysbiosis, altered microbiota and aggravated intestinal barrier dysfunction in DSS-induced colitis rats. *Nutrients* 15:782. doi: 10.3390/nu15030782

Terkeltaub, R. (2017). What makes gouty inflammation so variable? *BMC Med.* 15, 1–10. doi: 10.1186/s12916-017-0922-5

Tu, H. P., Tung, Y. C., Tsai, W. C., Lin, G. T., Ko, Y. C., and Lee, S. S. (2017). Alcohol-related diseases and alcohol dependence syndrome is associated with increased gout risk: a nationwide population-based cohort study. *Jt. Bone Spine* 84, 189–196. doi: 10.1016/j.jbspin.2016.02.024

Turnbaugh, P. J., Ley, R. E., Mahowald, M. A., Magrini, V., Mardis, E. R., and Gordon, J. I. (2006). An obesity-associated gut microbiome with increased capacity for energy harvest. *Nature* 444, 1027–1031. doi: 10.1038/nature05414

Vieira, A. T., Macia, L., Galvão, I., Martins, F. S., Canesso, M. C., Amaral, F. A., et al. (2015). A role for gut microbiota and the metabolite-sensing receptor GPR43 in a murine model of gout. *Arthritis Rheumatol.* 67, 1646–1656. doi: 10.1002/art.39107

Wan, Y., Wang, F., Yuan, J., Li, J., Jiang, D., Zhang, J., et al. (2019). Effects of dietary fat on gut microbiota and faecal metabolites, and their relationship with cardiometabolic risk factors: a 6-month randomised controlled-feeding trial. *Gut* 68, 1417–1429. doi: 10.1136/gutjnl-2018-317609

Wang, L., Fouts, D. E., Stärkel, P., Hartmann, P., Chen, P., Llorente, C., et al. (2016). Intestinal REG3 lectins protect against alcoholic steatohepatitis by reducing mucosa-associated microbiota and preventing bacterial translocation. *Cell Host Microbe* 19, 227–239. doi: 10.1016/j.chom.2016.01.003

Wang, G., Liu, Q., Guo, L., Zeng, H., Ding, C., Zhang, W., et al. (2018). Gut microbiota and relevant metabolites analysis in alcohol dependent mice. *Front. Microbiol.* 9:1874. doi: 10.3389/fmicb.2018.01874

Yang, Z., Ye, S., Xu, Z., Su, H., Tian, X., Han, B., et al. (2021). Dietary synbiotic ameliorates constipation through the modulation of gut microbiota and its metabolic function. *Food Res. Int.* 147:110569. doi: 10.1016/j.foodres.2021.110569

Zhang, J., Wang, M., Qi, X., Shi, L., Zhang, J., Zhang, X., et al. (2021). Predicting the postmortem interval of burial cadavers based on microbial community succession. *Forensic. Sci. Int. Genet.* 52:102488. doi: 10.1016/j.fsigen.2021.102488

frontiers | Frontiers in Microbiology

TYPE Original Research
PUBLISHED 10 October 2023
DOI 10.3389/fmicb.2023.1245042

OPEN ACCESS

EDITED BY
Fengjie Sun,
Georgia Gwinnett College,
United States

REVIEWED BY
Qinnan Yang,
University of Nebraska-Lincoln,
United States
Kishor Pant,
University of Minnesota Twin Cities,
United States

*CORRESPONDENCE
Muhamad Hanif Rawi
✉ hanifrawi@ums.edu.my

RECEIVED 23 June 2023
ACCEPTED 18 September 2023
PUBLISHED 10 October 2023

CITATION
Rawi MH, Tan HY and Sarbini SR (2023) Identification of acacia gum fermenting bacteria from pooled human feces using anaerobic enrichment culture. *Front. Microbiol.* 14:1245042. doi: 10.3389/fmicb.2023.1245042

Identification of acacia gum fermenting bacteria from pooled human feces using anaerobic enrichment culture

Muhamad Hanif Rawi[1]*, Hui Yan Tan[2] and Shahrul Razid Sarbini[2,3]

[1]Innovative Food Processing and Ingredients Research Group, Faculty of Food Science and Nutrition, Universiti Malaysia Sabah, Kota Kinabalu, Sabah, Malaysia, [2]Department of Crop Science, Faculty of Agricultural Science and Forestry, Universiti Putra Malaysia Bintulu Campus, Bintulu, Sarawak, Malaysia, [3]Halal Products Research Institute, Universiti Putra Malaysia, Serdang, Selangor, Malaysia

Commercial acacia gum (AG) used in this study is a premium-grade free-flowing powder. It is a gummy exudate composed of arabinogalactan branched polysaccharide, a biopolymer of arabinose and galactose. Also known as food additive, acacia gum (E414), which is presently marketed as a functional dietary fiber to improve overall human gut health. The health effects may be related to the luminal pH regulation from the short-chain fatty acids (SCFA) production. Studies suggested that amylolytic and butyrogenic pathways are the major factors determining the SCFA outcome of AG in the lower gut. However, the primary bacteria involved in the fermentation have not been studied. This study aimed to investigate the putative primary degraders of acacia gum in the gut ecosystem. Isolation and identification of gum-fermenting bacteria were performed through enrichment culture fermentation. The experiment was conducted in an anaerobic chamber for 144 h in three stages. The study was conducted in triplicate using an anaerobic chamber system. This culture system allows specific responses to support only bacteria that are responsible for gum fermentation among the gut microbiota. Five bacterial strains were isolated and found to be gum-fermenting bacteria. Based on the 16s RNA sequence, the isolates matched to butyrate-producing *Escherichia fergusonii*, ATCC 35469.

KEYWORDS

gum arabic, *Acacia senegal*, gut microbiota, *Escherichia*, isolation, metabolism, butyrate

1. Introduction

Despite the development of culture techniques and fast-moving molecular identification technology, there is still a substantial amplitude of uncultured microbial diversity within the gut ecosystem, a vast number of gut microbes yet to be characterized (Lu et al., 2014; Shin et al., 2019). As reviewed by Rawi et al. (2020), human gut bacteria largely classified into *Bacteroides*, *Prevotella*, and *Ruminococcus*, which predominantly inhabit by phyla *Firmicutes* and *Bacteroidetes* (Walker et al., 2011). Another recent metagenomic analysis conducted by Forster et al. (2019) revealed that the most frequent genomes were *Ruminococcus bromii*, *Alistipes putredinis*, and *Eubacterium rectale*. All are known to colonize the human gut (Rajilić-Stojanović and deVos, 2014), confirming that these species are common members of the intestinal microbiota. These data suggest that, despite being known colonizers of the intestinal microbiota, these clades still contain considerable uncultured diversity. Therefore, the detection of many

uncultured species assigned to this genus may reflect the current taxonomic limitations rather than biological signals. A review also suggested that specific microbial strains are responsible for the metabolism of certain substrates. Giving the impression that the gut environment is similar to the ecosystem will make the microbiome relationship within the gut more sensible. It can be postulated that the gut bacteria can be compared to the animal kingdom, while prebiotics or other indigestible substances in the colon serve as sources of food, similar to producers in an ecosystem. Just like in a food chain, a combination of food chains makes up a food web. The various undefined linkages between gut bacteria can be explained by their cross-feeding situation, which leads to both competitive and cooperative relationships through the intermediate fermentation products from one or more bacterial species to another. In the animal kingdom, there is a hierarchy of creatures, where prey and predators are further differentiated, and the prey typically includes primary to tertiary consumers. On the other hand, the bacteria could be categorized either as commensal, pathogenic or beneficial species. If an imbalance exists in the ecosystem, the condition of the colon is called gut dysbiosis (DeGruttola et al., 2016).

Enrichment culture is a closed system that can isolate organisms that utilize a specific nutrient substrate among complex microbial communities (Kishimoto et al., 2006). The enrichment culture employed a liquid growth medium containing acacia gum, creating an environment strictly desirable to isolating the primary substrate-utilizing organisms. This approach facilitates the isolation and subsequent study of the targeted microbes. Anaerobic enrichment culture techniques, as described by Beck (1971), are effective in isolating a variety of obligate and facultative anaerobic bacteria. The biological phenomena of the isolated bacteria were observed using enrichment culture techniques. The essence of this technique is to provide growth conditions that are favorable for the organism of interest and as unfavorable as possible for competing organisms. Simultaneously, an enrichment culture can be applied by modifying the media.

At least two decades of gut research have passed, and many of the unknowns before scientists now become clearer. Together with the host immune system, the gut microbiota acts as a barrier and prevents the invasion of pathogenic bacteria in the gastrointestinal tract. FOS has been extensively studied as a prebiotic that regulates and selectively stimulates bacterial populations in the colon (Tuohy et al., 2001; Palframan et al., 2002; Hidalgo et al., 2012; Cueva et al., 2013). Fermentation of AG results in bacterial proliferation (May et al., 1994). Thus, an increased population of colonic bacteria promotes the production of beneficial metabolites, such as short-chain fatty acids (SCFA), which play an important role in many physiological effects. The study involved observations on selective agar medium, with culture-dependent techniques dominating assessment methods during that period. Thus, selective media that only targeted beneficial bacteria were not sufficient to verify the fermentability of AG by colonic bacteria. In addition, AG been reported to break down in the colon of rats and humans (Ross et al., 1984; Walter et al., 1988; Phillips, 1998). While these studies were evaluated *in vivo*, there is no direct proof to support the findings since the parameters were only evaluated after the administration of the candidate after being fed AG during the study. In 2006, an animal study by Kishimoto et al. (2006) found that the predominant microbes from pooled cecal inocula of pigs responsible for AG fermentation and contributing to propionate production were *Prevotella ruminicola*-like bacteria. In contrast, studies using human and porcine fecal inoculum with 2% acacia gum isolated *Bifidobacterium longum* and *Bacteroides ovatus, Bacteroides oris, Bacteroides buccae,* and *Prevotella ruminicola*-like bacteria (Wyatt et al., 1986). While the study utilized human fecal samples, the conclusions drawn were primarily derived from culture plating techniques rather than molecular-based DNA sequencing. Notably, the latter method, which emerged in the 1970s, might not have been accessible in their laboratory during that period. Therefore, the traditional detection of many uncultured species assigned to this genus may reflect the current taxonomic limitations rather than biological signals. The chemical composition of AG varies slightly based on origin, sources, climate, season, tree age, and species (Williams and Phillips, 2009). The high carbohydrate content within these complex polysaccharides serves as the basis for evaluating the prebiotic potential of acacia gum. Species differences in AG were considered to determine the extent to which the species affected the fermentation performance of the colon. Thus, the evaluation of SCFA production and bacterial composition changes due to the input of AG as a substrate is the foundation for the benefits of human colon health. The limitation of simulating the interaction between the host and gut microbes in a fermentation system may also be one of the criteria for a fermentation system.

In this study, the enrichment technique was applied to AG in nutrient medium. A microbial strain that specifically utilized acacia gum as a nutrient source was isolated using an anaerobic enrichment culture fermentation system. Therefore, this study addressed possible pathways of AG fermentation by colonic bacteria. Investigation of the putative primary degrader of acacia gum based on enrichment culture was used to generate more information on the relationships between different microbial species in the gut. Hence, through this study, it is possible to enhance our understanding of the prebiotic applications of acacia gum in various industries, particularly nutraceuticals. Despite this, the current study is the first to show new insights towards the old knowledge about the prebiotic potential of AG. This study also opens the new perspectives on substrate-species relationship in the metabolism of food products.

2. Materials and methods

2.1. Acacia gum (AG) as the substrate

In this study, *Acacia senegal* gum (obtained from Natural Prebiotic Sdn. Bhd., Malaysia), which is a water-soluble, free-flowing powder. This commercially available product, marketed as a dietary fiber drink, consists of *A. senegal* gum in its raw form. Notably, the highly branched structure of this gum, composed of β-(1,3)-galactopyranose chains forming the backbone with branched side chains linked through the 1,6 positions comprising galactose, arabinose, rhamnose, and glucuronic acid, renders it resistant to human gut hydrolysis. These complex structures are not available as free sugar molecules for bacteria.

2.2. Anaerobic enrichment culture

The following methods was based on the study of Kishimoto et al. (2006) with modification. The experiment was conducted in a

Bactronez-2 (*Sheldon* Lab, United States) anaerobic chamber following the manufacturer's operating procedure. Fecal inoculum was obtained from three healthy human volunteers who fulfilled all the exclusion criteria as described previously. A portion of fecal material (10 g) from healthy volunteers was pooled and homogenized in a stomacher with buffer (1:10 w/v, pH 6.5, 1X PBS) at a normal speed for 2 min. An amount of 40 mL pre-reduced basal medium (pH 6.8) consisting of (peptone water (2 g/1), yeast extract (2 g/1), NaCl (0.1 g/1), K_2HPO_4 (0.04 g/1), KH_2PO_4 (0.04 g/1), $NaHCO_3$ (2 g/1), $MgSO_4$•$7H_2O$ (0.01 g/L), $CaC1_2$•$6H_2O$ (0.01 g/1), tween 80 (2 mL/1), hemin (50 mg/1), vitamin Kl (10 µL), L-cysteine HCl (0.5 g/1), bile salts (0.5 g/1), resazurin (0.25 g/L) (4.0 mL) with 1% AG was added into 100 mL Schott bottles and were autoclaved before transferred into the anaerobic chamber.

The 10 mL of fecal slurry prepared was inoculated into the (40 mL) medium and placed in an incubator at 37°C and subjected to continuous stirring. Three independent vessels were run in parallel and served as replicates. An additional set of vessels containing only media, without AG (as negative control), is concurrently run alongside the treatments to verify and validate culture growth. An amount of 1 mL of the culture was sampled from each vessel at 0 (start of incubation), 6, 12, 18, 24, 30, 36, and 48 h after the beginning of incubation. At the end of the culture period (48 h), 10 mL of the culture was transferred to fresh medium, and the culture and sampling were repeated. At the end of the second incubation (48 h), 10 mL of the culture was transferred to fresh medium, and culture and sampling were repeated for the last stage.

2.3. Chemical and molecular ecological analyzes

The sampled culture (1 mL) was centrifuged at high speed of 13,000 rpm for 10 min. The resulting supernatant was used for SCFA analysis using ion-exclusion HPLC, as described previously. Bacterial genomic DNA was extracted using the GF-1 Bacterial DNA Extraction Kit (*Vivantis*) following the manufacturer's protocol. First, 1 mL of the sample was centrifuged at 6000 × g for 2 min. The supernatant was completely removed, and the pellet was resuspended in 100 µL of Buffer R1 and aspirated with a pipette. The sample was treated with 10 µL lysozyme (50 mg/mL) and incubated at 37°C for 20 min. The cell suspension was centrifuged at 10000 × g for 3 min. The supernatant was completely decanted. The pellet was resuspended in 180 µL Buffer R2 and 20 µL Proteinase K. The suspension was denatured at 65°C for 20 min with occasional mixing every 5 min. Bacterial genomic DNA buffer (two volumes) was added to each sample. The suspension was homogenized and incubated at 65°C for 10 min. The samples were precipitated using 200 µL of absolute ethanol. The samples were transferred to a spin column assembled in a clean collection tube. The sample was centrifuged at 10000 × g for 1 min. Wash buffer was added before the second centrifugation with the same parameters. The flow-through was discarded. The pellet was eluted with preheated elution buffer (50 µL) and centrifuged (10,000 × g for 1 min) in a clean microcentrifuge tube. The extracted DNA was stored at 4°C until further analysis.

2.4. Polymerase chain reaction

The universal primers 27F (5′AGAGTTTGATCMTGGCTCAG) and 1492R (5'GGTTACCTTGTTACGACTT) from the first Base IDT were used to amplify the 16S rRNA gene regions of the extracted DNA. Amplification was performed with XP Cycle (*BioER*) using the following cycling conditions:94°C for 5 min; 27 cycles of 94°C for 1 min, 51.3°C for 1 min, 72°C for 1 min, and 72°C for 10 min. Amplicons were purified by agarose (*First Base*) gel electrophoresis using a PCR Purification Kit (*Qiagen, QIAquick*) prior to DNA sequencing to identify the strain species. The DNA ladder used was 100 bp plus (*Vivantis*) and pre-stained with 6X Loading Dye (*Vivantis*).

2.5. Organic acids analysis

The organic acid quantification was based on Rawi et al. (2021). The fermentation sample from each sampling period was pipetted into a 2 mL microcentrifuge tube for centrifugation (Centrifuge-5804, *Eppendorf*) at 13000 rpm for 10 min to obtain a clear supernatant. The supernatant was filtered through a 0.22 µm syringe filter unit (*Millipore*) into an HPLC vial (*Agilent Technologies,* Cheshire, United Kingdom). Prominence Series Liquid Chromatography (*Shimadzu Corp.,* Japan) using a reverse phase ion-exclusion C12 column (Rezex ROA, *Phenomenex*) was used for SCFA analysis. Analytes were detected using a UV detector at a wavelength of 210 nm. The isocratic mobile phase used was 0.25 mM sulphuric acid (H_2SO_4). A 15 µL sample was injected into the heated column (40°C) programmed to run in isocratic elution at a flow rate of 0.5 mL/min for 40 min. The peaks and response factors within the sample were calibrated and calculated using the LC Solutions software (*Shimadzu*). The standard solution contained of 12.5, 25, 50, 75, 100, 125, 150, 175, and 200 mM acetate, butyrate, propionate, and lactate.

2.6. Isolation of acacia gum fermenting bacteria

A portion (1 mL) of the culture was collected at the end of enrichment (144 h after commencement of the enrichment culture). This sample was subjected to serial 10-fold dilution (10^{-2}–10^{-6}) in anaerobic 1× PBS buffer. Diluted samples (100 µL) were plated on agar with the same constituents as the basal media, with the addition of AG and bacteriological agar (20.0 g). Incubation condition was at 37°C for 48 h. The developed colonies were randomly isolated and subjected to colony purification before being transferred to a fresh slant medium containing the same ingredients. Successfully isolated colonies were transferred to broth medium containing the same ingredients, except for agar. After incubation at 37°C for 48 h, organic acids were analyzed, and cell morphology was examined. This step is important for verifying the ability of the isolate to ferment acacia gum. The 16S rRNA gene sequences of selected isolates were examined.

2.7. Gram staining

Gram staining was performed as previously described (Coico, 2006). A thin layer of the cells was smeared onto a glass slide using a sterilized loop inside a drop of distilled water. The sample was heated over a spirit lamp and dried to fix onto a slide. Cells were stained with crystal violet and incubated for 1 min. Subsequently, the slide was rinsed under a gentle stream of water for approximately 5 s. The slides

were then shaken to remove excess water. Next, an iodine solution (iodine and potassium iodide) was added and incubated for 1 min. Subsequently, the slide was rinsed under a gentle stream of water for approximately 5 s. The slides were then shaken to remove excess water. Next, in a slightly tilted position on the slide, a few drops of ethyl alcohol were run through the sample until the last purple color ceased to wash away from the smear and rinse with a gentle stream of water for approximately 5 s. The slides were then shaken to remove excess water. Safranin was added to the smear and incubated for 1 min. Washed with a gentle stream of water for approximately 5 s and excess water is blotted around the ages of the smear with bibulous paper prior to microscopic observation.

3. Results

3.1. Anaerobic enrichment fermentation

Enrichment experiments of AG were conducted *in vitro,* using an anaerobic chamber to contain the culture. This study aimed to identify the first-hand microorganisms in human feces responsible for the fermentation of acacia gum. Furthermore, the putative isolates were verified for their ability to ferment acacia gum in monocultures. To the best of our knowledge, this is the first study on enrichment cultures using a complete anaerobic chamber. The benefit of using an anaerobic chamber is that it eliminates the possibility that the target bacteria may be exposed to perpetuate atmospheric oxygen during the transfer of the culture at any point. It is worth noting that any exposure to oxygen might reduce the chances or viability of anaerobic bacteria, especially strictly anaerobic ones. Therefore, keeping exposure to atmospheric air at a minimum, the probability of culturing bacteria that were once very difficult to grow *in vitro* was higher.

3.2. SCFA concentration from enrichment culture

Figure 1 shows different SCFA production during the 144 h of anaerobic enrichment by acacia gum. The enrichment culture consisted of three stages, where each stage indicates 48 h of incubation (stage 1:0–48 h, stage 2:48–96 h, and stage 3:96–144 h). The culture was transferred to fresh medium between stages (48 and 96 h). Acetate, propionate, and butyrate were the major SCFA produced during the incubation. At every stage, all the SCFA showed an incremental trend. The enrichment culture of acacia gum started with acetate and shifted towards health-promoting butyrate later in the incubation period. Acetate had the highest concentration at most of the time points in stages 1 and 2, whereas butyrate was the most abundant in stage 3. While the rate of acetate production decreased, that of butyrate production increased as enrichment progressed to stages 2 and 3. The molar proportion of propionate was very low and progressively diminished following the first and second medium transfer (Figure 1). A reduction in SCFA production was observed at every initial in each stage (0, 0–48, and 0–96 h). This can be expected from a multistage enrichment culture because the transferred culture to the subsequent stage contains a lower number of bacterial species. Therefore, lower bacterial compositions were present in the diluted samples transferred to the next series.

3.3. Monoculture fermentation of acacia gum by isolated strains

The isolated bacteria were assessed to verify their ability to ferment acacia gum in pure culture. All five isolated strains with putative gum-fermenting abilities were reconfirmed by anaerobic monoculture fermentation for 48 h (Figure 2). All five isolates produced butyrate during monoculture, conforming to butyrate elevation in stage 3 of the enrichment culture, with a small amount of acetate and propionate. The elevation was significant as soon as 6 h for Strain 2, and 5 before it remained stationary at the same concentration level and continued until the end of fermentation. The same trend was observed for butyrate concentration at 6 h in strain 1, but it ended with a significant spike at 48 h. Furthermore, our observations, based on both culture-dependent methods and metabolite analysis, have confirmed that the isolated strains cannot thrive in basal media broth and agar without the presence of AG or other essential nutrients. This mirrors the observations made in mixed-culture feces, which also require the addition of nutrients for sustained growth. Therefore, two of the isolates (S3 and S4) were chosen to have the best fermenting ability (achieved maximum butyrate levels compared to other strains, 197 mM, and 203 mM, respectively).

3.4. Homology analysis of isolates

Five bacterial strains (S1, S2, S3, S4, and S5) were isolated at the end of the enrichment period. Among these bacteria, an evaluation was performed to identify different isolates based on their growth morphology. These isolates were found to be gram-negative. Based on the results of the BLASTN search (Table 1) of the 16 s ribosomal rRNA sequences of the five isolated strains, all isolates were matched (100% identity) to complete the sequence of the type of strain (holotype) *Escherichia fergusonii* ATCC 35469, partial sequence of *E. fergusonii* strain NRBC 102419, partial sequence of *E. coli* strain JCM 1649, and partial sequence of *Shigella flexneri* strain ATCC 29903.

4. Discussion

4.1. Substrate-species specific pathways

Bifidobacterium spp. is considered an important reference to see the impact of tested prebiotic since immense worked have been involving the use of species from this group and suggested a favorable impact belongs to the genera in the large intestine (Rawi et al., 2021). It is well known that gut fermentation of prebiotic within the colon produced metabolites known as short chain fatty acids (SCFA) beneficial to enhance the colonic health and reduce the risk of colonic diseases and disorders such as colonic cancer, inflammatory bowel disease and irritable bowel syndrome (Roediger, 1980; Jenkins et al., 1999; Floch and Hong-Curtiss, 2002; Hijova and Chmelarova, 2007). SCFA comprises of one to six carbon atoms organic fatty acids derived from anaerobic bacterial fermentation such as polysaccharide, oligosaccharide, or arabinogalactans as its reactant substrate (Miller and Wolin, 1979; Cummings and Macfarlane, 1991). According to Macfarlane and Gibson (1997), the ingested organic matter is digested through pathways such as glycolytic pathway and pentose phosphate

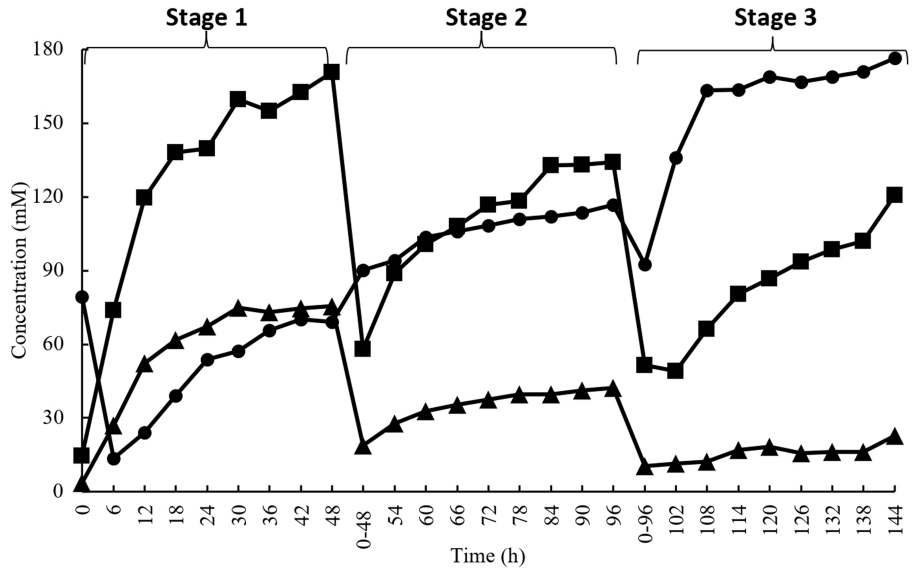

FIGURE 1
Short chain fatty acids concentration during enrichment culture on acacia gum (■, acetate; ▲, propionate; ●, butyrate). Transfer of culture to a fresh medium was performed at 48 h and 96 h.

pathway to transform into simple sugar molecules, pyruvate, energy for microbial growth and also other metabolites in the colon. From anaerobic fermentation of pyruvate, the process end up with a series of end products which include SCFA (Cummings, 1981). These SCFA are mainly metabolites such as acetate, propionate, butyrate, valerate and also other metabolites such as lactate, pyruvate, ethanol, succinate, gases of hydrogen, carbon dioxide and methane gas (Cummings, 1995; Levitt et al., 1995; Macfarlane and Macfarlane, 2003; Flint, 2006). The study of Macfarlane and Macfarlane (2003), Roberfroid (2005), and Cook and Sellin (1998) concluded that the production of SCFA is highly depending on the population of colonic microflora, gut transit time and also type of substrate. In other words, different sources of organic matter resulted in different composition of SCFA thus will affect colon physiology condition differently. The end fermentation products of AG include gases (methane, hydrogen, carbon dioxide) and short chain fatty acid (acetate, propionate, butyrate and valerate). Other intermediate products such as organic acids (lactate, succinate and formate), branch short chain fatty acid (BCFA) (isobutyrate and isovalerate), and alcohols (methanol and ethanol) are also produced with much smaller amount.

4.1.1. Amylolytic bacteria

In the human colon, there is a range of undigested starch content, varying from 10% to a maximum of 40%. This undigested starch is fermented by colonic bacteria with amylolytic activity, resulting in the production of beneficial metabolites such as acetate, propionate, and butyrate (Salyers, 1979; Roediger, 1980; Cummings, 1981; Cummings and Macfarlane, 1991; Mortensen and Clausen, 1996). Amylolytic lactic acid bacteria (ALAB), have the ability to degrade starch using amylase during fermentation. These bacteria are naturally found in starchy fermented foods derived from cassava, sweet potatoes, grains, and maize. The breakdown of starch involves enzymes such as α-amylase for α-1,4 linkage, type I pullulanase for α-1,6 linkage, and amylopullulanases for both 1,4 and 1,6 linkages (Erra-Pujada et al., 1999). Species from three major phyla, namely *Firmicutes*, *Bacteroidetes*, and *Actinobacteria*, are known to participate in starch fermentation. *Lactobacillus* strains are generally considered amylolytic bacteria, but some *Bifidobacterium* strains isolated from the human gastrointestinal tract also exhibit amylolytic activity (Ji et al., 1992; Lee et al., 1997, 1999). Additionally, Crittenden et al. (2001) identified two amylolytic strains, *Bifidobacterium pseudolongum* (ATCC 25526) and *Bifidobacterium adolescentis* (VTT E-001561), which prefer α-1,4-linked glucose sugars. Undigested starchy substrates that survive upper digestion undergo various pathways in the colon, ultimately contributing to lactic acid production. Starch is initially broken down into simpler sugars through enzymatic saccharification, acid or alkali hydrolysis, and the action of amylolytic microbes. This is followed by a second-step fermentation by lactic acid bacteria (LAB) to produce lactic acid. Notably, amylolytic lactic acid bacteria (ALAB) have the unique ability to directly metabolize starch into lactic acid without the need for the first hydrolysis step. This pathway is also observed in co-culture simultaneous saccharification and fermentation, involving a mixture of LAB and ALAB or the integration of two or more fermentation steps. Certain bacteria, such as *Butyrivibrio fibrisolvens*, *Roseburia inulinviorans*, and *Roseburia intestinalis*, produce cell-associated amylase and are known as butyrate-producing bacteria. Other predominant amylolytic lactic acid bacteria (ALAB) include *Lactococcus*, *Streptococcus*, *Pediococcus*, *Carnobacterium*, *Bacteroides*, *Fusobacterium*, and *Butyrivibrio* (Macfarlane and Englyst, 1986; Bhanwar and Ganguli, 2014). *Bacteroides vulgatus*, one of the most abundant strains in the human colon, is an amylolytic gram-negative anaerobic bacteria. *Bifidobacteria* produce amylase extracellularly, while *Bacteroides* strains like *B. vulgatus* and *B. ovatus* produce cell-bound amylase (Ji et al., 1992; Degnan et al., 1997). This partial hydrolysis of starchy material is efficiently converted into lactic acid by amylolytic bacteria in a single step, enhancing the economic feasibility of the fermentation process (Sanoja et al., 2000; Fossi and Tavea, 2013).

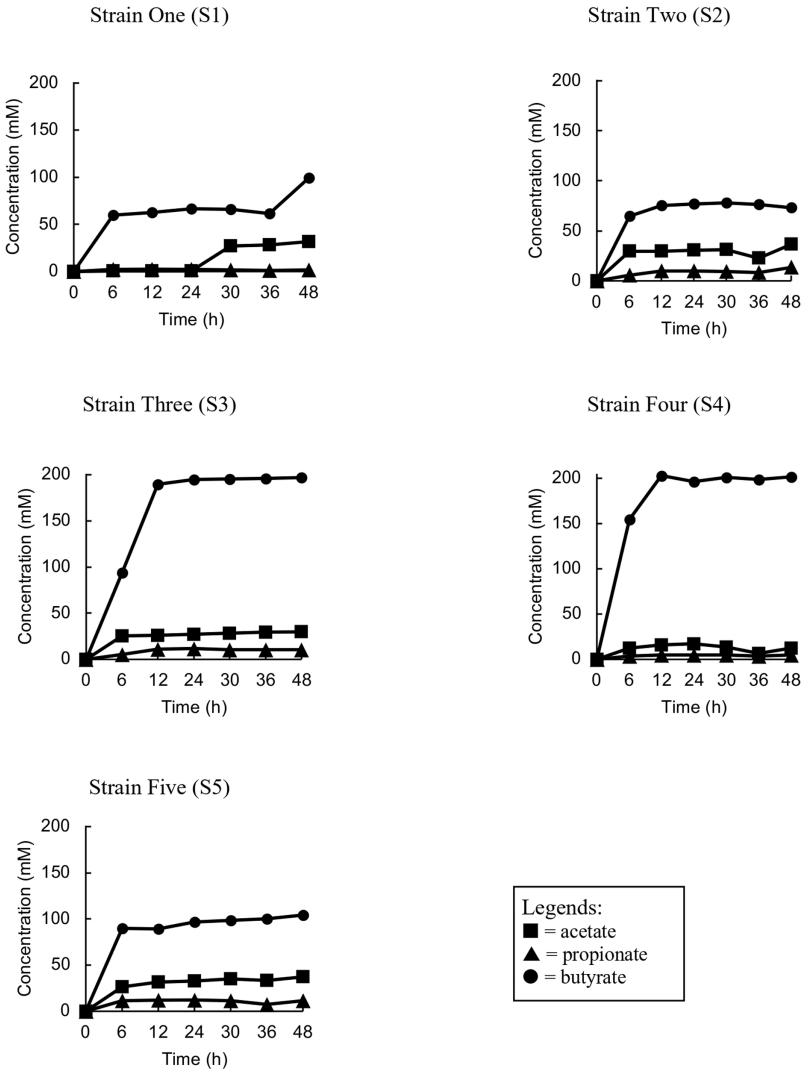

FIGURE 2
Trend analyses of the concentration of short chain fatty acids of each strain (S1, S2, S3, S4 and S5) during the monoculture fermentation.

TABLE 1 List of the sequences that showed similarity with the *Enterobacteriaceae* group.

16s rRNA gene	Strain	Accession no.	Sequence
Escherichia fergusonii	ATCC 35469	NR_074902.1	Complete
Escherichia fergusonii	NRBC 102419	NR_114079.1	Partial
Escherichia coli	JCM 1649	NR_112558.1	Partial
Escherichia fergusonii	ATCC 35469	NR_027549.1	Partial
Shigella flexneri	ATCC 29903	NR_026331.1	Partial

Values for the following parameters are identical for all sequences: Max Score and Total Score: 1664; Query cover: 100%; E value: 0.0; Identity: 100%.

4.1.2. Butyrogenic bacteria

Butyrate, a beneficial short-chain fatty acid (SCFA) metabolite, is produced by various commensal gram-positive microbes in the human gut. The identification of these butyrogenic bacteria is an important area of research. Butyrate is typically generated through the fermentation of colonic microbiota. The XIVa cluster, particularly related to *Eubacterium rectale*, *Eubacterium ramulus*, and *Roseburia cecicola*, is the most abundant group (42%) within this cluster (Barcenilla et al., 2000). Among the major butyrogenic colonic microbes frequently detected in human feces are those from the Clostridial group, primarily clusters IV and XIVa of the Firmicutes phylum. *Faecalibacterium prausnitzii* and *Eubacterium rectale* are included in Cluster IV, while *Roseburia* spp., *Eubacterium* spp., *Anaerostipes caccae*, *Butyrivibrio fibrisolvens*, and *Coprococcus* spp. are significant butyrogenic bacterial strains within Clostridium

Cluster XIVa. *Subdoligranulum variabile* and *Anaerotruncus colihominis* from Clostridium Cluster IV are also involved in butyrate production (Vital et al., 2014). These butyrogenic microbes produce butyrate by fermenting dietary fiber that survives upper gastrointestinal digestion. This process involves saccharolytic pathways related to carbohydrate metabolism and, to a lesser extent, proteolytic pathways associated with protein metabolism (Vital et al., 2014). Furthermore, butyrogenic bacteria exhibit specificity in fermenting unique types of dietary fiber (Moro et al., 2019).

Based on the results, in stage 1 (0–48 h) of the enrichment culture, the individual ratio of acetate:propionate:butyrate was 56:25:18, as shown in Figure 3, which is proportional to the ratio normally seen in the gut content. Different ratios were observed during stage 2 (48–96 h), and stage 3 (96–144 h) which are 44:14:42 and 32:6:62, respectively. Inevitably, a lower bacterial composition means lower production of SCFA compared to the previously cultured inoculum. This explains why the molar ratio of individual SCFA shifted to different proportions depending on which microorganisms were selected and could utilize acacia gum. As predicted, groups of amylolytic and butyrogenic bacteria were the major focus in determining the outcome of AG fermentation in the gut. Acetate, butyrate, and propionate exhibited an increasing trend from the beginning of every stage to the end of the same stage, but the gradient or the rate of production so to speak of acetate and propionate were significantly diminished compared to their respective times at the end of every stage (170 mM (48 h) > 134 mM (96 h) > 121 mM (144 h); 76 mM (48 h) > 42 mM (96 h) > 23 mM (144 h), whereas for butyrate, the opposite was observed, (69 mM (48 h) < 117 mM (96 h) < 176 mM (144 h). This explains why butyrate-producing bacteria were subsequently enriched, whereas others were screened out in the previous stage.

Two independent pathways have been described for butyrate production. The less common pathway, the pyruvate from the Embden-Meyerhof-Parnas (EMP) pathway is further transformed by bacteria into three components: acetyl-CoA, succinate, and lactate. For acetyl-CoA, proceed into butyrate kinase pathways (Zhu et al., 2005) and are transformed into either butyrate or acetate with reciprocal transition. The acetate produced may be utilized by butyryl-CoA:acetate-CoA transferase as a CoA acceptor in another butyrate synthesis cycle carried out by *Roseburia intestinalis* (Duncan et al., 2002).

4.2. Acacia gum fermenting bacteria

Sequence analyzes of certain isolates often suggested that the 16 s rRNA sequence was from multiple strain as it is not easily distinguished. The sequence matched the complete sequence of *Escherichia fergusonii* ATCC 35469, whereas the rest only matched partial sequences available in GenBank for the Enterobacteriaceae group. They are most closely related to *Escherichia coli*. *E. fergusonii* was first isolated from the clinical specimens of a one-year-old boy by Farmer et al. (1985). Another study isolated *E. fergusonii* from healthy cattle (Balqis et al., 2018), and this type of strain was described as a non-pathogenic species (non-virulent in a mouse model) (Forgetta et al., 2012). Therefore, it is deemed commensal. The *E. fergusonii* strains tested positive for indole production, methyl red, lysine decarboxylase, ornithine decarboxylase, and motility. *E. fergusonii* can metabolize several compounds such as d-glucose, adonitol, L-arabinose, L-rhamnose, maltose, d-xylose, trehalose, cellobiose, and d-arabitol. However, they lacked the ability to ferment lactose, sucrose, myo-inositol, d-sorbitol, raffinose, and a-methyl-D-glucoside. *E. fergusonii* was found to have both α- and β-galactosidase (Maheux

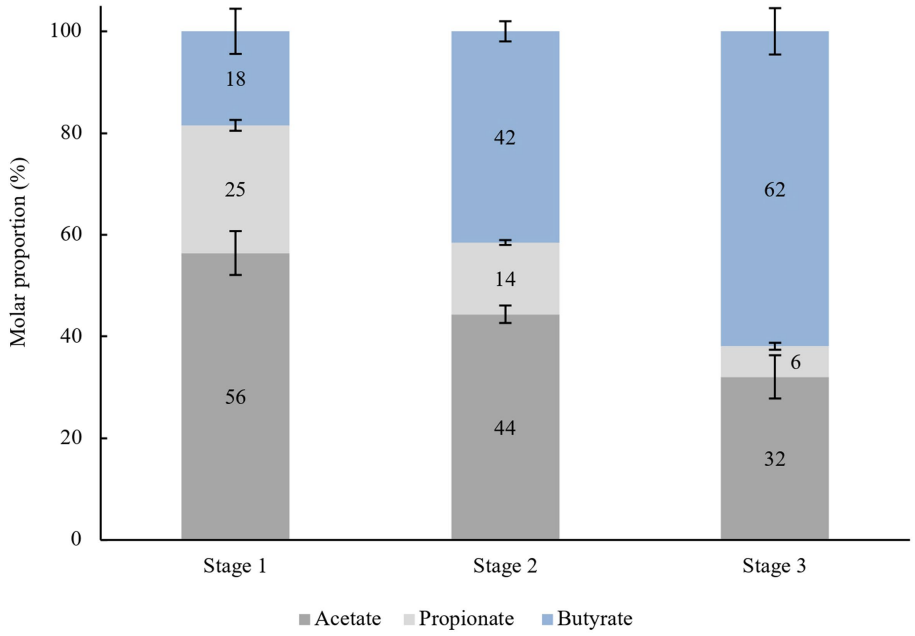

FIGURE 3
Average molar proportion of acetate, propionate and butyrate in every stage (48 h), *n* = 8.

et al., 2014), encoded by LacZ (Reznikoff and Miller, 1978). β-galactosidase has three enzymatic activities (Huber et al., 1976). First, it degrades lactose into glucose and galactose prior to being forwarded into glycolysis. Next, the enzyme catalyzes the transgalactosylation of lactose to allolactose. The last function is to further break the allolactose into monosaccharides. In this perspective, β-galactosidase is best recognized for its high specificity for the galactose part β-D-galactopyranosides linked to a substituted indole substrate (Juers et al., 2012). Apart from this strain, other *E. fergusonii* species have been isolated from many diseases associated with animals, humans, and food samples (Wragg et al., 2009; Weiss et al., 2011; Maifreni et al., 2013).

Findings emerged with various statement of suggesting *E. fergusonii or E. coli*-related species as an opportunistic bacterium, and prone to be pathogenic in high number as reviewed by Gastra et al. (2014). It is thus interesting to mention that *Escherichia fergusonii* could be another anti-inflammatory commensal bacterium as evident in *Faecalibacterium prausnitzii* (also a major butyrate-producer), based on human clinical data (Sokol et al., 2009; Miquel et al., 2013). The lack of a selective medium for the isolation of *E. fergusonii* from materials such as feces, which have high background flora, has been a major hurdle to its detection. This is a novel study on the isolation of gum-fermenting *E. fergusonii* and the first to employ complete enrichment techniques in an anaerobic chamber. The potential role of *E. fergusonii* in biodegradation should also not be neglected (Sriram et al., 2011; Pasumarthi et al., 2013). In our interpretation, it is proposed that *E. fergusonii* encoded LacZ for β-galactosidase in membrane-associated proteins; thus, we speculated that extracellular hydrolysis occurred in the presence of acacia gum molecules. As mentioned in a gene insertion of *E. fergusonii* close relation, *Escherichia coli* mutant, it was revealed that there were resulting mutants that showed β-galactosidase activity in membrane fractions (Komeda, 1988). This is the first study to show that *Escherichia fergusonii* is a gum-fermenting bacterium. β-Galactosidase can act on β-D-galactopyranosides linked to oxygen via glycosidic bonds (Lederberg, 1950; Cohn and Monod, 1951), nitrogen (Sinnott and Withers, 1974), or sulfur and fluorine, but with significantly reduced catalytic efficiency (Wallenfels and Weil, 1972). Its active site specificity targeting d-galactose (Brockhaus et al., 1979; Nam Shin et al., 1980; Huber and Gaunt, 1983) and orientation (2, 3, and 4 positions) for reactions to activate is especially important because only D-galactopyranose, L-arabinopyranose, D-fucopyranose, and D-galactal react in the reverse direction when D-glucose is the other reactant. The enzyme can also slowly react upon exposure to p-nitrophenyl- a-L-arabinopyranoside and p-nitrophenyl-b-D-fucopyranoside (which do not have O_6 hydroxyls) (Loeffler et al., 1979). All these studies conformed to the ability of *E. fergusonii* to break the complex chain of acacia gum polysaccharides in this study, considering the β-galactosidase specificity towards substrate structures. However, further studies are needed to understand the mechanism and capacity of *E. fergusonii* as an important commensal for fermenting complex polysaccharides.

4.3. Factors affecting the efficacy of *in vitro* fermentation

Previous research aimed at identifying acacia gum-fermenting bacteria found several different species and has not been consistent. Human and porcine fecal inocula with 2% acacia gum were used to isolate *Bifidobacterium longum*, *Bacteroides ovatus, Bacteroides oris, Bacteroides buccae,* and *Prevotella ruminicola*-like bacteria (Wyatt et al., 1986; Kishimoto et al., 2006). Kishimoto et al. (2006) reported that the isolated bacteria were propionate-producing bacteria. This highlights that propionate is the largest product of lactate metabolism (Stevani et al., 1991; Hove and Mortensen, 1995; Ushida and Hoshi, 2002). However, in our study, butyrate might have been derived from lactate as a precursor according to the monoculture isolates. Several factors can be ruled out to identify the differences between our study and the previous studies. *In vitro* fermentation systems are commonly used to simulate the human gastrointestinal environment for research purposes. To accurately mimic *in vivo* conditions, various factors need to be carefully controlled, including the type and concentration of substrate, preparation of inoculum, type, and components of the medium, incubation conditions, and stability of maintaining these conditions. The type and concentration of substrate used in prebiotic studies have a significant impact on the fermentation system. Different substrates react differently in the same system, and their physicochemical properties influence the availability of nutrients for bacterial growth and metabolism. Factors such as solubility, particle size, and nutritional composition of the substrates, as well as their structural properties, affect the accessibility of nutrients for bacteria. Soluble fiber is reported to have a higher influence on bacterial growth compared to insoluble fiber. Carbohydrate-type substrates lead to carbohydrate metabolism and the production of metabolites like lactate, acetate, butyrate, and propionate, while protein-type substrates contribute to protein metabolism and the production of branch chain fatty acids (BCFA).

The type and ratio of inoculum used in fermentation also affect the results. In general, inoculum can be saccharolytic (carrying out carbohydrate metabolism), proteolytic (carrying out protein metabolism), or a combination of both. Some bacteria can follow both pathways depending on substrate availability. Using a proteolytic inoculum for carbohydrate-based substrates can decrease the efficacy of fermentation conditions. It is also possible to use a mixture of various inoculum strains in an *in vitro* fermentation system. Overall, controlling the type and concentration of substrate, as well as the type and ratio of inoculum, is crucial for accurately simulating the human gastrointestinal environment in *in vitro* fermentation studies. Fundamentally, inoculum sources by Stevani et al. (1991), Ushida and Hoshi (2002) and by Kishimoto et al., 2006 were isolated from pigs, but in current study, feces were pooled from all healthy human volunteers. Next, different media preparations were used in all these studies. The composition was either from very simple media or a filtered fecal slurry, whereas this study used a more intricate medium, based on Gibson and Wang (1994), which was tested to support the growth of intestinal bacteria during incubation. Furthermore, the pH of the initial incubation is also an important issue to consider. Acidity can affect the regulation of lactate conversion by microbiota (Mackie and Gilchrist, 1979; Counotte and Prins, 1981). As such, more butyrate is produced at pH 5.8–6.0 as compared to pH 6.9 as lactate is converted into butyrate (Counotte et al., 1983). Butyrate production is linked to the transformation of other bacterial metabolites (Dominika et al., 2011). For example, *Megasphaera elsdenii* produces a wide range of

butyrate from lactate, depending on the environmental pH (Counotte and Prins, 1981). Alternatively, the pH effect may be due to the tolerance of lactate-utilizing bacteria to acidity (Mackie and Gilchrist, 1979). In the current study, an initial pH of 6.8 in the enrichment culture was set and was not further controlled as the culture progressed. This explains how much acid level had progressed during the fermentation process, which may contribute to the regulation of butyrate-producing bacteria.

Next, the composition of microbiota in individuals could contribute to different SCFA profiles, despite all replications being administered under the same controlled conditions. Based on our findings, in the *in vitro* colon model, among all the replications, the human microbiota did not have the same SCFA proportion, suggesting that the microbiome metabolized lactate in a different manner. Additionally, the pooled feces in the enrichment study also showed a different outcome (butyrate vs. propionate) compared to the mix of the three human microbiota, which may suggest a propionate-producing type (Hove and Mortensen, 1995). Overall, the current study will serve as a basis for developing selection strategies for the isolation of new butyrate-producing bacteria from the human intestinal microbiota. In addition, there has been recent interest in determining the exact role of butyrate in ameliorating colonic diseases. It is also important to consider inter-individual differences in the study of prebiotics making progress into the market.

Furthermore, acacia gum fermentation showed that these food components are not digestible but are very rapidly fermented once in the large intestine, where fermentation transiently induces accumulation of lactate and therefore could greatly affect butyrate production based on our enrichment study. Acacia gum is a very heterogeneous, and many methods used to demonstrate such as in fractional precipitation, ion exchange chromatography (IEC), gel permeation chromatography (GPC), and hydrophobic affinity chromatography (HAC). Different species and compositions can exert different prebiotic effects. Acacia gum polysaccharides were fractionated to yield three main fractions: arabinogalactan, arabinogalactan protein, and glycoprotein (Randall et al., 1989). These fractions differ in their molecular weights and chemical compositions. Among these fractions, arabinogalactan represented 88% of the total weight and had a low molecular weight. The arabinogalactan moieties were not distributed evenly, and different compositions were quantified throughout the various molecular components present. Furthermore, acacia gum resisted enzyme hydrolysis, suggesting that the arabinogalactan component is enclosed in the core of the molecule and is inaccessible to the enzyme active sites. *A. senegal* possess the higher branching structure than *A. seyal* (78.2% vs. 59.2%) including the galactopyranoses, shorter arabinosyl side branches, and more rhamnopyranoses in terminal position could explained the degree of resistance of AG1 is better than AG2 according to the percent of total carbohydrate reduction (3.63% vs. 11.59%) (Rawi et al., 2021). Many studies agree that it is a highly branched structure composed of β-(1,3)-galactopyranose chains as the backbone with branched side chains joined through the 1,6 positions comprising galactose, arabinose, rhamnose, and glucuronic acid (Anderson et al., 1966; Churms et al., 1983).

Research on acacia gum as a potential prebiotic in this study confirmed other *in vitro* studies and complemented other *in vivo* studies involving animal and human trials. Undoubtedly that prebiotic research has opened a formerly unknown health potential, which is now becoming an alternative approach for mediating gut illness. For example, an animal study on obese mice by Everard et al. (2011) reported that prebiotic feeding improved glucose tolerance and reduced fat accumulation, oxidative stress, and inflammation. In a simulated model of the human colon, the use of synbiotic can alter the dominant bacteria and the production of short-chain fatty acids (SCFAs) in the fecal microbiota (van Zanten et al., 2012). Thus, there is a need to understand the role of gut microbiota in nutrition and health (Valdes et al., 2018).

Data availability statement

The original contributions presented in the study are included in the article/supplementary materials, further inquiries can be directed to the corresponding author.

Ethics statement

The studies involving humans were approved by Universiti Research Ethics Committee, Universiti Putra Malaysia (JKEUPM). The studies were conducted in accordance with the local legislation and institutional requirements. The participants provided their written informed consent to participate in this study.

Author contributions

MHR, HYT, SRS contributed to conception and design of the study and wrote sections of the manuscript. MHR wrote the first draft of the manuscript. All authors contributed to the article and approved the submitted version.

Acknowledgments

The authors would like to express heartfelt gratitude towards the staff of UPM Bintulu Campus, as well as all peers for the valuable assistance in ensuring the success of this research.

Conflict of interest

The authors declare that the research was conducted in the absence of any commercial or financial relationships that could be construed as a potential conflict of interest.

Publisher's note

References

Anderson, D. M. W., Hirst, E., and Stoddart, J. F. (1966). Studies on uronic acid materials. Part XVII. Some structural features of *Acacia senegal* gum (gum arabic). *J. Chem. Soc. C Org.* 1959, 1959–1966. doi: 10.1039/j39660001959

Balqis, U., Hambal, M., Admi, M., Safika, M., Meutia, N., Sugito, D., et al. (2018). *Escherichia fergusonii* identified in preputial swabs from healthy Aceh cattle by phylogenetic 16S rRNA analysis. *Malays. J. Microbiol.* 14, 229–235. doi: 10.21161/mjm.107417

Barcenilla, A., Pryde, S. E., Martin, J. C., Duncan, S. H., Stewart, C. S., Henderson, C., et al. (2000). Phylogenetic relationships of butyrate-producing bacteria from the human gut. *Appl. Environ. Microbiol.* 66, 1654–1661. doi: 10.1128/AEM.66.4.1654-1661.2000

Beck, J. V. (1971). "[8] enrichment culture and isolation techniques particularly for anaerobic bacteria" in *Methods in enzymology*. eds. J. Abelson, M. Simon, G. Verdine and A. Pyle, vol. *22* (Cambridge, MA: Academic Press), 57–64.

Bhanwar, S., and Ganguli, A. (2014). α-Amylase and β-galactosidase production on potato starch waste by *Lactococcus lactis* subsp lactis isolated from pickled yam. *J. Sci. Ind. Res.* 73, 324–330. Available at: http://nopr.niscpr.res.in/handle/123456789/28740

Brockhaus, M., Dettinger, H. M., Kurz, G., Lehmann, J., and Wallenfels, K. (1979). Participation of HO-2 in the cleavage of β-d-galactosides by the β-d-galactosidase from *E. coli*. *Carbohydr. Res.* 69, 264–268. doi: 10.1016/S0008-6215(00)85773-0

Churms, S. C., Merrifield, E. H., and Stephen, A. M. (1983). Some new aspects of the molecular structure of *Acacia senegal* gum (gum arabic). *Carbohydr. Res.* 123, 267–279. doi: 10.1016/0008-6215(83)88483-3

Cohn, M., and Monod, J. (1951). Purification et propriétés de la β-galactosidase (lactase) D'*escherichia coli*. *Biochim. Biophys. Acta* 7, 153–174. doi: 10.1016/0006-3002(51)90013-3

Coico, R. (2006). Gram staining. *Curr. Protoc. Microbiol.* 3:A-3C. doi: 10.1002/9780471729259.mca03cs00

Cook, S., and Sellin, J. (1998). Review article: short chain fatty acids in health and disease. *Aliment. Pharmacol. Ther.* 12, 499–507. doi: 10.1046/j.1365-2036.1998.00337.x

Counotte, G. H. M., Lankhorst, A., and Prins, R. A. (1983). Role of DL-lactic acid as an intermediate in rumen metabolism of dairy cows. *J. Anim. Sci.* 56, 1222–1235. doi: 10.2527/jas1983.5651222x

Counotte, G. H., and Prins, R. A. (1981). Regulation of lactate metabolism in the rumen. *Vet. Res. Commun.* 5, 101–115. doi: 10.1007/BF02214975

Crittenden, R., Laitila, A., Forssell, P., Mättö, J., Saarela, M., Mattila-Sandholm, T., et al. (2001). Adhesion of bifidobacteria to granular starch and its implications in probiotic technologies. *Appl. Environ. Microbiol.* 67, 3469–3475. doi: 10.1128/AEM.67.8.3469-3475.2001

Cueva, C., Sánchez-Patán, F., Monagas, M., Walton, G. E., Gibson, G. R., Martín-Álvarez, P. J., et al. (2013). In vitro fermentation of grape seed flavan-3-ol fractions by human faecal microbiota: changes in microbial groups and phenolic metabolites. *FEMS Microbiol. Ecol.* 83, 792–805. doi: 10.1111/1574-6941.12037

Cummings, J. H. (1981). Short chain fatty acids in the human colon. *Gut* 22, 763–779. doi: 10.1136/gut.22.9.763

Cummings, J. H. (1995). "Short chain fatty acids" in *Human colonic Bacteria: Role in nutrition, physiology and pathology*. eds. G. R. Gibson and G. T. Macfarlane (Boca Raton, Florida: CRC Press Inc.), 101–130.

Cummings, J., and Macfarlane, G. (1991). The control and consequences of bacterial fermentation in the human colon. *J. Appl. Bacteriol.* 70, 443–459. doi: 10.1111/j.1365-2672.1991.tb02739.x

Degnan, B. A., Macfarlane, S., Quigley, M. E., and Macfarlane, G. T. (1997). Starch utilization by *Bacteroides ovatus* isolated from the human large intestine. *Curr. Microbiol.* 34, 290–296. doi: 10.1007/s002849900184

DeGruttola, A. K., Low, D., Mizoguchi, A., and Mizoguchi, E. (2016). Current understanding of dysbiosis in disease in human and animal models. *Inflamm. Bowel Dis.* 22, 1137–1150. doi: 10.1097/mib.0000000000000750

Dominika, Š., Arjan, N., Karyn, R. P., and Henryk, K. (2011). The study on the impact of glycated pea proteins on human intestinal bacteria. *Int. J. Food Microbiol.* 145, 267–272. doi: 10.1016/j.ijfoodmicro.2011.01.002

Duncan, S. H., Barcenilla, A., Stewart, C. S., Pryde, S. E., and Flint, H. J. (2002). Acetate utilization and butyryl coenzyme a (CoA): acetate-CoA transferase in butyrate-producing bacteria from the human large intestine. *Appl. Environ. Microbiol.* 68, 5186–5190. doi: 10.1128/AEM.68.10.5186-5190.2002

Erra-Pujada, M., Debeire, P., Duchiron, F., and O'Donohue, M. J. (1999). The type II pullulanase of *Thermococcus hydrothermalis*: molecular characterization of the gene and expression of the catalytic domain. *J. Bacteriol.* 181, 3284–3287. doi: 10.1128/JB.181.10.3284-3287.1999

Everard, A., Lazarevic, V., Derrien, M., Girard, M., Muccioli, G. G., Neyrinck, A. M., et al. (2011). Responses of gut microbiota and glucose and lipid metabolism to prebiotics in genetic obese and diet-induced leptin-resistant mice. *Diabetes* 60, 2775–2786. doi: 10.2337/db11-0227

Farmer, J. J., Fanning, G. R., Davis, B. R., O'Hara, C. M., Riddle, C., Hickman-Brenner, F. W., et al. (1985). Escherichia fergusonii and *Enterobacter taylorae*, two new species of Enterobacteriaceae isolated from clinical specimens. *J. Clin. Microbiol.* 21, 77–81. doi: 10.1128/jcm.21.1.77-81.1985

Flint, H. J. (2006). "The significance of prokaryote diversity in the human gastrointestinal tract" in *Prokaryotic diversity: Mechanisms and significance*. eds. N. A. Logan, H. M. Lappin-Scott and P. C. F. Oyston (Cambridge: Cambridge University Press), 65.

Floch, M. H., and Hong-Curtiss, J. (2002). Probiotics and functional foods in gastrointestinal disorders. *Curr. Treatm. Opt. Gastroenterol.* 5, 311–321. doi: 10.1007/s11938-002-0054-6

Forgetta, V., Rempel, H., Malouin, F., Vaillancourt, R. Jr., Topp, E., Dewar, K., et al. (2012). Pathogenic and multidrug-resistant *Escherichia fergusonii* from broiler chicken. *Poult. Sci.* 91, 512–525. doi: 10.3382/ps.2011-01738

Forster, S. C., Kumar, N., Anonye, B. O., Almeida, A., Viciani, E., Stares, M. D., et al. (2019). A human gut bacterial genome and culture collection for improved metagenomic analyses. *Nat. Biotechnol.* 37, 186–192. doi: 10.1038/s41587-018-0009-7

Fossi, B. T., and Tavea, F. (2013). *Application of amylolytic Lactobacillus fermentum 04BBA19 in fermentation for simultaneous production of thermostable alpha-amylase and lactic acid. In lactic acid Bacteria-R and D for food, Health and Livestock Purposes*, IntechOpen. London.

Gastra, W., Kusters, J. G., Van Duijkeren, E., and Lipman, L. J. A. (2014). Escherichia fergusonii. *Vet. Microbiol.* 172, 7–12. doi: 10.1016/j.vetmic.2014.04.016

Gibson, G., and Wang, X. (1994). Regulatory effects of Bifidobacteria on the growth of other colonic bacteria. *J. Appl. Bacteriol.* 77, 412–420. doi: 10.1111/j.1365-2672.1994.tb03443.x

Hidalgo, M., Oruna-Concha, M. J., Kolida, S., Walton, G. E., Kallithraka, S., Spencer, J. P., et al. (2012). Metabolism of anthocyanins by human gut microflora and their influence on gut bacterial growth. *J. Agric. Food Chem.* 60, 3882–3890. doi: 10.1021/jf3002153

Hijova, E., and Chmelarova, A. (2007). Short chain fatty acids and colonic health. *Bratisl Lek Listy* 108:354.

Hove, H., and Mortensen, P. B. (1995). Influence of intestinal inflammation (IBD) and small and large bowel length on faecal short-chain fatty acids and lactate. *Dig. Dis. Sci.* 40, 1372–1380. doi: 10.1007/BF02065554

Huber, R. E., and Gaunt, M. T. (1983). Importance of hydroxyls at positions 3, 4, and 6 for binding to the "galactose" site of β-galactosidase (*Escherichia coli*). *Arch. Biochem. Biophys.* 220, 263–271. doi: 10.1016/0003-9861(83)90409-5

Huber, R. E., Kurz, G., and Wallenfels, K. (1976). A quantitation of the factors which affect the hydrolase and transgalactosylase activities of β-galactosidase (*E. coli*) on lactose. *Biochemistry* 15, 1994–2001. doi: 10.1021/bi00654a029

Jenkins, D. J., Kendall, C. W., and Vuksan, V. (1999). Inulin, oligofructose and intestinal function. *J. Nutr.* 129, 1431S–1433S. doi: 10.1093/jn/129.7.1431S

Ji, G. -E., Han, H.-K., and Yun, S.-W. (1992). Isolation of amylolytic Bifidobacterium sp. Int-57 and characterization of amylase. *J. Microbiol. Biotechnol.* 2, 85–91.

Juers, D. H., Matthews, B. W., and Huber, R. E. (2012). LacZ β-galactosidase: structure and function of an enzyme of historical and molecular biological importance. *Protein Sci.* 21, 1792–1807. doi: 10.1002/pro.2165

Kishimoto, A., Ushida, K., Phillips, G. O., Ogasawara, T., and Sasaki, Y. (2006). Identification of intestinal bacteria responsible for fermentation of gum arabic in pig model. *Curr. Microbiol.* 53, 173–177. doi: 10.1007/s00284-005-0219-3

Komeda, Y. (1988). Isolation of fla-lacZ fusions in *Escherichia coli* K-12: most fusions result in soluble beta-galactosidase. *J. Bacteriol.* 170, 1980–1983. doi: 10.1128/jb.170.4.1980-1983.1988

Lederberg, J. (1950). The beta-d-galactosidase of *Escherichia coli*, strain K-12. *J. Bacteriol.* 60, 381–392. doi: 10.1128/jb.60.4.381-392.1950

Lee, S. K., Kim, Y. B., and Ji, G. E. (1997). Note: purification of amylase secreted from *Bifidobacterium adolescentis*. *J. Appl. Microbiol.* 83, 267–272. doi: 10.1046/j.1365-2672.1997.00145.x

Lee, J. H., Lee, S. K., Park, K. H., Hwang, I. K., and Ji, G. E. (1999). Fermentation of rice using amylolytic Bifidobacterium. *Int. J. Food Microbiol.* 50, 155–161. doi: 10.1016/S0168-1605(99)00086-0

Levitt, M. D., Gibson, G., and Christl, S. U. (1995). "Gas metabolism in the large intestine" in *Human colonic Bacteria: Role in nutrition, physiology and pathology*. eds. G. R. Gibson and G. T. Macfarlane (Boca Raton, Florida: CRC Press Inc), 131–154.

Loeffler, R. T., Sinnott, M. L., Sykes, B. D., and Withers, S. G. (1979). Interaction of the lacZ β-galactosidase of *Escherichia coli* with some β-d-galactopyranoside competitive inhibitors. *Biochem. J.* 177:145-152.1. doi: 10.1042/bj1770145

Lu, K., Abo, R. P., Schlieper, K. A., Graffam, M. E., Levine, S., Wishnok, J. S., et al. (2014). Arsenic exposure perturbs the gut microbiome and its metabolic profile in mice: an integrated metagenomics and metabolomics analysis. *Environ. Health Perspect.* 122, 284–291. doi: 10.1289/ehp.1307429

Macfarlane, G. T., and Englyst, H. N. (1986). Starch utilization by the human large intestinal microflora. *J. Appl. Bacteriol.* 60, 195–201. doi: 10.1111/j.1365-2672.1986.tb01073.x

Macfarlane, G. T., and Gibson, G. R. (1997). "Carbohydrate fermentation, energy transduction and gas metabolism in the human large intestine" in *Gastrointestinal microbiology* (London: Springer), 269–318.

Macfarlane, S., and Macfarlane, G. T. (2003). Regulation of short-chain fatty acid production. *Proc. Nutr. Soc.* 62, 67–72. doi: 10.1079/PNS2002207

Mackie, R. I., and Gilchrist, F. M. (1979). Changes in lactate-producing and lactate-utilizing bacteria in relation to pH in the rumen of sheep during stepwise adaptation to a high-concentrate diet. *Appl. Environ. Microbiol.* 38, 422–430. doi: 10.1128/aem.38.3.422-430.1979

Maheux, A. F., Boudreau, D. K., Bergeron, M. G., and Rodriguez, M. J. (2014). Characterization of Escherichia fergusonii and *Escherichia albertii* isolated from water. *J. Appl. Microbiol.* 117, 597–609. doi: 10.1111/jam.12551

Maifreni, M., Frigo, F., Bartolomeoli, I., Innocente, N., Biasutti, M., and Marino, M. (2013). Identification of the Enterobacteriaceae in Montasio cheese and assessment of their amino acid decarboxylase activity. *J. Dairy Res.* 80, 122–127. doi: 10.1017/S002202991200074X

May, T., Mackie, R. I., Fahey, G. C., Cremin, J. C., and Garleb, K. A. (1994). Effect of fibre source on short-chain fatty acid production and on the growth and toxin production by *Clostridium difficile*. *Scand. J. Gastroenterol.* 29, 916–922. doi: 10.3109/00365529409094863

Miller, T. L., and Wolin, M. (1979). Fermentations by saccharolytic intestinal bacteria. *Am. J. Clin. Nutr.* 32, 164–172. doi: 10.1093/ajcn/32.1.164

Miquel, S., Martín, R., Rossi, O., Bermúdez-Humarán, L. G., Chatel, J. M., Sokol, H., et al. (2013). Faecalibacterium prausnitzii and human intestinal health. *Curr. Opin. Microbiol.* 16, 255–261. doi: 10.1016/j.mib.2013.06.003

Moro, T., Rasmussen, H., and Hamaker, B. (2019). Potential of prebiotic butyrogenic fibres in Parkinson's disease. *Front. Neurol.* 10:663. doi: 10.3389/fneur.2019.00663

Mortensen, P. B., and Clausen, M. R. (1996). Short-chain fatty acids in the human colon: relation to gastrointestinal health and disease. *Scand. J. Gastroenterol.* 31, 132–148. doi: 10.3109/00365529609094568

Nam Shin, J. E., Maradufu, A., Marion, J., and Perlin, A. S. (1980). Specificity of α- and β-D-galactosidase towards analogs of D-galactopyranosides modified at C-4 or C-5. *Carbohydr. Res.* 84, 328–335. doi: 10.1016/s0008-6215(00)85562-7

Palframan, R. J., Gibson, G. R., and Rastall, R. A. (2002). Effect of pH and dose on the growth of gut bacteria on prebiotic carbohydrates in vitro. *Anaerobe* 8, 287–292. doi: 10.1006/anae.2002.0434

Pasumarthi, R., Chandrasekaran, S., and Mutnuri, S. (2013). Biodegradation of crude oil by Pseudomonas aeruginosa and *Escherichia fergusonii* isolated from the Goan coast. *Mar. Pollut. Bull.* 76, 276–282. doi: 10.1016/j.marpolbul.2013.08.026

Phillips, G. O. (1998). Acacia gum (Gum Arabic): A nutritional fibre; metabolism and calorific value. *Food Addit. Contam.* 15, 251–264. doi: 10.1080/02652039809374639

Rajilić-Stojanović, M., and deVos, W. M. (2014). The first 1000 cultured species of the human gastrointestinal microbiota. *FEMS Microbiol. Rev.* 38, 996–1047. doi: 10.1111/1574-6976.12075

Randall, R. C., Phillips, G. O., and Williams, P. A. (1989). Fractionation and characterization of gum from *Acacia senegal*. *Food Hydrocoll.* 3, 65–75. doi: 10.1016/s0268-005x(89)80034-7

Rawi, M. H., Abdullah, A., Ismail, A., and Sarbini, S. R. (2021). Manipulation of gut microbiota using acacia gum polysaccharide. *ACS Omega* 6, 17782–17797. doi: 10.1021/acsomega.1c00302

Rawi, M. H., Zaman, S. A., Pa'ee, K. F., Leong, S. S., and Sarbini, S. R. (2020). Prebiotics metabolism by gut-isolated probiotics. *J. Food Sci. Technol.* 57, 2786–2799. doi: 10.1007/s13197-020-04244-5

Reznikoff, W. S., and Miller, J. H. (Eds.). (1978). *The operon*. Cold Spring Harbor Laboratory. Cold Spring Harbor, NY

Roberfroid, M. B. (2005). Introducing inulin-type fructans. *Br. J. Nutr.* 93, S13–S25. doi: 10.1079/BJN20041350

Roediger, W. E. (1980). Role of anaerobic bacteria in the metabolic welfare of the colonic mucosa in man. *Gut* 21, 793–798. doi: 10.1136/gut.21.9.793

Ross, A. H. M., Eastwood, M. A., Brydon, W. G., Busuttil, A., McKay, L. F., and Anderson, D. M. (1984). A study of the effects of dietary gum arabic in the rat. *Br. J. Nutr.* 51, 47–56. doi: 10.1079/BJN19840008

Salyers, A. A. (1979). Energy sources of major intestinal fermentative anaerobes. *Am. J. Clin. Nutr.* 32, 158–163. doi: 10.1093/ajcn/32.1.158

Sanoja, R. R., Morlon-Guyot, J., Jore, J., Pintado, J., Juge, N., and Guyot, J. P. (2000). Comparative characterization of complete and truncated forms of *Lactobacillus amylovorus* α-amylase and role of the C-terminal direct repeats in raw-starch binding. *Appl. Environ. Microbiol.* 66, 3350–3356. doi: 10.1128/AEM.66.8.3350-3356.2000

Shin, W., Wu, A., Massidda, M., Foster, C., Thomas, N., Lee, D. W., et al. (2019). A robust longitudinal co-culture of obligate anaerobic gut microbiome with human intestinal epithelium in an anoxic-oxic interface-on-a-chip. *Front. Bioeng. Biotechnol.* 7:13. doi: 10.3389/fbioe.2019.00013

Sinnott, M. L., and Withers, S. G. (1974). The β-galactosidase-catalysed hydrolyses of β-d-galactopyranosyl pyridinium salts. Rate-limiting generation of an enzyme-bound galactopyranosyl cation in a process dependent only on aglycone acidity. *Biochem. J.* 143, 751–762. doi: 10.1042/bj1430751

Sokol, H., Seksik, P., Furet, J. P., Firmesse, O., Nion-Larmurier, I., Beaugerie, L., et al. (2009). Low counts of *Faecalibacterium prausnitzii* in colitis microbiota. *Inflamm. Bowel Dis.* 15, 1183–1189. doi: 10.1002/ibd.20903

Sriram, M. I., Gayathiri, S., Gnanaselvi, U., Jenifer, P. S., Raj, S. M., and Gurunathan, S. (2011). Novel lipopeptide biosurfactant produced by hydrocarbon degrading and heavy metal tolerant bacterium *Escherichia fergusonii* KLU01 as a potential tool for bioremediation. *Bioresour. Technol.* 102, 9291–9295. doi: 10.1016/j.biortech.2011.06.094

Stevani, J., Grivet, J. P., Hannequart, G., and Durand, M. (1991). Glucose and lactate catabolism by bacteria of the pig large intestine and sheep rumen as assessed by 13C nuclear magnetic resonance. *J. Appl. Bacteriol.* 71, 524–530. doi: 10.1111/j.1365-2672.1991.tb03827.x

Tuohy, K. M., Kolida, S., Lustenberger, A. M., and Gibson, G. R. (2001). The prebiotic effects of biscuits containing partially hydrolysed guar gum and fructo-oligosaccharides–a human volunteer study. *Br. J. Nutr.* 86, 341–348. doi: 10.1079/BJN2001394

Ushida, K., and Hoshi, S. (2002). 13 C-NMR studies on lactate metabolism in a porcine gut microbial ecosystem. *Microb. Ecol. Health Dis.* 14, 242–247. doi: 10.1080/08910600310002136

Valdes, A. M., Walter, J., Segal, E., and Spector, T. D. (2018). Role of the gut microbiota in nutrition and health. *BMJ* 361:k2179. doi: 10.1136/bmj.k2179

van Zanten, G. C., Knudsen, A., Röytiö, H., Forssten, S., Lawther, M., Blennow, A., et al. (2012). The effect of selected synbiotics on microbial composition and short-chain fatty acid production in a model system of the human colon. *PLoS One* 7:e47212. doi: 10.1371/journal.pone.0047212

Vital, M., Howe, A. C., and Tiedje, J. M. (2014). Revealing the bacterial butyrate synthesis pathways by analysing (meta) genomic data. *MBio* 5, e00889–e00814. doi: 10.1128/mBio.00889-14

Walker, A. W., Ince, J., Duncan, S. H., Webster, L. M., Holtrop, G., Ze, X., et al. (2011). Dominant and diet-responsive groups of bacteria within the human colonic microbiota. *ISME J.* 5, 220–230. doi: 10.1038/ismej.2010.118

Wallenfels, K., and Weil, R. (1972). "Beta-galactosidase" in *The enzymes VII*. ed. P. Boyer (New York: Academic Press)

Walter, D. J., Eastwood, M. A., Brydon, W. G., and Elton, R. A. (1988). Fermentation of wheat bran and gum arabic in rats fed on an elemental diet. *Br. J. Nutr.* 60, 225–232. doi: 10.1079/bjn19880094

Weiss, A. T. A., Lübke-Becker, A., Krenz, M., and van der Grinten, E. (2011). Enteritis and septicemia in a horse associated with infection by *Escherichia fergusonii*. *J. Equine Vet.* 31, 361–364. doi: 10.1016/j.jevs.2011.01.005

Williams, P. A., and Phillips, G. O. (2009). "Gum arabic" in *Handbook of hydrocolloids*. eds. G. O. Phillips and P. A. Williams (Sawston: Woodhead Publishing), 252–273.

Wragg, P., La Ragione, R. M., Best, A., Reichel, R., Anjum, M. F., Mafura, M., et al. (2009). Characterisation of *Escherichia fergusonii* isolates from farm animals using an *Escherichia coli* virulence gene array and tissue culture adherence assays. *Res. Vet. Sci.* 86, 27–35. doi: 10.1016/j.rvsc.2008.05.014

Wyatt, G. M., Bayliss, C. E., and Holcroft, J. D. (1986). A change in human faecal flora in response to inclusion of gum arabic in the diet. *Br. J. Nutr.* 55, 261–266. doi: 10.1079/BJN19860033

Zhu, Y., Liu, X., and Yang, S. T. (2005). Construction and characterization of pta gene-deleted mutant of *Clostridium tyrobutyricum* for enhanced butyric acid fermentation. *Biotechnol. Bioeng.* 90, 154–166. doi: 10.1002/bit.20354

frontiers | Frontiers in Microbiology

TYPE Original Research
PUBLISHED 16 October 2023
DOI 10.3389/fmicb.2023.1279029

OPEN ACCESS

EDITED BY
Huaxi Yi,
Ocean University of China, China

REVIEWED BY
Xi Liang,
Qingdao University, China
Youyou Lu,
Huazhong Agricultural University, China

*CORRESPONDENCE
Zheng Ruan
✉ ruanzheng@ncu.edu.cn

RECEIVED 17 August 2023
ACCEPTED 28 September 2023
PUBLISHED 16 October 2023

CITATION
Zou Y, Ding W, Wu Y, Chen T and Ruan Z (2023) Puerarin alleviates inflammation and pathological damage in colitis mice by regulating metabolism and gut microbiota. *Front. Microbiol.* 14:1279029. doi: 10.3389/fmicb.2023.1279029

Puerarin alleviates inflammation and pathological damage in colitis mice by regulating metabolism and gut microbiota

Yixin Zou, Wenjiao Ding, You Wu, Tingting Chen and Zheng Ruan*

State Key Laboratory of Food Science and Resources, School of Food Science, Nanchang University, Nanchang, China

Dysbiosis of gut microbiota and metabolic pathway disorders are closely related to the ulcerative colitis. Through network pharmacology, we found that puerarin is a potential ingredient that can improve the crypt deformation and inflammatory infiltration in mice, and decrease the levels of IL-1β, IL-6 and TNF-α significantly. *Listeria*, *Alistipes* and *P. copri* gradually became dominant bacteria in UC mice, which were positively correlated with inflammatory factors. Puerarin effectively improved dysbiosis by reducing the abundance of *Alistipes*, *P. copri* and *Veillonella*, and increasing the level of *Desulfovibrionacea*. Correlation network and metabolic function prediction analysis of the microbiota showed that they formed a tightly connected network and were widely involved in carbohydrate metabolism and amino acid metabolism. Specifically, we observed significant changes in the tryptophan metabolism pathway in DSS mice, with an increase in the abundance of *Bacteroidetes* and *Enterobacteriaceae* involved in tryptophan metabolism. However, this metabolic disorder was alleviated after puerarin treatment, including the reversal of 3-HAA levels and an increase in the abundance of *Rhodobacteraceae* and *Halomonadaceae* involved in kynurenine metabolism, as well as a significant increase in the purine metabolite guanosine. In conclusion, our study suggests that puerarin has a good therapeutic effect on UC, which is partially achieved by restoring the composition and abundance of gut microbiota and their metabolism.

KEYWORDS

puerarin, ulcerative colitis, network pharmacology, gut microbiota, untargeted metabonomics

1. Introduction

Ulcerative colitis (UC) is a relapsing disease characterized by chronic inflammation. Clinical symptoms include diarrhea, abdominal pain, and hematochezia. According to the latest data, the prevalence of UC was estimated to be 5 million cases around the world, and there is an increasing trend in some emerging industrialized countries (Le Berre et al., 2023; Liu J. et al., 2023).

The pathogenesis of UC is multifactorial, of which the epithelial barrier defects and disorder of immune response are important factors. Persistent inflammation in the gut can lead to dysbiosis of gut microbiota and abnormal accumulation of microbiota metabolites. These abnormal metabolites can further stimulate the immune system, ultimately resulting in impaired mucosal barrier function and exacerbated inflammation (Neurath, 2014).

The current mainstream treatment for UC is the use of salicylic acid drugs to inhibit the synthesis of prostaglandins and leukotrienes. However, they have significant side effects, such as nausea, rash and liver dysfunction, which make them unsuitable for long-term use (Kucharzik et al., 2020). Given the long course and high recurrence rate of UC, it is necessary to search other natural active substances for intervention to achieve a relieving effect.

Radix Puerariae is the dried root of the leguminous plant *Pueraria lobata*, which contains abundant isoflavones and has been widely used in the food and health product industries (Wang et al., 2022). Previous studies have found that water extracts containing *Radix Puerariae* can increase tight junction protein expression (Wang et al., 2023), lower NF-κB activation, reduce inflammatory factor expression in the colon and relieve oxidative stress (Li et al., 2016). These findings suggest that *Radix Puerariae* has a beneficial regulatory effect on intestinal barrier function and inflammation. However, its specific active ingredients and their effects on the composition of the intestinal microbiome and metabolite levels in UC have not been fully elucidated.

In recent years, with the proposal of disease network and systems pharmacology theory (Nogales et al., 2022), it has become a convenient and efficient method to systematically analyze and predict the "substance-gene-target-disease" action network and find potential effective active ingredients based on technologies such as genomics, high-throughput screening, network visualization, and network analysis (Wang et al., 2021).

Based on this, this article first uses network pharmacology to mine the single active ingredients in *Radix Puerariae*, and then establishes a DSS-induced colitis mouse model to verify its improvement effect. In order to further explore possible mechanisms of action, untargeted metabolomics and 16S rRNA technology are used to investigate the improvement of gut microbiota and metabolites by active ingredients.

2. Materials and methods

2.1. Virtual compound screening

We utilized the TCMSP database[1] to retrieve compounds by searching for '*Radix Puerariae*' as the primary keywords. To screen the active ingredients and corresponding targets, we applied OB ≥ 30% and DL ≥ 0.18 as screening conditions (Jiao et al., 2022). Additionally, we included substances with active ingredients that have been widely reported in *Radix Puerariae* for subsequent analysis. Then combined these active targets with compound active targets obtained from the Drugbank database[2] to obtain the total active targets for pueraria. Subsequently, we used uniprot database[3] to convert the corresponding gene names (Zhang H. et al., 2021).

For searching the disease targets, we used DisGeNET[4] and GeneCards database.[5] Then used Cytoscape software to map the cross-gene information between UC and *Radix Puerariae*. Additionally, we conducted PPI analysis using the STRING database,[6] as well as GO and KEGG analyses using the DAVID database[7] (Li et al., 2022).

2.2. Molecular docking

We searched the PubChem database[8] to obtain the 3D structure files of puerarin, genistein, formononetin, and daidzein. And downloaded the crystal structures of TNF-α, IL-1B, and IL-10 from the PDB database.[9] We then docked the small molecules with these proteins and visualized the results of small molecule-protein binding pockets and interactions between the small molecules and amino acid residues by using PyMol 2.5.5 software.

2.3. Animals and experimental treatment

C57BL/6J mice (male, 6–7 weeks old, 20–23 g) were obtained from Spafu Biotechnology (Beijing, China) and housed in a SPF animal facility with a 12 h light/dark cycle. The mice were provided with standard rodent feed and purified water, and the ambient relative humidity was maintained between 40 and 60% at a temperature of 25°C ± 2°C. The experiment was approved by the Animal Experimentation Ethical Committee of Nanchang University (License number: SYXK 2021-0001), and all animal feeding and procedures were conducted in accordance with the experimental animal welfare ethical code of Nanchang University.

The animal experiment procedures are depicted in Figure 1C. After 1 week of adaptive feeding, mice were randomly assigned to four groups: Control group (CON), Model group (UC), Positive group (Sulfasalazine, SASP), and Puerarin group (PUE). All mice were fed the same diet. During the first week, the Model group, Positive group, and Puerarin group received intragastric administration of DSS aqueous solution three times a day, while the Control group received an equivalent amount of normal saline. For the next 2 weeks, the Puerarin group received 200 mg/kg·BW puerarin via gavage, while the Positive group received 200 mg/kg·BW SASP via gavage (Huang et al., 2017). The Model and Control groups were administered an equivalent volume of normal saline via gavage. The weight and diet of all mice were monitored on a weekly basis.

2.4. Colitis induction and evaluation

To ensure that each mouse receives an equal dose of DSS during modeling, we induced colitis by gavage with DSS in this study. During the first week, mice in the model group were gavaged with 0.1 mL/g (0.23 mL) of 15% DSS water solution at 10:00, 15:00 and 20:00 each day until the end of modeling, with an average cumulative intake of DSS of 31.5 mg/g per mouse. After modeling, the DAI index was used for preliminary evaluation of the model (Peng et al., 2020). The detailed scoring criteria can be found in Supplementary Table S1.

1 https://old.tcmsp-e.com/tcmsp.php
2 https://go.drugbank.com/
3 https://www.uniprot.org/
4 https://www.disgenet.org/home/
5 https://www.genecards.org/
6 https://string-db.org/
7 https://DAVID.ncifcrf.gov/
8 https://pubchem.ncbi.nlm.nih.gov/
9 https://www.rcsb.org/

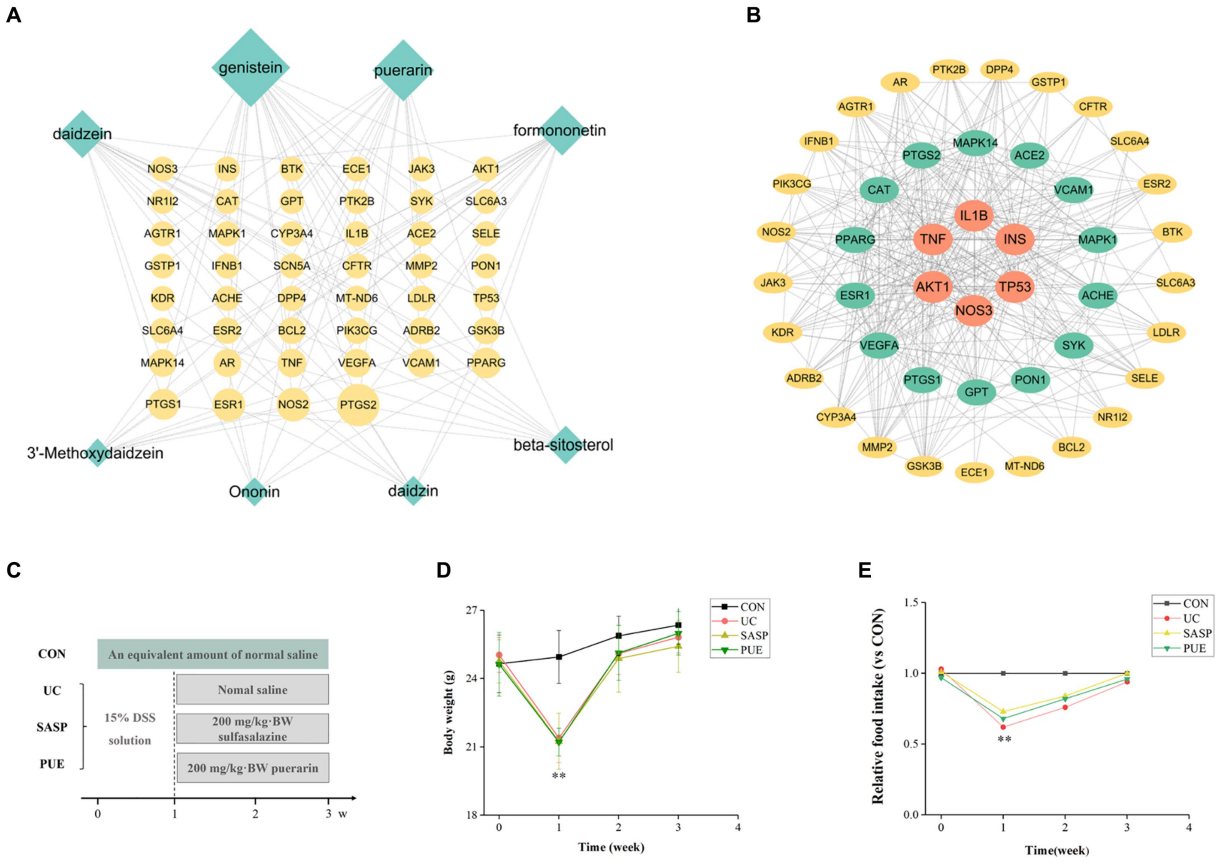

FIGURE 1
Active ingredient puerarin was screened out by network pharmacology, and it has a good effect on the growth performance of mice. **(A)** Diagram of overlapping genes' network between UC and active components in *Radix Puerariae*. **(B)** Protein–protein interaction analysis of overlapping genes. **(C)** Schematic diagram of mouse modeling. **(D)** Changes in body weight of mice during the experiment. **(E)** Changes of food intake of mice compared with CON group during the experiment. $^{**}p < 0.01$, compared to the CON group.

2.5. Biochemical assays of the serum

Whole blood was obtained by puncturing the submandibular vein. To be specific, we inserted a blood collection needle into the posterior aspect of the top of the mandible, where the vein was located, and collected blood. After that, we applied a dry cotton ball to the puncture site to stop bleeding. The whole blood of mice was placed in the tube and centrifuged at 3000 rpm for 15 min at 4°C to obtain serum. The concentrations of TNF-α, IL-6, and IL-1β in the serum were measured using an ELISA kit in accordance with the manufacturer's instructions (Zhao et al., 2021).

2.6. Hematoxylin and eosin staining

The colon tissue was fixed in 4% paraformaldehyde, embedded in paraffin to make 4 mm thick sections, stained with hematoxylin and eosin (H&E) staining solution, and observed under the orthostatic optical microscope (Zhang et al., 2022).

2.7. 16S rRNA and microbiota data analysis

We used QIAamp DNA Stool Kit (Qiagen, Hilden, Germany) and extracted the DNA according to the instructions. The V3-V4 region of the gene was amplified using primers with barcodes, and the resulting amplicons were sequenced on the Illumina NovaSeq platform (Yan et al., 2020).

The initial sequencing data were processed using QIIME2 (2021.8) to generate a sample metadata file (Ding et al., 2021). DADA2 was used for denoising analysis to obtain corresponding feature tables and ASVs data. A Venn diagram was constructed to display the diversity information of ASVs data, showing the abundance of different species and groups. Beta diversity analysis was performed to reveal differences in community structure among different sample groups using principal coordinates analysis (PCoA) and orthogonal partial least squares discriminant analysis (OPLS-DA). Linear discriminant analysis effect size (LEfSe) was used to identify significant differences in microbial composition between different groups (Xu et al., 2022).

2.8. Untargeted metabolomics

In untargeted metabolomics experiments, an X500R HPLC-Q-TOF/MS (SCIEX) was used with an XSelect Premier HSS T3 column (100 mm × 2.1 mm, Waters Corporation, Milford, Massachusetts, USA) for chromatographic separation (Jing et al., 2021). The mobile phase consisted of 0.1% formic acid in water (solvent A) and acetonitrile (solvent B), with a gradient duration of 18 min and a flow rate of 0.3 mL/min (Mi et al., 2023). ESI was used for ionization in both positive and negative ion modes, with ion source gasses 1 and 2 set at 55 psi and curtain gas at 35 psi. The ion source temperature was set to 550 C, while the positive and negative ion source voltages were set to 5,000 V and −4,500 V, respectively. TOF/MS scans were performed over a m/z range of 50–1,200 Da, while TOF/MS/MS scans were performed over a m/z range of 30–1,200 Da. MS/MS data was detected using information-dependent acquisition (IDA).

Data acquisition was controlled using SCIEX OS 2.0 software (AB SCIEX). Metabolite annotation was performed using MetDNA and SCIEX OS 2.0 software. Statistical analysis was conducted using unsupervised principal component analysis (PCA) and supervised orthogonal partial least squares discriminant analysis (OPLS-DA) in MetaboAnalyst 5.0[10] to identify differences in the studied metabolites and screen for potential biomarkers (Zhang Q. et al., 2021). After verifying the differential metabolites in the public database HMDB, we performed metabolic pathway analysis based on the KEGG database (Zhou et al., 2021).

2.9. Statistical analysis

The data collected in this study were analyzed by using SPSS statistical software (24.0). One-way analysis of variance (ANOVA) was used to compare mean differences among the groups, with significance set at $p < 0.05$. The results were expressed as mean ± SD.

3. Results

3.1. Puerarin is a potential ingredient that restored the growth performance of colitis mice

A total of 8 potential active components have been screened from *Radix Puerariae* (detailed information can be found in Supplementary Table S2) and identified 46 overlapping genes between core disease targets (1090) and active ingredient targets (113). Using Cytoscape software, we constructed a network diagram of the ingredient-disease-target interactions (Figure 1A), which revealed that genistein, puerarin, and daidzein had the highest degree of overlap with disease targets. We also performed protein interaction analysis on the overlapping genes and identified key genes such as IL1β, TNF, TP53, and INS (Figure 1B), and are involved in TNF, PI3K-Akt, and VEGF signaling pathways (Supplementary Figures S1–S3).

Subsequent molecular docking revealed that puerarin had the most stable docking with the core target (Figure 2; Supplementary Table S3). And considering the low OB and DL values of genistein (OB = 17.93%, DL = 0.21), we prioritized the use of puerarin, which showed similar good effect, for subsequent animal experiments.

As shown in Figures 1D,E, mice that were orally administered DSS in the first week exhibited a significant decrease in body weight and food intake compared to the control group ($p < 0.01$). However, after stopping the modeling and supplementing with puerarin or sulfasalazine, the body weight of mice gradually recovered, and their food intake also increased. After 2 weeks of oral administration, the food intake of mice in the modeling group gradually returned to normal levels and approached those of mice in the control group.

3.2. Puerarin alleviates the symptoms of DSS induced colitis in mice

We performed DAI scoring on mice at the end of both modeling and treatment (Figure 3A). Representative images of fecal samples from mice at the end of modeling/treatment are shown in Supplementary Figure S4A. The control group showed no abnormalities throughout the experiment, while severe bloody stools were observed in the other three groups after modeling. Some mice in the UC group still had mild red stool, while some mice in the PUE group had mild soft stools without blood and had returned to normal status.

Observation of colon tissue morphology revealed that DSS-induced colitis significantly shortened colon length ($p < 0.05$), while supplementation with puerarin significantly increased colon length compared to the UC group ($p < 0.05$), and showed no difference compared to the control and SASP groups (Figure 3B; Supplementary Figure S4B).

3.3. Puerarin improved colonic tissue morphology and reduced inflammatory factor expression

Figure 3C shows the HE staining of intestinal sections from mice in each group. In the control group, the colon tissue appeared normal, with intact crypt epithelial cells, goblet cells, and submucosa. However, in the UC group induced by DSS, ulcers appeared in the colon and spread to the mucosa and submucosa. The mucosal layer showed infiltration of inflammatory cells, and there was significant damage to the crypts with structural deformation. In contrast, mice treated with PUE did not show obvious colonic ulcers, and only a small amount of inflammatory cell infiltration was observed in the mucosal layer. The deformation of crypts also improved.

As shown in Figure 3D, compared to the CON group, the concentrations of IL-1β, IL-6 and TNF-α were significantly increased ($p < 0.01$) in the UC group. This suggests that there was significant inflammation in the intestines of UC mice. After treatment with SASP or PUE, the concentrations of these three cytokines significantly decreased ($p < 0.01$), but did not fully recover to normal levels (vs CON). Notably, PUE showed a more significant decrease in IL-1β and IL-6 compared to SASP, indicating that puerarin has a better effect on improving inflammation caused by DSS-induced cytokine surge.

10 http://www.metaboanalyst.ca

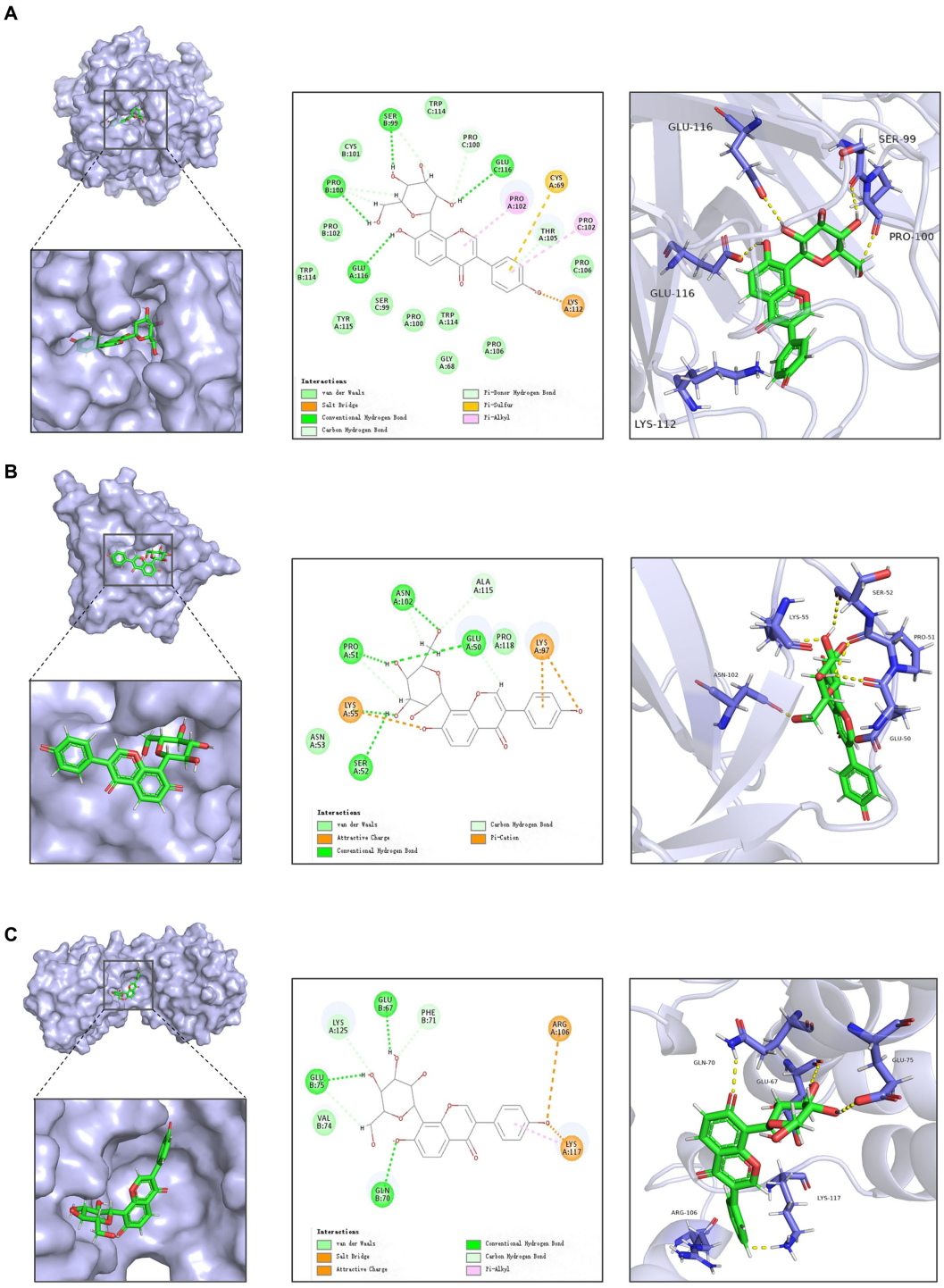

FIGURE 2
Docking of active ingredients in *Radix Puerariae* with target molecules. **(A)** Schematic diagram of docking of puerarin with TNF-α. **(B)** Schematic diagram of docking of Puerarin with IL1B. **(C)** Schematic diagram of docking of Puerarin with IL10.

3.4. Effect of puerarin on intestinal microorganisms in mice with colitis

By examining the species accumulation curve in microbial analysis (Supplementary Figure S5) and conducting α-diversity, β-diversity analysis on different microbial groups, the sample size and community richness were evaluated. The PCoA (Figure 4A) and NMDS plot (Figure 4B) showed significant separation between the UC group and the control group, indicating that DSS significantly altered the composition of the microbiota in mice, which was distinct from that of the control group. Moreover, there was no overlap between the PUE group, SASP group and UC group, suggesting that

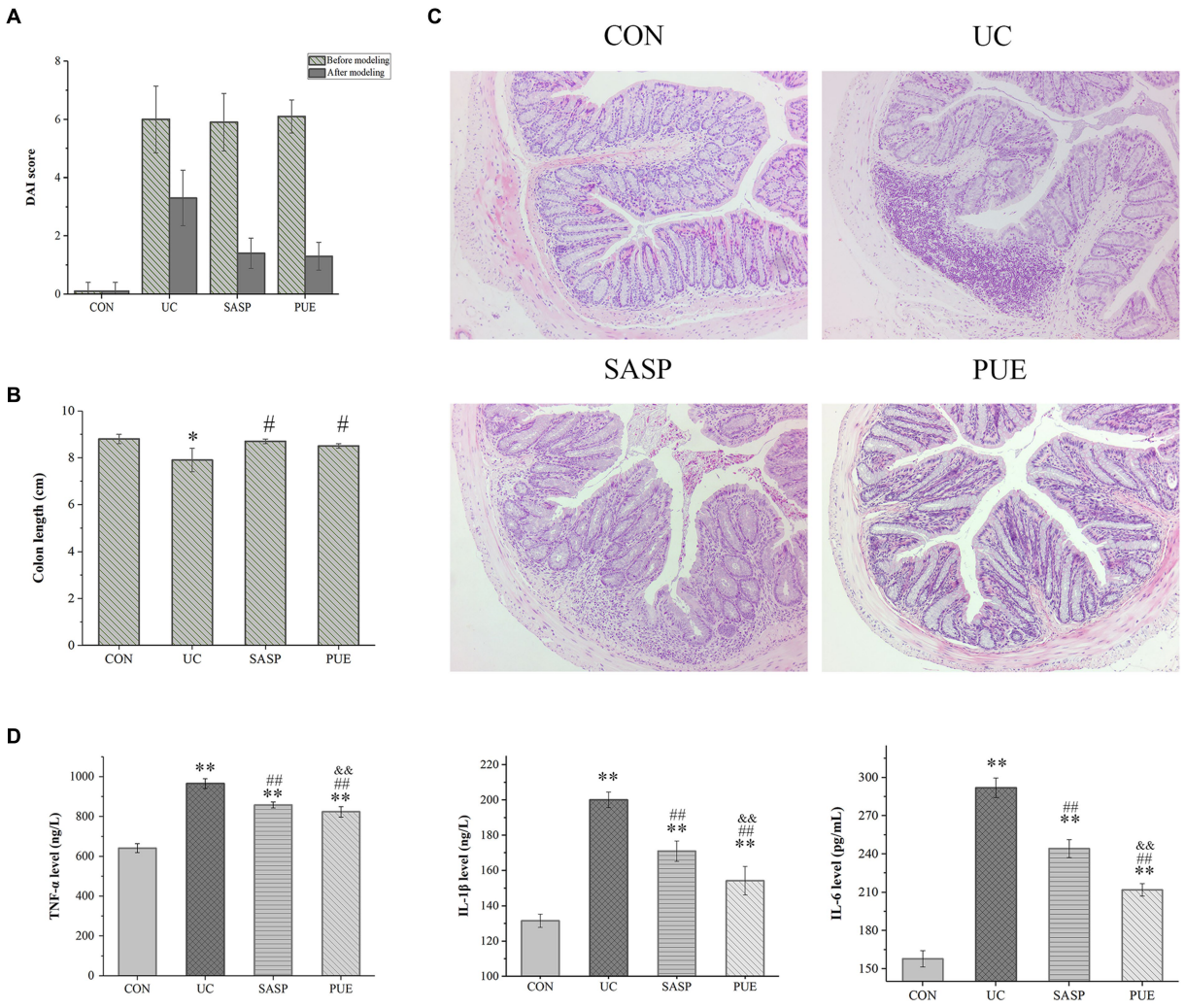

FIGURE 3
Puerarin improved disease score, colonic tissue morphology and reduced inflammatory factor expression in mice. **(A)** DAI score of each group at the end of modeling and administration. **(B)** Colon length of mice in each group. *$p < 0.05$, compared to the CON group; $^{\#}p < 0.05$, compared to the UC group. **(C)** HE section of colon of mice in each group. **(D)** The expression levels of IL-1β, IL-6 and TNF-α in each group ($n = 8$). **$p < 0.01$, compared to the CON group; $^{\#\#}p < 0.01$, compared to the UC group; $^{\&\&}p < 0.01$, compared to the SASP group.

administration induced significant changes in gut microbiota composition with a trend toward normalizing to that of the control group.

A Venn diagram was constructed to characterize the overlap of ASVs among the microbiota based on the ASV information table obtained from QIIME2 denoising analysis. As shown in Figure 4C, the four groups contained 264 (CON), 97 (UC), 147 (SASP), and 237 (PUE) unique ASVs respectively, with a total of 105 ASVs shared as their core microbiota. The results indicated that induced colitis significantly reduced gut species composition, while the number of ASVs increased after SASP intervention and was significantly higher after PUE intervention.

Figure 4D displays the changes in α-diversity of gut microbiota after modeling and intervention. It was observed that the Shannon, ACE, and Chao indices of mice in the UC group were significantly lower than those in the PUE group, indicating that puerarin intervention partially restored the species composition and abundance of gut microbiota in mice.

Furthermore, the top 5 species at the phylum level and top 10 species at the genus level were analyzed (Figures 4E,F). The major microbiota included *Firmicutes*, *Bacteroidetes*, *Proteobacteria*, *Deferribacteres* etc. DSS modeling increased the level of *Bacteroidetes* and decreased the level of *Firmicutes*. However, compared to the UC group, the PUE group reversed the change in F/B ratio and showed a trend toward normalization to that of the control group.

The major species at the genus level included *Allobaculum*, S24-7, *Lactobacillus*, *Prevotella*, *Bacteroides*, and *Turicibacter*. Comparing the changes in gut microbiota at the genus level revealed that DSS modeling significantly increased the levels of *Prevotella*, S24-7, *Bacteroides* and *Mucispirillum*, while decreased the levels of *Allobaculum* and *Lactobacillus*. Compared to the UC group, PUE intervention reversed the changes in *Allobaculum*, *Prevotella*, *Bacteroides*, and *Mucispirillum* levels while decreased S24-7 levels and moving toward a microbiota structure similar to that of the control group.

In addition, we used linear discriminant analysis effect size (LEfSe) to examine the differences in fecal species abundance between

10.3389/fmicb.2023.1279029

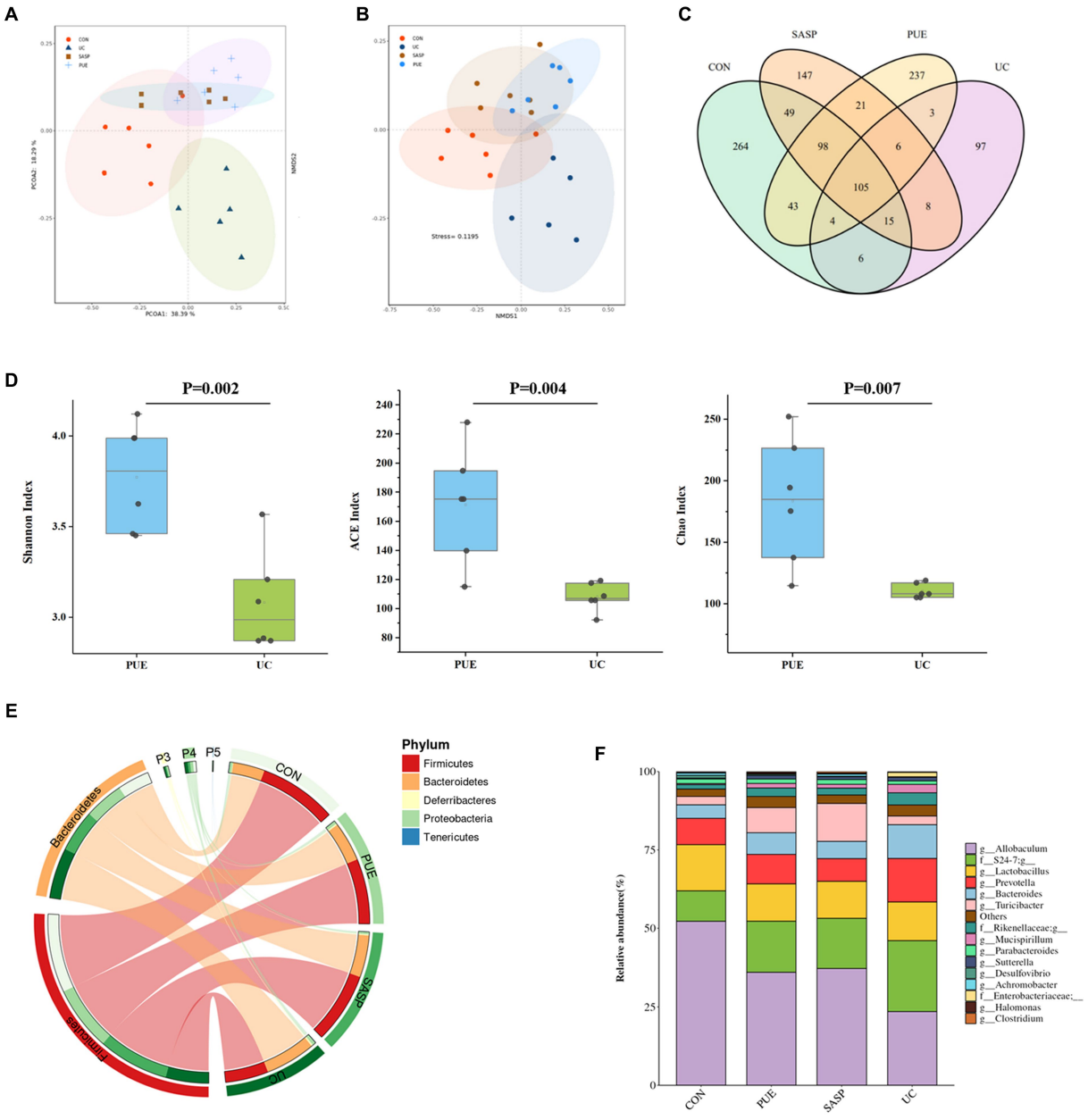

FIGURE 4
Changes of microbiota composition in mice after puerarin intervention. **(A)** PcoA diagram. **(B)** NMDS chart. **(C)** ASV Venn diagram of mice in each group. **(D)** Comparison of α diversity between UC and PUE groups. **(E)** Species composition at phylum level. **(F)** Species composition at genus level.

two groups of mice at different levels (Figures 5A,B). A total of 26 differentially abundant species were identified, including 11 in the UC group: *Prevotella*, S24-7, *Bacteroides*, *Veillonella*, *Veillonellaceae*, *Listeria*, *Eysipelotrichaceae*, *Ovatus*, *Alistipes*, *Copri* and *Enterobacteriaceae*. The PUE group had 6 differentially abundant species: *Rhodothermi*, *Alteromonadaceae*, *Halomonas*, *Halomonadaceae*, *Marinobacter* and *Bilophila*. The SASP intervention had 6 significant species: *Turicibacter*, *Turicibacteraceae*, *Turicibacterales*, *Reuteri*, *Parabacteroides*, and *Johnsonii*.

In order to further elucidate the potential relationships among gut microbiota, we conducted a correlation analysis of the gut microbiota in UC and PUE mice. The resulting visualization network diagram is shown in Figures 5C,D. Our analysis revealed that in the UC state, the abundance of *Allobaculum*, which is notably reduced in the UC state, exhibits a significant negative correlation with the dominant bacterium *Prevotella*. While various pathogenic bacteria such as *Alistipes*, *Listeria*, and *Rikenellaceaeg* formed a tightly connected network with multiple bacteria. After puerarin intervention, we observed a significant enrichment of *Halomonas*, while *Bilophila* and *Halomonas* were negatively correlated with *Prevotella*. Additionally, *Allobaculum* was negatively correlated with *Marinobacter* and *Marinimicrobium*. These correlation analysis results indicate that there are extensive connections among gut microbiota, and the dominance of different bacteria in different states may be due to their interactions with each other.

10.3389/fmicb.2023.1279029

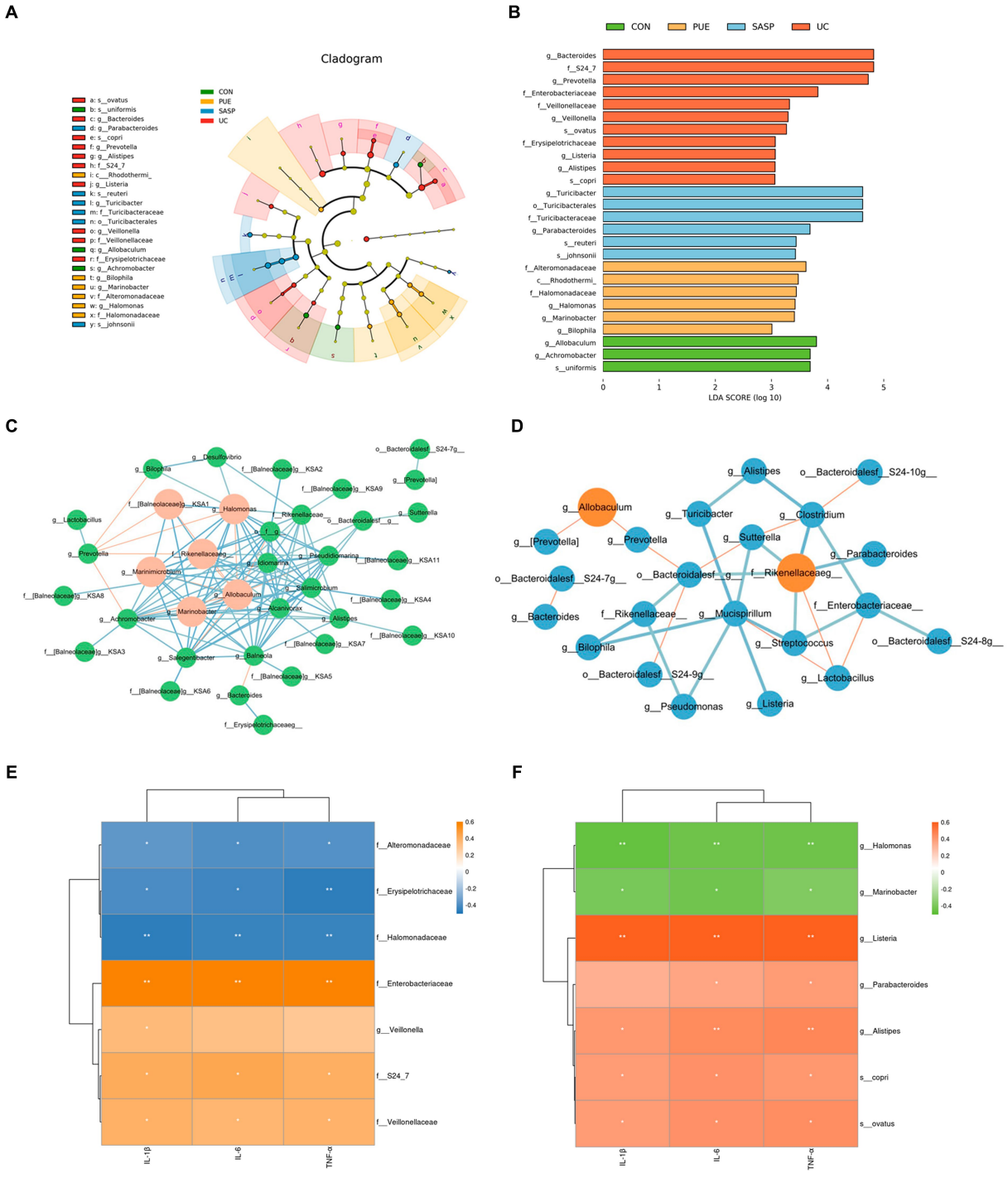

FIGURE 5
(A) Evolutionary branching diagram. **(B)** LEfSe multi-level species discrimination. **(C)** Correlation network of gut microbiota in PUE Group. **(D)** Correlation network of gut microbiota in UC Group. The red lines indicate negative correlation, while the blue lines indicate positive correlation. The red circles represent the bacteria with a larger number of associations. **(E,F)** The heat map of correlation analysis between inflammatory factors and significantly different microorganisms. * indicates $p < 0.05$; ** indicates $p < 0.01$.

Similarly, to understand the relationship between differentially abundant species and inflammatory factors, we conducted a correlation analysis between inflammatory factors and significantly different species (Figures 5E,F). We found that in the UC group, *Enterobacteriaceae*, *Alistipes* and *Listeria* ($p < 0.01$), *Copri*, *Veillonellaceae* and S24_7 ($p < 0.05$) were positively correlated with the concentration of pro-inflammatory factors, while *Eysipelotrichaceae* ($p < 0.01$) was negatively correlated with them. In the PUE group, *Alteromonadaceae* and *Halomonadaceae* ($p < 0.05$) were negatively correlated with the concentration of pro-inflammatory factors, while

Balneola and *Marinobacter* were negatively correlated with TNF-α ($p < 0.05$).

3.5. Effect of puerarin on intestinal metabolism in mice with colitis

In unsupervised mode (Figure 6A), the UC group was clearly separated from the control group, indicating significant differences in fecal metabolites between the two groups; PUE and SASP interventions caused their metabolite characteristics to move away from the UC group and toward the control group. At the same time, in the supervised OPLS-DA mode, each group could also be well separated (Figures 6B–D): UC vs. control group (R2 = 0.618, Q2 = 0.342), SASP vs. UC group (R2 = 0.793, Q2 = 0.364), PUE vs. UC group (R2 = 0.602, Q2 = 0.35). The results indicate that there are differences in metabolites in feces of each group.

By setting the conditions of FC >1 or FC <1/2 and $p < 0.1$, differentially abundant metabolites were screened out, and volcano plots were used to represent the differentially abundant metabolites obtained from different groups (Figures 6E–G). From the figure, it can be seen that compared to the CON group, there were 13 metabolites (such as 3-hydroxybenzoic acid, docosahexaenoic acid, indolelactic acid, etc.) increased and 18 metabolites decreased (such as azelaic acid, sebacic acid, uridine, etc.) in the UC group. Compared to the UC group, there were 7 metabolites increased and 1 metabolite (L-methionine) decreased in the SASP group; while there were 17 metabolites increased and 1 metabolite (docosahexaenoic acid) decreased in the PUE group. Specific information on differentially abundant metabolites can be found in Supplementary Tables S4–S6.

Further setting VIP value >1, 26 differentially abundant metabolites obtained from the secondary screening of the UC group were subjected to metabolic pathway analysis (Figure 6H), and it was found that these metabolites had a major impact on 7 metabolic pathways, including the biosynthesis of phenylalanine, tyrosine and tryptophan, D-glutamine and D-glutamate metabolism, taurine and hypotaurine metabolism, phenylalanine metabolism, alanine, aspartate and glutamate metabolism, arginine biosynthesis and cysteine and methionine metabolism.

To investigate the relationship between differentially abundant metabolites and differentially abundant species in gut microbiota, we performed correlation clustering analysis, as shown in Figure 7A. *Enterobacteriaceae* and *Listeria* were significantly negatively correlated with undecanedioic, sebacic acid, azelacic acid, sebaric acid, guanosine, and uridine. While *bilophila* was positively correlated with taurine, 4-Hydroxy-3-methylbenzoic acid and negtively correlated with various fatty acids levels. On the other hand, the enrichment of several bacterial taxa may affect the levels of 3-Hydroxybenzoic acid, azelaic acid and sebacic acid.

To gain a deeper understanding of the roles and functions of gut microbiota in mice, we conducted a comprehensive functional prediction analysis (Figure 7B). Our findings revealed that these gut microbiota are widely involved in various metabolic activities, including carbohydrate metabolism, amino acid metabolism, metabolism of cofactors and vitamins etc. These results reveal that gut microbiota play a significant role in maintaining the host's homeostasis and health, and this impact is closely related to their metabolic activities.

4. Discussion

Nowadays, there is a widespread and profound understanding of the role of natural products in disease intervention. Due to the large number and variety of small molecules, it is still necessary to seek more efficient and convenient methods to explore potential effective small molecule substances. Network pharmacology, which utilizes multiple databases and integrates various bioinformatics analyses, can effectively aid in addressing these issues (Wang et al., 2021).

In this study, we first utilized network pharmacology techniques to analyze the active ingredients in *Radix Puerariae*, and based on GO and PPI analysis, core protein targets for ulcerative colitis were identified, and molecular docking was performed between active ingredients and targets, resulting in the identification of puerarin as the most promising potential small molecule substance. We confirmed that it can effectively improve the pathological symptoms of DSS-induced colitis in mice, including restoring mouse weight and colon length, inhibiting intestinal tissue damage, and reducing DAI scores. In our experiments, the decrease in concentrations of IL-1β, IL-6 and TNF-α indicated that puerarin has an inhibitory effect on intestinal inflammation. Previous studies have also shown that puerarin can promote goblet cell secretion of mucin to rebuild the mucus layer, forming a barrier between bacteria and epithelial cells to alleviate colitis (Wu et al., 2021).

The microbial community inhabiting the gut plays an essential role in maintaining intestinal health. This study revealed that UC mice exhibited a reduction in *Firmicutes* levels and an increase in *Bacteroidetes* levels within their gut microbiota. The change in the F/B ratio is considered a manifestation of gut dysbiosis. *Firmicutes* are known to produce more energy from equivalent amounts of food compared to other bacterial groups, thus their reduction may lead to weight loss observed in colitis mice. Conversely, *Bacteroidetes* exhibit pro-inflammatory properties due to their lipopolysaccharides (Shen et al., 2018). The observed decrease in F/B ratio is closely associated with inflammatory bowel disease (Stojanov et al., 2020).

In DSS-induced colitis mice, *Alistipes*, *P. copri*, *Enterobacteriaceae*, *Veillonella* and other bacterial groups are significantly enriched. Studies have shown that they can enhance susceptibility to colorectal cancer and arthritis by interfering with IL-6/STAT3 signaling pathway and bile acid metabolism (David et al., 2014; Hofer, 2014; Parker et al., 2020). The differential bacteria *Listeria* has a higher infectivity for immunodeficient patients and also has a higher pathogenicity in IBD (Azimi et al., 2018). Recent studies have also suggested that *Enterobacteriaceae* can use mucosal inflammation to gain a competitive advantage in obtaining energy among symbiotic bacteria, thereby enriching and exacerbating the development of colitis (Garrett et al., 2010). In addition, our correlation analysis between inflammatory factors and differential species also shows a highly positive correlation between these inflammatory pathogenic bacteria and the concentrations of IL-1β, IL-6 and TNF-α. All of these indicate that the enrichment of these pathogenic and pro-inflammatory microorganisms as significant differential species in the UC group is a key factor leading to dysbiosis in the gut microbiota of colitis mice.

Compared with the UC group, after treatment with puerarin, the F/B ratio was restored, inflammation subsided, and the dominant pro-inflammatory bacterial groups were no longer present. Furthermore, it further reversed the significant changes in abundance of bacterial groups in the model group, such as increasing the level of

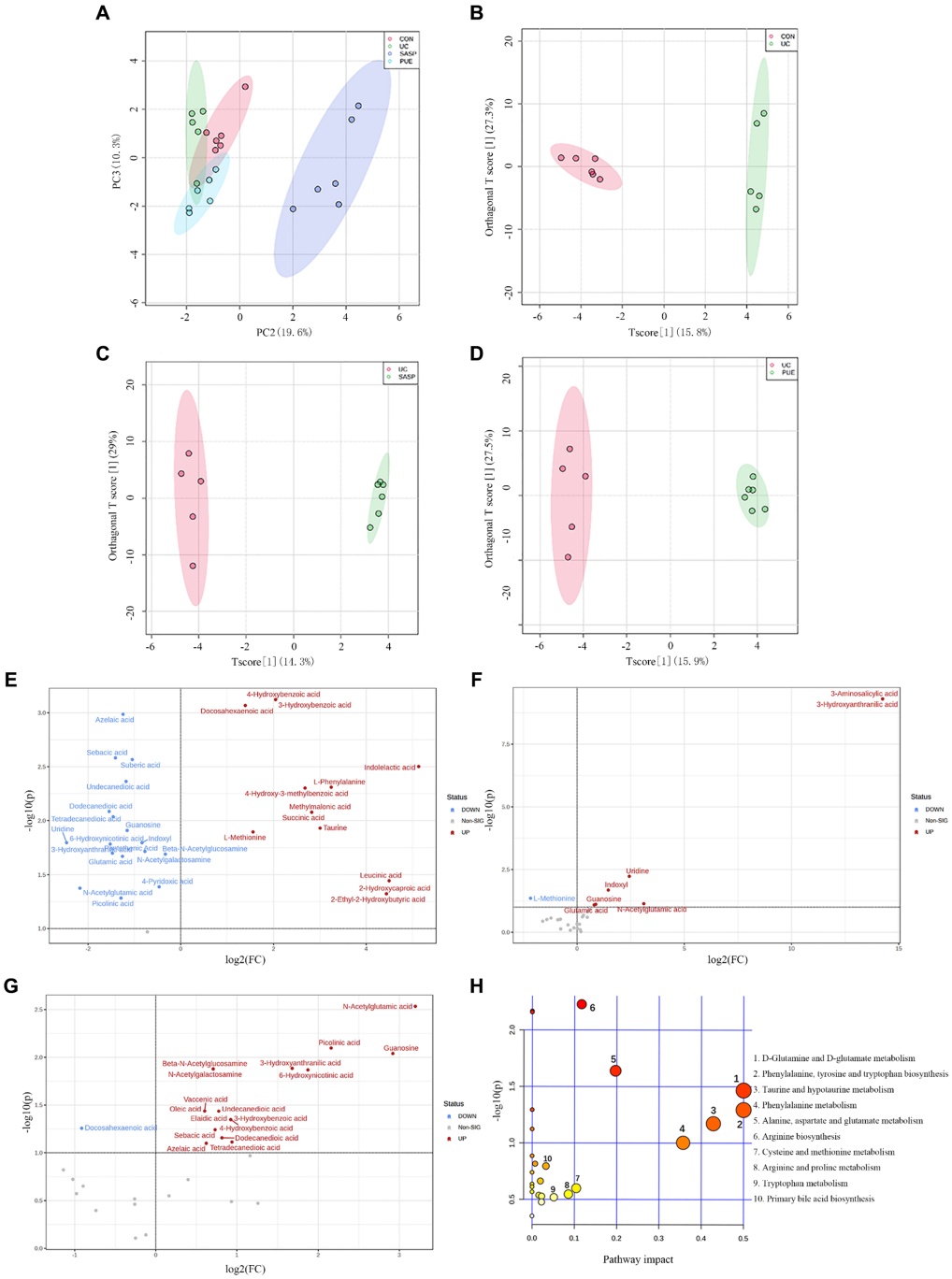

FIGURE 6
Changes of metabolite levels in each group. **(A)** PCA diagram between four groups. **(B–D)** OPLS-DA diagram between two groups. CON vs. UC; UC vs. SASP; UC vs. PUE. **(E)** Volcano plot of untargeted differential metabolites in UC mice compared to control group. **(F)** Volcano plot of differential metabolites in SASP mice compared to UC group. **(G)** Volcano plot of differential metabolites in PUE mice compared to UC group. **(H)** Bubble plot of differential metabolic pathways analysis in UC mice compared to control group.

Desulfovibrionaceae, which is also a type of bacteria that performs well in anti-inflammatory and anti-obesity aspects (Popli et al., 2022).

For better understanding the role of these bacteria in the gut and their interrelationships, we first conducted Spearman correlation analysis on the microbiota of mice in the model group and the puerarin intervention group. We found that the bacteria formed a tightly connected network. Interestingly, some bacteria that significantly decreased in disease, such as *Allobaculum*, showed significant negative correlations with pathogenic bacteria such as *Alistipes* and *Listeria*. This suggests that in a diseased state, bacteria may resist the growth of other bacterial species by taking advantage of their ecological niche, ultimately resulting in increased abundance, while bacteria negatively correlated with them decrease in abundance. In addition, using PICRUSt to predict the function of the mice

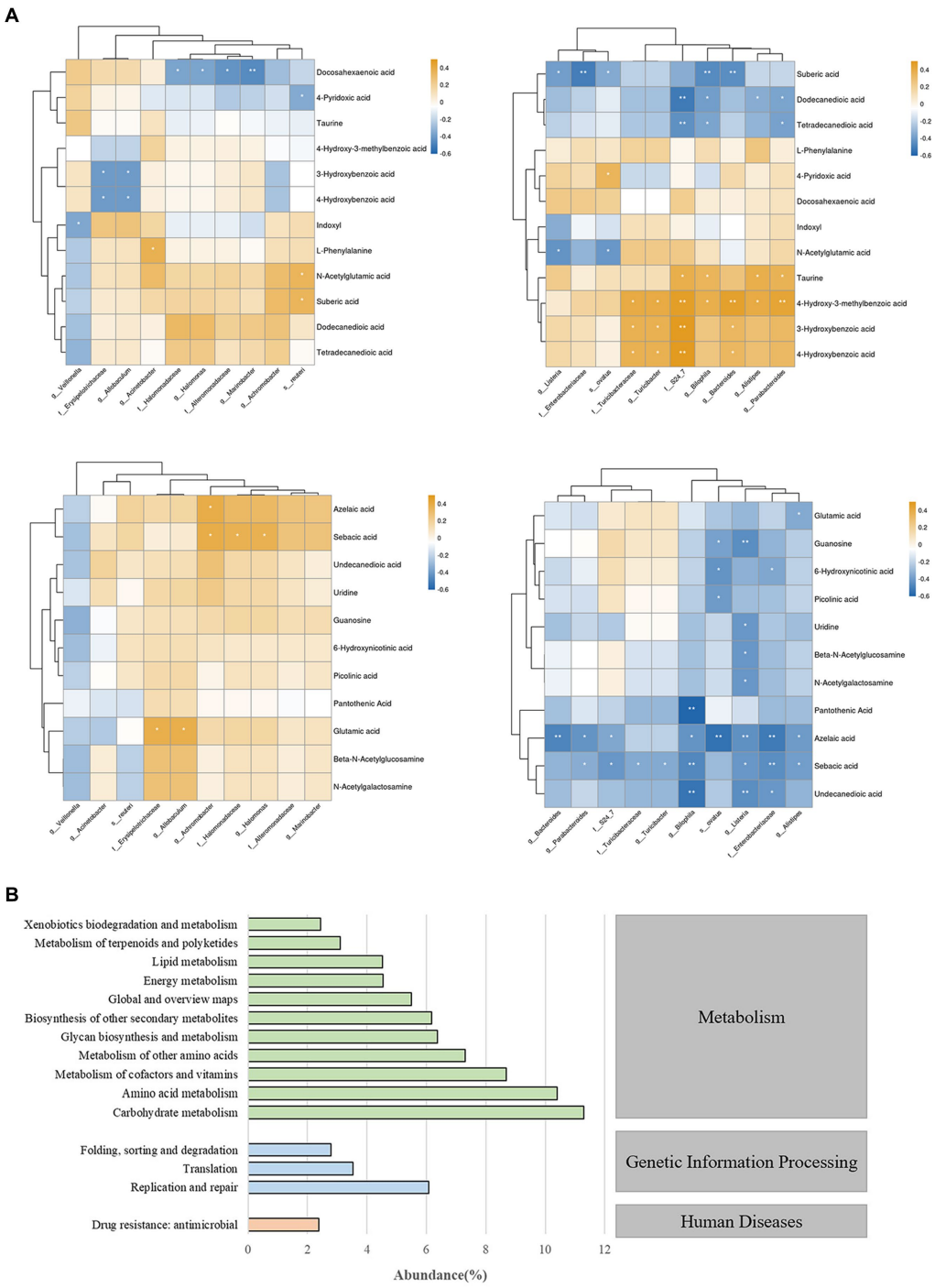

FIGURE 7
(A) Correlation analysis chart of gut microbiota and fecal metabolites. * indicates $p < 0.05$; ** indicates $p < 0.01$. **(B)** Prediction and analysis of gut microbiota function in mice.

microbiota, we found that the top-ranking abundance were involved in various metabolic activities, such as carbohydrate metabolism, amino acid metabolism, and metabolism of cofactors and vitamins. These results all indicate that the gut microbiota, as a special type of organism within the body, has a crucial impact on the host due to its close interrelationships and rich metabolic activities.

Recently, there have been continuous discussions about how metabolites from gut microbiota affect immune homeostasis, host energy metabolism and intestinal mucosal integrity in inflammatory bowel disease (Lavelle and Sokol, 2020). Our previous study found that indole-3-propionic acid derived from the tryptophan pathway can enhance mucous barrier by increasing secretion of mucin (MUC2 and MUC4) and goblet cell products (Li J. et al., 2021). Song et al. also reported that 3-oxo-deoxycholic acid, a bile acid metabolite, can regulate Foxp3 Treg cell homeostasis in the intestinal lamina propria to exert anti-inflammatory properties (Song et al., 2020). Although the

oral bioavailability of screened puerarin did not reach ideal standards, recent reports suggest that these polyphenolic small molecules can remain in the intestinal lumen and participate in gut microbiota metabolism to exert their functions (Luca et al., 2020).

In this experiment, it was found that levels of fecal metabolites such as glutamate and 4-pyridoxic acid decreased while taurine levels significantly increased in UC mice. Taurine is known to activate NLRP6 inflammasomes leading to inflammatory reactions in the intestinal mucosal layer and activation of vitamin B6 degradation pathways during cellular immune responses (Levy et al., 2015). However, no changes were observed in these metabolic pathways after treatment with puerarin. Additionally, tryptophan was not detected but its secondary metabolite indole derivative significantly increased in DSS-induced colitis mice.

Further metabolic pathway analysis of UC mice showed significant changes in the tryptophan metabolism pathway. In recent studies, it has similarly been found that DSS-induced colitis disrupts tryptophan/kynurenine metabolism through the regulation of the rate-limiting enzyme IDO1, and this phenomenon is closely associated with alterations in the gut microbiota (Zhao et al., 2023). Differential species analysis of fecal microbiota also revealed a significant increase in the abundance of the *Bacteroides* and *Enterobacteriaceae* in the UC group. Previous reports have suggested that *Bacteroides* is involved in many important metabolic activities in the colon, including carbohydrate fermentation, nitrogenous substance utilization, and biotransformation of bile acids and other steroids. Some species of *Bacteroides* can produce indole-3-lactic acid, indole-3-acetic acid, and tryptamine (Liu Y. et al., 2023; Nie et al., 2023). *Enterobacteriaceae* have also been reported to have the ability to metabolize tryptophan *in vivo* (Zhang J. et al., 2021). These findings suggest that there may be an imbalance and excessive utilization of tryptophan in the UC mice. Therefore, metabolic disorders such as the indole pathway, urea cycle, glutamate, vitamins, and taurine may exacerbate the development of intestinal inflammation in colitis mice.

After administration of puerarin, the abundance of the *Bacteroides* in the gut was found to be decreased, and the metabolic levels of 3-HAA, picolinic acid, and niacin metabolites were reversed. Among them, 3-HAA is a type of anti-inflammatory tryptophan metabolite, an increase in its concentration can inhibit the development of inflammation in collagen-induced arthritis models. Other studies have shown that 3-HAA can induce apoptosis in liver cancer cells as a ligand-activated transcription factor YY1 and has anti-cancer effects (Kolodziej, 2013; Shi et al., 2021). Puerarin may have an inhibitory effect on intestinal inflammation by regulating the tryptophan metabolism pathway. Yang et al. found that the active ingredient, theabrownin, in Fu Brick Tea can effectively correct intestinal damage in UC mice and promote the secretion of indole derivatives, which are downstream products of the tryptophan metabolic pathway (Yang et al., 2023). This effective improvement of the disease by alleviating the dysregulation of tryptophan metabolism in the microbiota was also observed after turmeric polysaccharides intervention (Yang et al., 2021).

In our results, the differential bacterial groups *Rhodobacteraceae* and *Halomonadaceae* after puerarin treatment contain enzymes that break down tryptophan into kynurenine and downstream metabolites (Vujkovic-Cvijin et al., 2013). Therefore, we speculate that the improvement effect of puerarin on UC may be partially achieved by restoring the function of gut microbiota and thus restoring tryptophan metabolism.

In addition, we correlated differential species and metabolites and found that *Enterobacteriaceae* and *Listeria* were significantly and negatively correlated with undecanedioic, sebacic acid, azelacic acid, sebaric acid, guanosine, and uridine, which are pathogenic bacteria that dominate under disease conditions. After treatment, we also observed a significant increase in purine metabolites such as uridine and guanosine, which have been reported in previous studies to activate the PPARγ signaling pathway in human colonic epithelial cells and restore mucosal barrier function (Li D. et al., 2021). These results well demonstrate that puerarin alleviates DSS-induced colitis by restoring the abundance and metabolic advantage of specific bacterial communities in mice.

Overall, our research indicates that puerarin intervention effectively reduced pathological damage and inflammatory status in DSS-induced colitis mice, and partially restored gut microbiota and metabolic disorders. Our study expands on the potential effects of puerarin in improving intestinal inflammation based on previous research, providing data support for the exploration and development of such natural small molecule substances in the future.

Data availability statement

The datasets presented in this study can be found in online repositories. The names of the repository/repositories and accession number(s) can be found in the article/Supplementary material.

Ethics statement

The animal study was approved by the Animal Experimentation Ethical Committee of Nanchang University (License number: SYXK 2021-0001). The study was conducted in accordance with the local legislation and institutional requirements.

Author contributions

YZ: Conceptualization, Data curation, Formal analysis, Investigation, Methodology, Software, Visualization, Writing – original draft. WD: Conceptualization, Data curation, Methodology, Visualization, Writing – original draft. YW: Methodology, Software, Supervision, Writing – original draft. TC: Data curation, Formal analysis, Investigation, Writing – original draft. ZR: Funding acquisition, Resources, Supervision, Validation, Writing – review & editing, Project administration.

Funding

The author(s) declare financial support was received for the research, authorship, and/or publication of this article. This study was supported by the National Natural Science Foundation of China (32060539).

Conflict of interest

The authors declare that the research was conducted in the absence of any commercial or financial relationships that could be construed as a potential conflict of interest.

Publisher's note

All claims expressed in this article are solely those of the authors and do not necessarily represent those of their affiliated organizations, or those of the publisher, the editors and the reviewers. Any product that may be evaluated in this article, or claim that may be made by its manufacturer, is not guaranteed or endorsed by the publisher.

Supplementary material

The Supplementary material for this article can be found online at: https://www.frontiersin.org/articles/10.3389/fmicb.2023.1279029/full#supplementary-material

References

Azimi, T., Nasiri, M. J., Chirani, A. S., Pouriran, R., and Dabiri, H. (2018). The role of bacteria in the inflammatory bowel disease development: a narrative review. *APMIS* 126, 275–283. doi: 10.1111/apm.12814

David, L. A., Maurice, C. F., Carmody, R. N., Gootenberg, D. B., Button, J. E., Wolfe, B. E., et al. (2014). Diet rapidly and reproducibly alters the human gut microbiome. *Nature* 505, 559–563. doi: 10.1038/nature12820

Ding, Y., Li, X., Liu, Y., Wang, S., and Cheng, D. (2021). Protection mechanisms underlying oral administration of chlorogenic acid against cadmium-induced hepatorenal injury related to regulating intestinal flora balance. *J. Agric. Food Chem.* 69, 1675–1683. doi: 10.1021/acs.jafc.0c06698

Garrett, W. S., Gallini, C. A., Yatsunenko, T., Michaud, M., DuBois, A., Delaney, M. L., et al. (2010). Enterobacteriaceae act in concert with the gut microbiota to induce spontaneous and maternally transmitted colitis. *Cell Host Microbe* 8, 292–300. doi: 10.1016/j.chom.2010.08.004

Hofer, U. (2014). Microbiome: pro-inflammatory Prevotella? *Nat. Rev. Microbiol.* 12:5. doi: 10.1038/nrmicro3180

Huang, Y. F., Zhou, J. T., Qu, C., Dou, Y. X., Huang, Q. H., Lin, Z. X., et al. (2017). Anti-inflammatory effects of Brucea javanica oil emulsion by suppressing NF-κB activation on dextran sulfate sodium-induced ulcerative colitis in mice. *J. Ethnopharmacol.* 198, 389–398. doi: 10.1016/j.jep.2017.01.042

Jiao, W., Mi, S., Sang, Y., Jin, Q., Chitrakar, B., Wang, X., et al. (2022). Integrated network pharmacology and cellular assay for the investigation of an anti-obesity effect of 6-shogaol. *Food Chem.* 374:131755. doi: 10.1016/j.foodchem.2021.131755

Jing, W., Dong, S., Luo, X., Liu, J., Wei, B., Du, W., et al. (2021). Berberine improves colitis by triggering AhR activation by microbial tryptophan catabolites. *Pharmacol. Res.* 164:105358. doi: 10.1016/j.phrs.2020.105358

Kolodziej, L. (2013). Systemic metabolism of tryptophan and its catabolites, kynurenine and 3-HAA, in mice with inflammatory arthritis. *Gene* 512, 23–27. doi: 10.1016/j.gene.2012.09.122

Kucharzik, T., Koletzko, S., Kannengiesser, K., and Dignass, A. (2020). Ulcerative colitis-diagnostic and therapeutic algorithms. *Dtsch. Arztebl. Int.* 117, 564–574. doi: 10.3238/arztebl.2020.0564

Lavelle, A., and Sokol, H. (2020). Gut microbiota-derived metabolites as key actors in inflammatory bowel disease. *Nat. Rev. Gastroenterol. Hepatol.* 17, 223–237. doi: 10.1038/s41575-019-0258-z

Le Berre, C., Honap, S., and Peyrin-Biroulet, L. (2023). Ulcerative colitis. *Lancet* 402, 571–584. doi: 10.1016/s0140-6736(23)00966-2

Levy, M., Thaiss, C. A., Zeevi, D., Dohnalová, L., Zilberman-Schapira, G., Mahdi, J. A., et al. (2015). Microbiota-modulated metabolites shape the intestinal microenvironment by regulating NLRP6 inflammasome signaling. *Cells* 163, 1428–1443. doi: 10.1016/j.cell.2015.10.048

Li, R., Chen, Y., Shi, M., Xu, X., Zhao, Y., Wu, X., et al. (2016). Gegen Qinlian decoction alleviates experimental colitis via suppressing TLR4/NF-κB signaling and enhancing antioxidant effect. *Phytomedicine* 23, 1012–1020. doi: 10.1016/j.phymed.2016.06.010

Li, D., Feng, Y., Tian, M., Ji, J., Hu, X., and Chen, F. (2021). Gut microbiota-derived inosine from dietary barley leaf supplementation attenuates colitis through PPARγ signaling activation. *Microbiome* 9:83. doi: 10.1186/s40168-021-01028-7

Li, X., Wei, S., Niu, S., Ma, X., Li, H., Jing, M., et al. (2022). Network pharmacology prediction and molecular docking-based strategy to explore the potential mechanism of Huanglian Jiedu decoction against sepsis. *Comput. Biol. Med.* 144:105389. doi: 10.1016/j.compbiomed.2022.105389

Li, J., Zhang, L., Wu, T., Li, Y., Zhou, X., and Ruan, Z. (2021). Indole-3-propionic acid improved the intestinal barrier by enhancing epithelial barrier and mucus barrier. *J. Agric. Food Chem.* 69, 1487–1495. doi: 10.1021/acs.jafc.0c05205

Liu, J., Di, B., and Xu, L. L. (2023). Recent advances in the treatment of IBD: targets, mechanisms and related therapies. *Cytokine Growth Factor Rev.* 71-72, 1–12. doi: 10.1016/j.cytogfr.2023.07.001

Liu, Y., Pei, Z., Pan, T., Wang, H., Chen, W., and Lu, W. (2023). Indole metabolites and colorectal cancer: gut microbial tryptophan metabolism, host gut microbiome biomarkers, and potential intervention mechanisms. *Microbiol. Res.* 272:127392. doi: 10.1016/j.micres.2023.127392

Luca, S. V., Macovei, I., Bujor, A., Miron, A., Skalicka-Woźniak, K., Aprotosoaie, A. C., et al. (2020). Bioactivity of dietary polyphenols: the role of metabolites. *Crit. Rev. Food Sci. Nutr.* 60, 626–659. doi: 10.1080/10408398.2018.1546669

Mi, Y., Xu, X., Zeng, F., Li, N., Tan, X., and Gong, Z. (2023). Prebiotics alleviates cartilage degradation and inflammation in post-traumatic osteoarthritis mice by modulating the gut barrier and fecal metabolomics. *Food Funct.* 14, 4065–4077. doi: 10.1039/D3FO00775h

Neurath, M. F. (2014). Cytokines in inflammatory bowel disease. *Nat. Rev. Immunol.* 14, 329–342. doi: 10.1038/nri3661

Nie, Q., Sun, Y., Li, M., Zuo, S., Chen, C., Lin, Q., et al. (2023). Targeted modification of gut microbiota and related metabolites via dietary fiber. *Carbohydr. Polym.* 316:120986. doi: 10.1016/j.carbpol.2023.120986

Nogales, C., Mamdouh, Z. M., List, M., Kiel, C., Casas, A. I., and Schmidt, H. (2022). Network pharmacology: curing causal mechanisms instead of treating symptoms. *Trends Pharmacol. Sci.* 43, 136–150. doi: 10.1016/j.tips.2021.11.004

Parker, B. J., Wearsch, P. A., Veloo, A. C. M., and Rodriguez-Palacios, A. (2020). The genus Alistipes: gut Bacteria with emerging implications to inflammation, Cancer, and mental health. *Front. Immunol.* 11:906. doi: 10.3389/fimmu.2020.00906

Peng, L., Gao, X., Nie, L., Xie, J., Dai, T., Shi, C., et al. (2020). Astragalin attenuates dextran sulfate sodium (DSS)-induced acute experimental colitis by alleviating gut microbiota Dysbiosis and inhibiting NF-κB activation in mice. *Front. Immunol.* 11:2058. doi: 10.3389/fimmu.2020.02058

Popli, S., Badgujar, P. C., Agarwal, T., Bhushan, B., and Mishra, V. (2022). Persistent organic pollutants in foods, their interplay with gut microbiota and resultant toxicity. *Sci. Total Environ.* 832:155084. doi: 10.1016/j.scitotenv.2022.155084

Shen, Z. H., Zhu, C. X., Quan, Y. S., Yang, Z. Y., Wu, S., Luo, W. W., et al. (2018). Relationship between intestinal microbiota and ulcerative colitis: mechanisms and clinical application of probiotics and fecal microbiota transplantation. *World J. Gastroenterol.* 24, 5–14. doi: 10.3748/wjg.v24.i1.5

Shi, Z., Gan, G., Xu, X., Zhang, J., Yuan, Y., Bi, B., et al. (2021). Kynurenine derivative 3-HAA is an agonist ligand for transcription factor YY1. *J. Hematol. Oncol.* 14:153. doi: 10.1186/s13045-021-01165-4

Song, X., Sun, X., Oh, S. F., Wu, M., Zhang, Y., Zheng, W., et al. (2020). Microbial bile acid metabolites modulate gut RORγ(+) regulatory T cell homeostasis. *Nature* 577, 410–415. doi: 10.1038/s41586-019-1865-0

Stojanov, S., Berlec, A., and Štrukelj, B. (2020). The influence of probiotics on the Firmicutes/Bacteroidetes ratio in the treatment of obesity and inflammatory bowel disease. *Microorganisms* 8:1715. doi: 10.3390/microorganisms8111715

Vujkovic-Cvijin, I., Dunham, R. M., Iwai, S., Maher, M. C., Albright, R. G., Broadhurst, M. J., et al. (2013). Dysbiosis of the gut microbiota is associated with HIV disease progression and tryptophan catabolism. *Sci. Transl. Med.* 5:193ra91. doi: 10.1126/scitranslmed.3006438

Wang, D., Bu, T., Li, Y., He, Y., Yang, F., and Zou, L. (2022). Pharmacological activity, pharmacokinetics, and clinical research progress of puerarin. *Antioxidants* 11:2121. doi: 10.3390/antiox11112121

Wang, X., Gao, Y., Wang, L., Yang, D., Bu, W., Gou, L., et al. (2021). Troxerutin improves dextran sulfate sodium-induced ulcerative colitis in mice. *J. Agric. Food Chem.* 69, 2729–2744. doi: 10.1021/acs.jafc.0c06755

Wang, Y., Zhang, J., Zhang, B., Lu, M., Ma, J., Liu, Z., et al. (2023). Modified Gegen Qinlian decoction ameliorated ulcerative colitis by attenuating inflammation and oxidative stress and enhancing intestinal barrier function in vivo and in vitro. *J. Ethnopharmacol.* 313:116538. doi: 10.1016/j.jep.2023.116538

Wu, Y., Li, J., Ding, W., Ruan, Z., and Zhang, L. (2021). Enhanced intestinal barriers by puerarin in combination with tryptophan. *J. Agric. Food Chem.* 69, 15575–15584. doi: 10.1021/acs.jafc.1c05830

Xu, D., Zhuang, L., Gao, S., Ma, H., Cheng, J., Liu, J., et al. (2022). Orally administered Ginkgolide C attenuates DSS-induced colitis by maintaining gut barrier integrity, inhibiting inflammatory responses, and regulating intestinal Flora. *J. Agric. Food Chem.* 70, 14718–14731. doi: 10.1021/acs.jafc.2c06177

Yan, X., Jin, J., Su, X., Yin, X., Gao, J., Wang, X., et al. (2020). Intestinal Flora modulates blood pressure by regulating the synthesis of intestinal-derived corticosterone in high salt-induced hypertension. *Circ. Res.* 126, 839–853. doi: 10.1161/circresaha.119.316394

Yang, C., Du, Y., Ren, D., Yang, X., and Zhao, Y. (2021). Gut microbiota-dependent catabolites of tryptophan play a predominant role in the protective effects of turmeric polysaccharides against DSS-induced ulcerative colitis. *Food Funct.* 12, 9793–9807. doi: 10.1039/d1fo01468d

Yang, W., Ren, D., Shao, H., Zhang, X., Li, T., Zhang, L., et al. (2023). Theabrownin from Fu brick tea improves ulcerative colitis by shaping the gut microbiota and modulating the tryptophan metabolism. *J. Agric. Food Chem.* 71, 2898–2913. doi: 10.1021/acs.jafc.2c06821

Zhang, R., Zhang, Q., Chen, Y., Zhao, Q., Zhang, B., Wang, L., et al. (2022). Combined treatment with Rg1 and adipose-derived stem cells alleviates DSS-induced colitis in a mouse model. *Stem Cell Res Ther* 13:272. doi: 10.1186/s13287-022-02940-x

Zhang, H., Zhang, Y., Li, Y., Wang, Y., Yan, S., Xu, S., et al. (2021). Bioinformatics and network pharmacology identify the therapeutic role and potential mechanism of melatonin in AD and Rosacea. *Front. Immunol.* 12:756550. doi: 10.3389/fimmu.2021.756550

Zhang, Q., Zhong, D., Ren, Y. Y., Meng, Z. K., Pegg, R. B., and Zhong, G. (2021). Effect of konjac glucomannan on metabolites in the stomach, small intestine and large intestine of constipated mice and prediction of the KEGG pathway. *Food Funct.* 12, 3044–3056. doi: 10.1039/d0fo02682d

Zhang, J., Zhu, S., Ma, N., Johnston, L. J., Wu, C., and Ma, X. (2021). Metabolites of microbiota response to tryptophan and intestinal mucosal immunity: a therapeutic target to control intestinal inflammation. *Med. Res. Rev.* 41, 1061–1088. doi: 10.1002/med.21752

Zhao, Y., Luan, H., Jiang, H., Xu, Y., Wu, X., Zhang, Y., et al. (2021). Gegen Qinlian decoction relieved DSS-induced ulcerative colitis in mice by modulating Th17/Treg cell homeostasis via suppressing IL-6/JAK2/STAT3 signaling. *Phytomedicine* 84:153519. doi: 10.1016/j.phymed.2021.153519

Zhao, L. P., Wu, J., Quan, W., Zhou, Y., Hong, H., Niu, G. Y., et al. (2023). DSS-induced acute colitis causes dysregulated tryptophan metabolism in brain: an involvement of gut microbiota. *J. Nutr. Biochem.* 115:109282. doi: 10.1016/j.jnutbio.2023.109282

Zhou, R., He, D., Xie, J., Zhou, Q., Zeng, H., Li, H., et al. (2021). The synergistic effects of polysaccharides and Ginsenosides from American ginseng (*Panax quinquefolius* L.) ameliorating cyclophosphamide-induced intestinal immune disorders and gut barrier dysfunctions based on microbiome-metabolomics analysis. *Front. Immunol.* 12:665901. doi: 10.3389/fimmu.2021.665901

frontiers | Frontiers in Microbiology

TYPE Original Research
PUBLISHED 06 February 2024
DOI 10.3389/fmicb.2024.1282932

OPEN ACCESS

EDITED BY
Xiaodong Xia,
Dalian Polytechnic University, China

REVIEWED BY
Bahtiyar Yilmaz,
University of Bern, Switzerland
Fengjie Sun,
Georgia Gwinnett College, United States

*CORRESPONDENCE
Soohyeon Lee
✉ soohyeon_lee@korea.ac.kr

†These authors have contributed equally to this work and share first authorship

RECEIVED 25 August 2023
ACCEPTED 22 January 2024
PUBLISHED 06 February 2024

CITATION
Kim B, Lee J, Jung ES, Lee S, Suh DH, Park YJ, Kim J, Kwak J-M and Lee S (2024) The impact of a modified microbiota-accessible carbohydrate diet on gut microbiome and clinical symptoms in colorectal cancer patients following surgical resection. *Front. Microbiol.* 15:1282932. doi: 10.3389/fmicb.2024.1282932

The impact of a modified microbiota-accessible carbohydrate diet on gut microbiome and clinical symptoms in colorectal cancer patients following surgical resection

Boyeon Kim[1,2†], Jiwon Lee[1,2†], Eun Sung Jung[3], Sunyoung Lee[3], Dong Ho Suh[3], Yu Jin Park[3], Jin Kim[4], Jung-Myun Kwak[4] and Soohyeon Lee[1,2*]

[1]Cancer Research Institute, Korea University College of Medicine, Seoul, Republic of Korea, [2]Division of Medical Oncology and Hematology, Department of Internal Medicine, Korea University College of Medicine, Seoul, Republic of Korea, [3]HEM Pharma Inc., Suwon, Gyeonggi, Republic of Korea, [4]Department of Surgery, Korea University College of Medicine, Seoul, Republic of Korea

A high-fiber diet is widely recognized for its positive effects on the gut microbiome. However, the specific impact of a high-fiber diet on the gut microbiome and bowel habits of patients with colon cancer remains poorly understood. In this study, we aimed to assess the effects of a modified microbiota-accessible carbohydrate (mMAC) diet on gut microbiota composition and clinical symptoms in colon cancer patients who underwent surgical resection. To achieve this, we enrolled 40 patients in two groups: those who received adjuvant chemotherapy and those who did not. Fecal samples were collected before and after dietary interventions for microbial and metabolite analyses. Each group was randomized in a 1: 1 ratio to follow either a 3-week conventional diet followed by a 3-week mMAC diet, or the reverse sequence. Although there were no significant differences in the microbial diversity data before and after the mMAC diet in both the non-chemotherapy and chemotherapy groups, distinct differences in gut microbial composition were revealed after the mMAC diet. Specifically, the abundance of *Prevotella*, which is associated with high-fiber diets, was further elevated with increased concentrations of acetate and propionate after the mMAC diet. Additionally, patients who experienced improved diarrhea and constipation after the mMAC diet exhibited an enrichment of beneficial bacteria and notable changes in metabolites. In conclusion, this study provides valuable insights into the potential benefits of the mMAC diet, specifically its impact on the gut microbiome and clinical symptoms in postoperative colorectal cancer (CRC) patients. These findings emphasize the potential role of a high-fiber diet in influencing the gut microbiome, and the clinical symptoms warrant further investigation.

KEYWORDS

modified MAC diet, colorectal cancer, microbiota, metabolites, bowel habit

1 Introduction

The human gut microbiome encompasses the genomic content of gut microbiota, consisting of a diverse array of microorganisms inhabiting the human gastrointestinal tract (GIT) (Sekirov et al., 2010; Clemente et al., 2012; Sender et al., 2016). This intricate ecosystem plays a pivotal role in various aspects of health, including digestion, immunity, and overall well-being, and even contributes to survival (Zheng et al., 2020; Wilmanski et al., 2021). These microorganisms perform distinct roles, which include the production of short-chain fatty acids (SCFAs), the metabolism of nutrients and drugs, the synthesis of vitamins, and defense against pathogens (Jandhyala et al., 2015). This complex microbial community also significantly influences the body's immune response, potentially impacting the risk and progression of cancer (Sadrekarimi et al., 2022). Studies have revealed that alterations in the composition, diversity, and function of the gut microbiota can contribute to the development and progression of CRC (Lopez et al., 2021). Gut microbial dysbiosis, with decreasing microbial diversity, induces cancer by disrupting the balance of beneficial and harmful bacteria in the GIT. Certain bacterial species, such as *Fusobacterium nucleatum, Bacteroides fragilis, and Escherichia coli*, have been found to be more prevalent in CRC tissues than in normal tissues, suggesting that they may play a role in cancer development (Whisner and Athena Aktipis, 2019). These harmful species are known to generate carcinogenic genotoxins/metabolites, induce inflammation, and foster immunosuppressive tumor microenvironment. On the other hand, beneficial bacteria like certain strains of *Bifidobacterium* and *Lactobacillus* have shown anti-inflammatory and anti-carcinogenic effects in the colon, by reversing gut dysbiosis and activating antitumor immune system (Wong and Yu, 2023). These findings underscore the intricate connection between the gut microbiota and cancer development.

Colorectal cancer (CRC) is the third most commonly diagnosed cancer in men and the second most common cancer in women worldwide, with an estimated 1.9 million new cases and 935,000 deaths in 2020, according to the World Health Organization. Past studies have shown that colon cancer is associated with environmental factors including diet, lifestyle, smoking and gut microbiome (Song et al., 2020). Numerous studies have demonstrated a strong link between dietary patterns and the risk of colon cancer, emphasizing the significance of adopting a healthy diet to mitigate the risk of developing this condition (Davies et al., 2011; Veettil et al., 2021). Red meat, processed meat and alcohol are associated with an increased risk of CRC, particularly for left-sided CRC (Cross et al., 2010; Baena and Salinas, 2015). Higher intakes of dietary fiber, calcium, and dairy products have been associated with reduced risk of CRC incidence (Veettil et al., 2021). Although the mechanism by which diet affects cancer is not fully elucidated, the microbiome has emerged as one possible factor in this relationship. Recent research has shed light on how diet influences the gut microbiome, potentially affecting cancer development (Spencer et al., 2021).

The formation and maintenance of a healthy gut microbiome are influenced by various factors, including age, diet, lifestyle, medication use (antibiotics and non-antibiotics), and genetics (Yang et al., 2021). Among these factors, diet plays a particularly important role in shaping the composition and diversity of the gut microbes (David et al., 2014; Singh et al., 2017). A diet rich in fiber and microbiota-accessible carbohydrate (MAC), such as whole grains, fruits, and vegetables, provides essential nutrients that support the growth of beneficial bacteria in the gut. These bacteria ferment fiber and MACs to produce SCFAs, which not only provide energy for gut lining cells, but also have anti-inflammatory effects (Koh et al., 2016). For example, butyrate levels, known for their anti-inflammatory effects and role in preventing primary cancer, were increased by fiber supplements (Scharlau et al., 2009; So et al., 2018). Despite the benefits of a high-fiber diet on the gut microbiome, it may present challenges due to the rapid gas production associated with certain fiber types, leading to abdominal discomfort (El-Salhy et al., 2017). Understanding the impact and feasibility of a high-fiber diet on the gut microbiome and bowel habits is crucial for gut health comprehension and reducing the risk of diseases linked to dysbiosis, such as colon cancer.

The objective of this study was to investigate the effects of a modified microbiota-accessible carbohydrate (mMAC) diet on the gut microbiome of colon cancer patients and its potential association with clinical symptoms. Additionally, the study aimed to assess the tolerability of the mMAC diet. By examining changes in the composition and function of the gut microbiota resulting from dietary interventions, this study sought to gain insights into the potential mechanisms underlying the impact of a mMAC diet on the gut microbiome of patients with early-stage CRC.

2 Results

2.1 Patient characteristics and nutritional analysis

Forty patients were enrolled in this study, and all participants completed the intervention. Figure 1 provides a comprehensive description of the study. Stool samples for 16S rRNA sequencing and metabolite analysis, as well as meal logs for nutritional analysis, were collected at the beginning and end of the dietary interventions (see Supplementary Figure 1A). Out of the 120 stool samples planned to be collected, 116 were successfully obtained. Among these, 113 samples met the quality control (QC) requirements for 16S rRNA sequencing, and all 116 samples underwent metabolite analysis (refer to Supplementary Figure 1B).

The baseline characteristics of the study population are summarized in Table 1, showing a median age of 61 years (range: 38–82 years). Among the patients, 29 (72.5%) had left-sided colon cancer, with 3, 21, and 16 patients having Stage I, II, and III disease, respectively. Twenty-two patients underwent chemotherapy following surgical resection, with 21 of them receiving oxaliplatin-based chemotherapy. Currently, 16 patients (40%) consumed alcohol and 5 (12.5%) were smokers.

During the analysis of food intake diaries over a 6-week study period, the overall compliance with the mMAC diet was 70.7%. Patients undergoing chemotherapy showed lower compliance (56.1%) compared to the non-chemotherapy group (86.1%). Relative to the conventional diet, there was an increase in average fiber intake during the mMAC diet period, from 22.38 g to 27.37 g ($p < 0.0001$), as well as increases in protein and fat intake, from 64.31 g to 85.97 g ($p < 0.0001$) and from 41.97 g to 50.79 g ($p < 0.0001$), respectively. Conversely, a reduction in sodium

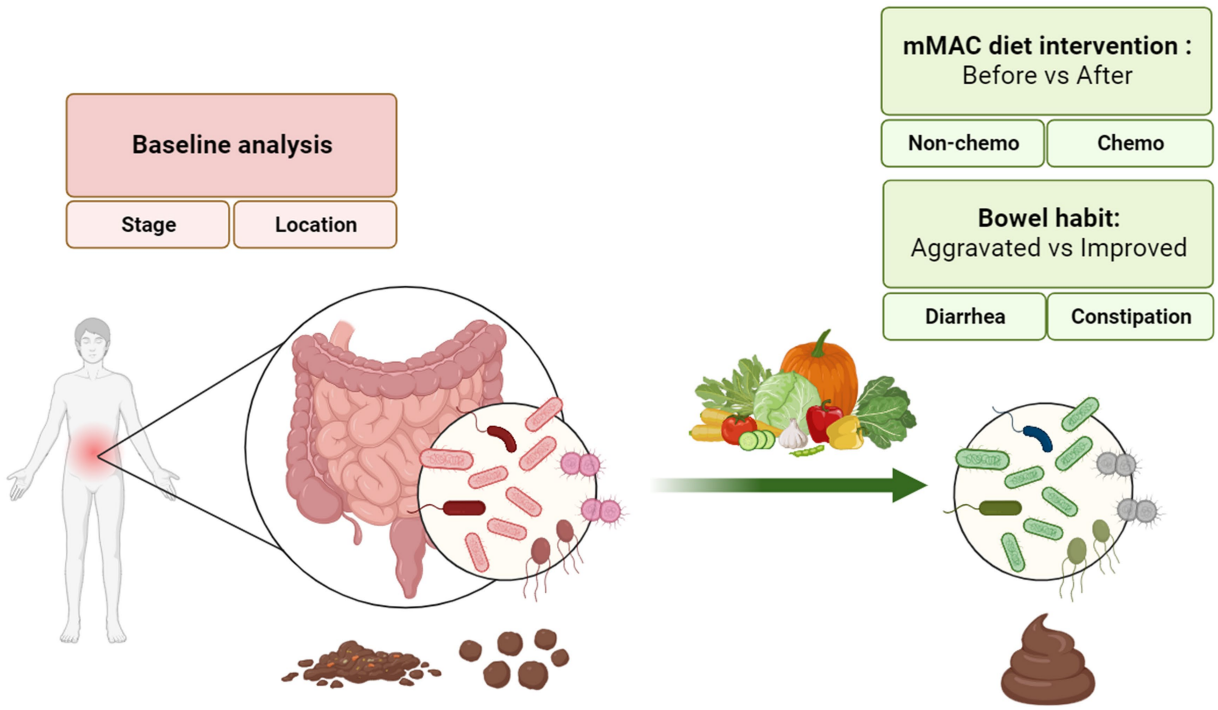

FIGURE 1
A description of the study.

consumption was observed, from 3456.42 mg to 3245.94 mg ($p = 0.0296$) (see Supplementary Figure 2). The percentage of diet composition consumed relative to the recommended daily intake is detailed in Supplementary Table 1.

2.2 Analysis of gut microbiota diversity and composition according to the baseline characteristics

Initially, we analyzed the microbial diversity and composition in relation to cancer stage and location. The cancer stage analysis involved classifying patients into either stage I and II or stage III. While little difference in alpha diversity was noted between these two groups, a significant difference in beta diversity was identified by weighted Unifrac distance ($p = 0.046$) (refer to Supplementary Figures 3A,B). The LEfSe analysis, conducted to identify distinct microorganisms for each group, revealed that *Rothia*, *Coprobacillus*, *Solobacterium*, [*Eubacterium*]*_eligens_group*, *Veillonella*, and *Lactobacillus* were significantly more abundant in stage III patients (see Supplementary Figures 3C–E).

Regarding the analysis based on location, no significant differences were found in alpha diversity between left and right-sided colon cancer (Supplementary Figure 4A). However, principal coordinate analysis (PCoA) using weighted Unifrac distance indicated a significant difference in beta diversity ($p = 0.023$) (Supplementary Figure 4B). In patients who underwent surgery for left-sided colon cancer, *Sellimonas*, [*Eubacterium*]*_eligens_group*, and *Anaerofustis* were significantly enriched. Conversely, in patients with right-sided cancer who underwent surgery, there was a significant increase in *Peptoniphilus*, *Lachnospiraceae_UCG-010*, [*Ruminococcus*]*_torques_group*, *Dorea*, *Blautia*, and *Holdemanella* (Supplementary Figures 4C–E).

2.3 The effect of mMAC diet on non-chemotherapy and chemotherapy groups

To evaluate the effects of a high-fiber diet on microbiome differences, we compared the diversity and microbial composition before and after the mMAC diet. Due to the compliance gap between the non-chemotherapy and chemotherapy groups, each group was analyzed separately. No significant differences were observed in alpha and beta diversity Before and After the mMAC diet in either group (Figures 2A,B,D,E). However, LEfSe analysis revealed distinct microbial differences between the Before and After mMAC diet groups. In the non-chemotherapy group, post-diet samples showed significant enrichment for *Lactococcus* while *UBA1819* and [*Eubacterium*]*_fissicatena_group* were decreased (Figure 2C and Supplementary Figures 5A,B). In the chemotherapy group, *Fusobacterium* and *Catabacter* were decreased in the After group (Figure 2F and Supplementary Figure 5C).

Precise LEfSe analysis up to the species level confirmed that the post-mMAC diet samples had an increased presence of several species belonging to the genera *Lactococcus*, *Lactobacillus*, and *Bifidobacteria* (Supplementary Figures 5D–I).

2.4 Short chain fatty acid analysis according to three dominant bacteria for enterotypes: *Prevotella*, *Bacteroides* and *Ruminococcus*

The human gut microbiome can be classified into one of three traditionally reported enterotypes of bacterial patterns: *Bacteroides*

10.3389/fmicb.2024.1282932

TABLE 1 Patients' baseline characteristics.

Baseline characteristics		Total ($N = 40$)	Chemotherapy	Non-chemotherapy
		n (%)	22	18
Sex	Male	26 (65)	14 (60)	12 (66.7)
	Female	14 (35)	8 (40)	6 (33)
Median age (range)		61 (38 ~ 82)	62 (46 ~ 82)	58 (38 ~ 79)
Age	<60	19 (47.5)	10	9
	≧60	21 (52.5)	12	9
BMI	<25	31 (77.5)	17	14
	≧25	9 (22.5)	5	4
ECOG PS	0	10 (25)	1	9
	1	30 (75)	21	9
	2	0	0	0
Smoking	Non-smoker	19 (47.5)	11	8
	Former-smoker	16 (40)	7	9
	Current-smoker	5 (12.5)	4	1
Alcohol	Non-drinker	20 (50)	11	9
	Former-drinker	4 (10)	1	3
	Current-drinker	16 (40)	10	6
Tumor location	Right colon	11 (27.5)	7	4
	Left colon	29 (72.5)	15	14
Cancer stage	I	3 (7.5)	0	3
	II	21 (52.5)	6	15
	III	16 (40)	16	0
Chemotherapy regimen	FOLFOX	15 (37.5)	15	
	XELOX	6 (15)	6	
	Capecitabine	1 (2.5)	1	

BMI, Body Mass Index; ECOG PS, Eastern Cooperative Oncology Group Performance status.

(enterotype 1), *Prevotella* (enterotype 2), and *Ruminococcus* (enterotype 3) (Arumugam et al., 2011; Gorvitovskaia et al., 2016).

We thus examined the abundance of *Bacteroides*, *Prevotella*, and *Ruminococcus* in individuals before and after adopting the mMAC diet. Notably, the abundance of *Prevotella* increased in the after group, particularly among those not undergoing chemotherapy ($p = 0.0218$). In contrast, the abundances of *Bacteroides* and *Ruminococcus* showed no significant differences (Figures 3A–C).

Furthermore, a positive correlation was observed between the abundance of *Prevotella* and two SCFAs, acetate and propionate, with R^2 values of 0.2298 and 0.5365, respectively ($p = 0.00984$ and $p < 0.0001$) (Figure 3D). Butyrate showed a weak positive correlation ($R^2 = 0.021$, $p = 0.4615$) (Supplementary Figure 6A). The correlations between *Bacteroides* or *Ruminococcus* and SCFAs were generally negative but weak, with only the correlation between *Bacteroides* and valerate reaching statistical significance ($R^2 = 0.0995$, $p = 0.007812$) (Supplementary Figures 6B,C).

2.5 The impact of mMAC diet on bowel habits and its association with the gut microbiome

Following the mMAC diet, 28 and 27 patients reported improvement in diarrhea and constipation, respectively, while 10 and 13 patients experienced worsening symptoms. To assess the relationship between the gut microbiome and symptom relief, we compared the microbial diversity and SCFAs in patients with either aggravated or improved diarrhea and constipation post-mMAC diet consumption. Notably, there were no significant differences in alpha and beta diversity between the Improved and Aggravated diarrhea groups (Figures 4A,B). However, the Chao1 and Observed ASV indices in the Improved constipation group tended to be higher compared to the Aggravated group (Figure 4D). Additionally, Bray Curtis and weighted Unifrac beta diversity indices showed significant differences between these two groups ($p = 0.008$ and $p = 0.069$) (Figure 4E). LEfSE analysis revealed an association between *Akkermansia* and the Improved diarrhea group (Figure 4C and Supplementary Figures 7A,B). Furthermore, the genera *Family_XIII_AD3011_group*, *Howardella*, *Bilophila*, *Paraprevotella*, *UCG-002*, *Subdoligranulum*, *Ruminococcus*, *Holdemanella*, *Catenibacterium*, and *Collinsella* were associated with Improved constipation (Figure 4F and Supplementary Figures 7D,E). In the metabolite analysis, levels of acetate and propionate were slightly increased in the Improved diarrhea group ($p = 0.0945$ for both) and valerate was significantly increased in the Improved constipation group ($p = 0.0118$) (Supplementary Figures 7C,F).

3 Discussion

This study examined the impact of the mMAC diet on the gut microbial composition of patients with early-stage CRC. Our primary objective was to ascertain any differences in the microbiome before and after the mMAC diet, considering factors

10.3389/fmicb.2024.1282932

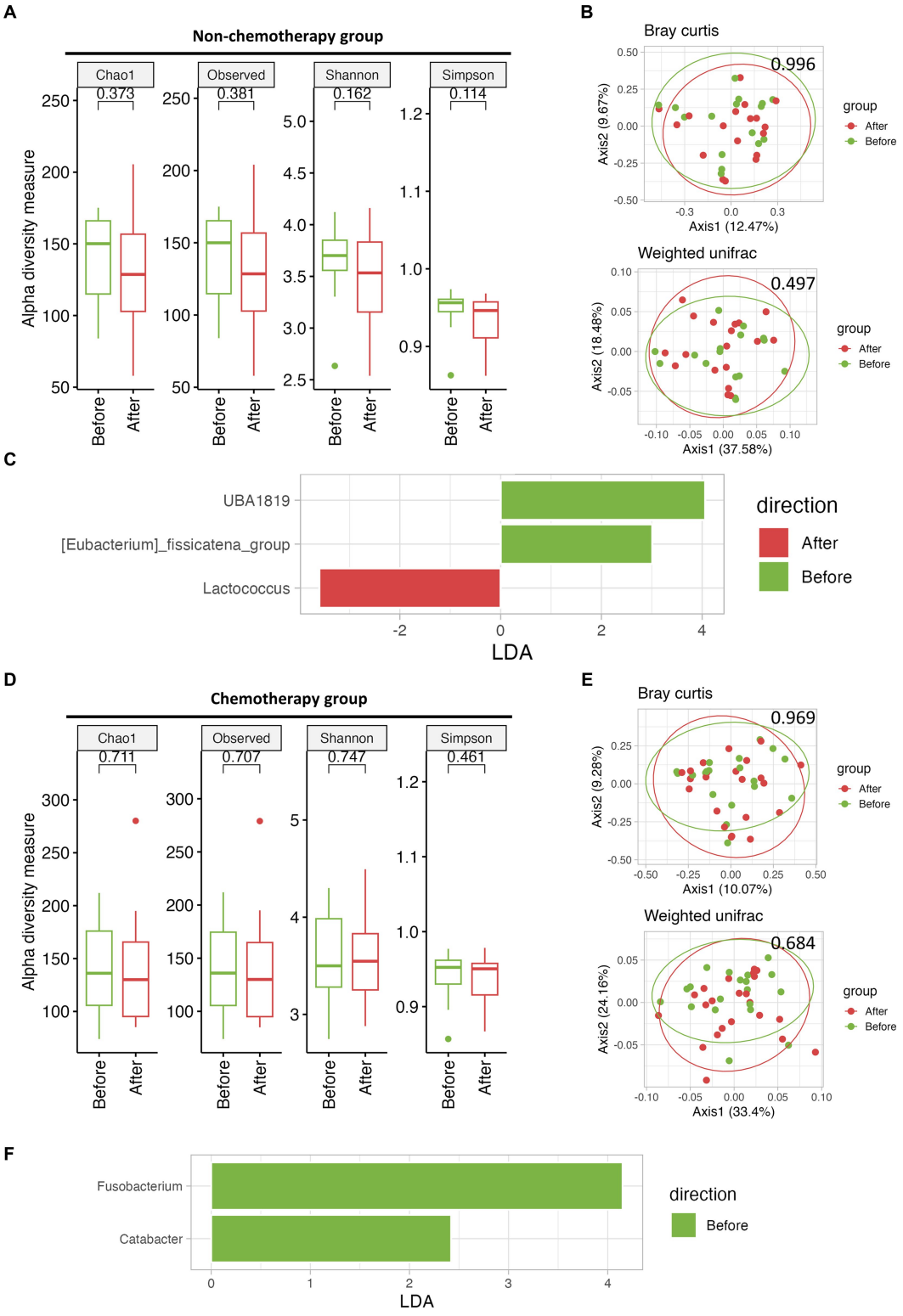

FIGURE 2
The effect of mMAC diet on microbial diversity and composition in non-chemotherapy and chemotherapy groups. **(A)** Alpha-diversity, as measured by the Chao1, Observed ASVs, Shannon, and Simpson indices, is depicted for the non-chemotherapy group both Before (green) and After (red) the mMAC diet. **(B)** PCoA plots represent beta-diversity, specifically Bray Curtis (top) and weighted Unifrac (bottom). In these plots, each point symbolizes a single sample, color-coded as Before (green) and After (red) the mMAC diet in the non-chemotherapy group. **(C)** Genus-level LEfSe analysis identified taxa with differential abundance Before (green) and After (red) the mMAC diet in the non-chemotherapy group. **(D)** Alpha-diversity metrics are plotted for the chemotherapy group Before (green) and After (red) the mMAC diet. **(E)** PCoA plots for this group also represent Bray Curtis (top) and weighted Unifrac (bottom) beta-diversity. **(F)** The genus-level LEfSe analysis in the chemotherapy group revealed significantly abundant taxa Before (green) the mMAC diet.

10.3389/fmicb.2024.1282932

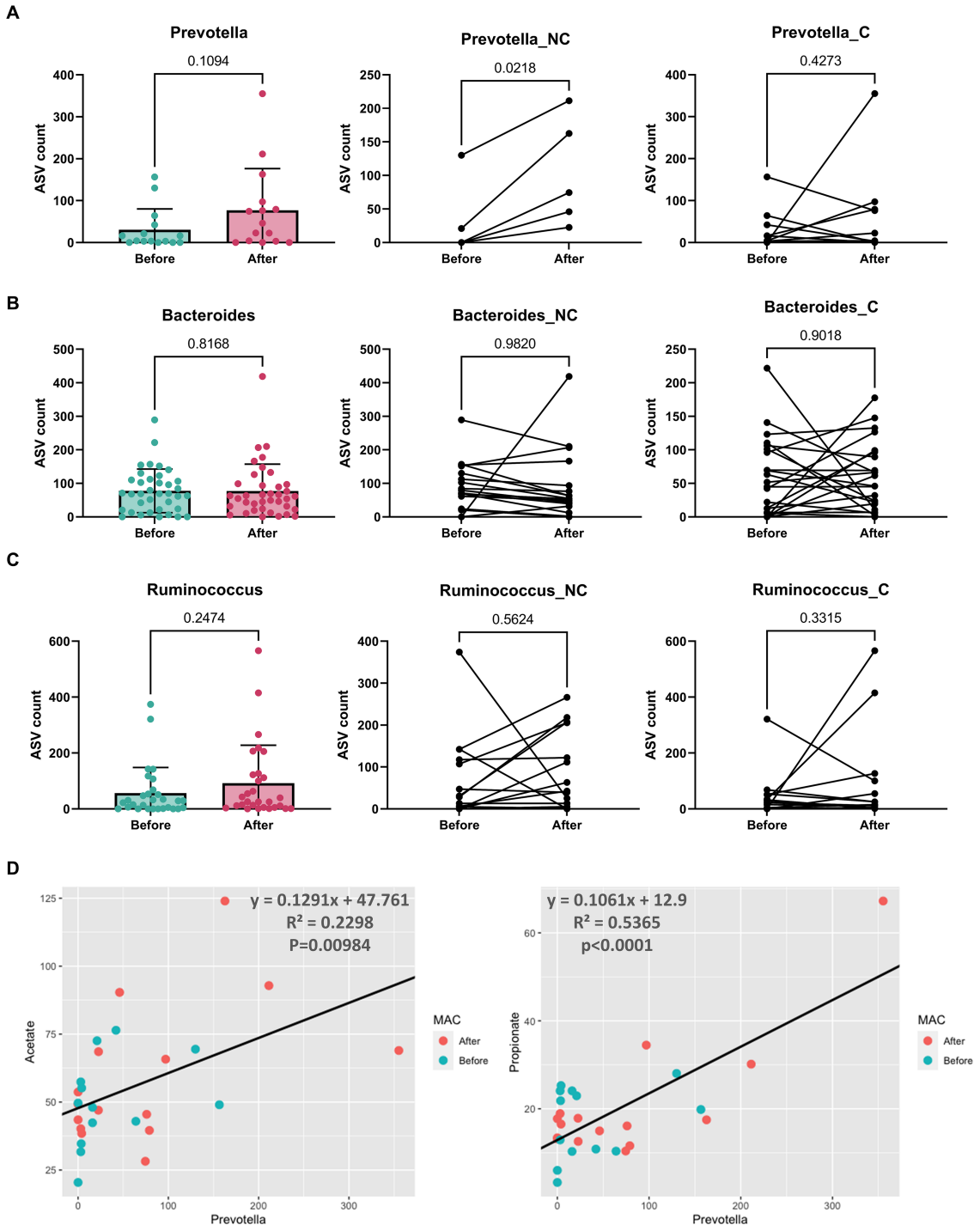

FIGURE 3
The abundance and correlation analysis of three enterotype dominant taxa and metabolites. **(A–C)** The abundance of *Prevotella* **(A)**, *Bacteroides* **(B)**, and *Ruminococcus* **(C)** in patients Before (green) and After (red) the mMAC diet. The comparison includes the entire patient cohort (left), the non-chemotherapy group (middle), and the chemotherapy group (right). **(D)** A correlation analysis was conducted between *Prevotella* and SCFAs (acetate and propionate). The analysis utilized *Prevotella*'s amplicon sequence variant (ASV) count and the concentration (μmol/g) of SCFAs. A black line on each graph represents the trend line for all samples, with the corresponding equation, R-squared (R^2) values, and *p*-values indicated.

such as chemotherapy and bowel habits. The findings revealed that a three-week mMAC diet regimen did not significantly alter the alpha and beta diversities of the gut microbiome in both the non-chemotherapy and chemotherapy groups. However, notable microbial differences were observed in both groups post-diet. Importantly, beneficial intestinal bacteria, including *Lactobacillus* and *Bifidobacterium*, were found to be enriched following the mMAC diet. Additionally, a significant increase in the abundance of *Prevotella* was observed in the non-chemotherapy group after following the mMAC diet. This increase in *Prevotella* was positively correlated with higher levels of SCFAs such as acetate and propionate.

3.1 Gut microbiome and tumor stages and locations

Previous studies have demonstrated variations in bacterial populations across different sites and stages of CRC (Nakatsu et al., 2015; Mima et al., 2016a). Distinct microbiome profiles have been observed between left-sided and right-sided CRC (Zhong et al., 2020; Miyake et al., 2021). However, the results obtained among various studies did not align or prove to be reproducible. It is likely that various factors influencing the microbiome played a role, as evidenced by a study that observed differences in microbiomes among different geographical regions in patients with CRC (Zhong et al., 2020). Among harmful microorganisms, *Fusobacterium nucleatum*, in particular, has been implicated in the carcinogenesis of right-sided CRC (Sheng et al., 2019; Yachida et al., 2019). Additionally, the levels of *Fusobacterium nucleatum* have been positively associated with advanced stages of CRC (Mima et al., 2016b). In our study, however, we observed no significant difference

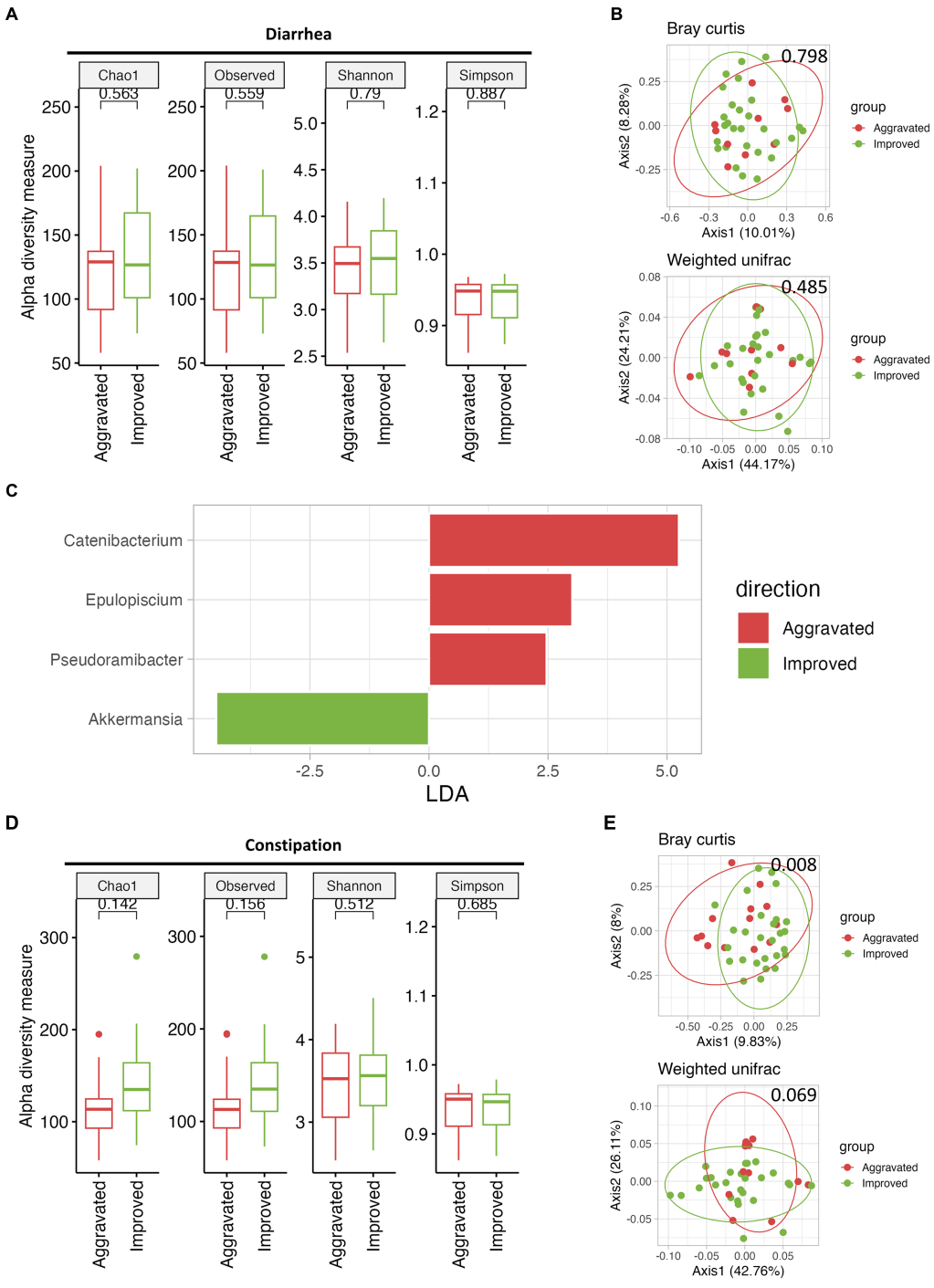

FIGURE 4 (Continued)

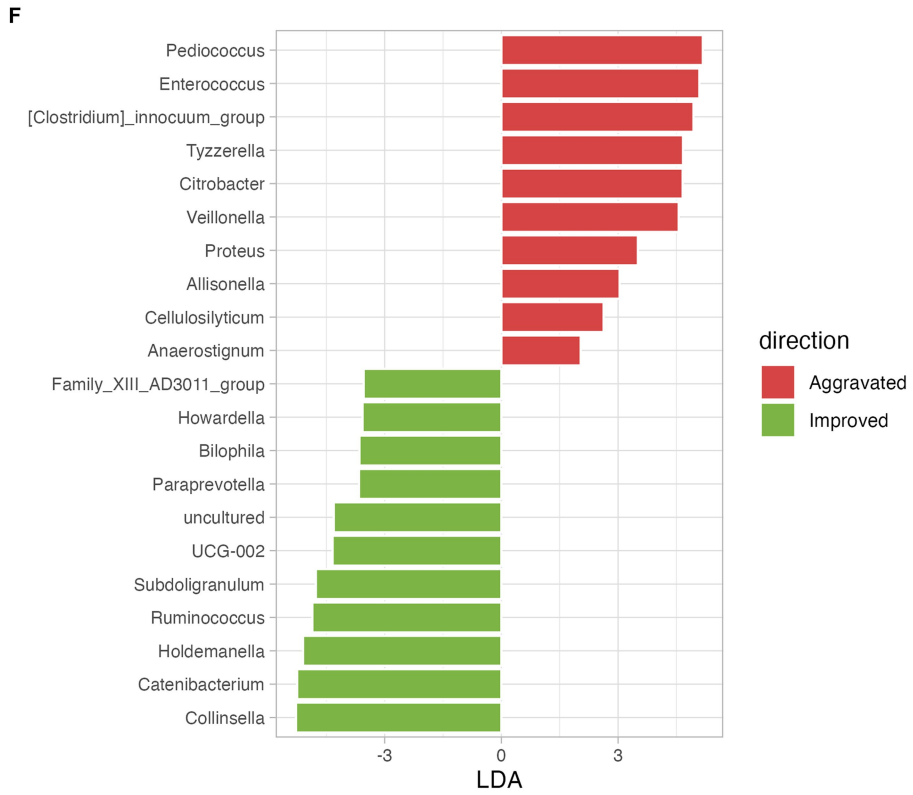

FIGURE 4
The effect of mMAC diet on microbial diversity and composition according to gastrointestinal (GI) symptom. **(A)** Alpha-diversity measurements are depicted for the Aggravated (red) and Improved (green) diarrhea groups following the mMAC diet. **(B)** PCoA plots illustrate beta-diversity using Bray Curtis (top) and weighted Unifrac (bottom) methods. **(C)** Genus-level LEfSe analysis identified significantly abundant taxa in both the Aggravated (red) and Improved (green) diarrhea groups. **(D)** Alpha-diversity plots are shown for the Aggravated (red) and Improved (green) constipation groups post-mMAC diet. **(E)** PCoA plots again represent Bray Curtis (top) and weighted Unifrac (bottom) beta-diversity for these groups. **(F)** The genus-level LEfSe analysis reveals significantly abundant taxa in the Aggravated (red) and Improved (green) constipation groups.

in *Fusobacterium nucleatum* levels across different stages and locations of CRC (data not shown). Our analysis was conducted using fecal samples, and it's possible, as noted in prior research, that the quantity of *Fusobacterium nucleatum* in fecal samples was insufficient compared to that in tumor tissues (Sheng et al., 2019).

In contrast to the majority of previous studies that analyzed the microbiome before surgical resection, we compared the microbiome of patients who underwent resection for CRC. We found that beta-diversity was significantly different, with distinct microbial profiles emerging after surgical resection of right-sided CRC compared to left-sided CRC. A previous study reported lower levels of *Gemellaceae* in patients who underwent right CRC resection, while the *Firmicutes* phylum was found to be abundant in those who underwent sigmoid colon cancer resection (Suga et al., 2022). Taken together, our results underscore the difference in microbiome composition based on the location of resection.

We also found distinct microbial profiles between Stages. Increased levels of *Rothia*, *Coprobacillus*, *Solobacterium*, [*Eubacterium*]*_eligens_group*, *Veillonella*, and *Lactobacillus* were found in patients with stage III CRC. *Rothia dentocariosa* and *Veillonella*, members of the oral microbiota, have been suggested to contribute to the pathogenesis of inflammatory bowel disease (IBD) and CRC (Koliarakis et al., 2019). Conversely, *Lactobacillus brevis* has been associated with suppressing the progression of CRC (Sakatani et al., 2016). Further research is necessary to explore the interactions between these beneficial and harmful bacteria and to understand how the overall microbial ecosystem influences the development and recurrence of CRC.

3.2 The impact of mMAC diet on gut microbiome and SCFA

MACs are carbohydrates that can be fermented by gut microbes, serving as the main source of energy. They are used in the production of various metabolites, including SCFAs, which play crucial roles in maintaining gut health and influencing various physiological processes MAC as novel gut microbiome modulators in noncommunicable diseases. In previous studies, reduced MAC intake was associated with decreased bacterial diversity leading to dysbiosis (Sonnenburg et al., 2016; Fehlbaum et al., 2018). This, in turn, suggests that a MAC-rich diet may increase bacterial diversity. But, clinical trials showed contradictory results and some have even demonstrated decreased alpha diversity after the use of MAC (Cantu-Jungles and Hamaker, 2023). This could be attributed to various factors that have been suggested to affect diversity, such as the number of microbes sharing the dietary fiber substrate, the initial abundance of bacterial taxa, and the composition of MACs. Despite the high fermentable fiber content of the mMAC diet used in this study, no significant changes in microbial diversity were observed before and after the MAC diet. It is possible that the three-week duration of the dietary

intervention was not long enough to affect a notable increase in microbial diversity.

In line with prior research (Wu and Kasper, 2020), we noted an increase in the abundance of *Prevotella* following the mMAC diet, especially in the non-chemotherapy group. This increase was positively correlated with two SCFAs, acetate and propionate. Up to now, the association of dietary fibers with SCFAs has not been fully elucidated (Vinelli et al., 2022). Further investigation is essential to elucidate the interplay among dietary fiber, SCFAs, and their effects on patients with CRC.

3.3 Feasibility and changes in bowel habits with the mMAC diet

In this study, we discovered that postoperative CRC patients are able to tolerate a high-fiber diet, specifically the mMAC diet, which includes a daily intake of 30 grams of fiber. Contrary to the initial concerns about potential discomfort, the compliance rate for the mMAC diet was notably high at 70% (Ioniță-Mîndrican et al., 2022). 28 patients (73.7%) experienced an improvement in diarrhea, while 27 patients (67.5%) showed improvement in constipation after mMAC diet. Previous studies have demonstrated that the gut microbiota, especially dysbiosis, significantly influences gastrointestinal symptoms such as diarrhea and constipation (Ohkusa et al., 2019; Li et al., 2021). Modulating the gut microbiota through interventions such as diet control, probiotics, prebiotics, and fecal transplantation has been attempted to control GI symptoms. Our study found distinct microbial profiles in improved groups compared to aggravated groups. Patients who experienced improvements in constipation showed a significant trend toward an increase in bacteria, such as *Paraprevotella*, Subdoligranulum and *Holdemanella*. Patients who experienced improved diarrhea showed higher *Akkermansia*. While the role of *Akkermansia muciniphila* in IBD is still a subject of debate, some studies have suggested its potential in regulating immune cells (Zhang et al., 2021). Given that our study included patients undergoing adjuvant chemotherapy, caution is needed when interpreting the results of the microbiome, as they may not solely be attributed to the effects of the mMAC diet. In subsequent studies, it is necessary to elucidate the respective impacts of cancer treatment and the mMAC diet on the gut microbiome in CRC patients.

3.4 Limitations of this study

Despite these intriguing findings, our study has several limitations. First, we did not assess the impact of the mMAC diet on critical clinical outcomes, such as cancer recurrence or survival, focusing solely on patients with early stage CRC within a limited timeframe. Secondly, the crossover of the dietary intervention may have influenced outcomes, as the former diet might have a carry-over effect. Thirdly, the small sample size limited the comprehensive assessment of changes in gut microbiome diversity, rendering the observed results exploratory in nature.

3.5 Conclusion

In conclusion, this study provides valuable insights into the potential benefits of the mMAC diet, specifically its impact on the gut microbiome and clinical symptoms in postoperative CRC patients. Although the mMAC diet did not lead to significant diversity, notable trends in microbial composition were observed in patients with improved diarrhea symptoms. These findings emphasize the potential role of a high-fiber diet in influencing the microbiome, and the clinical symptoms warrant further investigation.

4 Patients and methods

We conducted a prospective, randomized, crossover trial with dietary intervention in patients with localized CRC patients who underwent surgery. Written informed consent was obtained from all patients. This study was approved by our Institutional Review Board (2021AN0489) and was registered at ClinicalTrials.gov (NCT05039060). The trial procedures were performed in accordance with the Declaration of Helsinki and Guidelines for Good Clinical Practice.

4.1 Patient selection

The patients were enrolled in the group receiving adjuvant chemotherapy for half of the patients (chemotherapy group) and the other half for not receiving adjuvant chemotherapy (non-chemotherapy group) according to the postoperative stage from Korea University Anam Hospital. Each group was randomized separately in a 1: 1 ratio to start with one of two diet sequences: either a conventional diet followed by an mMAC diet or an mMAC diet followed by a conventional diet, with each diet lasting 3 weeks (see Supplementary Figure 1A). The inclusion criteria were Stage I to III CRC patients who underwent complete curative surgical resection, did not have an ileostomy, were appropriate for a solid diet, were above 19 years of age, and had Eastern Cooperative Oncology Group (ECOG) scores of 0 to 2. The exclusion criteria were Stage IV CRC, a history of antibiotics within 1 month, a history of food allergy, uncontrolled diabetes mellitus (HbA1c > 8.0 g/dL), and other medical conditions that impair the ability to adhere to diet intervention.

4.2 Subject characterization

Demographic and laboratory information were obtained for all subjects; including Sex, Age, BMI, ECOG performance status, body mass index, Tumor location, Cancer stage, adjuvant chemotherapy regimen. The clinical symptoms, including diarrhea and constipation, were assessed using The European Organization for Research and Treatment of Cancer (EORTC) Quality of Life Questionnaire, QLQ-C30 (version 3.0).

4.3 Dietary intervention

In each treatment group, the participants were further divided into two groups through random assignment and assigned to a 3-week mMAC diet group or a conventional diet group, followed by a diet switch for the next 3 weeks. During the 6-week study period, the patients kept records of their diets and defecation in their diaries. At the end of the study, diaries were collected to evaluate the participants' food intake and defecation status at the end of the study (Supplementary Figure 1).

The mMAC diet was designed to adapt to a high-fiber diet including 30 g of dietary fiber daily and delivered to the patient's home for 3 weeks as a meal kit supported by Dr. Kitchen Corp (Supplementary Table 2).

4.4 Stool sample collection and DNA extraction

All stool samples were kept in a participant's home freezer (−20°C) wrapped in ice packs until they were transferred on ice to the research laboratory and stored in a deep freezer (−80°C). After thawing, each sample was manually homogenized using a sterile tip and small aliquots of the sample were collected in a 2.0 mL microtube (0.2 g) for microbiome and metabolome analysis. Fecal bacterial genomic DNA extraction was performed using the Mag-Bind® Universal Pathogen Kit (Omega Bio-tek, Norcross, GA, US). Detailed stool DNA extraction and next generation sequencing methods are described in the Supplementary Methods section.

4.5 Next generation sequencing and metabolite analysis

Next generation sequencing (NGS) was performed to analyze the composition and diversity of the gut microbiota. Headspace sampler-gas chromatography-flame ionization detector (HSS-GC-FID) analysis was performed for microbial metabolite analysis. Detailed methods are described in the Supplementary Methods section.

4.6 Microbial diversity, taxonomic profiling and statistical analysis

Alpha diversity was quantified as the number of observed ASVs, Chao1, Shannon, and Simpson indices. Wilcoxon signed-rank tests were used to evaluate the differences in diversity among samples. Bray Curtis and weighted Unifrac distance matrices for beta diversity were obtained and q-values were calculated using QIIME2. Subsequently, these matrices were imported into R to obtain principal coordinate analysis (PCoA) plots. The Linear Discriminant Analysis (LDA) Effect Size (LEfSe) algorithm was applied to identify taxonomic biomarkers in genera and species level. Default parameters were used for significance ($p < 0.05$) and the linear discriminant analysis threshold (LDA score > 2.0). The Mann–Whitney test was applied to compare individual microbiota and SCFAs. SCFAs and microbial correlation was confirmed by linear regression with R^2 and value of p.

All analyses were performed using R packages (Qiime2R, Microbial, Microbiomeutilities) and GraphPad Prism (version 9.0).

Data availability statement

The datasets presented in this study can be found in online repositories. The names of the repository/repositories and accession number(s) can be found at: https://www.ncbi.nlm.nih.gov/, PRJNA1008784.

Ethics statement

The studies involving humans were approved by the Korea University Institutional Review Board. The studies were conducted in accordance with the local legislation and institutional requirements. The participants provided their written informed consent to participate in this study.

Author contributions

BK: Formal analysis, Investigation, Methodology, Visualization, Writing – original draft. JL: Data curation, Resources, Writing – original draft, Project administration. ESJ: Methodology, Writing – review & editing. SuL: Formal analysis, Writing – review & editing. DHS: Methodology, Writing – review & editing. YJP: Formal analysis, Writing – review & editing. JK: Resources, Writing – review & editing. J-MK: Resources, Writing – review & editing. SoL: Conceptualization, Project administration, Supervision, Writing – review & editing.

Funding

The author(s) declare financial support was received for the research, authorship, and/or publication of this article. This research was supported by a Korea University grant and Dr. Kitchen company.

Acknowledgments

This research was made possible by the generous research funding provided by Dr. Kitchen Company, and Dr. Kitchen and Hyejin Cho for technical support and sharing their expertise in developing mMAC diet plans for the study. Special thanks go to [HEM Pharma Inc. colleagues] for their technical assistance and support with raw data production and data analysis. Their expertise played a crucial role in the successful completion of this study.

Conflict of interest

ESJ, SuL, DHS, and YJP were employed by HEM Pharma Inc.

The remaining authors declare that the research was conducted in the absence of any commercial or financial relationships that could be construed as a potential conflict of interest.

Publisher's note

Supplementary material

The Supplementary material for this article can be found online at: https://www.frontiersin.org/articles/10.3389/fmicb.2024.1282932/full#supplementary-material

References

Arumugam, M., Raes, J., Pelletier, E., Le Paslier, D., Yamada, T., Mende, D. R., et al. (2011). Enterotypes of the human gut microbiome. *Nature* 473, 174–180. doi: 10.1038/nature09944

Baena, R., and Salinas, P. (2015). Diet and colorectal cancer. *Maturitas* 80, 258–264. doi: 10.1016/j.maturitas.2014.12.017

Cantu-Jungles, T. M., and Hamaker, B. R. (2023). Tuning expectations to reality: don't expect increased gut microbiota diversity with dietary fiber. *J. Nutr.* 153, 3156–3163. doi: 10.1016/j.tjnut.2023.09.001

Clemente, J. C., Ursell, L. K., Parfrey, L. W., and Knight, R. (2012). The impact of the gut microbiota on human health: an integrative view. *Cell* 148, 1258–1270. doi: 10.1016/j.cell.2012.01.035

Cross, A. J., Ferrucci, L. M., Risch, A., Graubard, B. I., Ward, M. H., Park, Y., et al. (2010). A large prospective study of meat consumption and colorectal cancer risk: an investigation of potential mechanisms underlying this association. *Cancer Res.* 70, 2406–2414. doi: 10.1158/0008-5472.CAN-09-3929

David, L. A., Maurice, C. F., Carmody, R. N., Gootenberg, D. B., Button, J. E., Wolfe, B. E., et al. (2014). Diet rapidly and reproducibly alters the human gut microbiome. *Nature* 505, 559–563. doi: 10.1038/nature12820

Davies, N. J., Batehup, L., and Thomas, R. (2011). The role of diet and physical activity in breast, colorectal, and prostate cancer survivorship: a review of the literature. *Br. J. Cancer* 105, S52–S73. doi: 10.1038/bjc.2011.423

El-Salhy, M., Ystad, S. O., Mazzawi, T., and Gundersen, D. (2017). Dietary fiber in irritable bowel syndrome (review). *Int. J. Mol. Med.* 40, 607–613. doi: 10.3892/ijmm.2017.3072

Fehlbaum, S., Prudence, K., Kieboom, J., Heerikhuisen, M., van den Broek, T., Schuren, F. H. J., et al. (2018). In vitro fermentation of selected prebiotics and their effects on the composition and activity of the adult gut microbiota. *Int. J. Mol. Sci.* 19:3097. doi: 10.3390/ijms19103097

Gorvitovskaia, A., Holmes, S. P., and Huse, S. M. (2016). Interpreting Prevotella and Bacteroides as biomarkers of diet and lifestyle. *Microbiome* 4:15. doi: 10.1186/s40168-016-0160-7

Ioniță-Mîndrican, C. B., Ziani, K., Mititelu, M., Oprea, E., Neacșu, S. M., Moroșan, E., et al. (2022). Therapeutic benefits and dietary restrictions of fiber intake: a state of the art review. *Nutrients* 14:2641. doi: 10.3390/nu14132641

Jandhyala, S. M., Talukdar, R., Subramanyam, C., Vuyyuru, H., Sasikala, M., and Nageshwar Reddy, D. (2015). Role of the normal gut microbiota. *World J. Gastroenterol.* 21, 8787–8803. doi: 10.3748/wjg.v21.i29.8787

Koh, A., De Vadder, F., Kovatcheva-Datchary, P., and Bäckhed, F. (2016). From dietary fiber to host physiology: short-chain fatty acids as key bacterial metabolites. *Cell* 165, 1332–1345. doi: 10.1016/j.cell.2016.05.041

Koliarakis, I., Messaritakis, I., Nikolouzakis, T. K., Hamilos, G., Souglakos, J., and Tsiaoussis, J. (2019). Oral bacteria and intestinal dysbiosis in colorectal cancer. *Int. J. Mol. Sci.* 20:4146. doi: 10.3390/ijms20174146

Li, Y., Xia, S., Jiang, X., Feng, C., Gong, S., Ma, J., et al. (2021). Gut microbiota and diarrhea: an updated review. *Front. Cell. Infect. Microbiol.* 11:625210. doi: 10.3389/fcimb.2021.625210

Lopez, L. R., Bleich, R. M., and Arthur, J. C. (2021). Microbiota effects on carcinogenesis: initiation, promotion, and progression. *Annu. Rev. Med.* 72, 243–261. doi: 10.1146/annurev-med-080719-091604

Mima, K., Cao, Y., Chan, A. T., Qian, Z. R., Nowak, J. A., Masugi, Y., et al. (2016a). *Fusobacterium nucleatum* in colorectal carcinoma tissue according to tumor location. *Clin. Transl. Gastroenterol.* 7:e200. doi: 10.1038/ctg.2016.53

Mima, K., Nishihara, R., Qian, Z. R., Cao, Y., Sukawa, Y., Nowak, J. A., et al. (2016b). *Fusobacterium nucleatum* in colorectal carcinoma tissue and patient prognosis. *Gut* 65, 1973–1980. doi: 10.1136/gutjnl-2015-310101

Miyake, T., Mori, H., Yasukawa, D., Hexun, Z., Maehira, H., Ueki, T., et al. (2021). The comparison of fecal microbiota in left-side and right-side human colorectal cancer. *Eur. Surg. Res.* 62, 248–254. doi: 10.1159/000516922

Nakatsu, G., Li, X., Zhou, H., Sheng, J., Wong, S. H., Wu, W. K., et al. (2015). Gut mucosal microbiome across stages of colorectal carcinogenesis. *Nat. Commun.* 6:8727. doi: 10.1038/ncomms9727

Ohkusa, T., Koido, S., Nishikawa, Y., and Sato, N. (2019). Gut microbiota and chronic constipation: a review and update. *Front Med* 6:19. doi: 10.3389/fmed.2019.00019

Sadrekarimi, H., Gardanova, Z. R., Bakhshesh, M., Ebrahimzadeh, F., Yaseri, A. F., Thangavelu, L., et al. (2022). Emerging role of human microbiome in cancer development and response to therapy: special focus on intestinal microflora. *J. Transl. Med.* 20:301. doi: 10.1186/s12967-022-03492-7

Sakatani, A., Fujiya, M., Ueno, N., Kashima, S., Sasajima, J., Moriichi, K., et al. (2016). Polyphosphate derived from *Lactobacillus brevis* inhibits colon cancer progression through induction of cell apoptosis. *Anticancer Res.* 36, 591–598.

Scharlau, D., Borowicki, A., Habermann, N., Hofmann, T., Klenow, S., Miene, C., et al. (2009). Mechanisms of primary cancer prevention by butyrate and other products formed during gut flora-mediated fermentation of dietary fibre. *Mutat. Res.* 682, 39–53. doi: 10.1016/j.mrrev.2009.04.001

Sekirov, I., Russell, S. L., Antunes, L. C., and Finlay, B. B. (2010). Gut microbiota in health and disease. *Physiol. Rev.* 90, 859–904. doi: 10.1152/physrev.00045.2009

Sender, R., Fuchs, S., and Milo, R. (2016). Revised estimates for the number of human and bacteria cells in the body. *PLoS Biol.* 14:e1002533. doi: 10.1371/journal.pbio.1002533

Sheng, Q., Du, H., Cheng, X., Cheng, X., Tang, Y., Pan, L., et al. (2019). Characteristics of fecal gut microbiota in patients with colorectal cancer at different stages and different sites. *Oncol. Lett.* 18, 4834–4844. doi: 10.3892/ol.2019.10841

Singh, R. K., Chang, H. W., Yan, D., Lee, K. M., Ucmak, D., Wong, K., et al. (2017). Influence of diet on the gut microbiome and implications for human health. *J. Transl. Med.* 15:73. doi: 10.1186/s12967-017-1175-y

So, D., Whelan, K., Rossi, M., Morrison, M., Holtmann, G., Kelly, J. T., et al. (2018). Dietary fiber intervention on gut microbiota composition in healthy adults: a systematic review and meta-analysis. *Am. J. Clin. Nutr.* 107, 965–983. doi: 10.1093/ajcn/nqy041

Song, M., Chan, A. T., and Sun, J. (2020). Influence of the gut microbiome, diet, and environment on risk of colorectal Cancer. *Gastroenterology* 158, 322–340. doi: 10.1053/j.gastro.2019.06.048

Sonnenburg, E. D., Smits, S. A., Tikhonov, M., Higginbottom, S. K., Wingreen, N. S., and Sonnenburg, J. L. (2016). Diet-induced extinctions in the gut microbiota compound over generations. *Nature* 529, 212–215. doi: 10.1038/nature16504

Spencer, C. N., McQuade, J. L., Gopalakrishnan, V., McCulloch, J. A., Vetizou, M., Cogdill, A. P., et al. (2021). Dietary fiber and probiotics influence the gut microbiome and melanoma immunotherapy response. *Science* 374, 1632–1640. doi: 10.1126/science.aaz7015

Suga, D., Mizutani, H., Fukui, S., Kobayashi, M., Shimada, Y., Nakazawa, Y., et al. (2022). The gut microbiota composition in patients with right-and left-sided colorectal cancer and after curative colectomy, as analyzed by 16S rRNA gene amplicon sequencing. *BMC Gastroenterol.* 22:313. doi: 10.1186/s12876-022-02382-y

Veettil, S. K., Wong, T. Y., Loo, Y. S., Playdon, M. C., Lai, N. M., Giovannucci, E. L., et al. (2021). Role of diet in colorectal cancer incidence: umbrella review of meta-analyses of prospective observational studies. *JAMA Netw. Open* 4:e2037341. doi: 10.1001/jamanetworkopen.2020.37341

Vinelli, V., Biscotti, P., Martini, D., Del Bo, C., Marino, M., Meroño, T., et al. (2022). Effects of dietary fibers on short-chain fatty acids and gut microbiota composition in healthy adults: a systematic review. *Nutrients* 14:2559. doi: 10.3390/nu14132559

Whisner, C. M., and Athena Aktipis, C. (2019). The role of the microbiome in cancer initiation and progression: how microbes and cancer cells utilize excess energy and promote one another's growth. *Curr. Nutr. Rep.* 8, 42–51. doi: 10.1007/s13668-019-0257-2

Wilmanski, T., Diener, C., Rappaport, N., Patwardhan, S., Wiedrick, J., Lapidus, J., et al. (2021). Gut microbiome pattern reflects healthy ageing and predicts survival in humans. *Nat. Metab.* 3, 274–286. doi: 10.1038/s42255-021-00348-0

Wong, C. C., and Yu, J. (2023). Gut microbiota in colorectal cancer development and therapy. *Nat. Rev. Clin. Oncol.* 20, 429–452. doi: 10.1038/s41571-023-00766-x

Wu, M., and Kasper, D. L. (2020). Fiber sets up the battleground for intestinal Prevotella. *Cell Host Microbe* 28, 776–777. doi: 10.1016/j.chom.2020.11.010

Yachida, S., Mizutani, S., Shiroma, H., Shiba, S., Nakajima, T., Sakamoto, T., et al. (2019). Metagenomic and metabolomic analyses reveal distinct stage-specific phenotypes of the gut microbiota in colorectal cancer. *Nat. Med.* 25, 968–976. doi: 10.1038/s41591-019-0458-7

Yang, J., Wu, J., Li, Y., Zhang, Y., Cho, W. C., Ju, X., et al. (2021). Gut bacteria formation and influencing factors. *FEMS Microbiol. Ecol.* 97:fiab043. doi: 10.1093/femsec/fiab043

Zhang, T., Ji, X., Lu, G., and Zhang, F. (2021). The potential of *Akkermansia muciniphila* in inflammatory bowel disease. *Appl. Microbiol. Biotechnol.* 105, 5785–5794. doi: 10.1007/s00253-021-11453-1

Zheng, D., Liwinski, T., and Elinav, E. (2020). Interaction between microbiota and immunity in health and disease. *Cell Res.* 30, 492–506. doi: 10.1038/s41422-020-0332-7

Zhong, M., Xiong, Y., Ye, Z., Zhao, J., Zhong, L., Liu, Y., et al. (2020). Microbial community profiling distinguishes left-sided and right-sided colon cancer. *Front. Cell. Infect. Microbiol.* 10:498502. doi: 10.3389/fcimb.2020.498502

frontiers | Frontiers in Microbiology

TYPE Original Research
PUBLISHED 27 February 2024
DOI 10.3389/fmicb.2024.1308866

OPEN ACCESS

EDITED BY
Xiaodong Xia,
Dalian Polytechnic University, China

REVIEWED BY
Abdulhadi Suwandi,
Hannover Medical School, Germany
Long Ding,
Northwest A&F University, China

*CORRESPONDENCE
Yang Cao
✉ hbdkcaoyang@163.com
Huacheng Tang
✉ byndthc@126.com

†These authors have contributed equally to this work

RECEIVED 07 October 2023
ACCEPTED 05 February 2024
PUBLISHED 27 February 2024

CITATION
Zang Y, Ge Y, Cao Y and Tang H (2024) Anti-diabetic effect of red quinoa polysaccharide on type 2 diabetic mellitus mice induced by streptozotocin and high-fat diet.
Front. Microbiol. 15:1308866.
doi: 10.3389/fmicb.2024.1308866

Anti-diabetic effect of red quinoa polysaccharide on type 2 diabetic mellitus mice induced by streptozotocin and high-fat diet

Yanqing Zang[1,2†], Yinchen Ge[1†], Yang Cao[2,3*] and Huacheng Tang[1,2*]

[1]College of Food Science and Engineering, Heilongjiang Bayi Agriculture University, Daqing, Heilongjiang, China, [2]Chinese National Engineering Research Center, Daqing, Heilongjiang, China, [3]College of Animal Science and Technology, Heilongjiang Bayi Agricultural University, Daqing, Heilongjiang, China

The purpose of this study was to explore the mechanism of red quinoa polysaccharide (RQP) in alleviating type 2 diabetes (T2D) through *in vivo* and *in vitro* experiments. Results of HPLC and FITR showed that RQP was a complex polysaccharide and contained more glucose, galactose and acarbose. *In vitro* experiments, RQP showed strong antioxidant capacity and inhibition on α-amylase and α-glucosidase. *In vivo* experiments, RQP was proved to induce a significant improvement of diabetes after 4 weeks of ingestion, including the abilities of lowering blood glucose, regulating lipid metabolism, anti-oxidation and promoting secretion of SCFAs. Furthermore, 16S rRNA study demonstrated that RQP transformed the intestinal microbiota composition in diabetic mice, decreased the abundance of *norank_f_Muribaculaceae* and *Lachnospiraceae_NK4A136_group*, and increased the relative abundance of *Akkermansia*, *unclassified_f_Lachnospiraceae*, *norank_f_Eubacterium_coprostanoligenes_group*, *unclassified_f_Atopobiaceae* and *norank_f_Lachnospiraceae*. The biosynthetic pathways, metabolic pathways and intestinal microbiome phenotypes in mice also changed accordingly. In conclusion, this study suggests that RQP can inhibit the development of diabetes by correcting the imbalance of intestinal flora.

KEYWORDS

red quinoa polysaccharides, high-fat diet, physicochemical properties, gut microbiota, antioxidant activity

1 Introduction

T2D is a serious health problem worldwide. It is defined by insulin insufficiency caused by pancreatic beta cell failure and insulin resistance in target organs (Chatterjee et al., 2017). The data showed that increased availability of high-calorie foods and decreased physical activity have led to lifestyle changes, that have resulted in a global increase in T2D and prediabetes (Saeedi et al., 2019). The International Diabetes Federation (IDF) Diabetes Map 2021, 10th edition, 537 million people have diabetes globally in 2021, and it will reach 783 million by 2045 (Magliano and Boyko, 2021). Researchers around the world are currently focusing on the causes, prevention, and treatment of T2D. Therefore, in this context, the beneficial role of polysaccharides in plant extracts in lowering blood glucose and inhibiting

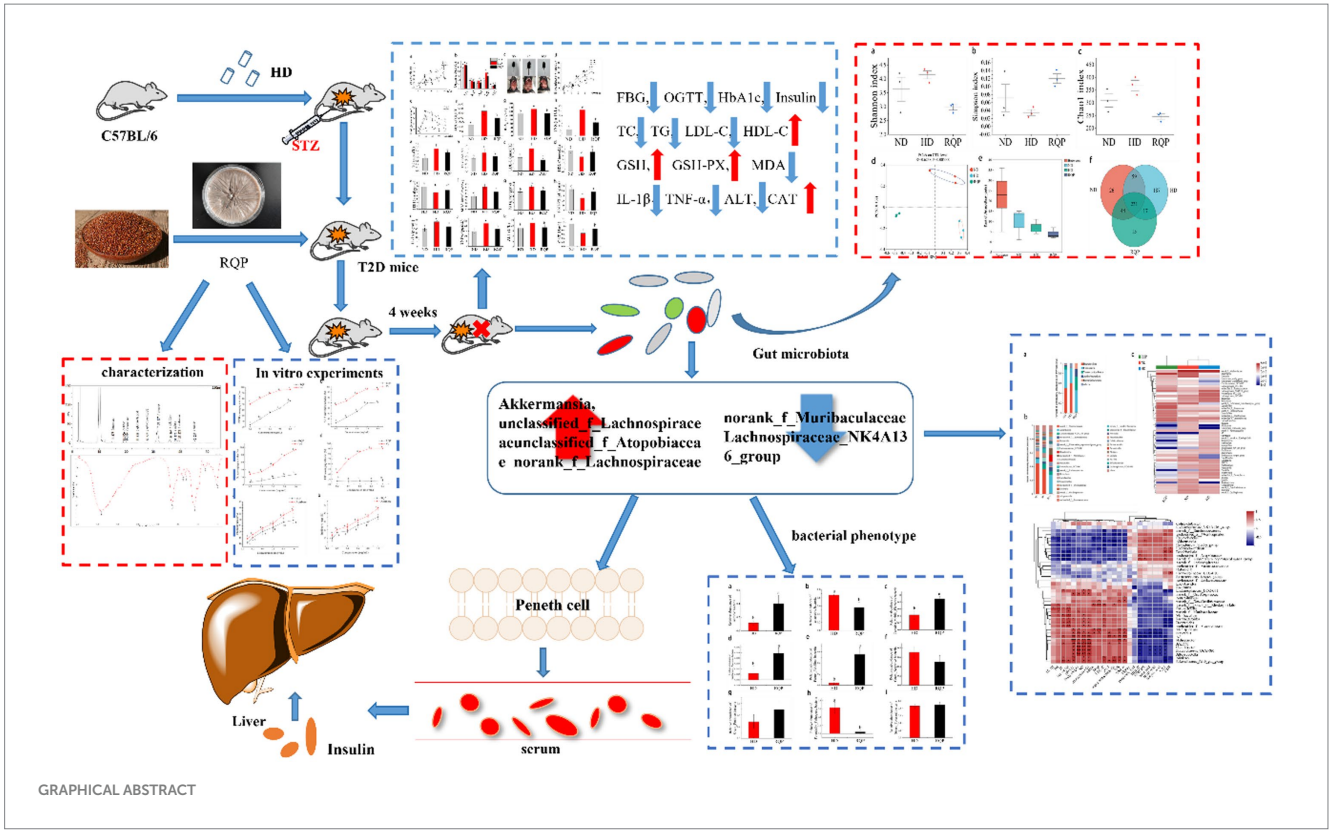

GRAPHICAL ABSTRACT

the development of diabetes mellitus has received extensive attention by researchers.

Quinoa (*Chenopodium quinoa* Wild, family Amaranthaceous) is a pseudo-cereal from the Andean region that was once called the "mother of grains" by the Incas and is now becoming increasingly popular because of its great nutritional value (Campos et al., 2018). Quinoa is rich in protein and has a balanced ratio of amino acids, with a nutritional value like milk, and is easily absorbed by the body (Ren et al., 2023). Studies have shown that quinoa also contains many biologically active substances such as flavonoids and polysaccharides. These substances have been shown to prevent many diseases such as cancer, inflammatory disease, and cardiovascular diseases (Ren et al., 2023). Some studies have proved the biological activities of quinoa polysaccharides (Cao et al., 2020). However, there are few reports on the health function of red quinoa polysaccharide.

According to a recent study, alterations in the composition of the gut microbiota are linked to the emergence of diabetes and are related to the other metabolic diseases (Salgaco et al., 2019). Numerous studies have demonstrated that controlling the intestinal microbiota of the host can reduce the symptoms of diabetes (Cani et al., 2008; Gurung et al., 2020). The host's energy homeostasis can be affected by gut microbiota through the method of altering the number of active substances, which in turn controls the production of insulin (Wu et al., 2021). The influence of red quinoa polysaccharide on modifying the make-up of the gut microbiota has not yet been properly clarified. We investigated whether red quinoa polysaccharide has hypoglycemic and lipid-lowering effects on C57BL/6 mice fed a high-fat diet (HD) in the current study.

2 Materials and methods

2.1 Materials

Red quinoa seeds were obtained from the Hexi Farm (Golmud City, Qinghai Province, China). We purchased 21 male C57BL/6 mice which were maintained in a specific-pathogen-free (SPF) place from Changsheng Biotechnology Co., Ltd. (Liaoning Province, China). Normal diet (ND) and high-fat diet (HD) were provided from Maohua Biotechnology Co., Ltd. (Liaoning Province, China). Assay kits were used to assess the serum's biochemical characteristics. Assay kits for total cholesterol (TC), triglyceride (TG), low density lipoprotein cholesterol (LDL-C), high density lipoprotein cholesterol (HDL-C), alpha-alanine aminotransferase (ALT), catalase (CAT), glycosylated hemoglobin (HbA_{1c}), insulin (INS), Tumor Necrosis Factor-α (TNF-α), interleukin -1β (IL-1β), nitric oxide (NO), reduced glutathione (GSH), glutathione peroxidase (GSH-PX) and malondialdehyde (MDA) were purchased from Nanjing Jiancheng Bioengineering Institute (Nanjing, Jiangsu Province, China). All other chemicals and reagents are analytically pure.

2.2 Preparation of RQP

The extraction and purification of polysaccharides from red quinoa was performed according to the methods described by Hu with a slight modification (Hu et al., 2017). Seeds of quinoa were ground into powder. The powder was passed through an 80-mesh sieve and extracted with petroleum ether (1:10, v/v) for 8 h to remove

lipids and pigments. The red quinoa powder was then extracted using ultrasonic-assisted extraction technology and distilled water (250 w, 40 KHz). The ultrasonic process took place at a temperature of 60°C for 51 min with a water to material ratio of 20 mL/g. Centrifuge and collect the supernatant, adjust the pH of the supernatant to 8, add protease, bathe in water at 37°C for 30 min, then bathe in water at 90°C for 30 min, cool and adjust the pH to 4.5, and place for 12 h.

Subsequently, the extract was centrifuged at 4,000 × g for 20 min and adjusted to pH 7. The supernatant was then reduced using a rotary evaporator to one tenth of its volume at 60°C and precipitated with 95% ethanol (1:4, v/v) for 12 h at room temperature. Centrifugation was used to gather the resultant precipitate, which included crude polysaccharides. The unprocessed polysaccharide was placed into the dialysis bag for 24 h of dialysis, and throughout that time, the pure water was changed frequently to remove other pollutants. The red quinoa polysaccharide was stored at −20°C after freeze drying.

2.3 Characterization of RQP

The structure of RQP was analyzed by FTIR spectrometer. The monosaccharide composition of RQP was measured by HPLC method (Tan et al., 2021). Briefly, RQP was dissolved in 3.0 mL of 2.0 M trifluoroacetic acid (TFA) and hydrolyzed at 120°C for 4 h in sealed glass tubes, respectively. After 4 h, the methanol was added and blow dry with nitrogen to completely remove the remaining TFA and then redissolve it in 3.0 mL of water. The 250 uL of RQP solution was mixed with 250 uL of 0.60 mol/L NaOH and 500 uL of 0.40 mol/L PMP-methanol in 5.0 mLEP tube. Then, the reaction was done at 70°C for 1 h and cooled in water for 10 min. The 500 uL of 0.30 mol/L HCL was added to neutralize and the 1.0 mL of chloroform was added to vortex for 1.0 min and centrifuge at 3,000 r/min for 10 min. The supernatant was extracted three times. The obtained supernatant was put into HPLC for determination.

2.4 *In vitro* experiments

2.4.1 *In vitro* antioxidant of RQP

The scavenging and reducing abilities of RQP on DPPH (1,1-diphenyl-2-picryl-hydrazyl radical), ABTS [2,2′-azino-bis (3-ethylbenzthiazoline-6-sulfonic acid)], OH (hydroxyl free radical), and O_2^- (superoxide anion) at various doses (0.20, 0.40, 0.60, 0.80, and 1.0 mg/mL, respectively; Ke et al., 2020). The vitamin C (VC) were determined as a comparative to aid with comprehension. The IC50 value, which was inversely associated with antioxidant activity and used to measure antioxidant activity. Each experiment was repeated three times to take the average value.

Inhibition of DPPH by RQP. The RQP solution 2.0 mL (0.20, 0.40, 0.60, 0.80, and 1.0 mg/mL) were mixed with 2.0 mL DPPH solution (2.0×10^{-4} mol/L, dissolved in anhydrous ethanol). The reaction was done for 20 min without light, and the absorbance was measure at 517 nm (A1). Anhydrous ethanol was used instead of DPPH as a control group (A2). Pure water was used as a blank group instead of polysaccharide samples (A0).

$$\text{The clearance of DPPH}(\%) = 1 - \left[(A1 - A2) / A0\right] \times 100$$

Inhibition of ABTS by RQP. The 0.20 g ABTS and 0.0344 g potassium persulfate were mixed in 52 mL of distilled water. Then stored at room temperature in the dark for 24 h as ABTS mother liquor and was measured at 734 nm (0.70 ± 0.02). 0.4 mL of RQP solution with different concentrations was taken from each test tube, and then 3.6 mL of ABTS solution was added and the reaction took 15 min at room temperature. The absorbance of samples with different concentrations was measured at 734 nm (A1). Distilled water is added to the RQP solution instead of the ABTS solution (A2). The absorbance of blank solution (A0).

$$\text{The clearance of ABTS}(\%) = 1 - \left[(A1 - A2) / A0\right] \times 100$$

Inhibition of ·OH by RQP. The RQP solution 1.0 mL (0.20, 0.40, 0.60, 0.80, and 1.0 mg/mL) were added with 1.0 mL 5 mmol/L $FeSO_4$, salicylic acid and H_2O_2 solution, respectively. The reaction was carried out at 37°C for 30 min, and the absorbance at 510 nm was measured (A1). Distilled water was added to the RQP solution instead of the H_2O_2 solution (A2). The absorbance of blank solution (A0).

$$\text{The clearance of ·OH}(\%) = 1 - \left[(A1 - A2) / A0\right] \times 100$$

Inhibition of O_2^- by RQP. The 5.0 mL 0.05 mol/L Tris–HCL buffer (pH 8.2) in a water bath at 25°C for 20 min. The above different concentrations of RQP solution 1.0 mL and pyrogallol solution 1.0 mL were added and shaken. The reaction was carried out in a water bath at 25°C for 5 min. Then, the reaction was terminated by adding 1 mL of 10 mol/L HCL, and the absorbance was measured at 320 nm (A1). Distilled water was added to the RQP solution instead of the o-toluene trios' solution (A2). The absorbance of blank solution (A0).

$$\text{The clearance of } O_2^- (\%) = 1 - \left[(A1 - A2) / A0\right] \times 100$$

2.4.2 Effects of RQP on inhibition of α-amylase and α-glucosidase

The previously published method was used to assess the α-amylase inhibitory activities of RQP at various concentrations (0.10, 0.20, 0.40, 0.60, 0.80, and 1.0 mg/mL) with a few minor modifications (Lv et al., 2021). Acarbose was selected as the positive control. Each experiment was repeated three times to take the average value.

Preparation of α-amylase and starch with phosphate buffer solution (0.10 mol/L PBS, pH 6.8). 0.50 mL of α-amylase (1 U/mL) and 1.0 mL of RQP at different concentrations were added to the test tubes and incubated for 10 min at 37°C. Then 2.5 mL of starch solution (10 g/L) was added and incubated for 8 min at 37°C. The 1.0 mL of DNS developer was added in the test tubes and incubated for 8 min at 95°C. After cooling to room temperature, the appropriate amount of distilled water was added to dilute and measured the absorbance value at 540 nm. The following formula was used to calculate the inhibitory activity of α-amylase:

$$\text{Inhibition rate}(\%) = \left[(A2 - As + Ab) / (A2 - A1)\right] \times 100$$

Where As was the absorbance of the test sample system, Ab was the absorbance of the test sample system without the enzyme solution, and A1 and A2 were the absorbances of the starch system and the starch system, respectively.

The polysaccharide's ability to block α-glucosidase was tested using this methodology, with a few minor modifications (Lv et al., 2021). The 2.0 mL of RQP solution (0.10, 0.20, 0.40, 0.60, 0.80, and 1.0 mg/mL) were mixed with 2.0 mL of 0.10 mol/L phosphate buffer solution (pH = 6.8) and 1.0 mL of 1.0 U/mL of α-glucosidase, respectively. The reaction was warmed in a water bath at 37°C for 15 min. 2.0 mL of 1 mmol/L PNPG was added and mixed thoroughly. 37°C water bath was used for 20 min. 3.0 mL of 0.20 mol/L Na_2CO_3 was added to terminate the reaction. The absorbance was measured at 405 nm. The formula below was used to calculate the inhibitory activity of α-glucosidase:

$$\text{Inhibitory rate}(\%) = \left[1 - (\text{As} - \text{Ab}) / \text{A0}\right] \times 100$$

Where As, Ab, and A0 stood for the absorbance of the test sample system, a mixture of polysaccharide and PNPG without an enzyme, and a combination of PNPG and an enzyme without a mixture of polysaccharide, respectively.

2.4.3 Simulated digestion of RQP

The simulated digestion of RQP was performed as the procedures described in the literature with minor modifications (Ma et al., 2022). RQP was reacted with saliva to simulate oral digestion (0, 1, and 2 h), and mixed with simulated gastric to reacted (0, 2, 4, and 6 h). The liquid after digestion of simulated gastric juice for 6 h was collected and added to simulated intestinal fluid to reacted (0, 2, 4, and 6 h). The samples collected at different time periods were inactivated in a boiling water bath for 5 min to determine the contents of reducing sugar.

2.5 Animal experiment

2.5.1 Experimental design

Animal experiments carried out in this study have complied with the ARRIVE guidelines and the U.K. Animals (Scientific Procedures) Act, 1986, EU Directive 2010/63/EU for animal experiments, and the National Research Council's Guide for the Care and Use of Laboratory Animals and were approved by the Experimental Animals Ethics Committee of Heilongjiang Bayi Agricultural University (Laboratory Animal Approval Number: SPXY2023001). 6 weeks old, 21 ± 1 g, specific pathogen-free male C57BL/6 J mice were subjected to the treatment after a week of acclimatization to the lab environment. The mice were kept in an animal home with free access to food and water under regulated circumstances (temperature: 22°C ± 2°C, relative humidity: 45% ± 5%, and a 12 h light/12 h dark cycle). Seven mice in the ND group were fed a standard pellet diet. Mice in the HD group (14 mice) were fed a high-fat diet (10% lard, 20% sucrose, 1% cholesterol, 0.2% sodium deoxycholate and 68.8% standard pellets) to induce diabetes in the mice. After 4 weeks, all mice were fasted overnight and given free access to water. Fresh STZ solution (0.10 mol/L citrate buffer, pH 4.5) was intraperitoneally given into the HD mice at a dose of 30 mg/kg body weight (Jiang et al., 2013; Zang et al., 2023). Citrate buffer was administered into mice in ND. After 72 h, the levels of fasting blood glucose (FBG) were measured using a glucometer (Sinocare, Changsha, China). Diabetic mice were defined as those with FBG levels over 11.1 mmol/L (Lan et al., 2023; Zhao et al., 2023).

The diabetic mice were then randomly split into two groups: HD with daily administration of dosage (800 mg·kg^{-1}·day^{-1}) red quinoa polysaccharide, and model control group with high-fat diet (Wang et al., 2016; Mao et al., 2020). After 12 h without food but with unlimited access to water, all mice had an anesthetic for anatomy after 4 weeks. Body weight, fasting blood sugar, and food intake were all monitored on a weekly basis. In the last day of treatment, after anaesthetized for anatomy the serum was separated from the abdominal aorta and centrifuged (4°C, 3,500 r/min, 10 min). For further study, liver and colon contents were immediately frozen in liquid nitrogen and transferred to a temperature of −80°C for storage.

2.5.2 Determination of serum and liver biochemical parameters

Serum markers (TC, TG, LDL-C, HDL-C, INS, HbA_{1c}, TNF-α, IL-1β) and markers in liver homogenate (GSH-PX, GSH, MDA, NO, ALT, CAT) were measured with the kit.

2.5.3 Determination of SCFAs in cecal contents

The content of SCFAs were determined by high performance liquid chromatography according to the method of Guo et al. (2022).

2.6 Gut microbiota detected by 16S rRNA gene sequencing technology

The DNeasy PowerSoil kit (QIAGEN) was used to extract total genomic DNA from fecal samples. Using Nanodrop (Thermo Scientific, NC2000) and agarose gel electrophoresis, the quantity and purity of DNA were verified. Then, using PCR as described in the prior study, the microbiota V3-V4 hypervariable areas of the 16S rRNA gene were amplified. Primer 338F 5-ACTCCTACGGGAG GCAGCAG-3 and Primer 806R 5-GGACTACHVGGGTWTCTAAT-3 were used in the current investigation. A six-base sequence that is exclusive to each sample makes up the barcode. The DNA libraries were created using the TruSeqTM DNA Sample Prep Kit after the PCR products were separated by gel electrophoresis, purified with the AxyPrep DNA Gel Extraction Kit (Axygen, AP-GX-500), and purified. For the library's quality assurance, the Agilent 2100 Bioanalyzer System (High Sensitive DNA Chip) was utilized. On the Illumina MiSeq platform, the pooled DNA product was paired-end sequenced in accordance with the recommended procedures.

After passing quality control, the Illumina MiSeq sequences were used in the analysis and uploaded to QIIME (Quantitative Insights into Microbial Ecology, v1.9.1) for additional research. The Simpson index, Chao1 index, and Shannon diversity index were calculated by Mothur (v1.30.2) using the operational taxonomy units of representative sequences and their relative abundance. The principal coordinates analysis (PCoA) with weighted and unweighted UniFrac analysis in R software was used to determine the abundance and diversity of the communities among the normal group, high fat group,

and red quinoa polysaccharide. Then, using the PCoA scores, MANOVA was used to evaluate the statistical significance of the difference between the groups. According to the LEfSe approach, which employed the Kruskal-Wallis and Wilcoxon rank sum test ($P<0.05$), mothur was utilized to identify significant communities that were crucial for differentiating the various treatment groups. The main communities of the gut microbiota and the serum and liver index were correlated using the Spearman analysis with a threshold p-value of 0.05.

2.7 Statistics and analysis

The software Origin 2022 (Origin Lab Corporation, Northampton, MA) was used to draw every single figure. Data from repeated measures were analyzed in SPSS 26 using one-way analysis of variance and Tukey's tests.

3 Results

3.1 Characterization of RQP

The yield of RQP is 1.57 ± 0.38%. Figures 1A,B show the HPLC chromatograms of the monosaccharide standards and RQP, respectively. The HPLC chromatogram in Figure 1B revealed that RQP was made up of 10 monosaccharides. Among them, glucose, galactose, and arabinose accounted for more than 90% of the monosaccharide composition of RQP (Table 1).

Figure 2 displays the FTIR spectroscopy data used to describe RQP. The spectra showed polysaccharide absorption peaks around 800–1,200, 1,300–1,800, and 3,200–3,600 cm^{-1}. At 3415.18 cm^{-1}, the hydroxyl group (O-H) displayed a recognizable broad stretch peak (Li et al., 2021). The presence of uronic acid in RQP can be inferred from the strong band at 1657.42 cm^{-1} and the weak band at 1402.2 cm^{-1} caused by the absorption of a carboxylic group (COO−; Ye et al., 2021). The frequency band at 1330.9 cm^{-1} is caused by the stretching vibration of C = O (Li et al., 2021). The 950–1,200 cm^{-1} FITR range that is utilized to pinpoint the location and strength of unique bands in polysaccharides (Ye et al., 2021). The band at 1108.98 and 848.10 cm^{-1}, respectively, verified the presence of pyranose rings and a-glycosidic connections in the monosaccharide blocks of RQP (Portincasa et al., 2022).

3.2 *In vitro* experiments

3.2.1 *In vitro* antioxidant

As shown in Figure 3, RQP had strong scavenging ability of DPPH and ABTS free radicals. In terms of DPPH and ABTS scavenging

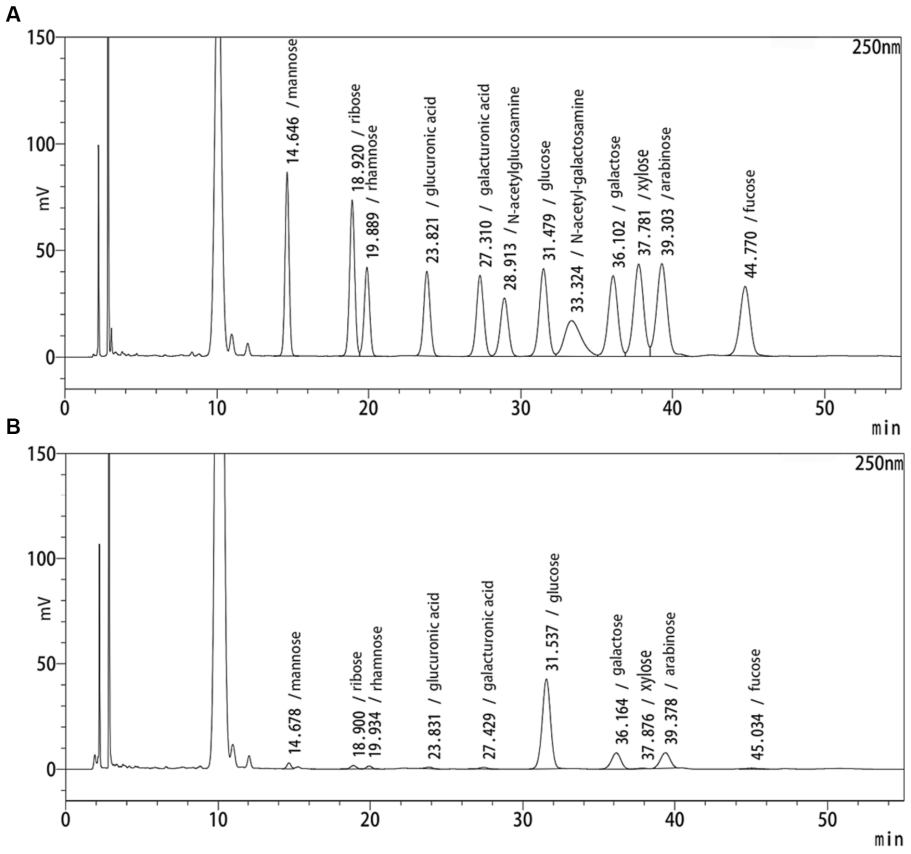

FIGURE 1
HPLC spectra of RQP. **(A)** monosaccharide standards; **(B)** RQP.

ability, the IC50 values of RQP were 0.51 mg/mL and 0.52 mg/mL. Furthermore, RQP have lower scavenging ability of O_2^- and ·OH, when compared to the VC group.

3.2.2 Inhibition of α-amylase and α-glucosidase by RQP and *in vitro* digestion of RQP

As shown in Figure 4, The inhibition rates of RQP on the activities of α-amylase and α-glucosidase increased with the increase of its concentration in a dose-dependent manner. When the concentration of polysaccharide was 1.0 mg/mL, The inhibition rates of RQP on α-amylase and α-glucosidase were 29.50% and 35.77%, respectively.

Through the preliminary experiment, we got the standard curve of reducing sugar: $y = 1.5151x - 0.0135$ ($R^2 = 0.9991$). To further explore the changes of reducing sugar contents in RQP during digestion include oral cavity, stomach, and small intestine (Supplementary Table S1). As shown in Supplementary Table S1, RQP were not digested in the mouth, stomach, and small intestine. RQP can maintain its original morphology and interact with intestinal microorganisms in the large intestine.

TABLE 1 Monosaccharide composition.

Monosaccharide composition	Sample (%)	
	Monosaccharide standards	RQP
Man	8.950	2.174
Rib	9.608	1.758
Rha	5.748	1.371
GlcA	6.534	0.987
GalA	7.133	1.212
Nag	5.569	-
Glu	8.881	64.545
Nad	7.160	-
Gal	9.195	13.217
Xyl	10.959	0.543
Ara	11.694	13.153
Fuc	8.569	1.040

Man, mannose; Rib, ribose; Rha, rhamnose; GlcA, glucuronic acid; GalA, galacturonic acid; Nag, N-acetyl-glucosamine; Glu, glucose; Nad, N-acetyl-galactosamine; Gal, galactose; Xyl, xylose; Ara, arabinose; Fuc, fucose.

3.3 Animal experiments

3.3.1 Effects of RQP on mice body weight, organ index, FBG, OGTT, HbA1c and insulin level

After 4 weeks high fat diet feeding, a significant decline on body weight was found in the RQP group mice, when compared with the HD group (Figure 5A). Additionally, had decreased of epididymal fat and mesenteric fat, and increased brown fat were found in the RQP group mice, when compared with the HD group (Figures 5B,C).

The diabetic mice in the HD group showed a significant increase in blood glucose and HbA_{1c} levels (Figures 5D,G,H). However, this elevation was inhibited by treatment with RQP. In Figure 5H, RQP reduced insulin level compared with the HD group, which indicated that RQP may be able to minimize the stress caused by hyperglycemia. As shown in Figure 5E, The blood glucose levels in the HD and RQP groups peaked 30 min after loading glucose. Additionally, at each time point, the HD group's blood glucose level was higher than that of the other groups. The AUC's fluctuations throughout the OGTT are depicted in Figure 5F. The model group responded to oral glucose delivery with a considerable hyperglycemic response. When compared to the HD group, the AUC of the blood glucose response was considerably lower in the RQP group.

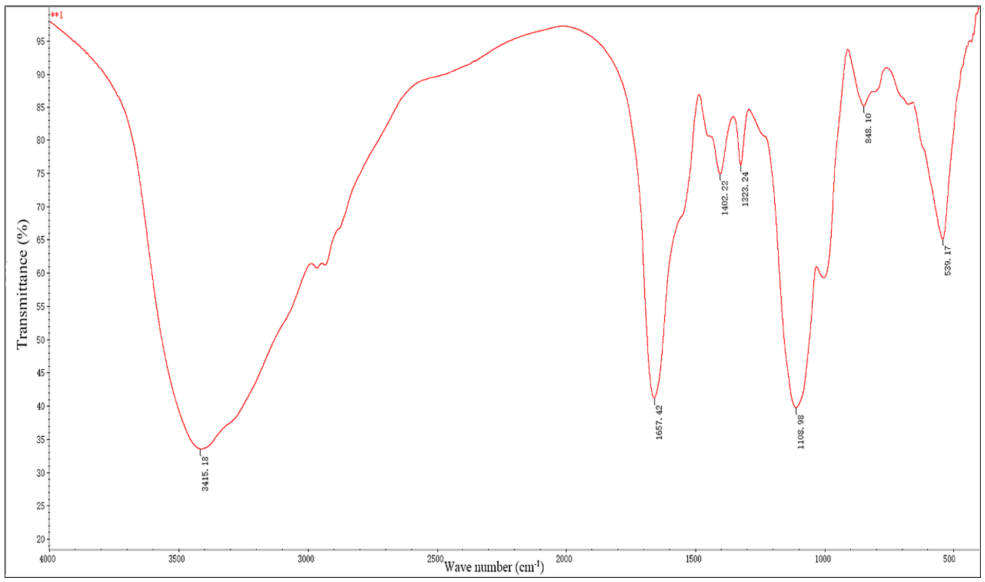

FIGURE 2
FTIR spectra of RQP.

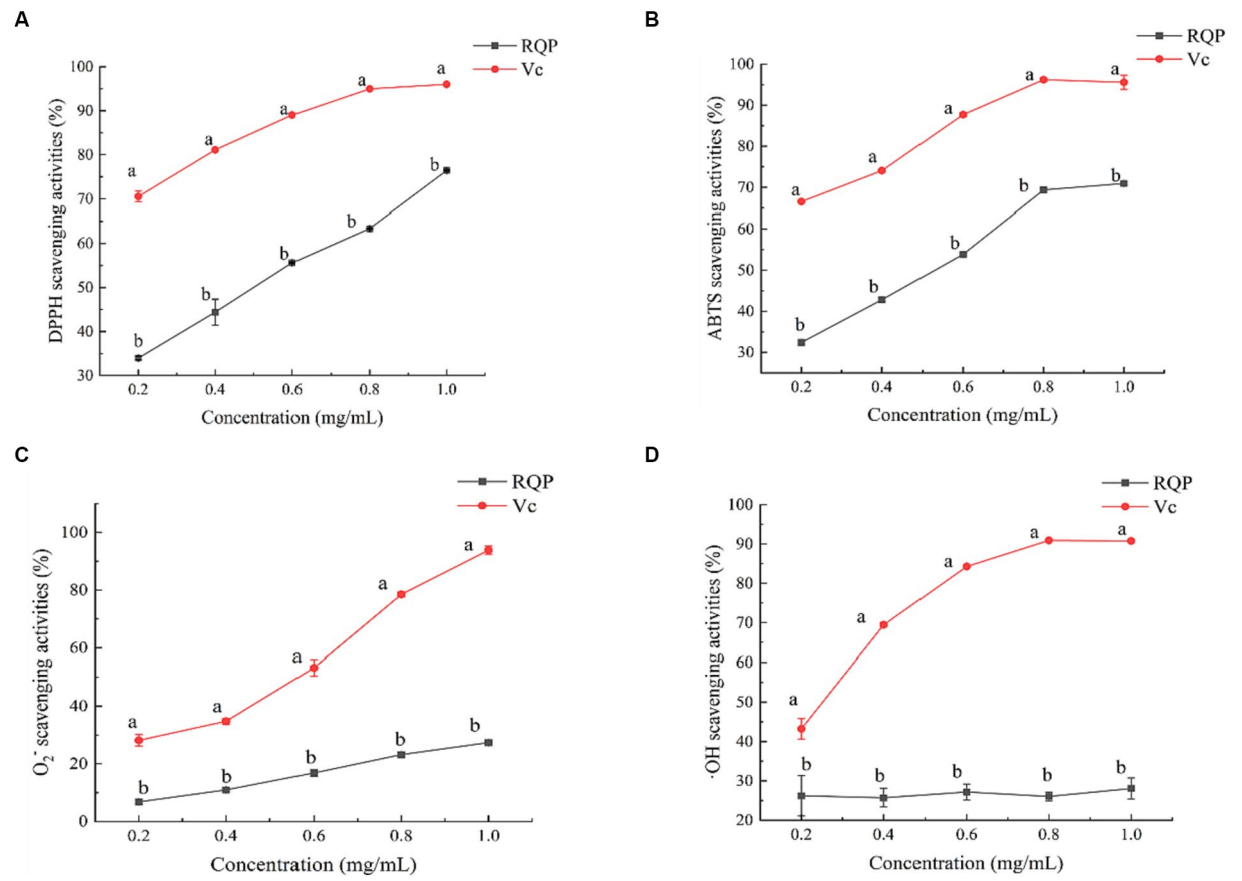

FIGURE 3
Antioxidant activities of RQP. **(A)** DPPH; **(B)** ABTS; **(C)** O_2^-; **(D)** OH. The values are expressed as means ± SD (n = 3). Data followed by the different letters are significantly different ($p < 0.05$) by Duncan's test.

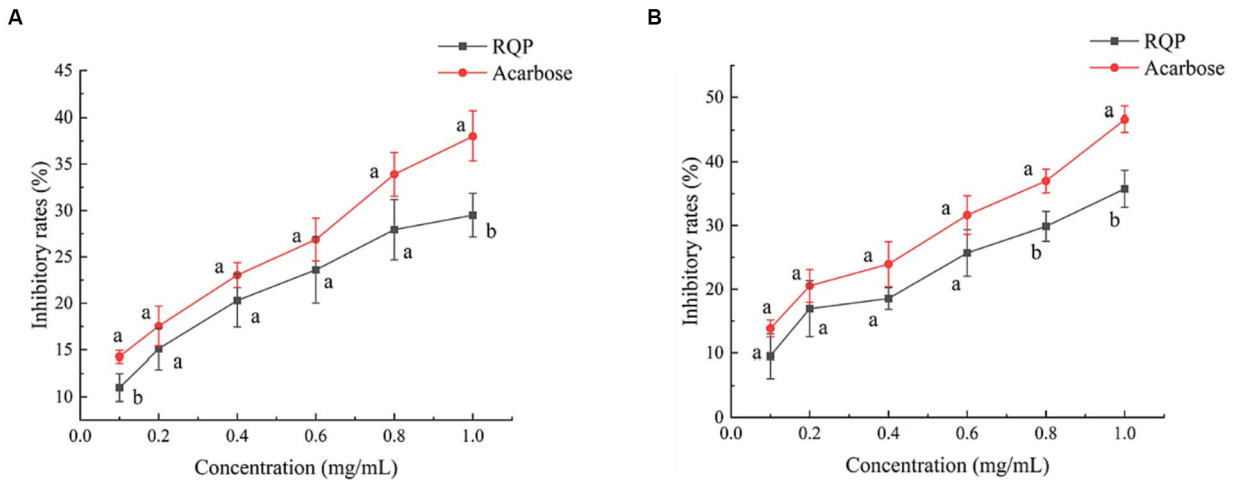

FIGURE 4
Inhibition on α-amylase **(A)** and α-glucosidase **(B)** activity of RQP. The values are expressed as means ± SD (n = 3). Data followed by the different letters are significantly different ($p < 0.05$) by Duncan's test.

3.3.2 Effects of RQP on lipid levels

TC, TG, and LDL-C levels were significantly lower in the RQP group compared with the HD group (Figures 6A–C). The TC content in the RQP group decreased by 16.82%, the TG content decreased by 19.0%, and the LDL-C content decreased by 50.0%. And as shown in Figure 6D, the HDL-C content in the RQP group was significantly increased, which was comparable to that of healthy mice.

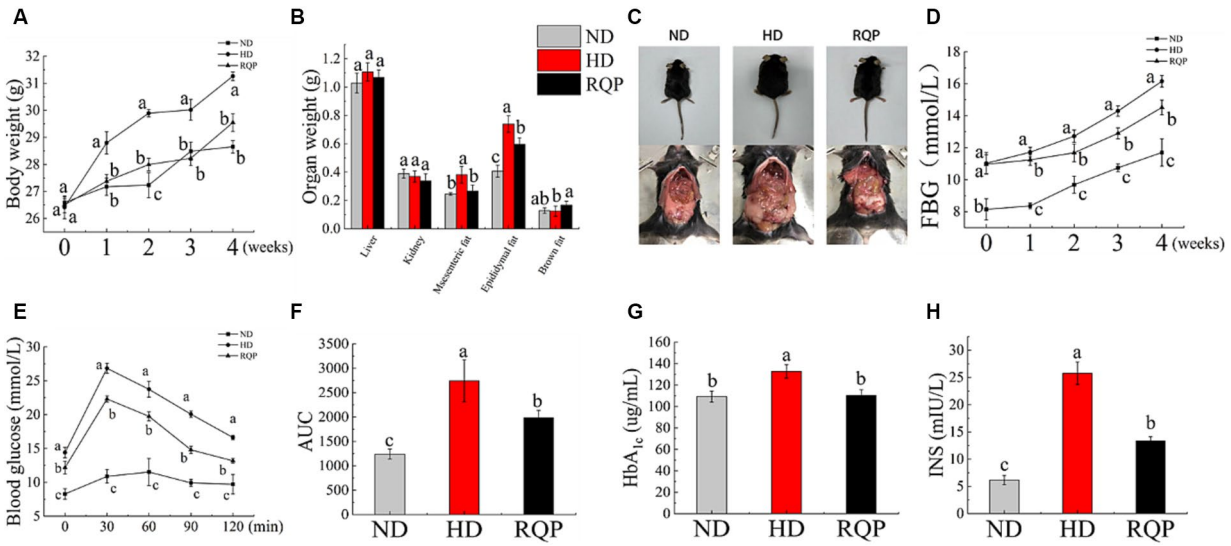

FIGURE 5
Effects of RQP on diabetic mice: **(A)** body weight; **(B)** organ weight; **(C)** representative images of mice; **(D)** FBG; **(E)** OGTT; **(F)** AUC; **(G)** HbA_{1c}; **(H)** INS. The values are expressed as means ± SD ($n = 5$). Data followed by the different letters are significantly different ($p < 0.05$) by Duncan's test.

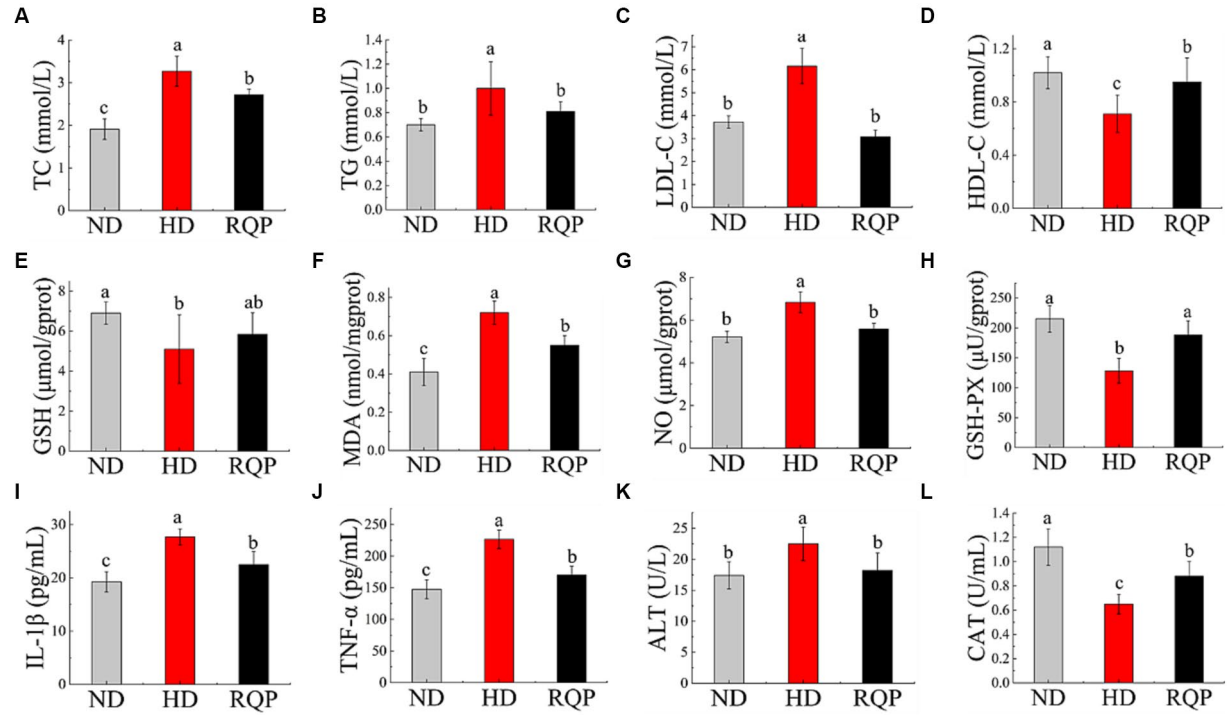

FIGURE 6
Effects of RQP on lipid level, antioxidant levels and inflammatory factors. **(A)** TC; **(B)** TG; **(C)** LDL-C; **(D)** HDL-C; **(E)** GSH; **(F)** MDA; **(G)** NO; **(H)** GSH-PX; **(I)** IL-1β; **(J)** TNF-α; **(K)** ALT; **(L)** CAT. The values are expressed as means ± SD ($n = 5$). Data followed by the different letters are significantly different ($p < 0.05$) by Duncan's test.

3.3.3 Effects of RQP on antioxidant levels in liver

Figures 6E,H show that the GSH-PX content was significantly reduced, but there was no significant difference in GSH content in the RQP group when compared with the HD group. Figure 6G shows that the NO content of RQP was significantly lower than that of HD group. Lipid peroxidation produces MDA, which elevated levels can cause inflammation, necrosis, and damage to cell membranes (Yuan et al., 2018). Figure 6F demonstrates that the MDA level in the HD group was substantially higher than that in the ND group, while it decreased significantly in the RQP group.

These findings showed that RQP had a significant impact on the antioxidant levels in diabetic mice.

3.3.4 Effects of RQP on inflammatory factors

TNF-α and IL-1β levels (Figures 6I,J) in the RQP group were significantly decreased compared with the HD group. In addition, the ALT content significantly decreased by while CAT significantly increased in the RQP group (Figures 6K,L), respectively. The results showed that RQP has the potential to improve liver cell injury.

3.3.5 Effects of RQP on SCFAs

When compared to the HD group, the concentrations of acetic acid and total acid in the cecal contents of RQP increased significantly, while propionic acid and butyric acid levels increased slightly (Figure 7). The results showed that feeding RQP increased SCFAs levels, which had a potential effect on improving intestinal function of diabetic mice.

3.3.6 Effects of RQP on diversities of gut microbiota

According to the findings, fecal samples from the ND, HD, and RQP groups were chosen for 16S rRNA sequencing to examine the variations in gut microbiota. Figures 8A–C demonstrate that the RQP group's microbial community's species diversity and abundance were lower than those of the HD group. For β-diversity, PCoA analysis, analysis of similarities (ANOSIM) and PLS-DA analysis were performed (Figures 8D–F). The results demonstrated the existence of three distinct clusters within the microbial community, each of which contained a concentrated distribution of samples. Both high-fat diet and RQP had a significant effect on gut microbiological composition, which was demonstrated by more significant between-group changes than within-group differences ($p < 0.05$).

The relative abundances of several bacterial taxa in each sample were counted at the phylum and genus levels to determine the impact of RQP on the make-up of the bacterial community. In the RQP group, the composition of the gut microbiota considerably changed at the phylum and genus levels (Figure 9A). Compared with the ND group, the *Bacteroidota* level increased and the *Firmicutes*, *Verrucomicrobiota*, *Actinobacteriota* levels were decreased in the HD group. However, compared to the HD group, the RQP group had significantly higher abundances of *Firmicutes*, *Verrucomicrobiota*, *Actinobacteriota*, and *Desulfobacterota*, and significantly decreased abundances of *Bacteroidota*. As shown in Figure 9B at genus level. After RQP treatment, the abundance of *norank_f_Muribaculaceae* decreased from 36.38% to 0.71% as well as the prevalence of the *Lachnospiraceae_NK4A136_group* from 7.49% to 4.93%. On the other hand, the abundances of *unclassified_f_Lachnospiraceae* increased from 2.95% to 6.38%, while the abundances of *Akkermansia* increased to 27.23%. Additionally, *norank_f_Lachnospiraceae*, *unclassified_f_Atopobiaceae*, and *norank_f_Eubacterium_coprostanoligenes_group* in the RQP group were significantly higher than those in the HD group. The results showed that RQP directly impacted the intestinal microbiota of diabetic mice. For further understanding the differences in intestinal flora at the genus level, heat map analysis was performed on the ND, HD, and RQP groups (Figure 9C). *Verrucomicrobia* decreased, because of RQP's enhanced *Akkermansia* abundance in comparison to the HD group. RQP inhibited the increase of harmful intestinal flora in diabetes mice by reducing the abundance of *A2*, *Odoribacter*, *norank_f_norank_o_Rhodospirillales*, *Ruminococcus*, *Muribaculum*, *Mucispirillum*, *Rikenellaceae_RC9_gut_group*, *Parabacteroids*, *Parasutterella*, *Prevotella*, *Alloprevotella*, *unclassified_f_Prevotellaceae* and *Alistipes*. In addition, the abundance of some beneficial bacteria increased after RQP treatment, such as *Eubacterium_brachy_group*, *Eubacterium_xylanophilum_group*, *Coriobacteriaceae UCG-002*, *Ruminococcus_torques_group* and *Faecalibaculum*.

In addition, LEfSe analysis highlights the core bacterial phenotype from phylum to genus, to understand the changes in microbial composition. As shown in Figures 10A,B, there was no significant difference among the three groups in *Proteobacteria*, *Bacteroidota*, *Firmicutes*, *Actinobacteriota*, *Cyanobacteria*. However, the ND group were enriched with the phylum *Spirochaetota*, the class *Spirochaetia*, the order *Spirochaetales* and *Bifidobacteriales*, the family *Spirochaetacea* and *Bifidobacteriaceae*, the genus *Treponema*, *Spirochaetia*, *Spirochaetales*, *Spirochaetaceae*, *Bifidobacteriales*, *Bifidobacteriaceae*, *Bifidobacterium*, *Faecalibaculum* and *Lachnospiraceae_UCG-010*. The HD group were enriched with the class *Cyanobacteriia* and *Alphaproteobacteria*, the order *Chloroplast*, the family *Chloroplast* and *Prevotellaceae*, the genus *Cyanobacteriia*, *Chloroplast*, *f_norank_o_Chloroplast*, *g_Prevotellaceae_UCG-001*, *Alphaproteobacteria*, *g_Prevotellaceae_UCG-001*, *f_Prevotellaceae*, *g_Alloprevotella*, *g_unclassified_f_Prevotellaceae*, *g_Butyricimonas*, *g-Muribaculum*, *g_Alistipes*, *g_Rikenellaceae_RC9_gut_group*, *g_Candidatus_Arthromitus*, *g_norank_f_Prevotellaceae*. The above results showed that the intestinal flora of mice fed with high-fat diet changed significantly. The gut microbiota enriched in the RQP group were the phylum *Verrucomicrobiota*, the class *Verrucomicrobiae*, the order *Verrucomicrobiales*, the family *Akkermansiaceae* and *f_unclassified_o_Oscillospirales*, the genus *f_Akkermansiaceae*, *p_Verrucomicrobiota*, *c_Verrucomicrobiae*, *o_Verrucomicrobiales*, *f_unclassified_o_Oscillospirales*, *g_Akkermansia*, *g_Parvibacter*, *g_unclassified_o_Oscillospirales*.

According to the evolutionary relationship among the species in the sample, the phylogenetic tree was constructed to reveal the genetic relationship of the species in the sample during the evolution process from the perspective of molecular evolution. As shown in Figure 11,

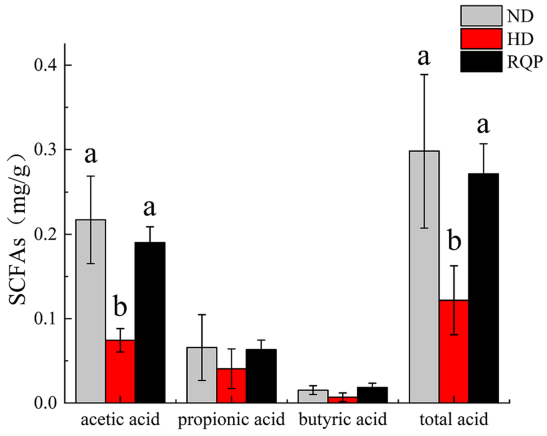

FIGURE 7
Effects of RQP on SCFAs of C57BL/6 J mice. The values are expressed as means ± SD ($n = 5$). Data followed by the different letters are significantly different ($p < 0.05$) by Duncan's test.

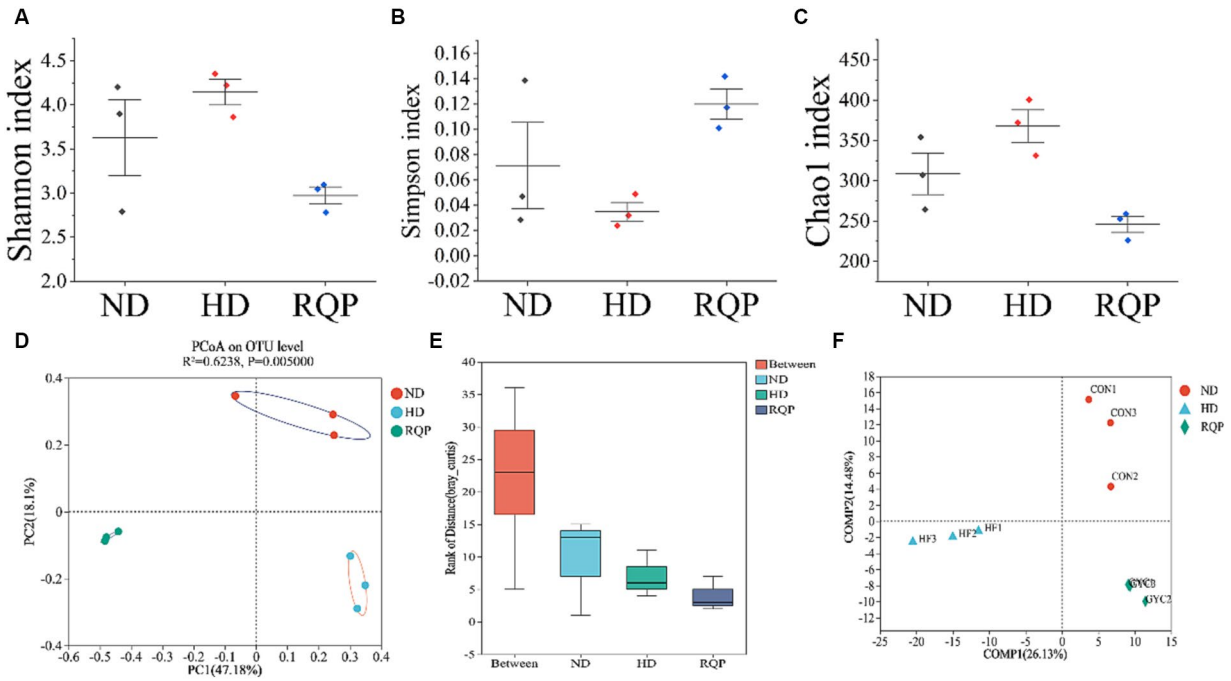

FIGURE 8
Effects of RQP on the diversity of gut microbiota in diabetic mice. **(A)** Shannon index; **(B)** Simpson index; **(C)** Chao1 index; **(D)** Principal co-ordinates analysis (PCoA); **(E)** Analysis of similarities (ANOSIM); **(F)** Venn analysis. Data are presented as the mean ± SD (n = 3).

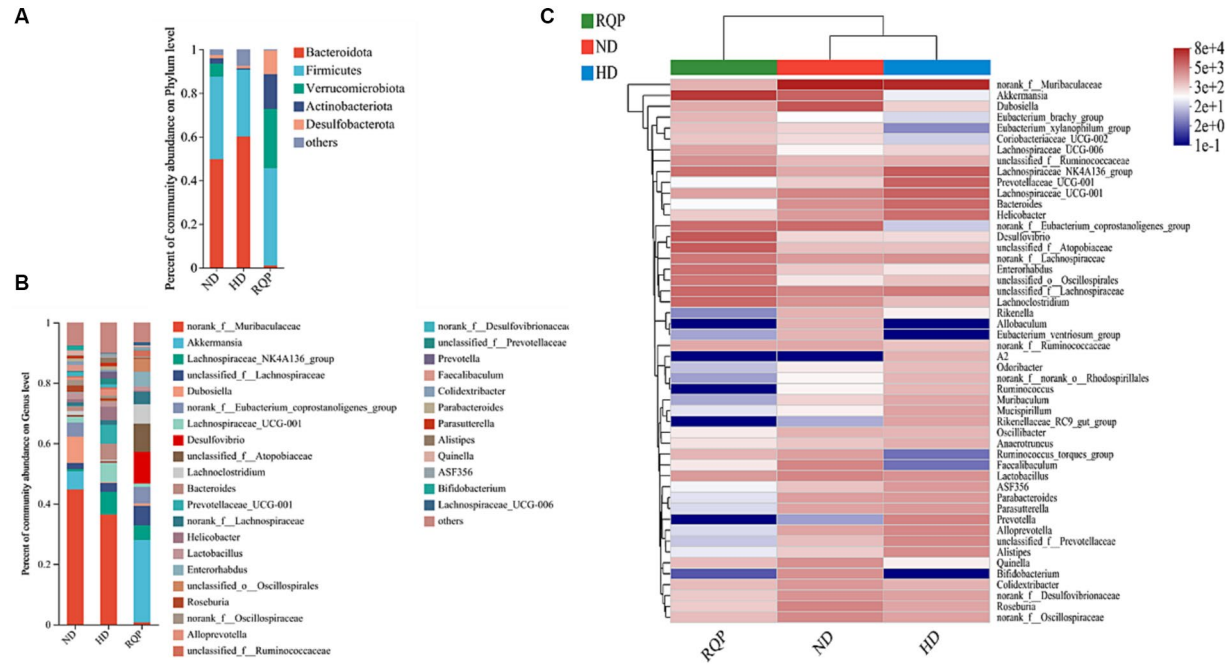

FIGURE 9
Effects of RQP on the gut microbiota composition in diabetic mice. **(A)** The relative abundance of gut microbiota at the phylum level; **(B)** genus level; **(C)** Community heatmap analysis on genus level. Data are presented as the mean ± SD (n = 3).

there are significant differences in the evolutionary distance between the bacteria, especially after RQP treatment. The results showed that RQP could change the disorders of intestinal microbiota in diabetic mice induced by high-fat diet.

To determine if RQP-induced alterations in the composition of the gut microbiota and the amounts of biochemical indicator molecules might be related, we used Spearman's correlation analysis (Figure 12). Specifically, *Akkermansia* are significantly positively correlated with

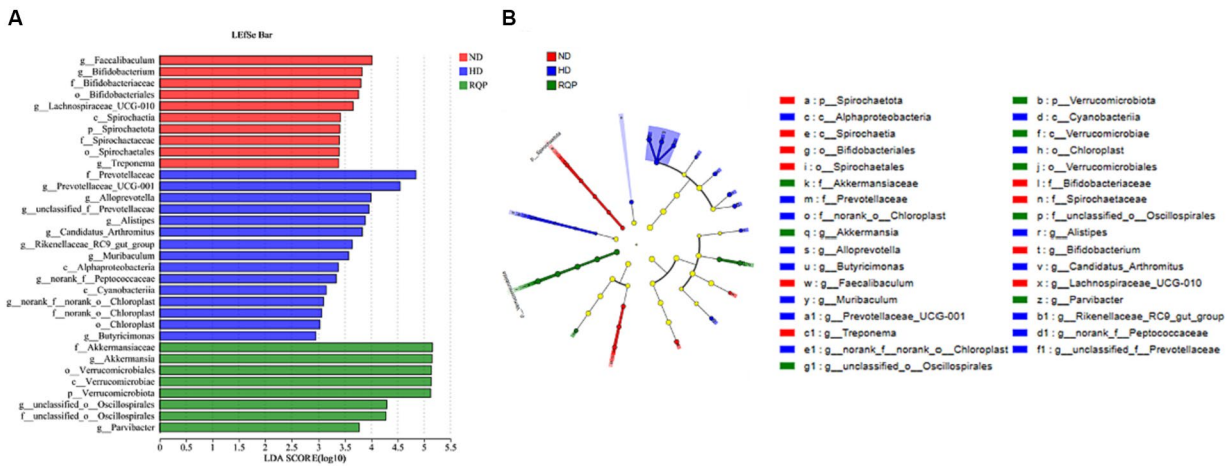

FIGURE 10
Core bacterial phenotype analysis in in diabetic mice (n = 3). **(A)** LDA scores of taxa enriched at different taxonomy levels (LDA significant threshold = 4); **(B)** Taxonomic cladogram generated by LEfSe analysis.

GSH-PX, negatively correlated with TNF-α, INS, ALT, LDL-C, ALT, MDA, TC, TG, brown fat and upper testis body fat. *Mucispirillum*, *Prevotella*, *A2*, *Helicobacter*, *ASF356*, *Oscillibacter*, *Prevotellaceae_UCG-001*, *Alloprevotella* are significantly positively correlated with HbA_{1c}, body weight, NO and mesenteric fat, negatively correlated with SCFAs.

3.3.7 BugBase phenotype prediction

The phenotype of the microbiome was studied. The relative abundance of aerobic bacteria and mobile elements bacteria is depicted in Figure 13, Facultatively_Anaerobic bacteria and Forms_Biofilms were lower. In contrast, Anaerobic bacteria, and microorganisms with potential for disease were more prevalent overall. However, the situation was the opposite in the RQP group. The relative abundance of Gram_Negative, Gram_Positive and Stress_Tolerant were not significantly difference between HD and RQP group. Therefore, RQP can also affect the composition of intestinal microorganisms by changing bacterial phenotypes.

3.3.8 PICRUSt1 and FAPROTAX function prediction

PICRUSt1 function prediction can be used for OTU annotation information at the functional level of COG and the abundance information of each function in different samples. FAPROTAX function prediction can be used to predict the metagenomic contribution of intestinal microbiota. As shown in Figure 14A, RQP significantly changed the abundance of OTU in the biosynthetic pathway and metabolic pathway, compared with the HD group. Figure 14B indicated that high-fat diet may lead to the production of potential pathogens, such as human_pathogens_pneumonia and human_pathogens_all. RQP can effectively inhibit the production of these two bacteria. The above experimental results further indicate that RQP can alleviate intestinal flora disorders and related metabolic dysfunction.

4 Discussion

In this study, we evaluated the hypoglycemic, hypolipidemic, and gut microbiota effects of RQP in diabetic mice. According to HPLC data, RQP in this study had a yield of 1.57 ± 0.38% and was a complex glycoconjugate. RQP is primarily composed of Man (2.17%), Rib (1.76%), Rha (1.37%), GlcA (0.90%), GalA (1.21%), Glu (64.55%), Gal (13.22%), Xyl (0.54%), Ara (13.15%), Fuc (1.04%). These findings are in line with the previous studies on RQP, and Glu, Gal, and Ara are prevalent in it (Tan et al., 2021). The results of monosaccharide composition, FITR and HPLC preliminarily revealed the composition and basic structure of RQP, which provided a framework for future research on the functional activity of RQP.

RQP was proved good antioxidant activities *in vitro*. Compared with O_2^- and ·OH, RQP showed higher antioxidant effects on DPPH and ABTS radicals, which may be due to the different antioxidant systems and different antioxidant mechanisms (Huang et al., 2017; Mu et al., 2021). The good antioxidant activities may be connected with low molecular weight of polysaccharides, which contributed by ultrasound-assisted extraction, and reported to be easier to transfer electrons from uronic acid groups (Huang and Huang, 2020) Another explanation is RQP contains high proportion of glucose, acarbose, and galactose, which was proved to contribute to higher effects on DPPH and ABTS scavenging (Huang and Huang, 2020). Inhibitors of α-amylase and α-amylase were essential for delaying human carbohydrate absorption and reducing the release of glucose from carbohydrates (Lv et al., 2021). A previous study has shown that the arabinose and xylose content of polysaccharides determines the inhibitory effect of polysaccharides on α-glucosidase and α-amylase (Lv et al., 2021). In the present study, the arabinose and xylose contents of RQP were 13.15% and 0.54%, respectively. This could be the reason for the lower inhibition of α-amylase and α-glucosidase by RQP. In this study, the inhibitory effects on both α-glucosidase and α-amylase may partly contribute to the improvement of hyperglycemia and hyperlipidemia in mice (Zhang et al., 2019). To function as prebiotics, polysaccharides must pass through the digestive tract and saliva to reach the colon. Previous studies have shown that polysaccharides are not hydrolyzed by digestive enzymes in saliva, gastric juice, and small intestinal fluid, which are consistent with our findings (Ding et al., 2019; Ma G. et al., 2022).

T2D is a persistent medical condition distinguished by elevated blood glucose levels, often accompanied by cardiovascular disease, renal

FIGURE 11
Phylogenetic tree on Genus level.

disease, eye disease, and other consequences. These complications arise from the impaired functionality of islet β cells within the body, leading to insulin resistance (Chatterjee et al., 2017). Long-term intake of high-fat diet can lead to weight gain, fat accumulation and elevated blood glucose in diabetic mice, resulting in insulin resistance, which makes the mice endocrine more insulin to maintain normal glucose and lipid metabolism in the body (Luo et al., 2021). We found that body weight, organ index, and FBG were significantly decreased in diabetic mice after 4 weeks RQP treatment. These results indicated that RQP effectively regulates glycolipid metabolism in an *in vivo* setting by enhancing glucose absorption and utilization in mice with T2D. The average blood glucose levels of the three groups of mice during the experiment were indicated by the OGTT and HbA_{1c} readings (Liu et al., 2018). Compared with the HD group, RQP improved OGTT and significantly reduced HbA_{1c} level in diabetes mice, indicated that the intake of RQP improved insulin resistance, helps maintain blood sugar homeostasis in the body (Yang et al., 2021). Disorders of lipid metabolism are another prominent feature of diabetes (Kane et al., 2021). Following consumption of a high-fat diet, the mice mostly displayed an increase in serum levels of TC, TG, LDL-C, while exhibiting a decrease in HDL-C (Athyros et al., 2018). This study found that RQP significantly improved the dyslipidemia caused by high fat-diet, decreased the contents of serum TC, TG, LDL-C, and increased HDL-C of diabetic mice. The findings suggest that RQP could modulate lipid metabolism and concurrently preserve blood glucose stability, hence exerting a partial inhibitory effect on diabetic outcomes.

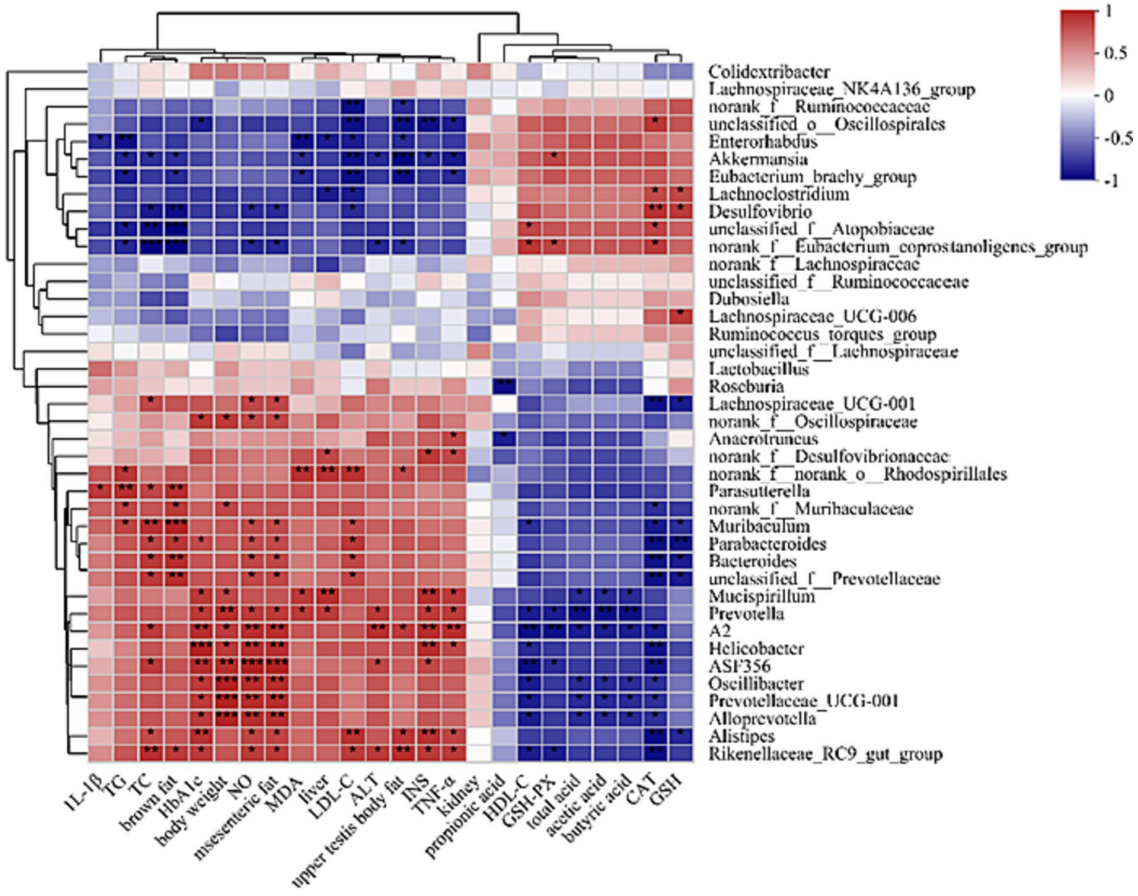

FIGURE 12
Spearman correlation heatmap between gut microbes and physiological indicators in mice at the genus level.

Previous studies have indicated a strong association between oxidation and diabetes, whereby oxidative stress is heightened, hence exacerbating the advancement of T2D and its associated consequences (Rehman and Akash, 2017; Yaribeygi et al., 2020). Prolonged consumption of a high-fat diet can lead to an alteration in the equilibrium of free radicals inside the human body, leading to an excessive generation of free radicals and subsequently triggering a reaction of oxidative stress (Pasaoglu et al., 2004). In the context of T2D, it was observed that the high-fat diet administered to mice resulted in an elevation of lipid oxidation, hence contributing to oxidative damage (Yaribeygi et al., 2020). The antioxidative properties of RQP were demonstrated by its capacity to reduce the levels of MDA, NO, and GSH, while simultaneously increasing the levels of GSH-PX and CAT in the bloodstream. Further, significant decreases in IL-1β, TNF-α and ALT activities were also found in mice of the RQP group, which were inflammatory factors and play vital role in the development of insulin resistance in T2D cases (Liu et al., 2016). The findings of this study indicated that the treatment of the RQP has the potential to mitigate oxidative damage and inflammatory levels resulting from hyperglycemia and hyperlipidemia.

Based on the above findings, this experiment further found that RQP intake significantly increased the content of SCFAs. SCFAs are important metabolites that regulate intestinal inflammation and metabolism, which were produced by microorganisms and difficult-to-digest polysaccharides (Sivaprakasam et al., 2016). SCFAs have the capacity to influence glucose homeostasis and modulate blood glucose levels through their regulatory effects on glucose absorption and utilization inside the human body (Rauf et al., 2022). Polysaccharides are fermented by the intestinal flora in the large intestine, where they are converted into different short-chain fatty acids due to their different structures and monosaccharide composition (Zhang et al., 2020). Acetic acid is produced mainly by the fermentation of glucuronic acid, xylose, galactose, and galacturonic acid, propionic acid is produced by the fermentation of glucose, xylose, and arabinose, and butyric acid is produced from xylose, glucuronic acid, galactose, and galacturonic acid. Acetate, propionate, and butyrate serve as metabolic substrates in the process of cholesterol production (Wang et al., 2019). In addition, propionate can also inhibit the synthesis of cholesterol and fatty acids in the liver (Portincasa et al., 2022). In this study, RQP increased the content of acetic acid and total acid compared with the HD group, indicated that RQP could improve the intestinal function of diabetic mice by increasing the contents of SCFAs, thereby regulating lipid metabolism, reducing blood glucose and lipid accumulation (Portincasa et al., 2022).

There is a growing body of evidence supporting the significant involvement of gut bacteria in the development and progression of lipid metabolic diseases (Ma et al., 2019). The composition of gut microbiota plays a crucial role in the manifestation and progression of metabolic syndrome through its impact on host energy metabolism, immune system function and inflammatory response (Wu et al.,

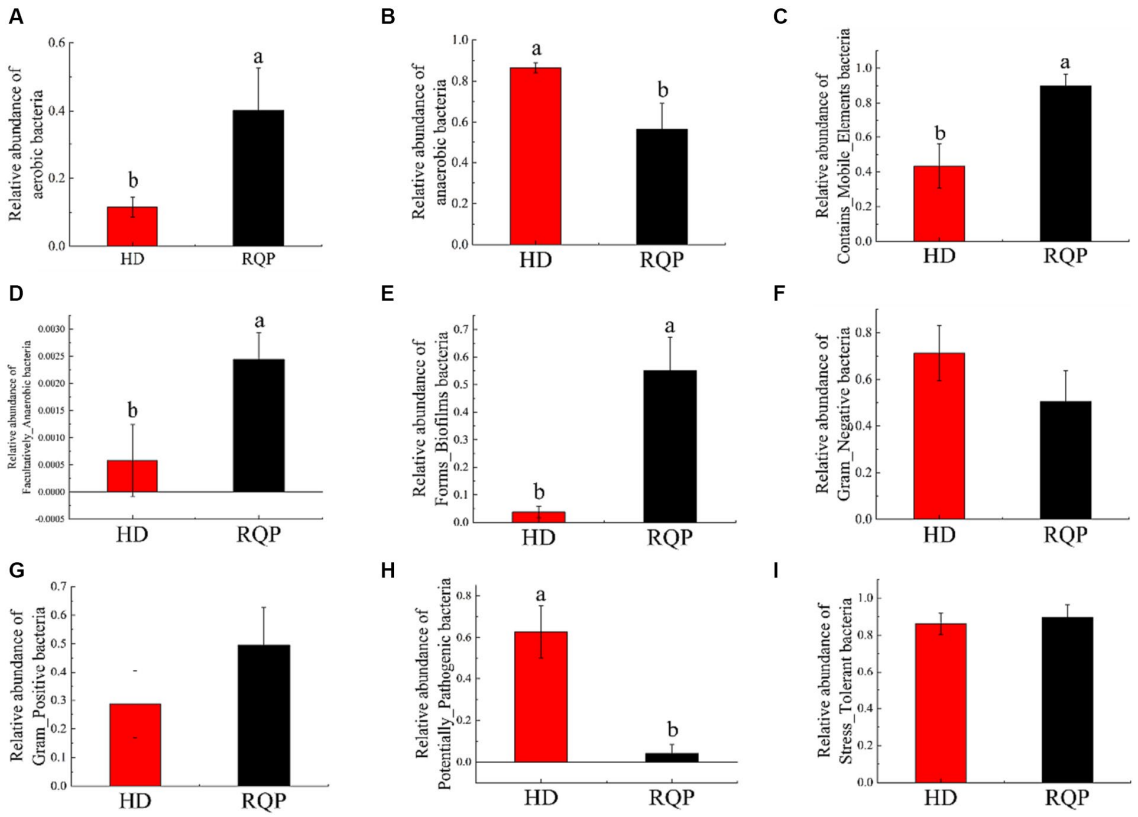

FIGURE 13
Effects of RQP on microbiome phenotypes. **(A)** aerobic bacteria; **(B)** anaerobic bacteria; **(C)** Contains_Mobile_Elements bacteria; **(D)** Facultatively_Anaerobic bacteria; **(E)** Forms_Biofilms bacteria; **(F)** Gram_Negative; **(G)** Gram_Positive; **(H)** Potentially_Pathogenic; **(I)** Stress_Tolerant. Data are presented as the mean ± SD ($n = 3$). Data followed by the different letters are significantly different ($p < 0.05$) by Duncan's test.

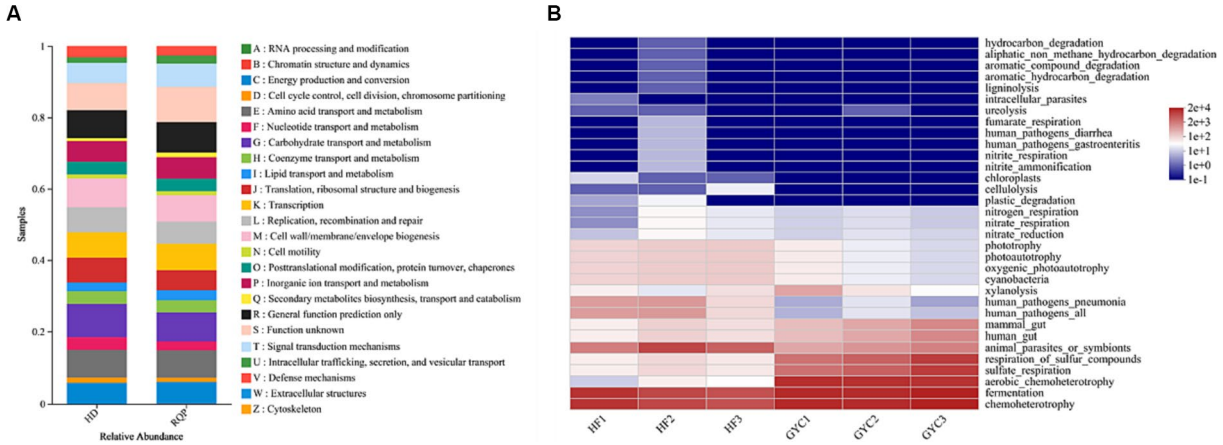

FIGURE 14
PICRUSt1 and FAPROTAX function prediction. **(A)** PICRUSt1 function prediction results stacked bar chart; **(B)** The prediction of intestinal microbiota function between HD and RQP by heatmap analysis.

2021). We investigated the regulatory effect of RQP on intestinal microflora by comparing special bacteria. The results showed that RQP intervention reversed the abundance of Bacteroidetes and Firmicutes, indicated that it could improve the proportion of bacteria in the body, inhibit the growth of some pathogenic bacteria and reduce inflammation (Ma Q. et al., 2022). Our study also found that *Akkermansia* was the dominant bacteria after RQP intervention, which was reported to produce SCFAs in the metabolic process, and expected to be a potential target for improving metabolic diseases such as obesity, diabetes, liver disease and cardiac metabolic disorders (Rodrigues et al., 2022). Another study showed that *Akkermansia* can also produce *Amuc _ 1100*, *P9* and other proteins which directly

involved in the regulation of glucose and lipid metabolism and immune response, while as stimulates glucagon-like peptide 1 (GLP-1) secretion by producing short-chain fatty acids such as acetic acid and propionic acid to regulate host energy balance and improve glucose homeostasis in mice (Yoon et al., 2021). In this study, increased *Akkermansia* may be one of the reasons that RQP intervention, could regulate glycolipid metabolism and inhibit the development of diabetes.

This study employed the PICRUSt1 approach to assess the abundance of OTUs at the functional level. Additionally, the BugBase analytic method was utilized to investigate the impact RQP on microbial phenotype. After RQP treatment, the abundance of biosynthetic and metabolic pathways was change, such as carbohydrate transport and metabolism and translation, ribosomal structure, and biogenesis. The observed decline in the abundance of anaerobic bacteria and potentially pathogenic bacteria inside the intestinal tract of the RQP group suggests that RQP has the capacity to mitigate the quantity of pathogenic bacteria and promote the restoration of intestinal health. The above results indicate that RQP can improve the biosynthetic pathway in diabetic mice, reduce intestinal metabolic disorders in mice, and reverse the potential risks of related pathogens.

5 Conclusion

In this study, RQP is a complex polysaccharide composed of a variety of monosaccharides, which has good antioxidant activity and α-amylase and α-glucosidase inhibitory activity *in vitro*. At the same time, this study indicated that RQP showed effective antioxidant and hypoglycemic activity in obese diabetic mice and regulated the structure of intestinal flora. Specifically, the supplementation of RQP reduced the weight gain of obese mice feed with a high-fat diet, which has regulated lipid metabolism and inhibited insulin resistance to reduce blood glucose. RQP also improved the antioxidant capacity of the body reduced inflammation and promoted the production of SCFAs in diabetic mice. Furthermore, structural alterations of the gut microbiota induced by high-fat diet were modulated by RQP, which would be one of the important hypoglycemic lipid-lowering mechanism. Our findings indicate that polysaccharides from red quinoa may possess potential health properties in alleviating the symptoms associated with T2D.

Data availability statement

The original contributions presented in the study are included in the article/Supplementary material, further inquiries can be directed to the corresponding authors.

Ethics statement

The animal study was approved by Experimental Animals Ethics Committee of Heilongjiang Bayi Agricultural University. The study was conducted in accordance with the local legislation and institutional requirements.

Author contributions

YZ: Conceptualization, Funding acquisition, Project administration, Resources, Writing – review & editing. YG: Formal analysis, Investigation, Software, Validation, Visualization, Writing – original draft. YC: Project administration, Supervision, Writing – review & editing. HT: Project administration, Supervision, Writing – review & editing.

Funding

The author(s) declare financial support was received for the research, authorship, and/or publication of this article. This work was supported by National Natural Science Foundation of China (32171676) and National Key Research and Development Program of China (2021YFD2100903).

Conflict of interest

The authors declare that the research was conducted in the absence of any commercial or financial relationships that could be construed as a potential conflict of interest.

Publisher's note

Supplementary material

The Supplementary material for this article can be found online at: https://www.frontiersin.org/articles/10.3389/fmicb.2024.1308866/full#supplementary-material

References

Athyros, V. G., Doumas, M., Imprialos, K. P., Stavropoulos, K., Georgianou, E., Katsimardou, A., et al. (2018). Diabetes and lipid metabolism. *Hormones* 17, 61–67. doi: 10.1007/s42000-018-0014-8

Campos, D., Chirinos, R., Galvez Ranilla, L., and Pedreschi, R. (2018). Bioactive potential of Andean fruits, seeds, and tubers. *Adv. Food Nutr. Res.* 84, 287–343. doi: 10.1016/bs.afnr.2017.12.005

Cani, P. D., Bibiloni, R., Knauf, C., Waget, A., Neyrinck, A. M., Delzenne, N. M., et al. (2008). Changes in gut microbiota control metabolic endotoxemia-induced inflammation in high-fat diet-induced obesity and diabetes in mice. *Diabetes* 57, 1470–1481. doi: 10.2337/db07-1403

Cao, Y., Zou, L., Li, W., Song, Y., Zhao, G., and Hu, Y. (2020). Dietary quinoa (*Chenopodium quinoa* Willd.) polysaccharides ameliorate high-fat diet-induced hyperlipidemia and modulate gut microbiota. *Int. J. Biol. Macromol.* 163, 55–65. doi: 10.1016/j.ijbiomac.2020.06.241

Chatterjee, S., Khunti, K., and Davies, M. J. (2017). Type 2 diabetes. *Lancet* 389, 2239–2251. doi: 10.1016/S0140-6736(17)30058-2

Ding, Y., Yan, Y., Peng, Y., Chen, D., Mi, J., Lu, L., et al. (2019). In vitro digestion under simulated saliva, gastric and small intestinal conditions and fermentation by human gut microbiota of polysaccharides from the fruits of *Lycium barbarum*. *Int. J. Biol. Macromol.* 125, 751–760. doi: 10.1016/j.ijbiomac.2018.12.081

Guo, J., Zhang, M., Wang, H., Li, N., Lu, Z., Li, L., et al. (2022). Gut microbiota and short chain fatty acids partially mediate the beneficial effects of inulin on metabolic disorders in obese Ob/Ob mice. *J. Food Biochem.* 46:e14063. doi: 10.1111/jfbc.14063

Gurung, M., Li, Z., You, H., Rodrigues, R., Jump, D. B., Morgun, A., et al. (2020). Role of gut microbiota in type 2 diabetes pathophysiology. *EBioMedicine* 51:102590. doi: 10.1016/j.ebiom.2019.11.051

Hu, Y., Zhang, J., Zou, L., Fu, C., Li, P., and Zhao, G. (2017). Chemical characterization, antioxidant, immune-regulating and anticancer activities of a novel bioactive polysaccharide from *Chenopodium quinoa* seeds. *Int. J. Biol. Macromol.* 99, 622–629. doi: 10.1016/j.ijbiomac.2017.03.019

Huang, H., and Huang, G. (2020). Extraction, separation, modification, structural characterization, and antioxidant activity of plant polysaccharides. *Chem. Biol. Drug Des.* 96, 1209–1222. doi: 10.1111/cbdd.13794

Huang, G., Mei, X., and Hu, J. (2017). The antioxidant activities of natural polysaccharides. *Curr. Drug Targets* 18, 1296–1300. doi: 10.2174/1389450118666170123145357

Jiang, S., Du, P., An, L., Yuan, G., and Sun, Z. (2013). Anti-diabetic effect of Coptis Chinensis polysaccharide in high-fat diet with STZ-induced diabetic mice. *Int. J. Biol. Macromol.* 55, 118–122. doi: 10.1016/j.ijbiomac.2012.12.035

Kane, J. P., Pullinger, C. R., Goldfine, I. D., and Malloy, M. J. (2021). Dyslipidemia and diabetes mellitus: role of lipoprotein species and interrelated pathways of lipid metabolism in diabetes mellitus. *Curr. Opin. Pharmacol.* 61, 21–27. doi: 10.1016/j.coph.2021.08.013

Ke, J., Jiang, G., Shen, G., Wu, H., Liu, Y., and Zhang, Z. (2020). Optimization, characterization and rheological behavior study of pectin extracted from chayote (*Sechium edule*) using ultrasound assisted method. *Int. J. Biol. Macromol.* 147, 688–698. doi: 10.1016/j.ijbiomac.2020.01.055

Lan, T., Tang, T., Li, Y., Duan, Y., Yuan, Q., Liu, W., et al. (2023). FTZ polysaccharides ameliorate kidney injury in diabetic mice by regulating gut-kidney axis. *Phytomedicine* 118:154935. doi: 10.1016/j.phymed.2023.154935

Li, F., Pak, S., Zhao, J., Wei, Y., Zhang, Y., and Li, Q. (2021). Structural characterization of a neutral polysaccharide from Cucurbia moschata and its uptake behaviors in Caco-2 cells. *Food Secur.* 10:2357. doi: 10.3390/foods10102357

Liu, C., Feng, X., Li, Q., Wang, Y., Li, Q., and Hua, M. (2016). Adiponectin, TNF-alpha and inflammatory cytokines and risk of type 2 diabetes: a systematic review and meta-analysis. *Cytokine* 86, 100–109. doi: 10.1016/j.cyto.2016.06.028

Liu, G., Liang, L., Yu, G., and Li, Q. (2018). Pumpkin polysaccharide modifies the gut microbiota during alleviation of type 2 diabetes in rats. *Int. J. Biol. Macromol.* 115, 711–717. doi: 10.1016/j.ijbiomac.2018.04.127

Luo, D., Dong, X., Huang, J., Huang, C., Fang, G., and Huang, Y. (2021). *Pueraria lobata* root polysaccharide alleviates glucose and lipid metabolic dysfunction in diabetic db/db mice. *Pharm. Biol.* 59, 382–390. doi: 10.1080/13880209.2021.1898648

Lv, Q. Q., Cao, J. J., Liu, R., and Chen, H. Q. (2021). Structural characterization, alpha-amylase and alpha-glucosidase inhibitory activities of polysaccharides from wheat bran. *Food Chem.* 341:128218. doi: 10.1016/j.foodchem.2020.128218

Ma, Q., Li, Y., Li, P., Wang, M., Wang, J., Tang, Z., et al. (2019). Research progress in the relationship between type 2 diabetes mellitus and intestinal flora. *Biomed. Pharmacother.* 117:109138. doi: 10.1016/j.biopha.2019.109138

Ma, G., Xu, Q., Du, H., Muinde Kimatu, B., Su, A., Yang, W., et al. (2022). Characterization of polysaccharide from Pleurotus eryngii during simulated gastrointestinal digestion and fermentation. *Food Chem.* 370:131303. doi: 10.1016/j.foodchem.2021.131303

Ma, Q., Zhai, R., Xie, X., Chen, T., Zhang, Z., Liu, H., et al. (2022). Hypoglycemic effects of *Lycium barbarum* polysaccharide in type 2 diabetes mellitus mice via modulating gut microbiota. *Front. Nutr.* 9:916271. doi: 10.3389/fnut.2022.916271

Magliano, D. J., and Boyko, E. J.IDF Diabetes Atlas 10th edition scientific committee; (2021). *IDF diabetes Atlas*, *10th* Edn. Brussels: International Diabetes Federation

Mao, D., Tian, X. Y., Mao, D., Hung, S. W., Wang, C. C., Lau, C. B. S., et al. (2020). A polysaccharide extract from the medicinal plant Maidong inhibits the IKK–NF-κB pathway and IL-1β–induced islet inflammation and increases insulin secretion. *J. Biol. Chem.* 295, 12573–12587. doi: 10.1074/jbc.RA120.014357

Mu, S., Yang, W., and Huang, G. (2021). Antioxidant activities and mechanisms of polysaccharides. *Chem. Biol. Drug Des.* 97, 628–632. doi: 10.1111/cbdd.13798

Pasaoglu, H., Sancak, B., and Bukan, N. (2004). Lipid peroxidation and resistance to oxidation in patients with type 2 diabetes mellitus. *Tohoku J. Exp. Med.* 203, 211–218. doi: 10.1620/tjem.203.211

Portincasa, P., Bonfrate, L., Vacca, M., De Angelis, M., Farella, I., Lanza, E., et al. (2022). Gut microbiota and short chain fatty acids: implications in glucose homeostasis. *Int. J. Mol. Sci.* 23:1105. doi: 10.3390/ijms23031105

Rauf, A., Khalil, A. A., Rahman, U. U., Khalid, A., Naz, S., Shariati, M. A., et al. (2022). Recent advances in the therapeutic application of short-chain fatty acids (SCFAs): An updated review. *Crit. Rev. Food Sci. Nutr.* 62, 6034–6054. doi: 10.1080/10408398.2021.1895064

Rehman, K., and Akash, M. S. H. (2017). Mechanism of generation of oxidative stress and pathophysiology of type 2 diabetes mellitus: how are they interlinked? *J. Cell. Biochem.* 118, 3577–3585. doi: 10.1002/jcb.26097

Ren, G., Teng, C., Fan, X., Guo, S., Zhao, G., Zhang, L., et al. (2023). Nutrient composition, functional activity and industrial applications of quinoa (*Chenopodium quinoa* Willd.). *Food Chem.* 410:135290. doi: 10.1016/j.foodchem.2022.135290

Rodrigues, V. F., Elias-Oliveira, J., Pereira, I. S., Pereira, J. A., Barbosa, S. C., Machado, M. S. G., et al. (2022). Akkermansia muciniphila and gut immune system: a good friendship that attenuates inflammatory bowel disease, obesity, and diabetes. *Front. Immunol.* 13:934695. doi: 10.3389/fimmu.2022.934695

Saeedi, P., Petersohn, I., Salpea, P., Malanda, B., Karuranga, S., Unwin, N., et al. (2019). Global and regional diabetes prevalence estimates for 2019 and projections for 2030 and 2045: results from the international diabetes federation diabetes Atlas, 9(th) edition. *Diabetes Res. Clin. Pract.* 157:107843. doi: 10.1016/j.diabres.2019.107843

Salgaco, M. K., Oliveira, L. G. S., Costa, G. N., Bianchi, F., and Sivieri, K. (2019). Relationship between gut microbiota, probiotics, and type 2 diabetes mellitus. *Appl. Microbiol. Biotechnol.* 103, 9229–9238. doi: 10.1007/s00253-019-10156-y

Sivaprakasam, S., Prasad, P. D., and Singh, N. (2016). Benefits of short-chain fatty acids and their receptors in inflammation and carcinogenesis. *Pharmacol. Ther.* 164, 144–151. doi: 10.1016/j.pharmthera.2016.04.007

Tan, M., Zhao, Q., and Zhao, B. (2021). Physicochemical properties, structural characterization and biological activities of polysaccharides from quinoa (*Chenopodium quinoa* Willd.) seeds. *Int. J. Biol. Macromol.* 193, 1635–1644. doi: 10.1016/j.ijbiomac.2021.10.226

Wang, C., Yin, Y., Cao, X., and Li, X. (2016). Effects of Maydis stigma polysaccharide on the intestinal microflora in type-2 diabetes. *Pharm. Biol.* 54, 3086–3092. doi: 10.1080/13880209.2016.1211153

Wang, G., Yu, Y., Wang, Y. Z., Wang, J. J., Guan, R., Sun, Y., et al. (2019). Role of SCFAs in gut microbiome and glycolysis for colorectal cancer therapy. *J. Cell. Physiol.* 234, 17023–17049. doi: 10.1002/jcp.28436

Wu, J., Wang, K., Wang, X., Pang, Y., and Jiang, C. (2021). The role of the gut microbiome and its metabolites in metabolic diseases. *Protein Cell* 12, 360–373. doi: 10.1007/s13238-020-00814-7

Yang, Y., Chang, Y., Wu, Y., Liu, H., Liu, Q., Kang, Z., et al. (2021). A homogeneous polysaccharide from *Lycium barbarum*: structural characterizations, anti-obesity effects and impacts on gut microbiota. *Int. J. Biol. Macromol.* 183, 2074–2087. doi: 10.1016/j.ijbiomac.2021.05.209

Yaribeygi, H., Sathyapalan, T., Atkin, S. L., and Sahebkar, A. (2020). Molecular mechanisms linking oxidative stress and diabetes mellitus. *Oxid. Med. Cell. Longev.* 2020:8609213. doi: 10.1155/2020/8609213

Ye, G., Li, J., Zhang, J., Liu, H., Ye, Q., and Wang, Z. (2021). Structural characterization and antitumor activity of a polysaccharide from Dendrobium wardianum. *Carbohydr. Polym.* 269:118253. doi: 10.1016/j.carbpol.2021.118253

Yoon, H. S., Cho, C. H., Yun, M. S., Jang, S. J., You, H. J., Kim, J. H., et al. (2021). *Akkermansia muciniphila* secretes a glucagon-like peptide-1-inducing protein that improves glucose homeostasis and ameliorates metabolic disease in mice. *Nat. Microbiol.* 6, 563–573. doi: 10.1038/s41564-021-00880-5

Yuan, R., Tao, X., Liang, S., Pan, Y., He, L., Sun, J., et al. (2018). Protective effect of acidic polysaccharide from Schisandra chinensis on acute ethanol-induced liver injury through reducing CYP2E1-dependent oxidative stress. *Biomed. Pharmacother.* 99, 537–542. doi: 10.1016/j.biopha.2018.01.079

Zang, Y., Du, C., Ru, X., Cao, Y., and Zuo, F. (2023). Anti-diabetic effect of modified 'Guanximiyou' pummelo peel pectin on type 2 diabetic mice via gut microbiota. *Int. J. Biol. Macromol.* 242:124865. doi: 10.1016/j.ijbiomac.2023.124865

Zhang, Z., Fan, S., Huang, D., Xiong, T., Nie, S., and Xie, M. (2020). Polysaccharides from fermentedAsparagus officinaliswithLactobacillus plantarumNCU116 alleviated liver injuryviamodulation of glutathione homeostasis, bile acid metabolism, and SCFA production. *Food Funct.* 11, 7681–7695. doi: 10.1039/D0FO01435D

Zhang, Y., Luo, L., Li, Z., Li, H., Yao, X., and Luo, R. (2019). Anti-lipid peroxidation,α-glucosidase andα-amylase inhibitory effects of the extract of Capitula ofCoreopsis tinctoriaNutt. And protection effects on high-fat/high-sugar and Streptozotocin-induced type 2 diabetes in mice. *Chem. Biodivers.* 16:e1900514. doi: 10.1002/cbdv.201900514

Zhao, H., Li, M., Liu, L., Li, D., Zhao, L., Wu, Z., et al. (2023). Cordyceps militaris polysaccharide alleviates diabetic symptoms by regulating gut microbiota against TLR4/NF-κB pathway. *Int. J. Biol. Macromol.* 230:123241. doi: 10.1016/j.ijbiomac.2023.123241

frontiers | Frontiers in Microbiology

TYPE Original Research
PUBLISHED 18 March 2024
DOI 10.3389/fmicb.2024.1305617

OPEN ACCESS

EDITED BY
Xiaodong Xia,
Dalian Polytechnic University, China

REVIEWED BY
Mongkol Thirabunyanon,
Maejo University, Thailand
Zhigang Liu,
Northwest A&F University, China

*CORRESPONDENCE
She-Ching Wu
✉ scwu@mail.ncyu.edu.tw
Bao-Hong Lee
✉ bhlee@mail.ncyu.edu.tw

RECEIVED 02 October 2023
ACCEPTED 26 February 2024
PUBLISHED 18 March 2024

CITATION
Hsiao Y-K, Lee B-H and Wu S-C (2024) *Lactiplantibacillus plantarum-encapsulated* microcapsules prepared from okra polysaccharides improved intestinal microbiota in Alzheimer's disease mice. *Front. Microbiol.* 15:1305617. doi: 10.3389/fmicb.2024.1305617

Lactiplantibacillus plantarum-encapsulated microcapsules prepared from okra polysaccharides improved intestinal microbiota in Alzheimer's disease mice

Yao-Kun Hsiao[1,2], Bao-Hong Lee[3]* and She-Ching Wu[2]*

[1]King Long Guan Company Ltd., Chiayi, Taiwan, [2]Department of Food Sciences, National Chiayi University, Chiayi, Taiwan, [3]Department of Horticultural Science, National Chiayi University, Chiayi, Taiwan

Background: Okra contains a viscous substance rich in water-soluble material, including fibers, pectin, proteoglycans, gum, and polysaccharides. This study explored the use of okra polysaccharides by microorganisms and their potential to improve microbiota.

Methods: The regulation of microcapsules prepared from okra polysaccharides with or without *L. plantarum* encapsulation on intestinal microbiota was assessed through 16S metagenomic analysis and short-chain fatty acids (SCFAs) in App$^{NL\text{-}G\text{-}F/NL\text{-}G\text{-}F}$ mice (Alzheimer's disease; AD model).

Results: We found that *Lactobacillaceae* and *Lactobacillus* were majorly regulated by microcapsules prepared from okra polysaccharides in AD mice. Similarly, microcapsules prepared from okra polysaccharides with *L. plantarum* encapsulation markedly elevated the abundance of *Lactobacillaceae* and *Lactobacillus* and increased SCFAs in AD mice.

Conclusion: Our results suggest that microcapsules prepared from okra polysaccharides with or without *L. plantarum* encapsulation may improve intestinal microbiota by elevating *Lactobacillus* levels in AD mice.

KEYWORDS

okra polysaccharides, microcapsules, microbiota, short-chain fatty acids, Alzheimer's disease

1 Introduction

There are approximately 10^{13}–10^{14} microbial cells in the human gastrointestinal tract, which is 10 times the total number of human cells; the total number of genes expressed by microorganisms exceeds the total number of human genes expressed by approximately 150 times or more (Qin et al., 2020). In terms of taxonomy, 50 phyla of microorganisms have been discovered and defined, of which 10 are found in the gut, including primarily *Bacteroides* spp., followed by *Actinobacteria* and *Proteobacteria* (Rajilic-Stojanovic et al., 2011).

The goblet cells and enterocytes in the gut produce mucin and mucus, and many gut microbes can use these substances as a source of growth nutrients (prebiotics) for their own growth and reproduction and to produce short-chain fatty acids (e.g., acetic acid, propionic acid, butyric acid, and valeric acid). Microorganisms that have this ability (e.g., *Akkermansia muciniphila* and *Faecalibacterium prausnitzii*) are known as next-generation probiotics, and their role is valued due to the ability of short-chain fatty acids to inhibit intestinal pathogens (Machiels et al., 2014; De la Cuesta-Zuluaga et al., 2017).

In addition to being consumed as a vegetable, okra (*Abelmoschus esculentus*) is also used in traditional medicine (Lengsfeld et al., 2004; Sengkhamparn et al., 2009; Sami et al., 2013). Okra contains a viscous substance that is rich in polysaccharides. Studies have reported that okra contains water-soluble fibers, such as pectin, proteoglycans, and gum arabic, which can be used as thickeners in cooking and food preparation (Woolfe et al., 1977; BeMiller et al., 1993), and have the characteristics of high viscosity, strong stability, and good suspension (Romanchik-Cerpovicz et al., 2002). Chemical analysis revealed that okra polysaccharides are composed of rhamnose, xylose, galactose, and arabinose (Sami et al., 2013). An early study extracted viscous substances from okra via acid hydrolysis and found that galactose, rhamnose, and galacturonic acid are the major carbohydrates in okra (Whistler and Conrad, 1954). It has also been suggested that the viscous substances extracted from okra are composed of acidic polysaccharides, proteins, and minerals. After hydrolysis, the ratios of galacturonic acid, galactose, rhamnose, and glucose obtained by colloidal chromatography were 1.3:1.0:0.1:0.1, respectively (Woolfe et al., 1977). In recent years, many research reports have pointed out that okra polysaccharides have neuroprotective functions, which can reduce nerve damage caused by amyloid beta and metabolic syndrome (Huang et al., 2020; Yan et al., 2020b; Huang et al., 2023). Due to the increasing attention to the relationship between neurodegenerative diseases and gut microbiota (Zhou et al., 2012), although there are relevant literature reports on the effect of okra polysaccharides on neurological diseases, the potential of okra polysaccharides to regulate gut microbiota to alleviate neurodegenerative diseases still needs further evaluation. Therefore, this study utilized $App^{NL\text{-}G\text{-}F/NL\text{-}G\text{-}F}$ mice to investigate the ability of okra polysaccharides to modulate the gut microbiota composition.

To date, large numbers of studies have explored the relationship between gut microbiota and Alzheimer's disease (AD), and many intestinal microbes have been found to accelerate its progression (Zhou et al., 2012). These microbes are often associated with metabolic diseases; a high proportion of Firmicutes/Bacteroidetes microbes is linked to intestinal inflammation and an increase in the incidence of AD (Soscia et al., 2010; Cowan et al., 2014; Chen et al., 2016). In the $App^{NL\text{-}G\text{-}F/NL\text{-}G\text{-}F}$ mouse model, in which Aβ accumulates without the overexpression of APP, leading to artificial phenotypes, Aβ deposition starts at 2 months of age, and plaques accumulate over time (Sakakibara et al., 2018). There are three mutations within the Aβ sequence in APP peptides, Aβ amyloidosis is aggressively accelerated, and neuroinflammation is observed in subcortical structures and cortical regions. These observations consistently indicate that $App^{NL\text{-}G\text{-}F/NL\text{-}G\text{-}F}$ mice represent a model for preclinical AD and are useful for studying AD prevention rather than treatment after neurodegeneration (Sakakibara et al., 2018). Several studies have explored the relationship between intestinal flora and AD. Many intestinal microorganisms have been found to accelerate AD progression, and these microorganisms are usually associated with metabolic diseases. Chen et al. (2016) confirmed that the amyloid protein produced by microorganisms in the intestine enters the central nervous system through the bloodstream and increases the aggregation and deposition of Aβ.

Because okra polysaccharides are mucin-like polysaccharides, these macromolecules are similar to mucin and mucus secreted by human intestinal cells (enterocytes and goblet cells) and may maintain the intestinal barrier and prevent the penetration of microorganisms into the intestinal lumen. When harmful bacteria exist in large quantities in the intestinal tract, the epithelial cells of the intestinal tract lose their normal physiological functions, resulting in inflammation and increased permeability of intestinal cells (gut permeability), a phenomenon known as leaky gut (Turner, 2009). The viscous substance in okra contains polysaccharides, which can be used as a material to promote the growth of probiotics to improve intestinal health. Okra polysaccharides have the ability to modulate the gut microbiome and thus are able to inhibit inflammation (Yan et al., 2020a,b). Microcapsules are materials with encapsulating structures that can protect their contents. In many healthy products, microcapsules are used to encapsulate probiotics to increase their survival ability in the intestine. Carbohydrates and polysaccharides are commonly used materials for preparing microcapsules. In this study, okra polysaccharides were used as a common material for encapsulating probiotic (*Lactiplantibacillus plantarum*) microcapsules. Additionally, the intestinal protective effect of okra polysaccharides against gut microbiota dysfunction was evaluated in this study.

2 Methods

2.1 The preparation of okra polysaccharides

The dried experimental okra stored at 4°C was taken out and pulverized, and the extraction was carried out with hot water for 3 h with double distilled water. After extraction, sedimentation was carried out with 4-fold the volume of 95% ethanol, and finally, the sediment was dried in a freeze dryer; the obtained powder is okra crude polysaccharide, which is stored in a 4°C refrigerator for the determination of polysaccharide content and subsequent experiments. To ensure whether the crude okra polysaccharide has residual protein, take 50 μL of okra polysaccharide aqueous solution, mix it with 200 μL of protein quantitative analysis solution (Bio-Rad, United States) in a 96-well culture plate, and observe its color change for 2 min. The original solution of protein quantitative analysis solution is reddish-brown, and the Coomassie Brilliant Blue G-250 contained in it will combine with protein and turn into blue, which can confirm no protein contamination in crude okra polysaccharide.

2.2 Assay for polysaccharides properties

Polysaccharide concentrations were determined using the phenol–sulfuric acid method (Dubois et al., 1956). Glucose solutions (0, 25, 50, 75, 100, and 125 mg/L) were prepared for use as standards. Then, 1 mL of glucose standard solutions (different concentrations) or sample (okra polysaccharides) were mixed with 0.5 mL of 5% phenol

and 2.5 mL of sulfuric acid and allowed the reaction for 20 min at room temperature. The absorbance was measured at 490 nm with spectrophotometer, and the concentration of polysaccharides was calculated from the standard curve. The molecular weight of okra polysaccharides was identified by nuclear magnetic resonance (NMR). The okra polysaccharides were fluorescently labeled according to the manual (SugarLighter, New Taipei City, Taiwan). In brief, adlay polysaccharide powder (1 mg) was mixed with hydrolysis solution (1 mL) for reaction at 80°C for 2 h. The solution was mixed with 2 mg 2,3-naphthalenediamine, 1 mg iodine, and 1 mL acetic acid (stirring for 1 h) for monosaccharide fluorescent labeling (Lin et al., 2010). The molecule weight was measured by diffusion ordered NMR spectroscopy (DOSY, Bruker AV600) at 600 MHz to obtain the diffusion coefficient and H1 profile (Lee et al., 2023).

2.3 *Lactiplantibacillus plantarum* culture

Lactiplantibacillus plantarum were purchased from the Bioresource Collection and Research Center (BCRC11697) in Taiwan (Hsinchu, Taiwan). These lactic acid bacteria were inoculated into MRS broth (BD Biosciences, San Jose, Calif., United States) or MRS agar at 37°C and transferred monthly. This strain has been reported to exhibit anti-cancer (Liu and Pan, 2010) and use in fermentation (Kuo et al., 2021).

2.4 Preparation of okra polysaccharide microencapsules

The okra polysaccharides were mixed with sodium alginate (4.5, 5, and 5.5%) in different proportions to prepare wall material solution. Subsequently, the core material solution (2 x 10^{10}CFU/mL lactic acid bacteria suspension) was mixed with wall material solution at 1: 1 (w/w). This mixed solution was transported and separated by gas and solidify by 5% $CaCl_2$ for 20 min for microcapsulation (Nasiri et al., 2021). The crystal microcapsules were washed and frozen-dried.

2.5 Analysis of microencapsule properties

For encapsulation efficiency, the okra polysaccharides were used as the stock solution and diluted with deionized water into five different concentrations, and then, the absorbance was measured with a spectrophotometer to make a standard calibration. The absorbance of okra polysaccharide microcapsules was measured, and the encapsulation efficiency was calculated according to a study by Nasiri et al. (2021). For swelling capacity, the 0.3 g of sample into a 10 mL graduated cylinder, add 10 mL of distilled water and let stand at room temperature for 24 h, then read the volume of the impregnated sample (Ralet and Della, 1993). For the mechanical strength test, the microencapsules (3 g) were stained by crystal violet and add 30 mL of deionized water. This microcapsules solution was stirred at 400 ± 10 rpm for 180 min, and the morphology and broken were observed and calculated.

2.6 Animals treatment

The $App^{NL\text{-}G\text{-}F/NL\text{-}G\text{-}F}$ mice contained a humanized amyloid beta (Aβ) region and introduced the Swedish mutation and the Beyreuther/Iberian mutation into the mouse amyloid precursor protein (APP) gene. This mouse model will overexpression Aβ42 and a high Aβ42/40 ratio, which causes cognitive decline at 6 months. Animals (10 months old) were divided into three groups ($n = 6$/group), including Group-A: transgenic (TG) mice group ($App^{NL\text{-}G\text{-}F/NL\text{-}G\text{-}F}$ mice), Group-B: TG mice administered with microcapsules (200 mg/kg bw) prepared from okra polysaccharides were mixed with sodium alginate (5%), and Group-C: TG mice administered with *L. plantarum*-encapsulated microcapsules (200 mg/kg bw) prepared from okra polysaccharides were mixed with sodium alginate (5%). The dosage (200 mg/kg bw) of okra polysaccharides was accorded to a study, which could show bioactivity (Liao et al., 2019). All animals were kept in the cages at 25 ± 2°C under the 12-h/12-h light/dark cycle, and the relative humidity was 55 ± 10% with free to water and fed. Experimental animals used in this study had been reviewed and approved by the Institutional Animal Care and Use Committee (IACUC) in National Cheng Kung University in Taiwan with IACUC approval No. 108317. At the end of the experiment, the mice were deprived of food for 12 h and were euthanized with carbon dioxide. Intestinal feces were collected and stored at −20°C until analyzed.

2.7 Assays for intestinal microbiota

Feces in the colon of each mouse (n = 6) were collected and immediately soaked in liquid nitrogen and stored at −80°C for subsequent use. The total genomic DNA from samples was extracted using QIAamp PowerFecal DNA Kit (Qiagen) for 16S gene sequencing. V3–V4 region was amplified by specific primer set (319F, 5'-CCTACGGGNGGCWGCAG-3′, 806R, 5'-GACTACHVGGGT ATCTAATCC-3′) according to Illumina MiSeq PE300 platform. In brief, 12.5 ng of gDNA was used for the PCR reaction under the conditions: 95°C for 3 min; 25 cycles of: 95°C for 30 s, 55°C for 30 s, 72°C for 30 s; 72°C for 5 min and hold at 4°C. 16S analysis using QIIME2 alignment platform[1] with SILVA132 annotation database.

2.8 Assay for short-chain fatty acids

The levels of SCFAs such as acetic acid, propionic acid, and butyric acid were performed by gas chromatography–flame ionization detection (GC-FID) that used the Shimadzu GC-2010 (Shimadzu Corp, Tokyo, Japan) with a capillary column (BP21 FFAP 30 m × 0.53 mm i.d., 0.50 μm film thickness, Trajan, Melbourne, Australia). The carrier gas was nitrogen, and the split less injection volume was 1 μL. Auxiliary gasses for the flame ionization detector were hydrogen (30 mL/min of flow rate) and dry air (300 mL/min of flow rate). The temperatures of the injector and detector were 220°C and 240°C, respectively. The temperature of the GC oven was first set at 90°C for 1 min and elevated to 150°C at 10°C/min, then to 200°C

1 v2019.7.0; https://qiime2.org/

at 20°C/min, and following held for 1 min. Triplicate repeats were analyzed, and the obtained data were normalized to the concentrations of external standards and are shown in μM (Lee et al., 2021a).

2.9 Statistical analysis

The experiments were performed in five repeats, and the results are expressed as the mean ± standard error of mean. The results were examined by using one-way analysis of variance and Duncan's multiple range tests, and the significance of differences between sample means was calculated. A p-value of ≤0.05 was considered significant. For β diversity of microbiota analysis, pairwise analysis of similarities (ANOSIM) with permutations were conducted and evaluated using principal coordinate analysis (PCoA) based on different distance matrices, where p-values were reported after Benjamini–Hochberg multiple testing correction. The value corresponding to the heatmap represents the Z-score obtained by the abundance of each species in all groups. The Z-score of a sample on a certain classification is the value of the average abundance of the sample on the category and all samples in the classification. Linear discriminant analysis (LDA) effect size (LEfSe) uses non-parametric factorial Kruskal–Wallis (KW) sum-rank test to find species with significant differences in abundance and uses linear regression discriminant analysis (LDA) to estimate the impact of abundance of each species to find out the communities or species that have a significant difference in the sample division. LEfSe analysis of the screening value of LDA score is set to 4.

3 Results

3.1 Molecular weight of okra polysaccharides

On analysis of the composition of okra polysaccharides, the proportion of water-soluble polysaccharides was found as 84% (W/W). The okra monosaccharide composition was composed of glucose (20.1%), mannose (16.7%), galactose (19.2%), arabinose (13.5%), xylose (5.7%), fructose (16.7%), and rhamnose (4.2%) (Table 1). The molecular weight distribution of okra polysaccharides by NMR spectrum has been performed. The molecular weight of polysaccharides ranges from 1 KDa to 2,767 KDa, and the highest peak of diffusion coefficient is the molecular weight of 1 KDa. The spectrum of 18 Da is solvent (H_2O) (Figure 1).

TABLE 1 Monosaccharide composition.

Monosaccharide composition	Ratio (%)
Glucose	20.1 ± 1.5
Mannose	16.7 ± 2.1
Galactose	19.2 ± 1.4
Arabinose	13.5 ± 0.8
Xylose	5.7 ± 0.3
Fructose	16.7 ± 2.7
Rhamnose	4.2 ± 0.6

Data are shown as mean ± SD (n = 3).

3.2 Analysis of microcapsules properties

The microcapsules were prepared from okra polysaccharides with different concentration of sodium alginate (4.5, 5, and 5.5%). We found that low concentration (4.5%) of sodium alginate resulted in serious tailing phenomenon in microcapsules, which may cause of low viscosity to lead to incomplete formation. From these results, it can be concluded that the mixed colloid with a sodium alginate concentration of 5.0% is the most suitable condition for the preparation of okra polysaccharide microcapsules (Figure 2A). The encapsulation efficiency, swelling capacity, and mechanical strength test of microcapsules prepared from okra polysaccharides with different concentration of sodium alginate were evaluated (Figure 2B). The encapsulation efficiency is related to the concentration of the wall material, the properties of the wall material, and the interaction between chemical molecules. The results showed that highest encapsulation efficiency (79.86%) could be found in microcapsules prepared from okra polysaccharides with 5% sodium alginate. The microcapsules were mixed with water, and then, the swelling capacity was investigated. The results for moisture content and particle size of microcapsules prepared from okra polysaccharides with sodium alginate are shown in Supplementary Table S1. The different particle sizes (214 μm, 237 μm, and 248 μm) were found in microcapsules by various concentrations of sodium alginate (4.5, 5, and 5.5%). We found that the concentration of sodium alginate markedly affected swelling capacity (4.5% > 5.5% > 5%) in microcapsules prepared from okra polysaccharides. In addition, the mechanical strength test was evaluated, which suggested that 5 and 5.5% sodium alginate could elevate resistance against microcapsules broken (Figure 2B).

3.3 Effects of administration with microcapsules prepared from okra polysaccharides with or without *Lactiplantibacillus plantarum* encapsulation on intestinal microbial diversity in App$^{NL\text{-}G\text{-}F/NL\text{-}G\text{-}F}$ mice

The intestinal flora is closely related to the health of the human body and the development of diseases. In healthy individuals, the microbiota in the intestinal environment originally has a balanced bacterial composition, with imbalance arising in conjunction with aging, stress, environment, and dietary habits. The composition of the intestinal flora changes and causes some flora to form dominant species in the intestinal ecological environment. To assess whether okra polysaccharides have potential to regulate intestinal microbiota *in vivo*, the fecal bacteria of mice were subjected to 16S metagenomic analysis in this study. The Simpson index was used to evaluate microbial alpha diversity in the intestine, and the index was negatively correlated with diversity. The AD mice were administered with microcapsules prepared from okra polysaccharides with or without *L. plantarum* encapsulation which increased bacterial alpha diversity compared to the AD mice (Figure 3A). Moreover, 233, 109, and 116 different bacteria (operational taxonomic units; OTU) were found in

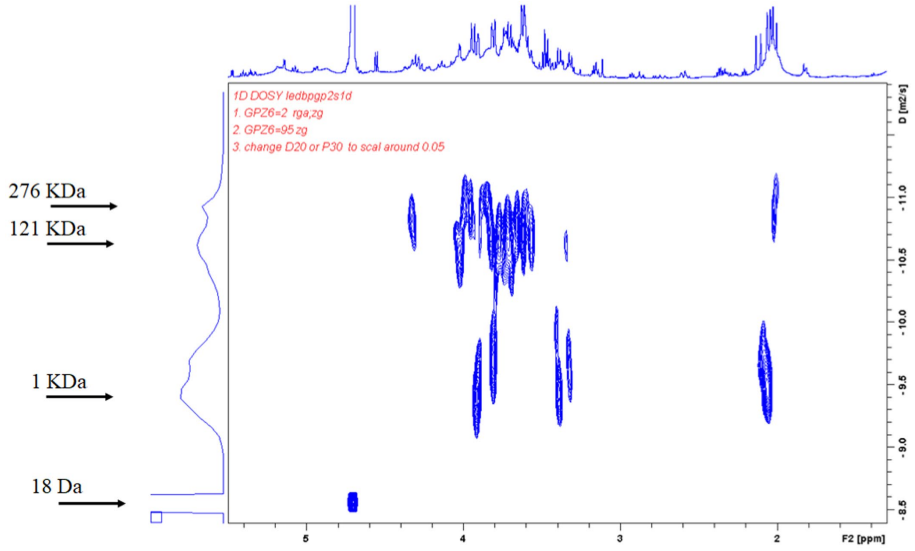

FIGURE 1
Diffusion-ordered NMR spectroscopy (DOSY) spectrum of adlay polysaccharides. Average molecular weight of purified adlay polysaccharides was determined and shown by 2D DOSY spectra. The horizontal axis represents the peak of NMR hydrogen ion absorption, and the vertical axis represents the self-diffusion coefficients. The molecular weight of polysaccharides ranges from 1 KDa to 2,767 KDa, and the highest peak of diffusion coefficient is the molecular weight of 1 KDa. The spectrum of 18 Da is solvent (H_2O).

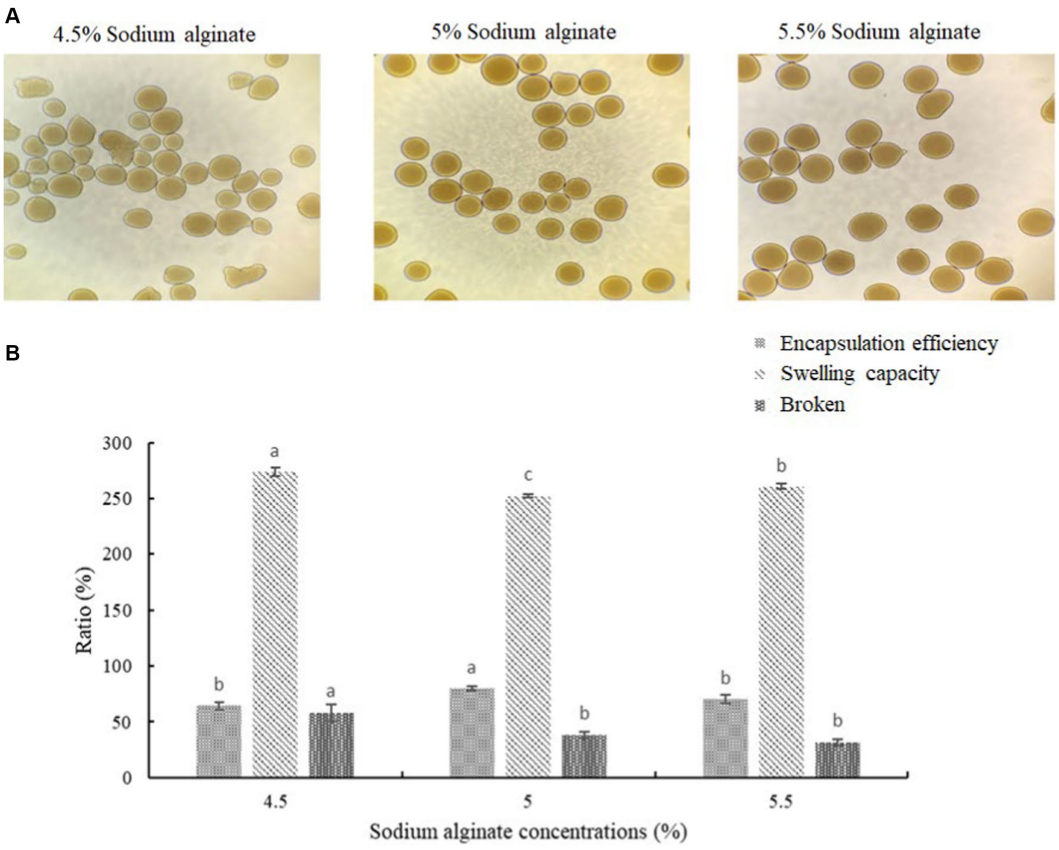

FIGURE 2
Effects of different sodium alginate concentrations on appearance of okra polysaccharide microcapsules. **(A)** Morphology of microcapsules prepared by 4.5, 5%, or 5.5% sodium alginate with okra polysaccharides. **(B)** Encapsulation efficiency, swelling capacity, and mechanical strength test (broken) of okra polysaccharide microcapsules with different sodium alginate concentrations. *Each value is expressed as mean ± S.D. ($n = 3$). Each value on the top right of means in the same column bearing of different letters is significantly different ($p < 0.05$).

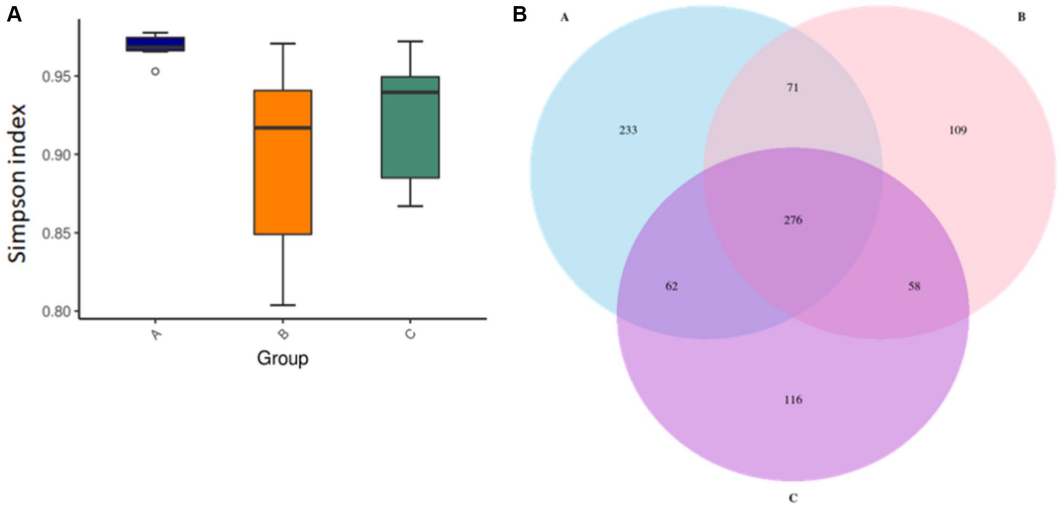

FIGURE 3
Assay for alpha diversity in intestinal microbiota in mice administered with microcapsules prepared from okra polysaccharides with or without *L. plantarum* encapsulation. **(A)** The Simpson indexes of alpha diversity obtained from the analysis of bacterial microbiota between groups. **(B)** Venn diagrams of analysis for the microbial OTU in each group. A: App$^{NL\text{-}G\text{-}F/NL\text{-}G\text{-}F}$ transgenic mice; B: App$^{NL\text{-}G\text{-}F/NL\text{-}G\text{-}F}$ transgenic mice administered with microcapsules (200 mg/kg bw) prepared from okra polysaccharides were mixed with sodium alginate (5%); C: App$^{NL\text{-}G\text{-}F/NL\text{-}G\text{-}F}$ transgenic mice administered with *L. plantarum*-encapsulated microcapsules (200 mg/kg bw) prepared from okra polysaccharides were mixed with sodium alginate (5%).

AD mice (Group-A), AD mice administered with microcapsules (200 mg/kg bw) (Group-B), and AD mice administered with *L. plantarum*-encapsulated microcapsules (200 mg/kg bw) (Group-C). However, there are 276 bacteria co-occurred among these three groups (Figure 3B). Beta diversity is a differential analysis of the microbial composition between different groups. According to the species annotation, the ASV information was merged for members belonging to the same classification group to obtain the species abundance. We used non-metric multidimensional scaling (NMDS), partial least squares discriminant analysis (PLSDA), and principal component analysis (PCA), including correlation matrix (PCA_corr) and covariance matrix (PCA_cov), to assess beta diversity. Our results indicate that both microcapsules prepared from okra polysaccharides (200 mg/kg bw) and *L. plantarum*-encapsulated microcapsules (200 mg/kg bw) could increase beta diversity in AD mice (Figure 4).

3.4 Effects of administration with microcapsules prepared from okra polysaccharides with or without *Lactiplantibacillus plantarum* encapsulation on intestinal microbiota in App$^{NL\text{-}G\text{-}F/NL\text{-}G\text{-}F}$ mice

Among the top-10 most abundant microbial families and genera, our results indicated that the levels of *Lachnospiraceae*, *Ruminococcaceae*, and *Bacteroidaceae* in AD mice were higher than that in AD mice administered with microcapsules prepared from okra polysaccharides with or without *L. plantarum* encapsulation. However, the administration of microcapsules prepared from okra polysaccharides with or without *L. plantarum* encapsulation elevated *Lactobacillaceae* (family) and *Lactobacillus* (genus) levels in AD mice (Figure 5). We performed an analysis of intestinal microbiota at the genus and species level using a heatmap showing the ratio of intestinal microbiota in mice administered with microcapsules prepared from okra polysaccharides with or without *L. plantarum* encapsulation compared to the AD mice. Figure 6 shows the top 35 families and genera in each group included in the heatmap plot. The results indicated an increase in the intestinal abundance of *Burkholderiaceae*, *Rikenellaceae*, *Bacteroidaceae*, *Desulfovibrionaceae*, *Peptococcaceae*, *Lachnospiraceae*, *Ruminococcaceae*, *Tannerellaceae*, *Christensenellaceae*, *Anaeroplasmataceae*, *Peptostreptococcaceae*, *Defluvitaleaceae*, *Deferribacteraceae*, and *Clostridiales_vadin* BB60_ group (family) in AD mice. We also observed a greater abundance of genera including *Alistipes*, *Ruminiclostridium*_5, *Marvinbryantia*, *Ruminiclostridium*_9, *Oscillibacter*, *Anaerotruncus*, *Parabacteroides*, *Lachnospiraceae*_UCG_001, *Blautia*, *Butyricicoccus*, *Rikenellaceae*_RC9_gut_group, *Ruminiclostridium*_6, *Ruminococcaceae*_UCG-014, *Parasutterella*, *Lachnospiraceae*_NK4A136_group, *Bacteroides*, and *Desulfovibria* in AD mice. However, these bacteria were suppressed in AD mice administered with microcapsules prepared from okra polysaccharides with or without *L. plantarum* encapsulation, even though populations of *Alloprevotella, Muribaculum, Odoribacter*, and *Lactobacillus* were increased in AD mice treated by microcapsules prepared from okra polysaccharides. We also found that the *Lachnospiraceae*_UCG_006, *Lactobacillus, Candidatus saccharimonas, Dorea, Rikenella,* and *Enterorhabdus* levels were increased in AD mice by administering microcapsules prepared from okra polysaccharides with *L. plantarum* encapsulation. *Lactobacillaceae* and *Lactobacillus* are mainly affected by microcapsules prepared from okra polysaccharides treating AD mice. Similarly, microcapsules prepared from okra polysaccharides with *L. plantarum* encapsulation markedly elevated the abundance of *Lactobacillaceae* and *Lactobacillus* in AD mice (Supplementary Figure S1). A study has also reported similar results, administration of lactic acid bacteria elevated the abundance of *Bifidobacterium*, *Bacteroides*, *Alistipes*, and *Alloprevotella*, but the

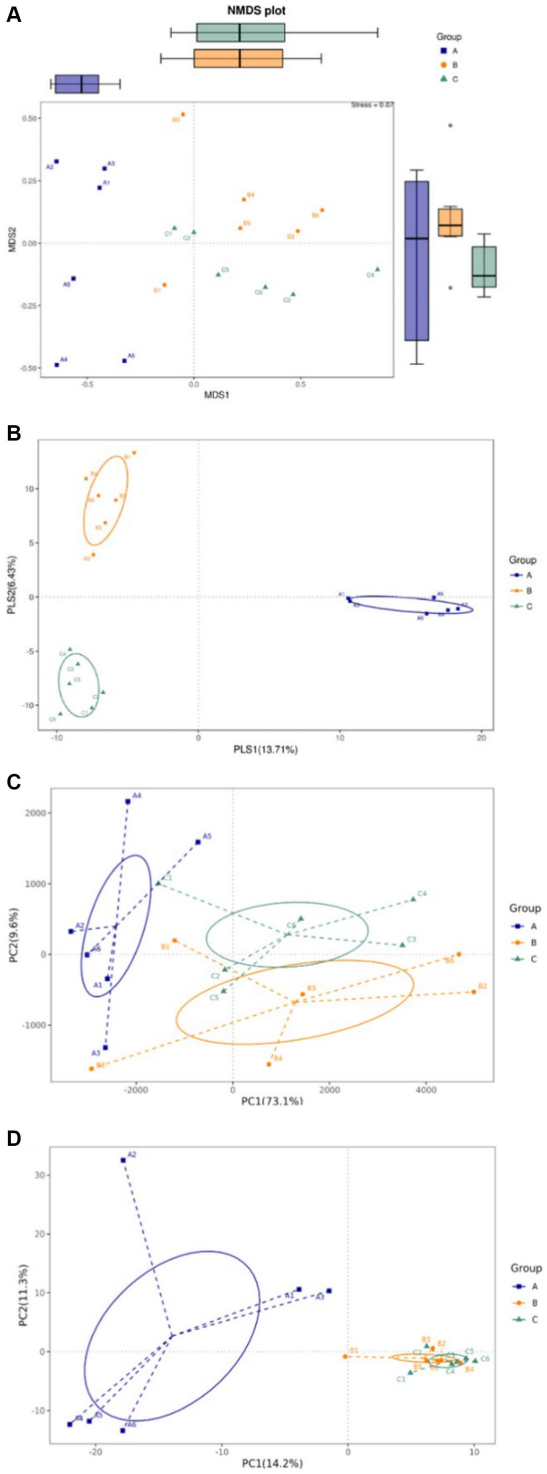

FIGURE 4
Assay for beta diversity in intestinal microbiota in mice administered with microcapsules prepared from okra polysaccharides with or without *L. plantarum* encapsulation. **(A)** Non-metric multidimensional scaling (NMDS), **(B)** partial least squares discriminant analysis (PLSDA), **(C)** principal component analysis (PCA)-covariance matrix, and **(D)** PCA correlation matrix. A: App$^{NL\text{-}G\text{-}F/NL\text{-}G\text{-}F}$ transgenic mice; B: App$^{NL\text{-}G\text{-}F/NL\text{-}G\text{-}F}$ transgenic mice administered with microcapsules (200 mg/kg bw) prepared from okra polysaccharides were mixed with sodium alginate (5%); C: App$^{NL\text{-}G\text{-}F/NL\text{-}G\text{-}F}$ transgenic mice administered with *L. plantarum*-encapsulated microcapsules (200 mg/kg bw) prepared from okra polysaccharides were mixed with sodium alginate (5%).

numbers of *Parabacteroides, Lachnoclostridium, Lachnospiraceae* UCG-006, *Eubacterium,* and *Romboutsia* were reduced in high-fat diet-induced mice (Li et al., 2020). Our results suggested that microcapsules prepared from okra polysaccharides with or without *L. plantarum* encapsulation elevated the levels of lactic acid bacteria (*Lactobacillales, Lactobacillaceae,* and *Lactobacillus*) and maintain intestinal microbiota (*Atopobiaceae, Actinobacteria, Coriobacteriia*, and *Coriobacteriales*) in AD mice.

The abundance of significant differences in species was evaluated by linear discriminant analysis (LDA) effect size (LEfSe) assay. The predominant microbial groups in AD mice including *Lachnospiraceae, Ruminococcaceae, Clostridia,* and *Clostridiales* are significantly elevated and potentially serve as biomarkers. However, these bacteria are all decreased in the gut of AD mice by administration with microcapsules prepared from okra polysaccharides with or without *L. plantarum* encapsulation, respectively (Figure 7). Furthermore, bacterial populations such as *Lachnospira, Blautia, Lachnospiraceae_*UCG_001, and *Peptococcus*, although not the most abundant in terms of richness, are notably suppressed by the administration with microcapsules prepared from okra polysaccharides with or without *L. plantarum* encapsulation (Figure 8). These results indicate that okra polysaccharides themselves possess the potential to regulate the gut microbiota of AD mice.

3.5 Effects of microencapsules prepared from okra polysaccharides with *Lactiplantibacillus plantarum* on fecal short-chain fatty acid (SCFA) in App$^{NL\text{-}G\text{-}F/NL\text{-}G\text{-}F}$ mice

We evaluated the fecal SCFA levels (including acetate, propionic acid, and butyrate) of AD mice after administering microcapsules prepared from okra polysaccharides with *L. plantarum* encapsulation (Table 2). Our results indicated that microcapsules prepared from okra polysaccharides with or without *L. plantarum* encapsulation markedly elevated acetate and propionic acid levels in AD mice, but only butyrate levels were increased by microcapsules prepared from okra polysaccharides with *L. plantarum* encapsulation. Similar to other studies, the SCFA levels *in vivo* were promoted by okra supplementation (Zhang et al., 2019).

4 Discussion

A bacterial amyloid known as curli is produced by *Escherichia coli*, and it is clearly seen through the sub-mock system that bacterial amyloids, such as prions, accelerate host Aβ aggregation (Zhou et al., 2012). Many other microorganisms have also been found to produce amyloids. For example, *Pseudomonas fluorescens* produces FapC, *Staphylococcus aureus* produces phenol-soluble modulins, *Streptomyces coelicolor* produces chaplins, and *Klebsiella pneumonia* produces MccE492, all of which are similar to human amyloid proteins (Schwartz and Boles, 2013). Studies have reported that extracellular Aβ produced by bacteria (*Escherichia coli*, *Salmonella enterica*, *Salmonella* Typhimurium, *Bacillus subtilis*, *Mycobacterium tuberculosis*, *Staphylococcus aureus*) also forms fibrous plaques after being released into the intestine (Pistollato et al., 2016). A study

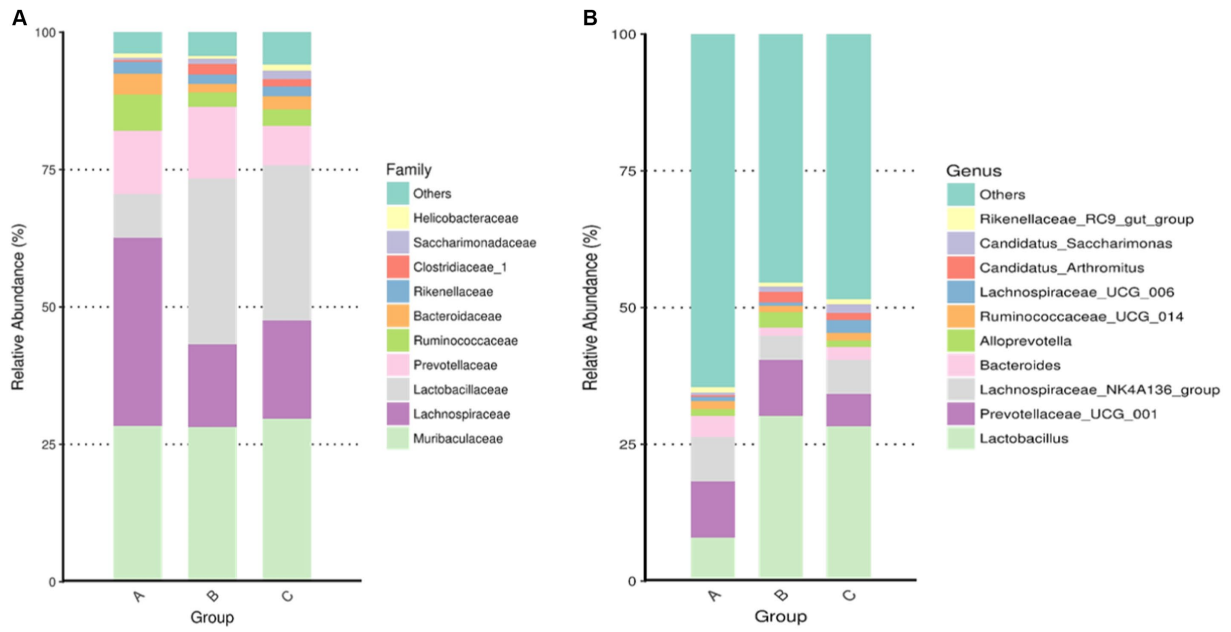

FIGURE 5
Assay for intestinal microbiota in mice administered with microcapsules prepared from okra polysaccharides with or without *L. plantarum* encapsulation. The top-10 abundance from taxa analysis of microbiota composition at **(A)** family and **(B)** genus. A: App$^{NL\text{-}G\text{-}F/NL\text{-}G\text{-}F}$ transgenic mice; B: App$^{NL\text{-}G\text{-}F/NL\text{-}G\text{-}F}$ transgenic mice administered with microcapsules (200 mg/kg bw) prepared from okra polysaccharides were mixed with sodium alginate (5%); C: App$^{NL\text{-}G\text{-}F/NL\text{-}G\text{-}F}$ transgenic mice administered with *L. plantarum*-encapsulated microcapsules (200 mg/kg bw) prepared from okra polysaccharides were mixed with sodium alginate (5%).

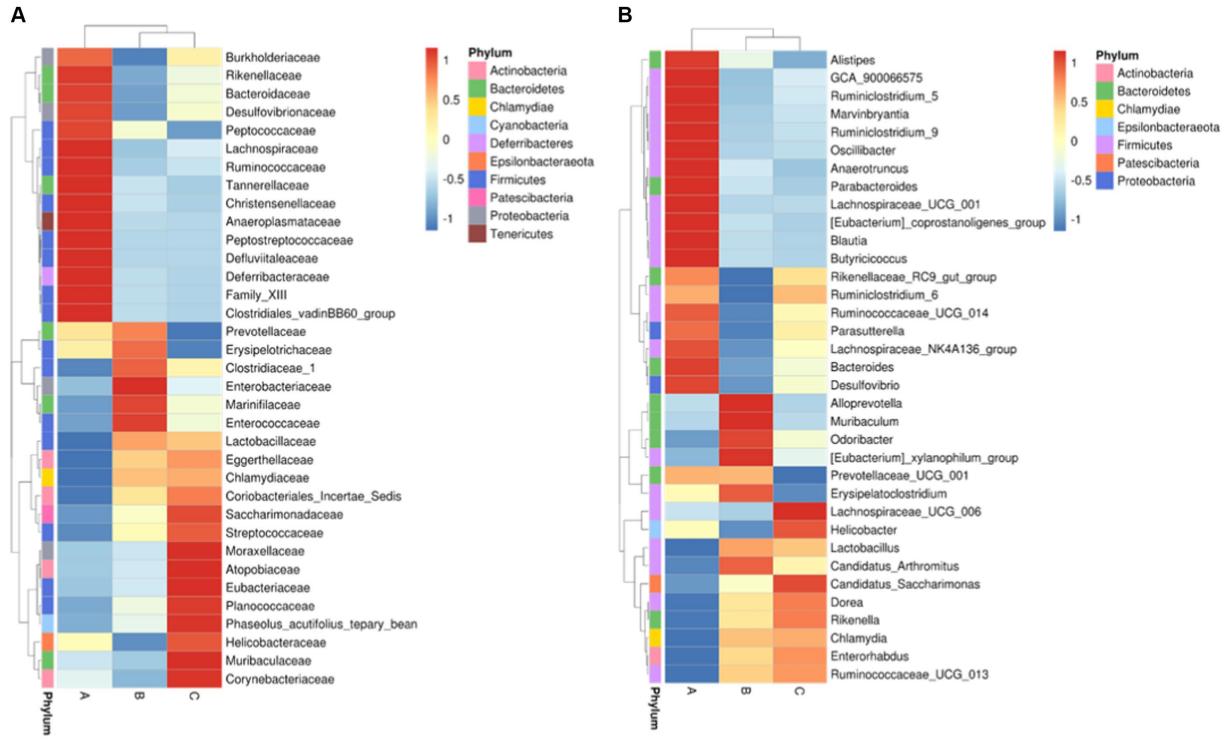

FIGURE 6
Intestinal taxa microbiota composition for **(A)** family level and **(B)** genus level in mice administered with microcapsules prepared from okra polysaccharides with or without *L. plantarum* encapsulation by heatmap. A: App$^{NL\text{-}G\text{-}F/NL\text{-}G\text{-}F}$ transgenic mice; B: App$^{NL\text{-}G\text{-}F/NL\text{-}G\text{-}F}$ transgenic mice administered with microcapsules (200 mg/kg bw) prepared from okra polysaccharides were mixed with sodium alginate (5%); C: App$^{NL\text{-}G\text{-}F/NL\text{-}G\text{-}F}$ transgenic mice administered with *L. plantarum*-encapsulated microcapsules (200 mg/kg bw) prepared from okra polysaccharides were mixed with sodium alginate (5%).

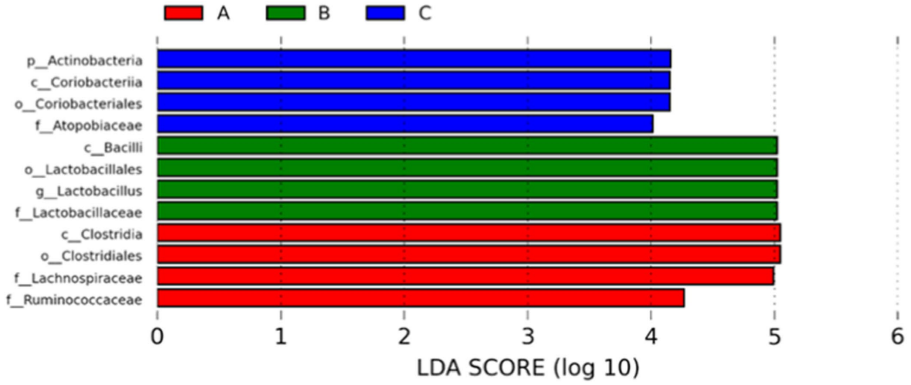

FIGURE 7
Use the non-parametric factorial Kruskal–Wallis (KW) sum-rank test to find species with significant differences in abundance by linear discriminant analysis (LDA) effect size (LEfSe) assay. Linear regression discriminant analysis (LDA) was used to estimate the magnitude of the effect of each species abundance on the difference. A: App$^{NL\text{-}G\text{-}F/NL\text{-}G\text{-}F}$ transgenic mice; B: App$^{NL\text{-}G\text{-}F/NL\text{-}G\text{-}F}$ transgenic mice administered with microcapsules (200 mg/kg bw) prepared from okra polysaccharides were mixed with sodium alginate (5%); C: App$^{NL\text{-}G\text{-}F/NL\text{-}G\text{-}F}$ transgenic mice administered with *L. plantarum*-encapsulated microcapsules (200 mg/kg bw) prepared from okra polysaccharides were mixed with sodium alginate (5%).

TABLE 2 **Productions of short-chain fatty acid productions in fecal of TG mice administered with okra polysaccharides or lactic acid bacteria-fermented okra polysaccharides.**

Groups	Acetate	Propionic acid	Butyrate
	Concentration (μM)		
A	68.0 ± 6.1^{c}	20.4 ± 0.8^{b}	737.4 ± 103.6^{b}
B	118.4 ± 8.4^{b}	39.3 ± 4.5^{a}	892.1 ± 81.0^{b}
C	163.1 ± 13.8^{a}	42.1 ± 3.7^{a}	1224.7 ± 91.4^{a}

Data are shown as mean ± SD (n = 3). Significant difference are indicated by different letters (a, b, and c).

confirmed that amyloid proteins produced by microorganisms in the gut enter the central nervous system through the bloodstream and increase the accumulation and deposition of Aβ (Chen et al., 2016). A bacterial-derived amyloid called curli, which is produced by *Escherichia coli* and accelerates Aβ aggregation, similar to what occurs with prions, has been clearly observed in the sub-simulation system (Zhou et al., 2012). There are also many other microorganisms that have been found to produce amyloid-like peptides, for example, *Pseudomonas fluorescens* can produce FapC; *Staphylococcus aureus* can produce phenol-soluble modulins; *Streptomyces coelicolor* can produce chaplins; and *Klebsiella pneumonia* can produce MccE492. These proteins are considered to have human amyloid protein characteristics (Schwartz and Boles, 2013). Furthermore, other bacteria also generate extracellular Aβ, thereby forming fibrous plaques after being released, including *Escherichia coli*, *Salmonella enterica*, *Salmonella* Typhimurium, *Bacillus subtilis*, *Mycobacterium tuberculosis*, and *Staphylococcus aureus* (Pistollato et al., 2016).

Okra polysaccharides have been found to reverse metabolic disorders and cognitive function in AD mice and improve gut microbiota to protect against depression (Yan et al., 2020a,b). Many microorganisms in the gut affect host behavior and emotional performance by producing brain neurotransmitters (Foster, 2013). The probiotic bacteria *Bifidobacterium infantis*, when administered in germ-free mice by fecal transplantation or oral routes, can restore cranial nerve damage and cause behavioral changes (Sudo et al., 2004). In another experiment, the spatial memory and learning abilities of germ-free mice following fecal transplantation or probiotic treatment were significantly better compared with that of a control group (Gareau et al., 2011). Numerous studies have found that microbes in the gut may potentially interact to influence their growth or distribution (Zhang et al., 2013). These studies found that such changes in the intestinal microbiota could improve neuronal activity.

Microorganisms of *Lachnospiraceae* can cause diabetes in germ-free mice (Kameyama and Itoh, 2014). Therefore, microorganisms in this family may contain bacteria belonging to probiotics or opportunistic bacteria that cause disease. After feeding mice with lactic acid bacteria, the distribution of intestinal flora of the *Lachnospiraceae* NK4A136 group and *Lachnospiraceae* UCG-006 was increased and inhibited, respectively (Li et al., 2020), suggesting that the functions of various microorganisms within the *Lachnospiraceae* family may be opposing (Vacca et al., 2020). An increase in the gastric vagus nerve activity in association with *Lactobacillus johnsonii* has been reported (Tanida et al., 2005). Moreover, *Lactobacillus rhamnosus*-derived metabolites have the potential to ameliorate neuronal inflammation (Bravo et al., 2011). Recently, the effects of various polysaccharides on intestinal microbiota have been investigated, including polysaccharides derived from pitaya, *Cordyceps militaris*, and other edible fungal polysaccharides (Liang et al., 2021; Lee et al., 2021b, 2022; Sun et al., 2023).

Fecal microbiota transplantation or oral administration of the probiotic *Bifidobacterium infantis* to germ-free mice restored cranial nerve damage and led to behavioral changes (Sudo et al., 2004). In another experiment, germ-free mice that received fecal microbiota transplantation or probiotics had significantly better spatial memory and learning abilities than the controls (Gareau et al., 2011). A high bacterial phylum ratio of Firmicutes/Bacteroidetes can lead to intestinal inflammation and influence the attack rate of AD, whereas probiotics in the gut can reduce the bacterial growth of the Firmicutes phylum and increase the bacterial growth of the Bacteroidetes phylum, reducing the risk of AD (Gareau et al., 2011). Although researchers currently do not fully understand the role of intestinal flora in the

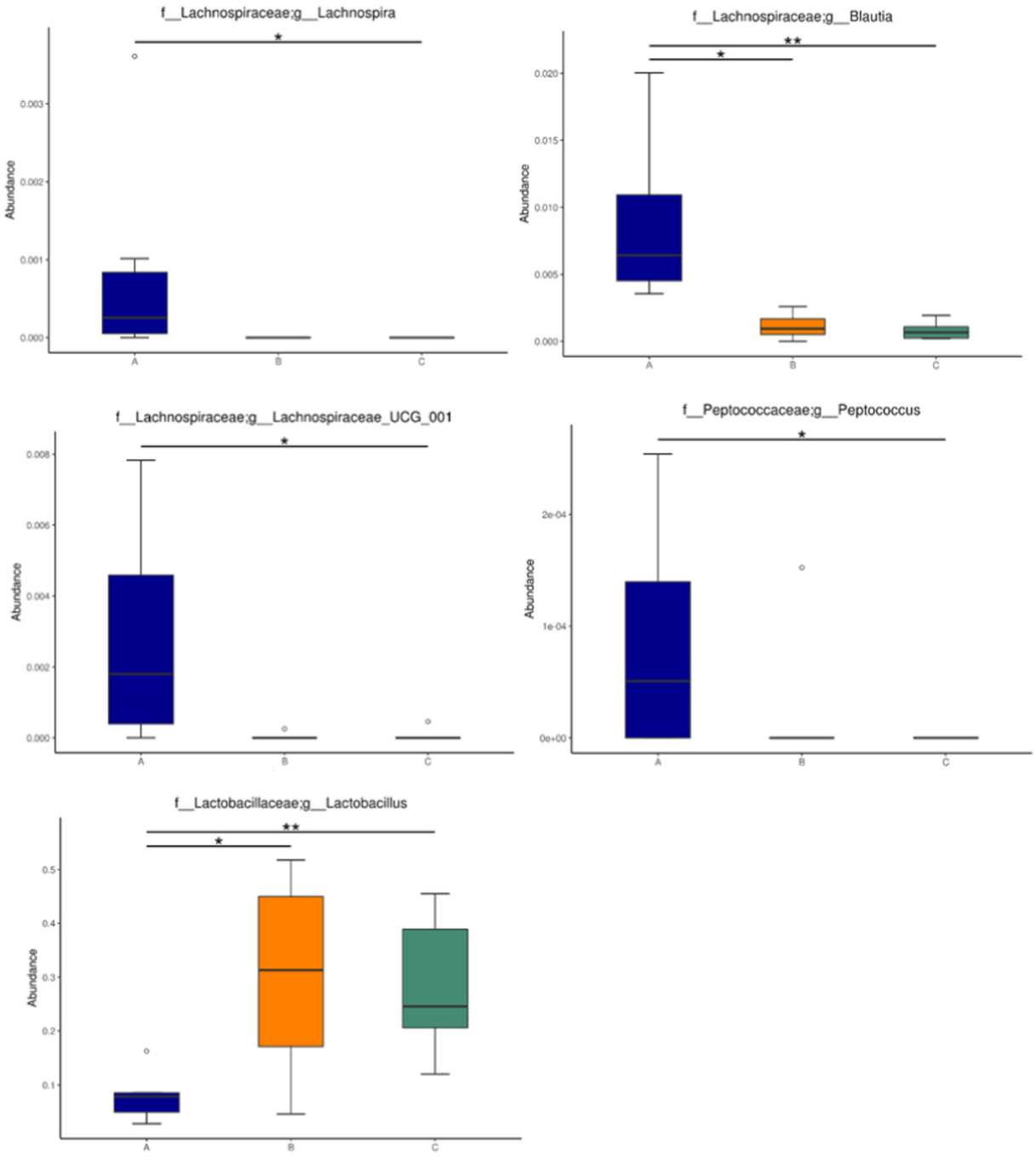

FIGURE 8
Relative abundance of the gut microbiota in mice administered with microcapsules prepared from okra polysaccharides with or without *L. plantarum* encapsulation. Abundance of *Lachnospira, Blautia, Lachnospiraceae*_UCG_001, *Peptococcus,* and *Lactobacillus* changed significantly among the groups. $*p < 0.05$ and $**p < 0.01$. A: App$^{NL\text{-}G\text{-}F/NL\text{-}G\text{-}F}$ transgenic mice; B: App$^{NL\text{-}G\text{-}F/NL\text{-}G\text{-}F}$ transgenic mice administered with microcapsules (200 mg/kg bw) prepared from okra polysaccharides were mixed with sodium alginate (5%); C: App$^{NL\text{-}G\text{-}F/NL\text{-}G\text{-}F}$ transgenic mice administered with *L. plantarum*-encapsulated microcapsules (200 mg/kg bw) prepared from okra polysaccharides were mixed with sodium alginate (5%).

prevention and control of AD in healthy people, it is also impossible to know whether AD symptoms lead to changes in intestinal flora, or whether intestinal flora themselves can influence the development of this disease. However, the above results show that intestinal bacteria play an extremely important role in the occurrence of AD by okra (Supplementary Figure S2). Taken together, probiotics in the intestinal flora can reduce the growth of *Firmicutes* and *Bacteroidetes* bacteria, consequently reducing the risk of AD (Cowan et al., 2014; Doroszkiewicz et al., 2021; Duan et al., 2021). In another study, a low-calorie diet promoted healthy gut flora, including bacteria of the genus *Lactobacillus* (Zhang et al., 2013).

The SCFAs were always produced from *Lachnospiraceae* (Vacca e al., 2020) and *Ruminococcaceae* (Xie et al., 2022), but the levels of these two bacteria were lowered in TG mice treated with samples. We found that

the *Lactobacillaceae* was elevated by okra polysaccharide microcapsules with or without encapsulated-lactic acid bacteria. Recently, lactic acid bacteria that generated SCFAs *in vitro* (Kang et al., 2021) and promoted intestinal SCFAs *in vivo* (Ni et al., 2021) have been reported. We hypothesized that okra polysaccharides may be as prebiotics for upregulating lactic acid bacteria growth and SCFA production.

Taken together, the results showed that the microcapsules prepared from okra polysaccharides with or without *L. plantarum* encapsulation had similar effects on regulating *Lactobacillus* population in AD mice. Moreover, the microcapsules prepared from okra polysaccharides with or without *L. plantarum* encapsulation also elevated intestinal SCFA level of AD mice. According to the above, microcapsules prepared from okra polysaccharides with or without *L. plantarum* encapsulation have the potential to act as a dietary supplement and health food via intestinal regulation.

Data availability statement

The raw data supporting the conclusions of this article will be made available by the authors, without undue reservation.

Ethics statement

The animal study was approved by National Cheng Kung University in Taiwan with IACUC approval no. 108317. The study was conducted in accordance with the local legislation and institutional requirements.

Author contributions

Y-KH: Data curation, Formal analysis, Funding acquisition, Writing – original draft. B-HL: Writing – original draft, Writing – review & editing. S-CW: Funding acquisition, Investigation, Methodology, Project administration, Writing – review & editing.

Funding

The author(s) declare that no financial support was received for the research, authorship, and/or publication of this article.

Conflict of interest

Y-KH was employed by King Long Guan Company Ltd.

The remaining authors declare that the research was conducted in the absence of any commercial or financial relationships that could be construed as a potential conflict of interest.

Publisher's note

Supplementary material

The Supplementary material for this article can be found online at: https://www.frontiersin.org/articles/10.3389/fmicb.2024.1305617/full#supplementary-material

References

BeMiller, J. N., Whistler, R. L., Barbalowm, D. G., and Chen, C. C. (1993). "Aloe, Chia, Flaxseed, Okra, psyllium seed, quince seed, and tamarind gums" in *Industrial gums. Polysaccharide and their derivatives*. eds. L. W. Roy and J. N. BeMiller. *3rd* ed (San Diago: Academic Press), 235–255.

Bravo, J. A., Forsythe, P., Chew, M. V., Escaravage, E., Savignac, H. M., Dinan, T. G., et al. (2011). Ingestion of Lactobacillus strain regulates emotional behavior and central GABA receptor expression in a mouse via the vagus nerve. *Proc. Natl. Acad. Sci. U. S. A.* 108, 16050–16055. doi: 10.1073/pnas.1102999108

Chen, S. G., Stribinskis, V., Rane, M. J., Demuth, D. R., Gozal, E., Roberts, A. M., et al. (2016). Exposure to the functional bacterial amyloid protein curli enhances alpha-synuclein aggregation in aged Fischer rats and *Caenorhabditis elegans*. *Sci. Rep.* 6:34477. doi: 10.1038/srep34477

Cowan, T. E., Palmnas, M. S. A., Yang, J., Bomhof, M. R., Ardell, K. A., Reimer, R. A., et al. (2014). Chronic coffee consumption in the diet-induced obese rat: impact on gut microbiota and serum metabolomics. *J. Nutr. Biochem.* 25, 489–495. doi: 10.1016/j.jnutbio.2013.12.009

De la Cuesta-Zuluaga, J., Mueller, N. T., Corrales-Agudelo, V., and Escobar, J. S. (2017). Metformin is associated with higher relative abundance of mucin-degrading *Akkermansia muciniphila* and several short-chain fatty acid producing microbiota in the gut. *Diabetic Care* 40, 54–62. doi: 10.2337/dc16-1324

Doroszkiewicz, J., Groblewska, M., and Mroczko, B. (2021). The role of gut microbiota and gut-brain interplay in selected diseases central nervous system. *Int. J. Mol. Sci.* 22:10028. doi: 10.3390/ijms221810028

Duan, M., Liu, F., Fu, H., Lu, S., and Wang, T. (2021). Preoperative microbiomes and intestinal barrier function can differentiate prodromal Alzheimer's disease from normal neurocognition in elderly patients scheduled to undergo orthopedic surgery. *Front. Cell. Infect. Microbiol.* 11:592842. doi: 10.3389/fcimb.2021.592842

Dubois, M., Gilles, K. A., Hamilton, J. K., Rebers, P. T., and Smith, F. (1956). Colorimetric method for determination of sugars and related substances. *Anal. Chem.* 28, 350–356. doi: 10.1021/ac60111a017

Foster, J. A. (2013). Gut feelings: bacteria and the brain. *Cerebrum* 2013:9.

Gareau, M. G., Wine, E., Rodrigues, D. M., Cho, J. H., Whary, M. T., Philpott, D. J., et al. (2011). Bacterial infection causes stress-induced memory dysfunction in mice. *Gut* 60, 307–317. doi: 10.1136/gut.2009.202515

Huang, C. N., Lin, C. L., Li, H. H., Tsou, S. H., and Peng, C. H. (2023). *Abelmoschus esculentus* (okra) prevents insulin resistance and restores neuron autophagy by regulating dipeptidyl peptidase-4 and thus improving hippocampal function. *J. Med. Food* 26, 462–469. doi: 10.1089/jmf.2023.K.0014

Huang, C. N., Wang, C. J., Lin, C. L., Li, H. H., Yen, A. T., and Peng, C. H. (2020). *Abelmoschus esculentus* subfractions attenuate Aβ and tau by regulating DPP-4 and insulin resistance signals. *BMC Complement. Med. Ther.* 20:370. doi: 10.1186/s12906-020-03163-4

Kameyama, K., and Itoh, K. (2014). Intestinal colonization by a Lachnospiraceae bacterium contributes to the development of diabetes in obese mice. *Microb. Environ.* 29, 427–430. doi: 10.1264/jsme2.ME14054

Kang, C. J., Kim, K. S., Park, H. M., Kim, S., and Paek, N. S. (2021). Antioxidant activity and short-chain fatty acid production of lactic acid bacteria isolated from Korean individuals and fermented foods. *3 Biotech* 11:217. doi: 10.1007/s13205-021-02767-y

Kuo, H. C., Kwong, H. K., Chen, H. Y., Hsu, H. Y., Yu, S. H., Hsieh, C. W., et al. (2021). Enhanced antioxidant activity of Chenopodium formosanum Koidz. By lactic acid bacteria: optimization of fermentation conditions. *PLoS One* 16:e0249250. doi: 10.1371/journal.pone.0249250

Lee, B. H., Chen, C. H., Hsu, Y. Y., Chuang, P. T., Shih, M. K., and Hsu, W. H. (2021a). Polysaccharides obtained from *Cordyceps militaris* alleviate hyperglycemia by regulating gut microbiota in mice fed a high-fat/sucrose diet. *Food Secur.* 10:1870. doi: 10.3390/foods10081870

Lee, B. H., Hsu, K. T., Chen, Y. Z., Tain, Y. L., Hou, C. Y., Lin, Y. C., et al. (2022). Polysaccharide extracts derived from defloration waste of fruit pitaya regulates gut microbiota in a mice model. *Fermentation* 8:108. doi: 10.3390/fermentation8030108

Lee, B. H., Hsu, W. H., Chien, H. Y., Hou, C. Y., Hsu, Y. T., Chen, Y. Z., et al. (2021b). Applications of *Lactobacillus acidophilus*-fermented mango protected *Clostridioides difficile* infection and developed as an innovative probiotic jam. *Food Secur.* 10:1631. doi: 10.3390/foods10071631

Lee, B. H., Huang, S. C., Hou, C. Y., Chen, Y. Z., Chen, Y. H., Hazeena, S. H., et al. (2023). Effect of polysaccharide derived from dehulled adlay on regulating gut microbiota and inhibiting *Clostridioides diffcile* in an vitro colonic fermentation model. *Food Chem.* 410:135410. doi: 10.1016/j.foodchem.2023.135410

Lengsfeld, C., Titgemeyer, F., Faller, G., and Hensel, A. (2004). Glycosylated compounds from okra inhibit adhesion of *Helicobacter pylori* to human gastric mucosa. *J. Agric. Food Chem.* 52, 1495–1503. doi: 10.1021/jf030666n

Li, H., Liu, F., Lu, J., Shi, J., Gua, J., Yan, F., et al. (2020). Probiotic mixture of *Lactobacillus plantarum* strains improves lipid metabolism and gut microbiota structure in high fat diet fed mice. *Front. Microbiol.* 11:512. doi: 10.3389/fmicb.2020.00512

Liang, J., Zhang, M., Wang, X., Ren, Y., Yue, T., Wang, Z., et al. (2021). Edible fungal polysaccharides, the gut microbiota, and host health. *Carbohydr. Polym.* 273:118558. doi: 10.1016/j.carbpol.2021.118558

Liao, Z., Zhang, J., Liu, B., Yan, T., Xu, F., Xiao, F., et al. (2019). Polysaccharide from okra [*Abelmoschus esculentus* (L.) Moench] improves antioxidant capacity via PI3K/Akt pathways and Nrf2 translocation in a type 2 diabetes model. *Molecules* 24:1906. doi: 10.3390/molecules24101906

Lin, C., Hung, W. T., Kuo, C. Y., Liao, K. S., Liu, Y. C., and Yang, W. B. (2010). I2-catalyzed oxidative condensation of aldoses with diamines: synthesis of aldonaphthimidazoles for carbohydrate analysis. *Molecules* 15, 1340–1353. doi: 10.3390/molecules15031340

Liu, C. F., and Pan, T. M. (2010). In vitro effects of lactic acid bacteria on cancer cell viability and antioxidant activity. *J. Food Drug Anal.* 18, 77–86.

Machiels, K., Joossens, M., Claes, K., Verhaegen, J., Rutgeerts, P., and Vermeire, S. (2014). A decrease of the butyrate-producing species *Roseburia hominis* and *Faecalibacterium prausnitzii* defines dysbiosis in patients with ulceratie colitis. *Gut* 63, 1275–1283. doi: 10.1136/gutjnl-2013-304833

Nasiri, H., Golestan, L., Shahidi, S. A., and Darjani, P. (2021). Encapsulation of *Lactobacillus casei* in sodium alginate microcapsules: improvement of the bacterial viability under simulated gastrointestinal conditions using wild sage seed mucilage. *J. Food Meas. Charact.* 15, 4726–4734. doi: 10.1007/s11694-021-01022-5

Ni, C., Li, X., Wang, L., Li, X., Zhao, J., Zhang, H., et al. (2021). Lactic acid bacteria strains relieve hyperuricaemia by suppressing xanthine oxidase activity via a short-chain fatty acid-dependent mechanism. *Food Funct.* 12, 7054–7067. doi: 10.1039/D1FO00198A

Pistollato, F., Sumalla Cano, S., Elio, I., Masias Vergara, M., Giampieri, F., and Battino, M. (2016). Role of gut microbiota and nutrients in amyloid formation and pathogenesis of Alzheimer disease. *Nutr. Rev.* 74, 624–634. doi: 10.1093/nutrit/nuw023

Qin, J., Li, R., Raes, J., Arumugam, M., Burgdorf, K. S., Manichanh, C., et al. (2020). A human gut microbial gene catalogue established by metagenomic sequencing. *Nature* 464, 59–65. doi: 10.1038/nature08821

Rajilic-Stojanovic, M., Biagi, E., Heilig, H. G., Kajander, K., Kellonen, R. A., Tims, S., et al. (2011). Global and deep molecular analysis of microbiota signatures in fecal samples from patients with irritable bowel syndrome. *Gastroenterology* 141, 1792–1801. doi: 10.1053/j.gastro.2011.07.043

Ralet, M. C., and Della, G. J. F. (1993). Thibault: raw and extruded fibre from pea hulls. Part I: composition and physico-chemical properties. *Carbohyd. Polym.* 20, 17–23. doi: 10.1016/0144-8617(93)90028-3

Romanchik-Cerpovicz, J. E., Tilmon, R. W., and Baldree, K. A. (2002). Moisture retention and consumer acceptability of chocolate bar cookies prepared with okra gum as a fat ingredient substitute. *J. Am. Diet. Assoc.* 102, 1301–1303. doi: 10.1016/S0002-8223(02)90287-7

Sakakibara, Y., Sekiya, M., Saito, T., Saido, T. C., and Iijima, K. M. (2018). Cognitive and emotional alterations in app knock-in mouse models of Aβ amyloidosis. *BMC Neurosci.* 19:46. doi: 10.1186/s12868-018-0446-8

Sami, R., Lianzhou, J., Yang, L., Ma, Y., and Jing, J. (2013). Evaluation of fatty acid and amino acid compositions in okra (*Abelmoschus esculentus*) grown in different geographical locations. *Biomed. Res. Int.* 2013:574283, 1–6. doi: 10.1155/2013/574283

Schwartz, K., and Boles, B. R. (2013). Microbial amyloids–functions and interactions within the host. *Curr. Opin. Microbiol.* 16, 93–99. doi: 10.1016/j.mib.2012.12.001

Sengkhamparn, N., Verhoef, R., Schols, H. A., Sajjaanantakul, T., and Voragen, A. G. (2009). Characteration of cell wall polysaccharides from okra [*Abelmoschus esculentus* (L.) Moench]. *Carbohydr. Res.* 344, 1824–1832. doi: 10.1016/j.carres.2008.10.012

Soscia, S. J., Kirby, J. E., Washicosky, K. J., Tucker, S. M., Ingelsson, M., Hyman, B., et al. (2010). The Alzheimer's disease-associated amyloid beta-protein is an antimicrobial peptide. *PLoS One* 5:e9505. doi: 10.1371/journal.pone.0009505

Sudo, N., Chida, Y., Aiba, Y., Sonoda, J., Oyama, N., Yu, X. N., et al. (2004). Postnatal microbial colonization programs the hypothalamic-pituitary-adrenal system for stress response in mice. *J. Physiol.* 558, 263–275. doi: 10.1113/jphysiol.2004.063388

Sun, Y., Ho, C. T., Zhang, Y., Hong, M., and Zhang, X. (2023). Plant polysaccharides utilized by gut microbiota: new players in ameliorating cognitive impairment. *J. Tradit. Complement. Med.* 13, 128–134. doi: 10.1016/j.jtcme.2022.01.003

Tanida, M., Yamano, T., Maeda, K., Okumura, N., Fukushima, Y., and Nagai, K. (2005). Effects of intraduodenal injection of *Lactobacillus johnsonii* La1 on renal sympathetic nerve activity and blood pressure in urethane-anesthetized rats. *Neurosci. Lett.* 389, 109–114. doi: 10.1016/j.neulet.2005.07.036

Turner, J. R. (2009). Intestinal mucosal barrier function in health and disease. *Nat. Rev. Immunol.* 9, 799–809. doi: 10.1038/nri2653

Vacca, M., Celano, G., Calabrese, F. M., Portincasa, P., Gobbett, M., and de Angelis, M. (2020). The controversial role of human gut Lachnospiraceae. *Microorganisms* 8:573. doi: 10.3390/microorganisms8040573

Whistler, R. L., and Conrad, H. E. (1954). 2-O-(D-galactopyranosyluronic acid)-L-rhamnose from okra mucilage. *J. Am. Chem. Soc.* 76, 3544–3546. doi: 10.1021/ja01642a057

Woolfe, M. L., Chaplin, M. F., and Otchere, G. (1977). Studies on the mucilages extracted from okra fruit (*Hibiscus eaculentus* L.) and baobab (*Adansonia* L.). *J. Sci. Food Agric.* 28, 519–529. doi: 10.1002/jsfa.2740280609

Xie, J., Li, L. F., Dai, T. Y., Qi, X., Wang, Y., Zheng, T. Z., et al. (2022). Short-chain fatty acids produced by Ruminococcaceae mediate α-linolenic acid promote intestinal stem cells proliferation. *Mol. Nutr. Food Res.* 66:e2100408. doi: 10.1002/mnfr.202100408

Yan, T., Nian, T., Liao, Z., Xiao, F., Wu, B., Bi, K., et al. (2020a). Antidepressant effects of a polysaccharide form okra [*Abelmoschus esculentus* (L) Moench] by anti-inflammation and rebalancing the gut microbiota. *Int. J. Biol. Macromol.* 144, 427–440. doi: 10.1016/j.ijbiomac.2019.12.138

Yan, T., Nian, T., Wu, B., Xiao, F., He, B., Bi, K., et al. (2020b). Okra polysaccharides can reverse the metabolic disorder induced by high-fat diet and cognitive function injury in Aβ1-42 mice. *Exp. Gerontol.* 130:110802. doi: 10.1016/j.exger.2019.110802

Zhang, C., Li, S., Yang, L., Huang, P., Li, W., Wang, S., et al. (2013). Structural modulation of gut microbiota in life-long calorie-restricted mice. *Nat. Commun.* 4:2163. doi: 10.1038/ncomms3163

Zhang, J., Zhao, Y., Ren, D., and Yang, X. (2019). Effect of okra fruit powder supplementation on metabolic syndrome and gut microbiota diversity in high fat diet-induced obese mice. *Food Res. Int.* 130:108929. doi: 10.1016/j.foodres.2019.108929

Zhou, Y., Smith, D., Leong, B. J., Brännström, K., Almqvist, F., and Chapman, M. R. (2012). Promiscuous cross-seeding between bacterial amyloids promotes interspecies biofilms. *J. Biol. Chem.* 287, 35092–35103. doi: 10.1074/jbc.M112.383737

frontiers | Frontiers in Microbiology

TYPE Original Research
PUBLISHED 04 April 2024
DOI 10.3389/fmicb.2024.1353015

OPEN ACCESS

EDITED BY
Fengjie Sun,
Georgia Gwinnett College, United States

REVIEWED BY
Jun-Xia Xiao,
Qingdao Agricultural University, China
Gang Liu,
Hunan Agricultural University, China

*CORRESPONDENCE
Ji Lijiang
✉ fsyy01041@njucm.edu.cn
Jiang Jie
✉ cheungchi@163.com

†These authors have contributed equally to this work

RECEIVED 09 December 2023
ACCEPTED 19 February 2024
PUBLISHED 04 April 2024

CITATION
Hua H, Yongtong W, Xufeng D, Fang L, Jing G, Fumao Z, Jie J and Lijiang J (2024) Hemp seeds attenuate loperamide-induced constipation in mice.
Front. Microbiol. 15:1353015.
doi: 10.3389/fmicb.2024.1353015

Hemp seeds attenuate loperamide-induced constipation in mice

Huang Hua[1†], Wang Yongtong[1†], Ding Xufeng[1], Li Fang[1], Gu Jing[1], Zeng Fumao[2], Jiang Jie[1*] and Ji Lijiang[1*]

[1]Department of Anorectal Surgery, Changshu Hospital Affiliated to Nanjing University of Chinese Medicine, Changshu, China, [2]School of Food Science and Resources, Nanchang University, Nanchang, China

Constipation is a common gastrointestinal disease that seriously affects human physical and mental health. Studies have reported that hemp seeds can improve constipation, however the specific mechanism is still unclear. This study investigates that hemp seed (HS) and its water-ethanol extract (HSE) attenuates loperamide-induced constipation in mice. The research results show that: the fecal water content and small intestinal transit rate of mice in the hemp seed group and hemp seed hydroalcoholic extract group were significantly increased compared with MC group, and the first red feces defecation time was significantly shortened; HS and HSE significantly influence serum levels of Gastrin (Gas), motilin (MTL), substance P (SP), and endothelin (ET), potentially mediating their effects on gastrointestinal motility. HS and HSE can improve colon inflammation in constipated mice with H&E staining. Compared with the model of constipation group, the content of short-chain fatty acids in the HS group and HSE group increased significantly. Gut microbiome studies have shown that the structure and abundance of intestinal flora are altered. HS and HSE changed the abundance of *Odoribacter, Bacteroide, Lactobacillus and Prevotella*. Together, these results suggest that HS have the potential to stimulate the proliferation of beneficial gut microbes and promote intestinal motility, thereby improving gut health and relieving symptoms of constipation.

KEYWORDS

hemp seed, hemp seed extract, constipation, intestinal flora, short-chain fatty acids

1 Introduction

Constipation, a term used to describe a variety of symptoms, including hard stools, over-stress, frequent bowel movements, abdominal distension and abdominal pain, is one of the most common gastrointestinal disorders worldwide (Camilleri et al., 2017). According to epidemiological data, the global prevalence of constipation in adults is 18.9% (Salari et al., 2023). It is well known that the occurrence of constipation imposes a significant economic burden and serious psychological impact on the patients. It is estimated that the cost of purchasing laxatives exceeds $800 million per year in the United States (Wang et al., 2022). Chronic constipation can induce the accumulation of pathogenic bacteria in the colon and is associated with an increased risk of gastrointestinal disorders, such as irritable bowel syndrome and colorectal cancer (Heidelbaugh et al., 2015). Currently, laxatives are the first choice for constipation. However, prolonged use of these laxatives will cause some adverse effects, such as abdominal cramps, rashes, excessive flatulence and dizziness (Ding et al., 2016), more than 50% of patients are not completely satisfied with the treatment of constipation (Huang et al., 2022). Therefore, it is of practical significance to develop a simple and affordable method to improve constipation.

Hemp seeds (HS) are the dried ripe fruit of *Cannabis sativa* L. (Moraceae). Hemp seeds have been utilized both as a food and medicinal ingredient in traditional Chinese medicine for at least 3,000 years (Yan et al., 2015). They have the effects of preventing constipation, promoting cardiovascular health, regulating immunity, and treating skin and gastrointestinal disorders. Hemp seeds have been listed as a Chinese herbal medicine of affinal drug and diet by the National Health Commission of the People's Republic of China. Hemp seeds are rich in nutrients and natural active ingredients. As one of the most commonly used traditional Chinese medicine for the treatment of constipation, hemp seeds are rich in plant proteins, unsaturated fatty acids, vitamins and other nutrients, containing up to 28% of dietary fiber (Opyd et al., 2020). Modern pharmacology has confirmed that hemp seeds contain fatty oil, which can stimulate the intestinal mucosa to increase secretion, promote peristalsis and reduce water absorption in the large intestine, thereby exerting a laxative effect. In a population-based cohort study of 216 patients by Zheng et al., Chinese patent drug Dama Wan (literally Cannabis pills) prepared from hemp seeds and other raw materials was shown to have a reliable and safe efficacy in functional constipation at a dose of 7.5 g bid (Cheng et al., 2011). Huang L. S. et al. (2018) reported the efficacy of Maziren Wan (literally hemp seed pills) in stimulating intestinal mucosa, reducing water absorption in the intestine, softening feces, restoring gastrointestinal homeostasis to increase intestinal peristalsis and relieve constipation. A study by Cheng et al. concluded that hemp seeds improved colonic transit, increased the bowel movement frequency, and reduced the severity of constipation in patients with functional constipation (Zhong et al., 2019).

Currently, hemp seeds are primarily used in the form of hemp seed oil (HSE) or traditional Chinese decoction, which leads to a low utility of many beneficial ingredients in hemp seeds and production of waste residue. Moreover, there are few research reports on utilization of complete hemp seed to treat constipation. Therefore, we aimed to study the protective effect of HS and HSE in mice with loperamide-induced constipation.

2 Materials and methods

2.1 Materials and instruments

Hemp seeds were purchased from Nanjing Traditional Chinese Medicine Market. Loperamide hydrochloride were purchased from Yifeng Pharmacy in Nanchang. Gastrin (Gas), motilin (MTL), substance P (SP), acetylcholinesterase (AchE), endothelin (ET), vasoactive intestinal peptide (VIP) enzyme-linked immunosorbent assay (ELISA) kit had been purchased from Shanghai Yuanju Biotechnology Center. Hematoxylin and eosin (H&E) dye, paraformaldehyde (Wuhan Qian Baidu Biotechnology Co., Ltd.). Short-chain fatty acids (SCFAs) standards: acetic acid, propionic acid, butyric acid, isobutyric acid, valeric acid, and isovaleric acid standards were purchased from Shanghai Aladdin Biochemical Technology Co., Ltd.

5804R refrigerated centrifuge, 5424R refrigerated centrifuge [Ebende (Shanghai) International Trade Co., Ltd.]; SB-02 high-speed multifunctional crusher (Shanghai Puheng Information Technology Co., Ltd.); RT-6000 microplate reader {Leica DM500 upright microscope [Leica Microsystems (Shanghai) Trading Co., Ltd.]; Agilent 7890B gas chromatograph [Agilent Technologies (China) Co., Ltd.]}.

2.2 Experimental methods

2.2.1 Preparation of feed supplemented with hemp seeds

Hemp seeds were added to the grinder and crushed into uniform particles for 3 min. Grind the maintenance feed for 3 min into powder. In every 90 g of maintenance feed, 10 g of crushed hemp seeds were evenly mixed to crush particles, then put into the mold for plasticity. The oven was heated at 60 degrees Celsius for 8 h to remove excess water and fix the shape, and 10% hemp seeds were made into added feed.

2.2.2 Preparation of hemp seed extract

We accurately weighed 20.0 g of hemp seed, ground them, and added 200 mL distilled water according to the solvent ratio of 1:10, vortexed and mixed it, ultrasonic at 40°C for 1 h, centrifuged at 4,500 rpm/min for 5 min, and pour the supernatant into a clean vial. Ethanol solution (200 mL) was added 1:10 to the residue, vortexed and mixed, and the above steps were repeated. Water extraction and alcohol extraction were repeated three times, respectively, and the above extracts were combined. Rotary evaporation was carried out at the temperature of 50°C and the to a constant volume of 30 mL at a speed of 25 and extract concentrate (30 ml) was obtained and stored at −20°C for subsequent experiments.

2.2.3 Animal experiment design

Forty specific pathogen-free (SPF) female BALB/c mice, 6–7 weeks old, weighing 16–19 g, were purchased from Spefford (Beijing) Biotechnology Co., Ltd. [license number: SCXK (Beijing) 2019–0010]; mouse maintenance feed was purchased from Jiangsu Synergy Biotechnology Co., Ltd. (Nanjing, China). The experimental animals were housed in a specific pathogen-free (SPF) facility, with unrestricted access to food and water, with a 12-h light-dark cycle, and the growth environment temperature was 23°C ± 2°C. After adaptive feeding for 3 days, the mice were randomly divided into four groups ($n = 10$): blank control group (CN: normal saline + maintenance feed), model of constipation group (MC: loperamide 10 mg/kg + maintenance feed), hemp seed group (HS: normal saline + 10% hemp seed powder added to feed), hemp seed extract group (HSE: hemp seed extract + maintenance feed). During the entire experiment, mice in the CN group were fed standard mouse chow without any treatment. After the adaptation period, mice in MC, HS, and HSE groups were intragastrically administered loperamide 10 mg/kg at 9:00 a.m. every day for 2 weeks (Huang et al., 2022). One week after modeling, the HSE group was intragastrically administered with the test substance (0.2 mL). The Hemp seed group were given free access to the maintenance feed containing with 10% hemp seed supplemented. When the number of defecation pellets of the mice in the constipation group is significantly different from the number of defecation pellets of the mice in the blank control group, it means that the constipation model has been successfully

established. During the experiment, the body weight and food intake of the mice were recorded twice a week; the physiological and fecal status of the mice were observed every day.

2.3 Moisture content of feces

After the constipation model was successfully established, mouse feces were collected every day and photos were taken to record the appearance of the feces. Each group of mice was placed in a clean cage, deprived of food and water, and allowed to defecate freely for 30 min. Fresh feces were collected in a 1.5 ml dry centrifuge tube, and the resolved samples were weighed using an electronic balance. All fecal samples were dried in an electric constant-temperature drying oven at 60°C until the samples had a constant weight. The formula for calculating feces water content is as follows:

Moisture content of feces (%) = (feces weight before drying—feces weight after drying)/feces weight before drying * 100

2.4 Defecation experiment

Preparation of red ink: a solution of 6 g phenol red in 100 ml 1% carboxymethylcellulose, which was stirred continuously and maintained at 37°C (Crowe and Kinsey, 2017).

This experiment was conducted after the 21st day, and all mice were fasted and water-free for 12 h. After the fasting, 0.2 ml of red ink was administered into the stomach and each mouse was individually transferred to a clean empty cage. The time when each mouse first discharged red stool was recorded.

2.5 Small intestinal transit rate

This experiment was conducted after the 22nd day, and all mice were fasted and water-free for 12 h. After fasting, 0.2 ml of red ink was administered into the stomach, and the eyes were anesthetized for 10 min to collect blood and then killed by neck dissection. Measure the distance traveled by the red ink and the total length of the small intestine. The gastrointestinal transit rate is calculated according to the formula:

Gastrointestinal transit rate (%) = red ink advancement distance/total length of small intestine*100

2.6 Distal colon histopathology

Colon tissue was fixed with 4% paraformaldehyde, embedded in paraffin, and cut into 4 μm thick sections. Fixed sections were dehydrocarbonated with xylene, hydrated with graded ethanol, and rinsed with distilled water. Hematoxylin and eosin (H&E) staining kit was used to detect morphological changes in the colon and ileum.

2.7 Serum biochemical analysis

After the intestinal transport experiment, the mice were anesthetized with isoflurane, and the eyeballs were enucleated and blood was collected. All blood samples were centrifuged at 4°C, 3,500 rpm (5804R desktop refrigerated centrifuge) for 15 min, and serum samples were obtained and stored in a −80°C ultra-low temperature refrigerator. According to the instructions of the enzyme-linked immunosorbent assay (ELISA) kit, the gastric motility protein (MTL), gastrin (Gas), endothelin (ET), substance P (SP), acetylcholinesterase (AChE), and blood vessels in the serum were measured. Viable intestinal peptide (VIP) levels.

2.8 Determination of short-chain fatty acid content

Gas chromatography was used to determine the contents of acetic acid, propionic acid, butyric acid, isobutyric acid, valeric acid and isovaleric acid. Mouse feces were collected, quickly frozen in liquid nitrogen, and placed in an 80°C freezer for testing. Weigh 200 mg of feces into a 1.5 ml centrifuge tube, add 1 ml of ultrapure water, add 10 μl of concentrated hydrochloric acid to acidify, homogenize for 3 min, let stand for 20 min after homogenization, centrifuge at 10,000 rpm for 10 min in a high-speed centrifuge at 4°C, and remove the supernatant The liquid is transferred to the injection bottle for testing.

2.9 Intestinal microbial 16s rRNA sequencing

Before the end of the experiment, the sterile feces of each mouse were collected, quickly frozen in liquid nitrogen, and then stored in an −80°C freezer for later use. Mouse fecal samples were taken out. Magnetic Soil and Stool DNA Kit (TianGen) was used to extract genomic DNA from the samples. The purity and concentration of DNA were detected by 1% agarose gel electrophoresis. Appropriate sample DNA was placed in a centrifuge tube and diluted to 1 ng/μL with sterile water. Then the PCR products were obtained and purified. The Library was constructed using NEB Next? Ultra™ II FS DNA PCR-free Library Prep Kit (New England Biolabs). The constructed library was quantified by Qubit and Q-PCR. Enable NovaSeq6000 to perform PE 250 on-machine sequencing. According to Barcode sequence and PCR amplification primer sequence, the sample data were separated from the disembarkation data. Qiime2 is used to analyze the raw data obtained and generate a graph of the analysis results on the Yun Tutu platform.

2.10 Data analysis

SPSS 13.0 statistical software was used for analysis, and GraphPad Prism 9.0 software was used for graphing. Data were

10.3389/fmicb.2024.1353015

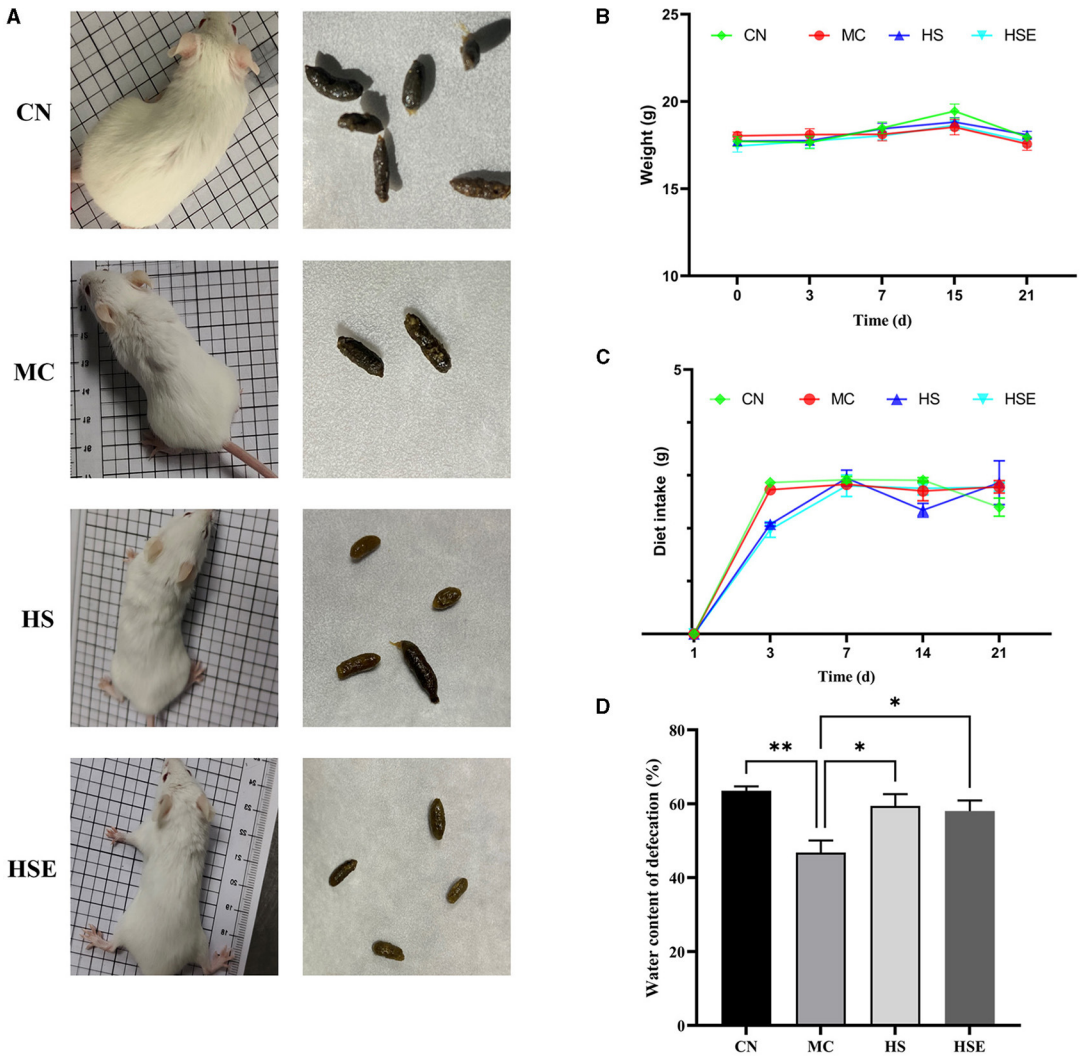

FIGURE 1
Effects of hemp seeds on the growth parameters and moisture content of feces in mice with constipation **(A)** Physiological status and feces of mice **(B)** Weight variation of mice **(C)** Food consumption of mice, and **(D)** Moisture content of feces. Results are provided as mean ± SEM ($n = 4–6$) $^{*}P <$ 0.05, and $^{**}P < 0.01$ compared to constipation group.

expressed as Mean ± standard error of the mean (SEM). One-way analysis of variance was used for comparison between groups. P<0.05 is considered as statistically significant.

3 Results

3.1 Effects of hemp seeds on physiological parameters in mice with constipation

The status and fecal morphology of the mice are shown in Figure 1A. Mice in the CN group appeared to be behaviorally active, with shiny hair and normal fecal pellets in size with a smooth and moist surface. In contrast, mice in the MC group were found to be less behaviorally active by curling themselves up, with fluffy hair and dark hard stools with a rough dry surface after induced constipation. After 2 weeks of treatment with HS and HSE, improvement in physiological state was observed in both HS and HSE groups. Mice in the HS group appeared to be behaviorally active, with fecal pellets that were smooth and soft, while mice in the HSE group were in a good mental state, with smaller fecal pellets that were smooth on surface and less hard. As shown in Figures 1B, C, there was no significant difference in weight variation and food consumption across the four groups. As shown in Figure 1D, there was a significant difference in water content of feces between the CN group and the MC group, that is, a significant increase in moisture content of feces was observed for mice in the HS and HSE groups after treatment with HS and HSE, respectively ($P < 0.05$).

3.2 Effects of hemp seeds on intestinal tract

The time to first bowel movement and small intestinal transit rates of the mice are provided in Figures 2A, B, D. After induced constipation, the time to first bowel movement was significantly

10.3389/fmicb.2024.1353015

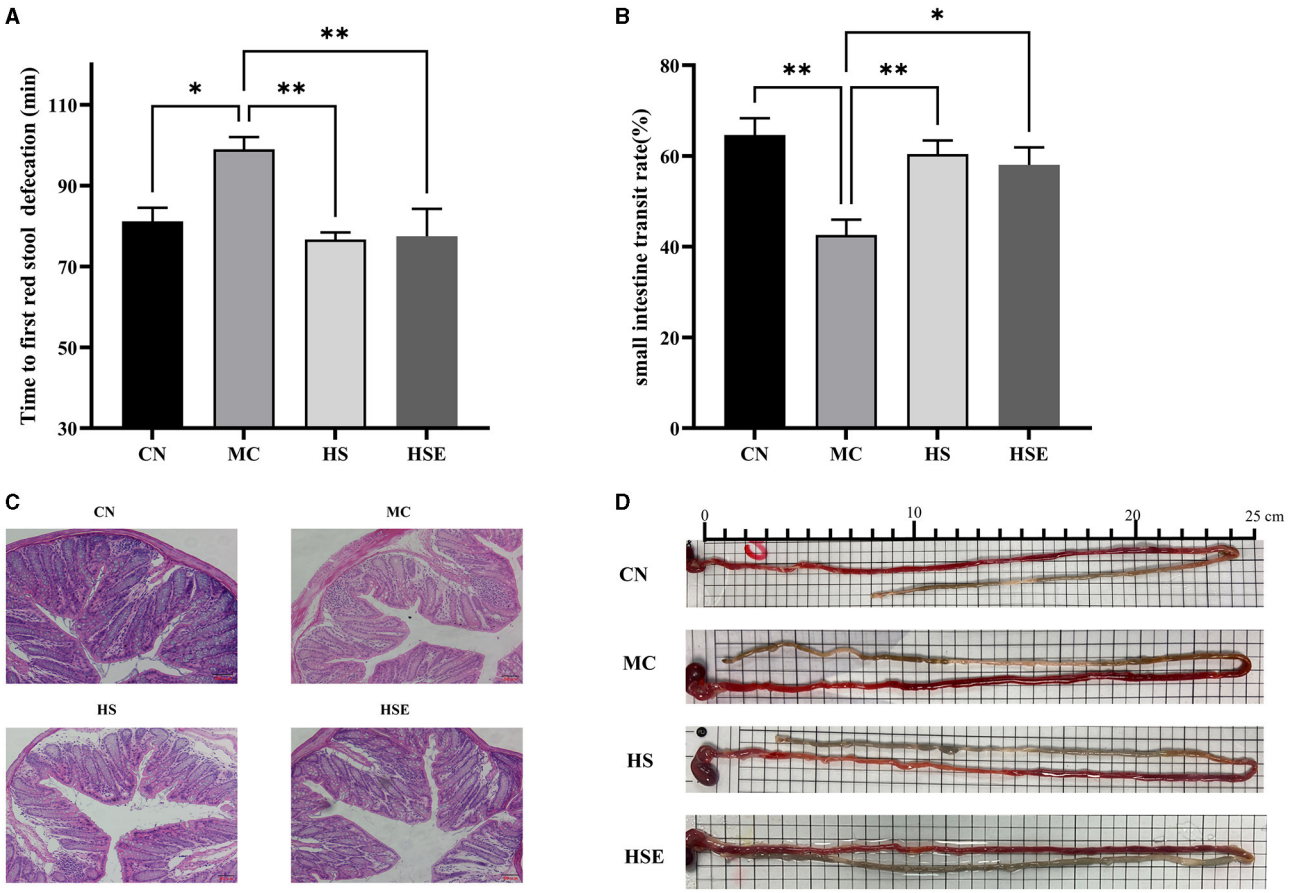

FIGURE 2
Effects of hemp seeds treatment on intestinal transit and protective effects on colonic tissue in mice with constipation **(A)** Time to discharge of the first red fecal pellet **(B)** Small intestinal transit rate **(C)** HE staining in the colon of mice, and **(D)** Image of assay on small intestinal transit rate (each cell in the picture is 0.5 cm long). Results are provided as mean ± SEM ($n = 5–6$) *$P < 0.05$ and **$P < 0.01$ compared with constipation group.

prolonged in the MC group compared with the CN group ($P < 0.05$), while the small intestinal transit rate was significantly decreased ($P < 0.01$), conforming to the characteristics of constipation in mice. After treatment with HS and HSE, the time to first bowel movement was significantly reduced in the HS and HSE groups ($P < 0.01$). In terms of improvement of small intestinal transit rate, the HS group showed an extremely significant change ($P < 0.01$) whereas the HSE group showed a significant change ($P < 0.05$). The experimental results showed that HS was superior to HSE in terms of the effects of reducing the time to bowel movement and promoting small intestinal transit. To further investigate the protective effects of HS and HSE on the intestinal tract in mice with constipation, we observed the histomorphological changes of the distal colon by histological staining. As shown in Figure 2C, increased infiltration of inflammatory cells, shorter crypts, fewer goblet cells and greater muscularis-crypt distance were observed in the colon of the MC group compared with the CN group. After treatment with HS and HSE, decreased inflammatory cell infiltration and increased goblet cells were noticed, indicating that constipation induced colitis in the mice and HS/HSE could relieve the inflammatory reaction caused by constipation.

3.3 Effects of hemp seeds on serum levels of neurotransmitters relating to gastrointestinal regulation

To further evaluate the effects of HS and HSE on constipation, serum parameters were measured. As shown in Figure 3, the levels of MTL, GAS and SP in the MC group were significantly lower than those in the CN group (*$P < 0.05$ for MTL, *$P < 0.05$ for GAS, and **$P < 0.01$ for SP), while the levels of ET and VIP increased but were not significantly different from those in the CN group, and the level of AchE decreased but was not significantly different from that in the CN group. After treatment with HS, the levels of MTL and GAS were significantly increased (*$P < 0.05$), and the level of ET was significantly decreased (**$P < 0.01$), but there were no significant differences in the levels of SP, VIP and AchE. In contrast, HSE-treated mice were observed with significant increases in the levels of MTL, GAS, and SP (**$P < 0.01$ for MTL, **$P < 0.01$ for GAS, and ***$P < 0.001$ for SP), and a significant decrease in the level of ET (*$P < 0.05$), whereas there were no significant differences in the levels of VIP and AchE.

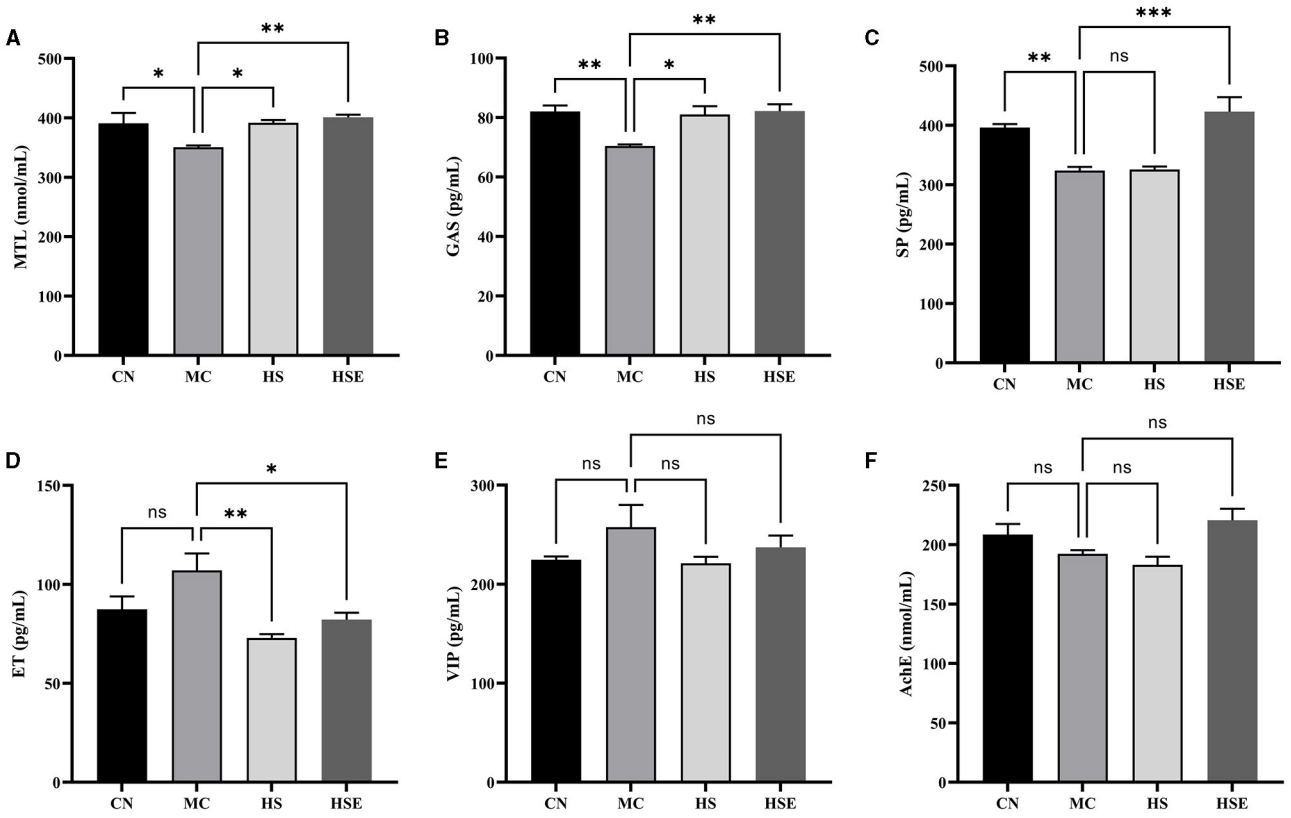

FIGURE 3
Effects of hemp seeds treatment on serum levels of neurotransmitters relating to gastrointestinal regulation in mice with constipation. **(A–F)** represents MTL, GAS, SP, ET, VIP, and AchE, respectively. Results are provided as mean ± SEM ($n = 4$) *$P < 0.05$, **$P < 0.01$, and ***$P < 0.001$ compared with constipation group.

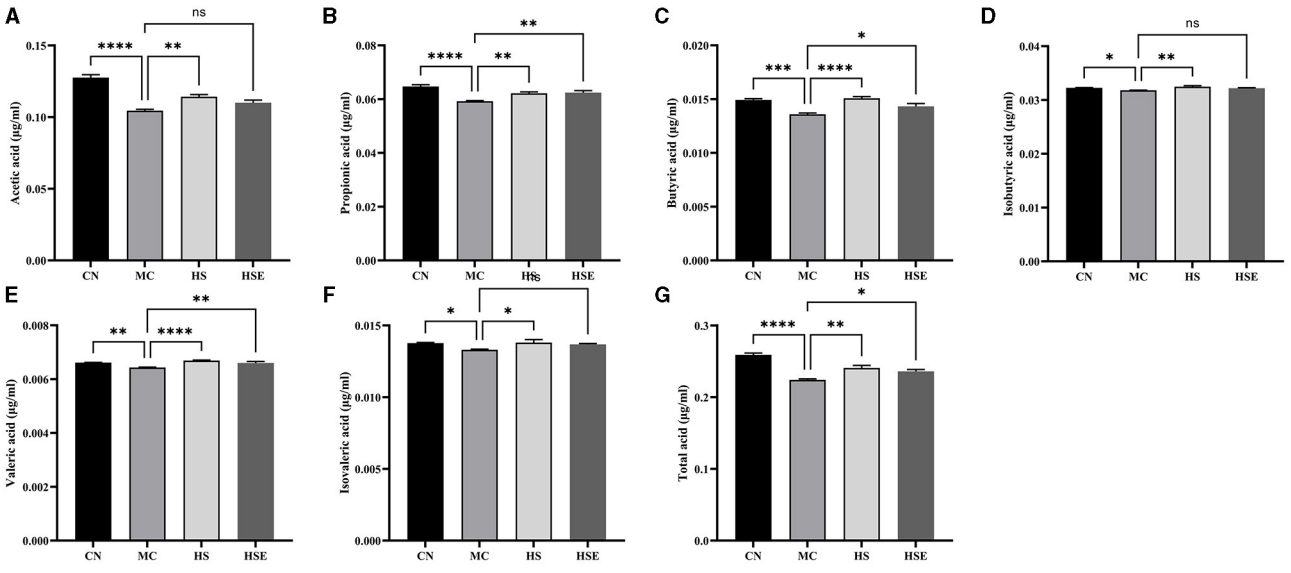

FIGURE 4
Effects of hemp seeds treatment on short-chain fatty acids (SCFAs) in the mice with constipation. **(A–G)** represents acetic acid, propionic acid, butyric acid, isobutyric acid, valeric acid, isovaleric acid and total acids, respectively. Results are provided as mean ± SEM ($n = 6$) *$P < 0.05$, **$P < 0.01$, ***$P < 0.001$, and ****$P < 0.0001$ compared with constipation group.

3.4 Effects of hemp seeds on short-chain fatty acids

SCFAs are the main products from the fermentation of indigestible carbohydrates by symbiotic bacteria. In addition to the effects of inhibiting the growth of pathogenic microorganisms and increasing the absorption of certain nutrients, SCFAs were also reported to regulate intestinal neurons and affect gastrointestinal motility. The fecal concentrations of SCFAs in this study are provided in Figure 4. The fecal concentrations of acetic acid, propionic acid, butyric acid, isobutyric acid, valeric acid, isovaleric acid and total acids were significantly lower in the MC group than in the CN group. After HS treatment, the HS group was observed with a significant increase in the fecal concentrations of the six short-chain fatty acids, while the HSE group was noticed with a significant increase in the fecal concentrations of propionic acid, butyric acid, valeric acid and total acids compared with the MC group, without no significant change in the fecal concentrations of acetic acid, isobutyric acid and isovaleric acid. The results showed that HS/HOS treatment led to a change in the content of SCFAs, which was possibly the protective mechanism of HS and HSE on the mice with constipation.

3.5 Effects of hemp seeds on the composition of intestinal microorganisms

To assess the effects of hemp seeds on the microbiota in intestinal feces, we performed metagenomic analysis of 16SrRNA gene sequences to examine changes in intestinal microorganisms after prophylaxis with hemp seeds (HS, HSE) and to characterize the effects on intestinal microbiota in mice after loperamide treatment. Alpha diversity (encompassing multiple indexes) is used as a measure of microbiota diversity (Cao et al., 2021). Totally 24 samples from four groups were evaluated. After sequence optimization, a total of 22,711,313 readable sequences were generated, with an average of 112,972 readable sequences per group. The results and the calculated α-diversity indexes of microbiota are shown in Figures 5A, B. At the OUT level, after Loperamide induced constipation, the Shannon and pielou_evenness indexes of intestinal microbiota in the MC group were higher than those in other groups, but there was no significant difference between groups as compared, indicating that HS and HSE treatment had no significant effect on the α-diversity of microbiota. As shown by the results of β-diversity (as measured by the Bray-Curtis distance) in Figure 5C, a trend toward segregation was observed with mice in the CN and MC group, whereas the HS and HSE groups were largely segregated from the MC group.

Taxonomically, Figure 6A presents the distribution of fecal flora at the phylum level. Although a total of 11 phyla were identified in the feces from all mice, the fecal flora was mostly composed of *Firmicutes/Bacteroides*. Therefore, we further conducted a discussion on changes in the proportion of the two phyla. Compared with the CN group, the proportion of *Bacteroides* was decreased and that of *Firmicute* was increased in the MC group, and the *Firmicutes/Bacteroides* ratio was 1.14 in the MC group, being higher than the ratio of 0.99 in the CN group, without a significant difference. After treatment with HS/HSE, the proportion of *Firmicutes* increased in the HS group, and interestingly, the number of *Bacteroides* also showed a trend toward increasing in the HS group compared with the MC group, but the *Firmicutes/Bacteroides* ratio in the HS group was almost equal to that in the MC group. On the other hand, the proportion of firmicutes decreased but that of *Bacteroides* increased in the HSE group compared with the MC group, and therefore the *Firmicutes/Bacteroides* ratio in the HSE group was lower than that in the MC group, but there was not a significant difference, which was consistent with the study findings (Lin et al., 2022). At the genus level, as shown in Figures 6B–F, the proportions of *Bacteroides* and *Odoribacter* were significantly lower in the MC group than in the CN group. Interestingly, the microbial change trend was basically identical between HS and HSE group. Compared with the MC group, an increased proportion of *Odoribacter* and of *Bacteroides* was observed with HS and HSE group. On the other hand, the proportion of *Lactobacillus* genus increased significantly in the HSE group, but there was no significant increase in HS group. Compared with the MC group, the abundance of *Precotella* in HS and HSE groups decreased significantly. Finally, we inferred that HS and HSE exerted effects on constipation by affecting different genera of bacteria to influence intestinal microbiota.

We next addressed differential changes in the relative content of microorganisms. As shown in Figure 7A, *Clostridium* was the most significantly enriched genus in the CN group, *Roseburia* and *Lachnospiraceae* were significantly enriched in the MC group, whilst *Rikenella*, *Ruminococcus*, *Anaerotruncus*, *Allobaculum* and *Desulfovibrio* were the significantly enriched genus in the HS group.

The results of linear discriminant analysis (LDA) provided in Figure 7B showed that *Clostridium* was the dominant genus in the NC group, *Roseburia* was the genus enriched in the MC group, and interestingly, *Allobaculum* was the genus enriched significantly in the HS group after HS treatment.

4 Discussion

There is a steady rise in the number of people with constipation in China with improvement of the living standards. Constipation, a functional gastrointestinal disorder that involves altered bowel movements, will seriously affect daily living and work and has become a common concern in the medical field (Rao et al., 2016). Loperamide is a drug intended for diarrhea control approved by the US Food and Drug Administration. It is often used as a model inducer for the treatment of constipation, by prolonging the duration of emptying, inhibiting peristalsis and reducing mucus in the colon. The feasibility and stability of loperamide in constipation model have been widely acknowledged (Wang et al., 2017). Fecal moisture content, time to first bowel movement, and intestinal charcoal propulsion rate are important measures used to assess gastrointestinal function (Fernández-Bañares, 2006). As one of traditional Chinese medicine with a long history in China, hemp seeds are one of the resources of affinal drug and diet, Meanwhile, hemp seeds have demonstrated potential for treating constipation, but it is still limited in popularization as a human food. This study discusses the effect

10.3389/fmicb.2024.1353015

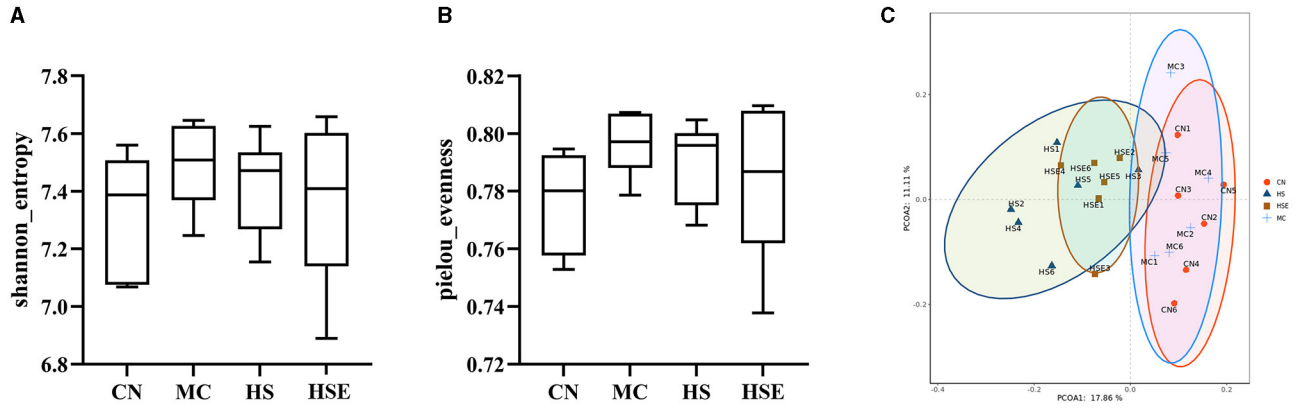

FIGURE 5
Review on the composition and diversity of intestinal microbiota in mice treated with hemp seeds for constipation. **(A)** Shannon Index, **(B)** Evenness Index, and **(C)** Plot of Principal Coordinate Analysis (PCoA) Score. Data are provided as mean ± SEM ($n = 6$).

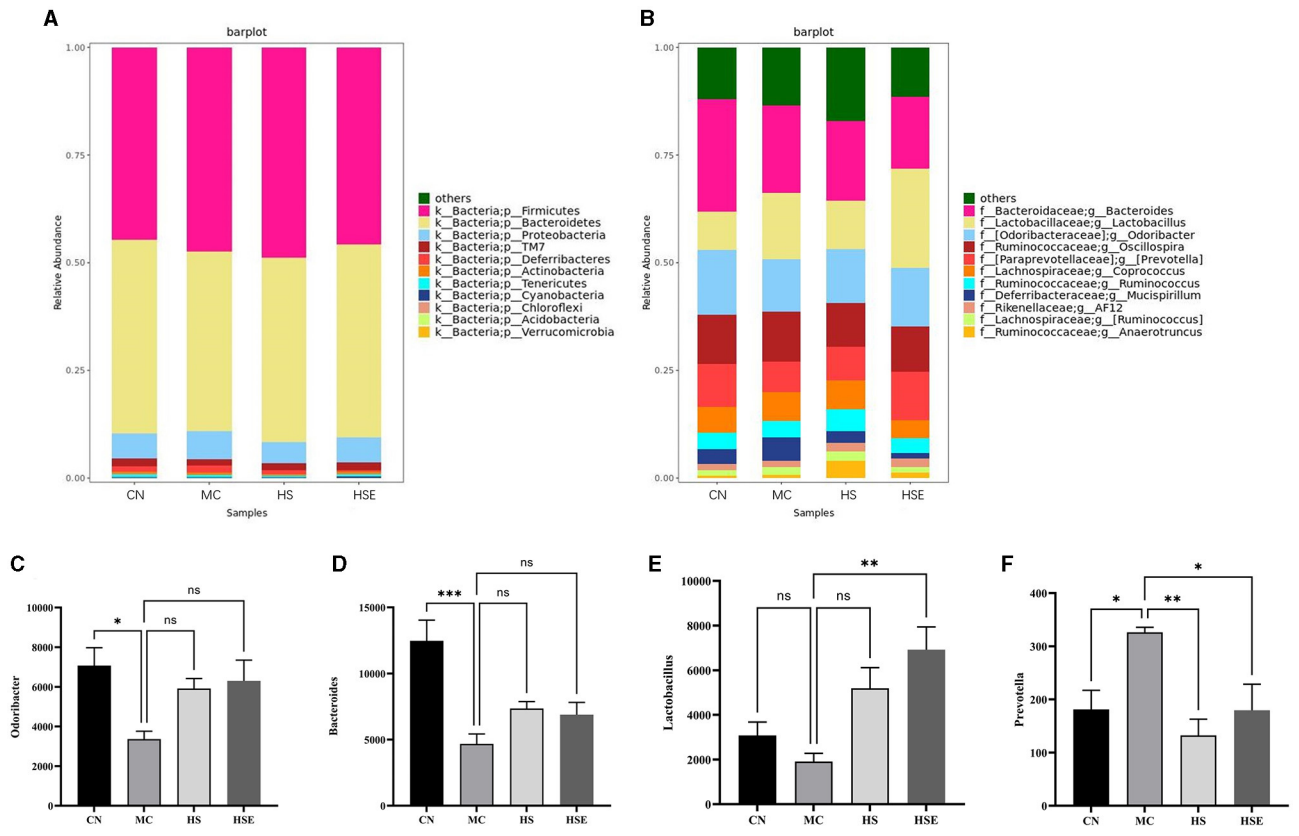

FIGURE 6
review on relative abundance of intestinal microbiota in mice treated with hemp seeds for constipation- composition of the microbiota. **(A)** phylum and **(B)** genus levels, **(C)** Relative abundance of *Odoribacter*, **(D)** Relative abundance of *Bacteroides*, **(E)** Relative abundance of *Lactobacillus*, **(F)** Relative abundance of *Prevotella*. Data are provided as mean ± SEM $^{*}P < 0.05$, $^{**}P < 0.01$, and $^{***}P < 0.001$ compared with constipation group.

of hemp seeds and water/ethanol extracts from hemp seeds in improving constipation in mice. The results showed that both hemp seeds and hemp seed extracts significantly improved the defecation parameters in mice, including fecal moisture content and time to first bowel movement. Parameters reflecting intestinal peristalsis are related to multiple aspects, such as fecal weight, fecal moisture content, time to fecal discharge, gastrointestinal transit time, small intestinal propulsion rate, and intestinal contractile activity (Gu et al., 2022). The improvement in defecation parameters indicates, to some extent, the effect of HS and HSE on intestinal peristalsis. In addition, the results of colon staining showed that HS/HSE improved to some extent the

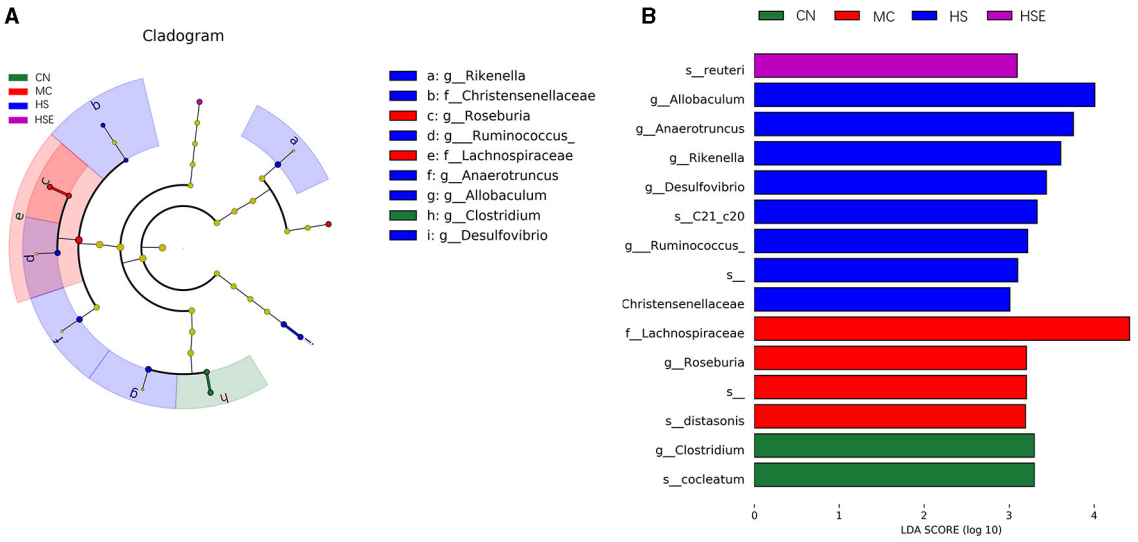

FIGURE 7
Differential classification of microorganisms in mice treated with hemp seeds for constipation. **(A)** Linear discriminant analysis effect size (LEfSe), and **(B)** Linear discriminant analysis (LDA). Data are provided as mean ± SEM ($n = 6$).

inflammatory reactions caused by constipation, which was possibly one of the reasons why hemp seeds have the effect of improving intestinal peristalsis.

We also studied the effects of hemp seeds on the serum levels of neurotransmitters and gastrointestinal hormones. MTL and GAS play an important role in regulating gastrointestinal peristalsis by stimulating the secretion of gastric acid and pepsin, promoting pyloric sphincter relaxation, gastrointestinal peristalsis and gastric emptying (Iijima et al., 2015). SP is an excitatory peptide neurotransmitter that stimulates intestinal peristalsis (Suo et al., 2014). Some studies have reported that SP stimulates interstitial cells of Cajal, induces contraction of gastrointestinal smooth muscles, and promotes gastrointestinal peristalsis (Faussone-Pellegrini, 2006). ET plays an important role in maintaining basal vascular tone and basic cardiovascular system. Constipation not only causes disorders (including intestinal obstruction and other serious diseases), but also induces or aggravates cardiovascular and cerebrovascular diseases in the elderly (Fevang et al., 2001).

In our study, after loperamide induced constipation, the levels of MTL, GAS and SP in the serum of mice in MC group were significantly lower than those in CN group, indicating that the occurrence of constipation is related to these neurotransmitters. After preventive treatment with hemp seeds and water/ethanol extracts from hemp seeds, hemp seed significantly increased the levels of MTL and GAS in serum of mice in HS group, and decreased the levels of ET, while hemp seed extract significantly increased the levels of MTL, GAS and SP in serum of mice in HSE group, and decreased the levels of ET. Extracts from hemp seeds demonstrated a stronger effect in regulating serum levels of neurotransmitters and gastrointestinal hormones. The differences observed were possibly a result of increased utility of the active ingredients in the extracts following extraction from hemp seeds. Variation in the levels of these gastrointestinal hormones would lead to a change in gastrointestinal peristalsis. We inferred that the improved intestinal propulsion rate and the shortened time to bowel movement were closely related to variation in the serum levels of such gastrointestinal hormones and neurotransmitters, suggesting that hemp seeds may alleviate the symptoms of constipation by regulating neurotransmitters and gastrointestinal hormones to stimulate intestinal peristalsis.

Disturbance of the intestinal microbiota is one of the characteristics of patients with constipation (Tian et al., 2020),It was revealed in the study by Huang et al. that patients with chronic functional constipation (CFC) had abnormalities in the number and composition of intestinal microbiota (Huang T. et al., 2018). Some studies suggested that changes in the intestinal microorganisms may alleviate or worsen constipation (Dimidi et al., 2017). In a study of pentose extracted from human milk to improve constipation in mice, it was shown that constipation was improved by increasing beneficial bacteria such as *Lactobacillus*, *Ruminococcaceae_UCG-014* and *Bacteroidales_S24-7* to improve the composition of intestinal microorganisms (Huang et al., 2020). In addition, hemp seeds have been widely reported to have effects on the intestinal microbiota. Changes in the intestinal microbiota in mice are primarily detected by changes in bacteria in the feces (Wang et al., 2017). Therefore, this study was of research significance by investigating whether hemp seeds could improve constipation by improving the intestinal microbiota. The results showed that after loperamide-induced constipation, significant differences in intestinal microbiota were observed between the CN and MC groups at the genus level. Our results showed that the intestinal microbiota was primarily composed of *Firmicutes and Bacteroides* and secondarily of Proteobacteria, and there was not a significant difference in the proportion of Firmicutes or Bacteroides at the genus level across the four groups, which was consistent with the study findings by (Gu et al., 2022). At the genus level, HS and HSE groups were observed with an increase in the proportion of *Odoribacter, Bacteroides* and *Lactobacillus*, and interestingly, the HS group and the HSE group were observed with a lower proportion of *Precotella* compared with the MC group.

These results suggest that hemp seeds regulate the symptoms of constipation by increasing the proportion of beneficial bacteria at the genus level. *Lactobacillus* works to decompose oligosaccharides in the intestinal tract, produce organic acids (including butyric acid, acetic acid, and propionic acid), improve intestinal peristalsis, and reduce the time to bowel movement. In addition, lactobacillus produces a great amount of volatile fatty acids and inhibit the excessive production of aerobic harmful bacteria, thereby maintaining the balance of intestinal microbiota (Cao et al., 2018). It has been found that butyric acid can be used as a carbon source for intestinal microbiota to produce acetic acid (Zhuang et al., 2019).

Hemp seeds are able to regulate the intestinal microbiota, one ability of intestinal bacteria is to produce SCFAs, but this process is influenced by the number of bacteria, pH, and substrate in the intestinal tract (Liu and Zhi, 2021). SCFAs are the metabolites of dietary fiber fermented by intestinal microorganisms. There is also a strong association between SCFAs and constipation. They affect the intestinal secretion function and enhance the intestinal mucosal barrier by regulating the functions of cell subsets like enterocytes (proliferation and differentiation) and enteroendocrine cells through different mechanisms. Organic acids act on the intestinal wall to lower pH in the intestinal tract and regulate gastrointestinal peristalsis and gastrointestinal function (Malagelada et al., 2017). Acetic acid acts to up-regulate the barrier function of enterocytes of the host (Fukuda et al., 2011),whilst propionate reduces fat production, serum cholesterol levels, and carcinogenesis in other tissues (Hosseini et al., 2011). Butyrate, which is a major source of metabolic energy in the large intestine, is the most important SCFAs and help to maintain the integrity of the large intestine, control intestinal inflammation, and support the genomic stability (Jiang et al., 2020). In a study reported on hemp seed, hemp seed increased the concentration of short-chain fatty acids in intestinal contents to improve intestinal health (Jurgoński et al., 2020). SCFAs can promote the secretion of intestinal fluids, accelerate colonic motility and are even considered as candidates for the treatment of constipation (Nicholson et al., 2012). In our study, the HS group was found to have significantly higher concentrations of the six SCFAs compared with the MC group, and the HSE group was observed with higher levels of propionic acid, butyric acid and valeric acid than the MC group, but HSE (an extract from hemp seeds) appeared inferior to HS in terms of the effect of increasing the levels of SCFAs. This was possibly because that production of SCFAs is affected by the quantity of microorganisms, the ambient pH value and the substrate concentration. The amounts and proportions of SCFAs produced by different substrate vary (Ritzhaupt et al., 1998). After extraction, HSE was inferior to HS in terms of both the type and concentration of substrate, and this was possibly one of the reasons for differences in the levels of SCFAs between the HS and HSE groups.

5 Conclusions

This study investigated the effects of hemp seeds and hemp seed extracts in the mice with constipation. The results showed that both hemp seeds and hemp seed extracts significantly improved the moisture content of feces, shortened the time to bowel movement, and promoted intestinal peristalsis in the mice with constipation. Hemp seeds were superior to hemp seed extracts in terms of the above effects. Both affected the levels of gastrointestinal hormones in the serum, whilst hemp seed extracts exhibited a stronger effect than hemp seeds. In contrast, hemp seed extracts had less effects on the levels of SCFAs than hemp seeds. In conclusion, both hemp seeds and hemp seed extracts provide protective effects in the mice with constipation to some extent.

Data availability statement

The datasets presented in this study can be found in online repositories. The names of the repository/repositories and accession number(s) can be found in the article/supplementary material.

Ethics statement

The animal studies were approved by Animal Ethics Committee of Changshu Hospital Affiliated to Nanjing University of Chinese Medicine. The studies were conducted in accordance with the local legislation and institutional requirements. Written informed consent was obtained from the owners for the participation of their animals in this study.

Author contributions

HH: Writing – original draft, Conceptualization, Formal analysis, Investigation, Methodology, Resources, Software. WY: Data curation, Formal analysis, Methodology, Visualization, Writing – original draft. DX: Conceptualization, Data curation, Methodology, Writing – review & editing. LF: Data curation, Software, Writing – original draft. GJ: Methodology, Formal analysis, Writing – review & editing. JJ: Formal analysis, Supervision, Writing – review & editing. ZF: Data curation, Formal analysis, Methodology, Writing – original draft, Writing – review & editing. JL: Funding acquisition, Investigation, Supervision, Writing – original draft, Writing – review & editing.

Funding

The author(s) declare financial support was received for the research, authorship, and/or publication of this article. This study was supported by Changshu Municipal Science and Technology Bureau Supporting Project (Grant Number: CS202227), Changshu Health Commission Science and Technology Plan Project (Grant Number: CSWS202103), Jiangsu Traditional Chinese Medicine Science and Technology Development Project (Grant Number: MS2021058), and Open Project of Zhenjiang Traditional Chinese Medicine Spleen and Stomach Diseases Clinical Medicine Research Center (Grant Number: SSPW2022-KF08).

Conflict of interest

The authors declare that the research was conducted in the absence of any commercial or financial relationships that could be construed as a potential conflict of interest.

Publisher's note

References

Camilleri, M., Ford, A. C., Mawe, G. M., Dinning, P. G., Rao, S. S., Chey, W. D., et al. (2017). Chronic constipation. *Nat. Rev. Dis. Primers*. 3, 17095. doi: 10.1038/nrdp.2017.95

Cao, P. Q., Li, X. P., Ou-Yang, J., Jiang, R. G., Huang, F. F., Wen, B. B., et al. (2021). The protective effects of yellow tea extract against loperamide-induced constipation in mice. *Food Funct.* 12, 5621–5636. doi: 10.1039/d0fo02969f

Cao, Y. N., Feng, L. J., Wang, B. M., Jiang, K., Li, S., Xu, X., et al. (2018). Lactobacillus acidophilus and Bifidobacterium longum supernatants upregulate the serotonin transporter expression in intestinal epithelial cells. *Saudi J. Gastroenterol.* 24, 59–66. doi: 10.4103/sjg.SJG_333_17

Cheng, C. W., Bian, Z. X., Zhu, L. X., Wu, J. C., and Sung, J. J. (2011). Efficacy of a Chinese herbal proprietary medicine (Hemp Seed Pill) for functional constipation. *Am. J. Gastroenterol.* 106, 120–129. doi: 10.1038/ajg.2010.305

Crowe, M. S., and Kinsey, S. G. (2017). MAGL inhibition modulates gastric secretion and motility following NSAID exposure in mice. *Eur. J. Pharmacol.* 807, 198–204. doi: 10.1016/j.ejphar.2017.05.006

Dimidi, E., Christodoulides, S., Scott, S. M., and Whelan, K. (2017). Mechanisms of action of probiotics and the gastrointestinal microbiota on gut motility and constipation. *Adv. Nutrit.* 8, 484–494. doi: 10.3945/an.116.014407

Ding, C., Ge, X., Zhang, X., Tian, H., Wang, H., Gu, L., et al. (2016). Efficacy of synbiotics in patients with slow transit constipation: a prospective randomized trial. *Nutrients* 8, 605. doi: 10.3390/nu8100605

Faussone-Pellegrini, M. S. (2006). Relationships between neurokinin receptor-expressing interstitial cells of Cajal and tachykininergic nerves in the gut. *J. Cell. Mol. Med.* 10, 20–32. doi: 10.1111/j.1582-4934.2006.tb00288.x

Fernández-Bañares, F. (2006). Nutritional care of the patient with constipation. *Best Pract. Res. Clin. Gastroenterol.* 20, 575–587. doi: 10.1016/j.bpg.2005.11.002

Fevang, J., Ovreb,ø, K., Myking, O., Grong, K., and Svanes, K. (2001). Role of endothelin in the circulatory changes associated with small bowel strangulation obstruction in pigs: effects of the endothelin receptor antagonist bosentan. *J. Surg. Res.* 96, 224–232. doi: 10.1006/jsre.2000.6066

Fukuda, S., Toh, H., Hase, K., Oshima, K., Nakanishi, Y., Yoshimura, K., et al. (2011). Bifidobacteria can protect from enteropathogenic infection through production of acetate. *Nature* 469, 543–547. doi: 10.38/nature09646

Gu, Y., Qin, X., Zhou, G., Wang, C., Mu, C., Liu, X., et al. (2022). Lactobacillus rhamnosus GG supernatant promotes intestinal mucin production through regulating 5-HT4R and gut microbiota. *Food Funct.* 13, 12144–12155. doi: 10.1039/d2fo01900k

Heidelbaugh, J. J., Stelwagon, M., Miller, S. A., Shea, E. P., and Chey, W. D. (2015). The spectrum of constipation-predominant irritable bowel syndrome and chronic idiopathic constipation: US survey assessing symptoms, care seeking, and disease burden. *Am. J. Gastroenterol.* 110, 580–587. doi: 10.1038/ajg.2015.67

Hosseini, E., Grootaert, C., Verstraete, W., and Van de Wiele, T. (2011). Propionate as a health-promoting microbial metabolite in the human gut. *Nutr. Rev.* 69, 245–258. doi: 10.1111/j.1753-4887.2011.00388.x

Huang, J., Li, S., Wang, Q., Guan, X., Qian, L., Li, J., et al. (2020). Pediococcus pentosaceus B49 from human colostrum ameliorates constipation in mice. *Food Funct.* 11, 5607–5620. doi: 10.1039/d0fo00208a

Huang, J., Lin, B., Zhang, Y., Xie, Z., Zheng, Y., Wang, Q., et al. (2022). Bamboo shavings derived O-acetylated xylan alleviates loperamide-induced constipation in mice. *Carbohydr. Polym.* 276, 118761. doi: 10.1016/j.carbpol.2021.118761

Huang, L. S., Kong, C., Gao, R. Y., Yan, X., Yu, H. J., Wen, B., et al. (2018). Analysis of fecal microbiota in patients with functional constipation undergoing treatment with synbiotics. *Eur. J. Clini. Microbiol. Infect. Dis.* 37, 555–563. doi: 10.1007/s10096-017-3149-7

Huang, T., Ning, Z., Hu, D., Zhang, M., Zhao, L., Lin, C., et al. (2018). Uncovering the mechanisms of chinese herbal medicine (MaZiRenWan) for functional constipation by focused network pharmacology approach. *Front. Pharmacol.* 9, 270. doi: 10.3389/fphar.2018.00270

Iijima, K., Koike, T., Ara, N., Nakagawa, K., Kondo, Y., Uno, K., et al. (2015). Identification of a high-risk group for low-dose aspirin-induced gastropathy by measuring serum pepsinogen in H. pylori-infected subjects. *J. Gastroenterol.* 50, 305–312. doi: 10.1007/s00535-014-0976-5

Jiang, H., Dong, J., Jiang, S., Liang, Q., Zhang, Y., Liu, Z., et al. (2020). Effect of Durio zibethinus rind polysaccharide on functional constipation and intestinal microbiota in rats. *Food Res. Int.* 136, 109316. doi: 10.1016/j.foodres.2020.109316

Jurgoński, A., Opyd, P. M., and Fotschki, B. (2020). Effects of native or partially defatted hemp seeds on hindgut function, antioxidant status and lipid metabolism in diet-induced obese rats. *J. Funct. Foods*. 72, 104071. doi: 10.1016/j.jff.2020.104071

Lin, Q., Liu, M., Erhunmwunsee, F., Li, B., Mou, Y., Wang, S., et al. (2022). Chinese patent medicine shouhui tongbian capsule attenuated loperamide-induced constipation through modulating the gut microbiota in rat. *J. Ethnopharmacol.* 298, 115575. doi: 10.1016/j.jep.2022.115575

Liu, W., and Zhi, A. (2021). The potential of Quercetin to protect against loperamide-induced constipation in rats. *Food Sci. Nutrit.* 9, 3297–3307. doi: 10.1002/fsn3.2296

Malagelada, C., Nieto, A., Mendez, S., Accarino, A., Santos, J., Malagelada, J. R., et al. (2017). Effect of prucalopride on intestinal gas tolerance in patients with functional bowel disorders and constipation. *J. Gastroenterol. Hepatol.* 32, 1457–1462. doi: 10.1111/jgh.13733

Nicholson, J. K., Holmes, E., Kinross, J., Burcelin, R., Gibson, G., Jia, W., et al. (2012). Host-gut microbiota metabolic interactions. *Science* 336, 1262–1267. doi: 10.1126/science.1223813

Opyd, P. M., Jurgoński, A., Fotschki, B., and Juśkiewicz, J. (2020). Dietary hemp seeds more effectively attenuate disorders in genetically obese rats than their lipid fraction. *J. Nutr.* 150, 1425–1433. doi: 10.1093/jn/nxaa081

Rao, S. S., Rattanakovit, K., and Patcharatrakul, T. (2016). Diagnosis and management of chronic constipation in adults. *Nat. Rev. Gastroenterol. Hepatol.* 13, 295–305. doi: 10.1038/nrgastro.2016.53

Ritzhaupt, A., Wood, I. S., Ellis, A., Hosie, K. B., and Shirazi-Beechey, S. P. (1998). Identification and characterization of a monocarboxylate transporter (MCT1) in pig and human colon: its potential to transport L-lactate as well as butyrate. *J. Physiol.* 513, 719–732. doi: 10.1111/j.1469-7793.1998.719ba.x

Salari, N., Ghasemianrad, M., Ammari-Allahyari, M., Rasoulpoor, S., Shohaimi, S., and Mohammadi, M. (2023). Global prevalence of constipation in older adults: a systematic review and meta-analysis. *Wien. Klin. Wochenschr.* 135, 389–398. doi: 10.1007/s00508-023-02156-w

Suo, H., Zhao, X., Qian, Y., Li, G., Liu, Z., Xie, J., et al. (2014). Therapeutic effect of activated carbon-induced constipation mice with Lactobacillus fermentum Suo on treatment. *Int. J. Mol. Sci.* 15, 21875–21895. doi: 10.3390/ijms151221875

Tian, Y., Zuo, L., Guo, Q., Li, J., Hu, Z., Zhao, K., et al. (2020). Potential role of fecal microbiota in patients with constipation. *Therap. Adv. Gastroenterol.* 13, 1756284820968423. doi: 10.1177/1756284820968423

Wang, L., Hu, L., Xu, Q., Jiang, T., Fang, S., Wang, G., et al. (2017). Bifidobacteria exert species-specific effects on constipation in BALB/c mice. *Food Funct.* 8, 3587–3600. doi: 10.1039/c6fo01641c

Wang, L., Wu, F., Hong, Y., Shen, L., Zhao, L., and Lin, X. (2022). Research progress in the treatment of slow transit constipation by traditional Chinese medicine. *J. Ethnopharmacol.* 290, 115075. doi: 10.1016/j.jep.2022.115075

Yan, X., Tang, J., dos Santos Passos, C., Nurisso, A., Simões-Pires, C. A., Ji, M., et al. (2015). Characterization of lignanamides from hemp (Cannabis sativa L.) seed and their antioxidant and acetylcholinesterase inhibitory activities. *J. Agric. Food Chem.* 63, 10611–10619. doi: 10.1021/acs.jafc.5b05282

Zhong, L. L. D., Cheng, C. W., Kun, W., Dai, L., Hu, D. D., Ning, Z. W., et al. (2019). Efficacy of MaZiRenWan, a Chinese herbal medicine, in patients with functional constipation in a randomized controlled trial. *Clini. Gastroenterol. Hepatol.* 17, 1303–1310.e18. doi: 10.1016/j.cgh.2018.04.005

Zhuang, M., Shang, W., Ma, Q., Strappe, P., and Zhou, Z. (2019). Abundance of probiotics and butyrate-production microbiome manages constipation via short-chain fatty acids production and hormones secretion. *Mol. Nutr. Food Res.* 63, e1801187. doi: 10.1002/mnfr.201801187

frontiers | Frontiers in Microbiology

TYPE Original Research
PUBLISHED 09 April 2024
DOI 10.3389/fmicb.2024.1375384

OPEN ACCESS

EDITED BY
Xiaodong Xia,
Dalian Polytechnic University, China

REVIEWED BY
Corina-Diana Ceapă,
National Autonomous University of Mexico, Mexico
Malgorzata Ziarno,
Warsaw University of Life Sciences, Poland

*CORRESPONDENCE
Yongqing Ni
✉ niyqlzu@sina.com
Yan Zhang
✉ zhangyanzqgh@163.com

†These authors have contributed equally to this work and share first authorship

RECEIVED 23 January 2024
ACCEPTED 13 March 2024
PUBLISHED 09 April 2024

CITATION
Lan Z, Zhang X, Xu M, Kong J, Zuo X, Wang Y, Wang C, Teng Y, Ni Y and Zhang Y (2024) Whole-genome resequencing and transcriptional profiling association analysis revealed the intraspecies difference response to oligosaccharides utilization in *Bifidobacterium animalis* subsp. *lactis*. *Front. Microbiol.* 15:1375384. doi: 10.3389/fmicb.2024.1375384

Whole-genome resequencing and transcriptional profiling association analysis revealed the intraspecies difference response to oligosaccharides utilization in *Bifidobacterium animalis* subsp. *lactis*

Zhenghui Lan†, Xueling Zhang†, Meng Xu, Junkai Kong, Xuancheng Zuo, Yixuan Wang, Chenxi Wang, Yingdi Teng, Yongqing Ni* and Yan Zhang*

School of Food Science and Technology, Shihezi University, Shihezi, Xinjiang Province, China

Introduction: As prebiotics, oligosaccharides are frequently combined with *Bifidobacterium* to develop synbiotic products. However, a highly diverse gene repertoire of *Bifidobacterium* is involved in sugar catabolism, and even phylogenetically close species may differ in their sugar utilization capabilities. To further explore the mechanism underlying the differences in *Bifidobacterium animalis* subsp. *lactis* oligosaccharide metabolism.

Methods: This study screened strains with differential oligosaccharide metabolism. Subsequently, these strains were subjected to genome-wide resequencing and RT-qPCR.

Results: The resequencing results indicated that the subspecies of *B. animalis* subsp. *lactis* had a high genome similarity. The RT-qPCR results revealed that glycosidase genes exhibited consistency in the phenotype of metabolism at the transcriptional level; the better the growth of the strains on the oligosaccharides, the higher was the expression of glycosidase genes related to the oligosaccharides. Our results suggested that the differences in the gene transcription levels led to intraspecies differences in the ability of the strains to metabolize oligosaccharides even when they belonged to the same subspecies.

Discussion: Future studies with more sample size could generalizable the conclusion to all *B. animalis* subsp. *lactis* strains, thus would lay the theoretical foundation for the utilization of the *B. animalis* subsp. *lactis* strain as probiotics and the development of synbiotic products.

KEYWORDS

***Bifidobacterium animalis* subsp. *lactis*, oligosaccharide metabolism, genotype comparison, resequencing, real-time PCR**

1 Introduction

The members of the genus *Bifidobacterium* are common inhabitants of the gastrointestinal tracts of humans and other mammals, where they ferment several diet-derived carbohydrates that cannot be digested by their hosts (O'connell et al., 2013). Until date, most studies have investigated *Bifidobacterium* and product development, such as the transformation of plant isoflavones by *Bifidobacterium*, the production of *Bifidobacterium*-fermented milk, and microencapsulation of *Bifidobacterium* (Gaya et al., 2017; Lohrasbi et al., 2020; Yan et al., 2020). The strains of *B. animalis* subsp. *lactis* are well-known health-promoting probiotics that are used commercially (Bunesova et al., 2017). The *B. animalis* subsp. *lactis* genome also contains a large number of transporters that transport complex carbohydrates, as well as genes for intracellular or extracellular hydrolases that degrade the glycosidic bonds in complex carbohydrates, which, in turn, facilitates the cell's uptake of these complex carbon-hydrates and provides the bacterium with the energy required for growth, thereby adapting to a complex environment. The genome sequence of *B. animalis* subsp. *lactis Bl-04* reveals putative prebiotic transport and catabolic pathways, as reported elsewhere (Paineau et al., 2008), thereby implying that the bacterium is highly adapted to the gastrointestinal tract (GIT) and can utilize diet-derived complex oligosaccharides. Certain indigestible carbon sources (oligosaccharides) consumed daily stimulate the growth of *Bifidobacterium* in the gut, are commonly used as the main prebiotics (Hopkins et al., 1998). Changes in the dietary composition may affect health; therefore, it is important to study the ability of *Bifidobacterium* to utilize carbohydrates as a theoretical guide for the rational design of new symbiotic products ("prebiotic-probiotic").

Oligosaccharides are carbohydrates formed by 2–10 monosaccharide molecules connected by glycosidic bonds. Owing to the rich variety of monosaccharide molecules that constitute oligosaccharides and the variety of intermolecular connection types and connection positions, there are several types of oligosaccharides in the nature. They can be broadly categorized into common oligosaccharides and functional oligosaccharides based on their biological functions. Common oligosaccharides mainly include lactose, sucrose, and maltose, which are easily digested and absorbed by the intestinal tract and thereby provide energy for the body's metabolism, growth, and development (Vieira et al., 2020; Liu et al., 2023). Functional oligosaccharides, also known as non-digestible oligosaccharides, are difficult to digest and absorb because of the lack of an enzyme system in the human intestinal tract that directly degrades these functional oligosaccharides. The functional oligosaccharides developed so far mainly include xylo-oligosaccharides (XOS), galacto-oligosaccharides (GOS), fructo-oligosaccharides (FOS), inulin, and resistant starch (Tomás-Barberán and Mine, 2013; Belorkar and Gupta, 2016). Because functional oligosaccharides are not hydrolyzed by intestinal digestive enzymes but can be decomposed, absorbed, and utilized by beneficial microorganisms in the intestinal tract, they are often used in combination with Bifidobacteria to develop symbiotic products.

However, the main challenge of using *Bifidobacterium* cultures directly in the food is that different matrices and environments hinder their growth and survival in food (Moradi et al., 2021). To increase the survival rate of *Bifidobacterium*, combining probiotics and prebiotics (symbiotic) has become a research hotspot. Prebiotics are substrates that are selectively used by host microbes to confer a health benefit (Sanders et al., 2019). However, probiotic bacteria selectively ferment prebiotics comprising mainly non-digestible oligosaccharides (Abou et al., 2013). Therefore, research was needed to understand the factors and mechanisms that the *Bifidobacterium* exhibits intraspecies differences in oligosaccharide utilization The application of symbiotic products is limited by the fact that not all oligosaccharides are appropriate for all *Bifidobacterium*. The efficacy of specific combination warrants validation before use. A past study has shown that *Bifidobacterium* exhibits interspecies differences in oligosaccharide utilization (Garrido et al., 2015). For example, *B. longum* has been found to consume most oligosaccharides, and the *B. bifidum* strain utilizes GOS with degrees of polymerization (DP) of 2 and 3 and exhibits very limited use of FOS (Li et al., 2017). In addition, on examining three *Bifidobacterium* strains, the strains exhibited specificity in utilizing human milk oligosaccharides (LoCascio et al., 2007). The *B. longum* subsp. *infantis* are more inclined to have better capabilities to metabolize human milk oligosaccharides. The XOS, FOS, soya bean oligosaccharides, and malto-oligosaccharides are more effective in promoting the growth of *B. adolescentis*. However, surprisingly, the oligosaccharide utilization ability varies between different isolates of the same species (Garrido et al., 2015). The presence of intraspecies differences in *Bifidobacterium* creates further challenges when combining symbiotic products and using *Bifidobacterium*. Ang-Xin Song et al. recently reported strain-specific utilization of wheat arabinoxylan by *B. longum* (Song et al., 2020). Furthermore, a study demonstrated that several endogalactanase-positive ($GalA^+$) *B. breve* strains can utilize purified GOS (PGOS) components with a high DP, whereas endogalactanase-negative ($GalA^-$) strains cannot. This intraspecies difference has been ascribed to *galA* present in *B. breve* strains (O'Connell Motherway et al., 2013). *Bifidobacterium* strain specifically utilizes oligosaccharides; such discoveries have generated substantial interest in the scientific community. The characteristics of the strains must thus be considered while producing symbiotic products. While synthesizing symbiotic products, specific prebiotics must be designed to pair with specific probiotics that will consume them and exhibit improved functional outcomes. Therefore, revealing the mechanisms underlying *Bifidobacterium* intraspecies differences in the metabolism of oligosaccharides and explaining the regularity of these differences are highly warranted for the development of effective synbiotics.

Most of the current studies are based on genotype–phenotype to investigate interspecies differences in the metabolism of functional oligosaccharides by *Bifidobacterium* (Bottacini et al., 2018; He et al., 2021). In contrast, the genomic structures of *B. animalis* subsp. *lactis* strains are similar, therefore there is a lack of differences in the metabolism of functional oligosaccharides by *Bifidobacterium* that can be analyzed from the transcriptional level.

The present study focused on *B. animalis* subsp. *lactis* obtained from human fecal samples of two regions with significant dietary differences. Then, we investigated their strain specificity in terms of the oligosaccharide-utilization capacity at the subspecies level. Using genome resequencing technology explored the key loci associated with oligosaccharide metabolism, combined phenotypic and genotypic data, and identified gene sequences significantly associated with differences in the oligosaccharide metabolism. RT-qPCR was performed to determine the differential gene expression during the growth of *B. animalis* subsp. *lactis* on oligosaccharides. The purpose of this study was to explore differences in the utilization phenotypes of different carbon sources, and to associate possible gene clusters for revealing the strain metabolism difference of functional oligosaccharides in *B. animalis* at the subspecies level and provides a theoretical basis for the study of *B. animalis* subsp. *lactis* and the application of synbiotic products.

2 Materials and methods

2.1 Materials

FOS, GOS, XOS, isomalto-oligosacchrides (IMO), raffinose, stachyos, inulin, resistant starch (RS), and glucose (Glu) were all purchased from Shanghai Yuanye Bio-Technology Co., Ltd. All other chemicals used were of analytical grade.

2.2 Sample collection and treatment

In sterile containers, we collected the fecal samples of mothers and their infants residing in Hotan, Xinjiang, China and Hainan, China. The samples were collected at the participants' homes and immediately frozen (−20°C) in a portable freezer. These samples were then transported to the laboratory and processed immediately upon receipt. The participants were not on any special diet, and, as instructed, had not taken probiotics or antibiotics for 2 months before sampling.

2.3 Isolation of *Bifidobacterium* from fecal samples by using the culture method

The samples were serially diluted (10^{-1} to 10^{-4}) in an anaerobic chamber, and 0.1 mL of aliquot of the 10^{-2}, 10^{-3}, and 10^{-4} dilutions were plated on *Bifidobacterium* specific mMRS agar. The medium (per liter) was composed of yeast extract, 5 g; peptone, 10 g; beef paste, 10 g; Tween 80, 1 mL; sodium acetate anhydrous, 5 g; ammonium citrate dibasic, 2 g; K_2HPO_4, 2 g; $MgSO_4$, 0.58 g; $MnSO_4$, 0.25 g; glucose, 20 g; L-cysteine, 0.5 g (Blotopped, China); mupirocin, 0.05 g (Bomei, Hefei, China); nystatin, 0.025 g (Bomei, China), and powdered agar, 20 g (Ventura et al., 2006; Linares-Morales et al., 2022). All other reagents involved in the composition of the culture medium were purchased from Sinopharm Chemical Reagent Beijing Co., Ltd., China. These plates were subsequently incubated under an atmosphere of 10% H_2, 10% CO_2, and 80% N_2 in an anaerobic chamber (DG520; DWS UK) and incubated for 48 h at 37°C (Shahin et al., 2003). All colonies appearing on the dilution plates were picked in succession and inoculated into mMRS broth.

2.4 DNA extraction and bacterial strain identification

The sample DNA was isolated from 1 mL of culture by using the FastPure Bacteria DNA Isolation Mini Kit (Vazyme, Nanjing, China) according to the manufacturer's protocol. The purity and concentration of isolated DNA were measured using a micro nucleic acid quantitative instrument (Thermo Scientific, United States). DNA with a 260/280 nm ratio of >1.8 was used as the template DNA, and its integrity was determined using 1.2% agarose gels. Next, the strains were identified by conducting molecular biology assays, including 16S rRNA gene sequencing of genomic DNA and *Bifidobacterium* subspecies-specific PCR (*aptD* gene). PCR amplification of the 16S rRNA gene was performed with primers 27F (5′-AGAGTTT GATCCTGGCTCAG-3′) and 1492r (5′-CTACGGCTACCTT GTTACGA-3′) (Nomoto et al., 2017). To further identify the isolated strains, *atpD* was PCR amplified with primers atp-1 (5′-CACCC TCGAGGTCGAAC-3′) and atp-2 (5′-CTGCATCTTGTGCCAC TTC-3′) (Ventura et al., 2004). The PCR-amplified products were detected through 1.2% agarose gel electrophoresis and sequenced using GENEWIZ (Suzhou Jinweizhi Biotechnology Co., Ltd., China). The sequencing results were submitted to the GenBank of the National Center for Biotechnology Information (NCBI) for BLAST homology comparison. A phylogenetic tree was constructed using MAGE 7.0 software. For repetitive-element PCR (rep-PCR), the strain was grown on MRS broth under anaerobic conditions for 48 h, and DNA was extracted as described earlier. Rep-PCR was conducted to generate genomic amplification products of the test strains. Specifically, rep-PCR amplification was performed using the Tc-512 PCR gene amplification instrument (Techne, British) and BOXAIR primers (Masco et al., 2003). The gel was visualized and photographed under a UV transilluminator (Quantum CX5, France). The separation of rep-patterns was processed with CelCompar || version 6.6 (Applied Maths, Sint-Matenslatem, Belgium) and analyzed using the Pearson's correlation coefficient and the unweighted pair group method with arithmetic mean (UPGMA) clustering algorithm.

2.5 Carbohydrate utilization

After 48 h of culture, the *Bifidobacterium* cells were centrifuged at 5000 xg for 5 min and washed twice with 0.9% normal saline. The cell suspensions (approximately 10^6 CFU/mL) were used to prepare bacterial inoculants for the carbohydrate fermentation experiments.

The *in vitro* utilization experiment was conducted using oligosaccharides (FOS, GOS, XOS, IMO, raffinose, stachyos, inulin, RS) as the unique carbon source in a 96-well microplate (Kan et al., 2020). The carbohydrate solution with 1% final concentration was added to the medium, thereby replacing glucose as a carbon source. Four microliters of each resulting suspension were inoculated into 200 µL of the modified medium. The experiment was conducted thrice with triplicate wells (He et al., 2021). The medium in which glucose was added instead of oligosaccharides was used as the positive control, whereas the medium without any carbon source was used as the negative control. Moreover, 0.05% (w/v) L-cysteine was added to the medium to consume free oxygen and promote strain growth and reproduction. The cells were incubated at 37°C in an anaerobic chamber for 48 h. Each carbon source fermentation experiment was monitored by assessing OD at 600_{nm} by using a microplate reader (BioTek Instruments Inc., United States).

2.6 Statistical analysis of growth

The optical density (OD) obtained for each strain grown on different substrates was compared with that obtained for each strain in the absence of a sugar source. This difference in OD (ΔOD) was used as a parameter for evaluating each strain's ability to grow on different substrates.

2.7 Whole-genome resequencing

The strains were cultured under anaerobic conditions in MRS broth containing 0.05% [v/w] L-cysteine hydrochloride at 37°C for

36 h. Chromosomal DNA was extracted from pure bacterial cultures by using the FastPure Bacteria DNA Isolation Mini kit. After DNA was extracted, DNA quantity and purity were assessed using the NanoDrop ND-2000 spectrophotometer (NanoDrop Technologies, Wilmington, DE, United States).

Then, 1 μg of genomic DNA was used to generate the sequencing libraries for each strain, followed by sequencing with the Illumina NovaSeq PE150 (Shanghai Biotree Biomedical Technology Co., Ltd.). The sequencing libraries were generated using the NEBNext® Ultra™ DNA Library Prep Kit for Illumina (NEB, USA) following the manufacturer's recommendations, and the index codes were incorporated to attribute sequences to each sample. Briefly, the DNA sample was fragmented through sonication to achieve a size of 350 bp. The DNA fragments were then end-polished, A-tailed, and ligated with the full-length adaptor for Illumina sequencing, followed by PCR amplification. Finally, PCR products were purified (AMPure XP system). Libraries were analyzed for size distribution by using the Agilent 2,100 Bioanalyzer and quantified through real-time PCR.

After sequencing, sequence adapters, low-quality bases from paired reads, and reads with an average quality of <20 (<Q20) were first trimmed and filtered using fastp. Then, reads that passed quality-control filtering were aligned and assembled using SPAdes v3.15.3 with default k-mer sizes. Each assembly was annotated using prokka. The pairwise average nucleotide identity (ANI) values were calculated using pyANI v0.2.9 with default BLASTN+ settings (cut-off: ≥95% identity). Roary v.3.12.0 was used to obtain core genome data and perform multiple sequence alignment. The core genome phylogenetic tree was constructed using FastTree v2.1.9[1] with the GTR model having 1,000 bootstrap iterations. Whole-genome sequence alignments for single nucleotide polymorphisms (SNPs) and indel identifications were performed using Snippy v3.13. Publicly available gene sequences of *B. animalis* type strains were downloaded from the NCBI Genome database. All *Bifidobacterium* genomes were input into dbCAN2 v2.0.1 [47] to annotate carbohydrate utilization-related genes based on the carbohydrate-active enzymes database (amino acid identity ≥30%, E-value $\leq 1 \times 10^{-5}$). The *t*-test function implemented in SPSS v26 was used to calculate statistically significant differences between the average numbers of glycosyl hydrolase (GH) genes belonging to the predominant GH families ($p < 0.05$).

2.8 RNA preparation

Total RNA was isolated from 1 mL of *B. animalis* subsp. *lactis* cells (approximately 1×10^8 CFU/mL) in the log-phase cultures grown on oligosaccharides or glucose as the sole carbohydrate source. The samples were centrifuged at 8,000 rpm for 1 min at 4°C on a bench centrifuge to collect cell pellets. The pellets were washed twice with 500 μL of DEPC-treated ddH_2O to remove the culture medium and centrifuged at 10,000 rpm. To disrupt the collected cell pellets, they were ground in liquid nitrogen. The Spin Column Bacteria Total RNA Purification Kit (Sangon Biotech) was used for extracting the total RNA. The extracted RNA was eluted in DEPC-treated ddH_2O. RNA degradation and contamination were monitored through 1.2% agarose gel electrophoresis. The electrophoretic results of the extracted RNA revealed that the bands of 23S and 16S rRNAs were bright and clear and that of 5S rRNA was darker. This finding indicated that the RNA extracted from the strains had good integrity, was less degraded, and could be used for the follow-up experiments. The RNA sample concentration was measured using the micro nucleic acid quantitative instrument to calculate the volume required for reverse transcription. The RNA samples were then immediately stored at −80°C until further use.

2.9 Real-time quantitative PCR analysis

Reverse transcription was conducted using the PerfectStart® Uni RT&qPCR Kit (TransGen Biotech, China). The expression of oligosaccharide metabolism-related differential genes was detected through three RT-PCR replicates. Specific primers for each gene (Table 1) were designed using Primer Premier 6 software. The experiments were conducted using the Real-Time Q-PCR System (MX3000P, Stratagene, United States) in combination with the PerfectStart® Uni RT&qPCR Kit and the PerfectStart® Green qPCR SuperMix (TransGen Biotech, China).

The gene expression was normalized using the $\Delta\Delta C_T$ method, and groEL was used as the reference gene for the calculations. The control group consisted of strains cultured in MRS medium containing glucose as the carbon source, while the experimental group consisted of strains cultured in MRS medium containing each oligosaccharide as the carbon source. The experimental results were visualized by plotting heatmaps.

2.10 Statistical analysis

All experiments were three biological replicates. The data were statistically analyzed using SPSS V26 (IBM, Armonk, NY, United States). Data for all variables were normally distributed and allowed for parametric tests of significance. Equal variance data were analyzed by ANOVA, followed by Duncan's multiple range test with 95% confidence intervals; the differences were considered significant at $p < 0.05$. Evolutionary trees were analyzed by MEGA7.0 software. A heatmap and the principal component analysis (PCA) were constructed in R software (ver 4.0.4).

3 Results

3.1 Isolation and identification of strains

In total, 68 *Bifidobacterium* strains were obtained from different sources of fecal samples (Hotan Prefecture and Hainan Province) and 9 strains were screened through the rep-PCR and carbohydrate utilization, and the 16S rRNA gene sequence of 9 isolates was determined and compared with the published sequences obtained from the GenBank nucleotide database by using the BLAST algorithm. All 16S rRNA gene sequences reported in this study have been deposited at GenBank (Figure 1). Because our phylogenetic analysis based on 16S rRNA gene sequences revealed that all strains

1 http://tree.bio.ed.ac.uk/software/figtree/

10.3389/fmicb.2024.1375384

TABLE 1 Target gene oligonucleotide primers for RT-qPCR.

Gene (Locus tag)	Primer sequence (5′ → 3′)	Product size (bp)
Balac_0475	GCTGACGATGGGAATGAC	160
	GCTCGACGTGTTCTACTC	
Balac_0483	CGTCGGAGTTCTTGATGG	142
	CAGGCAGCCTATGACTTC	
Balac_0484	CATGCCATGGGCTCAGCATCCACACAACATC	1750
	CTAGCTAGCTCAGCGCCTGAACGC	
Balat_0888	TGCCGTCGTGCTTCTGTT	876
	GCTCGTTGCGTGTGATAGG	
Balat_1241	CGCGGATCCATGACGATGACGTTCCCGAAGGGC	1,200
	CCGGAATTCCTACTTGGCGGAGTGCTCGGCGAT	
Balat_0977	CTTCGTTGTGCTTCTCGTTA	955
	CCATATTCGGATTGCGTGAT	
Balat_0373	GTCGCTTCATCAACTACACCTACATT	951
	ACACGCCATCCATCTGCTCAA	
Balac_1593	CTAGCTAGCGCTTCATGGTGGAAAAATGCTGTTG	1,632
	CCGCTCGAGTTCAATTACTTTGCTTATGAAAGCCTC	
Balac_1599	GAATTCCATATGGGCAGCGGGCAGGTCACGCTC	1,201
	CGCGGATCCCTACTTGCGGAAGTCACGAGCC	
Balat_0076	CGACGAATACGGCTACGACTG	578
	CGGCGAATGCGACCTTGTT	
Balac_0511	AACACCTCGTCGCTCTTCA	902
	TAGTTGTTGATGGTCGCCTTC	
Balac_0521	GCGATGCGATGCTGTGGAA	932
	ATTGGTGTTGCGTAGCGTCAT	
Balat_0517	CGCGGATCCAACCGGGCCGCCGTTTC	1,600
	CCGCTCGAGTTCACTCAATTCGCGGTAATC	
Balac_0514	GGCTGACCTTGGATTCTT	145
	CTTCTCGCCCATGTAGTTG	

possessed high sequence similarities (99.5%) to *B. animalis* subsp. *lactis*, the isolates were tentatively identified as *B. animalis* subsp. *lactis*.

3.2 Growth of *Bifidobacterium animalis* subsp. *lactis* on different oligosaccharides

To investigate the intraspecies differences in oligosaccharide metabolism, we monitored the growth of *B. animalis* subsp. *lactis* strains on modified Rogosa medium containing 1% different oligosaccharides as the sole carbohydrate source. The results are shown in Figure 1, where strain-specificity exists in the utilization of sugars by different strains, but the general trend is that all strains exhibited vigorous growth on media containing FOS, XOS, Glu, GOS, raffinose, stachyose, and IMO as the sole carbon source. The higher growth performances of *B. animalis* subsp. *lactis* strains were noted on the media containing FOS, XOS, GOS, and IMO. HN5 exhibited poor growth on the medium containing FOS as the sole carbon source. HT20 and HN7 exhibited poor growth on the XOS-containing medium, whereas the other strains reached a high OD. When compared with FOS, XOS, GOS, and IMO, the strains grew moderately in raffinose and stachyose. Although most strains could utilize oligosaccharides, two exceptions were the utilization patterns of inulin and RS, where low or poor growth was observed in a few cases. HN5 and HN9 failed to grow in the media containing inulin and RS. All isolates from Hotan failed to grow in the inulin-containing medium. HN10 failed to grow in the RS-containing medium.

In order to assess whether there were area differences in oligosaccharide metabolism among the resequenced strains, PCA analyzed experimental data on carbohydrate utilization. As depicted in the PCA diagram (Figure 2), the strains were clustered depending on the area. The results demonstrated that the selected strains from different areas exhibited differences in metabolizing functional oligosaccharides. The strains from Hainan (HN9, HN10, HN16, and HN24) and the strains from Hotan (HT12, HT13, and HT20) were clustered separately.

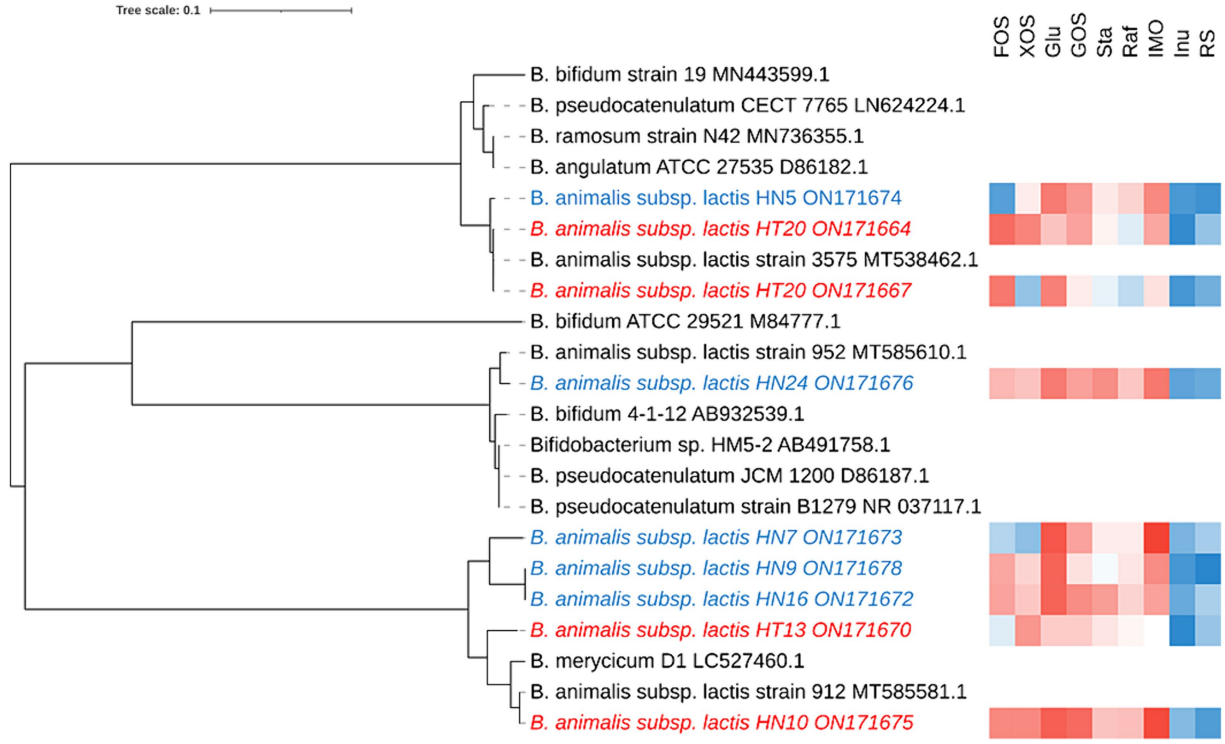

FIGURE 1
Phylogenetic tree and the functional oligosaccharide metabolism of *B. animalis* subsp. *lactis* strains. The color tending to red indicates that the strain grown better in the associated oligosaccharides, while that tending to blue indicates grown poorly in the associated oligosaccharides.

3.3 General features of *Bifidobacterium animalis* subsp. *lactis* isolates

To better comprehend the differences in the *B. animalis* subsp. *lactis* genomes, we resequenced 9 strains from China representing various geographical regions, including 3 strains from Hotan and 6 from Hainan. The results are shown in Table 2, and the genome size predicted for the strains ranged from 1.90 to 2.21 Mb. The genomes had an average G + C% content of 60.32%, an average predicted CDS number of 1,576, and the number of tRNA genes ranging from 53 to 59. In total, 1,452 core genes, 23 shell genes, and 171 cloud genes were identified in the *B. animalis* subsp. *lactis* genomes. The core genes, softcore genes, shell genes, and cloud genes were present in 99–100%, 95–99%, 15–95%, and 0–15% of the strains, respectively. The average nucleotide identity values were defined as the average base similarity between homologous segments of two microbial genomes. Nucleotide-level genomic similarities between the 9 genomes were determined using pyANI. The results indicated that *B. animalis* subsp. *lactis* ANI values ranged from 99.98 to 99.99% (Supplementary Table S1), indicating higher levels of sequence identity among all strains.

3.4 Glycobiome of the *Bifidobacterium animalis* subsp. *lactis* isolates

We further searched for the CAZymes profiles in *B. animalis* subsp. *lactis* genome. Of the 1736 gene families in the pangenome, 233 were determined to encode CAZymes, constituting 13.42% of functionally annotated genes, which reflects the saccharolytic character of the *B. animalis* subsp. *lactis*. These CAZymes included 315 glycosyl hydrolase (GH), 180 glycosyltransferases (GT), 36 carbohydrate esterases (CE), and 18 carbohydrate-binding motif-containing proteins (Figure 3). The most abundant CAZymes were GH13 (12 ± 0% GH genes per genome), followed by GT2 (8 ± 0% GH genes per genome), and GH43 and GH3 (3 ± 0% GH genes per genome). All these CAZymes encode enzymes associated with the hydrolysis plant-derived poly- and oligosaccharides, such as stachyose, raffinose and xylans, etc. And these poly- and oligosaccharides are major components of the adult diet. Studies have shown that the CAZymes profiles in *Bifidobacteria* genome are species and/or strain-specific, however, according to bioinformatic predictions, strain-specific CAZymes were not observed in this study (Genomics of the Genus *Bifidobacterium* Reveals Species-Specific Adaptation to the Glycan-Rich Gut Environment). On the contrary, regardless of the isolation source, all tested strains shared the same CAZyme repertoires.

We then explored the nucleotide-level differences in GH genes between the *B. animalis* subsp. *lactis* strains. The SNP analysis was conducted to compare the genomes of the 9 *B. animalis* subsp. *lactis* strains and *B. animalis* subsp. *lactis* DSM10140. Upon comparison of these 10 complete genome sequences, 493 validated SNPs were identified, and found that the *B. animalis* subsp. *lactis* strains exhibited low strain diversity, with the respective mean pairwise SNP distances of 46.73 ± 16.4 SNPs. Subsequently, these SNPs were functionally annotated. The results revealed that these SNPs were significantly associated with the transport and the metabolisms of carbohydrates (oligosaccharide). However, we found no significant SNPs that may

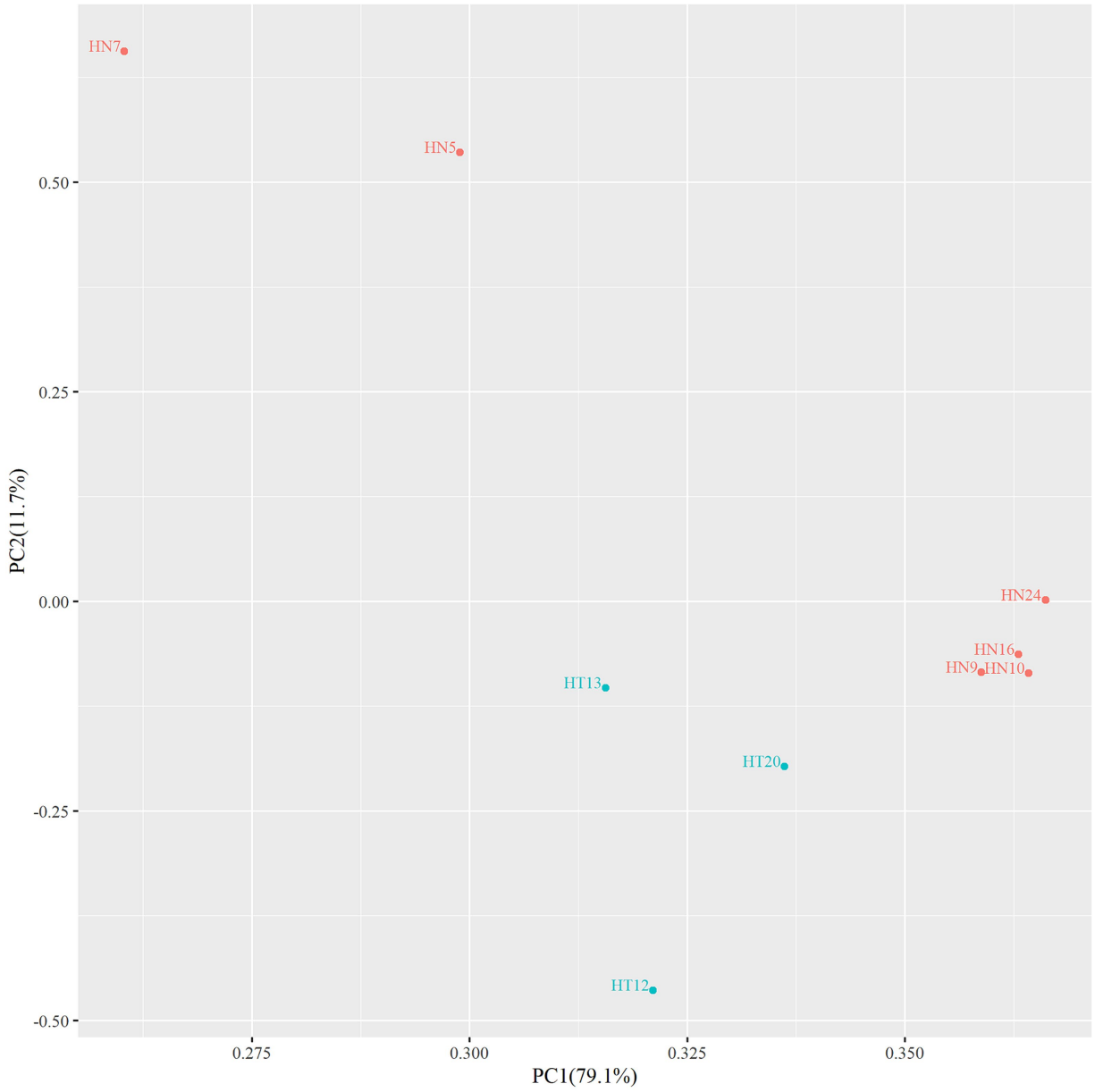

FIGURE 2
PCA diagram of functional oligosaccharide metabolism of resequenced strains.

cause functional changes in CAZyme genes. Interestingly, the experimental strains exhibited phenotypic differences in metabolizing different oligosaccharides. Therefore, we predicted that these SNPs were noncoding variants. Transcription factors play crucial roles in gene regulation by harboring these SNPs (Li et al., 2020).

3.5 Real-time quantitative PCR analysis

Thus, to reveal the phenotypic differences in the *B. animalis* subsp. *lactis* strains in metabolizing different oligosaccharides at the transcription level, total RNA isolated from the experimental strains was reverse-transcribed into cDNA, and then, the expression of relevant key enzyme genes was detected through real-time quantitative PCR (RT-qPCR). In the culture medium containing different functional oligosaccharides, the expression of the carbohydrate transporter gene changed to varying degrees at the mRNA level (Figure 4). The composition of oligosaccharides and monosaccharides are similar. However, their carbon chain lengths are different, and thus, they can induce the expression of the same or similar genes. On the other hand, a substrate can induce the expression of several carbohydrate metabolism genes. In this study, The results showed that the OD_{600nm} values of HN9, HN10, and HN16 strains were greater than 0.8 after 48 h of incubation in medium with FOS as the carbon source, and their relative expression of glycosidase genes (Balat_1241 and Balac_0888) related to FOS was higher than that of HN7, HT13, and HN5 (the OD_{600nm} values were 0.5 ± 0.04, 0.61 ± 0.01, and 0.26 ± 0.02, respectively). For GOS metabolism, the

TABLE 2 Genome information for publicly available *B. animalis* subsp. *lactis* DSM 10140 and nine *B. animalis* subsp. *lactis* strains used in this study.

Strains	Ecological origin	Genome size (Mb)	No. Of CDS	No.Of tRNAs	GC (%)	Accession
HN10	Human feces	1.90	1,572	55	59.4	SAMN40528426
HN16	Human feces	2.03	1,574	54	60.38	SAMN40528427
HN24	Human feces	1.95	1,564	53	60.01	SAMN40528428
HN5	Human feces	2.03	1,572	55	59.65	SAMN40528429
HN7	Human feces	1.94	1,558	55	59.57	SAMN40528430
HN9	Human feces	2.15	1,596	59	60.69	SAMN40528431
HT12	Human feces	2.15	1,585	58	59.93	SAMN40528432
HT13	Human feces	1.95	1,560	54	59.74	SAMN40528433
HT20	Human feces	2.21	1,604	55	60.17	SAMN40528434
B. animalis subsp. *lactis* DSM 10140	Human feces	1.94	1,635	52	61.37	SAMN09742860

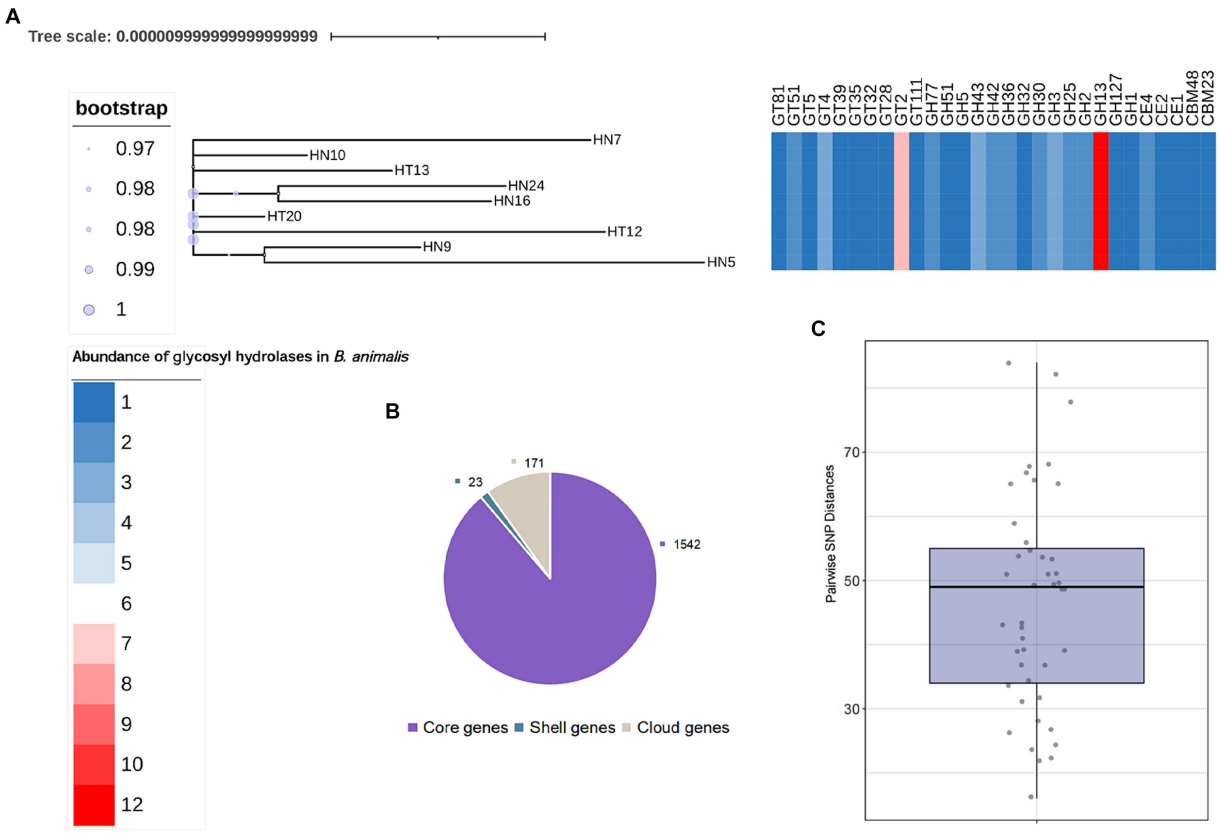

FIGURE 3
General Features of *B. animalis* subsp. *lactis* Genomes. **(A)** The maximum-likelihood trees were constructed based the core-genome alignment employing 'GTR'model with 1,000 bootstraps. Heatmap represents abundance of specific GH families. See also Supplementary Table S2. **(B)** Pan- and core genes of *B. animalis* subsp. *lactis*. **(C)** Pairwise SNP Distances between *B. animalis* subsp. *lactis*. Strains.

HT12 and HT13 strains exhibited a strong ability to metabolize than HN9, HT20, and the expression of genes (Balat_0483, Balat_0484, Balat_0475) related GOS metabolism higher than HN9, HT20 strains. The OD_{600nm} vanlues of HT12, HN24, HN7 and HT20 in the medium with XOS as carbon source were 1.05 ± 0.06, 0.87 ± 0.02, 0.42 ± 0.05 and 0.42 ± 0.05 respectively, and the expression levels of XOS-relevant metabolic genes (Balat_0517, Balac_0511, Balac_0514, and Balac_0521) of HT12 and HN24 higher than HN7 and HT20. However, the sample size of the resequencing and reverse transcription validation experimental strains in this study was small, and if further confirmation of intraspecies differences in metabolized oligosaccharides within the *B. animalis* subsp. *lactis* caused by transcriptional rather than the genetic levels is desired, the sample size of the experiments should be increased in subsequent studies in

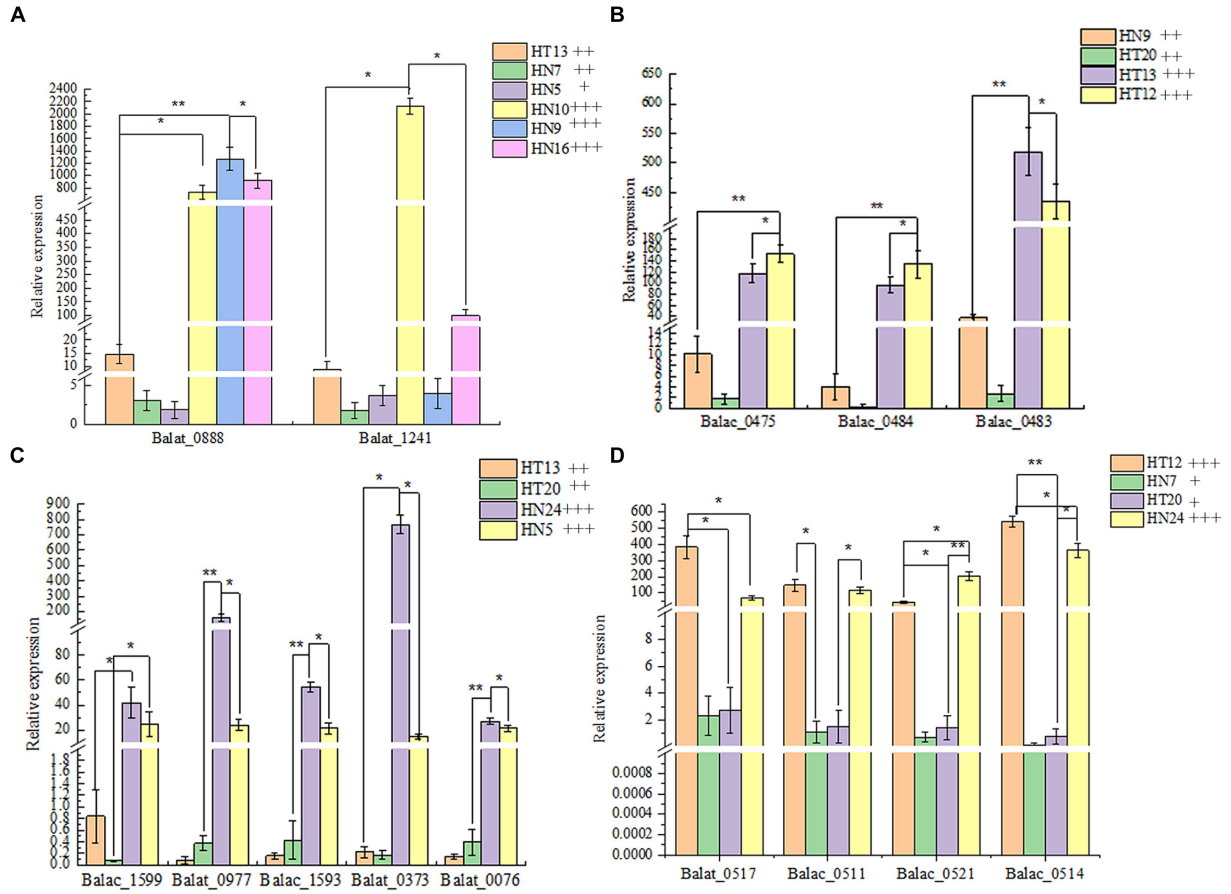

FIGURE 4
The relative expression of glycosidase genes in four oligosaccharides as the unique carbon source. **(A–D)**: Metabolic phenotypes of FOS, GOS, IMO and XOS and mRNA transcription levels of related genes by strains, respectively. The phenotype of metabolism was classified by the following labels: "+" OD600nm 0.25–0.5, low- level growth; "++" OD600nm 0.5–0.8, medium-level growth; "+++" OD600nm >0.8, high-level growth.

order to overcome the limitations caused by small sample sizes. And generalization of the conclusions to all strains of *B. animalis* subsp. *lactis*.

4 Discussion

B. animalis subsp. *lactis* are widely distributed in humans and other mammalian guts and are widely supplemented to multiple functional foods. Furthermore, *B. animalis* subsp. *lactis* possesses a saccharolytic lifestyle as well as the ability to utilize multiple oligosaccharides from a variety of host and dietary sources. Multi-omics techniques and the increased number of published *Bifidobacterium* sequences are beneficial for analyzing different strains of genomic multiplicity and the difference in functionality (Andersen et al., 2013; O'Connell Motherway et al., 2013; Nomoto et al., 2017). In this study, we explored the differences in the functional oligosaccharide metabolism of *B. animalis* subsp. *lactis* from three levels: phenotypic characteristics, gene level, and transcription level, and then analyzed the preference and utilization of different oligosaccharides by different strains so as to provide a theoretical reference for the development of suitable synbiotic ("probiotics-prebiotic") products.

In this study, *B. animalis* subsp. *lactis* were recovery from Hotan, Xinjiang, China and Hainan, China. The results of PCA analysis showed regional variability in the utilization of polysaccharides by *B. animalis* subsp. *lactis* isolated from Hotan and Hainan regions. It could be due to the growth of the *Bifidobacterium* strains may be affected by the environment and eating habits. According to the accumulating evidence, intraspecies differences might occur because of the human gastrointestinal environment (Holscher, 2020). Diet is considered the main environmental contributor to the gastrointestinal microbiota structure and function in humans and animals; therefore, can markedly influence the functionality of indigenous microbiota (Gibson et al., 2004; Hansen et al., 2018). This study resequenced analyzing the strains to explore the mechanism of metabolic oligomerization differences in *B. animalis* subsp. *lactis*.

Studies have shown that about 14% of the genes of Bifidobacteria genome are involved in carbohydrate metabolism (Genomics of the Genus *Bifidobacterium* Reveals Species-Specific Adaptation to the Glycan-Rich Gut Environment). The predominant CAZymes class found in this study were GH43, GT2, GH3, and GT13, which were responsible for the metabolism of multiple plant-derived carbohydrates (Lugli et al., 2019; Liang et al., 2023; Srivastava et al., 2023). In line with this result, our *in vitro* experiments showed that *B. animalis* subsp. *lactis* could assimilate several plant-derived

carbohydrates, such as IMO, GOS, and XOS, which may explain why *B. animalis* subsp. *lactis* could efficiently colonize several animal guts. According to *B. animalis* subsp. *lactis* glycobiome, all of the tested strains shared the same CAZymes profile. Nevertheless, our analysis detected strain-specific variation in carbohydrate utilization within 9 *B. animalis* subsp. *lactis*.

However, oligosaccharide utilization capacities of the *B. animalis* subsp. *lactis* strains differed because of the difference in the gene transcription level. In several studies, the *Bifidobacterium* genome functional annotation results revealed that most of the functions encoded by genes were related to carbohydrate metabolism (Milani et al., 2016). The oligosaccharide metabolism experiment combined with the PCR validation of functional genes indicated that the experimental strains could use 5–6 types of oligosaccharides and have genes encoding key enzymes involved in functional oligosaccharide metabolism. This finding suggests that the carbohydrate-utilizing ability of *Bifidobacterium* is crucial for its life activities. The study results are similar to those reported by Janer et al. (2004). In this past study, all experimental strains (*B. animalis* subsp. *lactis*) had genes encoding key enzymes involved in inulin metabolism, as determined through PCR amplification of the gene for β-fructosidase. However, almost none of the strains could metabolize inulin. This finding suggests that although strains possess key enzyme genes for metabolizing functional oligosaccharides, this finding does not confirm that they can surely metabolize relevant oligosaccharides, which could be because the associated genes are not expressed or less expressed. Global gene expression profiles were obtained for 9 *B. animalis* subsp. *lactis*, growing on 4 potential prebiotic oligosaccharides (FOS, GOS, XOS and IMO). RT-qPCR results unveiled that differentiation of gene expression regulation influences metabolic capabilities. HN9, HN10 and HN16 upregulated the expression of glycosyltransferase (Balat_0888) and β-fructofuranosidase (Balat_1241) which are allows to uptake FOS. HN24 and HN5 were observed to utilize IMO via upregulated ABC transporter (Balac_1599), isoamylase (Balat_0977), GH13_311, 6-α-Glucosidase (Balac_1593), 4-α-glucanotransferase (Balat_0373), and glucan phosphorylase (Balat_0076). Transporter differentially up regulated on XOS was also found in HT24, HN7, HT12 and HT20. Glycosidase genes exhibited consistency in terms of phenotype of functional oligosaccharide metabolism at the transcriptional level.

Similarly, the 16th International Symposium on Probiotics and Health reported that probiotics *B. animalis* subsp. *lactis* Probio-M8 and V9 shared similar carbohydrate metabolism-related genes, albeit their phenotypes of carbohydrate metabolism varied remarkably. As noted in the aforementioned report, our study results suggest that all experimental strains (*B. animalis* subsp. *lactis*) had similar genes related to the key enzymes involved in functional oligosaccharide metabolism, but their phenotypes of functional oligosaccharide metabolism were different. The difference in the phenotypes of metabolism may be caused by the difference in the gene transcription level and the protein translation level of relevant key enzymes. Differences were noted in the gene transcription of *Saccharomyces cerevisiae* in the presence of different long-chain fatty acids (Han Li et al., 2019). Moreover, the addition of glycerol effectively increased the transcription level of the lactone ring synthesis-related gene in *Streptomyces ambofaciens*. The relative transcript level of related genes unveiled that the increase in the oxygen supply level effectively promoted the relative transcription level of the forosamine synthesis-related gene. Thus, it was confirmed that the external growth environment can affect gene expression.

5 Conclusion

In this study, *B. animalis* subsp. *lactis* strains were isolated from human fecal samples collected from participants from across Hotan and Hainan. Comparison and analyses of their abilities were performed to utilize 8 types of functional oligosaccharides as well as their differences at the gene and transcription levels. The results indicated that, on one hand, the selected strains from different areas exhibited differences in metabolizing functional oligosaccharides. On the other hand, the ability of the strains to utilize the oligosaccharides was consistent with the transcript levels of the related glycosidase genes. This study provided a case for understanding functional diversity due to small gene expression changes within the *B. animalis* subsp. *lactis*. And the synbiotic formulations could be optimized through uncovered gene expression impacts phenotypic variations in *B. animalis* subsp. *lactis*. Subsequent studies could design targeted interventions through understanding the regulatory pathways involved in gene expression, thus developing more effective synbiotic products. This study may provide new ideas for the development of targeted bifidogenic functional oligosaccharides, for specific probiotic strains.

Data availability statement

The original contributions presented in the study are included in the article/Supplementary material, further inquiries can be directed to the corresponding authors.

Author contributions

ZL: Formal analysis, Writing – original draft, Writing – review & editing, Validation, Visualization. XZh: Formal analysis, Writing – original draft, Writing – review & editing, Data curation, Software. MX: Data curation, Methodology, Writing – original draft. JK: Writing – review & editing, Investigation. XZu: Investigation, Writing – review & editing. YW: Writing – review & editing, Data curation. CW: Writing – review & editing, Validation. YT: Writing – review & editing, Formal analysis. YN: Writing – review & editing, Resources. YZ: Resources, Writing – review & editing, Conceptualization, Funding acquisition, Project administration.

Funding

The author(s) declare financial support was received for the research, authorship, and/or publication of this article. This study was supported by the National Natural Science of China (Project No. 32260568).

Conflict of interest

The authors declare that the research was conducted in the absence of any commercial or financial relationships that could be construed as a potential conflict of interest.

Publisher's note

All claims expressed in this article are solely those of the authors and do not necessarily represent those of their affiliated organizations, or those of the publisher, the editors and the reviewers. Any product that may be evaluated in this article, or claim that may be made by its manufacturer, is not guaranteed or endorsed by the publisher.

Supplementary material

The Supplementary material for this article can be found online at: https://www.frontiersin.org/articles/10.3389/fmicb.2024.1375384/full#supplementary-material

References

Abou, H. M., Andersen, J. M., Barrangou, R., Møller, M. S., and Fredslund, F. (2013). Recent insight into oligosaccharide uptake and metabolism in probiotic bacteria. *Biocatal. Biotransformation* 31, 226–235. doi: 10.3109/10242422.2013.828048

Andersen, J. M., Barrangou, R., Abou Hachem, M., Lahtinen, S. J., Goh, Y. J., Svensson, B., et al. (2013). Transcriptional analysis of oligosaccharide utilization by *Bifidobacterium lactis* Bl-04. *BMC Genomics* 14:312. doi: 10.1186/1471-2164-14-312

Belorkar, S. A., and Gupta, A. K. (2016). Oligosaccharides: a boon from nature's desk. *Amb Express* 6, 11. doi: 10.1186/s13568-016-0253-5

Bottacini, F., Morrissey, R., Esteban-Torres, M., James, K., Van Breen, J., Dikareva, E., et al. (2018). Comparative genomics and genotype-phenotype associations in *Bifidobacterium breve*. *Sci. Rep.* 8:10633. doi: 10.1038/s41598-018-28919-4

Bunesova, V., Killer, J., Javurkova, B., Vlkova, E., Tejnecky, V., Musilova, S., et al. (2017). Diversity of the subspecies *Bifidobacterium animalis* subsp lactis. *Anaerobe* 44, 40–47. doi: 10.1016/j.anaerobe.2017.01.006

Garrido, D., Ruiz-Moyano, S., Lemay, D. G., Sela, D. A., German, J. B., and Mills, D. A. (2015). Comparative transcriptomics reveals key differences in the response to milk oligosaccharides of infant gut-associated bifidobacteria. *Sci. Rep.* 5:13517. doi: 10.1038/srep13517

Gaya, P., Peirotén, Á., and Landete, J. M. (2017). Transformation of plant isoflavones into bioactive isoflavones by lactic acid bacteria and bifidobacteria. *J. Funct. Foods* 39, 198–205. doi: 10.1016/j.jff.2017.10.029

Gibson, G. R., Probert, H. M., Loo, J. V., Rastall, R. A., and Roberfroid, M. B. (2004). Dietary modulation of the human colonic microbiota: updating the concept of prebiotics. *Nutr. Res. Rev.* 17, 259–275. doi: 10.1079/NRR200479

Han Li, H. L., Li Lei, L. L., Yang HouRong, Y. H., He PeiXin, H. P., and Huang Shen, H. S. (2019). Transcriptomic sequence analysis of the effect of three fatty acids with different chain length on gene transcription in *Saccharomyces cerevisiae*.Pdf. *Food Sci. Technol.* 40, 106–112. doi: 10.7506/spkx1002-6630-20180316-221

Hansen, L. B., Roager, H. M., Søndertoft, N. B., Gøbel, R. J., Kristensen, M., Vallès-Colomer, M., et al. (2018). A low-gluten diet induces changes in the intestinal microbiome of healthy Danish adults. *Nat. Commun.* 9:4630. doi: 10.1038/s41467-018-07019-x

He, Z., Yang, B., Liu, X., Ross, R. P., Stanton, C., and Zhao, J. (2021). Short communication: genotype-phenotype association analysis revealed different utilization ability of 2′-fucosyllactose in Bifidobacterium genus. *J. Dairy Sci.* 104, 1518–1523. doi: 10.3168/jds.2020-19013

Holscher, H. D. (2020). Diet affects the gastrointestinal microbiota and health. *J. Acad. Nutr. Diet.* 120, 495–499. doi: 10.1016/j.jand.2019.12.016

Hopkins, , Cummings, , and Macfarlane, (1998). Inter-species differences in maximum specific growth rates and cell yields of bifidobacteria cultured on oligosaccharides and other simple carbohydrate sources. *J. Appl. Microbiol.* 85, 381–386. doi: 10.1046/j.1365-2672.1998.00524.x

Janer, C., Rohr, L. M., Peláez, C., Laloi, M., Cleusix, V., Requena, T., et al. (2004). Hydrolysis of Oligofructoses by the recombinant β-Fructofuranosidase from *Bifidobacterium lactis*. *Syst. Appl. Microbiol.* 27, 279–285. doi: 10.1078/0723-2020-00274

Kan, Z. Y., Luo, B. L., Cai, J. J., Zhang, Y., Tian, F. W., and Ni, Y. Q. (2020). Genotyping and plant-derived glycan utilization analysis of Bifidobacterium strains from mother-infant pairs. *BMC Microbiol.* 20:277. doi: 10.1186/s12866-020-01962-w

Li, M., Yao, S., Duan, Y. Y., Zhang, Y. J., Guo, Y., Niu, H. M., et al. (2020). Transcription factor enrichment analysis in enhancers identifies EZH2 as a susceptibility gene for osteoporosis. *J. Clin. Endocrinol.Metab.* 105, e1152–e1161. doi: 10.1210/clinem/dgz270

Li, Q., Zhang, Y., Shi, J.-L., Wang, Y.-L., Zhao, H.-B., Shao, D.-Y., et al. (2017). Mechanism and anticancer activity of the metabolites of an endophytic Fungi from *Eucommia ulmoides* Oliv. *Anti Cancer Agents Med. Chem.* 17, 982–989. doi: 10.2174/1871520616666160923094814

Liang, T. T., Jiang, T., Liang, Z., Zhang, N., Dong, B., Wu, Q. P., et al. (2023). Carbohydrate-active enzyme profiles of Lactiplantibacillus plantarum strain 84-3 contribute to flavor formation in fermented dairy and vegetable products. *Food Chem. X* 20:101036. doi: 10.1016/j.fochx.2023.101036

Linares-Morales, J. R., Salmerón-Ochoa, I., Rivera-Chavira, B. E., Gutiérrez-Méndez, N., Pérez-Vega, S. B., and Nevarez-Moorillón, G. V. (2022). Influence of culture media formulated with Agroindustrial wastes on the antimicrobial activity of lactic acid Bacteria. *J. Microbiol. Biotechnol.* 32, 64–71. doi: 10.4014/jmb.2107.07030

Liu, N., Shen, H. B., Zhang, F., Liu, X., Xiao, Q. R., Jiang, Q., et al. (2023). Applications and prospects of functional oligosaccharides in pig nutrition: A review. *Animal Nutrition* 13, 206–215. doi: 10.1016/j.aninu.2023.02.002

LoCascio, R. G., Ninonuevo, M. R., Freeman, S. L., Sela, D. A., Grimm, R., Lebrilla, C. B., et al. (2007). Glycoprofiling of bifidobacterial consumption of human milk oligosaccharides demonstrates strain specific, preferential consumption of small chain glycans secreted in early human lactation. *J. Agric. Food Chem.* 55, 8914–8919. doi: 10.1021/jf0710480

Lohrasbi, V., Abdi, M., Asadi, A., Rohani, M., Esghaei, M., and Talebi, M. (2020). The effect of improved formulation of chitosan-alginate microcapsules of Bifidobacteria on serum lipid profiles in mice. *Microb. Pathog.* 149:104585. doi: 10.1016/j.micpath.2020.104585

Lugli, G. A., Mancino, W., Milani, C., Duranti, S., Mancabelli, L., Napoli, S., et al. (2019). Dissecting the evolutionary development of the species *Bifidobacterium animalis* through comparative genomics analyses. *Appl. Environ. Microbiol.* 85:16. doi: 10.1128/AEM.02806-18

Masco, L., Huys, G., Gevers, D., Verbrugghen, L., and Swings, J. (2003). Identification of Bifidobacterium species using rep-PCR fingerprinting. *Syst. Appl. Microbiol.* 26, 557–563. doi: 10.1078/072320203770865864

Milani, C., Turroni, F., Duranti, S., Lugli, G. A., Mancabelli, L., and Ferrario, C. (2016). Genomics of the genus Bifidobacterium reveals species-specific adaptation to the glycan-rich gut environment. *Appl. Environ. Microbiol.* 82, 980–991. doi: 10.1128/AEM.03500-15

Moradi, M., Molaei, R., and Guimarães, J. T. (2021). A review on preparation and chemical analysis of postbiotics from lactic acid bacteria. *Enzym. Microb. Technol.* 143:109722. doi: 10.1016/j.enzmictec.2020.109722

Nomoto, R., Takano, S., Tanaka, K., Tsujikawa, Y., Kusunoki, H., and Osawa, R. (2017). Isolation and identification of Bifidobacterium species from feces of captive chimpanzees. *Biosci. Microbiota Food Health* 36, 91–99. doi: 10.12938/bmfh.16-027

O'Connell Motherway, M., Kinsella, M., Fitzgerald, G. F., and Van Sinderen, D. (2013). Transcriptional and functional characterization of genetic elements involved in galacto-oligosaccharide utilization by *Bifidobacterium breve* UCC 2003. *Microb. Biotechnol.* 6, 67–79. doi: 10.1111/1751-7915.12011

O'connell, K. J., Motherway, M. O., O'callaghan, J., Fitzgerald, G. F., Ross, R. P., Ventura, M., et al. (2013). Metabolism of four α-Glycosidic linkage-containing oligosaccharides by *Bifidobacterium breve* UCC 2003. *Appl. Environ. Microbiol.* 79, 6280–6292. doi: 10.1128/AEM.01775-13

Paineau, D., Carcano, D., Leyer, G., Darquy, S., Alyanakian, M. A., Simoneau, G., et al. (2008). Effects of seven potential probiotic strains on specific immune responses in healthy adults: a double-blind, randomized, controlled trial. *FEMS Immunol. Med. Microbiol.* 53, 107–113. doi: 10.1111/j.1574-695X.2008.00413.x

Sanders, M. E., Merenstein, D. J., Reid, G., Gibson, G. R., and Rastall, R. A. (2019). Probiotics and prebiotics in intestinal health and disease: from biology to the clinic. *Nat. Rev. Gastroenterol. Hepatol.* 16, 605–616. doi: 10.1038/s41575-019-0173-3

Shahin, M., Jamal, W., Verghese, T., and Rotimi, V. O. (2003). Comparative evaluation of Anoxomat and conventional anaerobic gas Pak jar systems for the isolation of anaerobic bacteria. *Med. Princ. Pract.* 12, 81–86. doi: 10.1159/000069116

Song, A.-X., Li, L.-Q., Yin, J.-Y., Chiou, J.-C., and Wu, J.-Y. (2020). Mechanistic insights into the structure-dependant and strain-specific utilization of wheat

arabinoxylan by *Bifidobacterium longum*. *Carbohydr. Polym.* 249:116886. doi: 10.1016/j.carbpol.2020.116886

Srivastava, S., Bombaywala, S., Jakhesara, S. J., Patil, N. V., Joshi, C. G., Purohit, H. J., et al. (2023). Potential of camel rumen derived Bacillus subtilis and *Bacillus velezensis* strains for application in plant biomass hydrolysis. *Mol. Gen. Genomics.* 298, 361–374. doi: 10.1007/s00438-022-01987-y

Tomás-Barberán, F. A., and Mine, Y. (2013). A Key to Understanding the Effects of Food Bioactives in Health, Gut Microbiota. *Journal of Agricultural and Food Chemistry* 61, 9755–9757. doi: 10.1021/jf404354f

Ventura, M., Canchaya, C., Del Casale, A., Dellaglio, F., Neviani, E., Fitzgerald, G. F., et al. (2006). Analysis of bifidobacterial evolution using a multilocus approach. *Int. J. Syst. Evol. Microbiol.* 56, 2783–2792. doi: 10.1099/ijs.0.64233-0

Ventura, M., Canchaya, C., Van Sinderen, D., Fitzgerald, G. F., and Zink, R. (2004). *Bifidobacterium lactis* DSM 10140: identification of the atp (atp BEFHAGDC) operon and analysis of its genetic structure, characteristics, and phylogeny. *Appl. Environ. Microbiol.* 70, 3110–3121. doi: 10.1128/AEM.70.5.3110-3121.2004

Vieira, T. F., Corrêa, R. C. G., Peralta, R. A., Peralta-Muniz-Moreira, R. F., Bracht, A., and Peralta, R. M. (2020). An Overview of Structural Aspects and Health Beneficial Effects of Antioxidant Oligosaccharides. *Current Pharmaceutical Design* 26, 1759–1777. doi: 10.2174/1381612824666180517120642

Yan, S., Yang, B., Ross, R. P., Stanton, C., Zhang, H., and Zhao, J. (2020). *Bifidobacterium longum* subsp. longum YS108R fermented milk alleviates DSS induced colitis via anti-inflammation, mucosal barrier maintenance and gut microbiota modulation. *J. Funct. Foods* 73:104153. doi: 10.1016/j.jff.2020.104153

frontiers | Frontiers in Microbiology

TYPE Original Research
PUBLISHED 21 May 2024
DOI 10.3389/fmicb.2024.1356365

OPEN ACCESS

EDITED BY
Fengjie Sun,
Georgia Gwinnett College, United States

REVIEWED BY
Xiaoping Lv,
Guangxi Medical University, China
Tao Yi,
Hong Kong Baptist University,
Hong Kong SAR, China

*CORRESPONDENCE
Xiong-e Pi
✉ pixionge@163.com

RECEIVED 15 December 2023
ACCEPTED 06 May 2024
PUBLISHED 21 May 2024

CITATION
Wu Y, Fu H, Xu X, Jin H, Kao Q-j, Teng W-l, Wang B, Zhao G and Pi X-e (2024) Intervention with fructooligosaccharides, *Saccharomyces boulardii*, and their combination in a colitis mouse model. *Front. Microbiol.* 15:1356365. doi: 10.3389/fmicb.2024.1356365

Intervention with fructooligosaccharides, *Saccharomyces boulardii*, and their combination in a colitis mouse model

Yan Wu[1], Hao Fu[2], Xu Xu[3], Hui Jin[1], Qing-jun Kao[1], Wei-lin Teng[1], Bing Wang[1], Gang Zhao[1] and Xiong-e Pi[4]*

[1]Hangzhou Center for Disease Control and Prevention, Hangzhou, Zhejiang, China, [2]Institute of Plant Protection and Microbiology, Zhejiang Academy of Agricultural Sciences, Hangzhou, China, [3]School of Food Science and Biotechnology, Zhejiang Gongshang University, Hangzhou, Zhejiang, China, [4]Institute of Rural Development, Zhejiang Academy of Agricultural Sciences, Hangzhou, China

Objective: To examine the effects of an intervention with fructooligosaccharides (FOS), *Saccharomyces boulardii*, and their combination in a mouse model of colitis and to explore the mechanisms underlying these effects.

Methods: The effects of FOS, *S. boulardii*, and their combination were evaluated in a DSS-induced mouse model of colitis. To this end, parameters such as body weight, the disease activity index (DAI), and colon length were examined in model mice. Subsequently, ELISA was employed to detect the serum levels of proinflammatory cytokines. Histopathological analysis was performed to estimate the progression of inflammation in the colon. Gas chromatography was used to determine the content of short-chain fatty acids (SCFAs) in the feces of model mice. Finally, 16S rRNA sequencing technology was used to analyze the gut microbiota composition.

Results: FOS was slight effective in treating colitis and colitis-induced intestinal dysbiosis in mice. Meanwhile, *S. boulardii* could significantly reduced the DAI, inhibited the production of IL-1β, and prevented colon shortening. Nevertheless, *S. boulardii* treatment alone failed to effectively regulate the gut microbiota. In contrast, the combined administration of FOS/*S. boulardii* resulted in better anti-inflammatory effects and enabled microbiota regulation. The FOS/*S. boulardii* combination (10^9 CFU/ml and 10^7 CFU/ml) significantly reduced the DAI, inhibited colitis, lowered IL-1β and TNF-α production, and significantly improved the levels of butyric acid and isobutyric acid. However, FOS/*S. boulardii* 10^9 CFU/ml exerted stronger anti-inflammatory effects, inhibited IL-6 production and attenuated colon shortening. Meanwhile, FOS/*S. boulardii* 10^7 CFU/ml improved microbial regulation and alleviated the colitis-induced decrease in microbial diversity. The combination of FOS and *S. boulardii* significantly increased the abundance of *Parabacteroides* and decreased the abundance of *Escherichia–Shigella*. Additionally, it promoted the production of acetic acid and propionic acid.

Conclusion: Compared with single administration, the combination can significantly increase the abundance of beneficial bacteria such as *lactobacilli* and *Bifidobacteria* and effectively regulate the gut microbiota composition. These results provide a scientific rationale for the prevention and treatment of colitis using a FOS/*S. boulardii* combination. They also offer a theoretical

basis for the development of nutraceutical preparations containing FOS and *S. boulardii*.

KEYWORDS

fructooligosaccharides, *Saccharomyces boulardii*, gut microbiota, colitis, inflammatory bowel disease

1 Introduction

Inflammatory bowel disease (IBD) is a chronic inflammatory condition affecting the intestinal tract, and it includes ulcerative colitis and Crohn's disease (Wu et al., 2021). The clinical symptoms of IBD include celialgia, diarrhea, hematochezia, weight loss, and oxidative stress and patients with IBD are at an increased risk of colon cancer (Wang et al., 2019). The prevalence of IBD has been increasing year after year, making this disease an important global public health issue (Shi et al., 2020; Dong et al., 2022).

Several factors contribute to the pathogenesis of IBD including genetic susceptibility, intestinal barrier injury, environmental risk factors, and an imbalance of symbiotic flora (Liu et al., 2022; Yang et al., 2022). The three main goals of IBD management are to induce and maintain remission; prevent disease-related complications; and improve quality of life and minimize adverse events. The treatment strategies for IBD are based on the location and severity of inflammation, and account for the expected progression of the disease (Taleban et al., 2015). At present, colitis is mainly treated using clinical agents such as aminosalicylates, corticosteroids, immunosuppressants, and monoclonal antibodies. Of these, aminosalicylates are used to treat mild-to-moderate IBD. However, they cause adverse effects such as headache, nausea, and fatigue in 10 to 45% of treated patients. Additionally, they can induce allergic reactions such as rash, fever, Stevens-Johnson syndrome, hepatitis, pneumonitis, hemolytic anemia, and bone marrow suppression (Pithadia and Jain, 2011). Corticosteroids are effective at establishing but not maintaining remission in cases of moderate-to-severe IBD (Kornbluth et al., 2010). However, long-term corticosteroid use makes patients vulnerable to systemic side effects such as an increased risk of osteoporosis, opportunistic infections, and death (Toruner et al., 2008). Immunosuppressant drugs can serve as invaluable adjunct therapeutic agents for patients with intractable IBD or complex, inoperable perianal disease. Although immunosuppressant treatment causes some adverse effects, it is safer and more tolerable than long-term steroid hormone therapy. Notably, the adverse effects of immunosuppressants are rare and include leukopenia and hypersensitive interstitial pneumonitis, although long-term treatment can cause hepatic fibrosis (Pithadia and Jain, 2011). Monoclonal antibodies can also be an option in moderate-to-severe IBD, especially in steroid-dependent or steroid-resistant patients. Cottone et al. reported a 12% risk of serious infections including pneumonia and sepsis, in older patients under treatment with monoclonal antibodies. Overall, 3% of the patients in their cohort died due to septic shock (Cottone et al., 2011). In other studies, monoclonal antibodies have also been reported to cause dermatological problems, infusion reactions, and neurological sequelae. Hence, the current drugs used to treat colitis have several disadvantages such as serious adverse effects, and are not suitable for long-term use (Jeong et al., 2019; Qu Y. et al., 2021).

Fructooligosaccharides (FOS) are a typical prebiotics that can increase the diversity of the human intestinal microbiota, selectively promoting the growth of beneficial bacteria in the human gut, improving the intestinal environment and intestinal function, and decreasing the level of proinflammatory cytokines (Genda et al., 2017; Mao et al., 2018; Tandon et al., 2019). Relevant studies have shown that pretreatment with a mixture of FOS and galactooligosaccharides (GOS) can alleviate the symptoms of dextran sulfate sodium (DSS)-induced colitis in mice (Liu et al., 2021).

Saccharomyces boulardii is a subspecies of *Saccharomyces* yeast, and it is the only probiotic species of yeast discovered to date (Pais et al., 2020). Research on *S. boulardii* has gradually expanded in recent years, and many studies have shown that this yeast shows good efficacy in the treatment of various gastrointestinal diseases (Gao et al., 2023; Salazar-Parra et al., 2023).

Given the complexity of colitis and its etiology, treatment with FOS and *S. boulardii* alone has shown limited anti-colitis efficacy (Sivananthan and Petersen, 2018; Simoes et al., 2022). Moreover, there have been few studies on the combination of FOS and *S. boulardii* for colitis management. Hypothetically, the combination of FOS and *S. boulardii* could simultaneously provide a prebiotic and probiotic agent, synergistically enhancing the efficacy of colitis treatment (Wasilewski et al., 2015). Exploring the effects of this synbiotic combination in mouse models of colitis could provide a theoretical basis for its clinical development and application and create new therapeutic avenues for colitis management.

In this study, mice were pretreated with FOS, different concentrations of *S. boulardii*, and a combination of these agents. They were then treated with DSS to induce colitis. Parameters such as the disease activity index (DAI), the levels of SCFAs and proinflammatory cytokines, inflammation in the colon, and the composition of the gut microbiota were evaluated in the model mice after treatment. Accordingly, the preventive and therapeutic effects of FOS, *S. boulardii*, and their combination on colitis were evaluated and their regulatory effects on the mouse gut microbiota were delineated.

2 Experimental materials and instruments

2.1 Animals, microbes, reagents, and materials

The following animals, microbes, reagents, and materials were used in this study: male C57BL/6J mice (Jiangsu GemPharmatech Co., Ltd. license NO: SYXK (Zhejiang) 2020–0022), *S. boulardii*

(Angel Nutritech Co., Ltd. CAT.NO: 22011001), FOS (Baolingbao Biological Co., Ltd. CAT.NO: 22021012), DSS (MP Biomedicals Co., Ltd. CAT.NO: S7708), fecal occult blood qualitative detection kit (Shanghai Yuanye Bio-Technology Co., Ltd. CAT.NO: M03HR177092), and mouse tumor necrosis factor α (TNF-α) kit, interleukin-6 (IL-6) kit, and interleukin-1β (IL-1β) kit (Shanghai Enzyme-linked Biotechnology Co., Ltd. CAT.NO: YJ002095, YJ063159, YJ301814).

2.2 Instruments

The following equipment was used in this study: GC-2010 plus Gas Chromatographic instrument (Shimadzu Co., Ltd., Japan), DB-FFAP gas chromatographic column (Agilent Technologies, Inc., USA), JB-P5 embedding machine, JJ-12 J dehydrator, JB-L5 freezing table (Wuhan Junjie Electronics Co., Ltd.), KD-P water bath-slide drier (Jinhua Kedi Instrument Equipment Co., LTD.), RM2016 microtome (Leica Instrument Co., LTD.), DP260s dyeing machine (Shenzhen Dakewe Medical Technology Co., LTD.), ECLIPSE E100 microscope (NIKON Company, Japan), and Spectramax M2 Full Wavelength enzyme-labeling Apparatus (Molecular Devices, USA).

2.3 Methods

2.3.1 Mice and housing conditions

Forty-two healthy male SPF C57BL/6 J mice (8 weeks old; average body weight, 25.25 ± 0.7 g) were housed in cages at a room temperature of 21–25°C and relative humidity of 40–70%. The lights were artificially controlled to maintain a 12-h light/dark cycle, and the corncob bedding was changed twice a week.

2.3.2 Experimental protocol

The mice were randomly divided into seven groups of six mice each. These included the control group, DSS group, HSb group (High-*S. boulardii*), LSb group (Low-*S. boulardii*), FOS group, HFSb group (High-*S. boulardii* + FOS). and LFSb group (Low-*S. boulardii* + FOS). The experiment was carried out over a total duration of 17 days, including stage T1 (days 1–9) and stage T2 (days 10–17). On day 17, the mice were sacrificed, and samples (Stool, blood, and colon) were collected. Each treatment agent was administered to the mice via oral gavage (0.15 ml). The Ctrl group received the intragastric administration of sterile water, whereas the DSS group received sterile water at the T1 stage and 3% DSS at the T2 stage. Throughout the experimental period, the HSb group and the LSb group received 10^9 CFU/ml and 10^7 CFU/ml *S. boulardii* suspensions, respectively. Meanwhile, the FOS group was given a 0.8% FOS solution. The HFSb and LFSb groups received 0.8% FOS + 10^9 CFU/ml *S. boulardii* suspension and 0.8% FOS + 10^7 CFU/ml *S. boulardii* suspension, respectively. In addition, the Ctrl group was allowed to drink water freely throughout the experiment. Meanwhile, the other six groups drank water freely during the T1 stage, and the drinking water was changed to a 3% DSS solution (0.03 g/ml) during the T2 stage to induce colitis (Figure 1).

The DAI was recorded every day during the T2 stage. At the end of the experiment, stool samples were obtained to detect their short-chain fatty acid (SFCA) content. Moreover, blood samples were collected to detect serum proinflammatory cytokine levels, and colon contents were obtained for bacterial community analysis via 16S rRNA gene sequencing. Colon tissue samples were collected and stained for histological analysis.

2.3.3 Preparation of *Saccharomyces boulardii* suspensions

Saccharomyces boulardii was cultured in yeast liquid medium at 32°C and 160 rpm for 36 h. Subsequently, the culture medium was centrifuged at 4°C and 3,000 rpm for 5 min. The supernatant was discarded, and the pellet was suspended in sterile PBS. The procedure was repeated twice to remove any residual medium. Finally, the pellet was resuspended in sterile PBS, and the number of *S. boulardii* cells was measured using a hemocytometer. Finally, *S. boulardii* suspensions with concentrations of 10^9 CFU/mL and 10^7 CFU/mL were prepared.

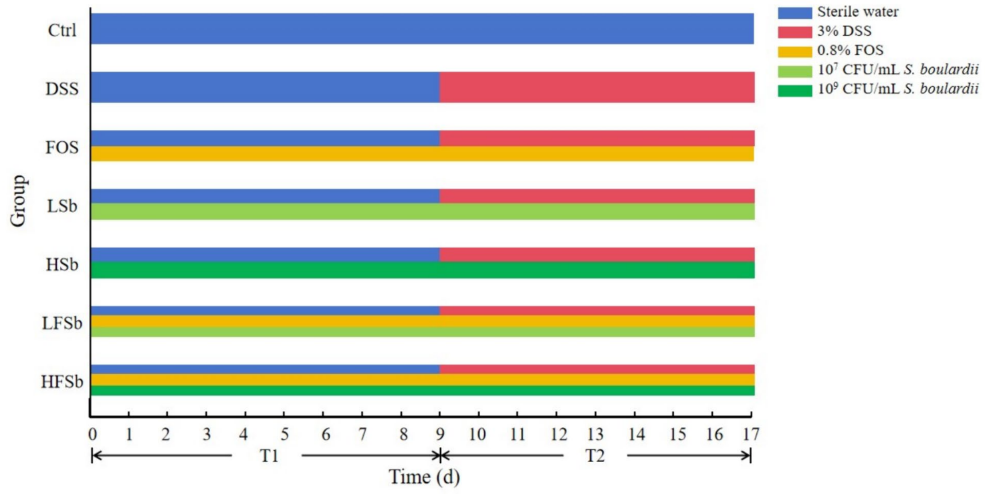

FIGURE 1
Schematic diagram of the experimental design.

2.3.4 Detection of proinflammatory cytokines in the serum

To detect the levels of TNF-α, IL-6, and IL-1β in the serum, standard, blank, and sample wells were set up on ELISA plates. Then, 50 μl of a standard solution was added to the standard well, 100 μl of the sample diluent was added to the blank well, and 40 μl of the sample diluent and 10 μl of serum were added to the sample well. The contents of each well were mixed, and subsequently, 100 μl of conjugate reagent was added to all wells except the blank wells. After incubation at 37°C for 60 min, the plates were washed five times. Then, 50 μl of color developer A and B were added successively to each well, and the color was developed at 37°C for 15 min, away from light. At the end of the color development phase, 50 μl of stop buffer was added to each well, and the absorbance of each well was measured at 400 nm. A standard curve was drawn, and the serum concentrations of the three proinflammatory cytokines were calculated.

2.3.5 Preparation, staining and histopathological analysis of colon sections

The colon tissues were fixed in formaldehyde and subsequently embedded in paraffin. Paraffin-embedded specimens were cut into 4-μm-thick sections and stained with hematoxylin and eosin (H&E). The presence and extent of neutrophil infiltration, cryptitis, crypt abscesses, epithelial erosion, and ulceration in the colon sections were evaluated based on the modified Riley score. The modified Riley score classifies histological activity as follows: 0 for neutrophils present in the epithelium but no crypt involvement; 1 for neutrophils present in the epithelium and <25% crypt involvement; 2 for neutrophils present in the epithelium and ≥25% to ≤75% crypt involvement; 3 for neutrophils present in the epithelium and >75% crypt involvement; 4 for neutrophils present in the lamina propria with a mild but unequivocal increase; 5 for neutrophils present in the lamina propria with a moderate increase; 6 for neutrophils present in the lamina propria with a marked increase; and 7 for erosion or ulceration (Ates et al., 2022).

2.3.6 Detection of SCFAs in fecal samples

Mouse feces were mixed with sterile water (1:10) and centrifuged for 5 min (4°C, 10000 rpm). Subsequently, the SCFA content in the supernatant was determined using gas chromatography. The column temperature was maintained at 80°C for 1 min and then increased to 190°C at a rate of 10°C/min. It was further increased to 240°C at 40°C/min, where it was maintained for 5 min. The vaporizing chamber and FID detector were maintained at 240°C. The flow rates of the three carrier gases were 400 ml/min (air), 40 ml/min (hydrogen), and 20 ml/min (nitrogen). A standard curve was plotted based on the peak area ratio between the standard solutions of SCFAs (acetic acid, propionic acid, isobutyric acid, butyric acid, isovaleric acid, and valeric acid) and crotonic acid, and the content of SCFAs in each sample was calculated.

2.3.7 16S rRNA sequencing

A DNA extraction kit was used to extract DNA from the colon contents of the mice. The V3-V4 hypervariable region of the 16S rRNA gene was amplified by PCR using the primers 341F (5'-CCTAYGGGRBGCASCAG-3′) and 806R (5'-GGACTACHVGGGTWTCTAAT-3′). Purified amplicons were paired-end sequenced on an Illumina NovaSeq PE250 platform. The raw sequencing reads were deposited into the NCBI Sequence Read Archive (SRA) database (Accession Number: PRJNA1040442).

2.4 Data and statistical analysis

SPSS 23 was used for statistical analysis, and GraphPad Prism 8.0.1 was used for mapping. Bacterial community analysis and mapping were carried out on the diversity cloud platform of Shanghai OE Biotech Co., Ltd. The Shapiro–Wilk test was used to assess the normality of data distribution. When comparing multiple groups, the Kruskal–Wallis test was performed to analyze data showing a non-normal distribution, and one-way ANOVA and Tukey's *post hoc* comparison test were performed on data showing a normal distribution.

3 Results

3.1 Analysis of body weight and DAI

The body weight changes in the mice during the experimental period are shown in Figure 2A. On day 10 (the end of T1), the average body weight of the mice increased in all other groups except the FOS group increased. On day 15 (day 6 after DSS intervention), the body weight of the mice in the other groups was significantly lower than that in the Ctrl group ($p < 0.05$), consistent with previous findings (Liu et al., 2023). On day 16 (day 7 after DSS intervention), all mice except those in the Ctrl group excreted loose and bloody stools. Their body weights decreased significantly, while their DAI values increased significantly. The DAI values of mice in all other groups were significantly higher than those in the Ctrl group on day 12 (day 3 after DSS intervention) (Figure 2B). On day 16 (day 7 after DSS intervention), only the DAI values in the LSb ($p = 0.017$), LFSb ($p = 0.012$), and HFSb groups ($p = 0.036$) were significantly lower than those in the DSS group.

3.2 Analysis of proinflammatory cytokine levels in the serum

The serum levels of proinflammatory factors were detected using ELISA in all groups of mice. The serum IL-1β concentration was significantly higher in mice from the DSS group ($p = 0.012$) and HSb groups ($p < 0.001$) than in those from the Ctrl group. Meanwhile, the serum IL-1β concentration was significantly lower in the FOS group ($p = 0.015$), LSb group ($p = 0.026$), LFSb group ($p = 0.018$), and HFSb group ($p = 0.013$) than in the DSS group (Figure 3A). Compared with the Ctrl group, the LSb group showed significantly elevated serum IL-6 levels ($p = 0.029$). Meanwhile, the serum IL-6 levels ($p = 0.032$) in the HFSb group were significantly lower than those in the DSS group (Figure 3B). Compared with the Ctrl group, the LFSb group showed significantly decreased serum TNF-α levels ($p = 0.005$), but the serum TNF-α levels were significantly increased in the HSb group ($p < 0.001$). The serum TNF-α levels in the LFSb group ($p = 0.018$) and the HFSb group ($p = 0.040$) were significantly lower than those in the DSS group (Figure 3C).

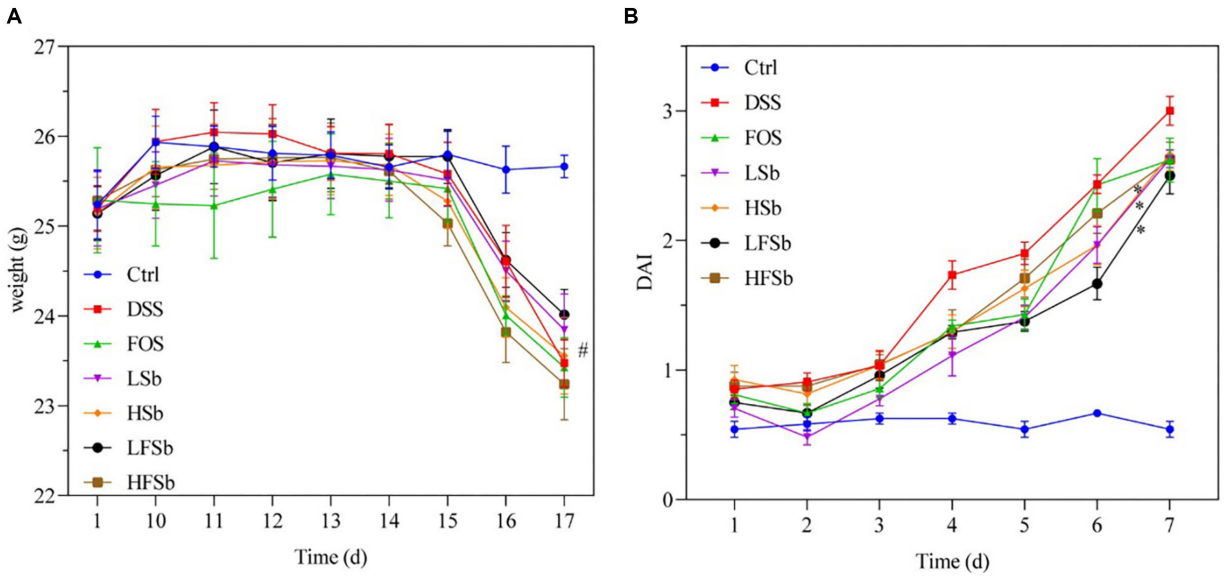

FIGURE 2
Effect of FOS and *Saccharomyces boulardii* on the body weight and disease activity index of the mice. **(A)** Body weight; **(B)** Disease activity index. Data are represented as the mean ± SEM. The Shapiro–Wilk test was used to evaluate whether the data were normally distributed. Subsequently, one-way ANOVA and Tukey's *post hoc* comparison test were conducted. # indicates a significant difference compared with the Ctrl group: # indicates $0.01 < p < 0.05$; * indicates a significant difference compared with the DSS group: * indicates $0.01 < p < 0.05$.

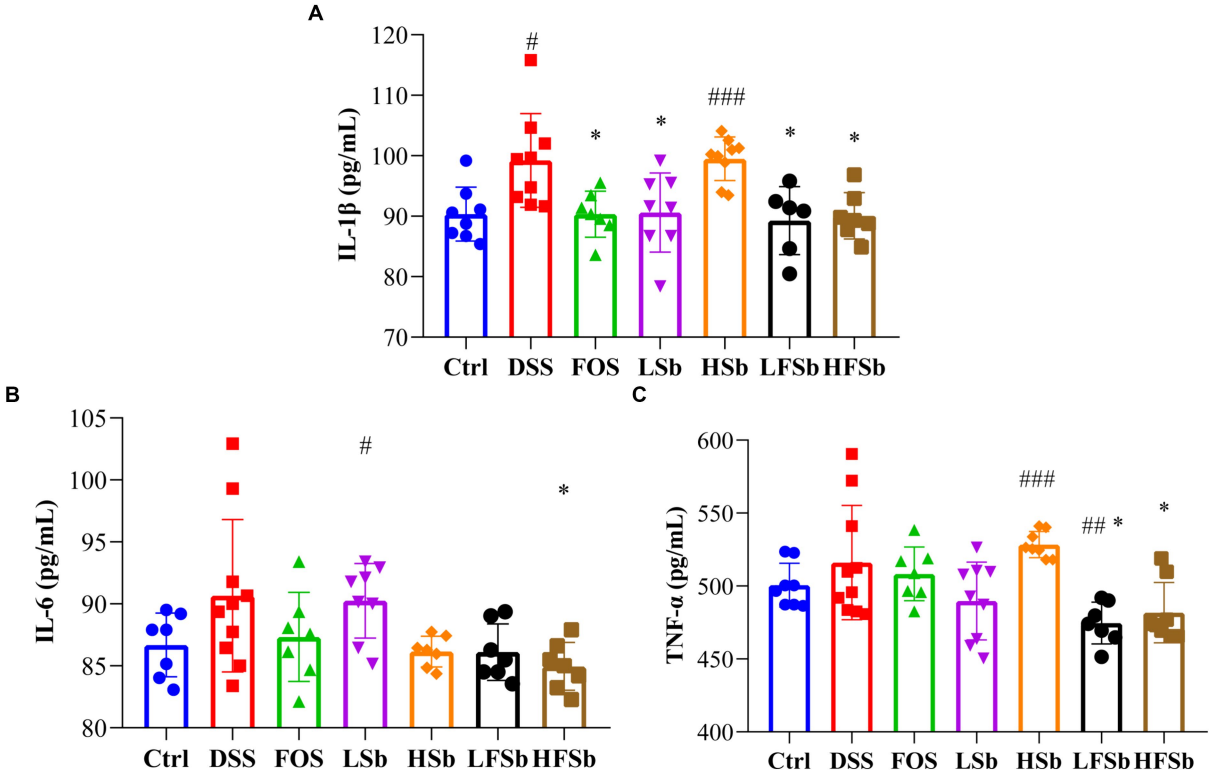

FIGURE 3
Serum levels of proinflammatory cytokines in the mice. **(A)** IL-1β; **(B)** IL-6; **(C)** TNF-α. Data are represented as the mean ± SD. The Shapiro–Wilk test was used to evaluate whether the data were normally distributed. Subsequently, one-way ANOVA and Tukey's *post hoc* comparison tests were conducted. # Indicates a significant difference compared with the Ctrl group; # indicates $0.01 < p < 0.05$, ## indicates $0.001 < p < 0.01$, and ### indicates $p < 0.001$; * indicates a significant difference compared with the DSS group: * indicates $0.01 < p < 0.05$.

3.3 Colon characteristics and histology

An important manifestation of DSS-induced colitis in mice is a shortened colon. The more severe the inflammation, the shorter is the colon length (Fonseca-Camarillo and Yamamoto-Furusho, 2015). Hence, colon length and morphology were compared among all groups in this study (Figure 4). Compared with the Ctrl group, the other groups showed a shorter colon length; notably, the colon length of mice in the DSS group ($p = 0.009$) and the FOS group ($p = 0.011$) was significantly reduced (Figure 4). Compared with the DSS group, the HSb group ($p = 0.021$) and HFSb group ($p = 0.023$) showed a significantly higher colon length, although no significant difference in colon length was observed between the LSb and LFSb groups (Figure 4).

By observing the microscopic morphology of colon tissues — such as intestinal villi, goblet cells, and crypts — the degree of inflammation can be estimated (Monk et al., 2018; Li M. X. et al., 2022). Therefore, colon tissues were histologically analyzed using H&E staining according to the modified Riley Scoring System (Figure 5). Healthy mice in the Ctrl group showed normal colon tissue morphology. However, DSS-induced colitis damaged the integrity of the colon mucosa. In animals with DSS-induced colitis, the goblet cells either decreased in number or completely disappeared. In these animals, the crypt was deformed, atrophied, or even absent. There were ulcers in the submucosa and neutrophil infiltration was also detected. These results indicated the successful establishment of the mouse colitis model.

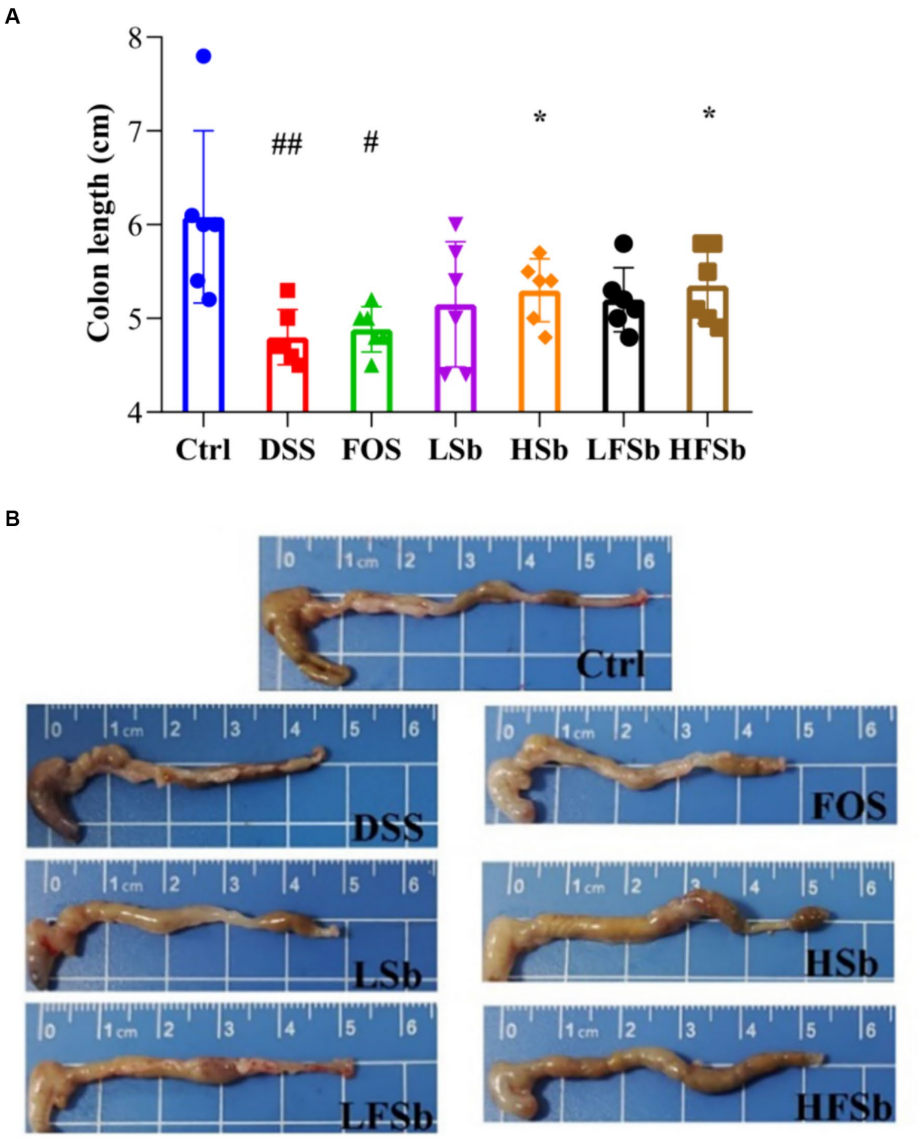

FIGURE 4
Colon length and colon morphology in mice from different groups. **(A)** Colon length; **(B)** Colon morphology. Data are represented as the mean ± SD. The Shapiro–Wilk test was used to evaluate whether the data were normally distributed. Subsequently, one-way ANOVA and Tukey's *post hoc* comparison tests were conducted. # Indicates a significant difference compared with the Ctrl group: # Indicates $0.01 < p < 0.05$, and ## indicates $0.001 < p < 0.01$; * indicates a significant difference compared with the DSS group: * indicates $0.01 < p < 0.05$.

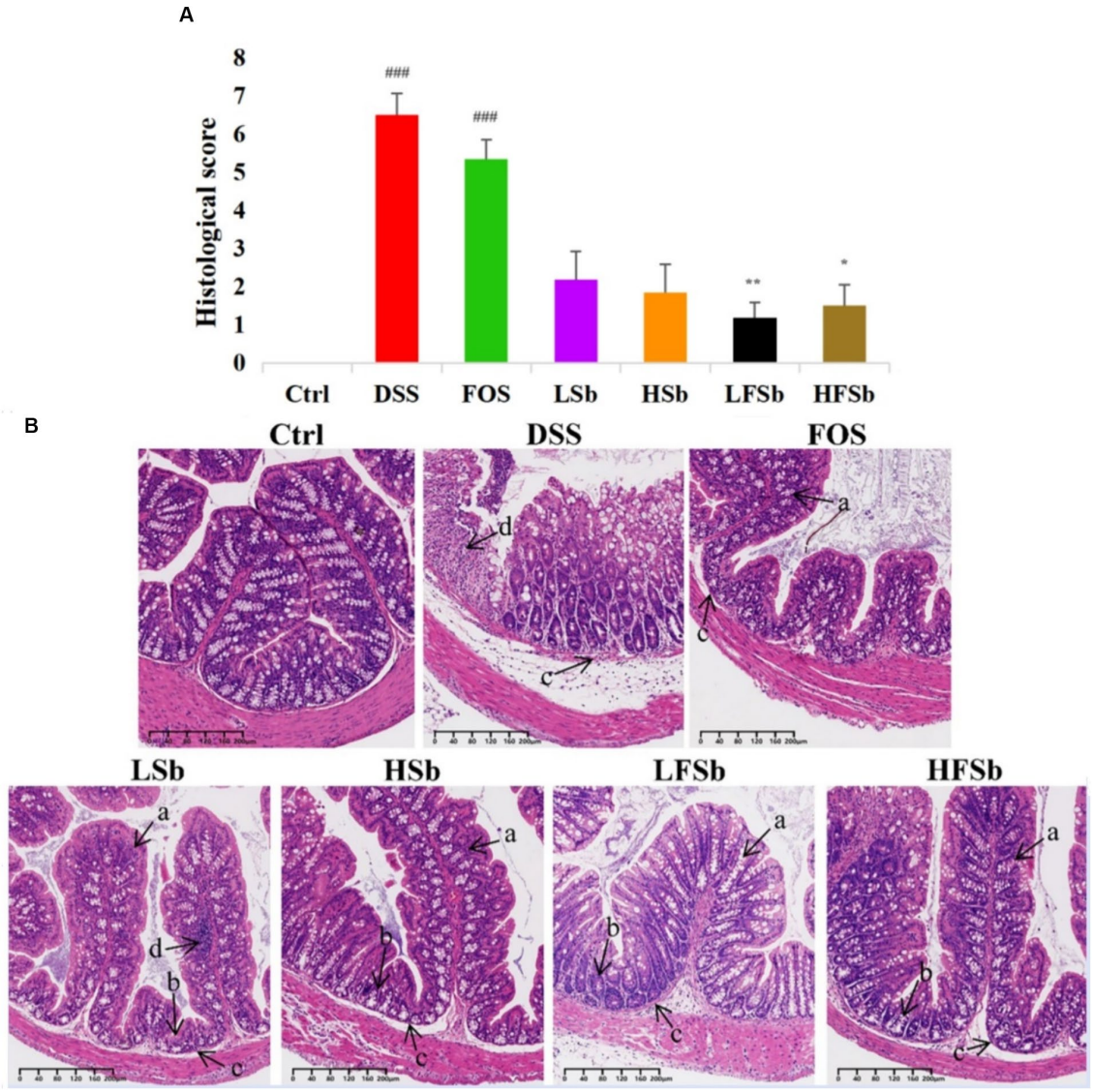

FIGURE 5
Histological analysis of the colon tissues of mice from different groups. **(A)** Histological scores; **(B)** Staining of colon tissues. Data are represented as the mean ± SEM. The Shapiro–Wilk test was used to evaluate whether the data were normally distributed. Subsequently, one-way ANOVA and Tukey's *post hoc* comparison test were conducted. # Indicates a significant difference compared with the Ctrl group: ### means $p < 0.001$; * indicates a significant difference compared with the DSS group: * indicates $p < 0.05$, ** Indicates $p < 0.01$. (a) Goblet cells; (b) Crypts; (c) Submucosa; (d) Neutrophils.

The colonic morphology of mice in the LFSb and HFSb groups showed the most significant improvement when compared with the DSS group. In these groups ($p<0.01$, $p<0.05$), goblet cells with mucus-secreting functions were largely preserved. Meanwhile, the structural integrity of the crypts and submucosa was also significantly improved, and inflammatory cell infiltration was only detected locally in the mucosa.

The colon morphology of mice in the LSb and HSb groups was also improved to a certain extent, with intestinal villi and cup cells being partially retained. However, in these groups, some crypts were deformed and atrophied, and considerable local inflammatory cell infiltration was detected. The histological scores in the LSb and HSb groups were not significantly better than those in the DSS group. In contrast, the villi in the FOS group were significantly atrophied. In this group, the goblet cells had largely disappeared, and the crypts were also deformed or had disappeared. With the exception of the DSS group, the FOS group had the highest histological score. Furthermore, the histological scores of the DSS and FOS groups were both significantly higher than those of the control group ($p<0.001$). In summary, a significant amelioration of colon injury was observed in the LFSb and HFSb groups. While the LSb and HSb groups also showed some degree of improvement, the improvement was not as high as that in the LFSb and HFSb groups.

3.4 Analysis of SCFA content in feces

The excrements of mice were collected, and six types of SCFAs were detected in mouse stool samples. Standard solutions for six

concentration gradients of the SCFAs (acetic acid, propionic acid, isobutyric acid, butyric acid, isovaleric acid, and valeric acid) were prepared. Subsequently, standard curves were generated based on the peak area ratio and concentration ratio between each SCFA and crotonic acid. Fecal samples were subjected to various hydrolysis and methyl esterification conditions (different durations, temperatures, and gas usage conditions) to obtain maximum extraction efficiency. The total SCFA content was significantly higher in the DSS ($p = 0.002$) and the LFSb group ($p = 0.006$) than in the Ctrl group. However, it was significantly lower in the LSb ($p = 0.030$) and the HSb group ($p = 0.006$) than in the DSS group (Figure 6A). The proportion of acetic acid in the fecal samples was much higher than that of the other SCFAs. The between-group differences in the levels of these individual SCFAs were similar to the between-group differences in the total SCFA content (Figure 6B). The propionic acid content in the LSb ($p = 0.015$) and LFSb groups ($p = 0.004$) was significantly higher than that in the Ctrl group. Moreover, the propionic acid levels in the LFSb group ($p = 0.047$) were significantly higher than those in the DSS group (Figure 6C). The contents of butyric acid and isobutyric acid in the DSS group and the other five experimental groups were significantly higher than those in the Ctrl group, while the contents of butyric acid in the LFSb ($p = 0.004$) and HFSb groups ($p = 0.038$) were significantly higher than those in the DSS group (Figures 6D,E). In addition, the contents of valeric acid ($p = 0.045$) and isovaleric acid ($p = 0.042$) in the LFSb group and the contents of isovaleric acid ($p = 0.028$) in the HFSb group were significantly higher than those in the DSS group (Figures 6F,G).

3.5 Analysis of gut microbial composition

The colon contents of mice were sequenced using 16S rRNA gene sequencing, and the composition of the gut microbiota in different groups of mice was analyzed. First. the α-diversity of the colon microbiota was examined (Figures 7A,B). Compared with Ctrl treatment, the DSS intervention significantly reduced the Chao1 index and Shannon index of the gut microbiota in mice. Thus, DSS-induced colitis significantly reduced the abundance and diversity of the gut microbiota. In addition, a significant decrease in the Shannon index was observed in all other treatment groups except the LFSb group. This indicated that LFSb could partly attenuate the decrease in gut microbiota diversity. However, there was no significant difference in the abundance and diversity of the gut microbiota between the other five experimental groups and the DSS group.

Principal coordinate analysis (PCoA) revealed a distinct separation between the β-diversity of the Ctrl group and that of the other six groups. This indicated that after the DSS intervention, a significant alteration in the gut microbiota was in all groups (when compared with the Ctrl group) (Figure 7C). However, there was a small difference between the DSS group and the other five experimental groups. In addition, there was no overlap between the FOS group and the LFSb group, indicating a significant variation in the composition of the gut microbiota between these two groups (Figure 7C).

The abundance of intestinal bacteria was examined at the phylum level. Firmicutes and Bacteroidota were the dominant phyla in the colons of healthy mice, accounting for more than 95% of the total microbes, followed by Actinobacteriota and Desulfobacterota (Figure 8A). The relative abundance of Deferribacterota increased significantly after DSS intervention, and this was one of the dominant phyla in the DSS group.

The mean relative abundance of Firmicutes in the LFSb group was higher than that in the other groups, but there was no significant difference in its abundance among the other groups. Notably, there were significant differences in the relative abundance of Bacteroidota and Proteobacteria among the groups. The abundance of Bacteroidota in all other groups except the LSb group was significantly lower than that in the Ctrl group (Figure 8B). Meanwhile, the relative abundance of Proteobacteria in the DSS group, FOS group, HSb group, and HFSb group was significantly higher than that in the Ctrl group. In contrast, the relative abundance of Proteobacteria in these five experimental groups was significantly lower than that in the DSS group (Figure 8C).

The top 30 genera (based on relative abundance) in the mouse gut are shown in Figure 9A. *Muribaculaceae* was the genus with the highest relative abundance in the colons of healthy mice, accounting for more than 50% of the total microbes. It was followed by *Lachnospiraceae_NK4A136_group* (13.35%), *Clostridia_UCG-014* (4.70%), and *Lactobacillus* (3.83%). The composition of the microbiota in the other groups was significantly different from that in the Ctrl group, with *Muribaculaceae* of Bacteroidota showing the most significant change (Figure 9B). The relative abundance of *Parabacteroides* in the FOS and LFSb groups was significantly higher than that in the Ctrl and DSS groups (Figure 9C). The relative abundance of *Escherichia-Shigella* was significantly elevated in all other groups except the LFSb group (Figure 9D). Meanwhile, the relative abundance of *Parasutterella* increased significantly in the DSS, HSb, and HFSb groups, when compared with the Ctrl group, and also tended to increase in the FOS, LSb, and LFSb groups (Figure 9E). The relative abundance of *Ileibacterium* in the FOS, LSb, HSb, and LFSb groups was significantly lower than that in the DSS group (Figure 9F).

4 Discussion

The present study found that typically, FOS and *S. boulardii* alone cannot prevent the occurrence of DSS-induced colitis. However, FOS/*S. boulardii* mixed suspensions (10^7 CFU/ml and 10^9 CFU/ml) and the 10^7 CFU/ml *S. boulardii* suspension may significantly attenuate the increased DAI in mice after DSS treatment and alleviate the clinical symptoms of colitis to a certain extent.

A previous study reported that 10^9 CFU/ml of *S. boulardii* may also reduce the DAI and prevent colon damage in DSS-induced mouse models of colitis. However, this study did not compare the effects of different concentrations of *S. boulardii* (Rodriguez-Nogales et al., 2018). Gao H et al. found that *S. boulardii* suspensions of 10^5 CFU/mL may significantly prevent weight loss in DSS-induced mouse models of colitis, improve the DAI, and reduce the colon weight/length ratio (Gao H. et al., 2021). Meanwhile, different concentrations of *S. boulardii* have also been shown to reduce colon inflammation to varying extents, and their combination with FOS has been found to enhance this improvement.

IL-1β, IL-6, and TNF-α are important cytokines that regulate inflammation and their release triggers and promotes the inflammatory response. Therefore, these cytokines are often used as inflammatory markers to estimate the severity of inflammation in the

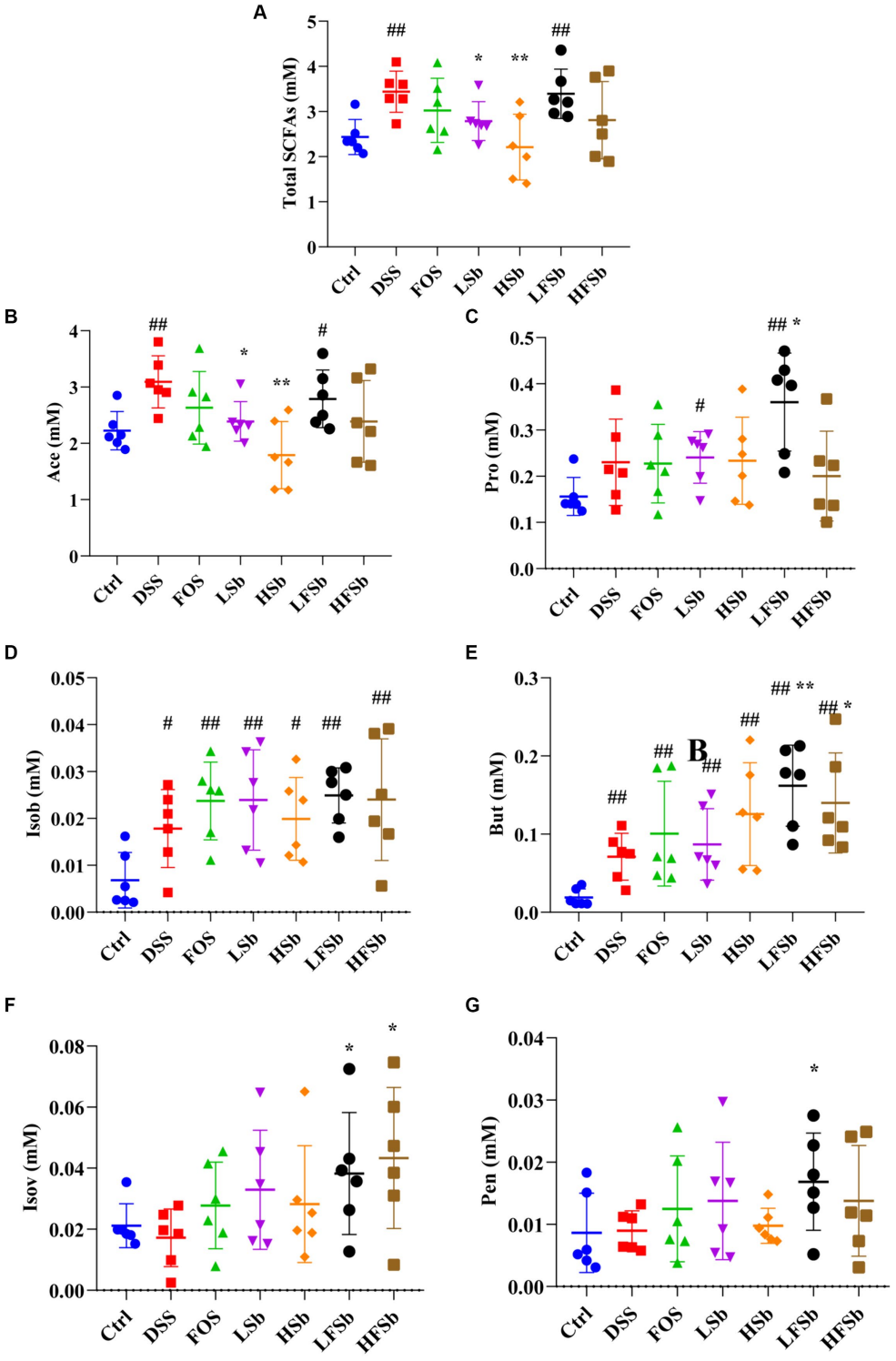

FIGURE 6
Effects of FOS and *S. boulardii* on short-chain fatty acid (SFCA) contents in the feces of different groups. **(A)** Total SCFA content, i.e., total contents of six SCFAs; **(B)** Ace (acetic acid); **(C)** Pro (propionic acid); **(D)** Isob (isobutyric acid); **(E)** But (butyric acid); **(F)** IsoV (Isovaleric acid); **(G)** Pen (valeric acid). Data are represented as the mean ± SD. The Shapiro–Wilk test was used to evaluate whether the data were normally distributed. Subsequently, one-way ANOVA and Tukey's *post hoc* comparison tests were conducted. # Indicates a significant difference compared with the Ctrl group: # indicates $0.01 < p < 0.05$, and ## indicates $0.001 < p < 0.01$; * indicates a significant difference compared with the DSS group: * indicates $0.01 < p < 0.05$, and ** indicates $0.001 < p < 0.01$.

body (Qu S. et al., 2021; Nakase et al., 2022). In the present study, the HFSb group showed significantly reduced levels of these proinflammatory cytokines. The anti-inflammatory effect was the strongest in the HFSb group, (significant reductions in IL-6, IL-1β, and TNF-α), followed by the LFSb group (significant reductions in IL-1β and TNF-α). Meanwhile, the FOS and LSb groups only exhibited

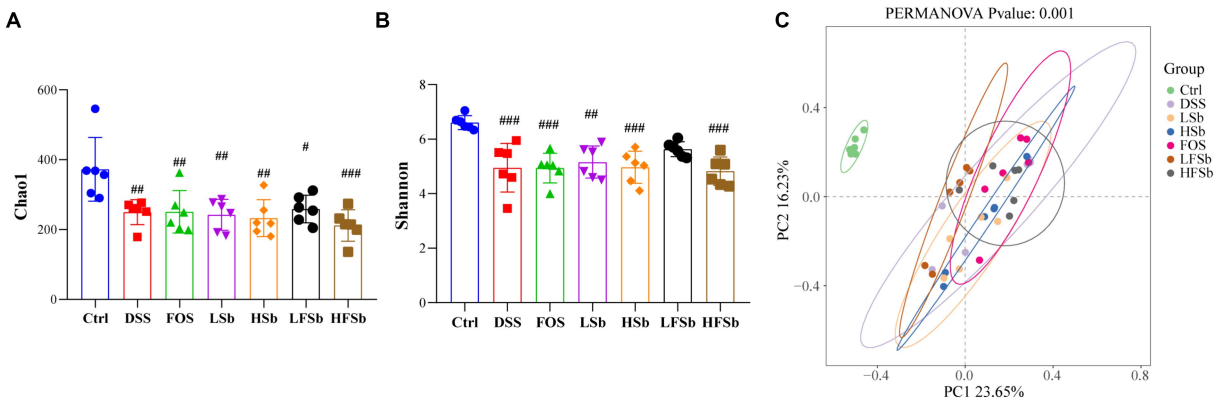

FIGURE 7
Microbial composition analysis of primary fecal samples and fermentation samples at the genus level. **(A)** Alpha-diversity analysis based on the Chao1 index; **(B)** Alpha-diversity analysis based on the Shannon index; **(C)** Beta-diversity analysis based on Bray-Curtis distances and PCoA; Data are represented as the mean ± SD. The Shapiro–Wilk test was used to evaluate whether the data were normally distributed. Subsequently, one-way ANOVA and Tukey's *post hoc* comparison tests were conducted. # Indicates a significant difference compared with the Ctrl group: # indicates $0.01 < p < 0.05$, ## indicates $0.001 < p < 0.01$, and ### indicates $p < 0.001$.

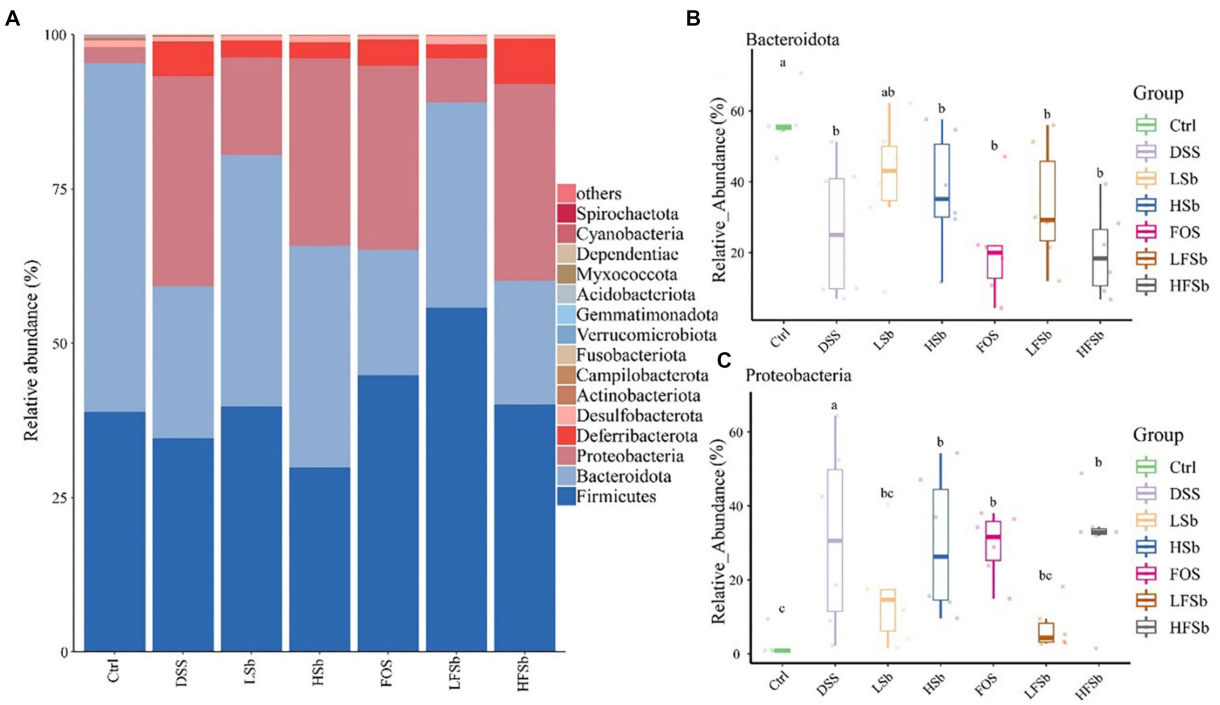

FIGURE 8
Colon microbiota composition and group differences at the phylum level. **(A)** Microbial composition at the phylum level; Differences in the relative abundance of Bacteroidota **(B)** and Proteobacteria **(C)** between different groups. Data are represented as the mean ± SD. The Shapiro–Wilk test was used to evaluate whether the data were normally distributed. Subsequently, the Kruskal-Wallis test was conducted. a, b, c: different lowercase letters represent significant differences between different groups.

significantly reduced levels of IL-1β, and the HSb group did not show any obvious alteration in proinflammatory cytokines. Gao et al. reported that *S. boulardii* suspensions of both 10^5 CFU/mL and 10^7 CFU/ml can reduce the levels of IL-1β, IL-6, and TNF-α. This indicates that a high concentration of *S. boulardii*, such as 10^9 CFU/ml, may indeed have a poor effect on improving inflammation (Gao H. et al., 2021). Zhang et al. discovered that FOS combined with GOS can decrease the serum levels of IL-1β, IL-6, IL-8, and TNF-α in mice with DSS-induced colitis (Zhang S. et al., 2023). Meanwhile, Rajkumar et al. found that the combination of *Lactobacillus salivarius* and FOS can significantly lower the serum levels of IL-1β, IL-6, IL-8, and TNF-α in adults, and combination treatment provides more obvious treatment effects than *Lactobacillus salivarius* alone (Rajkumar et al., 2015). Therefore, the combination of FOS and *S. boulardii* appears to

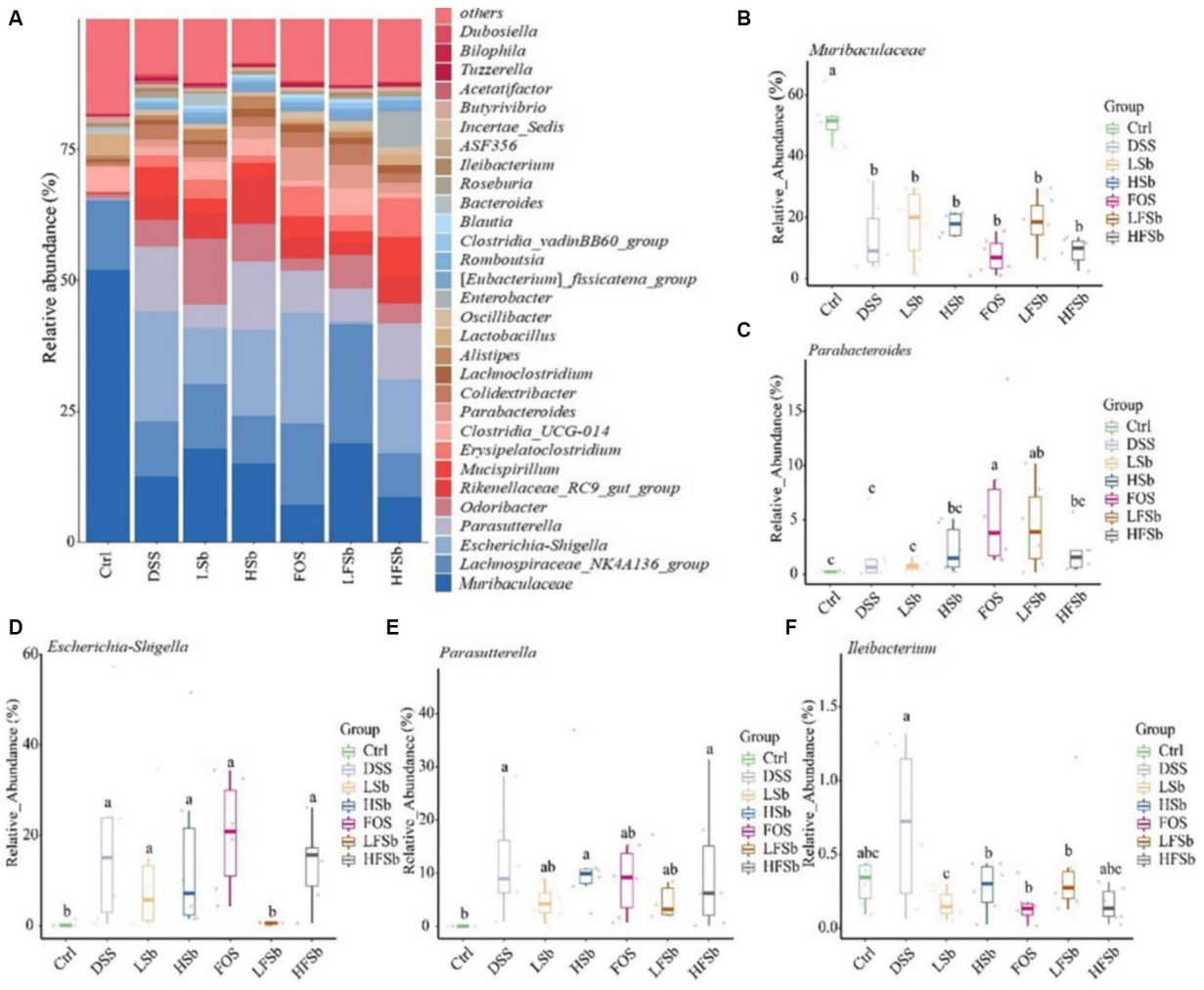

FIGURE 9
Colon microbiota composition and group differences at the genus level. **(A)** Microbial composition at the genus level; **(B–F)** Differences in *Muribaculaceae*, *Parabacteroides*, *Escherichia–Shigella*, *Parasutterella*, and *Ileibacterium* between groups. Data are represented as the mean ± SD. The Shapiro–Wilk test was used to evaluate whether the data were normally distributed. Subsequently, the Kruskal–Wallis test was conducted. a, b, c: different lowercase letters represent significant differences between different groups.

be more effective at inhibiting the release of proinflammatory cytokines than either of these agents alone. Moreover, the concentration of *S. boulardii* also seems to affect the inhibitory effect of this probiotic on proinflammatory cytokines.

The SCFAs present in mouse feces represent the residual products that are synthesized by gut microbes but not absorbed by the body. Notably, the integrity of the intestinal mucosa determines the absorption efficiency of SCFAs (Zhou et al., 2020; Guo et al., 2021). DSS-induced colitis can cause intestinal mucosal damage in mice, thus inhibiting nutrient absorption. This may partly explain the increase in SCFA content in the feces of mice from the DSS group (Niu et al., 2023; Wu et al., 2023). SCFAs, especially butyric acid, have a strong anti-inflammatory effect. Hence, they can help maintain the integrity of the intestinal mucosal barrier and thus improve colon health (Parada Venegas et al., 2019; Li W. et al., 2022). In this study, the content of butyric acid was significantly higher in the LFSb and HFSb groups than in the DSS group, which further explains why the intestinal damage was the least severe in these two groups. In addition to butyric acid, a variety of other SCFAs also showed significantly higher levels in fecal samples from the LFSb group than in those from the Ctrl group. The combination of FOS and *S. boulardii* promoted the production of SCFAs by intestinal microbes and the SCFA content in the LFSb group was higher than that in the LSb and FOS groups. These results indicated that FOS combined with *S. boulardii* was more effective at promoting fermentation than either agent alone. This result was consistent with the conclusion derived by Morales-Ferre C et al. regarding the preventive effects of probiotics and prebiotics on early rotavirus-induced diarrhea in rats. Combination of probiotics and prebiotics, such as FOS and *S. boulardii*, can significantly reduce intestinal permeability and increase the levels of SCFAs when compared with single-agent treatment (Morales-Ferre et al., 2022). However, in the present study, some differences were detected between the LSb group and HSb group and between the LFSb group and HFSb group, indicating that the concentration of *S. boulardii* also plays a key role in regulating fermentation activity in gut microbiota.

By examining the gut microbiota composition in mice, this study showed that DSS could inhibit Bacteroidota and promote the growth of Proteobacteria. Meanwhile, LSb could attenuate these changes and

maintain the balance of the gut microbiota. Notably, LFSb could also inhibit the growth of Proteobacteria and promote the growth of Firmicutes to a certain extent. These findings were consistent with the results obtained by Yu L et al. in their intervention study that focused on liver injury induced by D-Galactosamine in mice. These researchers found that *S. boulardii* significantly increases the relative abundance of Bacteroidota, and decreases the relative abundance of Firmicutes and Proteobacteria (Yu et al., 2017).

Compared with the Ctrl group, the other groups also showed a significantly reduced relative abundance of *Muribaculaceae* from the phylum Bacteroidota. Interestingly, *Muribaculaceae* is known to have a probiotic effect and can influence mucus layer formation and barrier function in the colon (Mu et al., 2021; Zhang Y. et al., 2023). In the present study, its mean relative abundance was the lowest in the DSS group and the FOS group, which may be one reason why colitis injury was more severe in these two groups. Furthermore, *Parabacteroides* from the phylum Bacteroidota has been shown to inhibit the inflammatory response by regulating IL-10 levels and Treg cells (Strandwitz et al., 2019; Koh et al., 2020). The relative abundance of *Parabacteroides* in the FOS and LFSb groups was significantly higher than that in the Ctrl and DSS groups, which may partly explain why inflammation was alleviated in the LFSb group. Although the abundance of *Parabacteroides* was also significantly increased in the FOS group, the other microbial indicators in this group were poor. Hence, the findings suggested that the anti-inflammatory effect in the FOS group was limited. *Muribaculaceae* and *Parabacteroides* have previously been identified as potential SCFAs-producing bacteria (Cui et al., 2022; Yang et al., 2023). Studies have demonstrated a strong positive correlation between *Muribaculaceae* and propionic acid production as well as a moderate association between *Muribaculaceae* and butyric acid production (Pei et al., 2023). Meanwhile, *Parabacteroides* has been shown to have a positive correlation with the level of acetic acid production (He et al., 2023).

Escherichia–Shigella from the phylum Proteobacteria can increase intestinal permeability and exacerbate colitis (Zorraquin-Pena et al., 2021). *Escherichia–Shigella are* negatively correlated with SCFA production (Huang et al., 2023). Among all the treatment groups in this study, only the LFSb group showed no significant increase in the abundance of *Escherichia–Shigella*. This suggested that LFSb effectively inhibited the growth of the harmful bacteria *Escherichia–Shigella*, thereby protecting the intestinal tract and reducing damage due to colitis. The relative abundance of *Parabacteroides* and *Escherichia–Shigella* was similar between the HFSb and DSS groups. However, HFSb did not provide the same effects as LFSb, which indicated that the concentration of *S. boulardii* affects the efficacy of microbiota regulation. Previously, the increase in *Parasutterella* (phylum Proteobacteria) in the gut has been linked to dysbiosis and decreased microbial diversity (Jang et al., 2019). In this study, although the FOS, LSb, and LFSb groups showed a higher relative abundance of *Parasutterella* than the Ctrl group, this difference was not significant. This may be one reason why the microbial diversity in the LFSb group did not decrease remarkably. Furthermore, the relative abundance of *Ileibacterium* in the FOS, LSb, HSb, and LFSb groups was significantly lower than that in the DSS group. *Ileibacterium* is a genus from the phylum Firmicutes, and it is a harmful group of bacteria. *Ileibacterium* has previously been linked to metabolic disorders and intestinal inflammation (Gao X. et al., 2021; Lin et al., 2022). However, some studies have shown that *Ileibacterium* and *Parasutterella* are positively correlated with butyric acid production (Huang et al., 2023; Cao et al., 2024). In the present study, the abundance of *Ileibacterium* and *Parasutterella* in the Ctrl group was significantly lower than that in the DSS group. This could explain why the butyric acid content in the Ctrl group was lower than that in the DSS group.

Although both the LFSb and HFSb groups showed a lower relative abundance of Proteobacteria than the DSS group, their levels were much lower in the LFSb group. In fact, the relative abundance of Proteobacteria was comparable between the LFSb group and the Ctrl group. Notably, only the relative abundance of *Escherichia–Shigella* and *Parasutterella* (both belonging to phylum Proteobacteria) was significantly lower in the LFSb group than in the DSS group, and there was no significant difference in the relative abundance of these bacteria between the LFSb group and the Ctrl group. The relative abundance of *Ileibacterium* (phylum Proteobacteria) in both groups was significantly lower than that in the DSS group, but only the LFSb group showed similar levels of *Ileibacterium* as the Ctrl group. In addition, compared with the DSS group, the relative abundance of *Parabacteroides* (phylum Bacteroidetes) was significantly elevated in the LFSb group, but not in the HFSb group. Overall, these results demonstrated that the concentration of *S. boulardii* has an important effect on modulating the reduction in intestinal inflammation and improving the gut microbiota, as suggested by several previous studies. Therefore, additional studies involving more concentration gradients of *S. boulardii* in combination with FOS are warranted. Overall, accurate evidence and theoretical confirmation are required for the combined use of these agents in clinical settings.

5 Conclusion

Intervention with DSS can cause a gut microbiota imbalance and reduce the richness and diversity of the gut microbes. By establishing a DSS-induced colitis mouse model, this study analyzed the correlation between the composition and characteristics of intestinal microbiota and the levels of proinflammatory cytokines in the serum and SCFAs in feces, while accounting for the severity of colitis. Therefore, this study provided a potential strategy for managing colitis by regulating the intestinal microbiota. This study showed that 10^7 CFU/ml of *S. boulardii* combined with FOS can reduce colitis-induced injury and protect the intestinal mucosal barrier by attenuating intestinal dysbiosis, promoting the growth of the beneficial bacteria *Parabacteroides*, and inhibiting the growth of the harmful bacteria *Escherichia–Shigella*. The effect of the combination was found to be obviously better than that of FOS or *S. boulardii* alone, and the concentration of *S. boulardii* appeared to be a key factor affecting the efficacy of the intervention. These results provide a scientific basis for the improved prevention and treatment of colitis using a FOS/*S. boulardii* combination. They also offer a theoretical basis for the development of preparations containing FOS combined with *S. boulardii*.

Data availability statement

The datasets presented in this study can be found in online repositories. The names of the repository/repositories and accession number(s) can be found at: https://www.ncbi.nlm.nih.gov/, PRJNA1040442.

Ethics statement

The animal study was approved by Institutional Animal Care and Use Committee (ACUC) of Zhejiang Academy of Agricultural Sciences (2022ZAASLA57). The study was conducted in accordance with the local legislation and institutional requirements.

Author contributions

YW: Data curation, Methodology, Writing – original draft, Writing – review & editing. HF: Data curation, Formal analysis, Methodology, Writing – review & editing. XX: Data curation, Investigation, Validation, Writing – review & editing. HJ: Investigation, Methodology, Project administration, Resources, Writing – review & editing. Q-jK: Investigation, Methodology, Project administration, Resources, Writing – review & editing. W-lT: Investigation, Methodology, Project administration, Resources, Writing – review & editing. BW: Project administration, Supervision, Writing – review & editing. GZ: Funding acquisition, Supervision, Writing – review & editing. X-eP: Methodology, Project administration, Supervision, Writing – review & editing.

Funding

The author(s) declare financial support was received for the research, authorship, and/or publication of this article. This work was supported by the Key Research Project of Agricultural and Social Development of Hangzhou (No. 202004A20).

Conflict of interest

The authors declare that the research was conducted in the absence of any commercial or financial relationships that could be construed as a potential conflict of interest.

Publisher's note

All claims expressed in this article are solely those of the authors and do not necessarily represent those of their affiliated organizations, or those of the publisher, the editors and the reviewers. Any product that may be evaluated in this article, or claim that may be made by its manufacturer, is not guaranteed or endorsed by the publisher.

References

Ates, B. B., Talim, B., Gulsen, H. H., Demir, H., Karaismailoglu, E., Ozen, H., et al. (2022). Significance of intestinal alkaline phosphatase in predicting histological activity of pediatric inflammatory bowel disease. *Turk. J. Pediatr.* 64, 1068–1076. doi: 10.24953/turkjped.2021.5413

Cao, C., Li, F., Ding, Q., Jin, X., Tu, W., Zhu, H., et al. (2024). Potassium sodium hydrogen citrate intervention on gut microbiota and clinical features in uric acid stone patients. *Appl. Microbiol. Biotechnol.* 108:51. doi: 10.1007/s00253-023-12953-y

Cottone, M., Kohn, A., Daperno, M., Armuzzi, A., Guidi, L., D'Inca, R., et al. (2011). Advanced age is an independent risk factor for severe infections and mortality in patients given anti-tumor necrosis factor therapy for inflammatory bowel disease. *Clin. Gastroenterol. Hepatol.* 9, 30–35. doi: 10.1016/j.cgh.2010.09.026

Cui, Y., Zhang, L., Wang, X., Yi, Y., Shan, Y., Liu, B., et al. (2022). Roles of intestinal Parabacteroides in human health and diseases. *FEMS Microbiol. Lett.* 369:fnac072. doi: 10.1093/femsle/fnac072

Dong, L., Xie, J., Wang, Y., Jiang, H., Chen, K., Li, D., et al. (2022). Mannose ameliorates experimental colitis by protecting intestinal barrier integrity. *Nat. Commun.* 13:4804. doi: 10.1038/s41467-022-32505-8

Fonseca-Camarillo, G., and Yamamoto-Furusho, J. K. (2015). Immunoregulatory pathways involved in inflammatory bowel disease. *Inflamm. Bowel Dis.* 21, 2188–2193. doi: 10.1097/MIB.0000000000000477

Gao, X., Du, L., Randell, E., Zhang, H., Li, K., and Li, D. (2021). Effect of different phosphatidylcholines on high fat diet-induced insulin resistance in mice. *Food Funct.* 12, 1516–1528. doi: 10.1039/d0fo02632h

Gao, H., Li, Y., Sun, J., Xu, H., Wang, M., Zuo, X., et al. (2021). *Saccharomyces boulardii* ameliorates dextran sulfate sodium-induced ulcerative colitis in mice by regulating NF-kappaB and Nrf2 signaling pathways. *Oxidative Med. Cell. Longev.* 2021:1622375. doi: 10.1155/2021/1622375

Gao, H., Li, Y., Xu, J., Zuo, X., Yue, T., Xu, H., et al. (2023). *Saccharomyces boulardii* protects against murine experimental colitis by reshaping the gut microbiome and its metabolic profile. *Front. Microbiol.* 14:1204122. doi: 10.3389/fmicb.2023.1204122

Genda, T., Sasaki, Y., Kondo, T., Hino, S., Nishimura, N., Tsukahara, T., et al. (2017). Fructo-oligosaccharide-induced transient increases in Cecal immunoglobulin a concentrations in rats are associated with mucosal inflammation in response to increased gut permeability. *J. Nutr.* 147, 1900–1908. doi: 10.3945/jn.117.253955

Guo, C., Wang, Y., Zhang, S., Zhang, X., Du, Z., Li, M., et al. (2021). *Crataegus pinnatifida* polysaccharide alleviates colitis via modulation of gut microbiota and SCFAs metabolism. *Int. J. Biol. Macromol.* 181, 357–368. doi: 10.1016/j.ijbiomac.2021.03.137

He, J., Gong, X., Hu, B., Lin, L., Lin, X., Gong, W., et al. (2023). Altered gut microbiota and short-chain fatty acids in Chinese children with constipated autism Spectrum disorder. *Sci. Rep.* 13:19103. doi: 10.1038/s41598-023-46566-2

Huang, Y., Wang, Z., Ye, B., Ma, J. H., Ji, S., Sheng, W., et al. (2023). Sodium butyrate ameliorates diabetic retinopathy in mice via the regulation of gut microbiota and related short-chain fatty acids. *J. Transl. Med.* 21:451. doi: 10.1186/s12967-023-04259-4

Jang, L. G., Choi, G., Kim, S. W., Kim, B. Y., Lee, S., and Park, H. (2019). The combination of sport and sport-specific diet is associated with characteristics of gut microbiota: an observational study. *J. Int. Soc. Sports Nutr.* 16:21. doi: 10.1186/s12970-019-0290-y

Jeong, D. Y., Kim, S., Son, M. J., Son, C. Y., Kim, J. Y., Kronbichler, A., et al. (2019). Induction and maintenance treatment of inflammatory bowel disease: a comprehensive review. *Autoimmun. Rev.* 18, 439–454. doi: 10.1016/j.autrev.2019.03.002

Koh, G. Y., Kane, A. V., Wu, X., and Crott, J. W. (2020). *Parabacteroides distasonis* attenuates tumorigenesis, modulates inflammatory markers and promotes intestinal barrier integrity in azoxymethane-treated A/J mice. *Carcinogenesis* 41, 909–917. doi: 10.1093/carcin/bgaa018

Kornbluth, A., and Sachar, D. B.Practice Parameters Committee of the American College of Gastroenterology (2010). Ulcerative colitis practice guidelines in adults: American college of gastroenterology, practice parameters committee. *Am. J. Gastroenterol.* 105, 501–523. doi: 10.1038/ajg.2009.727

Li, M. X., Li, M. Y., Lei, J. X., Wu, Y. Z., Li, Z. H., Chen, L. M., et al. (2022). Huangqin decoction ameliorates DSS-induced ulcerative colitis: role of gut microbiota and amino acid metabolism, mTOR pathway and intestinal epithelial barrier. *Phytomedicine* 100:154052. doi: 10.1016/j.phymed.2022.154052

Li, W., Zhang, L., Xu, Q., Yang, W., Zhao, J., Ren, Y., et al. (2022). Taxifolin alleviates DSS-induced ulcerative colitis by acting on gut microbiome to produce butyric acid. *Nutrients* 14:1069. doi: 10.3390/nu14051069

Lin, H., Ma, X., Yang, X., Chen, Q., Wen, Z., Yang, M., et al. (2022). Natural shikonin and acetyl-shikonin improve intestinal microbial and protein composition to alleviate colitis-associated colorectal cancer. *Int. Immunopharmacol.* 111:109097. doi: 10.1016/j.intimp.2022.109097

Liu, C., Huang, S., Wu, Z., Li, T., Li, N., Zhang, B., et al. (2021). Cohousing-mediated microbiota transfer from milk bioactive components-dosed mice ameliorate colitis by remodeling colonic mucus barrier and lamina propria macrophages. *Gut Microbes* 13, 1–23. doi: 10.1080/19490976.2021.1903826

Liu, J., Lin, H., Cao, M., Lin, T., Lin, A., Xu, W., et al. (2023). Shifts and importance of viable bacteria in treatment of DSS-induced ulcerative colitis mice with FMT. *Front. Cell. Infect. Microbiol.* 13:1124256. doi: 10.3389/fcimb.2023.1124256

Liu, C., Yan, X., Zhang, Y., Yang, M., Ma, Y., Zhang, Y., et al. (2022). Oral administration of turmeric-derived exosome-like nanovesicles with anti-inflammatory and pro-resolving bioactions for murine colitis therapy. *J. Nanobiotechnol.* 20:206. doi: 10.1186/s12951-022-01421-w

Mao, B., Gu, J., Li, D., Cui, S., Zhao, J., Zhang, H., et al. (2018). Effects of different doses of Fructooligosaccharides (FOS) on the composition of mice fecal microbiota, especially the Bifidobacterium composition. *Nutrients* 10:1105. doi: 10.3390/nu10081105

Monk, J. M., Wu, W., Hutchinson, A. L., Pauls, P., Robinson, L. E., and Power, K. A. (2018). Navy and black bean supplementation attenuates colitis-associated inflammation and colonic epithelial damage. *J. Nutr. Biochem.* 56, 215–223. doi: 10.1016/j.jnutbio.2018.02.013

Morales-Ferre, C., Azagra-Boronat, I., Massot-Cladera, M., Tims, S., Knipping, K., Garssen, J., et al. (2022). Preventive effect of a Postbiotic and prebiotic mixture in a rat model of early life rotavirus induced-diarrhea. *Nutrients* 14:1163. doi: 10.3390/nu14061163

Mu, Z., Yang, Y., Xia, Y., Wang, F., Sun, Y., Yang, Y., et al. (2021). Probiotic yeast BR14 ameliorates DSS-induced colitis by restoring the gut barrier and adjusting the intestinal microbiota. *Food Funct.* 12, 8386–8398. doi: 10.1039/d1fo01314a

Nakase, H., Sato, N., Mizuno, N., and Ikawa, Y. (2022). The influence of cytokines on the complex pathology of ulcerative colitis. *Autoimmun. Rev.* 21:103017. doi: 10.1016/j.autrev.2021.103017

Niu, C., Hu, X. L., Yuan, Z. W., Xiao, Y., Ji, P., Wei, Y. M., et al. (2023). *Pulsatilla* decoction improves DSS-induced colitis via modulation of fecal-bacteria-related short-chain fatty acids and intestinal barrier integrity. *J. Ethnopharmacol.* 300:115741. doi: 10.1016/j.jep.2022.115741

Pais, P., Almeida, V., Yilmaz, M., and Teixeira, M. C. (2020). *Saccharomyces boulardii*: what makes it tick as successful probiotic? *J. Fungi (Basel)* 6:78. doi: 10.3390/jof6020078

Parada Venegas, D., De la Fuente, M. K., Landskron, G., Gonzalez, M. J., Quera, R., Dijkstra, G., et al. (2019). Short chain fatty acids (SCFAs)-mediated gut epithelial and immune regulation and its relevance for inflammatory bowel diseases. *Front. Immunol.* 10:277. doi: 10.3389/fimmu.2019.00277

Pei, L., Liu, W., Liu, L., Wang, X., Jiang, L., Chen, Z., et al. (2023). Morel (Morchella spp.) intake alters gut microbial community and short-chain fatty acid profiles in mice. *Front. Nutr.* 10:1237237. doi: 10.3389/fnut.2023.1237237

Pithadia, A. B., and Jain, S. (2011). Treatment of inflammatory bowel disease (IBD). *Pharmacol. Rep.* 63, 629–642. doi: 10.1016/s1734-1140(11)70575-8

Qu, S., Fan, L., Qi, Y., Xu, C., Hu, Y., Chen, S., et al. (2021). *Akkermansia muciniphila* alleviates dextran sulfate sodium (DSS)-induced acute colitis by NLRP3 activation. *Microbiol. Spectr.* 9:e0073021. doi: 10.1128/Spectrum.00730-21

Qu, Y., Li, X., Xu, F., Zhao, S., Wu, X., Wang, Y., et al. (2021). Kaempferol alleviates murine experimental colitis by restoring gut microbiota and inhibiting the LPS-TLR4-NF-kappaB Axis. *Front. Immunol.* 12:679897. doi: 10.3389/fimmu.2021.679897

Rajkumar, H., Kumar, M., Das, N., Kumar, S. N., Challa, H. R., and Nagpal, R. (2015). Effect of probiotic *Lactobacillus salivarius* UBL S22 and prebiotic Fructo-oligosaccharide on serum lipids, inflammatory markers, insulin sensitivity, and gut Bacteria in healthy young volunteers: a randomized controlled single-blind pilot study. *J. Cardiovasc. Pharmacol. Ther.* 20, 289–298. doi: 10.1177/1074248414555004

Rodriguez-Nogales, A., Algieri, F., Garrido-Mesa, J., Vezza, T., Utrilla, M. P., Chueca, N., et al. (2018). Intestinal anti-inflammatory effect of the probiotic Saccharomyces boulardii in DSS-induced colitis in mice: impact on microRNAs expression and gut microbiota composition. *J. Nutr. Biochem.* 61, 129–139. doi: 10.1016/j.jnutbio.2018.08.005

Salazar-Parra, M. A., Cruz-Neri, R. U., Trujillo-Trujillo, X. A., Dominguez-Mora, J. J., Cruz-Neri, H. I., Guzman-Diaz, J. M., et al. (2023). Effectiveness of Saccharomyces Boulardii CNCM I-745 probiotic in acute inflammatory viral diarrhoea in adults: results from a single-Centre randomized trial. *BMC Gastroenterol.* 23:229. doi: 10.1186/s12876-023-02863-8

Shi, J., Du, P., Xie, Q., Wang, N., Li, H., Smith, E. E., et al. (2020). Protective effects of tryptophan-catabolizing *Lactobacillus plantarum* KLDS 1.0386 against dextran sodium sulfate-induced colitis in mice. *Food Funct.* 11, 10736–10747. doi: 10.1039/d0fo02622k

Simoes, C. D., Maganinho, M., and Sousa, A. S. (2022). FODMAPs, inflammatory bowel disease and gut microbiota: updated overview on the current evidence. *Eur. J. Nutr.* 61, 1187–1198. doi: 10.1007/s00394-021-02755-1

Sivananthan, K., and Petersen, A. M. (2018). Review of *Saccharomyces boulardii* as a treatment option in IBD. *Immunopharmacol. Immunotoxicol.* 40, 465–475. doi: 10.1080/08923973.2018.1469143

Strandwitz, P., Kim, K. H., Terekhova, D., Liu, J. K., Sharma, A., Levering, J., et al. (2019). GABA-modulating bacteria of the human gut microbiota. *Nat. Microbiol.* 4, 396–403. doi: 10.1038/s41564-018-0307-3

Taleban, S., Colombel, J. F., Mohler, M. J., and Fain, M. J. (2015). Inflammatory bowel disease and the elderly: a review. *J. Crohns Colitis* 9, 507–515. doi: 10.1093/ecco-jcc/jjv059

Tandon, D., Haque, M. M., Gote, M., Jain, M., Bhaduri, A., Dubey, A. K., et al. (2019). A prospective randomized, double-blind, placebo-controlled, dose-response relationship study to investigate efficacy of fructo-oligosaccharides (FOS) on human gut microflora. *Sci. Rep.* 9:5473. doi: 10.1038/s41598-019-41837-3

Toruner, M., Loftus, E. V. Jr., Harmsen, W. S., Zinsmeister, A. R., Orenstein, R., Sandborn, W. J., et al. (2008). Risk factors for opportunistic infections in patients with inflammatory bowel disease. *Gastroenterology* 134, 929–936. doi: 10.1053/j.gastro.2008.01.012

Wang, H. Y., Zhao, H. M., Wang, Y., Liu, Y., Lu, X. Y., Liu, X. K., et al. (2019). Sishen Wan((R)) ameliorated trinitrobenzene-sulfonic-acid-induced chronic colitis via NEMO/NLK signaling pathway. *Front. Pharmacol.* 10:170. doi: 10.3389/fphar.2019.00170

Wasilewski, A., Zielinska, M., Storr, M., and Fichna, J. (2015). Beneficial effects of probiotics, prebiotics, Synbiotics, and Psychobiotics in inflammatory bowel disease. *Inflamm. Bowel Dis.* 21, 1674–1682. doi: 10.1097/MIB.0000000000000364

Wu, Z., Huang, S., Li, T., Li, N., Han, D., Zhang, B., et al. (2021). Gut microbiota from green tea polyphenol-dosed mice improves intestinal epithelial homeostasis and ameliorates experimental colitis. *Microbiome* 9:184. doi: 10.1186/s40168-021-01115-9

Wu, Y., Ran, L., Yang, Y., Gao, X., Peng, M., Liu, S., et al. (2023). Deferasirox alleviates DSS-induced ulcerative colitis in mice by inhibiting ferroptosis and improving intestinal microbiota. *Life Sci.* 314:121312. doi: 10.1016/j.lfs.2022.121312

Yang, N., Lan, T., Han, Y., Zhao, H., Wang, C., Xu, Z., et al. (2023). Tributyrin alleviates gut microbiota dysbiosis to repair intestinal damage in antibiotic-treated mice. *PLoS One* 18:e0289364. doi: 10.1371/journal.pone.0289364

Yang, J., Pei, G., Sun, X., Xiao, Y., Miao, C., Zhou, L., et al. (2022). RhoB affects colitis through modulating cell signaling and intestinal microbiome. *Microbiome* 10:149. doi: 10.1186/s40168-022-01347-3

Yu, L., Zhao, X. K., Cheng, M. L., Yang, G. Z., Wang, B., Liu, H. J., et al. (2017). *Saccharomyces boulardii* administration changes gut microbiota and attenuates D-Galactosamine-induced liver injury. *Sci. Rep.* 7:1359. doi: 10.1038/s41598-017-01271-9

Zhang, S., Lv, S., Li, Y., Wei, D., Zhou, X., Niu, X., et al. (2023). Prebiotics modulate the microbiota-gut-brain axis and ameliorate cognitive impairment in APP/PS1 mice. *Eur. J. Nutr.* 62, 2991–3007. doi: 10.1007/s00394-023-03208-7

Zhang, Y., Tang, Y., Cai, L., He, J., Chen, L., Ouyang, K., et al. (2023). *Chimonanthus nitens* Oliv polysaccharides modulate immunity and gut microbiota in immunocompromised mice. *Oxidative Med. Cell. Longev.* 2023, –6208620. doi: 10.1155/2023/6208680

Zhou, C., Li, L., Li, T., Sun, L., Yin, J., Guan, H., et al. (2020). SCFAs induce autophagy in intestinal epithelial cells and relieve colitis by stabilizing HIF-1alpha. *J. Mol. Med. (Berl)* 98, 1189–1202. doi: 10.1007/s00109-020-01947-2

Zorraquin-Pena, I., Taladrid, D., Tamargo, A., Silva, M., Molinero, N., de Llano, D. G., et al. (2021). Effects of wine and its microbial-derived metabolites on intestinal permeability using simulated gastrointestinal digestion/colonic fermentation and Caco-2 intestinal cell models. *Microorganisms* 9:1378. doi: 10.3390/microorganisms9071378

frontiers | Frontiers in Microbiology

TYPE Original Research
PUBLISHED 21 May 2024
DOI 10.3389/fmicb.2024.1298432

OPEN ACCESS

EDITED BY
Fengjie Sun,
Georgia Gwinnett College, United States

REVIEWED BY
Rizaldy Taslim Pinzon,
Duta Wacana Christian University, Indonesia
Junqiong Chen,
Nanjing Normal University, China

*CORRESPONDENCE
Laurence Genton
✉ laurence.genton@hug.ch

RECEIVED 21 September 2023
ACCEPTED 06 May 2024
PUBLISHED 21 May 2024

CITATION
Lazarevic V, Teta D, Pruijm M, Stoermann C, Marangon N, Mareschal J, Solano R, Wurzner-Ghajarzadeh A, Gaïa N, Cani PD, Dizdar OS, Herrmann FR, Schrenzel J and Genton L (2024) Gut microbiota associations with chronic kidney disease: insights into nutritional and inflammatory parameters. *Front. Microbiol.* 15:1298432. doi: 10.3389/fmicb.2024.1298432

Gut microbiota associations with chronic kidney disease: insights into nutritional and inflammatory parameters

Vladimir Lazarevic[1], Daniel Teta[2], Menno Pruijm[3], Catherine Stoermann[4], Nicola Marangon[5], Julie Mareschal[6], Raquel Solano[2], Arlene Wurzner-Ghajarzadeh[3], Nadia Gaïa[1], Patrice D. Cani[7,8], Oğuzhan S. Dizdar[6,9], François R. Herrmann[10], Jacques Schrenzel[1,11] and Laurence Genton[6]*

[1]Genomic Research Laboratory, Geneva University Hospitals and University of Geneva, Geneva, Switzerland, [2]Nephrology, Hospital of Sion, Sion, Switzerland, [3]Nephrology, University Hospital of Lausanne and University of Lausanne, Lausanne, Switzerland, [4]Nephrology, Geneva University Hospitals and University of Geneva, Geneva, Switzerland, [5]Department of Nephrology, Geneva University Hospitals and Clinique of Champel, Geneva, Switzerland, [6]Clinical Nutrition, Geneva University Hospitals and University of Geneva, Geneva, Switzerland, [7]Metabolism and Nutrition Research Group, Louvain Drug Research Institute, UCLouvain, Université catholique de Louvain, Brussels, Belgium, [8]WELBIO-Walloon Excellence in Life Sciences and Biotechnology, WELBIO Department, WEL Research Institute, Wavre, Belgium, [9]Department of Internal Medicine and Clinical Nutrition Unit, Kayseri City Training and Research Hospital, University of Health Sciences, Kayseri, Türkiye, [10]Rehabilitation and Geriatrics, Geneva University Hospitals and University of Geneva, Geneva, Switzerland, [11]Infectious Diseases, Geneva University Hospitals and University of Geneva, Geneva, Switzerland

Introduction: The gut barrier, comprising gut microbiota, plays a pivotal role in chronic kidney disease (CKD) progression and nutritional status. This study aimed to explore gut barrier alterations in hemodialyzed (HD) patients, non-HD (NHD) CKD patients, and healthy volunteers.

Methods: Our cross-sectional study enrolled 22 HD patients, 11 NHD patients, and 11 healthy volunteers. We evaluated fecal microbiota composition (assessed via bacterial 16S rRNA gene sequencing), fecal IgA levels, surrogate markers of gut permeability, serum cytokines, appetite mediators, nutritional status, physical activity, and quality of life.

Results: HD patients exhibited significant alterations in fecal microbiota composition compared to healthy volunteers, with observed shifts in taxa known to be associated with dietary patterns or producing metabolites acting on human host. In comparison to healthy volunteers, individuals with HD patients exhibited elevated levels of inflammatory markers (CRP, IL-6 and TNF-α), glucagon-like peptide-2, and potential anorexigenic markers (including leptin and peptide YY). NHD patients had increased levels of CRP and peptide YY. Overall fecal microbiota composition was associated with height, soft lean mass, resting energy expenditure, handgrip strength, bone mineral content and plasma albumin and TNF-α.

Discussion: Compared to healthy volunteers, HD patients have an altered fecal microbiota composition, a higher systemic inflammation, and a modification in plasma levels of appetite mediators. While some differences align with previous findings, heterogeneity exists likely due to various factors including lifestyle and comorbidities. Despite limitations such as sample size, our study underscores

the multifaceted interplay between gut microbiota, physiological markers, and kidney function, warranting further investigation in larger cohorts.

KEYWORDS

appetite, gut permeability, handgrip strength, hormones, lean body mass, lipopolysaccharide, Metataxonomics 16S, nutritional state

Introduction

Chronic kidney disease (CKD) has a worldwide prevalence of 10 to 16% (Kazancioğlu, 2013). End-stage renal disease, which refers to an estimated glomerular filtration <15 mL/min/1.73m^2 (Vassalotti et al., 2016), is generally treated with dialysis. Over 2.5 million of patients receive renal replacement therapy and this number is expected to double within 10 years. A low glomerular filtration rate is related to complications such as protein-energy wasting (PEW), decreased physical function, cardio-vascular diseases, pulmonary edema, anemia, bone disease, and neuropathy (National Kidney Foundation, 2000). As PEW is highly prevalent and increases the risk of hospitalization and mortality (Huang et al., 2010; Mak et al., 2011), the National Kidney Foundation recommends routine assessment of the nutritional state in patients with end-stage kidney disease through measurements of body weight and composition, laboratory parameters, and nutritional intakes (National Kidney Foundation, 2019).

The gut barrier could be involved in the pathogenesis of CKD and its complications. It is secured by the gut epithelium and its tight junctions, the mucus, the gut-associated lymphoid tissue, and the microbiota (Magnotti and Deitch, 2005). Especially the gut microbiota encounters an increased interest in the scientific community. It can synthesize and/or metabolize uremic toxins (Popkov et al., 2022; Krukowski et al., 2023) which are substances that accumulate in the blood in case of CKD and have been related to cardio-vascular diseases and CKD progression (Vanholder et al., 2018). Thus, the gut microbiota composition and function may influence the outcome of CKD patients and be a therapeutic target (Sumida et al., 2021). Several studies suggest alterations of gut microbiota in CKD. In rats, uremia leads to gut dysbiosis, with a decreased abundance of Lactobacillaceae and Prevotellaceae (Vaziri et al., 2013a), and a disruption of intestinal tight junctions (Vaziri et al., 2013b). Cross-sectional human studies, summarized in a recent review, found alterations of the fecal microbiota composition and its metabolites in patients with advanced CKD, whether hemodialyzed (HD) or not, as compared to healthy persons (Chung et al., 2019). Most of these studies did not evaluate other parameters of the gut barrier and did not differentiate the impact of hemodialysis *per se* from uremia, although it may also affect the gut microbiota (Luo et al., 2021). If hemodialysis is associated with additional alterations in gut microbiota, the treatment of CKD progression and complications by gut microbiota modulation may be different in HD than in non-dialyzed patients with CKD (termed NHD) patients.

The first aim of the study was to compare the gut barrier and microbiota of HD patients, NHD, and healthy volunteers. We hypothesized that HD patients have an altered composition of fecal microbiota, an increased gut permeability and systemic inflammation, and an imbalance of plasma appetite mediators in favor of anorexigenic mediators, compared to the other groups. The second aim was to evaluate the associations between fecal microbiota and clinical and biological parameters, including nutritional parameters.

Methods

This cross-sectional analysis took place in the University Hospitals of Geneva and Lausanne, the Clinic of Champel Geneva, and the Hospital of Sion between August 1st 2016 and August 31st 2019. The protocol was accepted by the local Ethical Committees, registered under clinicaltrials.gov (NCT 02962089), and all participants signed an informed consent.

Study population

This post-hoc analysis encompasses three groups of subjects, i.e., 22 HD patients, 11 NHD patients and 11 healthy volunteers.

The inclusion criteria for the HD patients were maintenance HD ≥3 months and absence of systemic antibiotics for an acute infection in the previous month. This group consisted of 11 patients with features of PEW at screening (plasma albumin <38 g/L, or body weight loss >5% of dry body weight over the last 3 months; daily dietary intakes <30 kcal/kg and < 1 g protein/kg as calculated by 24 h dietary recall), recruited for an interventional nutritional study (Genton et al., 2021), and 11 patients without these features. Initially, the four groups (HD patients with PEW, without PEW, NHD patients and healthy volunteers) were matched for age (± 5 years) and sex. Features of PEW were assessed at screening. However, there were no significant differences in albumin and dietary intakes at the time of measurement between groups (Friedman ANOVA: albumin, Friedman test = 10.761, $p = 0.376$; dietary intakes, Friedman test = 7.500, $p = 0.6775$). Thus, we decided to pool the data of HP patients in a single group, which led to the loss of pairing. The NHD patients included non-dialyzed patients with CKD stage 4 or 5 with daily dietary intakes >30 kcal/kg as calculated by 24 h dietary recall. The healthy volunteers were included based on the following criteria: body mass index <30 kg/m^2, absence of chronic disease potentially leading to wasting such as chronic infections, cancer, rheumatoid arthritis, congestive cardiomyopathy, end stage renal disease, chronic obstructive disease, cystic fibrosis, Crohn's disease, or alcoholic liver disease.

The exclusion criteria were the same for all participants: cognitive impairment, life expectancy <1 year, enteral or parenteral nutrition, inadequate dialysis defined by sKt/V < 1.2 (if applicable), decreased plasma albumin levels related to liver failure or exudative enteropathy, nutritional supplements containing fibers since <1 month, drugs

influencing body composition since <1 month (systemic corticosteroids, insulin, testosterone, post-menopausal hormone therapy, injectable contraceptives), known endocrinological disorder leading to hypo- or hypermetabolism untreated or treated since <1 month, pregnancy and breast-feeding.

Measurements

We assessed clinical and routine biological parameters in the fasted state, as well as nutritional state, systemic inflammatory status, serum levels of appetite mediators, surrogate markers of gut permeability and fecal microbiota. The parameters of the HD patients with PEW were measured up to 6 weeks after screening, to allow them enough reflection time for their participation in the longitudinal study and for the organization of their baseline tests. The fecal microbiota composition and the biological parameters related to the study were determined in the University Hospitals of Geneva at the end of the study, while the routine biological parameters were performed in the local laboratories.

Clinical parameters

The weight and height were measured without shoes and in light clothes, immediately after dialysis for the HD participants, to calculate body mass index. Soft lean mass, bone mineral content, and fat mass were assessed by dual-energy x-ray absorptiometry (Hologic Discovery A®, Hologic, Waltham, MA, United States). In HD patients, this measurement was performed within 90 min of the end of the hemodialysis.

Energy and protein intakes of two weekdays and one day of the weekend were assessed through a 3-day food diary filled in by the patient and reviewed with a dietician. Resting energy expenditure was assessed after an overnight fast by indirect calorimetry (Quark RMR®, Cosmed, Pavone, Italy). Appetite was evaluated by a visual analog scale of 100 mm, ranging from 0 (no appetite) to 100 mm (excellent appetite) (Suneja et al., 2011).

Handgrip strength was measured with a hydraulic hand dynamometer (Baseline® 12–0240, White Plains, New York, USA), thrice with each hand. For analysis, we used the maximum value obtained from both hands (Leong et al., 2016).

Physical activity was assessed with a pedometry device worn at the waist for 7 consecutive days (Yamax Digiwalker SW-200®, London, United Kingdom) (Crouter et al., 2003; Schneider et al., 2003). For analysis, we considered the mean number of steps per day.

Quality of life was assessed with the RAND 36-item short form health survey (RAND Health Care, 2023). It evaluates eight health domains, each scoring from 0 (very unfavorable) to 100% (very favorable) (RAND Health Care, 2023): physical functioning, limitations due to physical health, limitations due to emotional health, energy/fatigue, emotional well-being, social functioning, pain, and general health.

Biological parameters

All participants underwent measurements of venous hemoglobin, prealbumin, urea, creatinine, bicarbonate, albumin, pre-albumin, and C-reactive protein (pre-dialysis if applicable). In the setting of this research, we additionally assessed the serum levels of cytokines, hormones involved in appetite regulation, and surrogate markers of gut permeability as glucagon-like peptide-2 (GLP-2) and lipopolysaccharides (LPS) (Szeto et al., 2018; Genton et al., 2021). ELISA allowed the determination of serum levels of interleukin (IL)-6, IL-10, tumor necrosis factor (TNF)-α, leptin, total ghrelin, total glucagon-like peptide-1, peptide YY (U-Plex metabolic group assays; MSD, Rockville, MD, USA), cholecystokinin (Antibodies-online, Aachen, Germany), GLP-2 and neuropeptide Y (Merck, Darmstadt, Germany) and active grehlin (Gentaur, Kampenhout, Belgium). Serum LPS levels were assessed by competitive inhibition enzyme immunoassay (Genton et al., 2021). Fecal IgA levels were measured by ELISA according to the instruction of the manufacturer (IBL International, Hamburg, Germany).

Fecal microbiota composition

Stool collection: The patients collected a nut-sized sample of their feces into Feces Tube (Sarstedt, Nürmbrecht, Germany), stored them in their fridge at 2–8°C, and transported them to the laboratory within 24 h. Stool samples were then aliquoted for fecal IgA measurements into 2 mL safe-lock Eppendorf tubes. The remaining material in the Feces Tube was used for DNA extraction. All tubes were kept frozen at −80°C. Processing of the samples occurred at the end of the study.

DNA extraction: DNA was extracted from 125 to 230 mg stool samples using ZymoBIOMICS DNA Miniprep Kit (Zymo Research, Irvine, CA, United States). Purified DNA was quantified using the Qubit dsDNA BR Assay Kit (Thermo Fisher Scientific, Carlsbad, CA, United States) and stored at −20°C. Three negative extraction controls (NECs) were performed previously (Genton et al., 2021) by extracting DNA using the same extraction procedure but omitting the addition of stools.

Amplicon sequencing: The V3–4 region of the bacterial 16S rRNA genes (positions 341–805 in *Escherichia coli* 16S rRNA gene) was amplified using 3 ng of extracted DNA in a 25 µL volume of ZymoTaq PreMix (Zymo Research) containing each of 0.4 µM forward primer 341F 5'-CCTACGGGNGGCWGCAG-3′ and reverse primer 805R 5'-GACTACHVGGGTATCTAAKCC-3′. The PCRs were carried out with an initial denaturation at 95°C for 10 min, 29 cycles at 95°C for 30 s, 51°C for 30 s and 72°C for 60 s, followed by a final extension at 72°C for 7 min. For each sample, duplicate PCRs were combined and run on a 2100 Bioanalyzer (Agilent Technologies, Santa Clara, CA, United States) for quality analysis and quantification. The amplicon barcoding/purification, library construction, 2 × 300 Illumina (San Diego, CA, USA) MiSeq sequencing, and library demultiplexing were performed as described previously (Lazarevic et al., 2016).

Sequence analysis: Paired reads were joined using PEAR v0.9.11 (-m 470 -n 390 -v 10 -p 0.0001 -u 0) (Zhang et al., 2014). Merged sequence reads were clustered into zero-radius operational taxonomic units (zOTUs) using UNOISE3 (Edgar, 2016) from USEARCH v10.0.240 package (Edgar, 2010). The zOTUs were defined using 181 samples and 3 negative controls collected during the interventional study (108 of which were analyzed in a previous contribution (Genton et al., 2021)). From zOTUs with >90% identity to reference EzBioCloud 16S database (Yoon et al., 2017) sequences (as of 19 August 2019) as revealed by USEARCH (-id 0.90 -query_cov 0.99),

we removed those with <10 reads in the whole dataset ($n = 784$), as well as those represented with >100x higher average relative abundance in NECs than in samples (n = 12). Remaining zOTUs ($n = 2,201$) were classified using EzBioCloud 16S database via MOTHUR (Schloss et al., 2009) (command classify.seq with the options method = wang and cutoff = 80). Sequencing data were submitted to European Nucleotide Archive (ENA; study number: PRJEB49241). Sequencing data from the 9 of 11 here analyzed HD patients with PEW have been previously submitted [PRJEB43505 (Genton et al., 2021)]. For the 44 samples analyzed, a total of 3,543,950 raw reads were obtained. After merging forward and reverse reads, zOTU clustering, removal of putative contaminant and low abundance zOTUs as well as zOTUs with no reasonable similarity to reference 16S rRNA sequences (see above), the dataset contained 3,358,342 (merged) reads with a median (per sample) of 78,015 (range 40,031–121,019).

Statistical methods

Sample size

The determination of the sample size was based on the study of Vaziri et al. (2013a). They showed significant differences in fecal microbiota when comparing 12 healthy volunteers and 24 HD patients, who were not matched for gender. At the time when the study was set up, no methodology was available to calculate sample size using microbiota as primary endpoint.

Non-metataxonomic data

Results are shown as median (IQR) or n (frequency). Continuous parameters were compared between the HD patients, NHD patients and healthy volunteers with Kruskal-Wallis H tests. Significance was set at $p < 0.05$ and corrected for multiple comparisons by the Benjamini-Hochberg method (Benjamini and Hochberg, 1995). In case of significance, the groups were compared two by two with the Wilcoxon rank sum tests.

Metataxonomic data

Principal coordinates analysis (PCoA) and hierarchical clustering (group average linking method) were performed to visualize variations in bacterial communities. These analyses, relying on Bray–Curtis similarity (Bray and Curtis, 1957) matrix, were based on the square-root-transformed relative abundance, and were performed in PRIMER (PRIMER-e, Auckland, New Zealand). We used permutational multivariate analysis of variance (PERMANOVA; 9,999 permutations) (Anderson, 2001) to assess the significance of microbiota differences and the PERMDISP (9,999 permutations) test to evaluate the homogeneity of multivariate dispersion among groups (Anderson, 2006).

Ecological indices (richness and Shannon diversity index (Shannon, 1948)) were calculated from the relative abundance of zOTUs after rarefying the dataset to the same sequencing depth (40,000) using the *rrarefy* function in the vegan v2.6–2 R v4.2.0 package. Values were compared with Wilcoxon rank sum tests.

The differences between groups in the relative abundance of individual taxa was tested using MaAsLin2 (Microbiome multivariate association with linear models) (Mallick et al., 2021). We used the default linear model (LM) with LOG transformation and filtered relative abundance (minimum 0.001%) and prevalence (minimum 25%). Benjamini-Hochberg corrected *p*-values <0.05 were considered significant.

Distance-based linear model (DISTLM, PRIMER) was used to analyze the association between the bacterial community profiles and continuous non-metataxonomic variables in the whole study population. In case of significant associations, we reformatted the symbols in the PCoA plots to visualize differences in bacterial communities after dichotomizing the subjects according to the median values of the relevant variables. The involved zOTUs were identified by Spearman tests.

Results

We included 22 white HD patients (6 female and 16 male), 11 NHD patients (3 female and 8 male) and 11 volunteers (3 female and 8 male), thus a similar proportion of males and females in each group. The etiologies of CKD in HD and in non-dialyzed patients were mostly hypertension (73 and 82%, respectively) and diabetes (50 and 27% respectively), and often multifactorial. The etiology of CKD for each patient and the drugs against hypertension and diabetes are shown for each patient in the Supplementary Tables 1, 2, respectively.

Non-metataxonomic data

Table 1 shows the clinical characteristics of the participants. The body composition and handgrip strength by sex is shown in Supplementary Table 3. After correction for multiple comparisons, HD patients had lower appetite rating, physical activity and general health than healthy volunteers, but their clinical characteristics did not significantly differ from NHD patients. Table 2 highlights the abnormal routine blood parameters in HD and NHD patients, as expected. Compared to healthy volunteers, HD patients had higher serum levels of inflammatory makers (CRP, IL-6, TNF-α), GLP-2, and of some possible anorexigenic (leptin, peptide YY) and orexigenic mediators (Neuropeptide YY). Compared to NHD patients, HD patients demonstrated higher levels of CRP, LPS and peptide YY.

Metataxonomic data

The most abundant bacterial families constituting the gut microbiota were Lachnospiraceae, Ruminococcaceae, and Bacteroidaceae, which are typical of gut microbiota. Figure 1 provides a summary of the variation in bacterial taxonomic profiles across individuals and studied groups. The PCoA plot revealed a trend in differentiating microbiota from healthy volunteers and patients (Figure 2A). Notably, a substantial proportion of HD samples were situated outside the area formed by healthy volunteer samples, and vice versa. PERMANOVA analysis further confirmed significant dissimilarities between HD patients and healthy volunteers ($p = 0.0038$, $R^2 = 0.0506$, $F = 1.6923$). The PCoA plot implies that the observed significance in the PERMANOVA test is likely attributed, at least in part, to differences in community composition, despite a distinction in multivariate dispersion between HD patients and healthy volunteers (PERMDISP $p = 0.0037$).

TABLE 1 Clinical characteristics of the participants [median (interquartile range)].

	HD patients	NHD patients	Healthy volunteers	H test*	*p**
	n = 22 (6 female, 16 males)	*n* = 11 (3 females, 8 males)	*n* = 11 (3 females, 8 males)		
Age (years)	63.2 (14.3)	62.6 (17.5)	58.6 (21.5)	0.022	0.989
Height (cm)	168.6 (15.0)	170.0 (9.8)	173.0 (10.2)	1.082	0.583
Body weight (kg)	83.3 (25.7)	76.2 (16.5)	78.7 (16.9)	1.986	0.370
Body mass index (kg/m^2)	29.9 (6.8)	25.4 (7.2)	26.0 (5.3)	5.682	0.058
Soft lean mass (kg)	53.7 (18.2)	49.3 (13.0)	49.9 (13.6)	0.221	0.895
Bone mineral content (kg)	2.4 (0.7)	2.1 (0.9)	2.3 (0.6)	1.030	0.599
Fat mass (kg)	26.3 (12.4)	23.3 (6.3)	23.9 (10.9)	3.503	0.174
Lean mass index (kg/m^2)	18.5 (3.8)	17.2 (2.0)	18.1 (2.5)	1.565	0.457
Fat mass index (kg/m^2)	9.6 (3.6)	7.7 (4.5)	8.1 (3.0)	4.474	0.107
Energy intake (kcal/kg)	20.3 (7.6)	26.7 (10.3)	27.8 (12.8)	5.779	0.056
Protein intake (g/kg)	0.9 (0.5)	1.1 (0.2)	1.0 (0.7)	1.133	0.567
Appetite rating (mm)	7.0 (1.0) [a]	8.0 (3.0) [a]	8.0 (2.0)	13.291	0.002
Resting energy expenditure (kcal)	1561.5 (644.0)	1563.0 (508.0)	1763.0 (494.0)	2.861	0.239
Handgrip strength (kg)	23.5 (11.0)	34.0 (23.0)	36.0 (12.0)	7.007	0.030
Pedometry (steps/d)	3037.2 (4061.9)[a]	5604.2 (8244.4)	5936.8 (4045.3)	10.667	0.005
General health (0 to 100%)	47.5 (25.0) [a]	40.0 (20.0) [a]	80.0 (25.0)	17.890	<0.001

HD: Hemodialysed patients; NHD: non-hemodialyzed patients with chronic kidney failure; Body mass index = weight (kg)/height (m)^2; Lean mass index = (soft lean mass + bone mineral content)/height (m)^2. *Kruskal-Wallis H tests, Chi-squared corrected for ties with 2 degrees of freedom. With the Benjamini–Hochberg method, significance was corrected to $p < 0.026$. [a]Significantly different from healthy volunteers; [b] significantly different from NHD patients (Wilcoxon rank sum tests).

Bray–Curtis similarity analysis underscored the highest homogeneity of the fecal microbiota in healthy volunteers and the lowest in HD patients (Figure 2B).

Visually, zOTUs richness and diversity seemed to be similar across the groups, although Shannon diversity index was significantly higher in the NHD patients compared to HD patients (Figure 3).

The MaAsLin2 analysis identified a larger number of differentially abundant zOTUs and higher-level taxa between HD and healthy volunteers in comparison to the differences between HD and NHD patients or NHD and healthy volunteers (Supplementary Table 4). Regarding short-chain fatty acid generating bacteria, we observed a decreased level of the unclassified *Oscillibacter* in NHD and HD versus heathy volunteers, and an increase in *Dialister invisus* in NHD patients as compared to healthy volunteers or HD patients. Eubacteriaceae had higher levels in both HD and NHD patients compared to healthy volunteers. *Clostridium scindens*, a bacterium involved in bile acid metabolism, exhibited higher levels in individuals with HD compared to healthy volunteers. However, after adjusting for multiple comparisons, none of the differences among groups remained statistically significant.

The overall zOTU composition was associated with height, soft lean mass, bone mineral content, resting energy expenditure, handgrip strength, and plasma levels of albumin and TNF-α (Table 3). The median values of these parameters in the whole study population were 170.0 (162.8–175.0) cm, 51.2 (32.9–66.1) kg, 2.3 (1.9–2.5) kg, 1,618 (917–2,445) kcal/day, 30.0 (11.0–50.0) kg, 43.0 (41.0–46.0) g/L, and 2.4 (0.5–5.7) pg/mL, respectively. The zOTUs associated with these variables are shown in Supplementary Table 5. Visually, the fecal microbiota communities seemed different between individuals dichotomized according to soft lean mass, resting energy expenditure, handgrip strength, and plasma albumin (Figure 4).

Discussion

This study showed that HD patients, as compared to healthy volunteers, display alterations in overall fecal microbiota composition and specific taxa, have higher blood levels of GLP-2, of inflammatory markers, and of several possible anorexigenic mediators, and impaired appetite, physical activity and general health. NHD patients also tended to show alterations in the gut barrier, although to a smaller extent than HD patients. Overall zOTU composition was significantly associated with several nutritional and inflammatory parameters.

A few cross-sectional studies have previously compared the fecal microbiota of adult patients with end-stage renal disease and healthy volunteers. At the phylum level, several studies described a higher proportion of Proteobacteria, Actinobacteria and Firmicutes (Vaziri et al., 2013a; Chao et al., 2023), and a lower abundance of Bacteroidetes (Hu et al., 2020; Wu et al., 2023) in HD patients. Although we could not confirm these differences, we found that the overall fecal microbiota composition was significantly altered in HD patients. The differences at the genus and OTU level were heterogeneous between the published studies, likely because of confounding factors like lifestyle, genetics, co-morbidities as for instance diabetes, and

TABLE 2 Biological characteristics of the participants [median (interquartile range)].

	HD patients	NHD patients	Healthy volunteers	H test*	*p**
	n = 22 (6 female, 16 males)	*n* = 11 (3 females, 8 males)	*n* = 11 (3 females, 8 males)		
Routine parameters					
Hemoglobin (g/L)	113.0 (14.0)[a]	120.0 (14.0)[a]	144.0 (14.0)	22.837	<0.001
Urea (mmol/L)	21.7 (7.5)[a]	24.9 (11.5)[a]	6.0 (2.3)	24.802	<0.001
Creatinin (umol/L)	632.5 (235.0)[a, b]	332.0 (202.0)	84.0 (29.0)	33.669	<0.001
Bicarbonate (mmol/L)	22.0 (2.8)[a]	22.8 (5.4)[a]	26.7 (4.1)	19.706	<0.001
Albumin (g/L)	41.0 (2.0)[a, b]	47.0 (3.0)	45.0 (5.0)	22.786	<0.001
Prealbumin (mg/L)	325.0 (63.0)	399.0 (105.0)[a]	289.0 (98.0)	8.727	0.013
C-reactive protein (g/L)	6.2 (8.50) [a, b]	1.5 (2.2)	1.4 (1.0)	23.942	<0.001
Intestinal permeability					
Serum lipopolysaccharides (ng/mL)	64.4 (40.1)[b]	37.4 (39.5)[a]	97.0 (30.5)	18.513	<0.001
Serum glucagon-like peptide 2 (ng/mL)	10.0 (4.4)[a]	8.3 (5.0)[a]	2.8 (0.8)	24.203	<0.001
Systemic inflammation					
Interleukin-6 (pg/mL)	1.4 (1.2)[a]	0.7 (0.8)	0.6 (0.6)	13.436	0.001
Interleukin-10 (pg/mL)	0.1 (0.1)	0.1 (0.2)	0.1 (0.1)	0.033	0.983
Tumor necrosis factor-α (pg/mL)	3.0 (1.6)[a]	2.4 (1.0)	1.5 (1.2)	17.124	<0.001
Fecal IgA (μg/mL)	1369.0 (4363.0)	738.0 (2800.0)	1200.0 (1725.0)	0.627	0.731
Appetite mediators					
Total ghrelin (pg/mL)	838.2 (403.0)	737.0 (713.9)	689.4 (581.1)	2.581	0.275
Active ghrelin (fmol/mL)	9.2 (12.8)	9.9 (8.3)	9.7 (11.4)	0.090	0.956
Leptin (pg/mL)	32643.4 (65775.8)[a]	20431.9 (53039.3)	10272.3 (10923.2)	9.518	0.009
Active glucagon-like peptide 1 (pM)	0.4 (1.0)[b]	0.1 (0.2)	0.1 (0.3)	6.764	0.034
Cholecystokinin (pg/mL)	360.7 (153.6)[a]	328.4 (161.9)	407.9 (87.4)	7.910	0.019
Neuropeptide Y (pg/mL)	61.9 (57.9)[a]	57.5 (30.0)	29.5 (15.5)	11.096	0.004
Peptide YY (pg/mL)	229.6 (107.9)[a,b]	121.7 (109.9)	54.3 (35.2)	27.672	<0.001

HD: hemodialyzed patients; NHD: non-hemodialyzed patients with chronic kidney failure. All parameters were measured in the blood besides the fecal IgA concentrations. *Kruskal–Wallis H-tests, Chi-squared corrected for ties with 2 degrees of freedom. With the Benjamini–Hochberg method, significance was corrected to $p < 0.026$.

[a]Significantly different from healthy volunteers.

[b]Significantly different from NHD patients (Wilcoxon rank sum tests).

treatments including hemodialysis. In our study, the protein and calorie intakes were not significantly different between groups and likely do not explain the gut microbiota differences. The HD and NHD patients were supplemented in micronutrients, advised to limit their dietary intake of sodium, and, if necessary, of other electrolytes as recommended by the National Kidney Foundation (Ikizler et al., 2020). The dietary restriction in potassium and acid through reduced intake of fruits and vegetable decreases the supply of fibers which may unfavorably affect the abundance and function of saccharolytic bacteria. Whether these dietary adaptations were indeed performed in our patients has not been determined.

Some studies report a depletion in short-chain fatty acid producing-bacteria in NHD patients vs. healthy controls (Wong et al., 2014; Jiang et al., 2016; Margiotta et al., 2020). We found a depletion in the butyrate-producer *Oscillibacter* species, known to be low also in diabetic patients (Wu et al., 2020). In contrast to other findings (Lau et al., 2021), the acetate- and propionate-producer *Dialister invisus* (Louis and Flint, 2017) was higher in our NHD patients. This anti-inflammatory bacterum has been associated with a dietary pattern rich in fruits, vegetables and fish (Shi et al., 2022). However, we did not evaluate long-term dietary patterns in our NHD patients and healthy volunteers. There is also an increasing interest in bacteria generating uremic toxins, such as p-cresyl sulfate for instance, which are associated with impaired prognosis. In our study, the abundance of Eubacteriaceae was higher in HD and NHD patients compared to the healthy controls. These bacteria of the Clostridia class, already described in patients with progressing IgA nephropathy (De Angelis et al., 2014), are known to produce p-cresyl sulfate (Gryp et al., 2017). Thus, their high levels may reflect severity of CKD. *Clostridium scindens*, the

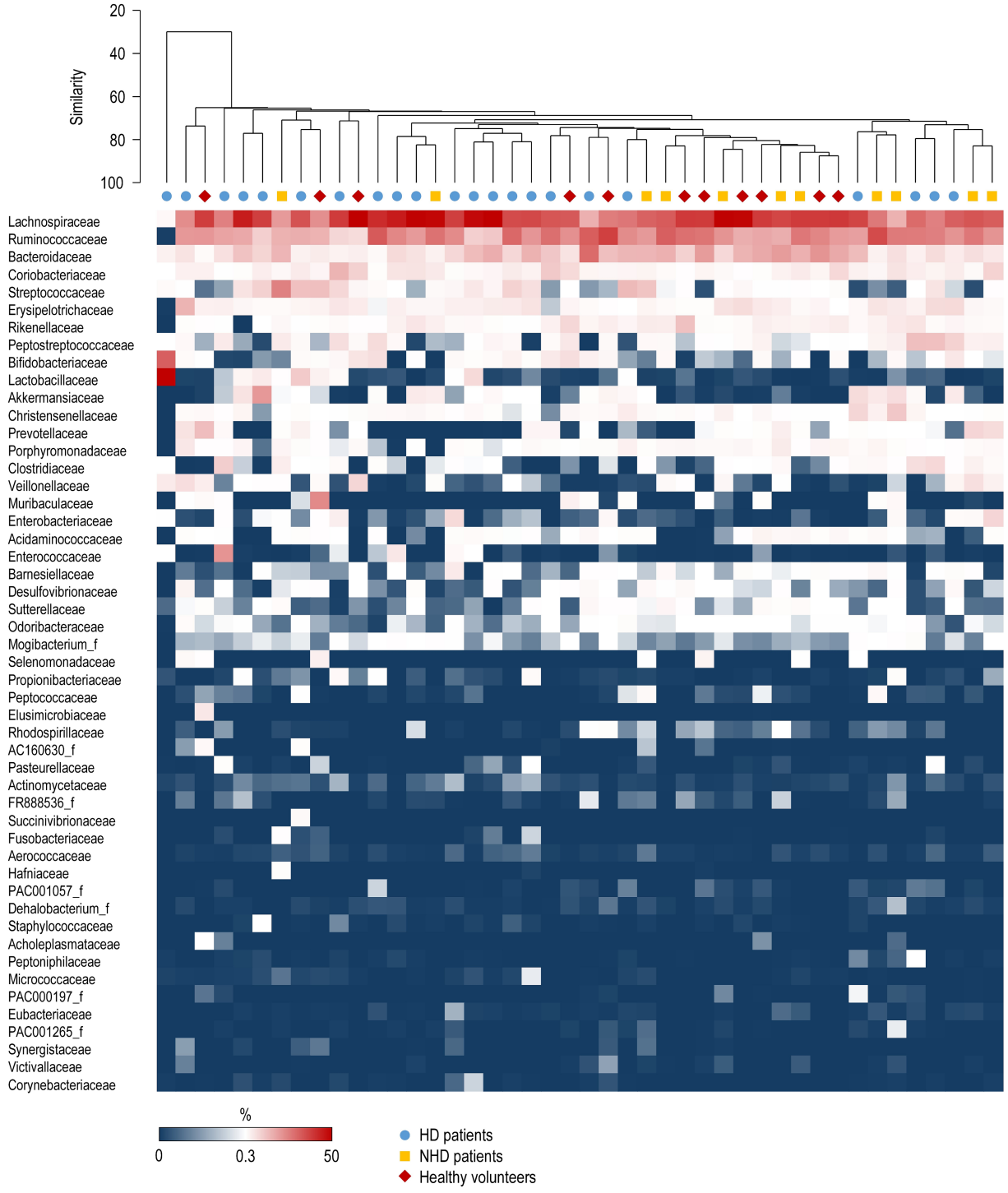

FIGURE 1
Variation in relative abundances of bacterial families among patients and control subjects. Each column corresponds to an individual patient. The top 50 families with the highest mean relative abundance are presented. The relative abundance scale is provided below the plot. The group average hierarchical clustering of samples is represented on the top. HD, hemodialyzed patients; HV, healthy volunteers; NHD, non-hemodialyzed patients with chronic kidney disease.

bacterial species with the ability to transform primary bile acids into secondary bile acids and convert glucocorticoids into androgens (Ridlon et al., 2013), was found to be more abundant in HD patients than in healthy controls. There is evidence of an association between the presence of this bacterium and the induction of remission in pediatric Crohn's disease through dietary interventions (Wang et al., 2019).

Regarding gut permeability, a cross-sectional study showed that circulating LPS, a surrogate marker of gut permeability, increased with worsening of the kidney function, correlated positively with

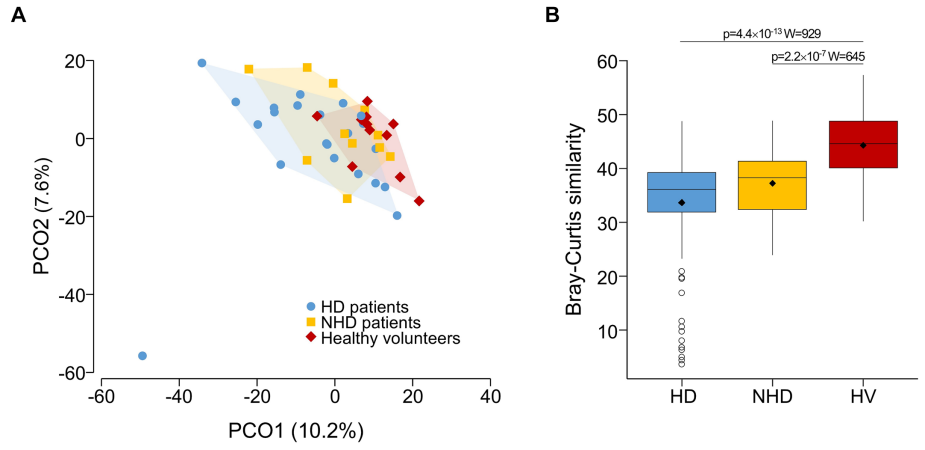

FIGURE 2
(A) PCoA plot of the fecal microbiota (zOTU-level) samples from hemodialysis (HD) patients, non hemodialyzed patients with chronic kidney disease (NHD) and healthy volunteers. It shows a trend of separation between the three groups. For clearer visual differentiation, the regions encompassing samples from each group (excluding one sample from the HD group) are shaded. **(B)** Bray–Curtis similarity analysis at the zOTU level depicting the similarity of individuals within each of the three studied groups. HV, healthy volunteers. Statistical analysis was performed using a Wilcoxon rank sum test.

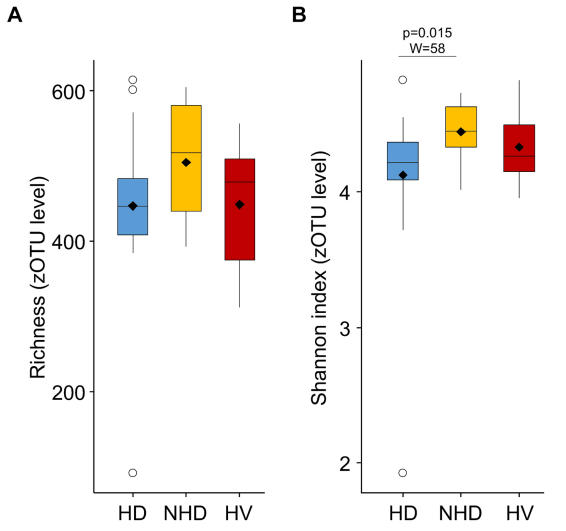

FIGURE 3
Richness **(A)** and Shannon diversity **(B)** index calculated from the relative abundance of zOTUs in hemodialysis (HD) patients, non-hemodialyzed patients with chronic kidney disease (NHD) and healthy volunteers (HV).

inflammation, and was highest in patients who recently started HD (McIntyre et al., 2011). In contrast, Wong et al. found that the intestinal permeability, assessed by sugar absorption tests, was not influenced by the dialysis procedure itself (Wong et al., 2019). Other studies which assessed gut permeability through different methods reported a higher gut permeability of NHD patients as compared to healthy controls (Magnusson et al., 1991; Wang et al., 2012). In our study, we found that LPS levels were not higher in HD and NHD patients, suggesting that LPS changes in these patients may not be responsive enough to assess gut permeability. The high serum levels of active GLP-2 in HD and NDH patients, a gut-trophic hormone produced by enteroendocrine intestinal L cells, was unexpected. It could represent an adaptative response to increased intestinal permeability, as high circulating levels of GLP-2 have been described in case of intestinal injury (Drucker, 2002).

Patients with CKD were reported to have higher plasma levels of CRP, IL-6 and TNF-α than controls (de Vinuesa et al., 2006; Borges et al., 2016). We could confirm the higher inflammatory markers in HD patients but not in the NHD patients. However, inflammation appears not to occur in all patients with CKD and is promoted mostly by the severity of kidney disease and the dialysis procedure (Cobo et al., 2018).

Levels of several possible anorexigenic hormones, such as leptin and peptide YY (Bossola et al., 2006), were higher in HD and NHD patients as compared to healthy volunteers, which is in line with their lower appetite. We would have also expected a lower level of Neuropeptide Y and a higher level of cholecystokinin in these patients. A recent review reports controversial results regarding plasma levels of leptin and ghrelin in patients with CKD (Wang et al., 2022). Thus, the explanation of low appetite in HD and uremia seems more complex than an imbalance of plasma appetite mediators.

Previous studies including NHD patients could not associate fecal microbiota composition with muscle mass and function (Margiotta et al., 2020, 2021). However, bacterial uremic toxins have been linked positively with inflammation (Borges et al., 2016), and negatively with body mass index and dietary intakes (Hu et al., 2022). As a novelty, we report an association of the overall microbiota composition with several nutritional parameters, as for instance soft lean mass and handgrip strength, and inflammatory parameters (C-reactive protein, IL-6, TNF-α, albumin), but these results need confirmation in larger studies.

Finally, the low physical activity and compromised health status in HD patients are not surprising as they have been described by others (Avesani et al., 2012; Zhou et al., 2018). A low handgrip strength has been linked with a low glomerular filtration rate, and a low muscle and fat mass (Zhou et al., 2018). Our HD patients tended

TABLE 3 Associations between overall zOTU-level microbiota composition and continuous variables by DISTLM.

Variables	*p*
Clinical characteristics	
Height (cm)	0.0020[a]
Body weight (kg)	0.1200
Body mass index (kg/m^2)	0.6943
Soft lean body mass (kg)	0.0006[a]
Bone mineral content (kg)	0.0046[a]
Fat mass (kg)	0.8312
Lean body mass index (kg/m^2)	0.0572
Fat mass index (kg/m^2)	0.4346
Energy intake (kcal/kg)	0.5390
Protein intake (g/kg)	0.4954
Appetite rating (mm)	0.1353
Resting energy expenditure (kcal/d)	0.0001[a]
Handgrip strength (kg)	0.0006[a]
Pedometry (steps/d)	0.1287
General health (0 to 100%)	0.1726
Biological characteristics	
Hemoglobin (g/L)	0.0150
Urea (mmol/L)	0.2579
Creatinin (umol/L)	0.0172
Bicarbonate (mmol/L)	0.1671
Albumin (g/L)	0.0052[a]
Prealbumin (mg/L)	0.6997
C-reactive protein (g/L)	0.0191
Serum lipopolysaccharides (ng/mL)	0.2754
Serum glucagon-like peptide 2 (ng/mL)	0.0259
Interleukin-6 (pg/mL)	0.0238
Interleukin-10 (pg/mL)	0.4803
Tumor necrosis factor-α (pg/mL)	0.0006[a]
Fecal IgA (μg/mL)	0.8555
Total ghrelin (pg/mL)	0.0213
Active ghrelin (fmol/mL)	0.2032
Leptin (pg/mL)	0.2856
Active glucagon-like peptide 1 (pM)	0.7765
Cholecystokinin (pg/mL)	0.2978
Neuropeptide Y (pg/mL)	0.0344
Peptide YY (pg/mL)	0.0384

[a]Significant after correction for multiple testing.

to have a lower handgrip strength than healthy volunteers. The unexpectedly similar soft lean mass index in HD patients compared to healthy volunteers could be due to their slightly higher body mass index.

The strength of this study were the comparisons of several gut barrier components in HD, NHD patients and healthy volunteers of similar age. Our study was limited by a relatively small population but our primary endpoint was a difference in fecal microbiota composition between groups which had been demonstrated in such small populations (Vaziri et al., 2013a).

Conclusion

Compared to healthy volunteers, HD patients have an altered composition of fecal microbiota, a higher systemic inflammation,

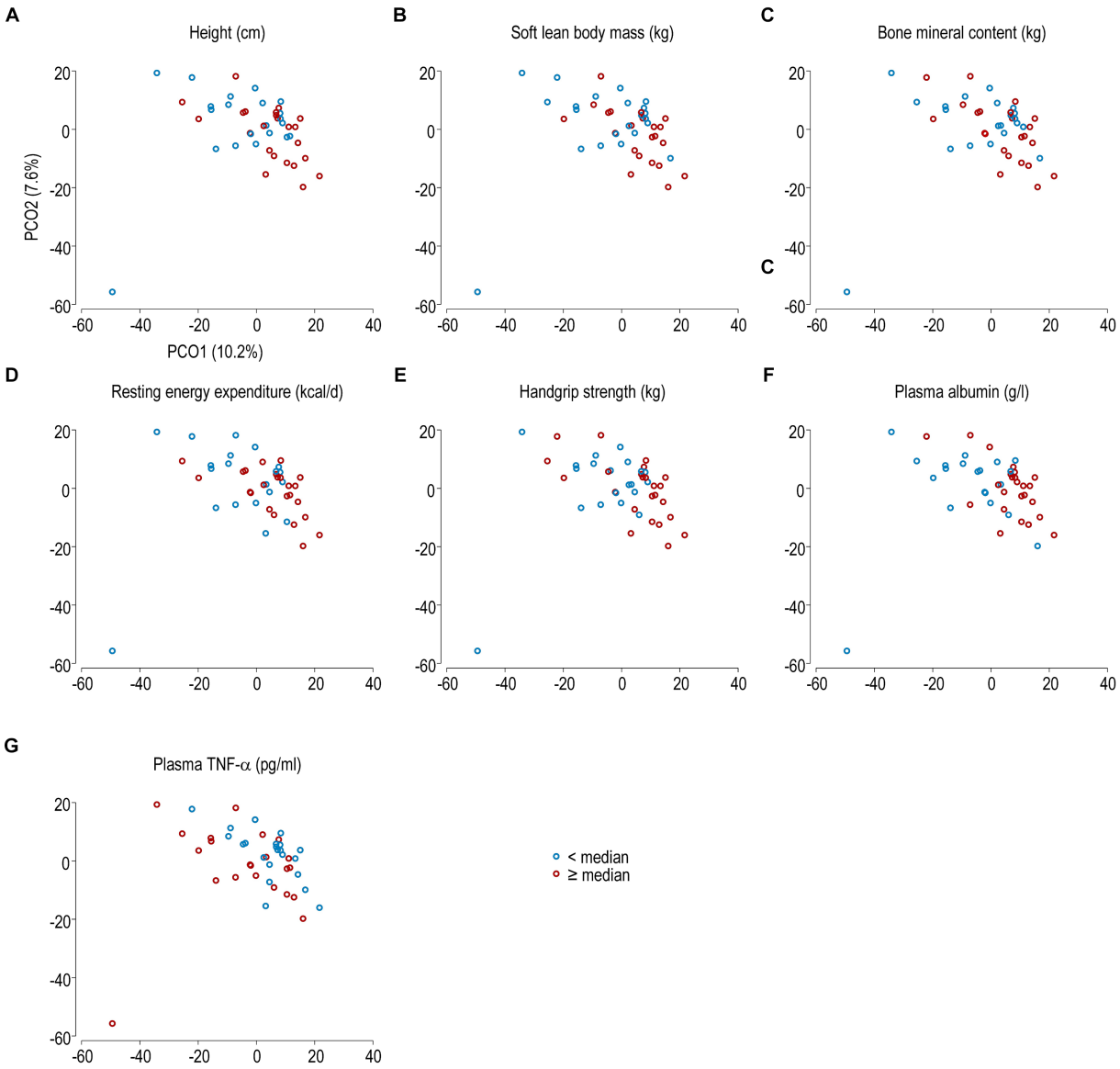

FIGURE 4
PCoA plot of the fecal microbiota samples at the zOTU level from all subjects. The subjects were categorized according to the median values of height **(A)**, soft lean body mass **(B)**, bone mineral content **(C)**, resting energy expenditure **(D)**, handgrip strength **(E)**, plasma albumin **(F)**, and plasma levels of TNF-α **(G)**. Bacterial communities of subjects with values below the median value are shown in blue, and the others in red.

and higher plasma levels of two anorexigenic appetite mediators, namely leptin and peptide YY. Overall bacterial composition was significantly associated with several nutritional and inflammatory parameters, but this association should be confirmed in larger studies.

Data availability statement

The datasets presented in this study can be found in online repositories. The names of the repository/repositories and accession number(s) can be found at: https://www.ebi.ac.uk/ena, PRJEB49241; https://www.ebi.ac.uk/ena, PRJEB43505.

Ethics statement

The studies involving humans were approved by Commission cantonale d'éthique de la recherche CCER (Geneva, Switzerland) and Commission cantonale d'éthique de la recherche sur l'être humain CER-VD (Lausanne, Switzerland). The studies were conducted in accordance with the local legislation and institutional requirements. The participants provided their written informed consent to participate in this study.

Author contributions

VL: Conceptualization, Formal analysis, Methodology, Writing – original draft, Writing – review & editing. DT: Conceptualization,

Data curation, Investigation, Methodology, Project administration, Writing – review & editing. MP: Data curation, Investigation, Methodology, Project administration, Writing – review & editing. CS: Investigation, Methodology, Writing – review & editing. NM: Investigation, Writing – review & editing. JM: Data curation, Investigation, Methodology, Project administration, Writing – review & editing. RS: Investigation, Project administration, Writing – review & editing. AW-G: Investigation, Project administration, Writing – review & editing. NG: Formal analysis, Methodology, Writing – review & editing. PC: Methodology, Writing – review & editing. OD: Writing – review & editing. FH: Conceptualization, Data curation, Formal analysis, Methodology, Writing – review & editing. JS: Formal analysis, Methodology, Project administration, Writing – review & editing. LG: Conceptualization, Data curation, Formal analysis, Funding acquisition, Investigation, Methodology, Project administration, Writing – original draft, Writing – review & editing.

Funding

The author(s) declare that financial support was received for the research, authorship, and/or publication of this article. Swiss National Foundation (Grant number 320030_163144), Alfred and Alice Lachmann Foundation and Fresenius Kabi Deutschland GmbH provided financial support for this study.

Acknowledgments

The authors are grateful to: at the Geneva University Hospitals: Giulio Conicella for performing the body composition measurements by dual-energy x-ray absorptiometry; Myriam Girard for performing DNA extractions and PCR; Pierre Lescuyer and Geraldine Poulain for helping with the SOP for blood sample, collection and storage of blood samples of the participating centers, and sending them to the different labs for analyses; Isabelle Ramseyer for taking care of the cytokine measurements; Pascale Roux-Lombard and Fabienne Mörch for taking care of the fecal IgA measurements. At the University Hospital of Lausanne: Didier Hans for performing the body composition measurements by dual-energy x-ray absorptiometry; Prof. Francesca Amati for performing the indirect calorimetries. At the Hospital of Sion: Bertrand Léger for performing the body composition measurements by dual-energy x-ray absorptiometry; Lorella Ciutto for performing the indirect calorimetries, dietary recalls and dietary reports; and Michel Rossier for his help in the collection and storage of blood samples of the Hospital of Sion.

Conflict of interest

PC is the research director at Fonds de la Recherche Scientifique (FNRS) and is a recipient of grants from FNRS. PC is an inventor on patent applications related to the use of bacteria in addressing metabolic disorders. PC was a co-founder of the Akkermansia Company SA and Enterosys.

Fresenius Kabi Deutschland GmbH had no authority over the purpose, methodology, and results of this investigator-initiated study.

The remaining authors declare that the research was conducted in the absence of any commercial or financial relationships that could be construed as a potential conflict of interest.

Publisher's note

Supplementary material

The Supplementary material for this article can be found online at: https://www.frontiersin.org/articles/10.3389/fmicb.2024.1298432/full#supplementary-material

References

Anderson, M. J. (2001). A new method for non-parametric multivariate analysis of variance. *Austral Ecol.* 26, 32–46.

Anderson, M. J. (2006). Distance-based tests for homogeneity of multivariate dispersions. *Biometrics* 62, 245–253. doi: 10.1111/j.1541-0420.2005.00440.x

Avesani, C. M., Trolonge, S., Deleaval, P., Baria, F., Mafra, D., Faxen-Irving, G., et al. (2012). Physical activity and energy expenditure in haemodialysis patients: an international survey. *Nephrol. Dial. Transplant.* 27, 2430–2434. doi: 10.1093/ndt/gfr692

Benjamini, Y., and Hochberg, Y. (1995). Controlling the false discovery rate: a practical and powerful approach to multiple testing. *J. R. Stat. Soc. Ser. B Stat. Methodol* 57, 289–300. doi: 10.1111/j.2517-6161.1995.tb02031.x

Borges, N. A., Barros, A. F., Nakao, L. S., Dolenga, C. J., Fouque, D., and Mafra, D. (2016). Protein-bound uremic toxins from gut microbiota and inflammatory markers in chronic kidney disease. *J. Ren. Nutr.* 26, 396–400. doi: 10.1053/j.jrn.2016.07.005

Bossola, M., Tazza, L., Giungi, S., and Luciani, G. (2006). Anorexia in hemodialysis patients: an update. *Kidney Int.* 70, 417–422. doi: 10.1038/sj.ki.5001572

Bray, R., and Curtis, J. T. (1957). An ordination of the upland forest communities of southern Wisconsin. *Ecol. Monogr.* 27, 325–349. doi: 10.2307/1942268

Chao, Y. T., Lin, Y.-K., Chen, L.-K., Huang, P., and Hsu, Y.-C. (2023). Role of the gut microbiota and their metabolites in hemodialysis patients. *Int. J. Med. Sci.* 20, 725–736. doi: 10.7150/ijms.82667

Chung, S., Barnes, J. L., and Astroth, K. S. (2019). Gastrointestinal microbiota in patients with chronic kidney disease: a systematic review. *Adv. Nutr.* 10, 888–901. doi: 10.1093/advances/nmz028

Cobo, G., Lindholm, B., and Stenvinkel, P. (2018). Chronic inflammation in end-stage renal disease and dialysis. *Nephrol. Dial. Transplant.* 33:iii35-iii40. doi: 10.1093/ndt/gfy175

Crouter, S. E., Schneider, P. L., Karabulut, M., and Bassett, D. R. Jr. (2003). Validity of 10 electronic pedometers for measuring steps, distance, and energy cost. *Med. Sci. Sports Exerc.* 35, 1455–1460. doi: 10.1249/01.MSS.0000078932.61440.A2

De Angelis, M., Montemurno, E., Piccolo, M., Vannini, L., Lauriero, G., Maranzano, V., et al. (2014). Microbiota and metabolome associated with immunoglobulin a nephropathy (IgAN). *PLoS One* 9:e99006. doi: 10.1371/journal.pone.0099006

de Vinuesa, S. G., Goicoechea, M., Kanter, J., Puerta, M., Cachofeiro, V., Lahera, V., et al. (2006). Insulin resistance, inflammatory biomarkers, and adipokines in patients with chronic kidney disease: effects of angiotensin II blockade. *J. Am. Soc. Nephrol.* 17, S206–S212. doi: 10.1681/ASN.2006080916

Drucker, D. J. (2002). Gut adaptation and the glucagon-like peptides. *Gut* 50, 428–435. doi: 10.1136/gut.50.3.428

Edgar, R. C. (2010). Search and clustering orders of magnitude faster than BLAST. *Bioinformatics* 26, 2460–2461. doi: 10.1093/bioinformatics/btq461

Edgar, R. C. (2016). UNOISE2: improved error-correction for Illumina 16S and ITS amplicon sequencing. *bioRxiv preprint*. doi: 10.1101/081257

Genton, L., Pruijm, M., Teta, D., Bassi, I., Cani, P. D., Gaia, N., et al. (2021). Gut barrier and microbiota changes with glycine and branched-chain amino acid supplementation in chronic haemodialysis patients. *J. Cachexia. Sarcopenia Muscle* 12, 1527–1539. doi: 10.1002/jcsm.12781

Gryp, T., Vanholder, R., Vaneechoutte, M., and Glorieux, G. (2017). P-Cresyl sulfate. *Toxins (Basel)* 9:52. doi: 10.3390/toxins9020052

Hu, C., Zhang, Y., Bi, X., Yao, L., Zhou, Y., and Ding, W. (2022). Correlation between serum trimethylamine-N-oxide concentration and protein energy wasting in patients on maintenance hemodialysis. *Ren. Fail.* 44, 1670–1677. doi: 10.1080/0886022X.2022.2131572

Hu, J., Zhong, X., Yan, J., Zhou, D., Qin, D., Xiao, X., et al. (2020). High-throughput sequencing analysis of intestinal flora changes in ESRD and CKD patients. *BMC Nephrol.* 21:12. doi: 10.1186/s12882-019-1668-4

Huang, C. X., Tighiouart, H., Beddhu, S., Cheung, A. K., Dwyer, J. T., Eknoyan, G., et al. (2010). Both low muscle mass and low fat are associated with higher all-cause mortality in hemodialysis patients. *Kidney Int.* 77, 624–629. doi: 10.1038/ki.2009.524

Ikizler, T. A., Burrowes, J. D., Byham-Gray, L. D., Campbell, K. L., Carrero, J. J., Chan, W., et al. (2020). KDOQI clinical practice guideline for nutrition in CKD: 2020 update. *Am. J. Kidney Dis.* 76, S1–S107. doi: 10.1053/j.ajkd.2020.05.006

Jiang, S., Xie, S., Lv, D., Zhang, Y., Deng, J., Zeng, L., et al. (2016). A reduction in the butyrate producing species Roseburia spp. and *Faecalibacterium prausnitzii* is associated with chronic kidney disease progression. *Antonie Van Leeuwenhoek* 109, 1389–1396. doi: 10.1007/s10482-016-0737-y

Kazancioğlu, R. (2013). Risk factors for chronic kidney disease: an update. *Kidney Int. Suppl.* 3, 368–371. doi: 10.1038/kisup.2013.79

Krukowski, H., Valkenburg, S., Madella, A. M., Garssen, J., van Bergenhenegouwen, J., Overbeek, S. A., et al. (2023). Gut microbiome studies in CKD: opportunities, pitfalls and therapeutic potential. *Nat. Rev. Nephrol.* 19, 87–101. doi: 10.1038/s41581-022-00647-z

Lau, W. L., Chang, Y., and Vaziri, N. D. (2021). The consequences of altered microbiota in immune-related chronic kidney disease. *Nephrol. Dial. Transplant.* 36, 1791–1798. doi: 10.1093/ndt/gfaa087

Lazarevic, V., Gaia, N., Girard, M., and Schrenzel, J. (2016). Decontamination of 16S rRNA gene amplicon sequence datasets based on bacterial load assessment by qPCR. *BMC Microbiol.* 16:73. doi: 10.1186/s12866-016-0689-4

Leong, D. P., Teo, K. K., Rangarajan, S., Kutty, V. R., Lanas, F., Hui, C., et al. (2016). Reference ranges of handgrip strength from 125,462 healthy adults in 21 countries: a prospective urban rural epidemiologic (PURE) study. *J. Cachexia. Sarcopenia Muscle* 7, 535–546. doi: 10.1002/jcsm.12112

Louis, P., and Flint, H. J. (2017). Formation of propionate and butyrate by the human colonic microbiota. *Environ. Microbiol.* 19, 29–41. doi: 10.1111/1462-2920.13589

Luo, D., Zhao, W., Lin, Z., Wu, J., Lin, H., Li, Y., et al. (2021). The effects of hemodialysis and peritoneal Dialysis on the gut microbiota of end-stage renal disease patients, and the relationship between gut microbiota and patient prognoses. *Front. Cell. Infect. Microbiol.* 11:579386. doi: 10.3389/fcimb.2021.579386

Magnotti, L. J., and Deitch, E. A. (2005). Burns, bacterial translocation, gut barrier function, and failure. *J. Burn Care Rehabil.* 26, 383–391. doi: 10.1097/01.bcr.0000176878.79267.e8

Magnusson, M., Magnusson, K. E., Sundqvist, T., and Denneberg, T. (1991). Impaired intestinal barrier function measured by differently sized polyethylene glycols in patients with chronic renal failure. *Gut* 32, 754–759. doi: 10.1136/gut.32.7.754

Mak, R. H., Ikizler, A. T., Kovesdy, C. P., Raj, D. S., Stenvinkel, P., and Kalantar-Zadeh, K. (2011). Wasting in chronic kidney disease. *J. Cachexia. Sarcopenia Muscle* 2, 9–25. doi: 10.1007/s13539-011-0019-5

Mallick, H., Rahnavard, A., McIver, L. J., Ma, S., Zhang, Y., Nguyen, L. H., et al. (2021). Multivariable association discovery in population-scale meta-omics studies. *PLoS Comput. Biol.* 17:e1009442. doi: 10.1371/journal.pcbi.1009442

Margiotta, E., Caldiroli, L., Callegari, M. L., Miragoli, F., Zanoni, F., Armelloni, S., et al. (2021). Association of sarcopenia and gut microbiota composition in older patients with advanced chronic kidney disease, investigation of the interactions with uremic toxins, inflammation and oxidative stress. *Toxins (Basel)* 13:472. doi: 10.3390/toxins13070472

Margiotta, E., Miragoli, F., Callegari, M. L., Vettoretti, S., Caldiroli, L., Meneghini, M., et al. (2020). Gut microbiota composition and frailty in elderly patients with chronic kidney disease. *PLoS One* 15:e0228530. doi: 10.1371/journal.pone.0228530

McIntyre, C. W., Harrison, L. E., Eldehni, M. T., Jefferies, H. J., Szeto, C. C., John, S. G., et al. (2011). Circulating endotoxemia: a novel factor in systemic inflammation and cardiovascular disease in chronic kidney disease. *Clin. J. Am. Soc. Nephrol.* 6, 133–141. doi: 10.2215/cjn.04610510

National Kidney Foundation (2000). Clinical practice guidelines for nutrition in chronic renal failure. Available at: https://www.kidney.org/professionals/guidelines (Accessed 1st September 2023).

National Kidney Foundation (2019). Clincal practice guideline for nutrition in chronic kidney disease: 2019 update. Available at: https://www.kidney.org/sites/default/files/Nutrition_GL%2BSubmission_101719_Public_Review_Copy.pdf

Popkov, V. A., Zharikova, A. A., Demchenko, E. A., Andrianova, N. V., Zorov, D. B., and Plotnikov, E. Y. (2022). Gut microbiota as a source of uremic toxins. *Int. J. Mol. Sci.* 23:483. doi: 10.3390/ijms23010483

RAND Health Care. (2023) 36-item short form survey from the RAND Medical Outcomes Study. Available at: https://www.rand.org/health-care/surveys_tools/mos/36-item-short-form.html (Accessed 1st September, 2023).

Ridlon, J. M., Ikegawa, S., Alves, J. M., Zhou, B., Kobayashi, A., Iida, T., et al. (2013). *Clostridium scindens*: a human gut microbe with a high potential to convert glucocorticoids into androgens. *J. Lipid Res.* 54, 2437–2449. doi: 10.1194/jlr.M038869

Schloss, P. D., Westcott, S. L., Ryabin, T., Hall, J. R., Hartmann, M., Hollister, E. B., et al. (2009). Introducing mothur: open-source, platform-independent, community-supported software for describing and comparing microbial communities. *Appl. Environ. Microbiol.* 75, 7537–7541. doi: 10.1128/AEM.01541-09

Schneider, P. L., Crouter, S. E., Lukajic, O., and Bassett, D. R. Jr. (2003). Accuracy and reliability of 10 pedometers for measuring steps over a 400-m walk. *Med. Sci. Sports Exerc.* 35, 1779–1784. doi: 10.1249/01.MSS.0000089342.96098.C4

Shannon, C. E. (1948). A mathematical theory of communication. *Bell Syst. Tech. J.* 27, 379–423. doi: 10.1002/j.1538-7305.1948.tb01338.x

Shi, H., Horst, R. T., Nielen, S., Bloemendaal, M., Jaeger, M., Joosten, I., et al. (2022). The gut microbiome as mediator between diet and its impact on immune function. *Sci. Rep.* 12:5149. doi: 10.1038/s41598-022-08544-y

Sumida, K., Lau, W. L., Kovesdy, C. P., Kalantar-Zadeh, K., and Kalantar-Zadeh, K. (2021). Microbiome modulation as a novel therapeutic approach in chronic kidney disease. *Curr. Opin. Nephrol. Hypertens.* 30, 75–84. doi: 10.1097/MNH.0000000000000661

Suneja, M., Murry, D. J., Stokes, J. B., and Lim, V. S. (2011). Hormonal regulation of energy-protein homeostasis in hemodialysis patients: an anorexigenic profile that may predispose to adverse cardiovascular outcomes. *Am. J. Physiol. Endocrinol. Metab.* 300, E55–E64. doi: 10.1152/ajpendo.00438.2010

Szeto, C. C., McIntyre, C. W., and Li, P. K. (2018). Circulating bacterial fragments as cardiovascular risk factors in CKD. *J. Am. Soc. Nephrol.* 29, 1601–1608. doi: 10.1681/ASN.2018010068

Vanholder, R., Pletinck, A., Schepers, E., and Glorieux, G. (2018). Biochemical and clinical impact of organic uremic retention solutes: a comprehensive update. *Toxins (Basel)* 10:33. doi: 10.3390/toxins10010033

Vassalotti, J. A., Centor, R., Turner, B. J., Greer, R. C., Choi, M., Sequist, T. D., et al. (2016). Practical approach to detection and management of chronic kidney disease for the primary care clinician. *Am. J. Med.* 129:e157, 153–162.e7. doi: 10.1016/j.amjmed.2015.08.025

Vaziri, N. D., Wong, J., Pahl, M., Piceno, Y. M., Yuan, J., Desantis, T. Z., et al. (2013a). Chronic kidney disease alters intestinal microbial flora. *Kidney Int.* 83, 308–315. doi: 10.1038/ki.2012.345

Vaziri, N. D., Yuan, J., and Norris, K. (2013b). Role of urea in intestinal barrier dysfunction and disruption of epithelial tight junction in chronic kidney disease. *Am. J. Nephrol.* 37, 1–6. doi: 10.1159/000345969

Wang, F., Jiang, H., Shi, K., Ren, Y., Zhang, P., and Cheng, S. (2012). Gut bacterial translocation is associated with microinflammation in end-stage renal disease patients. *Nephrology (Carlton)* 17, 733–738. doi: 10.1111/j.1440-1797.2012.01647.x

Wang, S., Martins, R., Sullivan, M. C., Friedman, E. S., Misic, A. M., El-Fahmawi, A., et al. (2019). Diet-induced remission in chronic enteropathy is associated with altered microbial community structure and synthesis of secondary bile acids. *Microbiome* 7:126. doi: 10.1186/s40168-019-0740-4

Wang, X. H., Mitch, W. E., and Price, S. R. (2022). Pathophysiological mechanisms leading to muscle loss in chronic kidney disease. *Nat. Rev. Nephrol.* 18, 138–152. doi: 10.1038/s41581-021-00498-0

Wong, J., Lenaerts, K., Meesters, D. M., Olde Damink, S. W. M., van Eijk, H. M. H., Vilar, E., et al. (2019). Acute haemodynamic changes during haemodialysis do not exacerbate gut hyperpermeability. *Biosci. Rep.* 39:BSR20181704. doi: 10.1042/BSR20181704

Wong, J., Piceno, Y. M., DeSantis, T. Z., Pahl, M., Andersen, G. L., and Vaziri, N. D. (2014). Expansion of urease- and uricase-containing, indole- and p-cresol-forming and contraction of short-chain fatty acid-producing intestinal microbiota in ESRD. *Am. J. Nephrol.* 39, 230–237. doi: 10.1159/000360010

Wu, H. Y., Lin, Y. T., Tsai, W. C., Chiu, Y. L., Ko, M. J., Yang, J. Y., et al. (2023). Microbiota analysis in the hemodialysis population - focusing on Enterobacteriaceae. *J. Microbiol. Immunol. Infect.* 56, 311–323. doi: 10.1016/j.jmii.2022.12.001

Wu, H., Tremaroli, V., Schmidt, C., Lundqvist, A., Olsson, L. M., Kramer, M., et al. (2020). The gut microbiota in prediabetes and diabetes: a population-based cross-sectional study. *Cell Metab.* 32:e373, 379–390.e3. doi: 10.1016/j.cmet.2020.06.011

Yoon, S. H., Ha, S. M., Kwon, S., Lim, J., Kim, Y., Seo, H., et al. (2017). Introducing EzBioCloud: a taxonomically united database of 16S rRNA gene sequences and whole-genome assemblies. *Int. J. Syst. Evol. Microbiol.* 67, 1613–1617. doi: 10.1099/ijsem.0.001755

Zhang, J., Kobert, K., Flouri, T., and Stamatakis, A. (2014). PEAR: a fast and accurate Illumina paired-end reAd mergeR. *Bioinformatics* 30, 614–620. doi: 10.1093/bioinformatics/btt593

Zhou, Y., Hellberg, M., Svensson, P., Hoglund, P., and Clyne, N. (2018). Sarcopenia and relationships between muscle mass, measured glomerular filtration rate and physical function in patients with chronic kidney disease stages 3-5. *Nephrol. Dial. Transplant.* 33, 342–348. doi: 10.1093/ndt/gfw466

Frontiers in Microbiology

Explores the habitable world and the potential of microbial life

The largest and most cited microbiology journal which advances our understanding of the role microbes play in addressing global challenges such as healthcare, food security, and climate change.

Discover the latest Research Topics

See more →

Frontiers

Avenue du Tribunal-Fédéral 34
1005 Lausanne, Switzerland
frontiersin.org

Contact us

+41 (0)21 510 17 00
frontiersin.org/about/contact